

Investigation of metal oxides mediated
construction and reactivity of polycyclic
aromatic hydrocarbons

Dissertation

zur Erlangung des Doktorgrades der Naturwissenschaften
(Dr. rer. nat.)

der

Naturwissenschaftlichen Fakultät II
Chemie, Physik und Mathematik

der Martin-Luther-Universität
Halle-Wittenberg

vorgelegt von

Herrn Andreas Förtsch

Gutachter

Prof. Dr. Konstantin Amsharov
Prof. Dr. Norbert Jux

Tag der Verteidigung

06.11.2023

Danksagung

Ich möchte mich herzlich bedanken bei Prof. Dr. Konstantin Amsharov für das Bereitstellen dieses interessanten Forschungsthemas. Außerdem hat er auch große Unterstützung bei Fragen oder Problemen geleistet.

Zudem gilt mein Dank allen Mitarbeitern seines Arbeitskreises, die mich sehr herzlich aufgenommen haben und mir immer mit Rat und Tat zur Seite gestanden haben. Besonders dankbar bin ich Vladimir Akhmetov für die Unterstützung bei der Festlegung und Ideensammlung der interessantesten Themen.

Zusätzlich möchte ich mich noch bei allen Angestellten des Institutes für Organische Chemie für die Unterstützung bedanken, vor allem Anne Hauptmann für alle organisatorischen Aufgaben.

Zum Schluss möchte ich mich noch bei meiner Familie bedanken, die mich nicht nur während der Doktorarbeit, sondern auch während des gesamten Studiums immer unterstützt und motiviert hat.

List of Symbols

δ	chemical shift (NMR)
λ	wavelength
J	coupling constant

List of Abbreviations

AcOH	acetic acid
aq.	Aqueous
amCFa	alumina-mediated C-F bond activation
Bz	benzyl
B ₂ pin ₂	bis(pinacolato)diboron
CDHF	cyclodehydrofluorination
¹³ C NMR	carbon 13 nuclear magnetic resonance
Cy	cyclohexyl
conc.	concentrated
d	doublet (NMR)
DBPO	dibenzoyl peroxide
DCM	dichloromethane
DDQ	4,5-dichloro-3,6-dioxocyclohexa-1,4-diene-1,2-dicarbonitrile
DME	dimethylether
DMF	dimethylformamide
DMA	dimethylacetamide
EtOAc	ethyl acetate
Et ₂ O	diethylether
¹⁹ F NMR	fluorine 19 nuclear magnetic resonance
FVP	flash vacuum pyrolysis
g	gram(s)
¹ H NMR	proton nuclear magnetic resonance
h	hour(s)
<i>hν</i>	light
HPLC	high performance liquid chromatography
Hz	Hertz

KOtBu	potassium <i>tert</i> -butoxide
L	liter
LDI	laser desorption ionization
LOI	Limiting Oxygen Index
LooP	ladderization of fluorinated oligophenylenes
m	multiplet (NMR)
M	molar
MALDI	matrix assisted laser desorption ionization
TOF	time of flight
MeOH	methanol
MHz	megahertz
mL	milliliter(s)
mmol	millimol(s)
mol	mol(s)
MS	mass spectrometry
<i>m/z</i>	mass-to-charge ratio
<i>n</i> -BuLi	<i>n</i> -butyllithium
NBS	<i>N</i> -bromosuccinimide
N ₄ (CH ₂) ₆	(1 <i>R</i> ,3 <i>s</i> ,5 <i>s</i>)-1,3,5,7-tetraazaadamantane
NGs	nanographenes
NMR	nuclear magnetic resonance
<i>o</i> -DCB	<i>ortho</i> -dichlorobenzene
PAH	polycyclic aromatic hydrocarbon
Pd(dppf)Cl ₂	[1,1'-bis(diphenylphosphino)ferrocene]dichloropalladium(II)
Pd-PEPPSI-Ipent	Dichloro-[1,3-bis-(2,6-di-3-pentylphenyl)-imidazol-2-yliden] (3-chloropyridyl)-palladium(II)
Pd(P(Ph) ₃) ₄	tetrakis(triphenylphosphine)palladium(0)
Pd(PPh ₃) ₂ Cl ₂	bis(triphenylphosphine)palladium(II) dichloride
³¹ P-NMR	phosphor nuclear magnetic resonance
ppm	parts per million
R _f	retention factor
R _t	retention time
rt	room temperature

s	singlet (NMR)
SA	surface area
sat.	saturated
SM	starting material
t	triplet (NMR)
<i>t</i> -Bu	<i>tert</i> -butyl
THF	tetrahydrofuran
TLC	thin layer chromatography
TMP	2,2,6,6-tetramethylpiperidine
UV/Vis	ultraviolet-visible

Table of Content

1. INTRODUCTION	1
1.1. Characterization of Relevant Polycyclic Aromatic Hydrocarbon Edge Structures	3
1.2. Synthesis of PAHs.....	4
1.2.1. Aryl-Aryl-Coupling by Oxidative Dehydrogenation	4
1.2.2. Aryl-Aryl coupling by C-F bond activation	8
1.2.3. Aryl-Aryl-coupling by γ -Al ₂ O ₃ -mediated CDHF	9
1.2.4. Defects in graphene: 7-membered ring formation.....	10
1.2.5. Zig-zag periphery by C _{sp} ³ -C _{aryl} coupling-Radical PAHs	15
1.2.6. Alumina-mediated terminal acetylene behavior	17
2. PROPOSAL	21
3. RESULTS AND DISCUSSION	22
3.1. Folding of Fluorinated Oligoarylenes into Non-alternant PAHs with Various Topological Shapes.....	22
3.1.1. Synthesis of 1,16-dehydrohexahelicene ⁷⁵	22
3.1.2. Synthesis of dibenzo[e,gh]dibenzo[4,5:6,7]-pleiadeno[2,1,12-pqa]pleiadene ⁷⁵	23
3.1.3. Synthesis of tribenzo[b,gh,pq]pleiadene	25
3.1.4. Synthesis of 14-methyldibenzo[gh,pq]pleiadene.....	26
3.1.5. Synthesis of 7-helicene-derivates and their opening on Al ₂ O ₃	27
3.1.6. Synthesis and reaction of 6,8,18,20-tetrafluorodiphenanthro[3,4-c:3',4'-l]chrysene.....	30
3.1.7. Synthesis of 12,12',14,14'-tetrafluoro-11,11'-bihexahelicene	32
3.2. Oxodefluorination of fluoroarenes	35
3.2.1. Synthesis of 2,8-bis(4-(tert-butyl)phenyl)dibenzo[b,d]furan	35
3.2.2. Synthesis of “smallest“ nanographene with bridge	36
3.3. Construction of zig-zag periphery by C _{sp} ³ -C _{aryl} coupling <i>via</i> AmCFA	40
3.3.1. Reactions with simple molecules	41
3.3.2. Synthesis of bi-[4]helicene derivates.....	46
3.4. Screening the reactivity of different functional groups on Al ₂ O ₃	48
3.5. Screening the reactivity of 2-ethynyl-1,1'-biphenyl on different metal oxides.....	51
3.6. Investigation for the soft π -Lewis acidity of different alumina's terminations	54
Commercially available.....	57
3.7. Homodimerization of terminal alkyne-model molecule under different temperatures	58
3.8. Hydrochlorination of terminal Alkynes on Al ₂ O ₃	62
4. SUMMARY	65

5. ZUSAMMENFASSUNG	67
6. EXPERIMENTAL PART	69
6.1. Instruments and Materials Data	69
6.2. Folding of Fluorinated Oligoarylenes into Non-alternant PAHs with Various Topological Shapes ⁷⁰	
6.2.1. Synthesis of 1,16-dehydrohexahelicene	74
6.2.2. Synthesis of dibenzo[e,gh]dibenzo[4,5:6,7]pleiaden[2,1,12-pqa]pleiadene	80
6.2.3. Synthesis of tribenzo[b,gh,pq]pleiadene	84
6.2.4. Synthesis of 1-(2,3-difluorophenyl)-8-(2-fluorophenyl)phenanthrene	87
6.2.5. Synthesis of 14-methyldibenzo[gh,pq]pleiadene	89
6.2.6. Synthesis of 7-helicene-derivates and their opening on Al ₂ O ₃	91
6.2.7. Synthesis and reaction of 6,8,18,20-tetrafluorodiphenanthro[3,4-c:3',4'-l]chrysene ⁹⁸	
6.2.8. Synthesis of 12,12',14,14'-tetrafluoro-11,11'-bihexahelicene	101
6.3. Oxodefluorination of fluoroarenes	107
6.3.1. Synthesis of 2,8-bis(4-(tert-butyl)phenyl)dibenzo[b,d]furan	107
6.3.2. Synthesis of „smallest“ nanographene with bridge	110
6.4. Construction of zig-zag periphery by C _{sp} ³ -C _{aryl} coupling <i>via</i> AmCFA	116
6.4.1. Reactions with small molecules	116
6.4.2. Synthesis of bi-[4]-helicene derivates	130
6.5. Screening the reactivity of different functional groups on Al ₂ O ₃	135
6.6. Screening the reactivity of 2-ethynyl-1,1'-biphenyl on different metal oxides	142
6.7. Investigation for the soft pi-Lewis acidity of different alumina's terminations	146
6.8. Homodimerization of terminal Alkyne- Model molecule with different temperatures	149
6.9. Hydrochlorination of terminal Alkynes on γ -Al ₂ O ₃	159
7. BIBLIOGRAPHY	161
8. APPENDIX	167
8.1 Folding of Fluorinated Oligoarylenes into Non-alternant PAHs with Various Topological Shapes ¹⁶⁷	
8.1.1. Synthesis of 1,16-dehydrohexahelicene	167
8.1.2. Synthesis of dibenzo[e,gh]dibenzo[4,5:6,7]pleiaden[2,1,12-pqa]pleiadene	176
8.1.3. Synthesis of tribenzo[b,gh,pq]pleiadene	180
8.1.4. Synthesis of 14-methyldibenzo[gh,pq]pleiadene	187
8.1.5. Synthesis of 7-helicene-derivates and their opening on Al ₂ O ₃	191
8.1.6. Synthesis and reaction of 6,8,18,20-tetrafluorodiphenanthro[3,4-c:3',4'-l]chrysene	214
8.1.7. Synthesis of 12,12',14,14'-tetrafluoro-11,11'-bihexahelicene	222
8.1.8. Synthesis of 1-(2,3-difluorophenyl)-8-(2-fluorophenyl)phenanthrene	237
8.2. Oxodefluorination of fluoroarenes	243
8.2.1. Synthesis of 2,8-bis(4-(tert-butyl)phenyl)dibenzo[b,d]furan	243
8.2.2. Synthesis of „smallest“ nanographene with bridge	248

8.3.	Construction of zig-zag periphery by Csp ³ -Caryl coupling via AmCFA	261
8.3.1.	Reactions with small molecules	261
8.3.2.	Synthesis of di-4-helicene derivates	288
8.4.	Screening the reactivity of different functional groups on Al ₂ O ₃	298
8.5.	Screening the reactivity of 2-ethynyl-1,1'-biphenyl on different metal oxides	309
8.6.	Investigation for the soft pi-Lewis acidity of different alumina's terminations	319
8.7.	Homodimerization of terminal Akyne- Model molecule with different temperatures	336
8.8.	Hydrochlorination of terminal Akynes on Al ₂ O ₃	358

Abstract

The groundbreaking achievements in graphene research by Geim and Novoselov^[1] have awakened interest in the synthesis and analysis of small model structures and fragments of graphene, so-called nanographenes or large polycyclic aromatic hydrocarbons (PAHs). Graphene is currently considered to be one of the leading materials due to its fascinating mechanical, electronic and optical properties.^[2] Therefore, scientists started to synthesize new nanographenes in order to examine their intriguing properties. Since the pioneering work of Clar many various synthetic routes towards planar and non-planar PAHs were proposed and realized. Alumina-mediated C-F bond activation (AmCFA) is one such valuable tool to control synthesis of nanographenes and formation of asymmetric molecules is possible.

This work uses this approach, which utilizes the advantages of the C-F bond chemistry for creation of large PAHs and nanographenes.^{[3],[4]} First, this thesis gives a general brief introduction about graphene, which is followed by an overview about carbon-based nanostructures and their edge terminology. Several of the most prolific approaches for the synthesis of large PAHs are discussed and compared, even though particular emphasis is placed on the synthesis of non-planar systems containing five- and seven-membered rings.

Secondly, the proposal introduces the goal and motivation of this thesis.

The third chapter initially deals with the synthesis of the fluorine substituted precursor molecules, preprogrammed for subsequent generation of the respective PAHs on activated γ -Al₂O₃ by cyclodehydrofluorination. Afterwards, the oxodefluorination of fluoroarenes and the formation of molecule with zig-zag periphery on alumina is discussed. After a short screening of different functional groups on alumina, reactivity of biphenylacetylene on other metal oxides were researched. The dimerization and hydrochlorination of terminal alkynes on alumina is described next. The investigation of different alumina's terminations on a model compound concludes this chapter.

Chapter four concludes the thesis and gives an outlook in possible future projects.

Following, the chapter five describes the experimental data and the synthesis details.

Lastly, HPLC chromatograms, MS, UV/vis, and NMR spectra of all compounds are given in the Appendix.

1. Introduction

Carbon is one of the most versatile elements on earth. Its ability to create long and stable chains of C-C bonds is essential for life to exist on earth. Not only the huge amount of different biological compounds is interesting for the scientific community, but also the synthesis, properties, and application of molecules such as fullerenes, single-wall carbon nanotubes or graphene. Two of these discoveries were awarded by Nobel Prizes in Chemistry and Physics (in 1996: "for discovery of fullerenes"¹ and in 2010: "for ground-breaking experiments regarding the two-dimensional material graphene"²). When Novoselov et al. discovered and isolated a stable single layer of graphene, a single layer honeycomb lattice of carbon, in 2004³, scientist around the world were astonished because it was assumed, that flat, two-dimensional and infinitely extended structures were impossible to exist, due to their verifiable thermodynamic instability.^{4,5} These groundbreaking and fundamental results opened up an immense number of directions for fundamental and applied research of chemists, physicists and material scientists.⁶ Because of its high chemical stability, optical transmittance⁷, elasticity, porosity, biocompatibility, specific surface area and tunable band gap, graphene is one of the most attractive nanomaterial, with its excellent thermal⁸, mechanical⁹, electronic¹⁰, and optical properties.^{5,7} Graphene consists of a single flat layer of graphite, in which each carbon atom is surrounded by three carbon atoms at an angle of 120° and a distance of 1.42 Å to form the typical honeycomb pattern (linked aromatic six-membered carbon rings) (Figure 1.1).

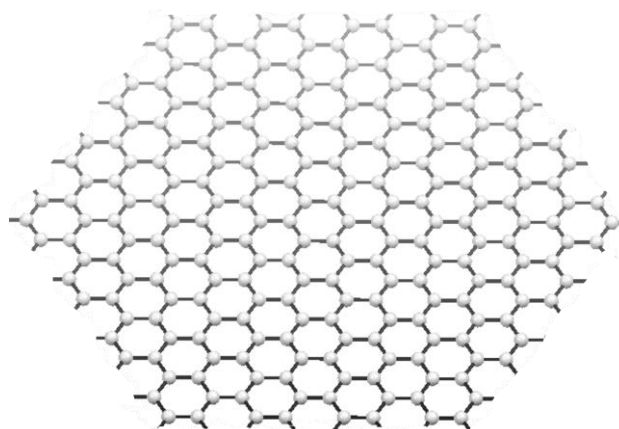


Figure 1.1: Structure of a graphene section.

Since all carbon atoms are sp^2 hybridized, each one forms three equivalent σ -bonds to neighbouring atoms. A π -bond is formed by the $2p_z$ -orbitals carrying one electron. The respective p-orbitals are perpendicular to the graphene plane and build up a delocalized π -system, which is responsible for most of the electrical properties of graphene. Traditional semiconductors show a finite bandgap greater than zero, but due to the meeting of conduction and valence band at the Dirac point, graphene is a zero-bandgap semiconductor.¹¹ Furthermore, graphene is an ultralight material, which is 100 times stronger than steel^{9,12} and due to interesting vibrational properties the material can efficiently conduct heat as well as electricity.¹³ Due to these intriguing properties, graphene is a suitable candidate for many interesting applications in electronic and optoelectronic devices such as transistors¹⁴ light-emitting diodes (LED)¹⁰, smart phones or solar cells^{15,16}. But also filtering membranes¹⁷, storage systems¹⁸ and sensors¹⁹ are possibilities.

In general, graphene can be understood as a polycyclic aromatic hydrocarbon (PAH) with infinite extent and therefore can be considered as “father” of all PAH molecules. Therefore, large PAH molecules, also called nanographenes, are often used as model compounds for graphene. Due to the correlation between size and topology of large aromatic systems with their electrical properties, a comparison with graphene is possible.^{20,21} These PAHs are becoming more and more important in the field of molecular electronics and optoelectronics including discotic liquid crystals (DLC) for light emitting diodes (LED), solar cells, donor-acceptor photovoltaics and optical field-effect transistors (OFET).^{20,22} One of the main reason for their success is the ability to tune and control properties of carbon materials by changing the shape, width and edge topologies.²³

1.1. Characterization of Relevant Polycyclic Aromatic Hydrocarbon Edge Structures

Zig-zag and armchair periphery are the two geometrically optimal arrangement in graphene. The simplest fragment of the zig-zag conformation is called the L-region. The K-region combined with the *bay*-region results in the armchair periphery. One defect in the armchair periphery leads to the *fjord-cavity*, while defects in zig-zag conformation result in *cove*- and *gulf*-regions, as it is shown in Figure 1.2.

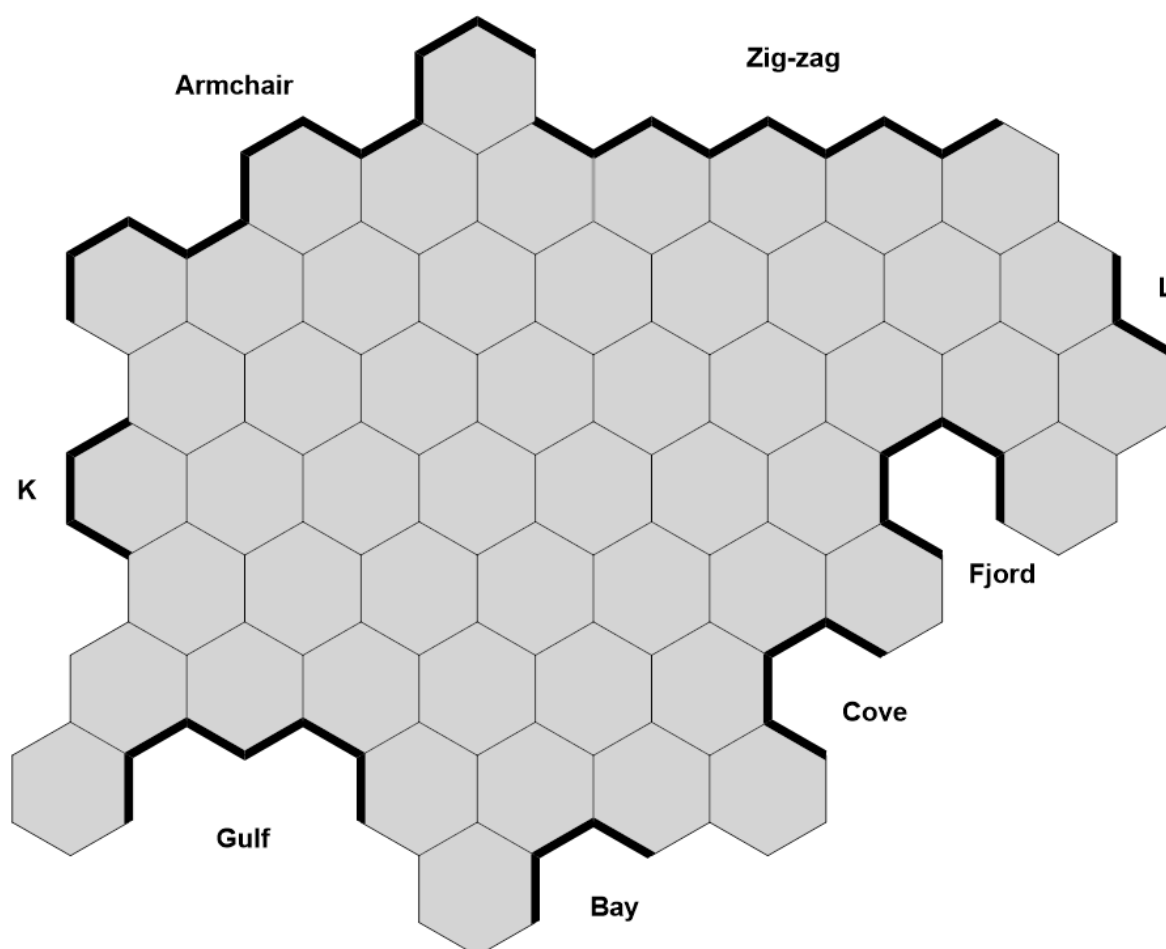


Figure 1.2: Schematic edge depiction and definitions of a graphene section.

The *bay*-, *cove*- and *fjord*-regions play a major role in PAH-chemistry, looking at the closure of these cavities to 5- or 6-member rings. The zig-zag periphery on the other hand is interesting for controlling the physical properties and therefore have found application in organic semiconductors with high charge mobilities²⁴, materials for non-

linear optics²⁵, photovoltaics²⁶, organic light-emitting diodes²⁷, liquid crystals²⁸, singlet fission²⁹, single-molecule spectroscopy³⁰ and molecular magnetism^{31,32}. In the next chapter, we discuss the known synthetic pathways of PAHs.

1.2. Synthesis of PAHs

Since the pioneering and fundamental research of Scholl, Clar, and Zander²⁰, who synthesized many small and fundamental PAHs under harsh reaction conditions, there has been huge interest in the development of alternative mild synthetic strategies. In this regard, the intramolecular aryl-aryl coupling has emerged as a very important and efficient method for the preparation of PAHs. Various approaches to PAHs were reported in literature, from which flash vacuum pyrolysis (FVP)³³, photocyclization³⁴, Pd-catalysed direct arylation^{35,36} and oxidative Scholl reaction³⁷ has to be mentioned as effective and general procedures. One of the most important reactions is the Scholl oxidation.

1.2.1. Aryl-Aryl-Coupling by Oxidative Dehydrogenation

Oxidative Scholl cyclodehydrogenation has been proven to be an efficient method for the synthesis of extremely large carbon-based nanostructures. Precursors for Scholl reaction^{22,38-40} such as dendritic and hyperbranched poly- and oligophenylenes were usually synthesized by intramolecular Diels-Alder cycloaddition of phenylene-vinylene derivatives³⁹ or trimerization of phenylene-ethynylene derivatives^{39,41} (Figure 3a). Furthermore, the intramolecular Diels-Alder reaction of phenylene-ethynylene derivatives with phenyl substituted cyclopentadienones was reported as another alternative synthetic route (Figure 3b).⁴⁰

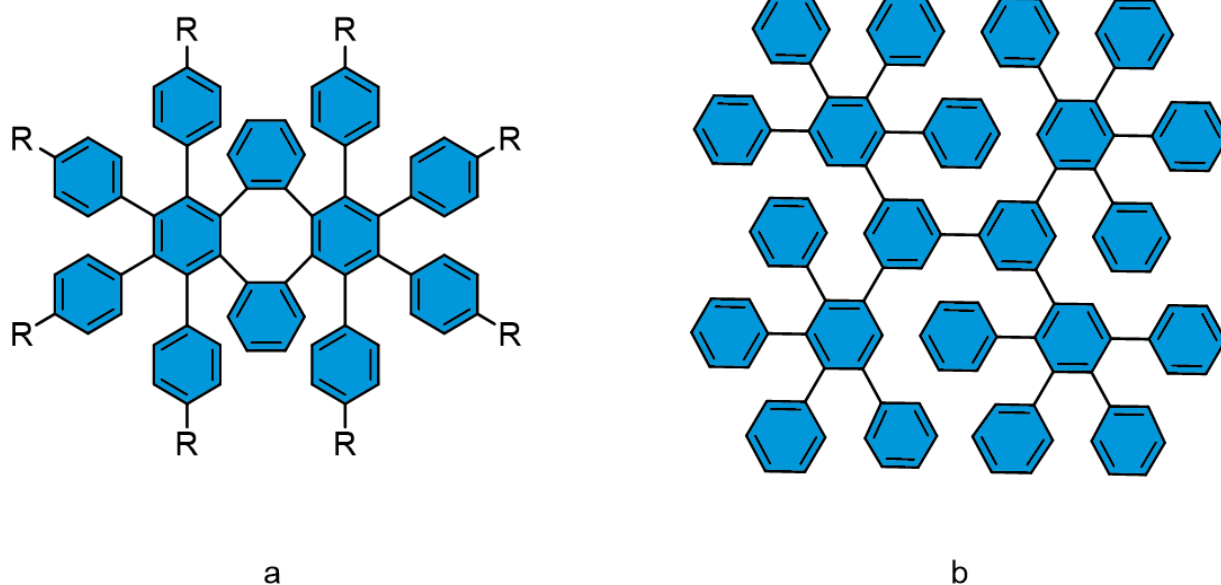


Figure 1.3: Structure of oligophenylene dendrimers $a^{21,22}$, b^{40} .

These compounds are readily soluble in common organic solvents due to their dendritic structure and can therefore be easily purified and characterized.^{22,38–40} After successful synthesis, the dendrimers were converted into their respective planar PAHs in multiple intramolecular oxidative cyclodehydrogenation steps (Scholl reaction) (Figure 1.4). Due to the low solubility of the respective planar PAHs, identification can only be done by mass spectrometry.

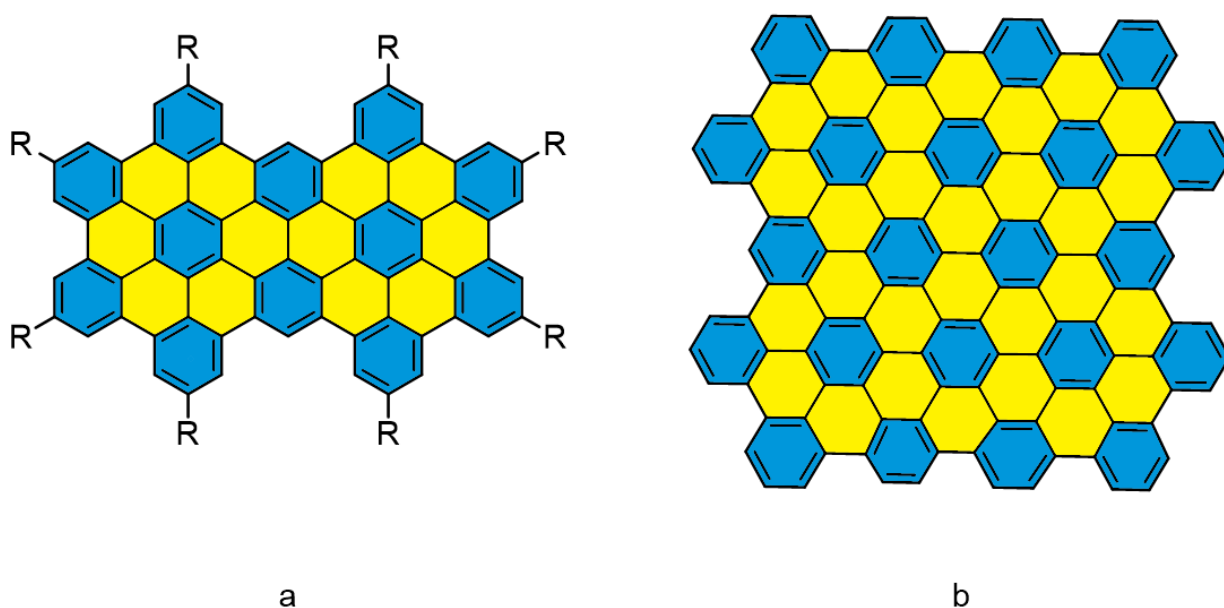


Figure 1.4: Corresponding PAHs; conditions applied for a: $\text{CuCl}_2/\text{AlCl}_3$, $80\text{ }^\circ\text{C}$, $\text{C}_2\text{H}_2\text{Cl}_4$, 12 h, quantitative yield³⁸; and for b: $\text{CuCl}_2/\text{AlCl}_3$, $\text{C}_2\text{H}_2\text{Cl}_4$, $100\text{ }^\circ\text{C}$, 9 h, 83 %⁴⁰.

The largest rationally synthesized nanographene was reported by Müllen *et al.* and was designated to C₂₂₂ by its number of carbon atoms as depicted in Figure 1.5.⁴¹

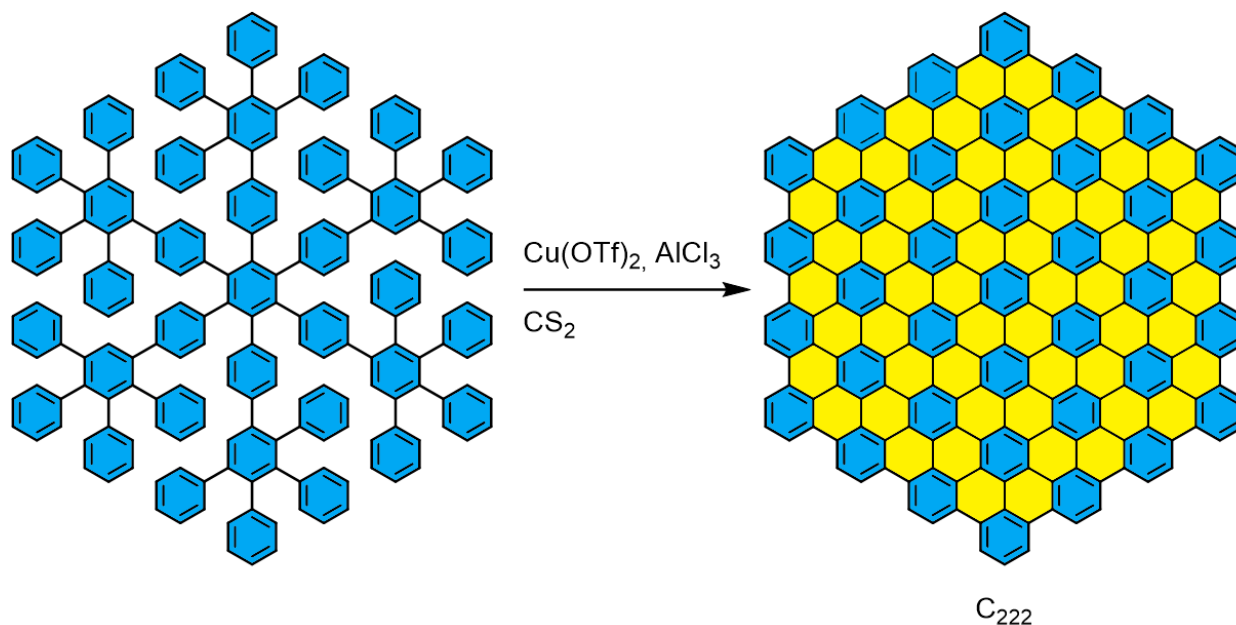


Figure 1.5: Synthesis of nanographene C₂₂₂ by oxidative cyclodehydrogenation.

The precursor showed good solubility due to a relatively spherical shape and behavior, but after removal of 108 hydrogen atoms planar PAH C₂₂₂ was completely insoluble in common solvents.⁴²

Large, well-defined and flat PAHs can be formed with almost quantitative yield,^{38,39} but it is highly restricted to the application of dendrimeric precursors with high packing density of benzene rings.⁴⁰ Precursors with linear oligomers or polymers chains show the limits of Scholl-reaction. For example, the report by King *et al.* in 2007 shows that ring closure of the small unsubstituted *o*-terphenyl did not only result in the formation of the triphenylene monomer but also leads to undesired oligomerization of the product.³⁷ The limits of oxidative cyclodehydrogenation were also shown by Hilt *et al.* in 2012, demonstrating that the reaction of an quinquephenyl derivative **1.1** with FeCl₃ as oxidizing agent did not yield desired **1.2** but exclusively yields the regioisomer **1.3** (Figure 1.6).⁴³

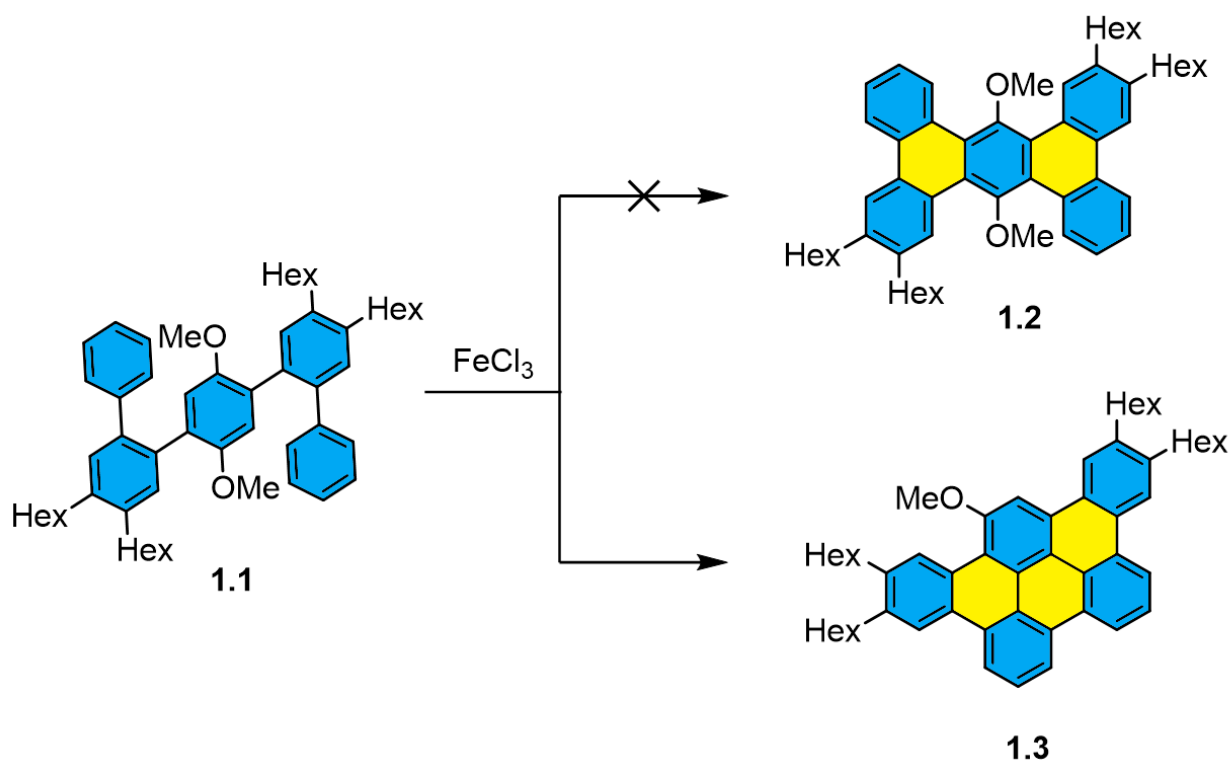


Figure 1.6: Alternative product formation with hexane (Hex) substituents.

These two examples show that the precursor molecules require a very well predefined or rigid structure with fixed orientation to yield the desired products by intramolecular oxidative cyclodehydrogenation. Control of regioselectivity during reaction is not possible otherwise. Normally, formation of non-hexagonal rings is also not effective. Therefore, highly interesting non-classical PAHs bearing pentagons and/or heptagons in the structure are difficult to obtain by Scholl reaction.

In order to perform reactions with more control over product formation, alternative approaches to this unique class of molecules must be developed. The following chapter reveals a brief insight into C-F bond activation as an alternative approach to the formation of nanostructures. In particular, a detailed introduction of the recently developed intramolecular cyclodehydrofluorination by Al_2O_3 -mediated CDHF is given.⁴⁴

1.2.2. Aryl-Aryl coupling by C-F bond activation

The fluorine-carbon bond is known to be the most stable bond to carbon and therefore is often considered as the least reactive functionality in organic chemistry.^{45,46} However, recent progress in the C-F bond activation has demonstrated the high potential of the C-F functionality in complex carbon-based nanostructure synthesis via intramolecular aryl-aryl coupling.

One example is the flash vacuum pyrolysis of halogen atoms such as bromine and chlorine, which have been shown to be effective promoters and were effectively used in the synthesis of small buckybowls.^{22,47} However, this approach reaches its limits in the case of large structures, due to their decomposition during sublimation. Fluorinated precursors were found to be more effective for the synthesis of large bowl-shaped PAHs and fullerenes.⁴⁷⁻⁴⁹ The main drawback of this method is related to the harsh reaction conditions, low conversion rate, poor functional group tolerance and the difficulty of scaling up the reaction.

These disadvantages can be overcome by liquid phase reactions such as the direct arylation of chlorinated and/or brominated precursors with Pd catalysts (Scheme 1.7).^{36,50}

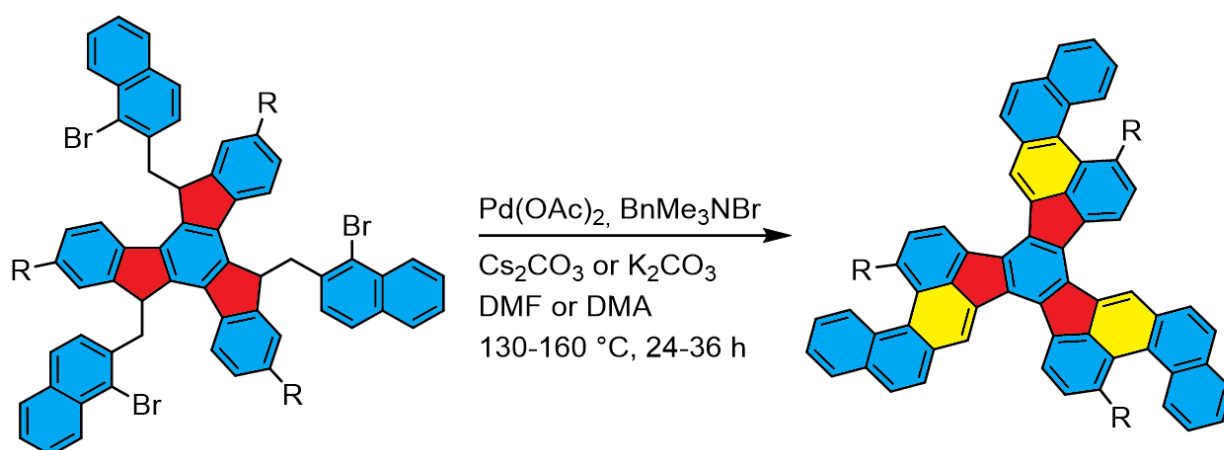


Figure 1.7: Palladium-catalyzed arylation of truxene-derivatives.⁵⁰

Despite of the C-F bond stability, activation under transitions-metal free conditions using silylium-carborane catalysts are possible, as reported by Siegel *et al.* for

intramolecular aryl-aryl coupling.⁵¹ However, both approaches display a low efficiency in the case of large nanostructures and cannot be performed in a domino-like fashion.⁴⁴

1.2.3. Aryl-Aryl-coupling by γ -Al₂O₃-mediated CDHF

Amsharov et al. published 2012 a highly effective method for the regio- and chemoselective intramolecular aryl-aryl coupling via alumina mediated C-F bond activation (AmCFA). This reaction offers several advantages over the previously described approaches.^{44,49,52} One advantage is the high chemoselectivity of the process, as C-Cl and C-Br bonds remain completely intact.⁵² Therefore, it is very well suited for the synthesis of rationally halogenated PAHs which can be further extended to the more complex structures via post-functionalization. Another advantage is the high regioselectivity, since only the C-F bonds in cove and fjord regions of a PAH molecule can undergo efficient cyclization, whereas C-F bonds in the periphery remain completely inactive.⁴⁴ High regioselectivity was explained by the close proximity of C-H bond, which is required for the transition state realization. This requirement also renders the approach applicable for the tandem cyclization via CDHF in a truly domino-like fashion as reported by Steiner and Amsharov in 2017.⁵³ Notably, this alumina-mediated HF-zipping approach allows the conversion of virtually linear fluorinated oligophenylenes into the desired target nanostructures with exceptional conversion. In the initial precursor structure only one H...F pair is "activated" for CDHF and can undergo coupling via CDHF. However, after first ring closure the next fluorine atom appears in close proximity to hydrogen and thus becomes "activated" for the next CDHF step (see Figure 1.8).⁵³

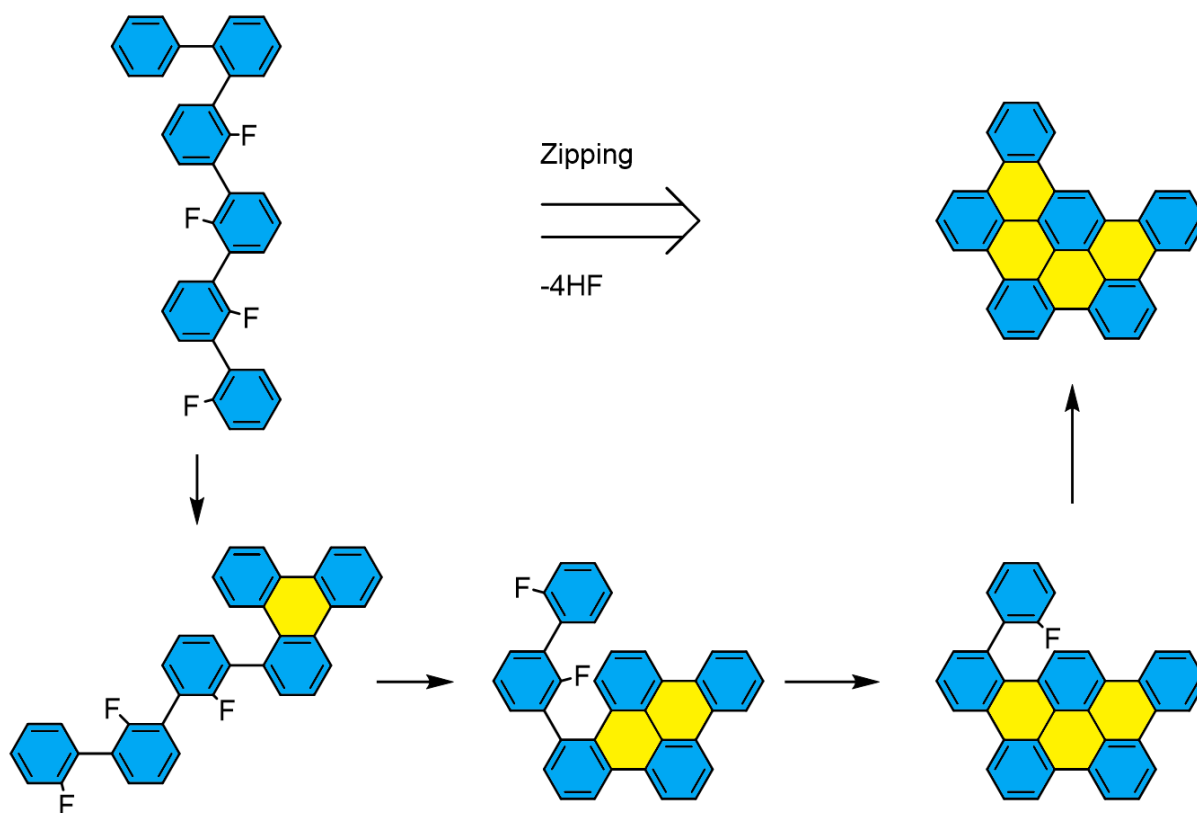


Figure 1.8: Synthesis of a small nanographene by HF-zipping approach (domino-like cyclodehydrofluorination on γ -alumina).⁵³

Furthermore, metal oxides besides alumina such as ZrO_2 and TiO_2 were found to be rather effective for the CDHF.⁵⁴

1.2.4. Defects in graphene: 7-membered ring formation

The two-dimensional structure of perfectly defined graphene exclusively consists of six-membered carbon rings. However, detailed investigations of real graphene samples revealed the presence of five- and seven-membered rings, which can have a huge impact on the mechanical, electrical, chemical, and optical properties of graphene.⁵⁵

Therefore, the synthesis of extended PAHs containing other ring sizes attracted renewed and widespread interest, since these molecules can generally mimic the defects in graphene sheets and thus, serve as model compounds in graphene research.⁵⁶ Moreover, as these compounds possess a highly distorted, non-planar geometry, they

are therefore frequently soluble in common organic solvents, greatly simplifying their study.⁵⁷ Furthermore as demonstrated by Wang *et al.*, the introduction of penta- and heptagons tends to narrow the HOMO-LUMO gap, which affects the optical absorption spectra of warped nanographenes by the participation of the rings in electronic transitions and/or by changing the composition of molecular orbitals that are involved in the excitation.⁵⁸

Several synthetic approaches towards PAHs containing five-membered rings have been reported.⁵⁶ One example is the cyclodehydrofluorination method. One of the most important advantages of the C-F bond activation strategy is tolerance to chlorine and bromine, which opens access to rationally halogenated bowl-shaped systems not accessible by other methods. In our group, variously halogenated indacenopicenes and diindeno-chrysenes were successfully synthesized by this approach showing unprecedented high efficiency and near quantitative conversion to the target molecules (Scheme 1.9).^{44,59}

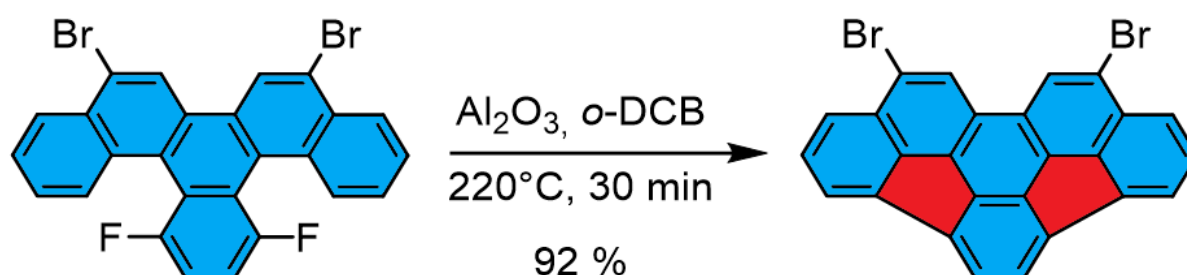


Figure 1.9: Synthesis of dibrominated indacenopicene by twofold HF-elimination.⁵⁹

The possibility to incorporate pentagons into NGs allows introduction of halogen functionalities at virtually any desired positions, making this approach superior to alternative methods for buckybowl synthesis. Moreover, peripheral halogen atoms allow possible post-functionalization and thus fine tuning of the physical–chemical properties.⁵⁹

Although PAHs containing five-membered rings and the synthetic approaches have already been extensively investigated, only scarce examples of PAHs with seven or eight-membered rings are reported in literature. One of the earliest examples for

successful heptagon formation includes the synthesis of hexa[7]circulene by Jessup *et al.* in 1975⁶⁰ and the synthesis of [7]circulene by Yamamoto *et al.* in 1983⁶¹ (Figure 1.10).

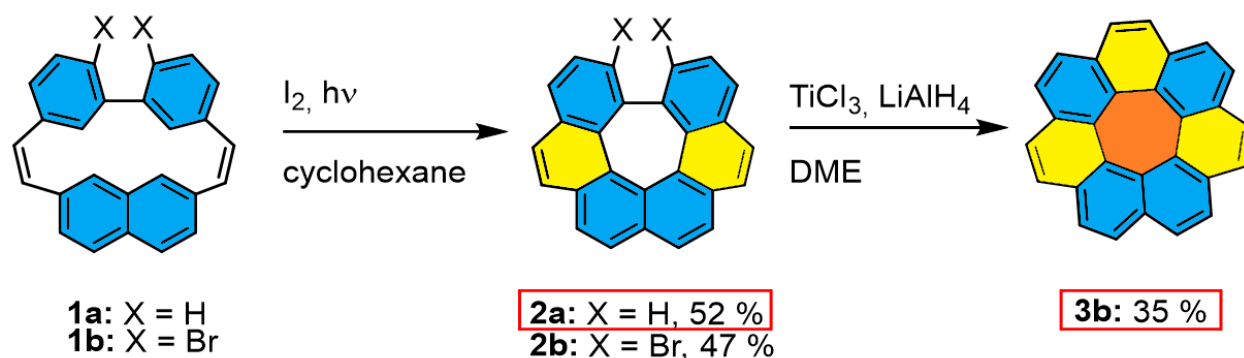


Figure 1.10: Synthesis of hexa[7]circulene (2a)⁶⁰ and [7]circulene (3b)⁶¹.

Nowadays, there are few general strategies towards the synthesis of heptagon containing PAHs. One of which starts with an already functionalized heptagonal carbocycle and the surrounding aromatic backbone is created afterwards. The second strategy includes the formation of seven-membered rings via an intramolecular cyclization reaction which can be accomplished in various ways. For example, Mughal and Kuck reported the successful synthesis of a cycloheptatriene unit by intramolecular ring closure via Scholl oxidation.⁶² Kawai *et al.* published the first synthesis of a propeller-shaped PAH with three seven-membered rings, implementing a Pd-catalyzed intramolecular arylation reaction (Scheme 1.11).⁶³

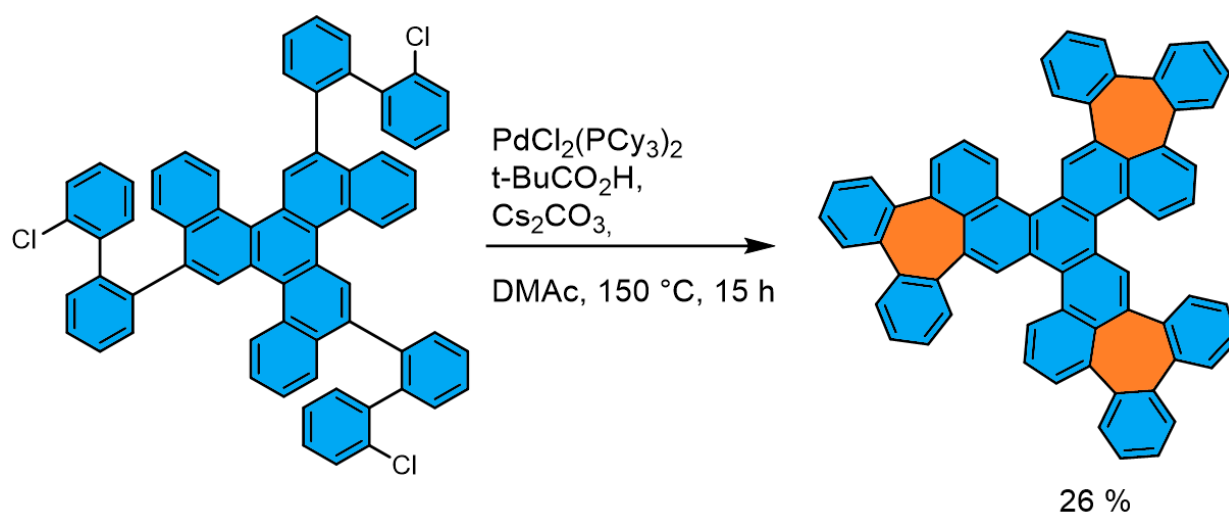


Figure 1.11: Formation of seven-membered rings by Pd-catalyzed intramolecular direct arylation.⁶³

Finally, the Scholl reaction is a third possible path for the synthesis of heptagonal carbocycles as reported by Miao *et al.* (Scheme 1.12).⁶⁴

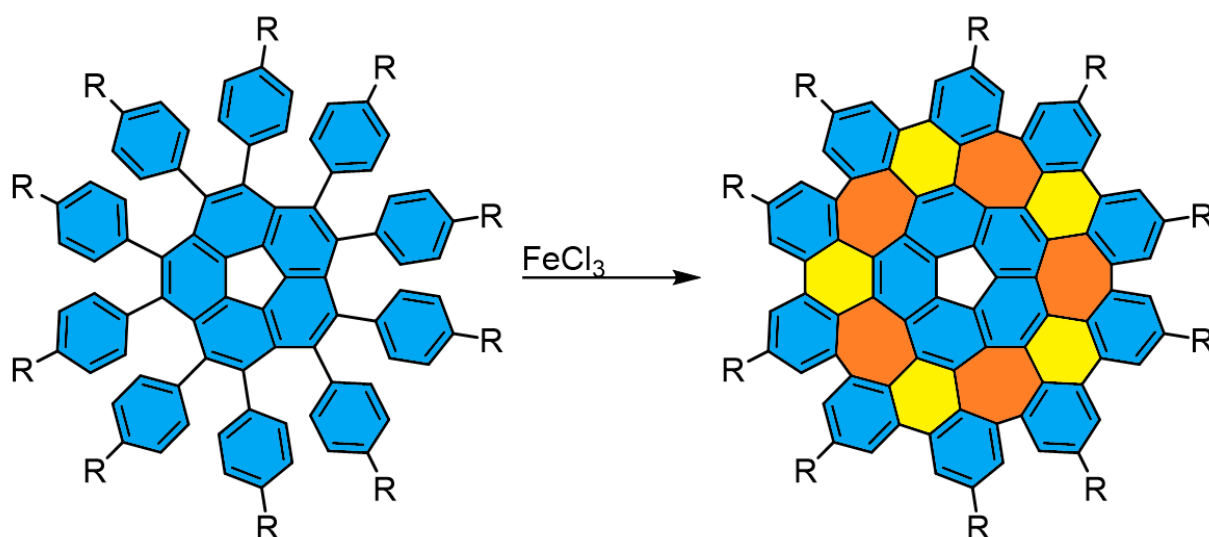


Figure 1.12: Formation of seven-membered rings by Scholl reaction.⁶⁴

Ring expansion of cyclohexanones and the intramolecular cyclotrimerization of alkynes should be mentioned as alternative approaches as well.⁶⁵ Despite the progress in the synthesis of 7-circulenes and their derivatives facile fabrication of heptagon containing NGs have remained elusive.⁵⁶

Due to big success in the pentagon formation by CDHF and effective synthesis of buckybowls demonstrated in our group, the approach seems to be a good alternative and promising approach towards the synthesis of nanographenes containing heptagonal carbocycles. The method is characterized by high chemo- and regioselectivity providing full control over C-C bond formation and thus appears to be a good prospective as a general strategy for the synthesis of elusive non-planar PAH architectures.^{44,45,49}

Specifically the [4]helicene derivate has proven to form non-planar PAHs with fluor in bay region. Therefore the [6]helicene appears to be the smallest model compound for seven member ring formation and [7]helicene forming the respective eight member ring seems to be possible as well. These ortho-condensed polycyclic aromatic compounds, in which benzene rings are angularly annulated to give helically-shaped chiral molecules, will be discussed in this thesis.

1.2.5. Zig-zag periphery by C_{sp^3} - C_{aryl} coupling-Radical PAHs

AmCFA forming 6-member rings is still nontrivial and worth investigating. One aspect of this is the synthesis of nanographenes with zig-zag periphery. A number of examples are highlighted on a graphene section (Figure 1.13).

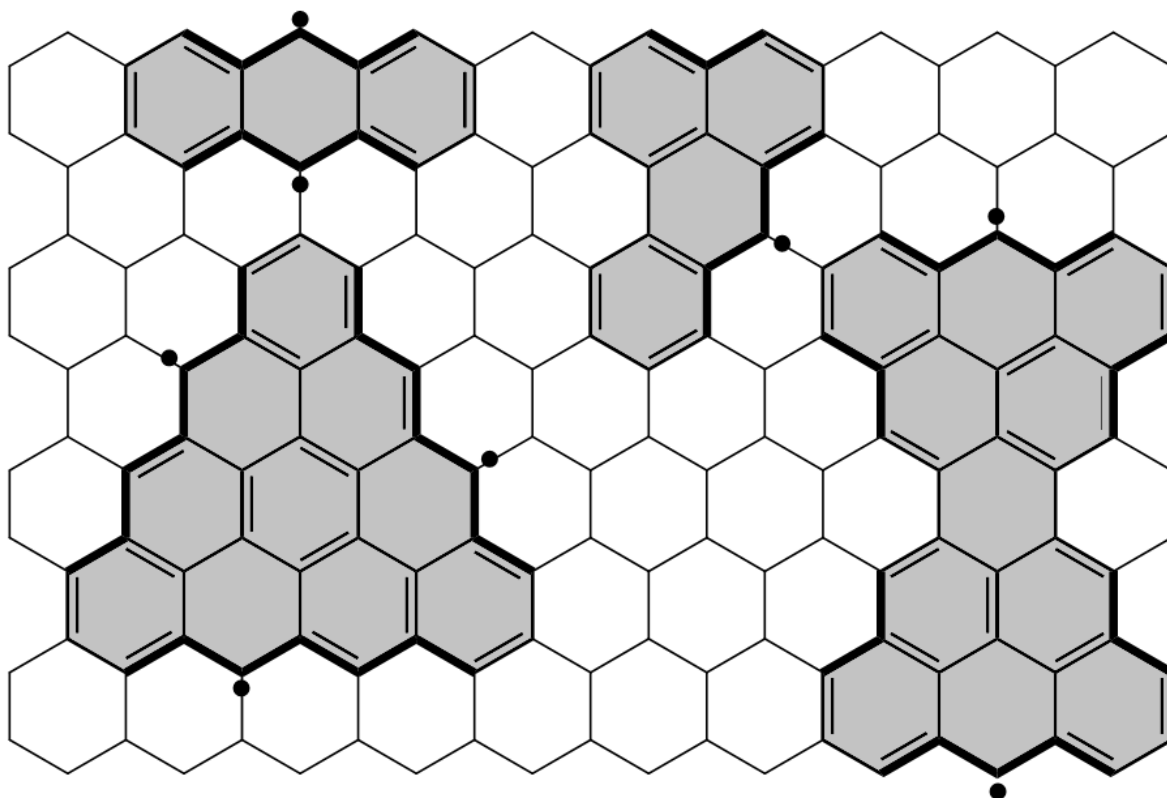


Figure 1.13: Graphene derivatives with zig-zag periphery.

This kind of molecules often have unpaired electrons i.e., open shell electronic structures and are intriguing for advanced applications in molecular electronics, spintronics and organic batteries, as well as other possible applications. Oxidative cyclodehydrogenation of a methyl group in cove region is the only reported method for synthesizing the zigzag periphery on the surface of metals. Fasel et al. have developed nanoribbons' synthesis with zigzag periphery via cyclodehydrogenation and oxidative ring-closure reactions upon annealing of methyl- substituted PAHs on Au(111) surface during the synthesis of graphene nanoribbons.⁶⁶ as simplified in Figure 1.14.

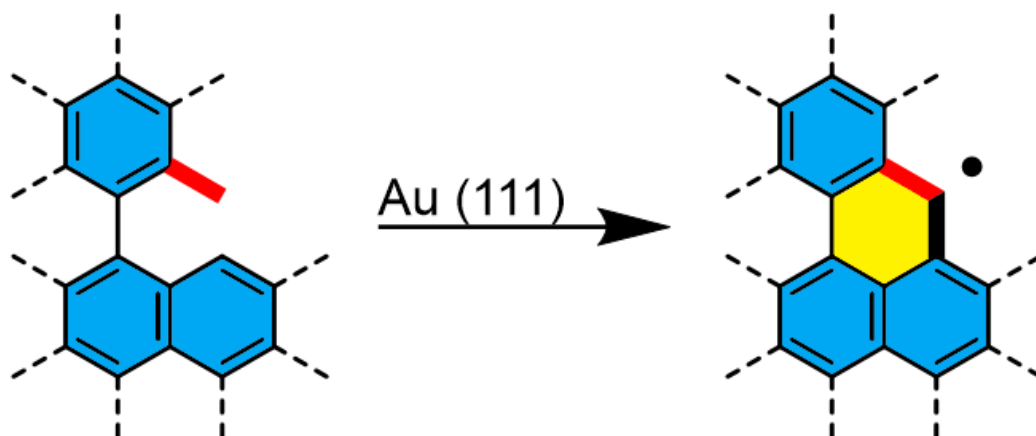


Figure 1.14: Synthesis of methyl- substituted PAHs on Au(111) surface.

Among them, diradicaloids have received growing attention due to the characteristic resonance structures between open-shell and closed-shell forms that lead to unique properties such as low energy bandgap and strong intermolecular spin–spin interaction. One of the most famous of these non-Kekulé structures is the antiferromagnetic Clar’s Goblet⁶⁷ (Figure 1.15).

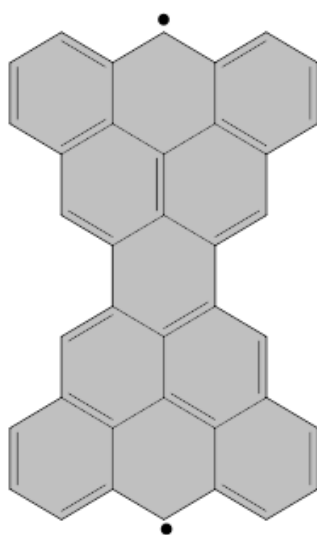


Figure 1.15: Structure of Clar’s Goblet.

but despite great interest from material scientists, zigzag PAHs suffer from significant insufficiency of synthetic methods, in contrast to the armchair periphery. In this work, we explore the alternative synthetic approach by AmCFA.

1.2.6. Alumina-mediated terminal acetylene behavior

Dewar–Chatt–Duncanson model⁶⁸ can explain the chemistry of acetylenes on novel metals such as gold⁶⁹ and platinum⁷⁰ -based catalysts. It is characteristic with its σ -donation of the HOMO-orbital to the empty p- or d- orbital of the transition metal and its π -back-donation of the filled d-orbitals to the antibonding LUMO of acetylene (Figure 1.16).

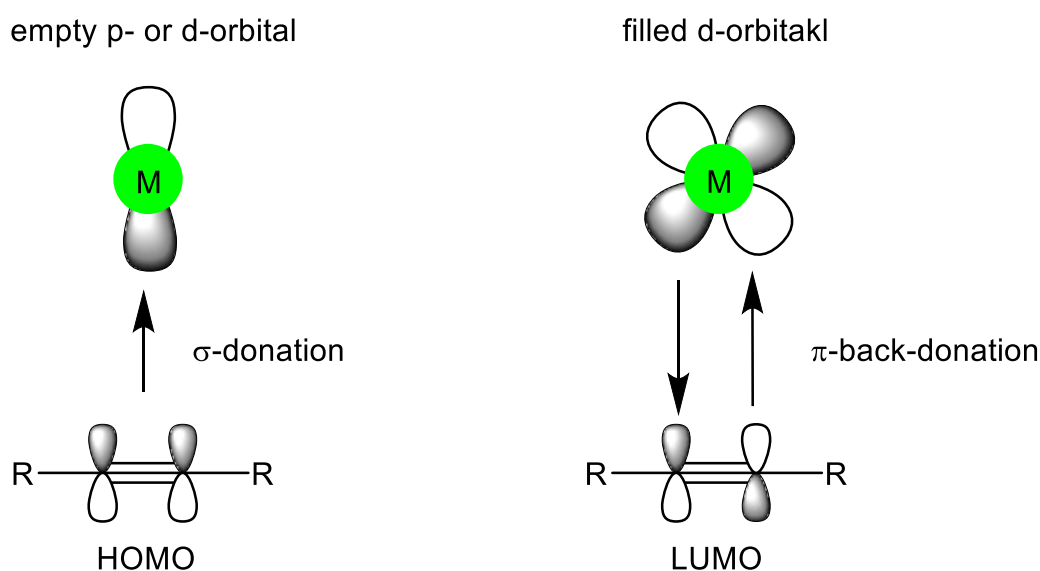


Figure 1.16: Interaction of acetylenes with metal.

This leads to a π -activation and the generation of an electrophilic center (Figure 1.17). This unique catalytic activity was believed to be an exclusive domain of noble metals, such as gold and platinum and inherently dependent on the presence of the d-orbitals. Moreover, selective activation of alkynes by gold and platinum catalysts is attributed to the relativistic effects,⁷¹ which reach a maximum in the periodic table with these metals and particularly with gold.^{72,73}

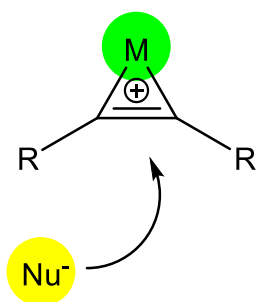


Figure 1.17: Generation of electrophilic center and nucleophile attack.

As will be shown in this thesis, thermally activated alumina shows behavior, that were typically assigned to the softest π -Lewis acids. The formation of phenanthrene from biphenylacetylene on alumina can be explained by an 6-endo attack on the electrophilic center (Figure 1.18). We show with this, that elements having no d-orbital are capable of a similar catalytic activity.

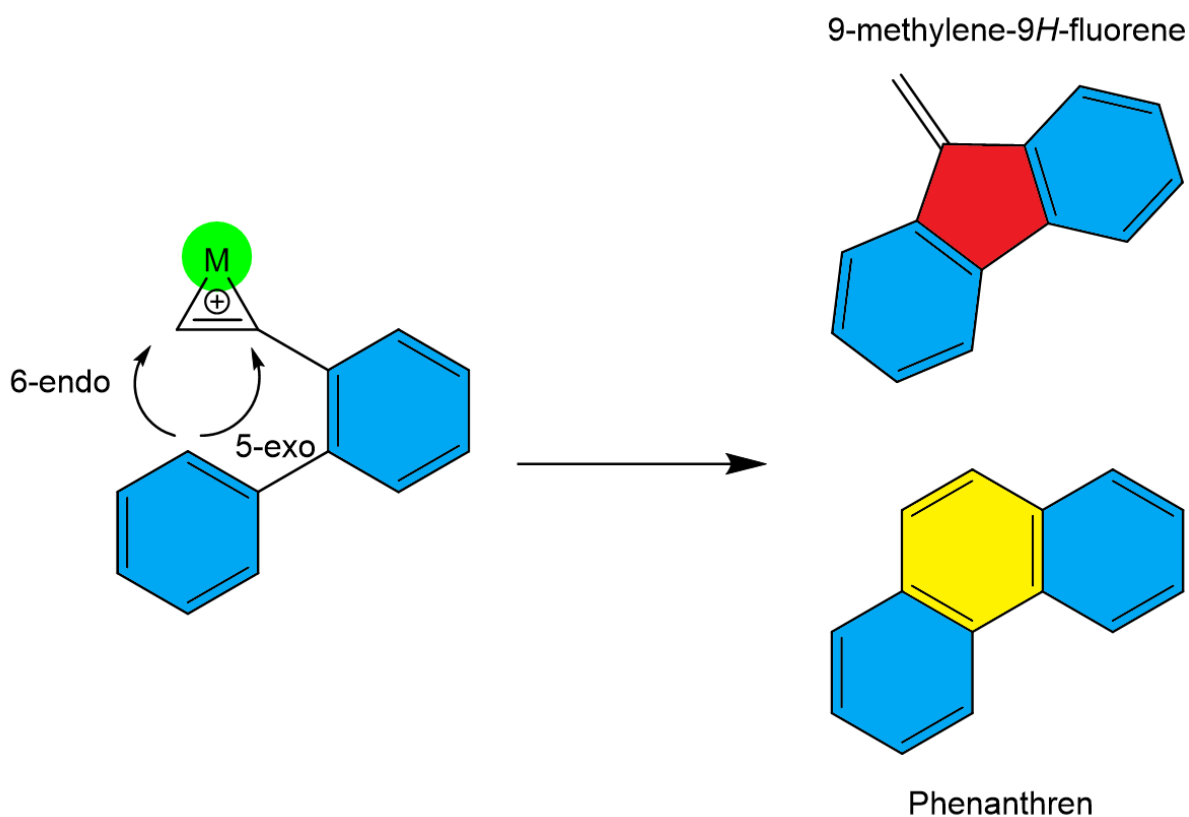


Figure 1.18: Formation of 9-methylene-9H-fluorene and phenanthrene through a 5-exo or 6-endo attack respectively.

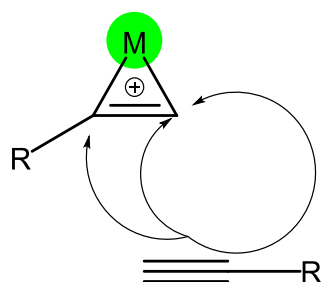


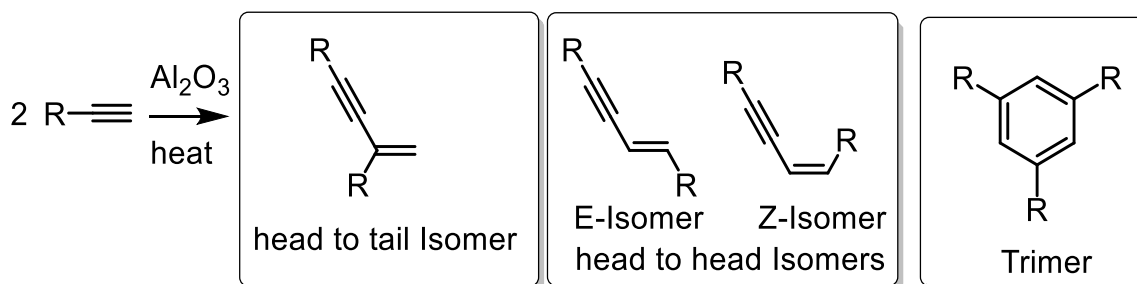
Figure 1.20: Dimerization of terminal acetylenes on alumina.

Depending on the position of the attacked terminal acetylene group three different isomers are formed.

Head-to-tail dimer: the last carbon of one acetylene attacks the carbon of another acetylene molecule, which is nearer to the aromatic part.

Head-to-head dimer: the last carbon of one acetylene attacks the last carbon of another acetylene molecule. In this formation, the E- and Z-isomers are possible.

The resulting Head-to-tail dimer may react further with another monomer to the trimer. (Scheme 1).



Scheme 1: Possible reaction products of terminal alkynes.

With the claim of electrophilic center formation solidified in the coming thesis, the question arises, if other electrophiles are possible to react with these terminal acetylenes on alumina. Chlorine in form of hydrochloric acid was chosen in this thesis. The chlorination of acetylenes is an important challenge in research as well as industry. The generation of vinyl chloride from acetylene is of utmost importance for the industrial production as a precursor of polyvinyl chloride (PVC). More details to this topic will be discussed in chapter 3.

2. Proposal

This work is oriented on the development of the synthesis of non-planar polycyclic aromatic hydrocarbons by introducing 7-member rings and 8-member rings through alumina-mediated C-F bond activation. The synthesis of these molecules will be tried through varying ways and complexity.

Oxodefluorination will be used to design complex molecules with oxygen in zig-zag periphery and afterwards pure hydrocarbons with zig-zag periphery will be synthesized by using AmCFA on molecules with aliphatic groups. This method allows the synthesis of molecules with high diradical character and can be used for further on-surface synthesis studies.

Next to this investigation, other possible reactions on alumina will be investigated, through a screening of different functional groups and especially the study of terminal acetylenes.

A limited evaluation of alumina in 2012 presented the possibility of using other metal oxides for cyclodehydrofluorination.⁵⁴ But as alumina makes other reactions possible, reactivity of other metal oxides is still unexplored. This thesis will shed some light on the possibility of using other metal oxides or even doped alumina in combination with acetylenes.

Lastly different alumina's terminations will be tested to investigate the soft or hard π -Lewis acidity. The behaviour of a model compound will be used to determine the degree of acidity.

With these objectives, the reactions on alumina will be explored and further unravel the mysteries of graphene-based alumina-chemistry.

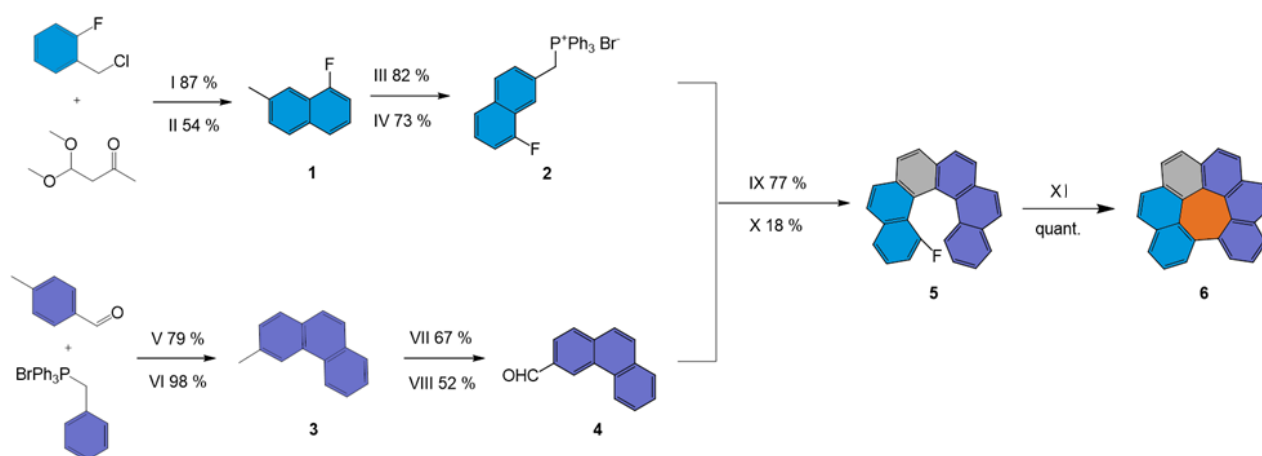
3. Results and discussion

In this chapter, all results will be discussed. First will be the formation of non-alternate PAHs by HF-Elimination. Afterwards the formation of an oxygen-bridge through two fluor-atoms in bay region and the reaction of fluor with methyl groups will be discussed. The fourth part will contain a screening of reactivity of different functional groups on Al_2O_3 . Next the closure of 2-ethynyl-1,1'-biphenyl on different oxides will be investigated. Afterwards, research of dimerization and chlorination of terminal alkynes on Al_2O_3 will be done. Lastly, the soft π -Lewis acidity of different alumina's terminations will be investigated.

3.1. Folding of Fluorinated Oligoarylenes into Non-alternant PAHs with Various Topological Shapes

After the successful closure of [4]helicene's cavity by cyclodehydrofluorination, leading to the formation of a pentagon⁷⁵, the formation of a heptagon with [6]helicene has been attempted.

3.1.1. Synthesis of 1,16-dehydrohexahelicene⁷⁵



Scheme 2: Synthesis of fluoro-6-helicene and AmCFA. I. Mg , I_2 , Et_2O . II. H_2SO_4 , AcOH . III. NBS , DBPO , fluorobenzene. IV. PPh_3 , toluene. V. KOH , CHCl_3 . VI. $h\nu$, I_2 , propyleneoxide,

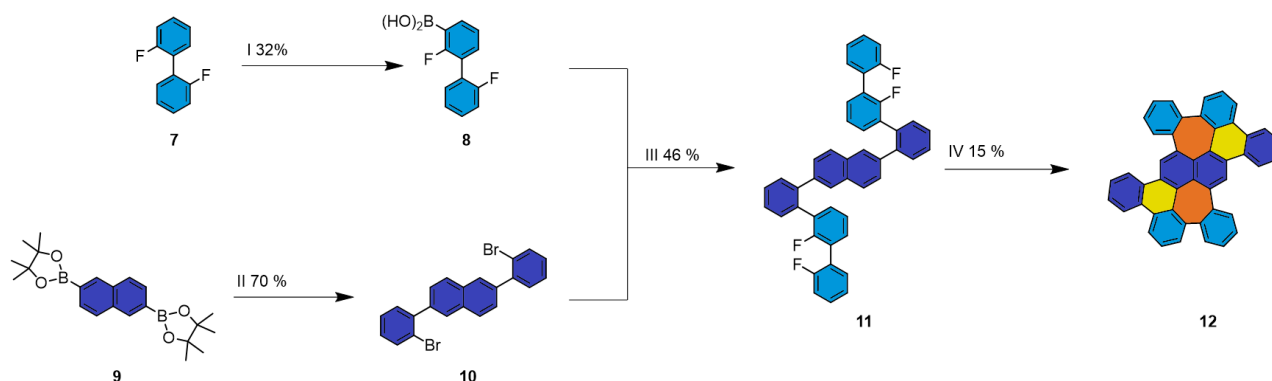
cyclohexane. VII. NBS, DBPO, CCl₄. VIII. hexamethylenetetramine, CHCl₃. IX. KOH, CHCl₃.
X. hv, I₂, propyleneoxide, cyclohexane. XI. Al₂O₃, 180 °C.

The pathway to [6]helicene with a fluorinated cavity includes the Wittig reaction of a 1-fluoro-7-methyl-naphthalene derivative with phenanthrene-3-carbaldehyde (**4**) and subsequent photocyclization of the obtained (Z/E)-alkenes. We were delighted to find that, like its successor fluorinated [4]helicene, **5** transforms into **6** in quantitative yield. Thus, AmCFA turns out to be the first C–C coupling technique to manage such a transformation (Scheme 1).^{60,75,76}

3.1.2. Synthesis of dibenzo[e,gh]dibenzo[4,5:6,7]-pleiadeno[2,1,12-pqa]pleiadene⁷⁵

The result of fluorinated [6]helicene inspired us to implement another feature of AmCFA to achieve rapid access to PAHs containing several seven-membered rings. The so-called HF-zipping approach, where the first C–C coupling transforms the previously “dormant” fluorine functionality into an “active” one, which can participate in intramolecular HF elimination.⁷⁷

To use this concept to incorporate non-hexagonal rings is as attractive as it is questionable since many methods commonly fail to achieve C–C coupling for non-alternant PAHs as effectively as for purely hexagonal PAHs. To test the viability of this concept, we investigated the folding of several fluoroarylenes.



Scheme 3: Synthesis of 2,6-bis(2',2''-difluoro-[1,1':3',1''-terphenyl]-2-yl)naphthalene (**11**) and AmCFA. I. 1-Fluoro-2-bromobenzene, 2-fluorophenylboronic acid, Cs₂CO₃, Pd(PPh₃)₂Cl₂, THF/H₂O (5:1). II. 1-bromo-2-iodobenzene, Cs₂CO₃, Pd(PPh₃)₂Cl₂, THF/H₂O (5:1). III. K₃PO₄, Pd(dppf)Cl₂, THF/H₂O (5:1). IV. Al₂O₃, 200°C.

(2,2'-Difluoro-[1,1'-biphenyl]-3-yl)boronic acid (**8**) has been proven to be a valuable block to direct the rolling up of fluorinated oligophenylenes into alternant PAHs.^{75,77} After synthesis by palladium catalyzed Miyaura borylation, (**8**) was reacted with 2,6-bis(2-bromophenyl)naphthalene (**10**), which was synthesized by Suzuki cross-coupling reaction^{78,79}.

The resulting 2,6-bis(2',2''-difluoro-[1,1':3',1''-terphenyl]-2-yl)naphthalene (**11**) was reacted by AmCFA in the zipping approach. First the fluor functionalized fjord region reacted in a HF-elimination to the carbon hexagon formation. This resulted in the second fluor to be in position for cyclodehydrofluorination, resulting in the formation of heptagons. It is noteworthy that four new C–C bonds are formed in one step during the cyclization of **11**. Moreover, the saddle-shaped PAH **12** can be easily purified, as the side products are mainly polar dibenzofuran derivatives.^{75,80}

The product structure was confirmed by single-crystal X-ray analysis, which shed some light on the topology of the obtained non-alternant PAH **12**. Single crystals were obtained from a diluted solution in DCM /hexane by slow evaporation of the solvents. Due to non-planar structure, the product possesses chirality, while the crystal structure contains a racemic mixture of both enantiomers (Figure 3.1).

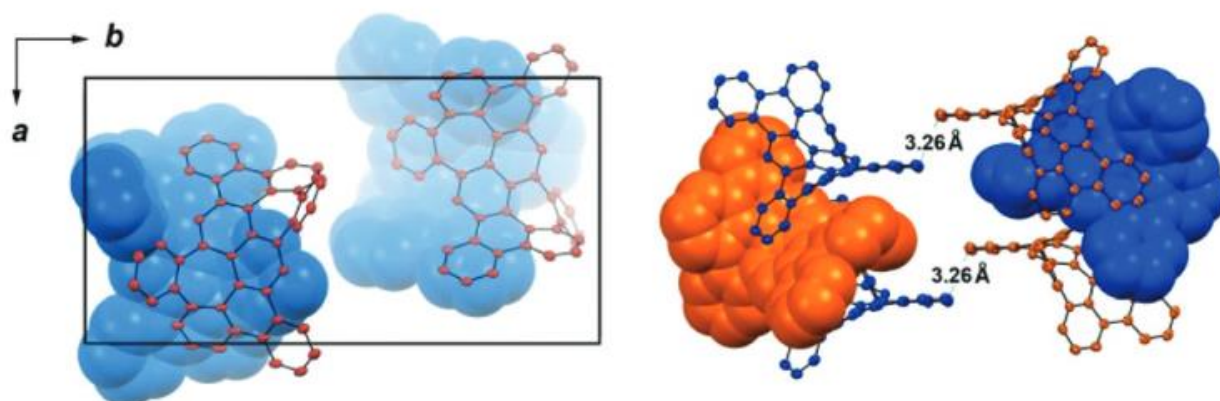


Figure 3.1: unit cell of **12** as viewed along the *c* axis; solvent molecules are removed for clarity (left) and molecular packing of **12**. Enantiomers are shown in orange and blue.

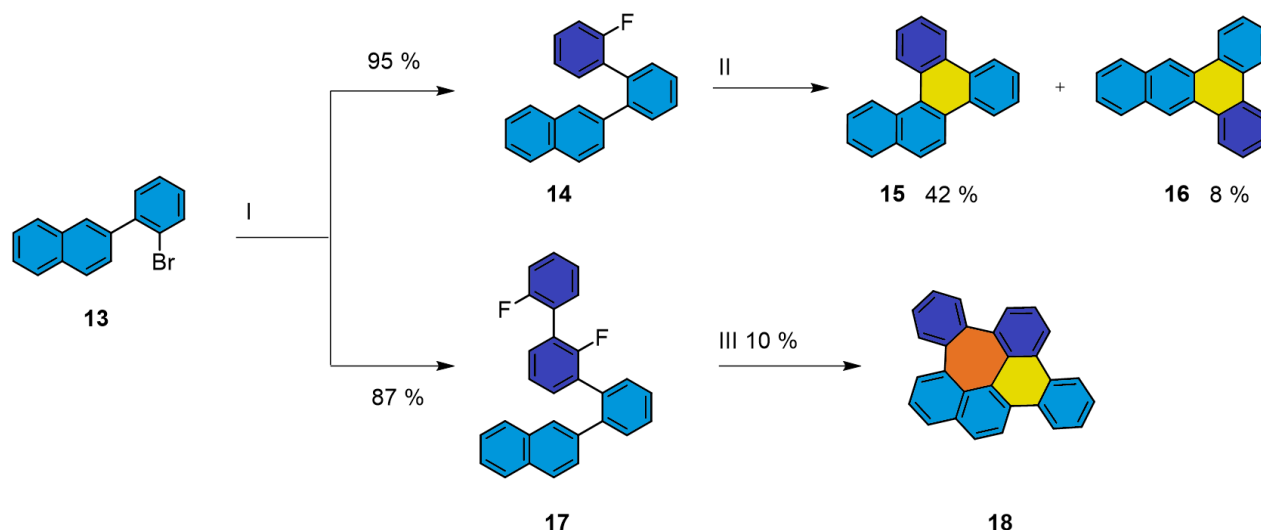
Hydrogen atoms are removed for clarity.⁷⁵

The molecule is processible in its pristine form and requires no solubilizing substituents, which generally prevent effective π -stacking in the crystal.⁸¹ The crystal structure

reveals very close C...C contacts not only within the columns (3.38 Å) but also between them (3.34 and 3.26 Å). At the same time, numerous C...H contacts with lengths of 2.68–2.88 Å indicate the existence of CH– π inter-actions⁸², the strongest one occurring between neighboring molecules in the direction of the crystallographic axis a. The C–C bond length analysis shows a uniform delocalization of π -electrons. Thus, the C–C bond between heptagons has a length of 1.424 Å.⁷⁵

3.1.3. Synthesis of tribenzo[b,gh,pq]pleiadene

To investigate the details of zipping of the compound **11**, small fragments **14** and **17** of the molecule were synthesized and investigated.



Scheme 4: Synthesis of 2-(2'-fluoro-[1,1'-biphenyl]-2-yl)naphthalene and 2-(2',2''-difluoro-[1,1':3',1''-terphenyl]-2-yl)naphthalene and their respective AmCFA. I. (2-fluorophenyl)boronic acid or (2,2'-difluoro-[1,1'-biphenyl]-3-yl)boronic acid, K_3PO_4 , $Pd(PPh_3)_2Cl_2$. II. Al_2O_3 , 220 °C. III. Al_2O_3 , 200°C.

After Suzuki cross-coupling reaction^{78,79} of 2-(2-bromophenyl)naphthalene (**13**), precursors 2-(2'-fluoro-[1,1'-biphenyl]-2-yl)naphthalene (**14**) and 2-(2',2''-difluoro-[1,1':3',1''-terphenyl]-2-yl)naphthalene (**17**) were synthesized. The cyclodehydrofluorination of **14** results in the main product benzo[g]chrysene (yield 42 %) and minor product benzo[f]tetraphene (yield 8 %). This represents not only the first step in the synthesis of tribenzo[b,gh,pq]pleiadene (**18**) but also compound **12** and

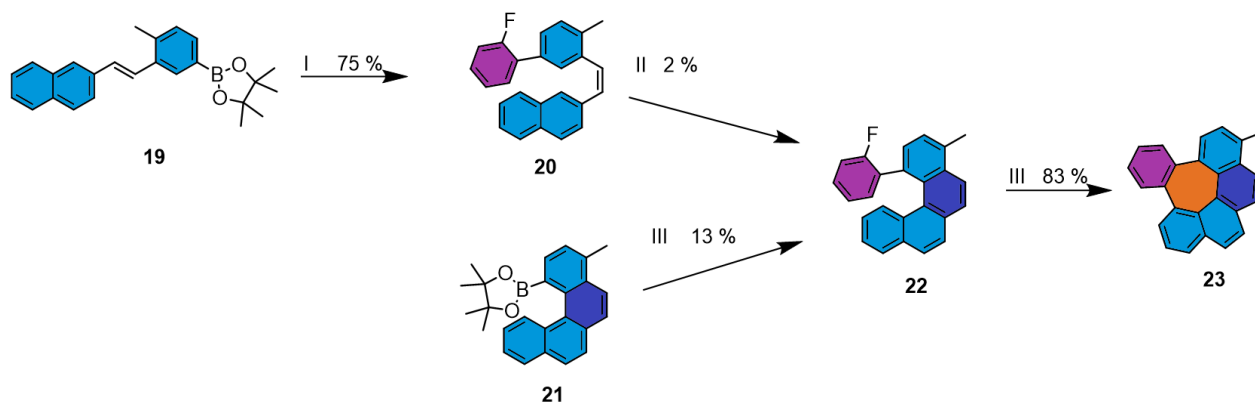
demonstrates the closure to **15** is favored in comparison to **16**. The HF-elimination of **17** yielded only 10 % of product **18**, which shows a more difficult formation of the 7-member ring with approximately 24 % yield of this step

$$0.42 \cdot x = 0.1 \quad x = 0.24.$$

The higher yield of **11** in comparison to **18** can be explained with the sterically hindered position for the formation of benzo[f]tetraphene derivatives. Looking at the results of chapter 3.1.1, 3.1.2 & 3.1.3, it can be concluded, that higher degree of flexibility of the precursor lowers the chance to form heptagonal rings in PAHs.

3.1.4. Synthesis of 14-methyldibenzo[gh,pq]pleiadene

This conclusion is further supported by another helicene derivate. 1-(2-fluorophenyl)-4-methylbenzo[c]phenanthrene (**22**) was aimed for, in the hope the methyl group would simplify the photocyclization and increase solubility of the end product 14-methyldibenzo[gh,pq]pleiadene (**23**) and have one more degree of flexibility in comparison to **5** through the rotating single bond to the fluorinated phenyl ring.



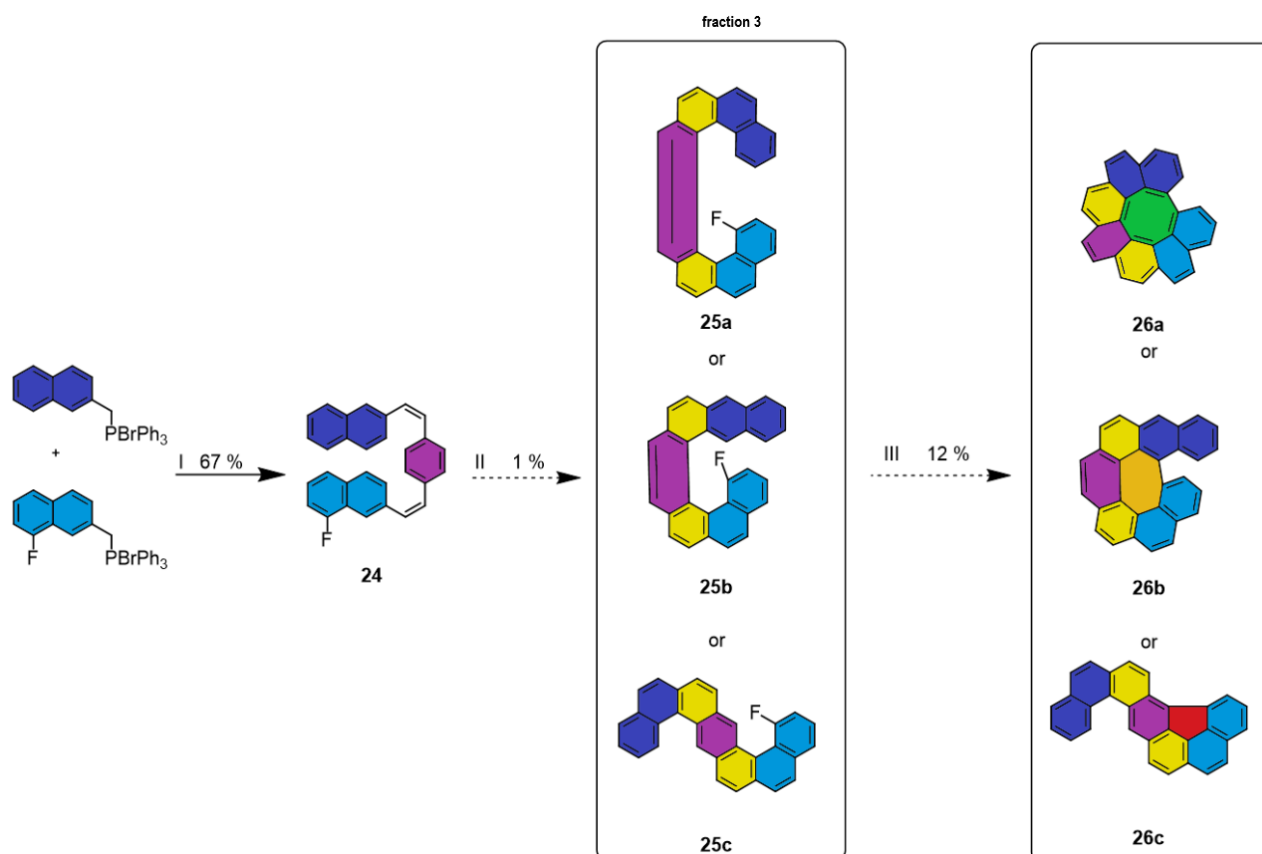
Scheme 5: Synthesis of 1-(2-fluorophenyl)-4-methylbenzo[c]phenanthrene and its respective AmCFA. I. 1-bromo-2-fluorobenzene, K_3PO_4 , $Pd(dppf)Cl_2$, THF/ H_2O (5/1). II. H ν , I_2 , propylene oxide, cyclohexane. III. 1-bromo-2-fluorobenzene, Cs_2CO_3 , $Pd(dppf)_2Cl_2$ THF/ H_2O (5:1). IV. Al_2O_3 , 220 °C.

After Suzuki cross-coupling reaction^{78,79} with 4,4,5,5-tetramethyl-2-(4-methylbenzo[c]phenanthren-1-yl)-1,3,2-dioxaborolane (**21**) and 1-bromo-2-fluorobenzene, compound **22** was synthesized. The pathway with a Suzuki reaction before a photocyclization

(compound **20**) proved less successful. Cyclodehydrofluorination of **22** yielded 83 % of molecule **23** without any side products. HPLC and mass spectrometry showed 100 % conversion.* As other helicene (**5**), the compound **22** showed high reactivity in HF-Elimination for the formation of the 7-member ring but due to the flexibility of phenyl ring the lower yield can be explained.

*Compound **19** and **21** were synthesized by Mikhail Feofanov from our group.

3.1.5. Synthesis of 7-helicene-derivates and their opening on Al₂O₃



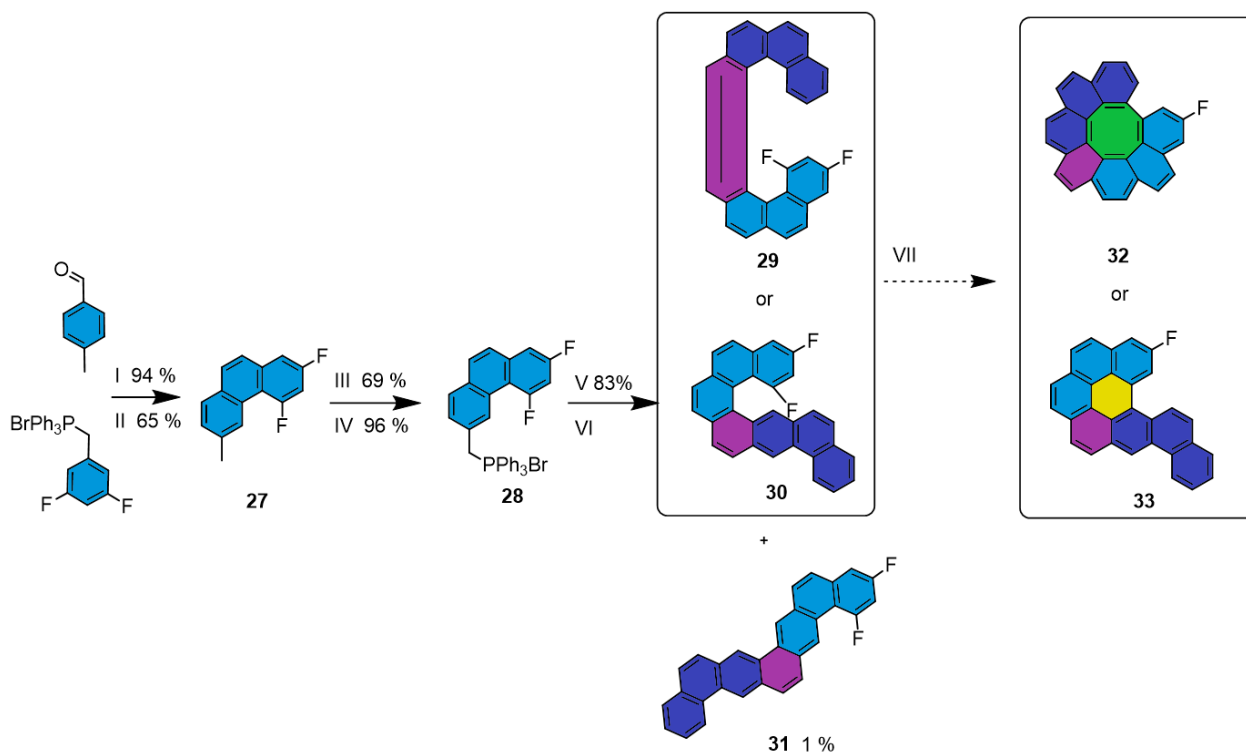
Scheme 6: Synthesis of 1-fluoro-[7]helicene (**25**) and its respective AmCFA. I.

Terephthalaldehyde, CHCl₃, KOH. II. hv, I₂, propylene oxide, cyclohexane. III. Al₂O₃, 200 °C.

After the successful closure of fluorinated [6] helicene to a 7-member ring, now we try to synthesize an 8-member ring by cyclodehydrofluorination of fluorinated [7] helicene (**25a**). 1-Fluoro-7-(4-(2-(naphthalen-2-yl)vinyl)styryl)naphthalene (**24**) was

synthesized by Wittig-reaction. The many Isomers were not possible to isolate and were all used in subsequent photocyclization reaction. The predictable problem of many side products for **25a**, could not easily be solved. To identify the product mass spectrometry was used, and fraction 2,3 and 4 showed 396 m/z of the product. In the ^{19}F -NMR, fraction 2 showed no fluor signal and could therefore be eliminated. Fraction 2 and 3 were both characterized by ^1H -, ^{19}F - and ^{13}C -NMR, but clear identification was not possible and further research must be done at this point. Both fraction 3 and 4 were used in AmCFA, but only fraction 3 formed a product with 376 m/z according to mass spectrometry. This indicates a formation of ether the desired product **26a** or formation of the smaller seven- or five-member ring in **26b** and **26c**. Characterization by ^1H -, and ^{13}C -NMR was done, but clear identification was not possible as the non-planar **26a** needn't have symmetrical signals (Scheme 6). As this approach proved to be not optimal, a second pathway was tried. This time instead of a naphthalene derivative, a phenanthrene derivative was chosen to only have one photocyclization reaction and therefore less possible isomers. Furthermore, two fluor in meta position should guaranty the correct position for HF-elimination in the final product.

Therefore, 2,4-difluoro-6-methylphenanthrene (**27**) was synthesized by Wittig reaction and subsequent photocyclization. After bromination and reaction with triphenylphosphine, the Wittig salt **28** was used in a Wittig reaction with **4**. The resulting E/Z-isomers were reacted in a photocyclization reaction. After separation, fraction 4 and 5 showed 414 m/z (m/z of **29**, **30**, **31**) using mass spectrometry. Characterization by ^1H -, ^{19}F - and ^{13}C -NMR was done, but clear identification was not possible. Both fractions were used in subsequent AmCFA, but only fraction 5 showed a reaction to product **32** or **33** by mass spectrometry (394 m/z). Therefore fraction 4 can be identified as (2,4-difluorodibenzo[c,m]pentaphene) (**31**). The question now is, if fraction 5 is our wanted product **29** or only the [5]helicene derivate **30**. Unfortunately, starting material was still present after reaction and further purification and therefore characterization proved unsuccessful. As shown in the next chapter, very low activity with compounds with two fluor in meta position in one benzyl ring was found, therefore this approach was discontinued.

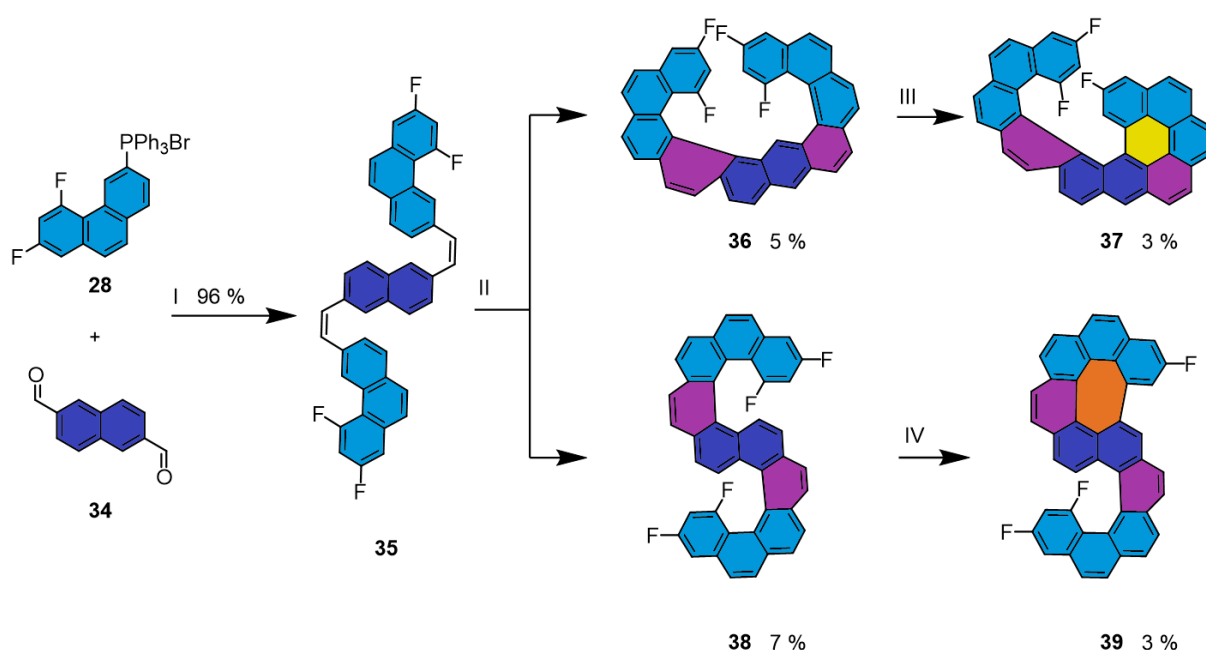


Scheme 7: Synthesis of 1,3-difluorobenzo[1,2-c:4,3-c']diphenanthrene (**29**) and its AmCFA. I. KOH, CHCl_3 . II. $h\nu$, I_2 , propylene oxide, cyclohexane. III. NBS, DBPO, CHCl_3 . IV. PPh_3 , toluene. V. phenanthrene-3-carbaldehyde (**4**), CHCl_3 , KOH. VI. $h\nu$, I_2 , propylene oxide, toluene. VII. Al_2O_3 , 200°C .

Overall, the synthesis of 7-helicene-derivates seems promising, but further research is needed to clearly identify the products. Crystallography might be one possible approach for this.

3.1.6. Synthesis and reaction of 6,8,18,20-tetrafluorodiphenanthro[3,4-c:3',4'-l]chrysenes

As the synthesis of small 7-member rings was very successful, synthesis of large and more complex nanographene structures with intriguing geometries and properties were tried. Molecule **38** possessing a helical geometry was chosen in respect to these criteria (Figure 3.2). As a non-planar molecule, the target should exhibit higher solubility and easier characterization than its planar relatives.



Scheme 8: Synthesis of tetrafluorodiphenanthro[3,4-c:3',4'-l]-chrysenes **38** and tetraphene **36** and their respective AmCFA. I. KOH , CHCl_3 . II. $h\nu$, I_2 , propylene oxide, toluene. III. Al_2O_3 , 200°C . IV. Al_2O_3 , 200°C .

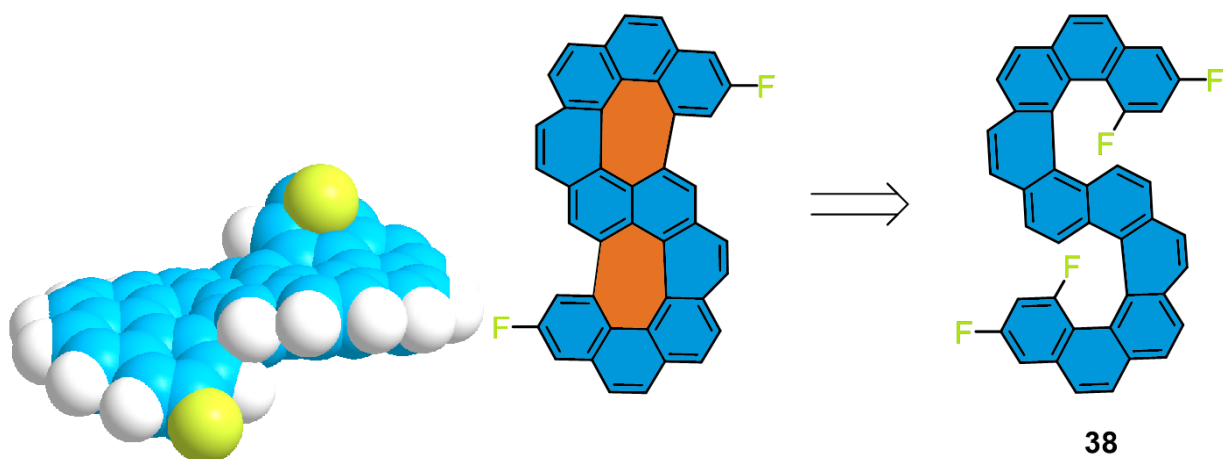


Figure 3.2: Structure of precursor **38** (right) and the corresponding product after AmCFA (middle) and its calculated 3D configuration's side view (left).

Therefore molecule **38** was synthesized by Wittig reaction of the naphthalene derivative (**34**) with corresponding phenanthrene like Wittig salt (**28**) and subsequent photocyclization. This photocyclization was expected to provide rather complex mixture because of the formation of 16 possible isomers (Figure 3.3). Nevertheless, we were able to isolate **38** from the mixture with 7 % yield.

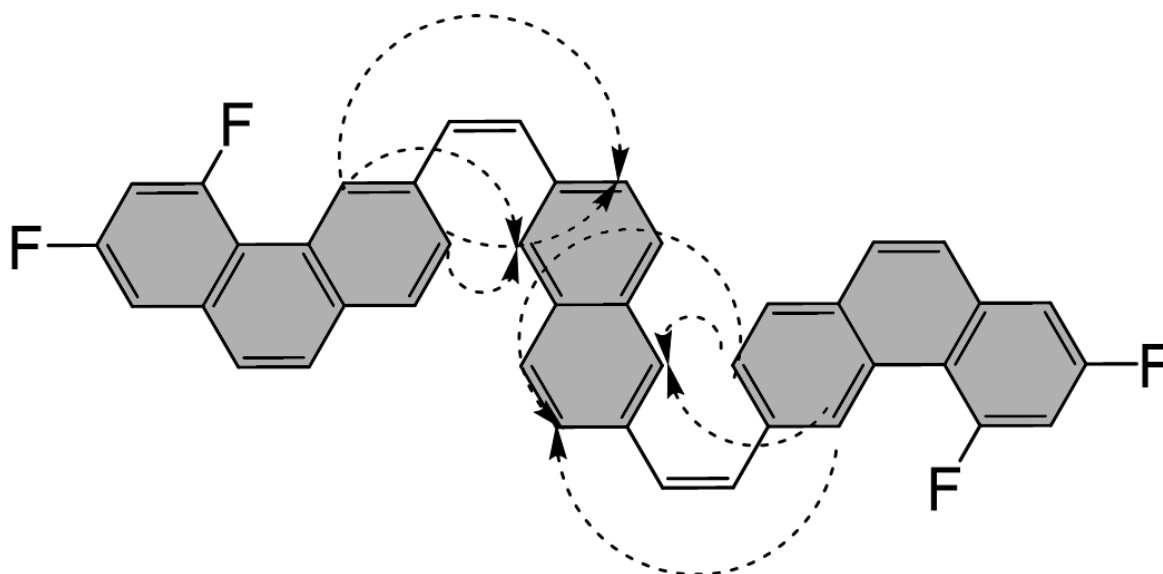


Figure 3.3: Possible photocyclization ring-closures of **35**.

After AmCFA in dry conditions, only the one-time closure product **39** was found in very low yield. Another interesting side product **36** was found and undergone AmCFA, which

resulted in another one-time closure product **37** in low yield (Scheme 8). As normal AmCFA of 7-helicene was very successful (s. chapter 3.1.1), we can conclude that the influence of two fluor atoms in meta position in the same ring is significantly detrimental for the HF-elimination.

3.1.7. Synthesis of 12,12',14,14'-tetrafluoro-11,11'-bihexahelicene

Another synthesis of large and more complex nanographene structures with intriguing geometries were tried. Molecule **47** possessing a helical geometry was chosen in respect to these criteria (Figure 3.4).

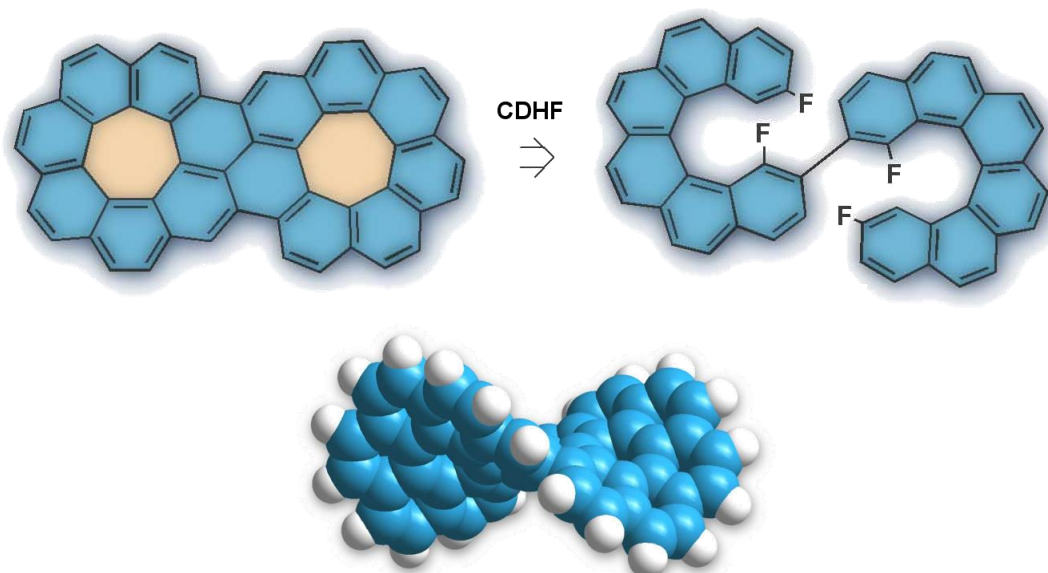
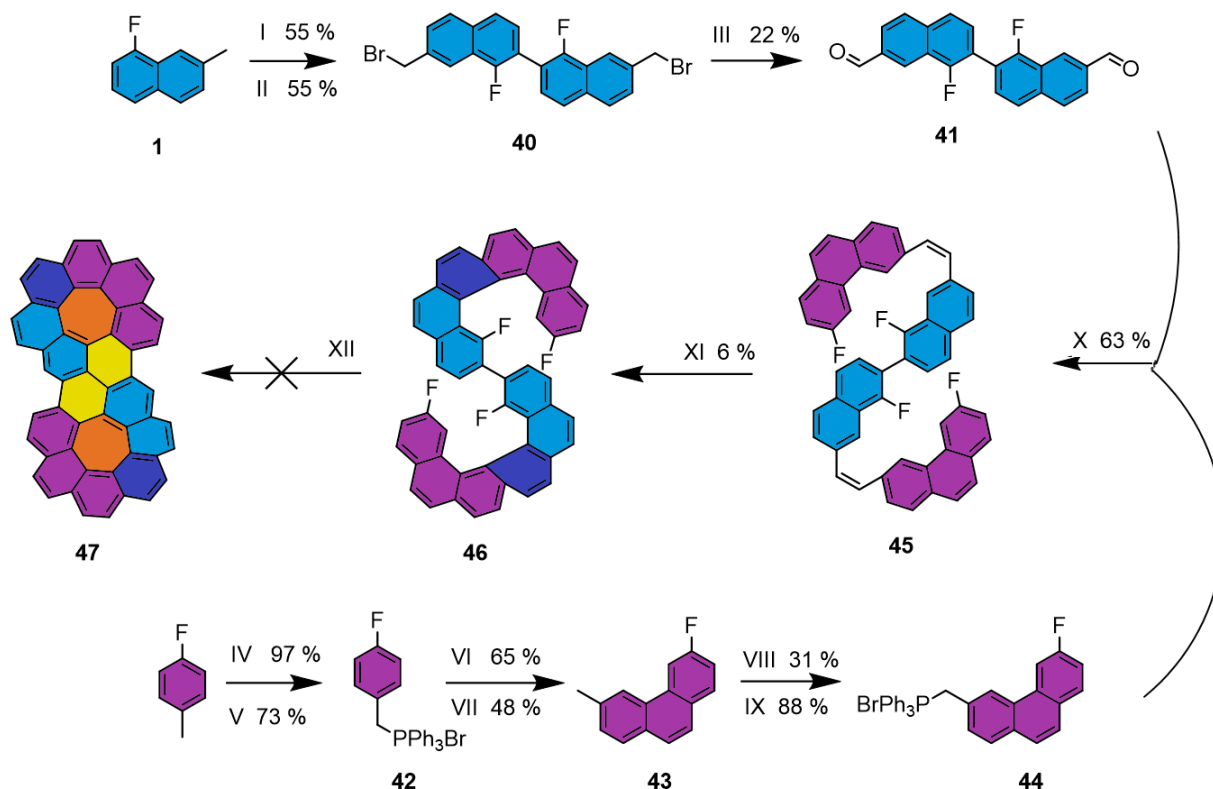


Figure 3.4: Structures of precursor **46** (right, top) and the corresponding product **47** (left, top) and its calculated 3D configuration (center, bottom).

Due to its very distorted nature, it is assumed to show interesting optical and electronic properties which maybe renders it applicable in future nanotechnologies.



Scheme 9: Synthesis of 12,12',14,14'-tetrafluoro-11,11'-bihexahelicene and its respective AmCFA. I. 1. TMP, THF, *n*-BuLi, 2. CuBr₂, 3. nitrobenzene. II. NBS, DBPO, fluorobenzene. III. CHCl₃, hexamethylenetetramine, AcOH/H₂O. IV. NBS, DDBPO, fluorobenzene. V. PPh₃, toluene. VI. 4-methylbenzaldehyde, KO^tBu, *i*-propanol. VII. hv, I₂, propylene oxide, cyclohexane. VIII. NBS, DBPO, fluorobenzene. IX. PPh₃, toluene. X. CHCl₃, KOH. XI. hv, I₂, propylene oxide, cyclohexane. XII. Al₂O₃, 190 °C.

The first building block was synthesized by dimerization of **1** and subsequent bromination to yield **40**. Formylation of **40** with hexamethylenetetramine yielded **41**. Second building block **44** was synthesized in a six-step organic synthesis route. First, bromination of commercially available 1-fluoro-4-methylbenzene and afterwards conversion into the respective Wittig salt **42**. Wittig reaction with 4-methylbenzaldehyde followed by stilbene photocyclization afforded phenanthrene derivative **43**. After bromination of the methyl substituent the corresponding phosphonium salt (**44**) was synthesized in the next step. Once both building blocks **41** and **44** have been successfully synthesized, they can be inserted as precursors in a Wittig reaction to form target compound **45**. Thereafter, subsequent photocyclization of **45** results in the formation of desired precursor **46**. Unfortunately the final reaction with AmCFA was unsuccessful (Scheme 9). The reason for this was solved in the next

chapter, as two fluor atoms in bay region undergo oxodefluorination (Figure 3.5) as published by our group⁸³.

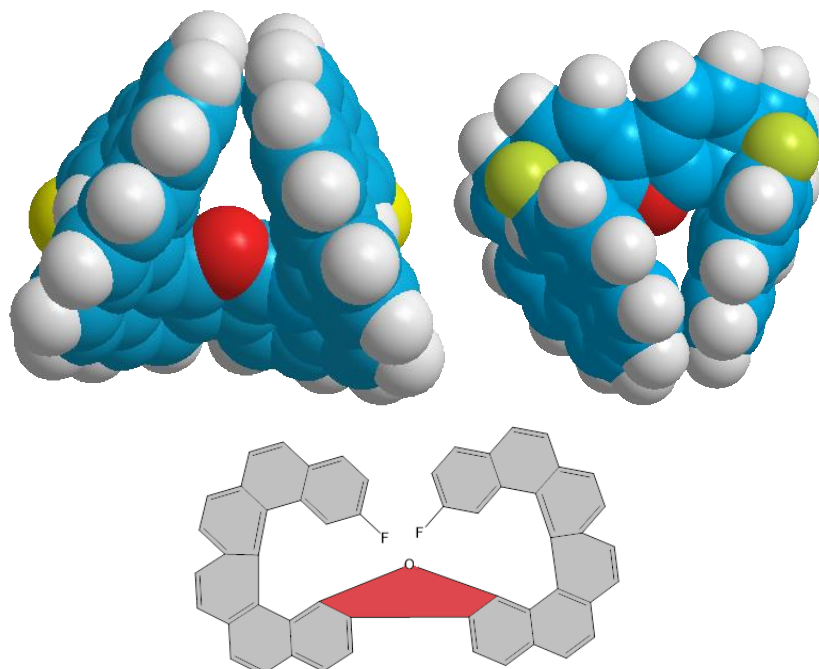


Figure 3.5: Structure of product **46** after oxodefluorination (right) and its calculated 3D configuration's top and back view (left).

Therefore, **46** is expected to show an oxodefluorination reaction on Al_2O_3 , which unfortunately could not be isolated. As no product or starting material at all was found, it can be concluded, that the separation from the alumina surface is very problematic in this case.

3.2. Oxodefluorination of fluoroarenes

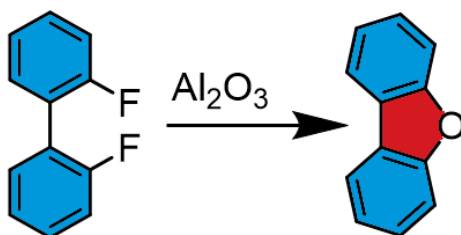
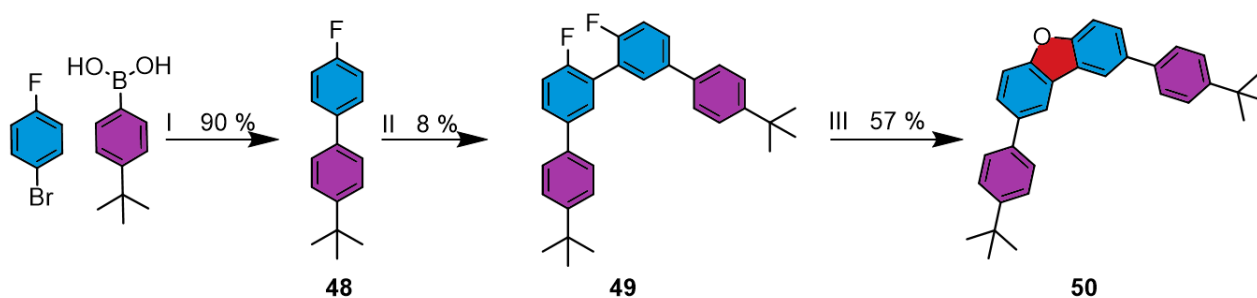


Figure 3.6: Oxodefluorination of 2,2'-difluoro-1,1'-biphenyl on Al_2O_3 .

The reaction of two fluor in bay region was proven by Vladimir Akhmetov et al. from our group in the simplest molecule 2,2'-difluoro-1,1'-biphenyl. This reacted on activated alumina to dibenzo[b,d]furan in 65 % yield.⁸³ This proved the viability of using two fluor in bay region in the synthesis of furan fragments. But as the usage of HMPA in a catalyst-free approach to a wide range of O-heteroacenes via “ladderization”⁸⁴ of fluorinated oligophenylenes (Loop) still proved superior⁸⁵, the method with HMPA was adapted in this chapter.

3.2.1. Synthesis of 2,8-bis(4-(tert-butyl)phenyl)dibenzo[b,d]furan

First the concept of two fluor in bay region with HMPA was extended in view of the project discussed in the following chapter. With the introduction of phenyl with a tert-butyl group, the general feasibility of the idea was tested.



Scheme 10: Synthesis of 4,4'''-di-tert-butyl-4',6''-difluoro-1,1':3',1'':3'',1'''-quaterphenyl (**49**) and its oxodefluorination. I. Cs_2CO_3 , THF/ H_2O (5:1), $\text{Pd}(\text{PPh}_3)_2\text{Cl}_2$. II. 1. THF, TMP, $n\text{-BuLi}$ 2. CuBr_2 , 3. nitrobenzene. III. KO^tBu , HMPA.

4,4''-di-tert-butyl-4',6''-difluoro-1,1':3',1'':3'',1'''-quaterphenyl (**49**) was used as a more complex precursor with two fluor atoms in bay region. The synthesis was achieved by Suzuki reaction (**48**) and subsequent dimerization with copper bromine and *n*-BuLi (Scheme 10). Oxodefluorination was done by LooP-reaction in good yield.

3.2.2. Synthesis of “smallest” nanographene with bridge

The aim of this chapter is to synthesize and characterize, two hexabenzocoronene derivatives, often called smallest graphene fragment,⁸⁶ linked with a bridge of furan fragments (Figure 3.7). Theoretically, the two planes of hexabenzocoronene will overlap due to the bridge and through variation of the bridge and therefore different degree of overlap, the product should exhibit different but adjustable properties. To synthesize this bridge, the oxodefluorination in bay region will be used. As proven in the previous chapter, the hexabenzocoronene fragment should have negligible influence of the LOOP-reaction in the last step.

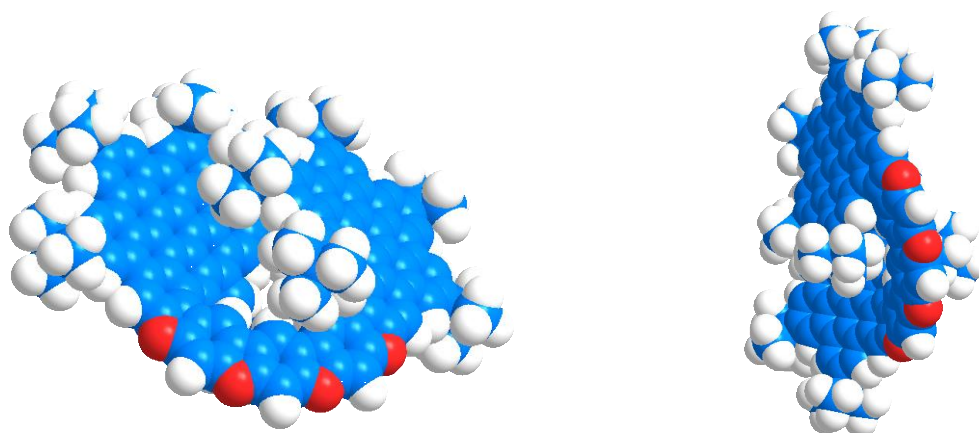


Figure 3.7: Structure of calculated 3D configuration's top and side view of product **55**.

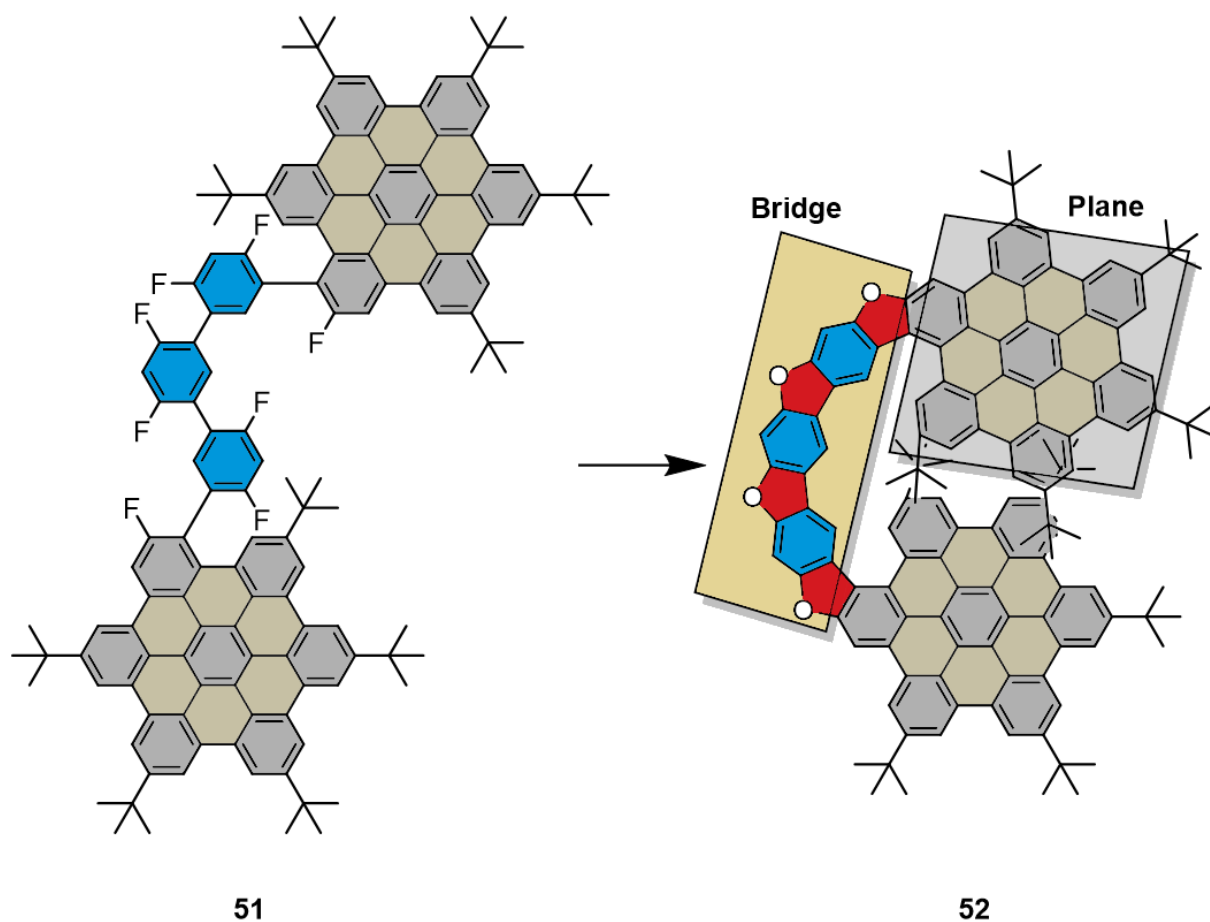
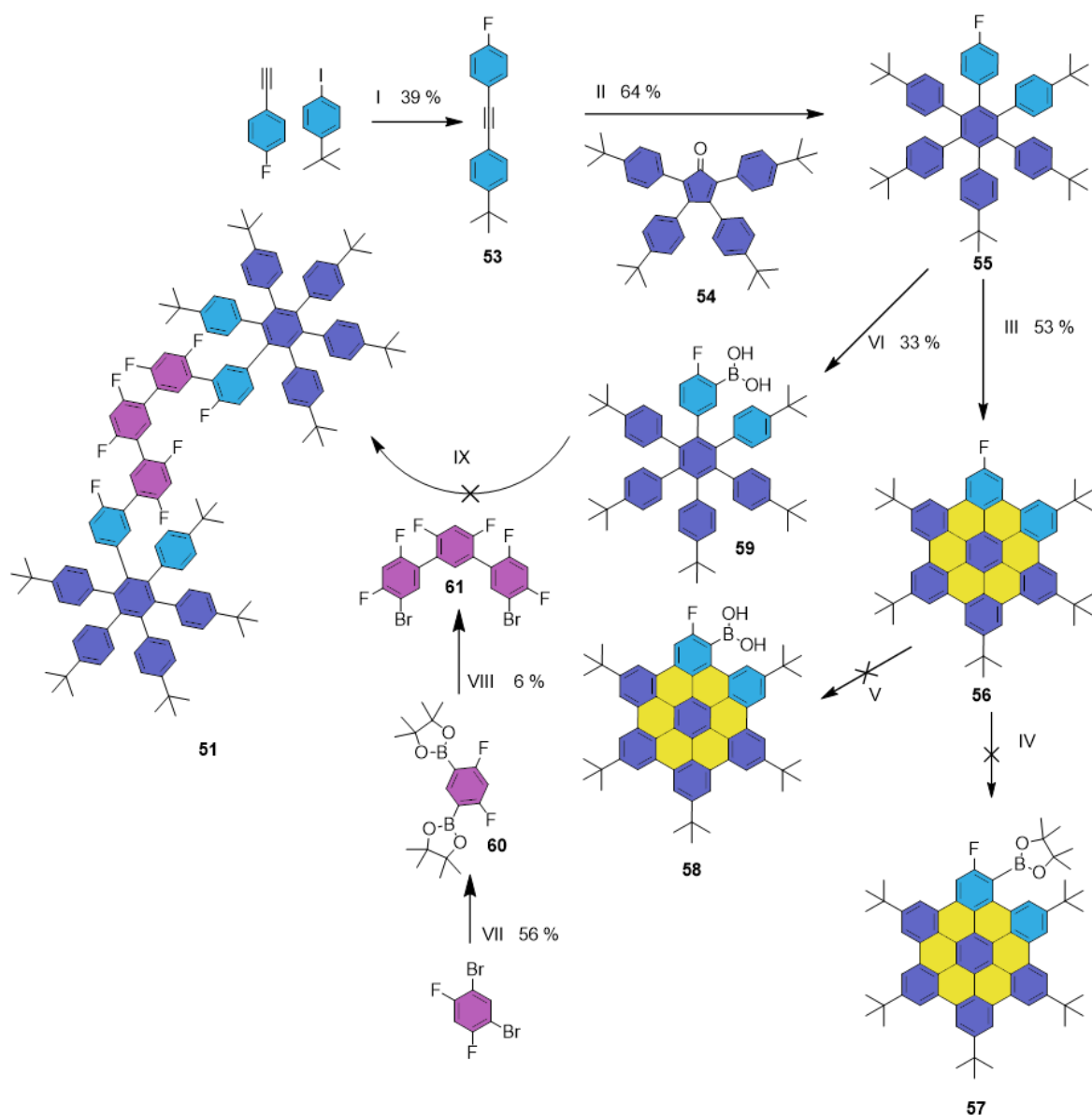


Figure 3.8: Structure of targeted precursor **51** and product **52**.

The closure of this molecule is promising, as the closure of only the bridge, with multiple oxodefluorination steps in one reaction, was done successfully already.⁸³

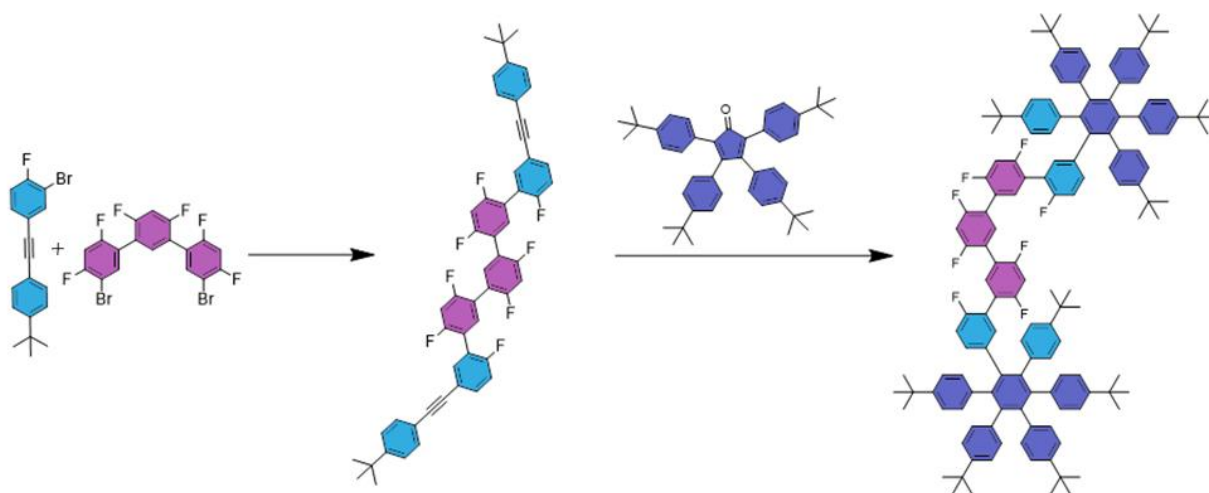


Scheme 11: Synthesis of 2,5,8,11,14-penta-tert-butyl-17-fluorohexabenzocoronene (**56**) and further failed reactions. I. *N*-methylpyrrolidinone, Cs_2CO_3 , CuI. II. Ph_2O , **54**. III. DDQ, $\text{F}_3\text{CSO}_3\text{H}$, DCM. IV. *N*-BuLi, TMP, 2-isopropoxy-4,4,5,5-tetramethyl-1,3,2-dioxaborolane. V. 1. TMP, THF, *n*-BuLi. 2. THF. 3. $\text{B}(\text{OMe})_3$. 4. HCl. VI. 1. TMP, THF, *n*-BuLi. 2. THF. 3. $\text{B}(\text{OMe})_3$. 4. HCl. VII. $\text{Pd}(\text{dppf})\text{Cl}_2$, B_2pin_2 , KOAc, 1,4-dioxane. VIII. 1,5-dibromo-2,4-difluorobenzene, K_2CO_3 , $\text{Pd}(\text{PPh}_3)_2\text{Cl}_2$, 1,4-dioxane/ H_2O 1:2. IX. **61**, $\text{Pd}(\text{PPh}_3)_2\text{Cl}_2$, Cs_2CO_3 , THF/ H_2O 5:1.

First, 1-(tert-butyl)-4-((4-fluorophenyl)ethynyl)benzene (**53**) was synthesized by copper-catalyzed cross-coupling reaction⁸⁷. Interestingly, the reaction only works in this combination. Reaction of fluoroiodobenzene with *t*butylphenylacetylene does not work. Here the +I-effect of *t*butyl-group and the -I-effect of fluor might be the decisive

factor for this problem. Afterwards **53** reacted with **54** (synthesized by Jux-group, Friedrich-Alexander-Universität Erlangen-Nürnberg) in biphenyl ether to **55**. One pathway uses first oxidative cyclodehydrogenation conditions with DDQ and triflic acid (Scholl oxidation) for the formation of hexabenzocoronene derivate **56** in good yield. Similar reactions were reported by Jux et. Al.⁸⁸. Borylation of **56** with 2-isopropoxy-4,4,5,5-tetramethyl-1,3,2-dioxaborolane or B(OMe)₃ were both unsuccessful because of sterical hindrance of the ^tbutyl-group, but which is essential for the solubility of the compound. In the hope borylation of the non-planar molecule **55**, with a bigger distance to the ^tbutyl-group, to be more successful, the reaction with B(OMe)₃ was successfully tried. To keep a higher reactivity, the compound **59** was not closed in a Scholl reaction. Instead, a linkage with the bridge-molecule **61** was tried in a Suzuki reaction. Unfortunately this was unsuccessful. **61** was synthesized by careful and short Suzuki reaction with 1,5-dibromo-2,4-difluorobenzene.

Another possible pathway would be the synthesis of 1-(tert-butyl)-4-((4-fluoro-3-bromo-phenyl)ethynyl)benzene (Yield 17 %) and further Suzuki reaction with a bridge molecule (Scheme 12).



Scheme 12: Second pathway to synthesize **51**.

This way or a variation of it, like LOOP reaction before reaction with the ketone, can be a future opportunity to realize this idea.

3.3. Construction of zig-zag periphery by $C_{sp^3}-C_{aryl}$ coupling *via* AmCFA

Open shell PAH's magnetic properties⁸⁹ offer future opportunities for application in spintronics.^{31,90} These molecule host unpaired electron densities, of which the Clar goblet is probably the most famous.⁹¹

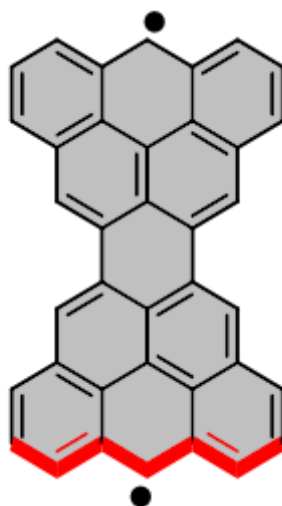


Figure 3.9: Structure of Clar goblet, a molecule with zig-zag periphery (red).

Graphene Zig-zag edges in particular are very interesting as they are intricately connected with their π -magnetism⁹², large magnetic exchange coupling^{67,93,94} and long coherence times due to weak spin-orbit and hyperfine coupling.⁹⁵ However, pure open-shell PAHs are extremely unstable and can only be obtained via difficult on-surface chemistry under ultra-high vacuum conditions.^{93,94,96} There, zig-zag edges are prepared via $C_{sp^3}-C_{aryl}$ coupling upon annealing on metallic substrates. These couple with the electronic states of the PAHs and prevent full physical characterization of open-shell PAHs. While this problem can be partially overcome via pulling PAHs on non-metallic islands^{66,67}, synthesis of open-shell PAHs or their hydrogenated precursors^{97,98} directly on technologically relevant substrates (e.g. metal oxides) is an important challenge that constrains further advances in the field.⁹⁹ Therefore, it is important to investigate novel chemical transformations catalyzed by non-metallic surfaces. Despite some recent successes in this area,¹⁰⁰ there are still few reported reactions enabling $C_{sp^3}-C_{aryl}$ coupling for synthesis of zig-zag edges in PAHs on non-metallic surfaces.

This chapter discusses the AmCFA method to induce C-H insertion leading to methylene-bridged PAHs. These molecules can serve as valuable precursors for non-Kekulé structures such as olympicene, since hydrogenated zig-zag edges can be easily oxidized during STM or AFM studies via tip manipulation.⁹⁷

3.3.1. Reactions with simple molecules

C-F bond activation was chosen as a model reaction for the study of the synthesis of zig-zag periphery on alumina. This can be obtained from fluorinated precursors via three different strategies (Figure 3.10). Therefore, we investigated intramolecular C-H insertion (**62**), C_{aryl}-C_{aryl} coupling (**63**), Friedel-Crafts coupling (**64***) on fluorene as a model compound.¹⁰¹

*This reaction was done by Mikhail Feofanov.

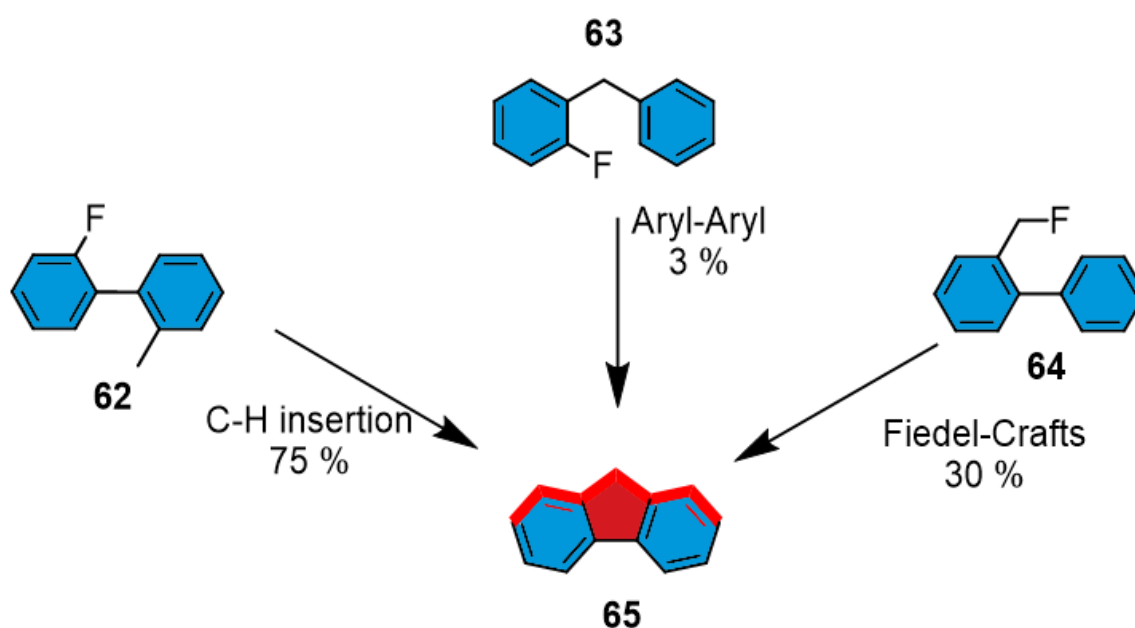


Figure 3.10: Synthetic approaches to fluorene (**65**) from the fluorinated precursors via AmCFA.

While the latter approach led to a multitude of products including **65** and Aryl-Aryl coupling did not allow an adequate conversion of **63**, **62** converted into fluorene in good yield. In principle, the C-H insertion isn't trivial and was previously known to be induced by expensive silyl carboranes,¹⁰² where the reaction occurs via the formation of

carbocation intermediates.¹⁰³ Like these studies, we proposed that alumina-mediated polarization of the C–F bond generates an electrophilic center, which reacts with the methyl group inducing C–H insertion (Figure 3.11).¹⁰¹

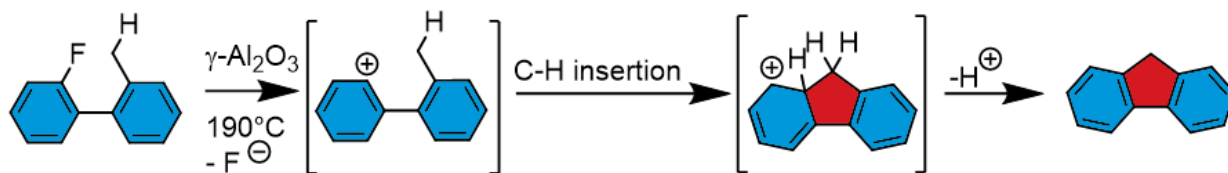
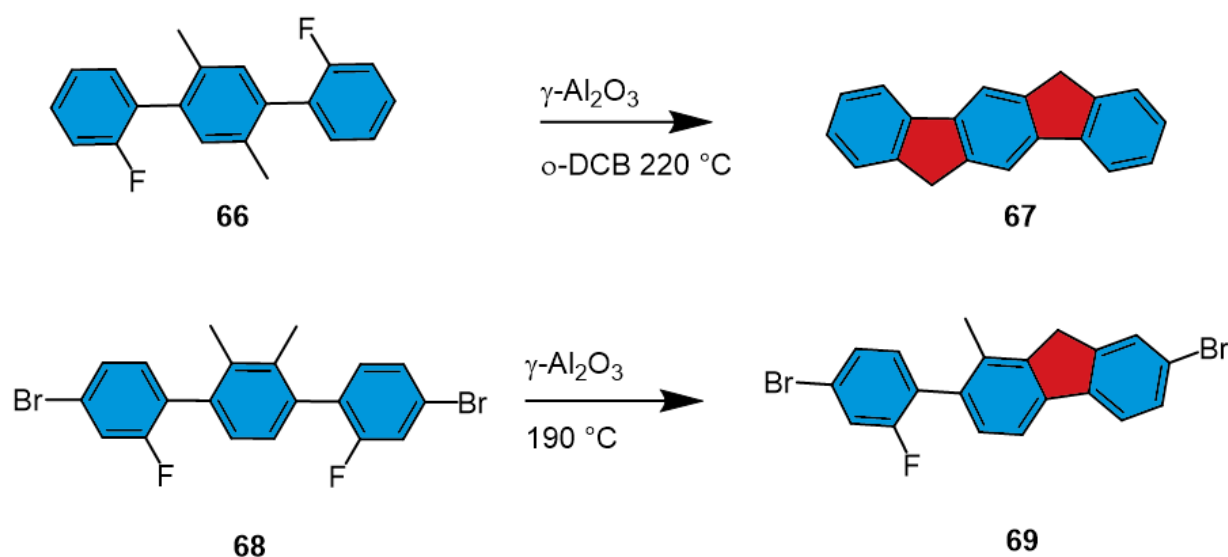


Figure 3.11: Proposed mechanism for AmCFA induced C-H insertion.

However, the precise mechanism is still not proven. The $C_{\text{aryl}}-C_{\text{aryl}}$ coupling of **63** yielded only 3 % of **65** and the main product was 2-benzylphenol (22 %). The hope of the synthesis of dibenzo[b,d]furan *via* reaction of 1-fluoro-2-phenoxybenzene on alumina yielded only 2-phenoxyphenol (38 %).



Scheme 13: Synthesis of dihydroindeno[1,2-b]fluorenes.

We investigated extended systems with longer zig-zag periphery with dihydroindeno[1,2-b]fluorene **67** from the precursor **66** through AmCFA. The wet chemistry of **66** was successful, but with very low yields, while dry conditions proved themselves a lot better (27 %). It is important that, the precursor doesn't contain a doubly fluorinated central moiety, in which case the reaction doesn't work as the electronic effects of two fluorine

atoms within the same phenyl moiety significantly destabilize the cationic species and increases energetic barriers for the C–F bond activation.¹⁰¹ The brominated precursor **68** was synthesized in hope of achieving an easy and straight forward synthesis of long chains of dihydroindenofluorenes. Unfortunately, the AmCFA of **68** only yielded the mono-closure of the compound even after repeated attempts (Scheme 13).

We tried a different alkyl substituent next. The isopropyl-substituted biphenyl **70** reacted under a cyclodehydrofluorination reaction to the methylated fluorene **71** in good yield (Figure 3.12). This predictable behavior is anticipated to be due to the higher acidity of benzyl C–H bonds.

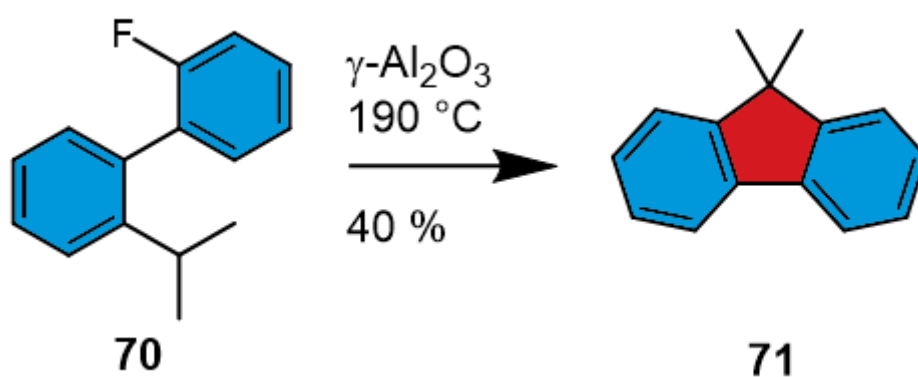
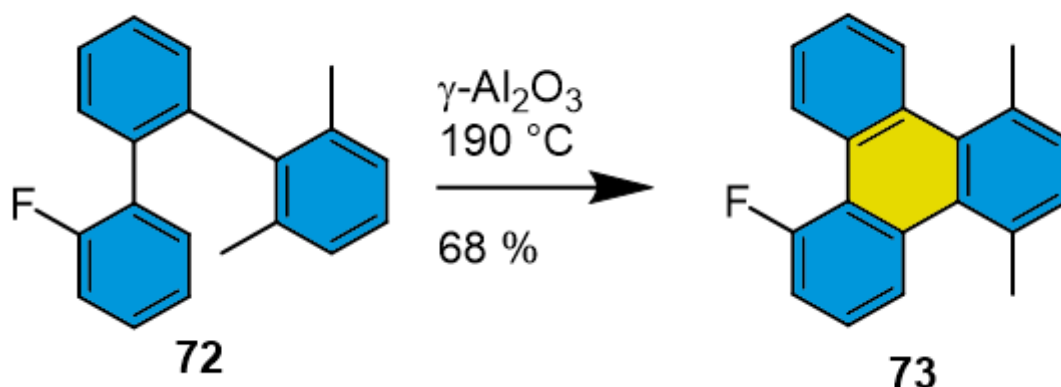


Figure 3.12: AmCFA of the isopropyl-substituted biphenyl.



*Figure 3.13: AmCFA of 2''-fluoro-2,6-dimethyl-1,1':2',1''-terphenyl **72**.*

We investigated the application of this method for the synthesis of non-alternant zig-zag PAH containing heptagon. The precursor **72** was synthesized, but after AmCFA,

unexpected hexagon formation in form of the triphenylene derivative **73** was detected. This transformation requires a 1,2-methyl shift (Figure 3.13).

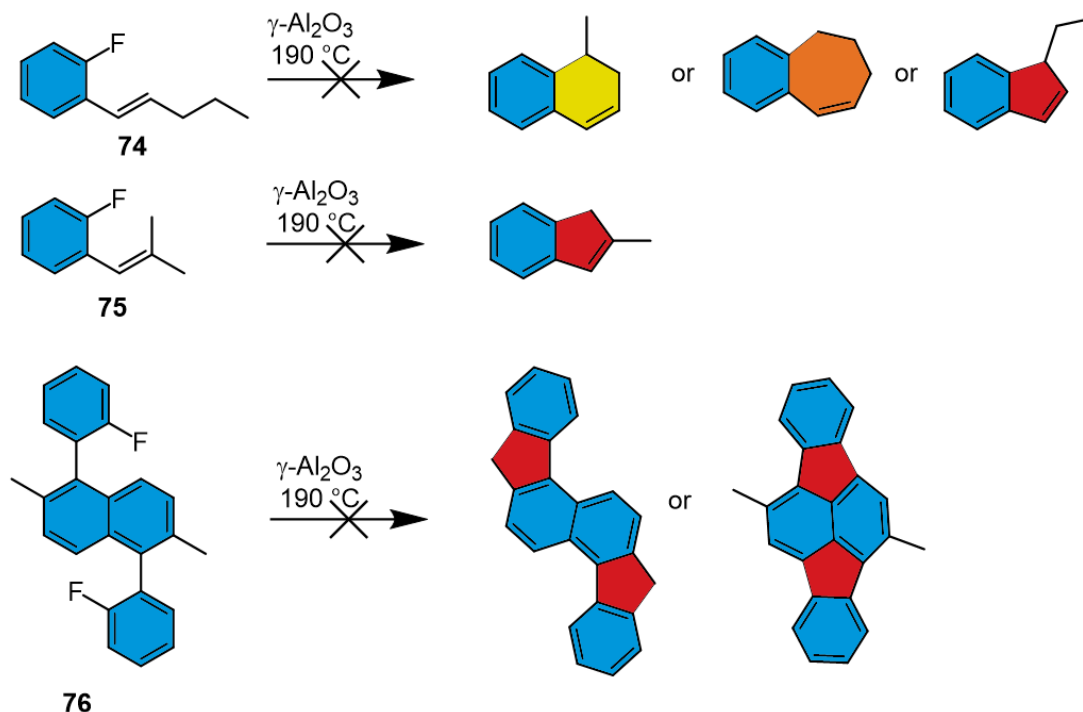


Figure 3.14: Unsuccessful reactions of fluorophenyl with alkene substituents **74** and **75** and 1,5-bis(2-fluorophenyl)-2,6-dimethylnaphthalene **76**.

The less stiff molecules **74** and **75** showed no reaction under exposure of Al_2O_3 . Unexpectedly **76** showed no reaction as well (Figure 3.14), although the same molecule without one fluorophenyl and methyl group reacted on Al_2O_3 ¹⁰¹. Neither the formation of a pentagon with the methyl-group nor the heptagon formation with the naphthalin position were detected. This reaction was tried at 90°C for 1 d, 190°C for 1 d and 190°C for 5 d, but only starting material was isolated.

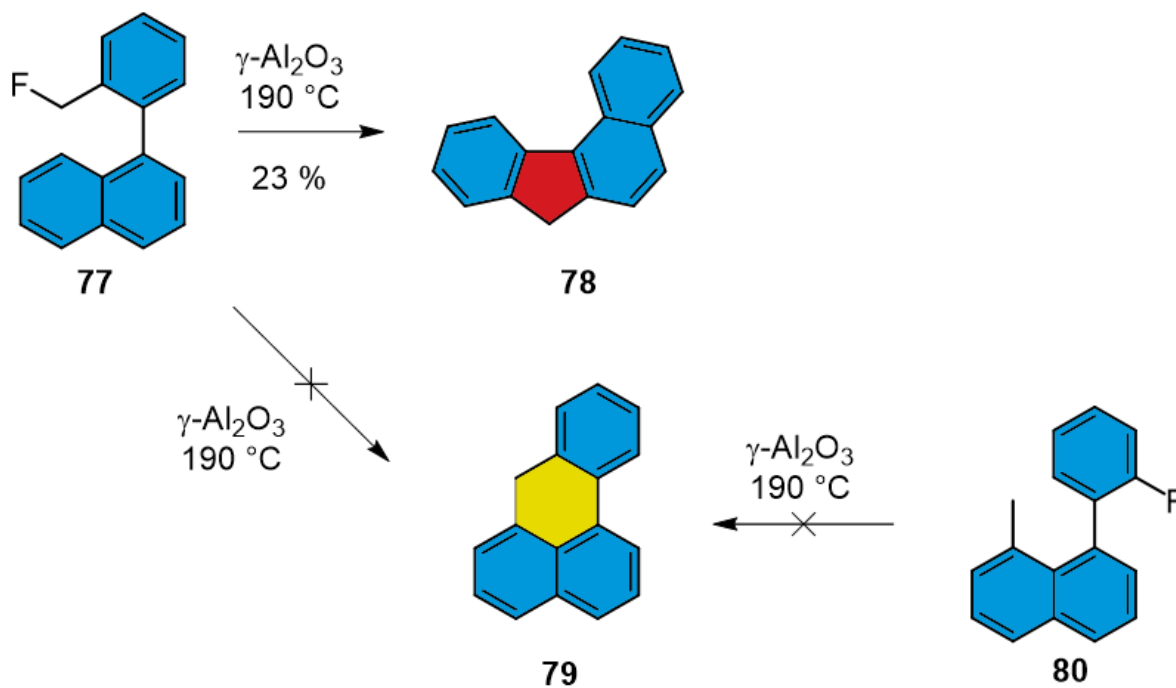


Figure 3.15: Synthesis of 7H-benzo[*c*]fluorene **71**.

Experiments with 1-(2-(fluoromethyl)phenyl)naphthalene (**77**) showed the formation of the pentagon (**78**) and only traces of 7H-benzo[*de*]anthracene (**79**). Even with only one possible reaction path, as is the case with 1-(2-fluorophenyl)-8-methylnaphthalene (**80**), no hexagon formation was observed (Figure 3.15). This observation is likely connected to the steric hindrance, which prevents a conformation favorable for the intramolecular coupling.

3.3.2. Synthesis of bi-[4]helicene derivatives

In the stiff precursor **81**, fluorine and methyl groups are located in the cavity of the [4]helicene, i.e. in the cove-region and form the hexagon carbon formation on alumina in good yield. Surprisingly, the dimer **83** of the same [4]helicene derivate oxidizes after closure to the ketone **84** (45 % Yield) and no pure hydrocarbon-molecule could be isolated after reaction on alumina (Figure 3.16).

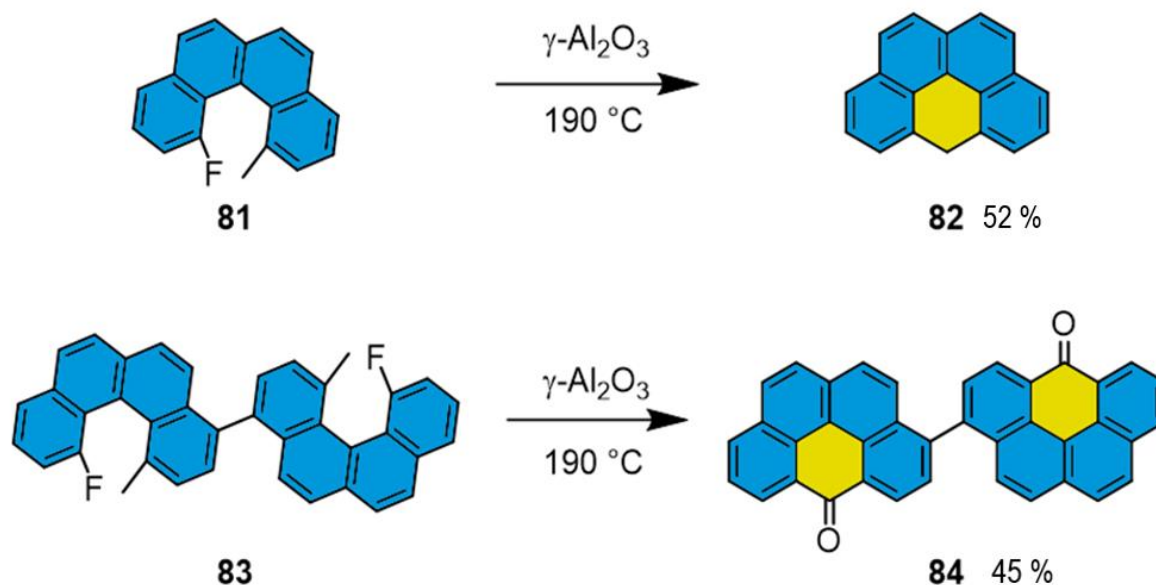
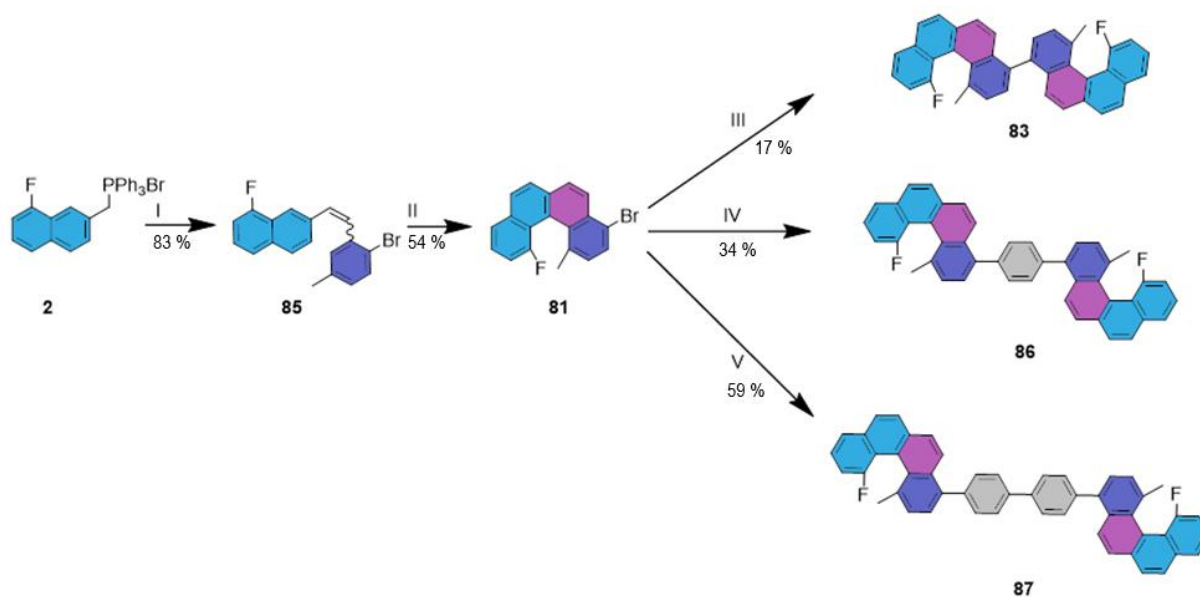


Figure 3.16: AmCFA of 1-fluoro-12-methylbenzo[*c*]phenanthrene **81**¹⁰¹ and its dimer **83**.

Nevertheless, precursor **83** and its derivatives **86** and **87** were synthesized for surface studies on metal oxides (Scheme 14). The closed products should be interesting to study due to their biradical character. The easily modifiable distance of the helicene section and therefore the two radicals, due to a polyphenyl-bridge promise an easy variation of properties.



Scheme 14: Synthesis of 4-bromo-12-fluoro-1-methylbenzo[*c*]phenanthrene **81**, its dimer **83**, its dimers with phenyl(**86**) and biphenyl linkage (**87**). I. 2-bromo-5-methylbenzaldehyde, CHCl_3 , KOH. II. $h\nu$, I_2 , propylene oxide, cyclohexane. III. Toluene, $t\text{-BuLi}$, Pd-PEPPSI-*Ipent*. IV. 1,4-phenylenediboronic acid, Cs_2CO_3 , THF/ H_2O (5:1), $\text{Pd}(\text{PPh}_3)_4$. V. [1,1'-biphenyl]-4,4'-diylidiboronic acid, Cs_2CO_3 , THF/ H_2O (5:1), $\text{Pd}(\text{PPh}_3)_4$.

The brominated species **81** of the published fluoromethyl[4]helicene¹⁰¹ has been synthesized by Wittig reaction of **2** with 2-bromo-5-methylbenzaldehyde and subsequent photocyclization. Afterwards dimerization yielded **83**. Suzuki reaction of **81** with phenyl-diboronic acid and biphenyl diboronic acid yielded **86** and **87**. These compounds were sent to Switzerland for further studies.

3.4. Screening the reactivity of different functional groups on Al₂O₃

After numerous additional reactions on alumina were observed, the question aroused if other functional groups are reactive on alumina and what significance this has for alumina chemistry. Therefore different functional groups were tested on γ -alumina and examined via ¹H-NMR spectrometry in a qualitative manner.

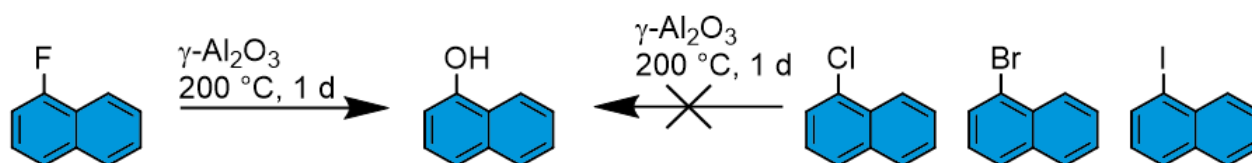


Figure 3.17: AmCFA of fluoronaphthalene and its other halogen derivatives.

First, halogen substituted naphthalene were investigated in the presence of aluminum oxide (Figure 3.17). 1-Fluoronaphthalene reacted to naphthalen-1-ol, but no other halogen compound showed a reaction. We can conclude, that other halogen-structures are stable in AmCFA and can be introduced for further reactions e.g., Suzuki reaction.

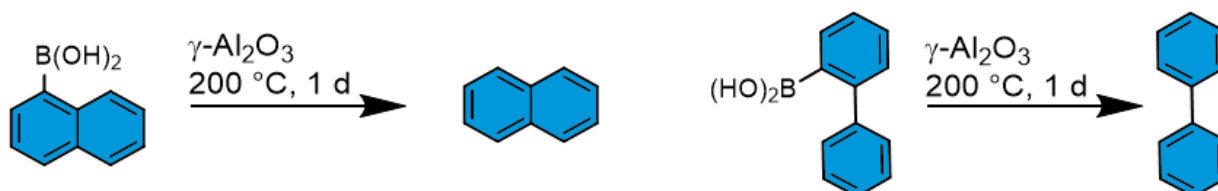


Figure 3.18: AmCFA of boronic acid of naphthalene (left) and biphenyl (right).

Boronic acids are valuable compounds for the PAH synthesis, therefore the reactivity on aluminum oxide was tested. Naphthalene boronic acid and biphenyl boronic acid showed a cleavage of the respective boronic acid group and only pure naphthalene and biphenyl was isolated (Figure 3.18).

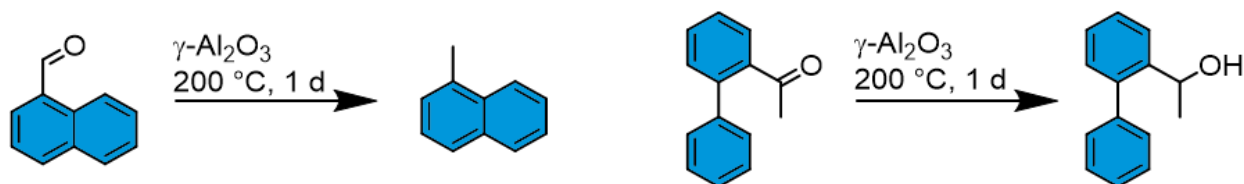


Figure 3.19: AmCFA of aldehyde and ketone group.

The carbonyl group is essential for Wittig-reaction and therefore an important molecule for PAH synthesis. Investigation into the reactivity of these compounds showed the instability of carbonyl-groups on alumina. 1-naphthaldehyde was reduced to 1-methylnaphthalene and the ketone 1-([1,1'-biphenyl]-2-yl)ethan-1-one was converted to the alcohol 1-([1,1'-biphenyl]-2-yl)ethan-1-ol (Figure 3.19).

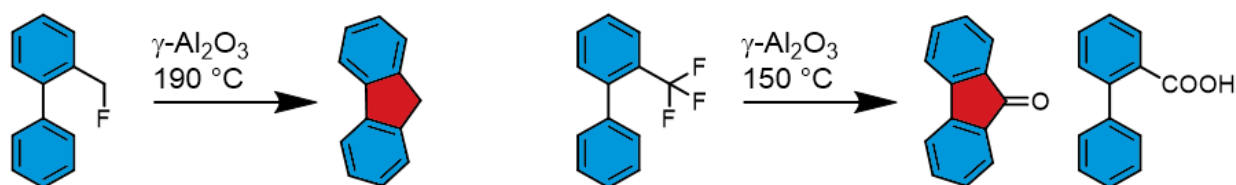


Figure 3.20: Published results of AmCFA of fluorinated methylbiphenyl¹⁰¹ (left) and triple fluorinated methylbiphenyl¹⁰⁴ (right).

As discussed in the previous chapter, 2-(fluoromethyl)-1,1'-biphenyl reacts to fluorene on aluminum oxide. 2-(Trifluoromethyl)-1,1'-biphenyl was reported by Papaianina et.al. in 2016 to transform into the ketone and carbonic acid (Figure 3.20).¹⁰⁴ But the twice fluor substituted biphenyl was yet to be investigated.

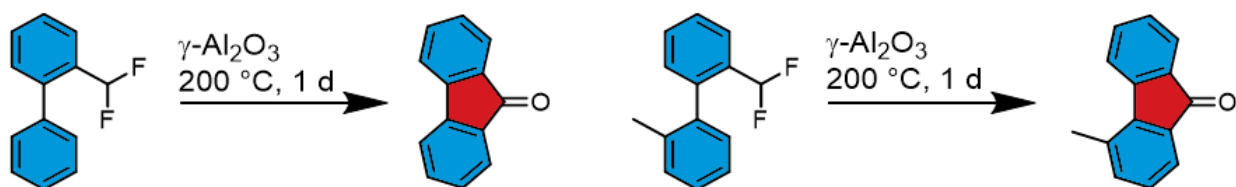


Figure 3.21: AmCFA of double fluorinated methylbiphenyl.

Therefore 2-(difluoromethyl)-1,1'-biphenyl was reacted on aluminum oxide, which yielded the ketone 9H-fluoren-9-one. To investigate the influence of alkyl groups, methyl was introduced in bay region, but showed no impact on the formation of the ketone (Figure 3.21).

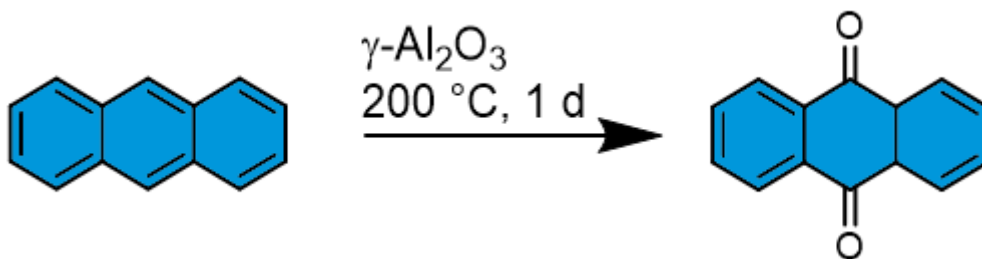


Figure 3.22: AmCFA of anthracene.

Anthracene surprisingly reacted on Al_2O_3 to anthraquinone (Figure 3.22). This oxidation reaction is therefore a possible alternative path for anthraquinone synthesis, other than using toxic chromic acid.¹⁰⁵ Unfortunately shortly after detection by $^1\text{H-NMR}$, the unstable compound decomposed. As was shown in Figure 3.19 the carbonyl group is not stable on alumina for a long time.

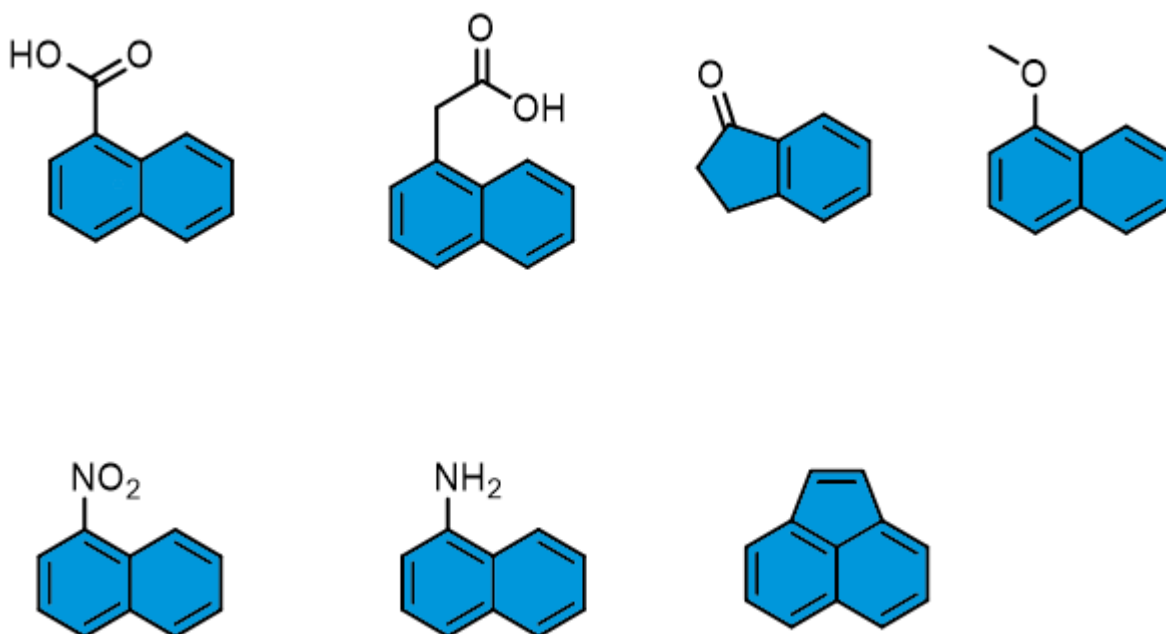
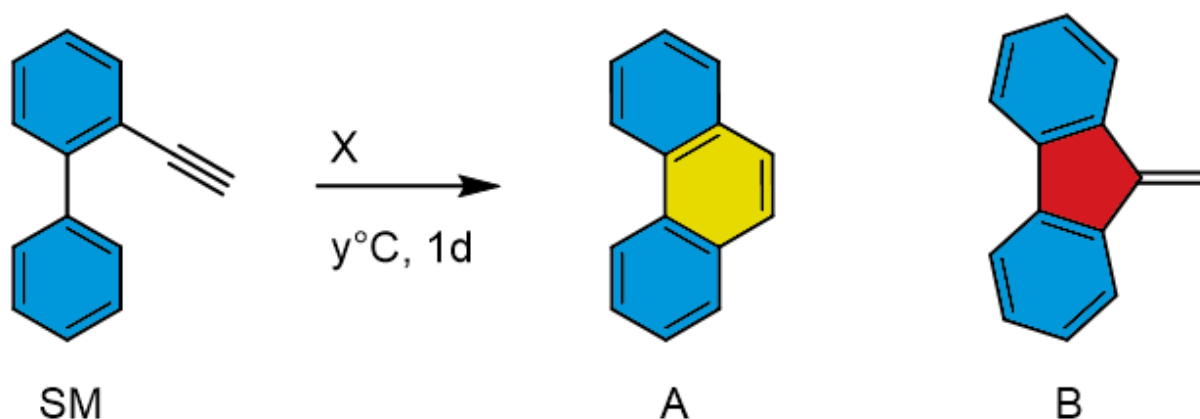


Figure 3.23: Compounds, which showed no reaction on Al_2O_3 .

Multiple compounds showed no reaction and partly could not be released after adsorption on alumina (Figure 3.23). 1-naphthoic acid, 2-(naphthalen-1-yl)acetic acid, 1-nitronaphthalene and naphthalen-1-amine adsorbed on aluminum oxide and could not, even with acetic acid, be isolated afterwards. 2,3-dihydro-1H-inden-1-one, 1-methoxynaphthalene and acenaphthylene could be dissolved in toluene or methanol and identified afterwards.

3.5. Screening the reactivity of 2-ethynyl-1,1'-biphenyl on different metal oxides

Konstantin Amsharov has done a small study on the reactivity of different metal oxides in 2016.⁵⁴ In conclusion γ -alumina has proven to be the best oxide material for cyclodehydrofluorination. But new results have been published, which call into question the reactivity of other metal oxides in connection to acetylenes. This represents an important path for potential bottom-up synthesis of sp^2 -carbon-based materials directly within a device.¹⁰⁶ Therefore multiple, easily commercially available metal oxides were tested on the model starting material biphenyl acetylene (**SM**) in a 5-exo-attack to 9-methylenefluorene (**B**) and 6-endo-attack to phenanthrene (**A**) under different temperatures (Scheme 15). Normally only phenanthrene is formed using activated alumina (s. Chapter 1.2.6.), which shows its soft π -Lewis character. Consequently, detection of 9-methylenefluorene indicated a hard π -Lewis character.



Scheme 15: Reaction of **SM** on different metal oxides (*X*) under different temperatures (*y*).

Surface material	90 °C General Procedure I	90 °C General Procedure II	200°C General Procedure II	400°C General Procedure II
Al ₂ O ₃	-	A	A	
TiO ₂ anatase	SM	SM	SM	
TiO ₂ rutil	SM	SM	SM	
SiO ₂	SM	SM	-	
a-Fe ₂ O ₃	SM	SM	-	
Ga ₂ O ₃	SM	SM, A, B*	A	
MgO	SM	SM	-	
ZrO ₂	SM	A, B	-	
Nb ₂ O ₅	B	SM	-	
In ₂ O ₃	SM	SM	A	
Ce ₂ O ₃	SM	SM	-	
MoS ₂	-	SM, A	-	
Zr20	SM, A*, B	A		A
Si5	SM	B*		A*, B
Si30	SM, B*	B		
Mg5	SM	SM		SM
Mg30	SM	SM		SM
Ce20	SM	SM		SM*, A

Table 1: Experimental results of different metal oxides with biphenyl acetylene (**SM**).

Activated Ga₂O₃ is one promising surface material, as the formation of phenanthrene at 200°C and even already at 90 °C showed. Trace amounts of **B** were detected at these low temperatures, which disappeared in high temperatures. Activated ZrO₂ showed the formation of both **A** and **B** at 90 °C but no reaction at 200 °C. Whereas activated In₂O₃ showed directly opposite behavior, with formation of **A** at 200 °C and no reaction at 90 °C. The 13th group with Al₂O₃, Ga₂O₃ and In₂O₃ showed therefore high reactivity to biphenyl acetylene (Table 1).

But the cheap prize of Al₂O₃ and high reactivity, still makes it the favorite candidate for non-specific PAH synthesis. But because of no selectivity of pure Al₂O₃, new doped aluminas from “SASOL” were investigated. Dopants deposited on the surface of pure alumina allows to adjust surface chemical properties like acidity or even to combine the beneficial physical properties of alumina with chemical properties of other oxides. Silica doped aluminas exhibit a higher degree of acidity than pure aluminas.¹⁰⁷

Therefore Si5 showed trace amount of **B** at 90 °C and trace amount of **A** at 400 °C with the main product being **B**. With higher amount of SiO₂ in Si30, **B** is synthesized at 90 °C and even without activation of the metal oxide, trace amount of **B** was detected. The lower loose bulk density and higher surface area (Table 2) might also be a factor for higher reactivity at lower temperatures. This shows a definite advantage of these doped alumina compared to the reactivity of pure alumina and pure SiO₂, which showed no reaction at all.

Typical chemical and physical properties		Si5 SIRAL 5	Si30 SIRAL 30	Zr 20 Puralox SCFa- 190 Zr20	Mg5 PURAL MG5	Mg30 PURAL MG30	Ce20 Puralox SCFa- 160/Ce20
Al ₂ O ₃ / SiO ₂	[%]	95/5	70/30	-			
Al ₂ O ₃ / ZrO ₂	[%]	-	-	80*/20			
Al ₂ O ₃ / MgO	[%]				95/5	70/30	
Al ₂ O ₃ / CeO ₂	[%]						80/20
LOI	[%]	25	20	3	25	35	3
Loose bulk density	[g/l]	450-650	250-450	600-800	300-600	300-600	600-800
Particle size (d50)	[mm]	35	35	30	40	40	30
Surface area (BET)	[m ² /g]	350	450	190	250	250	160
Pore volume	[ml/g]	0.7	0.9	0.5	0.5	0.5	0.5

Table 2: Technical data of doped alumina provided by SASOL. *here SASOL gave 97 %, but as this doesn't make sense, it was substituted for 80 %.¹⁰⁷

Activated Zr 20 showed formation of **A** at 400°C and 90°C and formation of **B** and trace amount of **A** without activation at 90 °C. This showed, that hydroxy groups on the surface, which can be removed by annealing, do not completely deactivate the reaction but switch the selectivity of the reaction to **B**. This surprising action were only before seen in Nb₂O₅, where **B** was synthesized without activation and with activation no reaction at all was detected. Therefore, we can conclude, that the hydroxy-group on

the oxide have significant impact not only on the overall activity but also selectivity of the reactions and therefore their π -Lewis character. Mg 5 and Mg 30 were tested with biphenyl acetylene but no reaction at all was determined to occur. This shows, that Mg has a highly deactivating impact on the reaction. Ce 20 shows only a reaction to **A** at 400 °C and therefore has no significant bearing on the activity of alumina.

The reactivity of different metal oxides, regarding cyclodehydrofluorination through C_{sp^3} - C_{aryl} coupling and oxodefluorination with two fluor in bay region, was investigated briefly but no reaction occurred with the examined oxides and therefore are not further mentioned in this thesis.

3.6. Investigation for the soft π -Lewis acidity of different alumina's terminations

Even with our normal γ -alumina and its soft π -Lewis acidity (s. Chapter 1.2.6.) the definite determination of the active catalytic centers and the assignment of their reactivity is difficult due to the diversity of the possible alumina terminations.⁷³ Therefore we studied different aluminas with different terminations on the surface, which can influence the Lewis acidity of π -electron systems and their reaction mechanisms. We investigate the soft π -Lewis acidity of these different aluminum oxides, via reaction of 7-(phenylethynyl)cyclohepta-1,3,5-triene dissolved in a toluene/*n*-hexane mixture (Figure 3.30). All experiments were done for 1 d at 40 °C, if not especially mentioned. The reason for this particular reaction was that not all π -activators act in the same manner.

As published by Echavarren et al., gold(I) complexes catalyze 7-alkynylcycloheptatrienes as an 1,6-enyne that undergoes skeletal reorganization into the regioisomeric indenenes via formation of fluxional barbaralyl cations.¹⁰⁸ This is a characteristic behaviour of soft π -Lewis acids.^{70,109} Common π -acids such as $PtCl_2$ and $GaCl_3$ were found to be catalytically inactive contrary to gold and now γ -alumina which induce regioselective isomerization of SM. Using this behaviour, Gandon et al. developed a test exploiting a chemical indicator, which allows assigning a π -Lewis acid

6.1	6	pure theta-alumina	75	has very little OH groups on the surface	20/60/20
6.2	6	pure theta-alumina	75	has very little OH groups on the surface	80/0/20
7.1	7	pure theta-alumina	75	is covered with OH groups	80/19/1
7.2	7	pure theta-alumina	75	is covered with OH groups	60/0/40
8.1	8	1 weight% Lanthanum/ γ -alumina			5/15/80
8.2	8	1 weight% Lanthanum/ γ -alumina			20/30/50
9.1	9	gamma-alumina, commercial	200		5/90/5
9.2	9	γ -alumina, commercial	200		20/30/50
10.1	10	γ -alumina, commercial	90		10/85/5
10.2	10	γ -alumina, commercial	90		95/0/5
11.1	11	α -alumina nanosheets	20		85/0/15
11.2	11	α -alumina nanosheets	20		95/0/5

Table 3: Characteristic of different Al_2O_3 samples used in reaction of 7-(phenylethynyl)cyclohepta-1,3,5-triene (**SM**) and approximate conversion using HPLC Contour view and spectra as reference.

Normally after activation, our γ -alumina reacts as a soft π -Lewis acid and forms 80 % of **2** and only traces of **1** were detected by HPLC (experiment 0).

γ -Alumina rods with a surface of 75 m^2/g showed slight increase of **1** but still about 80 % of **2** (experiment 1.2). After extraction, this alumina was reused and the same activity was detected. This showed the stability and possibility to use the same surface material multiple times. This is especially interesting for industrial usage. At room temperature, the activity decreases with 50 % starting material still on alumina and shows a hard Lewis acid character with 40 % formation of **1**.

γ -Alumina platelet with a surface of 72 m^2/g showed 85 % of **1** and only traces of **2**.

The activity decreases sharply with reusage of the platelets (experiment 2.2).

γ -Alumina with hexagonal arrangement displayed formation of 80 % of **2** and 15 % of **1**. This showed a similar reactivity to γ -alumina rods and normal γ -alumina, but reusage is not very successful with 80 % starting material (experiment 3.2).

Rhodium doped (0.1 %) γ -alumina induces formation of nearly an equal amount of **1** and **2** (experiment 4.1). After reusage, overall decreased activity was detected and a preferred formation of **1**.

Palladium doped (0.05 %) γ -alumina induces formation of mostly **1** but after using the sample again mostly **2** was detected.

Pure theta-alumina with very little hydroxy groups on the surface showed 60 % formation of **1** and 20% of **2** but after reusage no **1** was detected but a small amount of **2** (Experiment 6.2).

Lanthanum doped (1 %) γ -alumina induces formation of mostly **2** with small amount of **1** but after reusage the amount of **1** double and **2** decreases slightly (Experiment 8.2). Overall doped alumina shows high activity the first time but this decreases sharply after reusage.

Pure theta-alumina with hydroxy group coverage formed only a small amount of **1** and showed overall low activity. After reusage 40 % of **2** was detected (Experiment 7.2). One can see, the coverage of the surface deactivates reactions but after new activation at high temperatures the surface is less covered in hydroxy groups and activity increases.

Commercially available γ -alumina with 200 m²/g and 90 m²/g show exceptionally high formation of **1**. Compared to our alumina which generally generated only **2**. The reason for this might be a higher SA as commercially available γ -alumina with 200 m²/g showed higher formation of **2** after reusage (Experiment 9.2).

However, α -alumina nanosheets show overall low activity as a Lewis- Acid (Experiments 11).

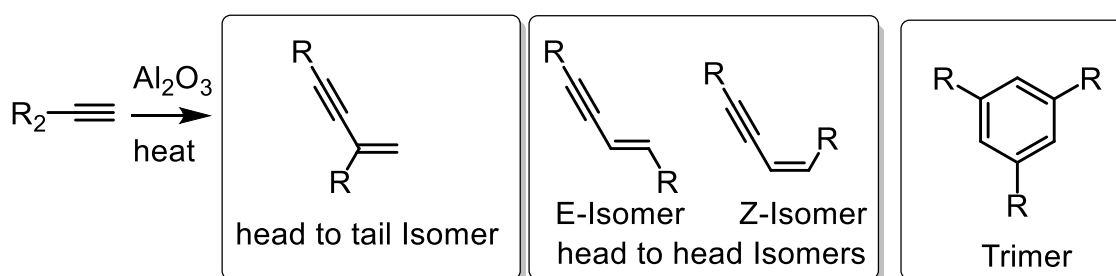
3.7. Homodimerization of terminal alkyne-model molecule under different temperatures

Terminal acetylenes, which are not in bay region to another benzyl-ring, undergo dimerization or trimerization on alumina (Scheme 16). Thereby four products are possible:

Head-to-tail dimer: the last carbon of one acetylene attacks the carbon of another acetylene molecule, which is nearer to the aromatic part.

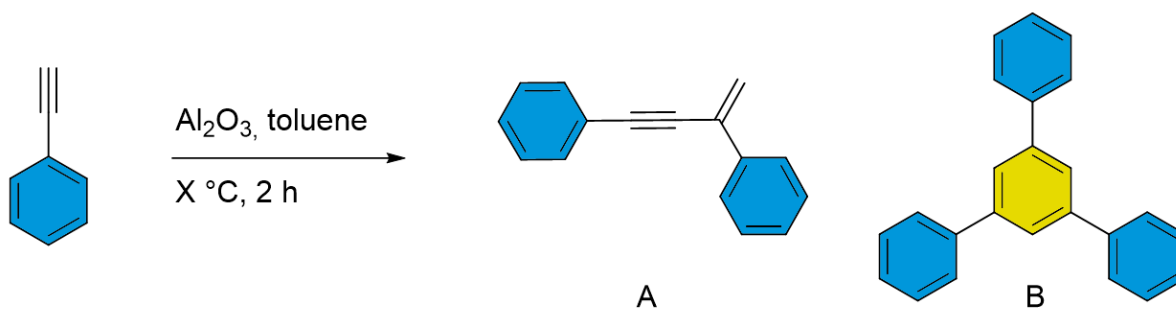
Head-to-head dimers: the last carbon of one acetylene attacks the last carbon of another acetylene molecule. In this formation, the E- and Z-isomers are possible.

Trimer: the head-to-tail isomer reacts further with one more acetylene molecule to the trimer under formation of a benzyl ring.



Scheme 16: Possible reactions of terminal alkynes.

Phenyl acetylene is the simplest aromatic system with a terminal acetylene group for AmCFA (Scheme 17), therefore it was used as a model compound for optimization of reaction conditions (Table 4).



Scheme 17: AmCFA of phenylacetylene at different temperatures.

Temperature [°C]	Reaction time	Ratio of A/B [%]
20	2d	68:32
40	2h	88:12
60	2h	94:6
60	6h	83:17
90	2h	0:100
120	2h	9:91
150	2h	19:81

Table 4: Results of AmCFA of phenylacetylene under varying temperatures.

No absolute yields for optimization of reaction conditions were necessary, therefore the ratio of head-to-tail dimer and trimer, based on ¹H-NMR data were analyzed. No head-to-head dimers were detected in these reactions. 60 °C was the best temperature for the formation of dimers and 90 °C for the complete reaction to the trimer. With increasing temperatures higher than 90 °C, the amount of dimer increases as well. On the other hand, decreasing temperatures lower than 60 °C increases the number of trimers, but as the overall activity decreases to an unacceptable degree, this can be ignored.

The influence of activated doped alumina was researched briefly. The reaction on Mg30 at 90 °C for 1 d resulted in the formation of the trimer (4 %), the head-to-tail dimer (51 %) and the Z-head-to-head dimer (45 %). Reaction on Si30 at 90 °C for 1 d resulted in the formation of only trimer. Reaction on Ce20 at 90 °C for 1 d resulted in the formation of the trimer (15 %), the E-head-to-head dimer (47 %) and the Z-head-

to-head dimer (38 %). As was discussed in the previous chapter as well, doping of alumina has a huge impact on the reaction selectivity. As these were all dry experiments, one reaction was tested under wet conditions.

Reaction on Ce20 at 120 °C in toluene for 5 h yielded the trimer (23 %) and the Z-head-to-head dimer (77 %). The influence of selectivity from the solvent can be clearly seen, as no E-isomer was detected.

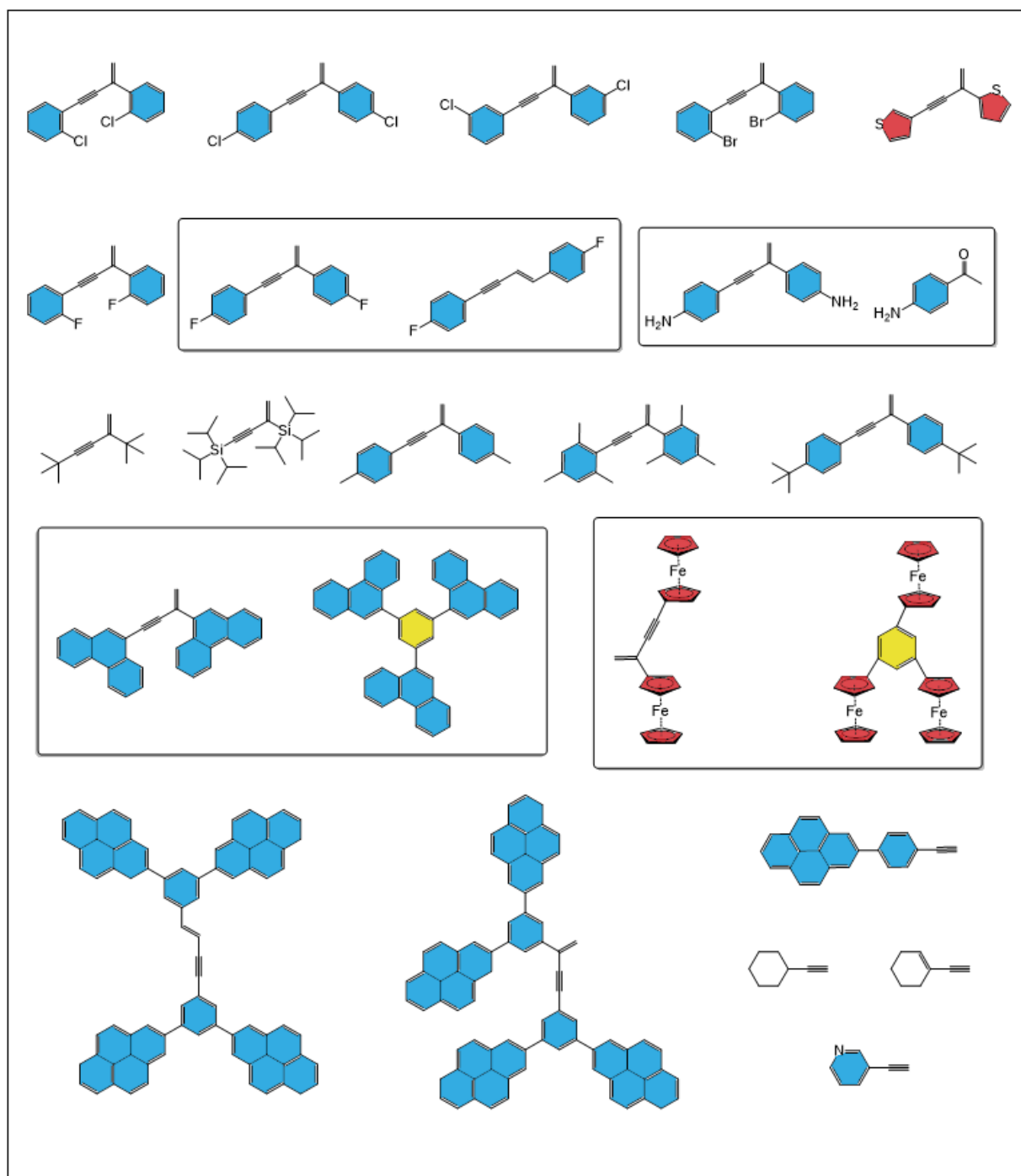
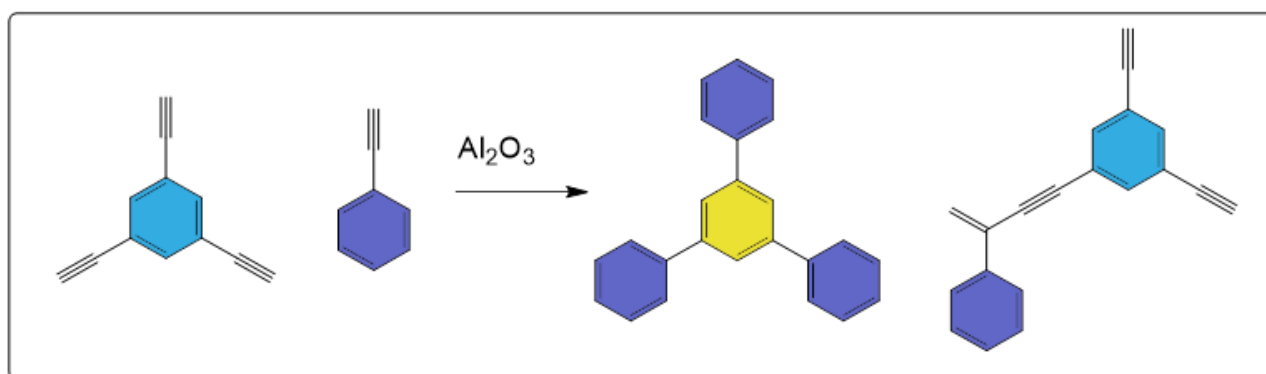


Figure 3.25: Scope of dimerization products on alumina.

Next, the influence of substituents on the aromatic ring were researched (Figure 3.24). Chlorine was introduced in ortho-, meta- and para-position. Thereby only the tail-to-head dimers were isolated in increasing yield. Afterwards fluorine in ortho and para position were investigated and an increased yield with fluorine in para-position. Brom in ortho position, yielded a higher amount compared to the other tested halogen compound. The introduction of Amino-group in para-position yielded the head to tail dimer and unexpectedly the ketone 1-(4-aminophenyl)ethan-1-one. Compounds with aliphatic groups were investigated next. Phenyl acetylene with methyl-, and tert-butyl-group in para position, yielded the head-to-tail dimer. The same happened with three methyl-groups in ortho and para-position. Compounds without aromatic rings were also detected to form head to tail dimers on alumina (3,3-dimethylbut-1-yne, ethynyltriisopropylsilane). 3-Ethynylthiophene was determined to also form the head-to-tail dimer only. On the other hand, 9-ethynylphenanthrene didn't just stop the reaction at the head-to-tail dimer but also formed its trimer. Traces of head-to-tail dimer and E-head to head dimer of 7,7'-(5-ethynyl-1,3-phenylene)bis(1,5a1-dihydropyrene) were detected by $^1\text{H-NMR}$. Ferrocene acetylene surprisingly also formed its trimer, next to the head-to-tail dimer. No products were found for 3-ethynylpyridine, 1-ethynylcyclohex-1-ene, ethynylcyclohexane and 2-(4-ethynylphenyl)pyrene on alumina. One reason for this might be the low boiling point for the non-aromatic compounds and therefore possible products were evaporated in the isolation process. Overall, a clear trend to head-to-tail dimers is clear but further reactions to the trimer proved difficult. This shows the impressive opportunity of doped aluminas, which determine selectivity in the reaction to also form head-to-head dimers, again.



Scheme 18: Hetero-dimerization on alumina.

A mixture of two different dimers was tried with 1 equivalent of 1,3,5-triethynylbenzene and three equivalent phenyl acetylene. But only the trimer of the latter and a simple dimer with the former were synthesized (Scheme 18). Further reaction of the dimer, which still has two terminal triple bonds, with phenylacetylene were unsuccessful.

3.8. Hydrochlorination of terminal Alkynes on Al_2O_3

The hydrochlorination of acetylene compounds were investigated among other things with zinc surfaces¹¹¹, Fe(0) particles¹¹² or copper salt impregnated borosilicate surfaces.¹¹³ Copper chlorides are for example important for surface-catalyzed chlorination reactions. In the Deacon reaction¹¹⁴, HCl is oxidized with oxygen in the presence of copper salts to chlorine, which reacts with acetylene at temperatures above 450 °C to yield tetrachloroethylene.^{113,115} As the chlorination of acetylenes is of great significance in industry and as sink for Cl and/or acetylene in the atmosphere¹¹⁶, alumina was tested as well.

Activated $\gamma\text{-Al}_2\text{O}_3$ was combined with the acetylene compounds in dry toluene at room temperature. Under Argon atmosphere, dry HCl-gas was led into the suspension. After extraction with toluene, the combined toluene fractions were reduced *in vacuo* and analysed by $^1\text{H-NMR}$.

Hydrochlorination of pure acetylene-gas was tried, in which acetylene gas was prepared by calcium carbide and water and purified in H_2SO_4 and CuSO_4 -solution. $^1\text{H-NMR}$ spectroscopy was used to determine the products as well as yields. Chlorinated acetylene species could not be identified by $^1\text{H-NMR}$ spectrometry. Even with d_6 -benzene as solvent instead of toluene, which circumvented the need of solvent removal *in vacuo* and therefore minimalizes loss of easily volatile products, reactions were unsuccessful according to $^1\text{H-NMR}$.

Therefore, only aromatic systems were successfully experimented on. Hydrochlorination of phenylacetylene at room temperature yielded tail-, E- and Z-substituted chlorovinyl benzene with ratio of 30/49/21 (Figure 3.25).

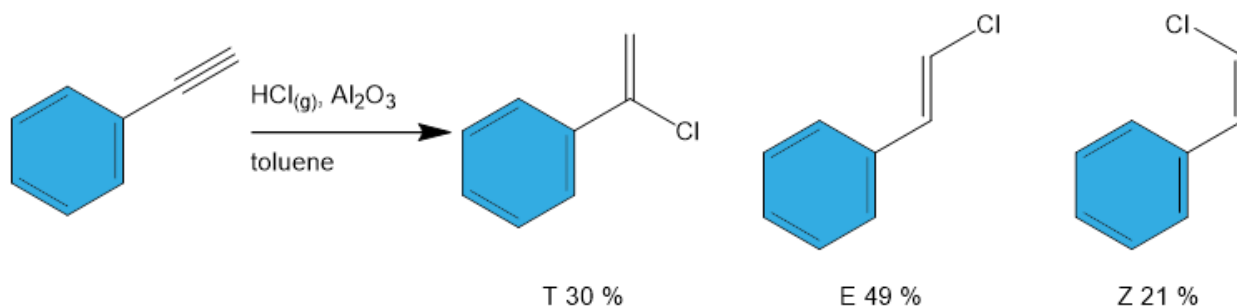


Figure 3.26: Hydrochlorination of phenyl acetylene on alumina at room temperature.

Fluoro-, chloro-, and bromo-substituted phenyl acetylene were investigated next. Here the ortho-fluorophenyl acetylene yielded Tail-, E-, and Z-products with ratio of 54/34/12 according to NMR (Figure 3.26). Here the influence of fluoro-substituent favored the formation of the tail-product, because of -I-effect of fluorine and therefore activation of the carbon near the aromatic ring.

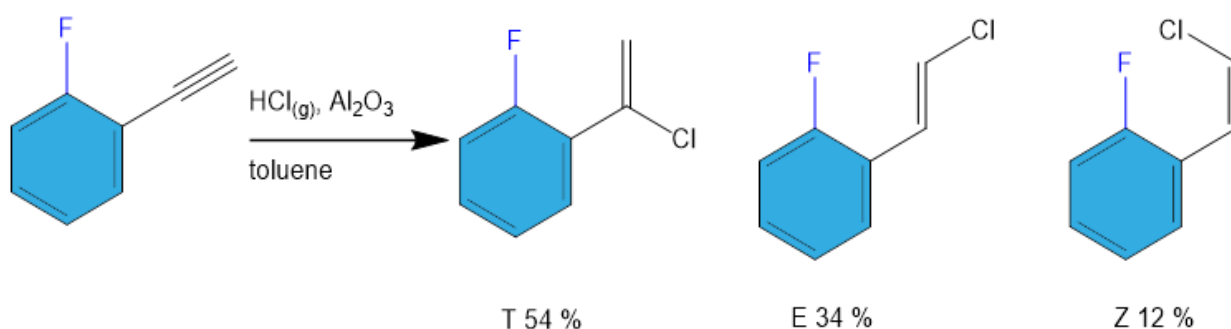


Figure 3.27: Hydrochlorination of 1-ethynyl-2-fluorobenzene on alumina.

1-Chloro-2-ethynylbenzene yielded only the Tail- and Z-Product with ratio of 17/83 as the lower electronegativity and bigger size of chlorine favors the formation of the Z-Isomer (Figure 3. 27).

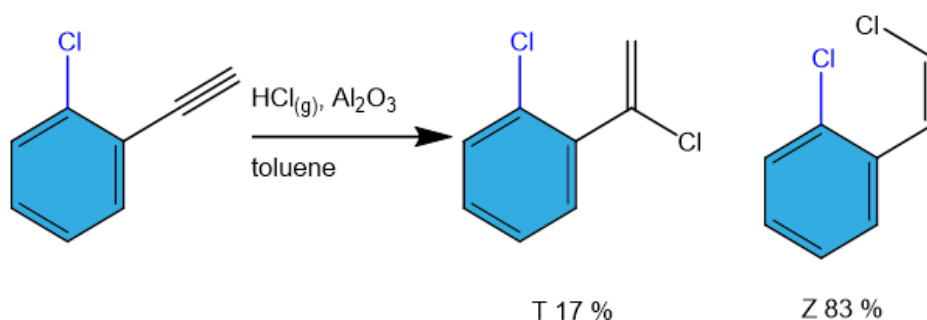


Figure 3.28: Hydrochlorination of 1-chloro-2-ethynylbenzene on alumina.

Bromo-substituted phenyl acetylene in para position favored the formation of the Z-Isomer, especially compared to phenylacetylene. The reaction yielded tail-, E- and Z-Isomers with ratio of 15/26/59 (Figure 3.28).

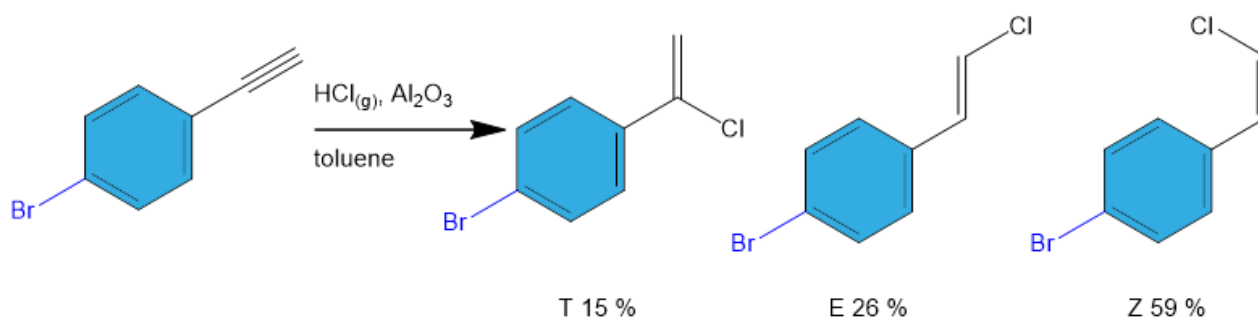


Figure 3.29: Hydrochlorination of 1-ethynyl-4-bromobenzene on alumina.

At last, the influence of aliphatic substituent in form of *tert*-butyl in para position was researched. The hydrochlorination of 4-(*tert*-butyl) phenylacetylene at room temperature yielded tail-, E- and Z-isomers with ratio of 44/19/37 (Figure 3.29). The +I-effect of the *tert*-butyl-group would suggest a decreasing formation of the tail-Isomer, which wasn't the case.

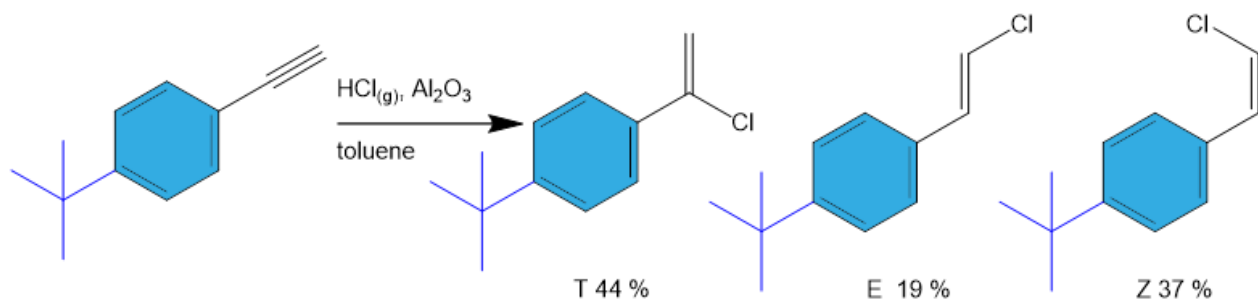


Figure 3.30: Hydrochlorination of 1-(*tert*-butyl)-4-ethynylbenzene on alumina.

We found the hydrochlorination of aromatic acetylenes on alumina already being successful at room temperature, which is a very promising result and can inspire future investigation into this topic.

4. Summary

The main objectives of this thesis were the development of alumina-mediated C-F activation to enable the facile synthesis of non-alternant PAHs and screening of other functional groups in relation to alumina-mediated reactions. Furthermore, the behavior of terminal acetylenes on different metal oxides were researched. Lastly the π -Lewis acidity of different alumina's terminations were investigated. The following summary briefly describes our achievements and observations made during the thesis.

First of all, the facile synthesis of heptagon-containing PAHs was achieved in quantitative yield. Further a scope of different molecules containing seven and eight member rings were synthesized, but deactivation effects of two fluor on one ring in meta position and oxodefluorination of fluoroarenes hindered progress on this front. First steps in the synthesis of bridged hexabenzocoronene derivatives via oxodefluorination were done and fluorene was investigated as a model compound for the study of the synthesis of zig-zag periphery on alumina. Reaction of fluorine with a methyl group via intramolecular C-H insertion proved the best method of construction. Therefore we investigated extended systems with longer zig-zag periphery and synthesized di[4]helicene derivatives with varying bridge length to enable investigation of surface behavior in later studies.

Next, different functional groups were investigated in view of alumina mediated reactions. Halogens other than fluorine, proved inactive on alumina. Boronic acids turned out to be great leaving groups and carbonyl groups proved unstable on alumina. Nevertheless, products with carbonyl groups could be isolated, such as the product of AmCFA of double fluorinated methylbiphenyl or even anthracene.

The behavior of terminal acetylenes on different metal oxides were investigated. First biphenyl acetylene was reacted in a 5-exo-attack to 9-methylenefluorene and 6-endo-attack to phenanthrene under different temperatures. Particular mention should be made of the high reactivity of Ga₂O and In₂O₃, as well as the doped alumina Zr20 and Si30, which resulted in formation of phenanthrene and 9-methylenefluorene at 90 °C respectively. As this indicates a different Lewis acidity depending on the forming product, the π -Lewis acidity of different alumina's terminations were investigated on a model compound. Afterwards aromatic terminal acetylenes without an aromatic ring in

ortho position underwent dimerization. The model molecule phenylacetylene even underwent trimerization. A bigger scope of similar materials was done to investigate the influence of different substituents. Special mention should be made for the introduction of an amino-group in para-position, which yielded the ketone 1-(4-aminophenyl)ethan-1-one next to the dimer.

Lastly, hydrochlorination of phenylacetylene at room temperature yielded tail-, E- and Z-substituted chlorovinyl benzene. Different substitutions on the phenyl ring resulted in changing the ratios of these three products.

5. Zusammenfassung

Die Hauptziele dieser Dissertation waren die Entwicklung einer Aluminiumoxid-vermittelten C-F-Aktivierung, um die einfache Synthese von nicht-alternierende polycyclische, aromatische Kohlenwasserstoffe zu ermöglichen, und das Screening anderer funktioneller Gruppen in Bezug auf Aluminiumoxid-vermittelten Reaktionen. Weiterhin wurde das Verhalten von endständigen Acetylenen auf verschiedenen Metalloxiden untersucht. Schließlich wurde die π -Lewis-Azidität verschiedener Aluminiumoxid-Oberflächen untersucht. Die folgende Zusammenfassung beschreibt kurz unsere Leistungen und Beobachtungen, die während der Dissertation gemacht wurden.

Zunächst gelang die einfache Synthese von Heptagon-haltigen polycyclische, aromatische Kohlenwasserstoffe in quantitativer Ausbeute. Darüber hinaus wurde eine Reihe verschiedener Moleküle mit sieben- und achtegliedrigen Ringen synthetisiert, aber die Deaktivierungseffekte von zwei Fluoratomen an einem Ring in meta-Position und die Oxodefleurierung von Fluorarenen behinderten den Fortschritt an dieser Front. Erste Schritte in der Synthese von verbrückten Hexabenzocoronon-Derivaten durch Oxodefleurierung wurden unternommen und Fluoren wurde als Modellverbindung für die Untersuchung der Synthesen von Zick-Zack-Peripherie auf Aluminiumoxid untersucht. Die Reaktion von Fluor mit einer Methylgruppe über eine intramolekulare CH-Insertion erwies sich als die beste Konstruktionsmethode. Daher untersuchten wir ausgedehnte Systeme mit längerer Zickzack-Peripherie und synthetisierten Di[4]helicen-Derivate mit unterschiedlicher Brückenlänge, um das Oberflächenverhalten in späteren Studien untersuchen zu können.

Als nächstes wurden verschiedene funktionelle Gruppen im Hinblick auf Aluminiumoxid-vermittelte Reaktionen untersucht. Andere Halogene als Fluor erwiesen sich gegenüber Aluminiumoxid als inaktiv. Boronsäuren erwiesen sich als hervorragende Abgangsgruppen, und Carbonylgruppen erwiesen sich auf Aluminiumoxid als instabil. Trotzdem konnten Produkte mit Carbonylgruppen isoliert werden, wie das Produkt von AmCFA aus doppelt fluoriertem Methylbiphenyl oder sogar Anthracen.

Das Verhalten von endständigen Acetylenen auf verschiedenen Metalloxiden wurde untersucht. Zunächst wurde Biphenylacetylen in einem 5-exo-Angriff zu 9-Methylenfluoren und einem 6-endo-Angriff zu Phenanthren bei unterschiedlichen Temperaturen umgesetzt. Besonders hervorzuheben ist die hohe Reaktivität von Ga₂O und In₂O₃

sowie des dotierten Aluminiumoxids Zr₂₀ und Si₃₀, die bei 90 °C zur Bildung von Phenanthren bzw. 9-Methylenfluoren führten. Da dies je nach entstehendem Produkt auf eine unterschiedliche Lewis-Azidität hindeutet, wurde die π -Lewis-Azidität verschiedener Aluminiumoxid-Terminierungen an einer Modellverbindung untersucht.

Anschließend wurden aromatische endständige Acetylene ohne aromatischen Ring in ortho-Position dimerisiert. Das Modellmolekül Phenylacetylen wurde sogar trimerisiert. Ein größerer Umfang ähnlicher Materialien wurde durchgeführt, um den Einfluss verschiedener Substituenten zu untersuchen. Besonders hervorzuheben ist die Einführung einer Aminogruppe in para-Position, die neben dem Dimer das Keton 1-(4-Aminophenyl)ethan-1-on ergab.

Schließlich ergab die Hydrochlorierung von Phenylacetylen bei Raumtemperatur Schwanz-, E- und Z-substituiertes Chlorvinylbenzol. Unterschiedliche Substitutionen am Phenylring führten zu veränderten Verhältnissen dieser drei Produkte.

6. Experimental part

6.1. Instruments and Materials Data

All chemicals and solvents were purchased in reagent grade from commercial suppliers (Acros®, Sigma-Aldrich® or Fluka®, Fluorochem®, Merck®, chemPur®) and used as received, unless otherwise specified. Solvents in HPLC grade were purchased from VWR® and Sigma-Aldrich®. γ -Al₂O₃ (neutral, 50–200 mm) was purchased from Acros®.

Microwave-assisted reactions were performed using Discover SP Microwave Synthesizer, CEM. **NMR spectra** were recorded on a Bruker Avance 400 operating at 400 MHz (¹H NMR), 100 MHz (¹³C NMR) and 377 MHz (¹⁹F NMR) at room temperature. The signals were referenced to residual solvent peaks (in parts per million (ppm) ¹H: CDCl₃, 7.26 ppm; CD₂Cl₂, 5.32 ppm; ¹³C: CDCl₃, 77.0 ppm, CD₂Cl₂, 53.8 ppm). Coupling constants were assigned as observed. The obtained spectra were evaluated with the program MestReNova. **LDI-MS spectra** were recorded on a Shimadzu Biotech AXIMA Confidence MALDI–TOF instrument. **Flash column chromatography** was performed on a Interchim PuriFlash 430 using flash grade silica gel from (Machery-Nagel 60 M (40–63 μ m, deactivated)). **Analytical HPLC measurements** were performed on a Shimadzu Prominence Liquid Chromatograph LC-20AT with communication bus module CBM-20A, diode array detector SPD-M20A, and column oven CTO-20AC. **Preparative HPLC** was performed on a Shimadzu Prominence Liquid Chromatograph LC-20AT with communication bus module CBM-20A, diode array detector SPD-M20A, degassing unit DGU-20A 5R, column oven CTO-20A, auto sampler SIL-20A HT and fraction collector FRC-10A. For analysis a Cosmosil PBr column (4.6ID x 250 mm) from Nacalai Tesque and for separation a Cosmosil PBr column (10ID x 250 mm) was used. The data obtained 67 (HPLC chromatograms and UV/vis spectra) were evaluated with the programs Shimadzu LCsolution and Shimadzu LabSolutions, respectively. **TLC analyses** were carried out with TLC sheets coated with silica gel with fluorescent indicator 254 nm from Machery-Nagel (ALUGRAM® SIL G/UV254) and visualized via UV-light of 254 nm or 366 nm. **Photochemical reactions**

were carried out in a photochemical reactor from Photochemical Reactors LTD. with a 400 W Mercury lamp under cooling with water. **X-RAY** High resolution APPI MS spectra were recorded on a Bruker ESI TOF maXis4G instrument. The data was evaluated with the program Bruker Compass DataAnalysis 4.2.

6.2. Folding of Fluorinated Oligoarylenes into Non-alternant PAHs with Various Topological Shapes

General procedure 1 – Suzuki cross-coupling reaction

A single-neck round-bottom flask equipped with a magnetic stirring bar was charged with aryl halide (1 equiv.), boronic acid (1.1 or 2.2 equiv.), K_3PO_4/Cs_2CO_3 (2 or 4 equiv.) and a mixture of THF/ H_2O 5:1. The mixture was degassed under dynamic vacuum (2x3 min.). Under a nitrogen atmosphere the catalyst $Pd(PPh_3)_4/Pd(PPh_3)_2Cl_2$ (0.02 equiv.) was added and the suspension degassed once again for 2 minutes under stirring. Under nitrogen atmosphere the reaction mixture was stirred under reflux for 16–48 h overnight. After cooling to rt water was added, phases were separated and the aqueous layer extracted with DCM. The combined organic fractions were dried over Na_2SO_4 , filtrated and the solvent removed *in vacuo*. The crude product was purified by flash column chromatography on silica gel to afford the desired product.

General procedure 2a – Wittig reaction with potassium *tert*-butoxide

A single-neck round-bottom flask equipped with a magnetic stirring bar was charged with aldehyde (1 equiv.), triphenyl phosphonium bromide (1.1 equiv.), potassium *tert*-butoxide (1.1 equiv.) and ethanol or iso-propanol. The mixture was degassed under dynamic vacuum (2 x 3 min). Under nitrogen atmosphere the reaction mixture was stirred under reflux for 16–24 h overnight. After cooling to room temperature water was added, phases were separated, and the aqueous layer extracted with CH_2Cl_2 . The combined organic fractions were dried over Na_2SO_4 , filtrated and the solvent removed *in vacuo*. The product was purified by flash column chromatography on silica gel to afford the desired Wittig product.

General procedure 2b – Wittig reaction with potassium hydroxide

A single-neck round-bottom flask equipped with a magnetic stirring bar was charged with aldehyde (1 equiv.), triphenylphosphonium bromide (1.1-1.5 equiv.) and chloroform. After degassing under dynamic vacuum (2 x 3 min) the mixture was stirred at room temperature under nitrogen atmosphere and an aqueous solution of KOH (50 %) was added dropwise. The mixture was heated to 80 °C and stirred for 18–24 h. After cooling to room temperature, water was added, phases were separated, and the aqueous layer extracted with CH₂Cl₂. The combined organic fractions were dried over Na₂SO₄, filtered and the solvent removed *in vacuo*. The product was purified by flash column chromatography on silica gel to afford the desired Wittig product.

General procedure 3 – Photocyclization

A 1 L photochemical reactor with a magnetic stirring bar was charged with stilbene derivative (1 equiv.) and dissolved in cyclohexane (800 mL). I₂ (1.1–1.3 equiv.) and propylene oxide (10 equiv.) were added and the reaction stirred for the indicated time under UV irradiation. The reaction progress was monitored by HPLC measurements and after completion of the reaction, cyclohexane was concentrated to 50 mL *in vacuo* and washed with a sat. aqueous solution of Na₂S₂O₅. Purification by flash column chromatography afforded the photocyclization product.

General Procedure 4-activated alumina mediated reaction

A glass tube was charged with 2-5 g of γ -Al₂O₃ (neutral, 50-200 micron) and preactivated at 450 °C for 3-4 hours. Then it was connected to a Schlenk line and heated at 500 °C under vacuum (10⁻³ mbar) for another 18 hours. The vessel was cooled down to r.t. and starting material was added under argon atmosphere. The tube containing the obtained mixture was sealed under vacuum and heated at 40-220 °C for 2-96 h (Figure 6.1). After cooling to room temperature, products were extracted with toluene and methanol or dichloromethane. Separation and final purification of the products were carried out by flash chromatography or HPLC of the respective extract.



Figure 6.1: Different dry reactions on alumina under vacuum by melting the glass-ampule.

General procedure 5- activated metal oxide mediated reaction

The oxide was activated by annealing at 400 °C for 4 h in air. Afterwards, it was activated by annealing at 400 °C under vacuum (10-2 mbar) for 18 h. After cooling to room temperature an ampule was filled with the compound and the previously activated oxide (5 g). The ampule was put under vacuum and sealed by melting the glass ampule. After reacting for 24 h at 90°C- 200 °C the ampule was opened and products extracted with toluol (100 mL) and methanol (100 mL) or dichloromethane. After removing the solvent *in vacuo* the residue was examined by ¹H-NMR spectroscopy.

General Procedure 6

An ampule was filled with 2-ethynyl-1,1'-biphenyl and the oxide (10 g). The ampule was put under vacuum and sealed by melting the glass ampule. After reacting for 18 h at 90 °C the ampule was opened and products extracted with toluol (100 mL) and methanol (100 mL).

General Procedure 7

The oxide was activated by annealing at 400 °C for 4 h in air. Afterwards, it was activated by annealing at 400 °C under vacuum (10-2 mbar) for 16 h. After cooling to room temperature an ampule was filled with 2-ethynyl-1,1'-biphenyl and the previously activated oxide (10 g). The ampule was put under vacuum and sealed by melting the

glass ampule. After reacting for 18 h at 90°C, 200°C or 400°C the ampule was opened and products extracted with toluol (100 mL) and methanol (100 mL).

General procedure 8- Al₂O₃-Mediated dimerization in Microwave

γ -Al₂O₃ was activated by annealing at 400 °C for 4 h in air. Afterwards, it was activated by annealing at 400 °C under vacuum (10-2 mbar) for 16 h. After cooling to room temperature an ampule was filled with the compound (100 mg), the previously activated oxide (2 g) and toluene (4 mL). The ampule was closed and stirred for 2-48 h at different temperatures in the microwave. After washing with toluene, dichloromethane and methanol, solvent was evaporated via vacuo and the residue was analyzed by ¹H-NMR spectroscopy.

General Procedure 9- Al₂O₃ with induced defects -Mediated dimerization in dry conditions

Aluminum oxide doped with different metals, was activated by annealing at 400 °C for 6 h in air. Afterwards, it was heated at 400 °C under vacuum (10-2 mbar) for 16 h. After cooling to room temperature, phenylacetylene was added under argon atmosphere. The tube containing the obtained mixture was sealed under vacuum and heated at 90 °C for 1 d. After cooling to room temperature, products were extracted with dichloromethane. Yields were determined by ¹H-NMR analysis.

General procedure 10

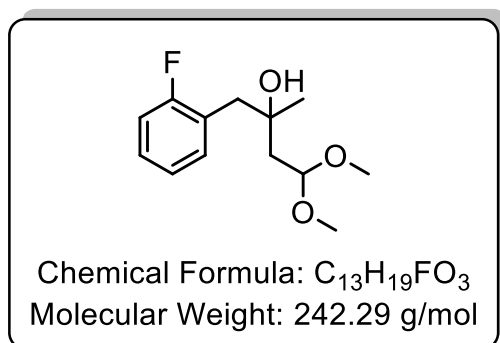
Aluminum oxide was activated by annealing at 400 °C for 6 h in air. Afterwards, it was heated at 400 °C under vacuum (10-2 mbar) for 16 h. After cooling to room temperature, the oxide (2g) and phenylacetylene-derivate (70 mg) was added to a two-neck flask under argon atmosphere. 12 mL dry toluene was added as a solvent and the reaction was started by flowing HCl-gas into the solution. The HCl-gas was prepared by adding HCl (3 mL) slowly to CaCl₂ and after heating with heatgun, transferred it through a plug of CaCl₂. No additional argon was necessary to transfer the gas into the solution. The addition of argon was counterproductive after starting the reaction. After 1h, the oxide was washed with toluene and methanol. The combined toluene fractions were reduced in vacuo and analysed by ¹H-NMR.

General Procedure 11

5 μ L 7-(phenylethynyl)cyclohepta-1,3,5-triene (**SM**) reacted in distilled hexane/dry toluene (0.25 mL/0.25 mL) on different activated alumina(50-70 mg) under inert conditions (Ar). The oxides were activated by annealing at 400 °C for 4 h in air. Afterwards, they were activated by annealing at 400 °C under vacuum (10-2 mbar) for 16 h. The mixture was diluted and filtered before injection into HPLC.

6.2.1. Synthesis of 1,16-dehydrohexahelicene

Synthesis of 1-(2-fluorophenyl)-4,4-dimethoxy-2-methylbutan-2-ol

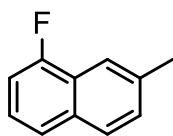


A flame-dried three-necked round-bottom flask was charged with magnesium (2.19 g, 89.9 mmol, 1.3 equiv.) which was activated with iodine (10 mg). After addition of Et₂O (10 mL) and 1 mL of 1-(chloromethyl)-2-fluorobenzene the reaction began and 7.22 mL of 1-(chloromethyl)-2-fluorobenzene (8.22 mL, 69.2 mmol, 1 equiv.)

in 25 mL Et₂O was added slowly. The mixture was stirred under reflux for 1 h and afterwards 4,4-dimethoxybutan-2-one (9.18 mL, 69.2 mmol, 1 equiv.) in Et₂O (25 mL) was added over period of 2 h. After cooling to 0 °C an aqueous solution of NH₄Cl (35 g) in H₂O (100 mL) was added and the product extracted with Et₂O (200 mL). The organic solution was dried over Na₂SO₄, filtrated and the solvent removed *in vacuo*. The product was obtained as orange oil (14.6 g, 87 %).

R_f = 0.46 (SiO₂, *n*-hexane/DCM 1:1). **¹H NMR** (400 MHz, chloroform-*d*) δ 7.37 – 7.27 (m, 1H), 7.27 – 7.15 (m, 1H), 7.13 – 6.96 (m, 2H), 4.77 – 4.64 (m, 1H), 3.36 (d, J = 10.8 Hz, 6H), 2.84 (s, 2H), 1.97 – 1.70 (m, 2H), 1.21 (s, 3H). **¹⁹F NMR** (377 MHz, chloroform-*d*) δ -116.40 (d, J = 8.3 Hz).

Synthesis of 1-fluoro-7-methylnaphthalene



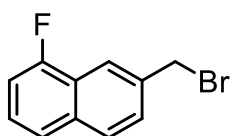
Chemical Formula: C₁₁H₉F
Molecular Weight: 160.19 g/mol

1-(2-fluorophenyl)-4,4-dimethoxy-2-methylbutan-2-ol (14.5 g, 59.9 mmol, 1 equiv.) was slowly added to a mixture of conc. H₂SO₄ (50 mL) and acetic acid (200 mL) at 100 °C. The reaction mixture was stirred for 20 min at 100 °C and 24 h at rt. The mixture was poured on ice and

the aqueous mixture extracted with hexanes (4 x 200 mL). The combined organic fractions were concentrated to 50 mL *in vacuo* by rotatory evaporation and the residue filtrated through silica (*n*-hexane). The product was obtained as colorless oil (5.17 g, 54 %).

R_f = 0.80 (SiO₂, hexanes) **¹H NMR** (400 MHz, CD₂Cl₂) δ 7.88 (s, 1H), 7.79 (dd, *J* = 8.4, 1.8 Hz, 1H), 7.61 (d, *J* = 8.3 Hz, 1H), 7.40 (dd, *J* = 8.5, 1.7 Hz, 1H), 7.35 (td, *J* = 8.0, 5.4 Hz, 1H), 7.17 – 7.10 (m, 1H), 2.55 (s, 3H). **¹⁹F NMR** (282 MHz, CD₂Cl₂) δ -123.10 – -125.88 (m, 1F). **¹³C NMR** (101 MHz, CD₂Cl₂) δ 158.8 (d, *J* = 250.1 Hz), 136.8, 133.7 (d, *J* = 5.0 Hz), 129.6, 127.8 (d, *J* = 3.1 Hz), 125.0 (d, *J* = 8.2 Hz), 124.2 (d, *J* = 16.1 Hz), 123.9 (d, *J* = 4.1 Hz), 119.5 (d, *J* = 5.0 Hz), 109.8 (d, *J* = 19.8 Hz), 22.0.

Synthesis of 7-(bromomethyl)-1-fluoronaphthalene



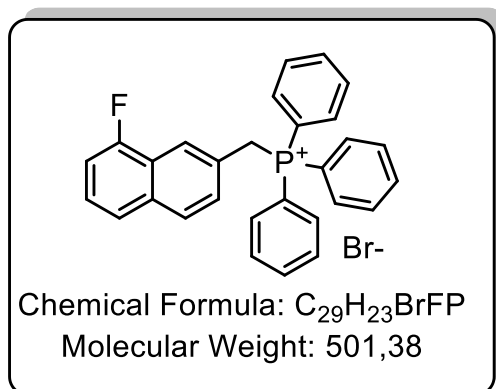
Chemical Formula: C₁₁H₈BrF
Molecular Weight: 239,09

1-Fluoro-7-methylnaphthalene (1.08 g, 6.76 mmol, 1 equiv.) and NBS (1.20 g, 6.76 mmol, 1 equiv.) were reacted with DBPO (44 mg, 0.135 mmol, 0.02 equiv.) in fluorobenzene (20 mL) under reflux for 4 h. The organic solution was washed with

water and brine and dried over Na₂SO₄. After filtration and evaporation of the solvent, the crude product was purified by flash column chromatography on silica gel (*n*-hexane) and isolated as yellow solid (1.33 g, 82 %).

¹H NMR (300 MHz, CD₂Cl₂) δ 8.09 (s, 1H), 7.89 (dd, *J* = 8.6, 1.6 Hz, 1H), 7.65 (d, *J* = 8.2 Hz, 1H), 7.58 (dd, *J* = 8.5, 1.8 Hz, 1H), 7.49 – 7.40 (m, 1H), 7.19 (ddd, *J* = 10.8, 7.7, 0.7 Hz, 1H), 4.71 (s, 2H). **¹⁹F NMR** (282 MHz, CD₂Cl₂) δ -123.20 – -123.30 (m, 1F). **¹³C NMR** (101 MHz, CD₂Cl₂) δ 159.3 (d, *J* = 251.6 Hz), 136.5, 135.0 (d, *J* = 4.3 Hz), 128.9 (d, *J* = 3.1 Hz), 128.4, 127.0 (d, *J* = 8.5 Hz), 124.1 (d, *J* = 3.9 Hz), 123.8 (d, *J* = 16.4 Hz), 120.8 (d, *J* = 5.0 Hz), 110.6 (d, *J* = 19.9 Hz), 34.2.

Synthesis of ((8-fluoronaphthalen-2-yl)methyl)triphenylphosphonium bromide

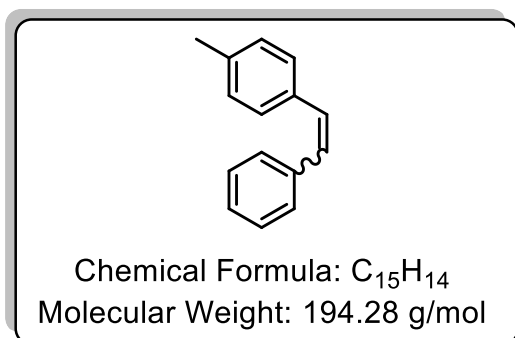


7-(Bromomethyl)-1-fluoronaphthalene (1.32 g, 5.52 mmol, 1 equiv.) and triphenylphosphine (2.17 g, 8.28 mmol, 1.5 equiv.) were reacted in toluene (20 mL) under reflux for 24 h. The resulting precipitate was collected by suction filtration, washed with toluene (50 mL) and dried *in vacuo*. ((8-Fluoronaphthalen-2-yl)methyl)triphenylphosphonium bromide was

obtained as white solid (2.01 g, 73 %).

¹H NMR (300 MHz, CD₂Cl₂) δ 7.90 – 7.70 (m, 10H), 7.70 – 7.55 (m, 9H), 7.49 – 7.35 (m, 2H), 7.10 (dd, *J* = 10.6, 7.7 Hz, 1H), 5.54 (d, *J* = 14.8 Hz, 1H). **¹⁹F NMR** (282 MHz, CD₂Cl₂) δ -123.40 (dd, *J* = 10.4, 5.3 Hz). **¹³C NMR** (101 MHz, CD₂Cl₂) δ 158.8 (d, *J* = 251.8 Hz), 135.7 (d, *J* = 2.8 Hz), 134.9 (d, *J* = 9.7 Hz), 130.6 (d, *J* = 12.6 Hz), 130.3 (d, *J* = 4.4 Hz), 128.9 (t, *J* = 2.5 Hz), 127.1 (d, *J* = 8.2 Hz), 126.1 (d, *J* = 8.3 Hz), 124.03, 123.7 (d, *J* = 6.7 Hz), 123.6 (d, *J* = 5.7 Hz), 123.5, 118.1 (d, *J* = 85.9 Hz), 110.5 (d, *J* = 19.9 Hz), 31.6 (d, *J* = 47.3 Hz).

Synthesis of 1-methyl-4-styrylbenzene

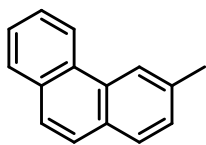


An aqueous solution of KOH (50 %, 40 mL) was added dropwise to a solution of 4-methylbenzaldehyde (1.03 mL, 8.74 mmol, 1 equiv.) and benzyltriphenylphosphonium bromide (4.17 g, 9.61 mmol, 1.1 equiv.) in CHCl₃ (80 mL) and. The mixture was heated to 65 °C and stirred for 1h. After cooling to rt, it was washed with water

and brine, dried over Na₂SO₄. After filtration and evaporation of the solvent, the crude product was purified by flash column chromatography on silica gel (*n*-hexane:DCM 9:1,) and pure 1-methyl-4-styrylbenzene isolated as white solid (1.32 g, 79 %).

R_f = 0.71, 0.55 (SiO₂, *n*-hexane:DCM 10:1). **¹H NMR** (400 MHz, chloroform-*d*) δ 7.70 – 7.46 (m, 1H), 7.42 (d, *J* = 8.1 Hz, 1H), 7.36 (dd, *J* = 8.4, 6.8 Hz, 1H), 7.23 – 7.11 (m, 6H), 7.08 (d, *J* = 2.5 Hz, 1H), 7.03 (d, *J* = 7.8 Hz, 2H), 6.56 (s, 2H), 2.37 (s, 2H), 2.32 (s, 3H).

Synthesis of 3-methylphenanthrene



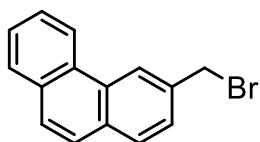
Chemical Formula: C₁₅H₁₂
Molecular Weight: 192.26 g/mol

1-Methyl-4-styrylbenzene (1.10 g, 5.66 mmol, 1 equiv.), iodine (1.44 g, 5.66 mmol, 1 equiv.) and propylene oxide (3.98 mL, 56.6 mmol, 10 equiv.) were reacted in cyclohexane (1 L) for 7 h according to general procedure 3. The product was purified by flash column chromatography

on silica gel (*n*-hexane) and isolated as white solid (1.06 g, 98 %).

$R_f = 0.67$ (SiO₂, *n*-hexane/DCM 5:1). ¹H NMR (400 MHz, chloroform-*d*) δ 8.67 (s, 1H), 8.48 (s, 1H), 7.86 (s, 1H), 7.78 (s, 1H), 7.74 – 7.48 (m, 4H), 7.43 (d, *J* = 7.3 Hz, 1H), 2.62 (s, 3H).

Synthesis of 3-(bromomethyl)phenanthrene



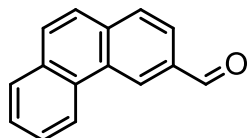
Chemical Formula: C₁₅H₁₁Br
Molecular Weight: 271.16 g/mol

3-Methylphenanthrene (1.00 g, 5.20 mmol, 1 equiv.) and NBS (1.02 g, 5.72 mmol, 1.1 equiv.) were reacted with DBPO (25.2 mg, 0.104 mmol, 0.02 equiv.) in carbon tetrachloride (50 mL) for 5 h under reflux. After cooling to rt, the mixture was washed with water and dried over Na₂SO₄. After

filtration and evaporation of the solvent, the crude product was purified by flash column chromatography on silica gel (*n*-hexane) and isolated as white solid (477 mg, 67 %).

$R_f = 0.33$ (SiO₂, hexanes/DCM 10:1). ¹H NMR (400 MHz, chloroform-*d*) δ 8.76 – 8.63 (m, 2H), 8.04 – 7.82 (m, 2H), 7.82 – 7.56 (m, 5H), 4.78 (s, 2H).

Synthesis of phenanthrene-3-carbaldehyde



Chemical Formula: C₁₅H₁₀O
Molecular Weight: 206.24 g/mol

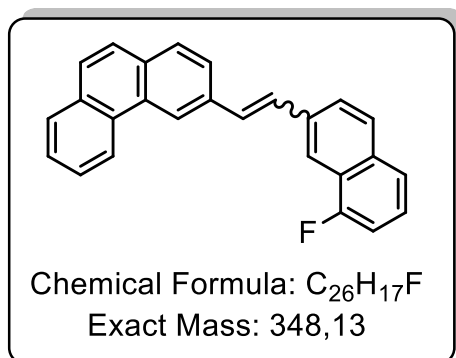
A solution of 3-(bromomethyl)phenanthrene (477 mg, 1.76 mmol, 1 equiv.) and (1R,3s,5s)-1,3,5,7-tetraazaadamantane (370 mg, 2.64 mmol, 1.5 equiv.) in chloroform (20 mL) was stirred under reflux for 3 h. After cooling to rt, the solvent was removed *in vacuo* and a mixture of AcOH and H₂O

(15 mL, 1:1) was added and stirred under reflux for 1 h. After cooling to rt the mixture was stirred for 16 h and afterwards washed with an aqueous solution of NaHCO₃ and

water. The organic phase was dried over Na₂SO₄, filtered and solvent removed *in vacuo*. After purification via flash column chromatography on silica gel (*n*-hexane/EtOAc 9:1), the product was isolated as yellow solid (0.190 g, 52 %).

R_f = 0.35 (SiO₂, hexanes/EtOAc 5:1). **¹H NMR** (400 MHz, chloroform-*d*) δ 10.28 (d, *J* = 0.5 Hz, 1H), 9.20 (s, 1H), 8.80 (d, *J* = 8.2, 1.3, 0.6 Hz, 1H), 8.09 (dd, *J* = 8.2, 1.5 Hz, 1H), 8.02 (dd, *J* = 8.2, 0.6 Hz, 1H), 7.99 – 7.88 (m, 2H), 7.85 – 7.72 (m, 2H), 7.72 – 7.63 (m, 1H). **¹³C NMR** (100 MHz, chloroform-*d*) δ 192.49, 136.15, 134.36, 132.31, 130.60, 130.48, 130.22, 129.63, 129.00, 127.62, 127.52, 127.32, 126.49, 125.24, 122.82.

Synthesis of 3-(2-(8-fluoronaphthalen-2-yl)vinyl)phenanthrene

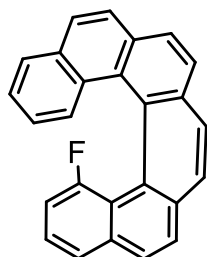


To solution of phenanthrene-3-carbaldehyde (100 mg, 0.485 mmol, 1 equiv.) and [(8-fluoro-2-naphthalenyl)methyl]triphenylphosphonium bromide (267 mg, 0.533 mmol, 1.1 equiv.) in CHCl₃ (4 mL) aqueous solution of KOH (50 %, 1.6 mL) was added dropwise under inert atmosphere. The mixture was heated to 80 °C and stirred 18 h. After the end of

the reaction mixture was cooled to room temperature, water was added, phases were separated and the aqueous layer was extracted with DCM. The combine organic frictions were dried over Na₂SO₄, and the solvent was evaporated under reduced pressure. The residue was purified by flash column chromatography on silica gel (*n*-hexane→*n*-hexane:DCM 9:1) yielding 3-(2-(8-fluoronaphthalen-2-yl)vinyl)phenanthrene as white solid (130 mg, 77 %).

¹H NMR (400 MHz, CDCl₃) δ 8.63 (s, 1H), 8.37 (d, *J* = 7.9 Hz, 1H), 8.09 (s, 1H), 7.89 – 7.83 (m, 1H), 7.75 – 7.66 (m, 3H), 7.63 – 7.43 (m, 6H), 7.36 (td, *J* = 8.0, 5.4 Hz, 1H), 7.11 (dd, *J* = 10.7, 7.7 Hz, 1H), 7.03 – 6.89 (m, 2H). **¹⁹F NMR** (377 MHz, CDCl₃) δ -123.15 (m, 1F)

Synthesis of 12-fluorohexahelicene



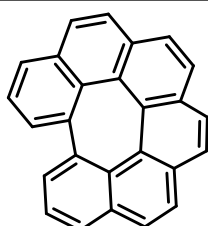
Chemical Formula: $C_{26}H_{15}F$
Exact Mass: 346,12

Solution of 3-(2-(8-fluoronaphthalen-2-yl)vinyl)phenanthrene (133 mg, 0.382 mmol) in 800 ml of cyclohexane was irradiated in the presence of I_2 (104 mg, 0.41 mmol) and methylpropyleneoxide (0.26 mL) for 3 h. After completion of reaction, cyclohexane was evaporated under reduced pressure, washed with $Na_2S_2O_3$ solution, dried over Na_2SO_4 . The residue

was purified by column chromatography (*n*-hexane) and HPLC (DCM/MeOH 1:1) yielding 12-fluorohexahelicene as yellow solid in 18 % (24 mg).

1H NMR (400 MHz, CD_2Cl_2) δ 8.15 (d, $J = 8.1$ Hz, 1H), 8.07 – 8.03 (m, 3H), 8.02 – 7.99 (m, 2H), 7.98 – 7.93 (m, 2H), 7.86 (dd, $J = 7.9, 1.0$ Hz, 1H), 7.75 (dd, $J = 7.9, 1.1$ Hz, 1H), 7.26 (td, $J = 7.8, 4.9$ Hz, 1H), 7.22 – 7.16 (m, 2H), 6.59 (ddd, $J = 8.4, 6.9, 1.4$ Hz, 1H), 6.40 (ddd, $J = 13.0, 7.8, 1.2$ Hz, 1H). **^{19}F NMR** (377 MHz, CD_2Cl_2) δ -101.95 (dd, $J = 13.0, 4.7$ Hz, 1F). **^{13}C NMR** (101 MHz, CD_2Cl_2) δ 159.2 (d, $J = 253.9$ Hz), 134.3 (d, $J = 4.2$ Hz), 132.8, 132.5, 132.2, 130.4 (d, $J = 1.7$ Hz), 130.0 (d, $J = 8.8$ Hz), 129.1 (d, $J = 7.6$ Hz), 128.2, 128.0, 127.89, 127.7 (d, $J = 1.0$ Hz), 127.6 (d, $J = 3.1$ Hz), 126.80, 126.76, 126.7, 126.6, 126.5, 126.4, 125.6, 124.2, 123.9 (d, $J = 3.2$ Hz), 123.5 (d, $J = 3.3$ Hz), 121.3 (d, 24 Hz), 111.68 (d, $J = 24.4$ Hz).

Synthesis of 1,16-dehydrohexahelicene



Chemical Formula: $C_{26}H_{14}$
Molecular Weight: 326,40

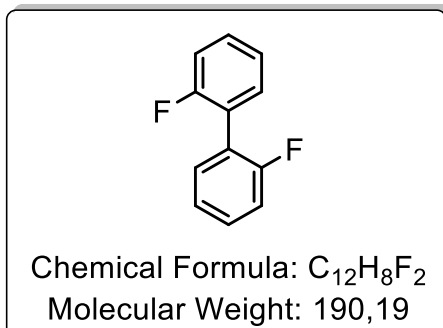
The compound was obtained according to the General Procedure 4 using 12-fluorohexahelicene (15 mg). Yield 14 mg (99 %)

1H NMR (400 MHz, CD_2Cl_2) δ 7.91 (d, $J = 8.3$ Hz, 2H), 7.86 (d, $J = 8.6$ Hz, 2H), 7.84 – 7.79 (m, 4H), 7.76 (d, $J = 8.6$ Hz, 1H), 7.68 – 7.61 (m, 2H), 7.24 (dd, $J = 7.3, 1.5$ Hz, 2H). **^{13}C NMR** (101 MHz,

CD_2Cl_2) δ 141.6, 136.3, 135.2, 133.7, 133.0, 132.3, 131.2, 130.9, 129.1, 128.7, 128.5, 128.0, 127.7, 126.7. **UV/Vis** (DCM, 293 K): λ [nm] 245, 260, 304, 323.

6.2.2. Synthesis of dibenzo[e,gh]dibenzo[4,5:6,7]plei- adeno[2,1,12-pqa]pleiadene

Synthesis of 2-fluoro-2'-fluoro-1,1'-biphenyl

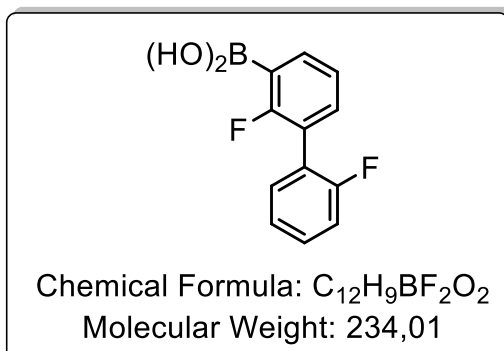


1-Fluoro-2-bromobenzene (2.00 g, 11.4 mmol, 1.25 mL, 1 equiv.), 2-fluorophenylboronic acid (1.76 g, 12.6 mmol, 1.1 equiv.) Cs₂CO₃ (7.45 g, 22.9 mmol, 2 equiv.) were reacted in THF/H₂O (60 mL, 5:1) with Pd(PPh₃)₂Cl₂ (160 mg, 0.228 mmol, 0.02 equiv.) for 18 h according to general procedure 1. The product was purified by flash

column chromatography on silica gel (*n*-hexane) and isolated as white solid (1.83 g, 84 %).

¹H NMR (400 MHz, chloroform-*d*) δ 7.37 – 7.24 (m, 4H), 7.18 – 7.12 (m, 2H), 7.13 – 7.06 (m, 2H). ¹⁹F NMR (377 MHz, chloroform-*d*) δ -114.85 (s).

Synthesis of (2,2'-difluoro-[1,1'-biphenyl]-3-yl)boronic acid

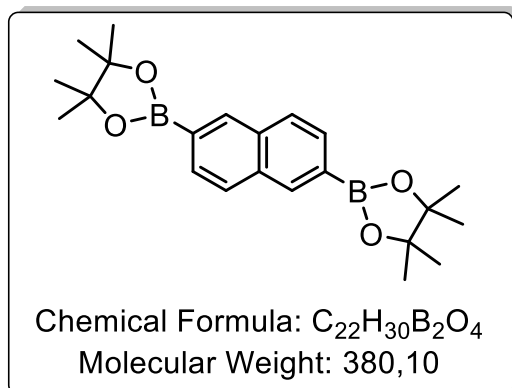


2,2,6,6-Tetramethylpiperidine (2.75 mL, 16.2 mmol, 1.6 equiv.) was added to THF (7 mL) at -78 °C. Afterwards *n*-butyllithium (2.5 M in hexane, 6.12 mL, 15.3 mmol, 1.5 equiv.) was added dropwise. After stirring for 30 min at 78 °C, a solution of 2-fluoro-2'-fluoro-1,1'-biphenyl (1.94 g, 10.2 mmol, 1 equiv.) in THF (12 mL)

was added dropwise and stirred for 30 min. Trimethyl borate (5.79 mL, 51.0 mmol, 5 equiv.) was added dropwise, the solution was allowed to warm to rt and stirred for 3 h. After quenching with HCl (1 M, 12 mL) and stirring for 30 min, the organic phase was separated. The aqueous phase was extracted with DCM (2 x 40 mL). The combined organic phases were dried over Na₂SO₄ and after filtrating, the solvent was removed *in vacuo*. The residue was dissolved in *n*-hexane and plugged through silica gel using a solvent gradient (*n*-hexane → *n*-hexane/DCM 1:1 → DCM → DCM/EtOAc 20:1 → DCM/EtOAc 10:1 → DCM/EtOAc 5:1 → DCM/EtOAc 1:1) and a yellow oil was yielded. After addition of hexanes (10 mL) the product precipitated from solution. The resulting

solid was collected by suction filtration and washed with hexanes (30 mL) to yield pure product (2,2'-difluoro-[1,1'-biphenyl]-3-yl)boronic acid as a brown solid (764 mg, 32 %). $R_f = 0.14$ (SiO₂, DCM/EtOAc 20:1).

Synthesis of 2,6-bis(4,4,5,5-tetramethyl-1,3,2-dioxaborolan-2-yl)naphthalene

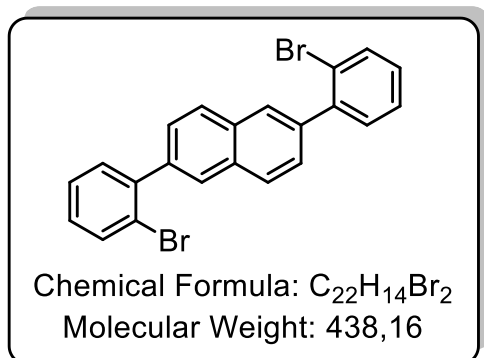


Under nitrogen atmosphere, 2,6-dibromonaphthalene (0.500 g, 1.75 mmol, 1 equiv.), bis(pinacolato)diboron (1.33 g, 5.25 mmol, 3 equiv.), potassium acetate (0.686 g, 6.99 mmol, 4 equiv.) were reacted in 1,4-dioxane (12 mL) with Pd(dppf)Cl₂ (8.4 mg, 11.4 μmol, 0.02 equiv.) under reflux for 20 h. After cooling to rt water was added, phases were separated

and the aqueous layer extracted with CH₂Cl₂ (3 x 50 mL). The combined organic fractions were dried over Na₂SO₄, filtered and the solvent removed *in vacuo*. The crude product was purified by flash column chromatography on silica gel (DCM/ *n*-hexane = 1:1). After washing the solid with methanol, the product **19** was yielded as a white solid (497 mg, 76 %).

$R_f = 0.60$ (SiO₂, *n*-hexane/DCM = 1:1). ¹H NMR (400 MHz, chloroform-*d*) δ 8.35 (s, 2H), 7.96 – 7.68 (m, 4H), 1.39 (s, 24H). ¹³C NMR (100 MHz, CDCl₃) δ 136.13, 134.47, 130.49, 127.83, 84.11, 25.09.

Synthesis of 2,6-bis(2-bromophenyl)naphthalene

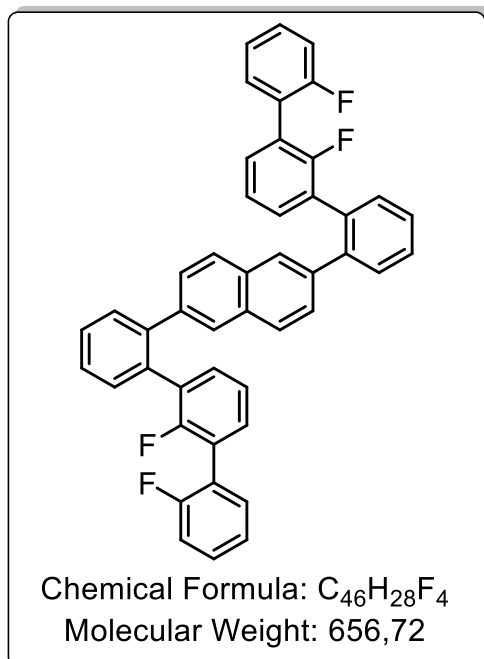


2,6-Bis(4,4,5,5-tetramethyl-1,3,2-dioxaborolan-2-yl)naphthalene (217 mg, 0.571 mmol, 1 equiv.), 1-bromo-2-iodobenzene (220 mL, 1.71 mmol, 3 equiv.), Cs₂CO₃ (744 mg, 2.28 mmol, 4 equiv.) were reacted in THF/H₂O (6 mL, 5:1) with Pd(PPh₃)₂Cl₂ (8.0 mg, 11.4 μmol, 0.02 equiv.) for 48 h according general procedure 1. The product

was purified by flash column chromatography on silica gel (*n*-hexane/DCM = 9:1) and isolated as white solid (175 mg, 70 %).

¹H NMR (400 MHz, CDCl₃) δ 7.84 (d, *J* = 8.4 Hz, 1H), 7.81 (d, *J* = 1.8 Hz, 1H), 7.62 (dd, *J* = 8.0, 0.9 Hz, 1H), 7.51 (dd, *J* = 8.3, 1.7 Hz, 1H), 7.335-7.28 (m, 2H), 7.19 – 7.11 (m, 1H). **¹³C NMR** (101 MHz, CDCl₃) δ 142.4, 139.1, 133.2, 132.2, 131.5, 128.9, 128.07, 128.04, 127.7, 127.5, 122.8.

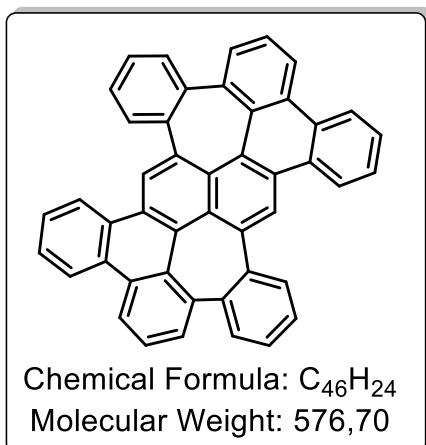
Synthesis of 2,6-bis(2',2''-difluoro-[1,1':3',1''-terphenyl]-2-yl)naphthalene



(2,2'-Difluoro-[1,1'-biphenyl]-3-yl)boronic acid (160 mg, 0.678 mmol, 4 equiv.) 2,6-bis(2-bromophenyl)naphthalene (75 mg, 0.172 mmol, 1 equiv.), K₃PO₄ (145 mg, 0.678 mmol, 4 equiv.) were reacted in THF/H₂O (6 mL, 5:1) with Pd(dppf)Cl₂ (2.4 mg, 3.4 μmol, 0.02 equiv.) for 20 h according to general procedure 1. The product was purified by flash column chromatography on silica gel (*n*-hexane/DCM = 9:1) and isolated as white solid (52.0 mg, 46 %).

¹H NMR (400 MHz, CD₂Cl₂) δ 7.66 (d, *J* = 1.7 Hz, 2H), 7.60 – 7.55 (m, 4H), 7.50 (dtd, *J* = 10.4, 7.5, 2.7 Hz, 6H), 7.32 (tt, *J* = 8.3, 2.6 Hz, 2H), 7.27 – 7.20 (m, 4H), 7.14 (dd, *J* = 7.0, 1.8 Hz, 2H), 7.09 (dd, *J* = 7.7, 3.5 Hz, 6H), 7.05 (t, *J* = 7.6 Hz, 2H). **¹⁹F NMR** (376 MHz, CD₂Cl₂) δ -115.32 – -115.58 (m, 2F), -117.18 (dt, *J* = 16.3, 6.8 Hz, 2F). **¹³C NMR** (101 MHz, CD₂Cl₂) δ 160.2 (d, *J* = 239 Hz), 142.0, 139.3, 134.9, 132.46 (d, *J* = 3.5 Hz), 132.4, 132.07 – 131.85 (m), 131.4 (d, *J* = 1.3 Hz), 131.0 (dd, *J* = 3.0, 1.4 Hz), 130.8, 130.2, 130.1, 128.8, 128.1, 127.7, 124.4 (d, *J* = 3.7 Hz), 124.04 – 123.93 (m), 116.0 (d, *J* = 22.3 Hz).

Synthesis of dibenzo[e,gh]dibenzo[4,5:6,7]pleiaden[2,1,12-pqa]pleiadene



The compound was obtained according to the General Procedure 4 at 200°C using 2,6-bis(2',2''-difluoro-[1,1';3',1''-terphenyl]-2-yl)naphthalene (40 mg). Yield 5 mg (15%).

1H NMR (400 MHz, $CDCl_3$) δ 8.64 – 8.58 (m, 2H), 8.56 (s, 2H), 8.45 – 8.35 (m, 4H), 7.64 (dd, $J = 7.3, 1.3$ Hz, 2H), 7.58 – 7.52 (m, 6H), 7.40 (ddd, $J = 11.9, 9.1, 5.4$ Hz, 4H), 7.24 (dd, $J = 7.4, 1.6$ Hz, 2H), 7.15 (dd, $J = 7.6, 1.5$ Hz, 2H).

^{13}C NMR was not recorded due to low solubility of dibenzo[e,gh]dibenzo[4,5:6,7]pleiaden[2,1,12-pqa]pleiadene. **UV/Vis** (DCM-MeOH, 1-1, 293 K): λ [nm] = 266, 298, 356.

Synchrotron X-ray diffraction data was collected at 100 K on beamline BL14.2 at the BESSY II electron storage ring (Berlin, Germany) using a hybrid pixel detector Pilatus3S 2M ($\lambda = 0.8266$ Å). All structures were solved and anisotropically refined using the SHELX package. Selected crystallographic data and CCDC deposition numbers are given in Table 5.⁷⁵

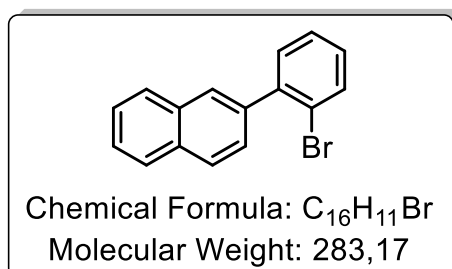
Compound	dibenzo[e,gh]dibenzo[4,5:6,7]pleiaden[2,1,12-pqa]pleiadene
Formula	$C_{46}H_{24} \cdot 0.58 CH_2Cl_2$
Mr	626.12
crystal system	monoclinic
space group	P21/c
a [Å]	12.746(1)
b [Å]	24.782(2)
c [Å]	9.402(1)
α [°]	90
β [°]	91.33(1)
γ [°]	90
V [Å ³]	2969.0(5)
Z	4
D _c [g cm ⁻³]	1.401
refls collected/R _{int}	28692/0.049
data / parameters	8121 / 470
R ₁ (I ≥ 2σ(I))	0.082/0.219

$\Delta\rho_{\max/\min}$ [$e \text{ \AA}^{-3}$]	0.59 / -0.51
CCDC	1970885

Table 5: Selected X-ray diffraction data of compound *dibenzo[e,gh]dibenzo[4,5:6,7]pleiadenol[2,1,12-pqa]pleiadene*.

6.2.3. Synthesis of tribenzo[b,gh,pq]pleiadene

Synthesis of 2-(2-bromophenyl)naphthalene

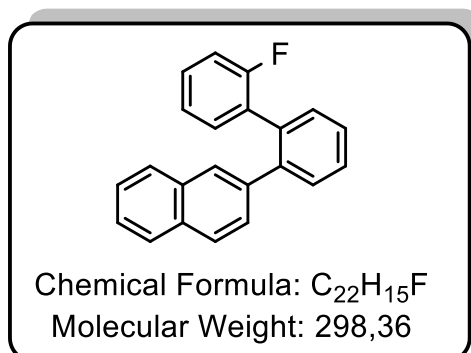


2-Naphthylboronic acid (1.00 g, 5.81 mmol, 1 equiv.), 1-Bromo-2-iodobenzene (0.822 mL, 6.39 mmol, 1.1 equiv.), K_3PO_4 (2.47 g, 11.6 mmol, 2 equiv.) were reacted in THF/ H_2O (24 mL, 5:1) with $Pd(PPh_3)_2Cl_2$ (0.02 equiv.) for 40 h according general procedure 1. The product was purified by flash

column chromatography on silica gel (*n*-hexane) and isolated as white solid (1.32 g, 80 %).

$R_f = 0$. (SiO₂, hexanes). 1H NMR (400 MHz, chloroform-*d*) δ 7.95 – 7.87 (m, 4H), 7.74 (dd, $J = 8.1, 1.1$ Hz, 1H), 7.59 (dd, $J = 8.5, 1.8$ Hz, 1H), 7.54 (dd, $J = 6.2, 3.2$ Hz, 2H), 7.47 – 7.39 (m, 2H), 7.28 – 7.24 (m, 1H). ^{13}C NMR (101 MHz, $cdCl_3$) δ 142.53, 138.63, 133.13, 133.06, 132.61, 131.51, 128.79, 128.21, 128.14, 127.70, 127.58, 127.39, 127.35, 126.22, 126.20, 122.79.

Synthesis of 2-(2'-fluoro-[1,1'-biphenyl]-2-yl)naphthalene



2-(2-bromophenyl)naphthalene (200 mg, 706,29 μ mol, 1 equiv.), (2-fluorophenyl)boronic acid (109 mg, 776 μ mol, 1.1 equiv.), K_3PO_4 (300 mg, 1.41 mmol, 2 equiv.) were reacted in THF/ H_2O (6 mL, 5:1) with $Pd(PPh_3)_2Cl_2$ (0.02 equiv.) for 24 h according general procedure 1. The product was purified by flash column chroma-

tography on silica gel (*n*-hexane) and isolated as white solid (200 mg, 95 %).

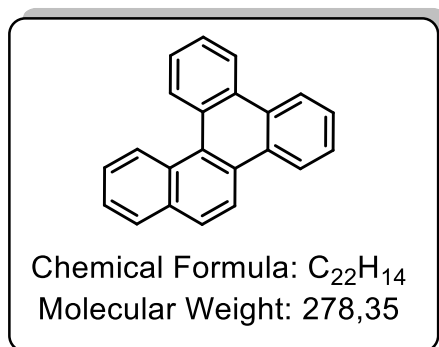
1H NMR (400 MHz, $cdCl_3$) δ 7.79 – 7.68 (m, 3H), 7.66 – 7.55 (m, 2H), 7.53 – 7.40 (m, 5H), 7.27 – 7.13 (m, 3H), 6.99 (td, $J = 7.7, 1.1$ Hz, 1H), 6.94 – 6.86 (m, 1H). ^{19}F NMR

(376 MHz, cdcl_3) δ -114.91 – -115.03 (m). ^{13}C NMR (101 MHz, cdcl_3) δ 160.79, 158.34, 141.52, 138.91, 134.58, 133.21, 132.18, 132.15, 132.08, 131.08, 131.07, 130.48, 129.18, 129.03, 128.88, 128.80, 128.21, 128.02, 128.01, 127.59, 127.51, 127.24, 127.11, 125.85, 125.72, 123.74, 123.70, 115.58, 115.36.

Reaction of 2-(2'-fluoro-[1,1'-biphenyl]-2-yl)naphthalene on Al_2O_3

2-(2'-fluoro-[1,1'-biphenyl]-2-yl)naphthalene (11.0 mg, 36.9 μmol) were reacted on Al_2O_3 according to general procedure 4 at 220 °C for 20 h. HPLC separation yielded benzo[g]chrysene (4.55 mg, 42 %) and benzo[f]tetraphene (0.83 mg, 8%).

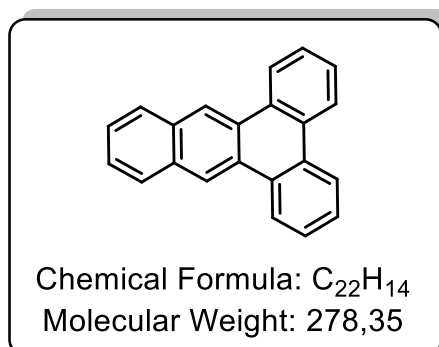
benzo[g]chrysene:



^1H NMR (400 MHz, CD_2Cl_2) δ 9.04 – 8.92 (m, 2H), 8.84 – 8.76 (m, 2H), 8.76 – 8.72 (m, 1H), 8.71 – 8.65 (m, 1H), 8.13 – 8.05 (m, 2H), 7.84 – 7.62 (m, 6H).
 ^{13}C NMR (101 MHz, CD_2Cl_2) δ 133.59, 130.80, 130.13, 129.90, 129.69, 129.36, 129.32, 128.33, 128.10, 128.00, 127.69, 127.39, 127.22, 127.15, 126.71, 126.15, 126.06, 125.93, 123.71, 123.43,

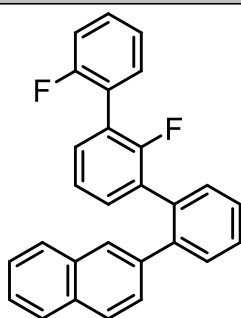
123.09, 120.70.

benzo[f]tetraphene:



^1H NMR (400 MHz, CD_2Cl_2) δ 9.18 (s, 2H), 8.89 – 8.81 (m, 2H), 8.70 – 8.62 (m, 2H), 8.20 – 8.14 (m, 2H), 7.78 – 7.68 (m, 4H), 7.66 – 7.61 (m, 2H).

Synthesis of 2-(2',2''-difluoro-[1,1':3',1''-terphenyl]-2-yl)naphthalene

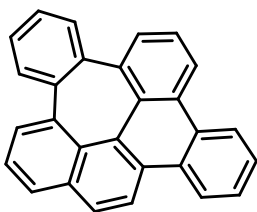


Chemical Formula: $C_{28}H_{18}F_2$
Molecular Weight: 392,45

2-(2-bromophenyl)naphthalene (111 mg, 0.392 mmol, 1 equiv.), (2,2'-difluoro-[1,1'-biphenyl]-3-yl)boronic acid (92 mg, 0.392 mmol, 1 equiv.), K_3PO_4 (166 mg, 784 μ mol, 2 equiv.) were reacted in THF/H₂O (6 mL, 5:1) with $Pd(PPh_3)_2Cl_2$ (mg, μ mol, 0.02 equiv.) for 72 h according general procedure 1. The product was purified by flash column chromatography on silica gel (*n*-hexane:DCM = 9:1) and isolated as colorless oil (134 mg, 87 %).

¹H NMR (400 MHz, CDCl₃) δ 7.81 – 7.75 (m, 1H), 7.75 – 7.70 (m, 2H), 7.67 (d, J = 8.5 Hz, 1H), 7.61 – 7.55 (m, 1H), 7.54 – 7.39 (m, 5H), 7.33 – 7.27 (m, 2H), 7.24 – 7.18 (m, 1H), 7.16 – 7.10 (m, 1H), 7.10 – 6.98 (m, 4H). **¹⁹F NMR** (377 MHz, CDCl₃) δ -114.84 (dd, J = 16.5, 9.8 Hz), -116.32 (dd, J = 15.2, 7.1 Hz). **¹³C NMR** (101 MHz, cdcl₃) δ 161.00, 158.52, 157.95, 155.47, 141.63, 138.82, 134.62, 133.26, 132.17, 132.01, 131.98, 131.56, 131.54, 131.53, 131.51, 131.07, 131.06, 130.56, 130.55, 130.53, 130.52, 130.43, 129.66, 129.60, 129.52, 129.50, 128.29, 128.16, 128.05, 127.63, 127.50, 127.26, 127.23, 125.88, 125.74, 123.87, 123.84, 123.74, 123.63, 123.57, 123.53, 123.49, 123.47, 115.78, 115.56. HPLC (PBr column, 1.0 mL/min, 35 °C, MeOH/DCM 8:2) t_R 5.7 min.

Synthesis of tribenzo[b,gh,pq]pleiadene



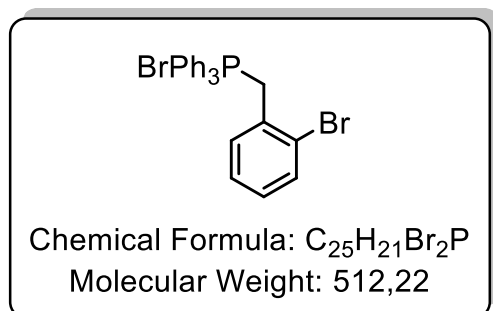
Chemical Formula: $C_{28}H_{16}$
Molecular Weight: 352,44

8 mg of 2-(2',2''-difluoro-[1,1':3',1''-terphenyl]-2-yl)naphthalene was reacted on Al₂O₃ (5 g) under dry conditions for 6 d at 200°C according to general procedure 4. After extraction of alumina with toluene, the products were isolated by preparative HPLC (toluene/methanol 40:60). The product was yielded as solid (0.69 mg, 10 %).

¹H NMR (400 MHz, CD₂Cl₂) δ 8.59 – 8.52 (m, 1H), 8.49 – 8.40 (m, 3H), 7.89 – 7.79 (m, 2H), 7.76 (ddd, J = 7.3, 2.5, 1.5 Hz, 2H), 7.72 – 7.60 (m, 4H), 7.44 – 7.33 (m, 2H), 7.19 – 7.11 (m, 1H), 7.11 – 7.05 (m, 1H). HPLC (PBr column, 1.0 mL/min, 35 °C, MeOH/DCM 6:4) t_R 9.4 min. **UV/vis** (DCM) λ_{max} 352, 283, 264, 246 nm.

6.2.4. Synthesis of 1-(2,3-difluorophenyl)-8-(2-fluorophenyl)phenanthrene

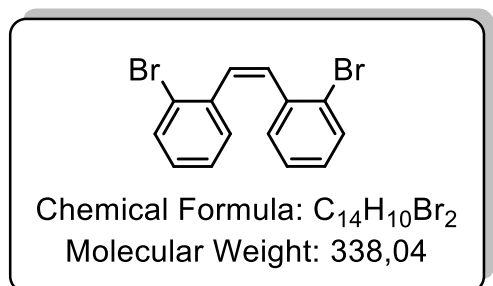
Synthesis of bromo(2-bromobenzyl)triphenyl-λ5-phosphane



1-bromo-2-(bromomethyl)benzene (10 g, 40.0 mmol, 1 equiv.) and triphenylphosphane (15.7 g, 60.0 mmol, 1.5 equiv.) were reacted in toluene (150 mL) for 24 h under reflux. After extracting with toluene, the product was isolated as a white solid (20.0 g, 98 %).

¹H NMR (400 MHz, cdcl₃) δ 7.86 – 7.43 (m, 15H), 7.35 (d, *J* = 7.9 Hz, 1H), 7.21 – 6.97 (m, 2H), 5.61 (dd, *J* = 40.0, 12.6 Hz, 2H). **³¹P NMR** (162 MHz, cdcl₃) δ 22.73 – 22.52 (m). **¹³C NMR** (101 MHz, cdcl₃) δ 135.16, 135.13, 134.39, 134.30, 133.23, 133.18, 132.93, 132.90, 130.27, 130.20, 130.14, 128.45, 128.41, 127.71, 127.62, 127.22, 127.15, 117.85, 117.00, 31.24, 30.76.

Synthesis of 1,2-bis(2-bromophenyl)ethene

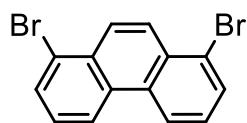


(2-bromobenzyl)triphenyl-λ4-phosphane (5.00 g, 11.6 mmol, 1 equiv.), 2-bromobenzaldehyde (1.34 mL, 11.6 mmol, 1 equiv.) were reacted in chloroform (100 mL) und addition of KOH (50%, 20 mL) for 18 h under reflux according to general procedure 2b. The product was purified by flash

column chromatography on silica gel (*n*-hexane) and isolated as a white solid (2.99 g, 76 %).

¹H NMR (400 MHz, cdcl₃) δ 7.61 – 7.56 (m, 2H), 7.09 – 6.97 (m, 6H), 6.80 (s, 2H). **¹³C NMR** (101 MHz, cdcl₃) δ 136.99, 136.82, 133.08, 132.59, 130.94, 130.12, 129.20, 128.76, 127.65, 127.15, 126.89, 124.25, 124.02.

Synthesis of 1,8-dibromophenanthrene



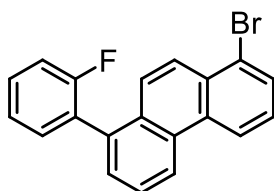
Chemical Formula: C₁₄H₈Br₂
Molecular Weight: 336,03

1,2-bis(2-bromophenyl)ethene (3.00 g, 8.87 mmol, 1 equiv.) in 600 ml of cyclohexane was irradiated in the presence of iodine (2.48 g, 9.76 mmol, 1.1 equiv.) I₂ (307 mg, 1.2 mmol) and methylpropyleneoxide (6.21 mL, 88.8 mmol, 10 equiv.) for 4 h. After completion of reaction half of

cyclohexane was evaporated under reduced pressure, washed with Na₂S₂O₃ solution, dried over Na₂SO₄. Cyclohexane was evaporated under reduced pressure and residue was purified by column chromatography (*n*-hexane) yielding 1,8-dibromophenanthrene (850 mg, 29 %).

¹H NMR (400 MHz, cdcl₃) δ 8.73 – 8.59 (m, 2H), 8.34 – 8.17 (m, 1H), 7.90 (ddd, *J* = 27.8, 13.9, 5.2 Hz, 2H), 7.72 – 7.60 (m, 2H), 7.50 (dd, *J* = 15.1, 7.4 Hz, 1H). **¹³C NMR** (101 MHz, cdcl₃) δ 132.02, 131.90, 131.66, 131.34, 130.71, 130.56, 130.51, 129.93, 128.66, 128.47, 127.35, 127.20, 127.08, 126.85, 125.27, 123.82, 123.70, 122.87, 122.56, 122.32.

Synthesis of 1-bromo-8-(2-fluorophenyl)phenanthrene



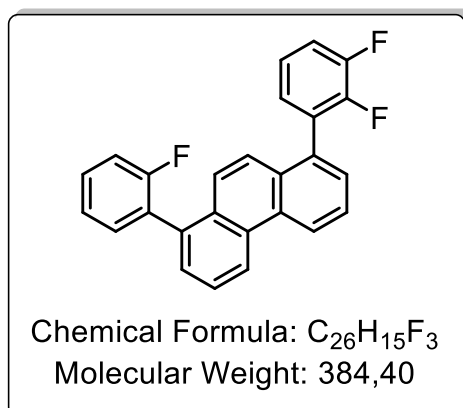
Chemical Formula: C₂₀H₁₂BrF
Molecular Weight: 351,22

1,8-dibromophenanthrene (850 mg, 2,53mmol, 1 equiv.), (2-fluorophenyl)boronic acid (354 mg, 2.53 mmol, 1 equiv.) and K₂CO₃ (1.05 g, 7.59 mmol, 3 equiv.) were reacted in 1,4-dioxane/H₂O (30 mL/20 mL) with Pd(PH₃)₄ (0.02 equiv.) for 3 h under reflux according to general procedure 1. The crude product was purified by flash column

chromatography on silica gel with *n*-hexane to afford 1-bromo-8-(2-fluorophenyl)phenanthrene (100 mg, 11 %).

¹H NMR (400 MHz, cdcl₃) δ 8.79 – 8.71 (m, 2H), 8.16 (d, *J* = 9.5 Hz, 1H), 7.90 (dd, *J* = 7.6, 0.9 Hz, 1H), 7.74 (dt, *J* = 11.2, 5.6 Hz, 1H), 7.70 (dd, *J* = 9.5, 2.4 Hz, 1H), 7.61 (d, *J* = 7.2 Hz, 1H), 7.55 – 7.40 (m, 3H), 7.34 – 7.21 (m, 2H). **¹⁹F NMR** (376 MHz, cdcl₃) δ -113.90 – -114.16 (m). **¹³C NMR** (101 MHz, cdcl₃) δ 161.25, 158.80, 134.70, 132.38, 132.34, 132.07, 130.84, 130.32, 130.20, 130.18, 129.72, 129.64, 129.05, 128.00, 127.83, 126.99, 126.44, 125.95, 125.94, 125.54, 124.19, 124.15, 123.68, 123.06, 122.59, 115.88, 115.66.

Synthesis of 1-(2,3-difluorophenyl)-8-(2-fluorophenyl)phenanthrene



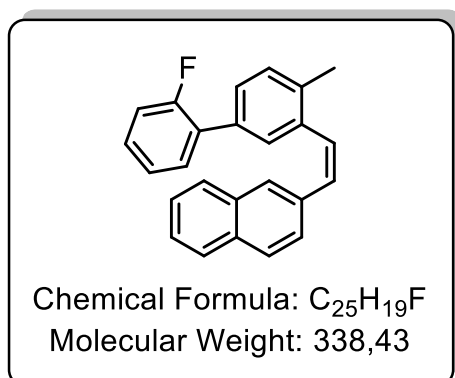
1-bromo-8-(2-fluorophenyl)phenanthrene (100 mg, 285 μ mol, 1 equiv.), (2,3-difluorophenyl)boronic acid (58.4 mg, 370 μ mol, 1.3 equiv.) and K₂CO₃ (78.7 mg, 569 μ mol, 2 equiv.) were reacted in THF/H₂O (12 mL 5:1) with Pd(PH₃)₄ (7 mg, 5.69 μ mol, 0.02 equiv.) for 24 h under reflux according to general procedure 1. The crude product was purified by flash column chromatography on silica

gel with *n*-hexane to afford 1-(2,3-difluorophenyl)-8-(2-fluorophenyl)phenanthrene (28.5 mg, 26 %) as a solid.

¹H NMR (400 MHz, cdcl₃) δ 8.86 (t, *J* = 8.5 Hz, 2H), 7.80 – 7.70 (m, 2H), 7.65 – 7.49 (m, 4H), 7.48 – 7.37 (m, 2H), 7.31 – 7.13 (m, 5H). **¹⁹F NMR** (376 MHz, cdcl₃) δ -113.59 – -114.61 (m), -137.38 – -138.21 (m), -138.66 – -139.55 (m). **¹³C NMR** (101 MHz, cdcl₃) δ 134.53, 132.42, 132.35, 130.65, 130.59, 130.50, 130.46, 130.02, 129.85, 129.57, 129.49, 128.66, 128.51, 128.18, 128.01, 127.11, 126.19, 126.04, 124.93, 124.21, 124.11, 123.99, 123.53, 123.08, 116.65, 116.48, 115.85, 115.72, 115.50.

6.2.5. Synthesis of 14-methyldibenzo[gh,pq]pleiadene

Synthesis of 2-(2-(2'-fluoro-4-methyl-[1,1'-biphenyl]-3-yl)vinyl)naphthalene



4,4,5,5-tetramethyl-2-(4-methyl-3-(2-(naphthalen-2-yl)vinyl)phenyl)-1,3,2-dioxaborolane* (220 mg, 594 μ mol), 1-bromo-2-fluorobenzene (0.1 mL, 891 μ mol, 1.5 equiv.) and K₃PO₄ (250 mg, 1.19 mmol, 2 equiv.) were reacted with Pd(dppf)Cl₂ (9.70 mg, 11.9 μ mol, 0.02 equiv.) in THF/H₂O (15 mL/3 mL) under reflux for 18 h according to general procedure

1. After Extraction, the crude product was purified by flash column chromatography on silica gel with *n*-hexane/DCM 1:1 to afford the product (151 mg, 75 %).

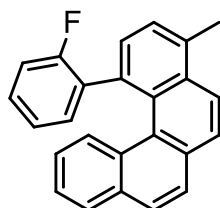
¹H NMR (400 MHz, CDCl₃) δ 7.77 – 7.67 (m, 4H), 7.67 – 7.62 (m, 1H), 7.58 (t, *J* = 5.8 Hz, 1H), 7.45 – 7.38 (m, 3H), 7.20 (ddd, *J* = 7.2, 4.8, 1.9 Hz, 1H), 7.12 – 7.06 (m, 1H),

6.82 – 6.74 (m, 1H), 6.67 (ddd, $J = 15.2, 6.9, 2.8$ Hz, 3H), 4.40 (s, 1H), 2.22 (s, 3H).

^{19}F NMR (377 MHz, CDCl_3) δ -113.40 – -113.57 (m), -114.46 – -114.61 (m), -117.11 – -117.24 (m), -117.28 – -117.40 (m).

*4,4,5,5-tetramethyl-2-(4-methyl-3-(2-(naphthalen-2-yl)vinyl)phenyl)-1,3,2-dioxaborolane was prepared by Vladimir Akhmetov from our group.

Synthesis of 1-(2-fluorophenyl)-4-methylbenzo[c]phenanthrene



Chemical Formula: $\text{C}_{25}\text{H}_{17}\text{F}$
Molecular Weight: 336,41

Method 1: 4,4,5,5-tetramethyl-2-(4-methylbenzo[c]phenanthren-1-yl)-1,3,2-dioxaborolane (140 mg, 380 μmol) and 1-bromo-2-fluorobenzene (0.06 mL, 570 μmol , 1.5 equiv.) and Cs_2CO_3 (248 mg, 760 μmol , 2 equiv.) were reacted in THF/ H_2O (18 mL, 5:1) with $\text{Pd}(\text{dppf})_2\text{Cl}_2$ (14 mg, 19.0 μmol , 0.05 equiv.) for 48 h under reflux. After cooling to rt, water was added, phases were separated

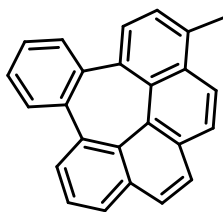
and the aqueous layer extracted with DCM. The combined organic fractions were dried over Na_2SO_4 , filtrated and the solvent removed in vacuo. The crude product was purified by flash column chromatography on silica gel with *n*-hexane:DCM 9:1 to afford the product as a white solid.(16.8 mg, 13 %).

Method 2: 2-(2-(2'-fluoro-4-methyl-[1,1'-biphenyl]-3-yl)vinyl)naphthalene (267 mg, 788 μmol) was reacted with iodine (220 mg, 867 μmol , 1.1 equiv.) and propylene oxide (552 mmL, 7.89 mmol, 10 equiv.) according to general procedure 3. The crude product was purified by flash column chromatography on silica gel with *n*-hexane:DCM 9:1 to afford the product as a white solid (5 mg, 2%).

^1H NMR (400 MHz, CD_2Cl_2) δ 8.04 (t, $J = 12.0$ Hz, 1H), 7.92 (dd, $J = 29.4, 16.9$ Hz, 1H), 7.86 – 7.26 (m, 6H), 7.27 – 6.70 (m, 4H), 6.30 – 6.03 (m, 1H), 5.82 (t, $J = 7.1$ Hz, 1H), 2.78 (s, 3H). **^{19}F NMR** (377 MHz, CD_2Cl_2) δ -113.58 (s), -118.15 (s).

4,4,5,5-tetramethyl-2-(4-methylbenzo[c]phenanthren-1-yl)-1,3,2-dioxaborolane was prepared by Vladimir or Misha.

Synthesis of 14-methyldibenzo[gh,pq]pleiadene



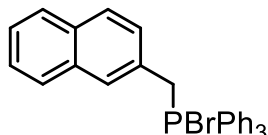
Chemical Formula: C₂₅H₁₆
Molecular Weight: 316,40

1-(2-fluorophenyl)-4-methylbenzo[c]phenanthrene (16.8 mg, 47.6 μmol) were reacted on activated Al₂O₃ according to general procedure 4 at 220 °C for 18 h. After extracting with toluene only product (13.9 mg, 83 %) could be found by HPLC and Mass spectrometry (100 % conversion).

¹H NMR (400 MHz, CD₂Cl₂) δ 7.93 (q, *J* = 8.9 Hz, 1H), 7.88 – 7.74 (m, 2H), 7.74 – 7.62 (m, 1H), 7.62 – 7.43 (m, 3H), 7.44 – 7.23 (m, 4H), 7.21 – 7.15 (m, 1H), 7.08 (ddd, *J* = 9.5, 7.3, 4.4 Hz, 1H), 2.69 (s, 3H). ¹³C NMR (101 MHz, CD₂Cl₂) δ 133.15, 133.07, 131.72, 131.49, 131.29, 130.42, 130.01, 129.84, 129.81, 129.79, 129.46, 128.88, 128.84, 128.62, 128.58, 127.88, 127.63, 127.52, 127.18, 127.14, 127.02, 127.00, 126.48, 122.78, 30.08.

6.2.6. Synthesis of 7-helicene-derivates and their opening on Al₂O₃

Synthesis of bromo(naphthalen-2-ylmethyl)triphenyl-15-phosphane

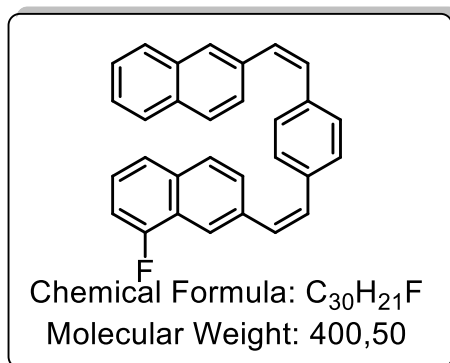


Chemical Formula: C₂₉H₂₄BrP
Molecular Weight: 483,39

2-(bromomethyl)naphthalene (7.68 g, 34.4 μmol, 1 equiv.) and triphenylphosphine (13.5 g, 51.6 μmol, 1.5 equiv.) were reacted in toluene (200 mL) under reflux for 24 h. The resulting precipitate was collected by suction filtration, washed with toluene (200 mL) and dried *in vacuo*. The Product

was obtained as white solid (11.1 g, 67 %).

Synthesis of 1-fluoro-7-(-4-(-2-(naphthalen-2-yl)vinyl)styryl)naphthalene

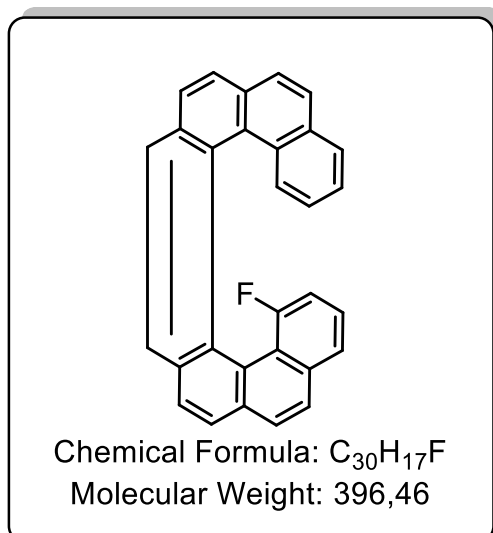


Terephthalaldehyde (500 mg, 3.73mmol, 1 equiv.), bromo(naphthalen-2-ylmethyl)triphenylphosphane (1.8 g, 3.73mmol, 1 equiv.) and bromo((8-fluoronaphthalen-2-yl)methyl)triphenylphosphane (2.24 g, 4.47mmol) were dissolved in 150 mL chloroform. After degassing twice, KOH solution(50 %, 80 mL) was added and degassed

again. The mixture was stirred under reflux for 18 h. After cooling to rt, it was washed with water (3x100 mL), dried over Na₂SO₄. After filtration and evaporation of the solvent, the crude product was analyzed first by TLC (*n*-hexane:DCM 1:1). The multiple Isomers (1.0 g, 67 %) were detected and it was decided to only analyze further with mass spectrometry.

¹H NMR (400 MHz, cdcl₃) δ 8.09 – 7.27 (m, 17H), 5.79 (d, *J* = 14.8 Hz, 4H). **¹⁹F NMR** (376 MHz, cdcl₃) δ -122.83 – -122.91 (m), -123.19 (ddd, *J* = 15.7, 10.7, 5.4 Hz), -123.30 – -123.37 (m). **¹³C NMR** (101 MHz, cdcl₃) δ 134.92, 134.89, 134.46, 134.36, 133.09, 132.12, 132.05, 132.02, 131.89, 131.87, 130.19, 130.06, 128.52, 128.40, 126.90, 118.41, 117.56.

Synthesis of “1-fluorobenzo[1,2-c:4,3-c']diphenanthrene”



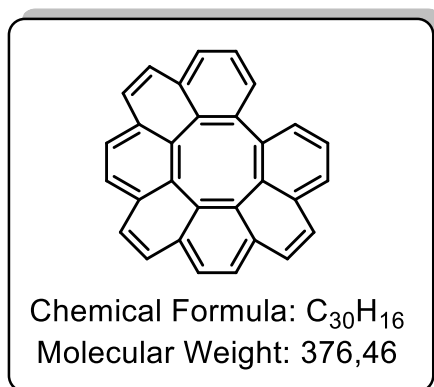
The isomer-mixture of 1-fluoro-7-(-4-(-2-(naphthalen-2-yl)vinyl)styryl)naphthalene (1.00 g, 2.50 mmol, 1 equiv.), iodine (1.39 g, 5.49 mmol, 2.2 equiv.) and propylene oxide (3.49 mL, 49.9 mmol, 20 equiv.) were reacted in cyclohexane (1 L) for 6 h according to general procedure 3. The product was purified according to general procedure 3 and further by flash column chromatography on silica gel (*n*-hexane:DCM 9:1 to 2:8). The product was further

purified by HPLC (PBr 1ml/min Tol/MeOH 30/70 40 °C) into 6 fractions. Mass spectrometry showed 396 m/z of the product at fraction 2 (6mg), 3 (13 mg) and 4 (89 mg). Fraction 2 had no ¹⁹F-NMR signal.

3. Fraction:

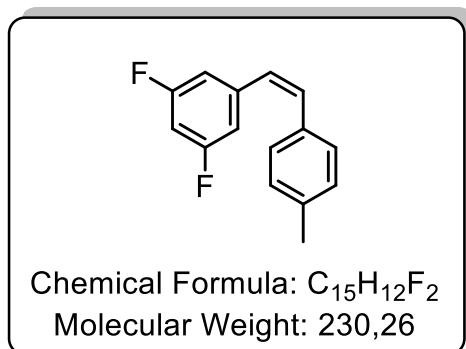
¹H NMR (400 MHz, c_6d_6) δ 9.56 (d, $J = 17.8$ Hz, 1H), 9.30 (dd, $J = 22.7, 8.2$ Hz, 1H), 8.98 (d, $J = 15.0$ Hz, 1H), 7.88 – 7.35 (m, 6H), 7.35 – 7.25 (m, 1H), 7.25 – 7.15 (m, 2H), 6.84 (d, $J = 7.7$ Hz, 1H), 6.74 (t, $J = 7.3$ Hz, 1H), 6.54 (dd, $J = 12.6, 7.7$ Hz, 1H), 6.29 (t, $J = 7.7$ Hz, 1H), 6.13 (dd, $J = 12.3, 7.8$ Hz, 1H). **¹⁹F NMR** (376 MHz, c_6d_6) δ -98.06 – -98.45 (m), -105.45 – -105.67 (m). **¹³C NMR** (101 MHz, c_6d_6) δ 133.67, 132.03, 131.39, 131.14, 130.77, 129.98, 129.82, 129.42, 128.61, 128.40, 128.26, 127.19, 127.05, 126.96, 126.85, 126.77, 126.74, 126.72, 126.50, 126.46, 126.41, 126.38, 126.29, 126.22, 126.19, 126.10, 125.93, 125.85, 125.64, 125.04, 124.94, 124.45, 124.19, 124.16, 123.74, 123.49, 122.50, 122.47, 112.65, 112.41, 110.88, 110.64.

Synthesis of “tribenzo[def,jkl,pqr]tetraphenylene”



1-fluorobenzo[1,2-c:4,3-c']diphenanthrene (Fraction 3) was reacted on activated Al_2O_3 according to general procedure 4 at 200 °C for 18 h. The product (1.5 mg, 12 %) was identified by mass spectrometry. **¹H NMR** (400 MHz, c_6d_6) δ 9.56 (d, $J = 14.3$ Hz, 1H), 9.17 (d, $J = 7.7$ Hz, 1H), 8.53 – 8.47 (m, 1H), 8.09 (d, $J = 6.9$ Hz, 1H), 7.86 – 7.57 (m, 5H), 7.57 – 7.36 (m, 2H), 7.08 (dd, $J = 7.7, 1.6$ Hz, 2H), 7.02 – 6.94 (m, 3H). **¹³C NMR** (101 MHz, c_6d_6) δ 138.84, 137.90, 134.53, 133.73, 133.31, 132.49, 132.37, 132.10, 131.96, 131.34, 130.55, 130.29, 129.34, 129.16, 128.91, 128.85, 128.77, 128.57, 127.55, 127.14, 126.66, 126.44, 126.28, 126.14, 125.81, 125.72, 125.70, 125.58, 124.39.

Synthesis of 1,3-difluoro-5-(4-methylstyryl)benzene



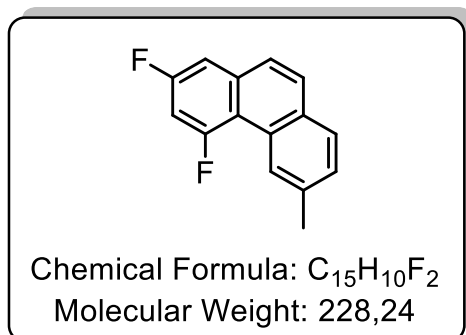
An aqueous solution of KOH (50 %, 30 mL) was added dropwise to a solution of 4-methylbenzaldehyde (0.981 mL, 8.32 mmol, 1 equiv.) and 2,4-Difluorobenzyltriphenylphosphonium bromide (5.86 g, 12.5 mmol, 1.5 equiv.) in $CHCl_3$ (150 mL). The mixture was heated to 65 °C and stirred for 18h. After cooling to rt, it was washed with water

(3x100 mL), dried over Na₂SO₄. After filtration and evaporation of the solvent, the crude product was purified by flash column chromatography on silica gel (*n*-hexane). The product was isolated as white solid and clear liquid (1.80 g, 94 %).

Liquid isomer: $R_f = 0.69$ (SiO₂, *n*-hexane) **¹H NMR** (500 MHz, Chloroform-*d*) δ 7.13 – 7.05 (m, 4H), 6.78 – 6.73 (m, 2H), 6.67 – 6.59 (m, 2H), 6.43 (d, $J = 12.2$ Hz, 1H), 2.33 (s, 3H). **¹⁹F NMR** (470 MHz, Chloroform-*d*) δ -110.58 (t, $J = 8.6$ Hz).

Solid isomer: $R_f = 0.51$ (SiO₂, *n*-hexane) **¹H NMR** (500 MHz, Chloroform-*d*) δ 7.40 (d, $J = 8.1$ Hz, 2H), 7.19 (d, $J = 7.8$ Hz, 2H), 7.14 – 7.04 (m, 2H), 7.04 – 6.92 (m, 3H), 2.37 (s, 3H). **¹⁹F NMR** (470 MHz, Chloroform-*d*) δ -110.43 (t, $J = 8.5$ Hz). **¹³C NMR** (101 MHz, cdcl₃) δ 164.56, 164.43, 162.10, 161.97, 140.98, 138.42, 133.54, 131.21, 129.49, 126.70, 125.54, 125.51, 125.48, 109.00, 108.93, 108.81, 108.74, 102.70, 102.44, 102.19, 21.27.

Synthesis of 2,4-difluoro-6-methylphenanthrene

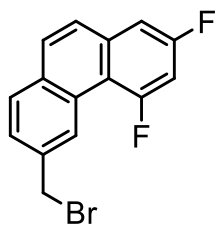


1,3-Difluoro-5-(4-methylstyryl)benzene (1.80 g, 7.82 mmol, 1 equiv.), iodine (2.18 g, 8.60 mmol, 1 equiv.) and propylene oxide (5.47 mL, 78.2 mmol, 10 equiv.) were reacted in cyclohexane (1 L) for 7 h according to general procedure 3. The product was purified according to general procedure 3 and further flash column chromatography on silica gel

(*n*-hexane). The product was isolated as white solid (1.16 g, 65 %).

¹H NMR (400 MHz, Chloroform-*d*) δ 8.81 (s, 1H), 7.78 (d, $J = 8.1$ Hz, 1H), 7.71 (d, $J = 8.8$ Hz, 1H), 7.53 (dd, $J = 8.8, 2.2$ Hz, 1H), 7.46 (dd, $J = 8.1, 1.6$ Hz, 1H), 7.34 – 7.30 (m, 1H), 7.13 (ddd, $J = 13.9, 8.7, 2.6$ Hz, 2H), 2.64 (s, 3H). **¹⁹F NMR** (376 MHz, Chloroform-*d*) δ -104.66 – -104.99 (m), -113.19 (q, $J = 8.9$ Hz). **¹³C NMR** (101 MHz, cdcl₃) δ 163.14, 161.20, 161.06, 160.60, 158.75, 158.60, 137.40, 137.38, 135.29, 135.23, 131.20, 129.91, 129.49, 129.29, 128.38, 128.30, 128.29, 126.89, 126.70, 126.66, 125.50, 124.87, 124.83, 124.80, 108.99, 108.95, 108.79, 108.75, 103.30, 103.03, 103.01, 102.75, 102.44, 22.31, 21.27.

Synthesis of 6-(bromomethyl)-2,4-difluorophenanthrene



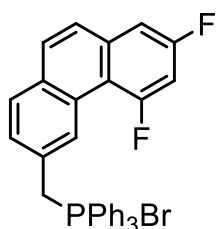
Chemical Formula: C₁₅H₉BrF₂
Molecular Weight: 307,14

2,4-difluoro-6-methylphenanthrene (1.14 g, 4.99 mmol) and NBS (978 mg, 5.49 mmol, 1.1 equiv.) were reacted with DBPO (34 mg, 99.9 μmol, 0.02 equiv.) in chloroform (50 mL) under reflux for 4 h. The organic solution was washed with water and brine and dried over Na₂SO₄. After filtration and evaporation of the solvent, the crude product was

purified by flash column chromatography on silica gel (hexanes) and isolated as white solid (1.06 g, 69 %).

¹H NMR (400 MHz, cdcl₃) δ 9.00 (s, 1H), 7.86 (d, *J* = 8.2 Hz, 1H), 7.73 (dd, *J* = 9.1, 4.5 Hz, 1H), 7.64 (ddd, *J* = 11.0, 8.5, 1.9 Hz, 2H), 7.37 – 7.31 (m, 1H), 7.20 – 7.11 (m, 1H), 4.75 (s, 2H). **¹⁹F NMR** (376 MHz, cdcl₃) δ -104.62 – -104.98 (m), -112.03 – -112.27 (m). **¹³C NMR** (101 MHz, cdcl₃) δ 164.02, 163.02, 162.89, 161.44, 161.30, 160.47, 160.35, 158.97, 158.83, 139.32, 136.87, 136.85, 136.35, 135.31, 135.25, 135.21, 135.15, 131.74, 130.43, 129.58, 129.51, 129.27, 128.98, 128.19, 128.13, 127.70, 127.54, 127.46, 127.22, 127.13, 126.50, 126.47, 126.43, 116.15, 116.12, 116.06, 116.03, 111.29, 111.10, 111.03, 109.25, 109.21, 109.05, 109.01, 104.73, 104.48, 104.23, 103.78, 103.51, 103.50, 103.23, 55.43.

Synthesis of bromo((5,7-difluorophenanthren-3-yl)methyl)triphenyl-λ⁵-phosphane



Chemical Formula: C₃₃H₂₄BrF₂P
Molecular Weight: 569,43

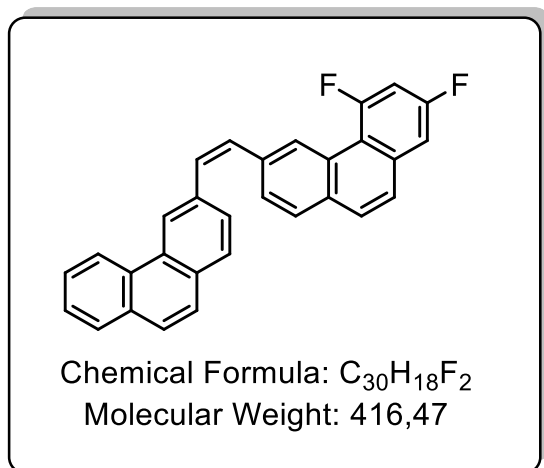
6-(bromomethyl)-2,4-difluorophenanthrene (1.06 g, 3.43 mmol) and triphenylphosphine (1.35g, 5,50 mmol, 1.6 equiv.) were reacted in toluene (100 mL) under reflux for 24 h. The resulting precipitate was collected by suction filtration, washed with toluene (200 mL) and dried *in vacuo*. The Product was obtained as

white solid (1.89 g, 96 %).

¹H NMR (400 MHz, cdcl₃) δ 8.40 (s, 1H), 7.86 – 7.71 (m, 9H), 7.69 – 7.55 (m, 6H), 7.26 (s, 4H), 7.20 – 7.15 (m, 5H), 7.05 – 6.96 (m, 1H), 5.75 (d, *J* = 14.6 Hz, 2H). **¹⁹F NMR** (376 MHz, cdcl₃) δ -105.30 (t, *J* = 11.8 Hz), -111.98 (q, *J* = 8.9 Hz). **³¹P NMR** (162 MHz,

cdcl₃) δ 23.33 (s). **¹³C NMR** (101 MHz, cdcl₃) δ 162.59, 161.33, 159.91, 158.86, 134.90, 134.87, 134.49, 134.39, 131.32, 130.44, 130.16, 130.03, 129.28, 129.07, 129.04, 128.93, 126.54, 126.48, 126.35, 118.22, 117.36, 109.05, 108.85, 103.54, 103.27, 102.99, 31.60, 31.14.

Synthesis of 2,4-difluoro-6-(2-(phenanthren-3-yl)vinyl)phenanthrene

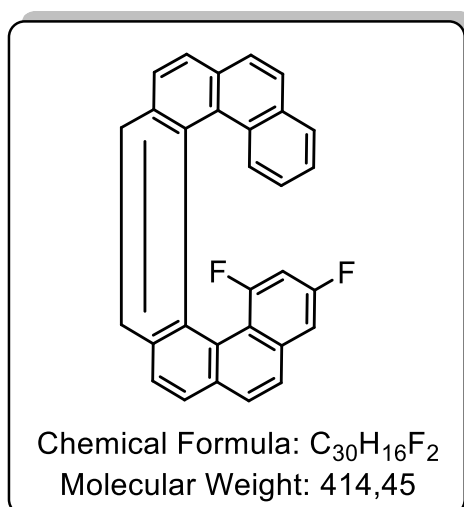


Phenanthrene-3-carbaldehyde (54.0 mg, 261.8 μmol, 1.0 equiv.) and bromo((5,7-difluorophenanthren-3-yl)methyl)triphenyl-λ⁵-phosphane (209 mg, 367 μmol, 1.4 equiv.) in chloroform (10 mL) was reacted with an aqueous solution of KOH (50 %, 4 mL) for 18 h according to general procedure 2b. The (E) and (Z)-products were purified by flash column chromatography on silica gel (*n*-hexane) and isolated as green solid (91 mg, 83 %), which glows blue in solution (fluorescence).

(fluorescence).

¹H NMR (400 MHz, cdcl₃) δ 9.05 (s, 1H), 8.85 – 8.78 (m, 1H), 8.66 (s, 1H), 8.38 (d, *J* = 8.1 Hz, 1H), 7.98 – 7.77 (m, 3H), 7.77 – 7.46 (m, 7H), 7.36 (dd, *J* = 8.2, 5.6 Hz, 2H), 7.00 (d, *J* = 3.0 Hz, 2H). **¹⁹F NMR** (376 MHz, cdcl₃) δ -104.79 – -104.95 (m), -112.76 (d, *J* = 8.9 Hz).

Synthesis of “1,3-difluorobenzo[1,2-c:4,3-c']diphenanthrene”



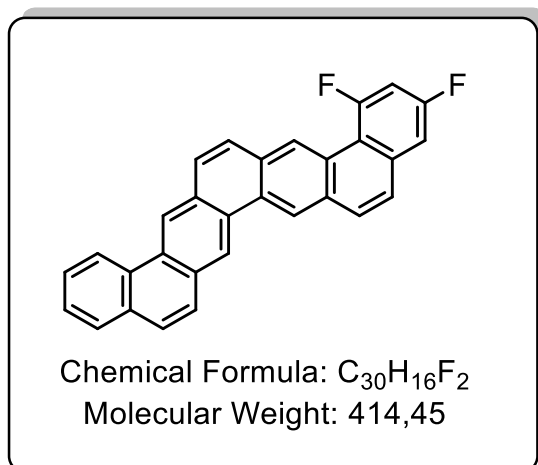
2,4-difluoro-6-(2-(phenanthren-3-yl)vinyl)phenanthrene (91 mg, 218,50 μmol, 1.0 equiv.), iodine (61 mg, 240 μmol, 1.1 equiv.) and propylene oxide (0.153 mL, 2.19 mmol, 10 equiv.) were reacted in toluene (1 L) for 4 h according to general procedure 3. The product was purified by flash column chromatography on silica gel (*n*-hexane/DCM 9:1) and isolated as yellow solid (4 mg, 4 %). It was further purified by HPLC (PBr 1ml/min Tol/MeOH 30/70 40 °C) into fractions.

Fraction 5

MS: 414 m/z

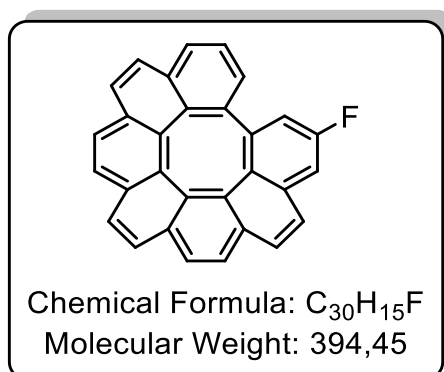
¹H NMR (400 MHz, c_6d_6) δ 7.77 – 7.63 (m, 5H), 7.58 (dd, $J = 8.2, 3.8$ Hz, 1H), 7.52 (d, $J = 8.5$ Hz, 1H), 7.38 (d, $J = 8.4$ Hz, 1H), 7.27 (d, $J = 8.5$ Hz, 1H), 7.17 (ddd, $J = 17.1, 8.8, 3.3$ Hz, 2H), 6.94 (dd, $J = 8.5, 1.8$ Hz, 1H), 6.74 (ddd, $J = 8.0, 6.9, 1.1$ Hz, 1H), 6.53 – 6.49 (m, 1H), 6.25 (ddd, $J = 8.4, 6.9, 1.4$ Hz, 1H), 5.92 (ddd, $J = 11.6, 8.9, 2.6$ Hz, 1H). **¹⁹F NMR** (376 MHz, c_6d_6) δ -101.20 (dd, $J = 11.3, 10.3$ Hz), -114.51 (q, $J = 9.1$ Hz). **¹³C NMR** (101 MHz, c_6d_6) δ 160.42, 160.30, 160.00, 159.88, 157.97, 157.84, 157.45, 157.33, 134.05, 134.00, 133.95, 133.90, 131.73, 131.55, 131.46, 131.34, 130.93, 129.74, 127.02, 126.77, 126.74, 126.28, 126.13, 126.05, 125.87, 125.77, 125.73, 125.70, 124.61, 123.85, 123.35, 106.72, 106.69, 106.52, 106.48, 101.23, 100.96, 100.68.

Fraction 4 (2,4-difluorodibenzo[*c,m*]pentaphene):



¹H NMR (400 MHz, cd_2cl_2) δ 9.86 (d, $J = 2.4$ Hz, 1H), 9.29 (d, $J = 9.3$ Hz, 1H), 9.16 (d, $J = 7.8$ Hz, 1H), 8.54 (d, $J = 3.9$ Hz, 2H), 8.39 (d, $J = 8.4$ Hz, 2H), 8.32 (q, $J = 8.6$ Hz, 3H), 8.18 (t, $J = 7.8$ Hz, 1H), 7.92 (d, $J = 9.2$ Hz, 1H), 7.57 (d, $J = 8.8$ Hz, 1H), 7.43 – 7.02 (m, 2H), 5.55 (s, 1H), 5.11 (s, 1H). **¹⁹F NMR** (376 MHz, cd_2cl_2) δ -105.53 (t, $J = 12.5$ Hz), -112.48 – -112.76 (m). **¹³C NMR:** not enough product

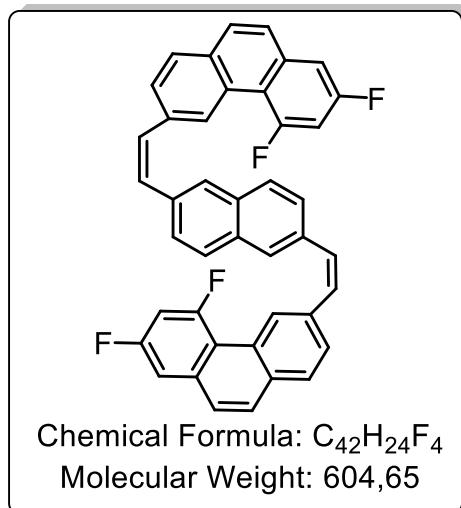
Synthesis of “8-fluorotribenzo[*def,jkl,pqr*]tetraphenylene“



2,4-difluoro-6-(2-(phenanthren-3-yl)vinyl)phenanthrene (5 mg, fraction 5) was reacted on dry Al_2O_3 according to general procedure 4 at 200 °C for 1 d. After washing with toluene (80 mL), the product was identified by mass spectrometry.

6.2.7. Synthesis and reaction of 6,8,18,20-tetrafluorodiphenanthro[3,4-c:3',4'-l]chrysene

Synthesis of 2,6-bis(-2-(5,7-difluorophenanthren-3-yl)vinyl)naphthalene



An aqueous solution of KOH (50 %, 8 mL) was added dropwise to a solution of bromo((5,7-difluorophenanthren-3-yl)methyl)triphenyl- λ 5-phosphane (464 mg, 815 μ mol, 2.2 equiv.) and naphthalene-2,6-dicarbaldehyde (68 mg, 370 μ mol, 1 equiv.) in chloroform (20 mL). The mixture was heated to 65 °C and stirred for 18 h. After cooling to r.t., it was washed with water (3x100 mL), dried over Na_2SO_4 . After filtration and evaporation of the solvent, the crude product was purified by flash

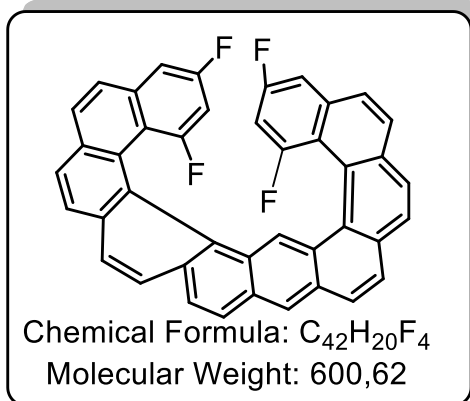
column chromatography on silica gel (*n*-hexane). The product was isolated as green-yellow solid (215 mg, 96 %).

MS: 604 m/z

Synthesis of 6,8,18,20-tetrafluorodiphenanthro[3,4-c:3',4'-l]chrysene and 17,19,21,23-tetrafluorodiphenanthro[4,3-a:3',4'-m]tetraphene

2,6-bis(-2-(5,7-difluorophenanthren-3-yl)vinyl)naphthalene (220 mg, 364 μ mol, 1 equiv.), iodine (203 mg, 800 μ mol, 2.2 equiv.) and propylene oxide (509 mmL, 7.28 mmol, 20 equiv.) were reacted in toluene (1 L) for 8 h according to general procedure 3. The product was purified according to general procedure 3 and further flash column chromatography on silica gel (*n*-hexane). The products 17,19,21,23-tetrafluorodiphenanthro[4,3-a:3',4'-m]tetraphene and 6,8,18,20-tetrafluorodiphenanthro[3,4-c:3',4'-l]chrysene were isolated as white solids.

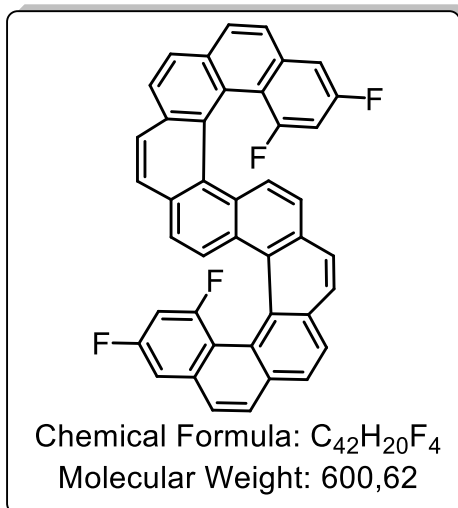
1. Fraction 17,19,21,23-tetrafluorodiphenanthro[4,3-a:3',4'-m]tetraphene (10 mg, 5 %)



1H NMR (500 MHz, $cdCl_3$) δ 8.09 (d, $J = 8.1$ Hz, 2H), 8.03 (t, $J = 9.1$ Hz, 4H), 7.93 (dd, $J = 11.5, 8.5$ Hz, 4H), 7.78 (d, $J = 8.2$ Hz, 2H), 7.46 (dt, $J = 16.7, 8.4$ Hz, 2H), 7.36 (d, $J = 8.7$ Hz, 2H), 7.11 (d, $J = 8.8$ Hz, 2H), 6.64 (ddd, $J = 14.1, 8.9, 2.5$ Hz, 2H). **^{19}F NMR** (470 MHz, $cdCl_3$) δ -92.78 (t, $J = 11.8$ Hz), -112.62 – -113.05 (m). **^{13}C NMR** (126 MHz, $cdCl_3$) δ 132.84, 131.24, 129.65, 128.78, 128.16, 127.89,

126.54, 126.45, 126.04, 123.77.

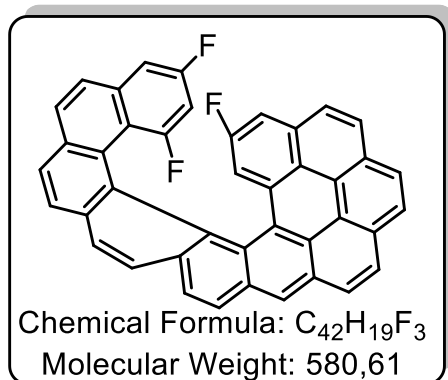
3. Fraction 6,8,18,20-tetrafluorodiphenanthro[3,4-c:3',4'-l]chrysene (15 mg, 7 %)



1H NMR (500 MHz, $cdCl_3$) δ 9.72 (s, 1H), 9.62 (s, 1H), 9.34 (d, $J = 8.8$ Hz, 1H), 8.17 (d, $J = 8.1$ Hz, 1H), 8.14 – 8.00 (m, 7H), 7.87 (d, $J = 8.3$ Hz, 1H), 7.73 (dd, $J = 9.0, 1.8$ Hz, 1H), 7.62 (d, $J = 8.6$ Hz, 1H), 7.45 (dd, $J = 8.6, 2.3$ Hz, 1H), 7.32 (dd, $J = 12.3, 5.5$ Hz, 2H), 7.26 – 7.19 (m, 4H), 7.05 (d, $J = 8.7$ Hz, 1H), 6.10 – 5.99 (m, 1H). **^{19}F NMR** (470 MHz, $cdCl_3$) δ -95.97 (t, $J = 11.3$ Hz), -104.91 – -105.26 (m), -112.06 (q, $J = 8.9$ Hz), -112.84 (dd, $J = 18.6, 8.9$ Hz). **^{13}C NMR** (126 MHz, $cdCl_3$) δ 132.73,

131.06, 130.34, 130.34, 129.97, 129.55, 128.75, 128.61, 128.43, 128.43, 128.03, 128.03, 127.86, 127.86, 127.46, 127.46, 127.15, 127.13, 127.13, 127.07, 127.07, 127.05, 126.86, 126.61, 126.61, 126.57, 126.44, 126.44, 126.42, 126.40, 125.92, 125.89, 124.02, 124.02.

Reaction of 17,19,21,23-tetrafluorodiphenanthro[4,3-a:3',4'-m]tetraphene

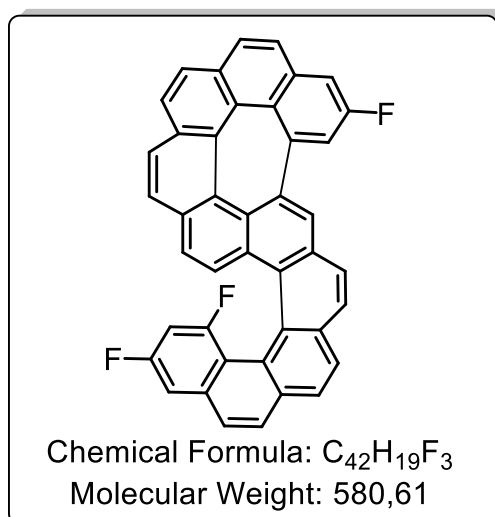


17,19,21,23-tetrafluorodiphenanthro[4,3-a:3',4'-m]tetraphene (10 mg) was reacted on activated Al_2O_3 according to general procedure 4 at 200 °C for 1 d. After extraction with toluene 17,19,21-trifluorobenzo[ghi]naphtho[1',2':5,6]phenanthro[4,3-a]perylene (0.3 mg, 3 %) was found by mass-spectrometry.

1H NMR (500 MHz, c_6d_6) δ 7.76 (d, $J = 8.0$ Hz, 1H), 7.67 (dd, $J = 12.5, 8.3$ Hz, 2H), 7.60 – 7.53 (m, 3H), 7.49 (d, $J = 8.7$ Hz, 1H), 7.41 (d, $J = 8.2$ Hz, 1H), 7.31 – 7.18 (m, 3H), 7.08 (d, $J = 5.3$ Hz, 1H), 6.93 (d, $J = 8.8$ Hz, 1H), 6.67 – 6.56 (m, 1H). **^{19}F NMR** (470 MHz, c_6d_6) δ -92.16 (d, $J = 11.7$ Hz), -112.55 (q, $J = 9.0$ Hz). **^{13}C NMR** (126 MHz, c_6d_6) δ 133.12, 129.46, 128.74, 128.14, 128.12, 127.15, 127.10, 126.74, 126.59, 126.32, 126.28, 126.21, 126.03, 125.99, 124.83, 123.94, 119.81, 118.15.

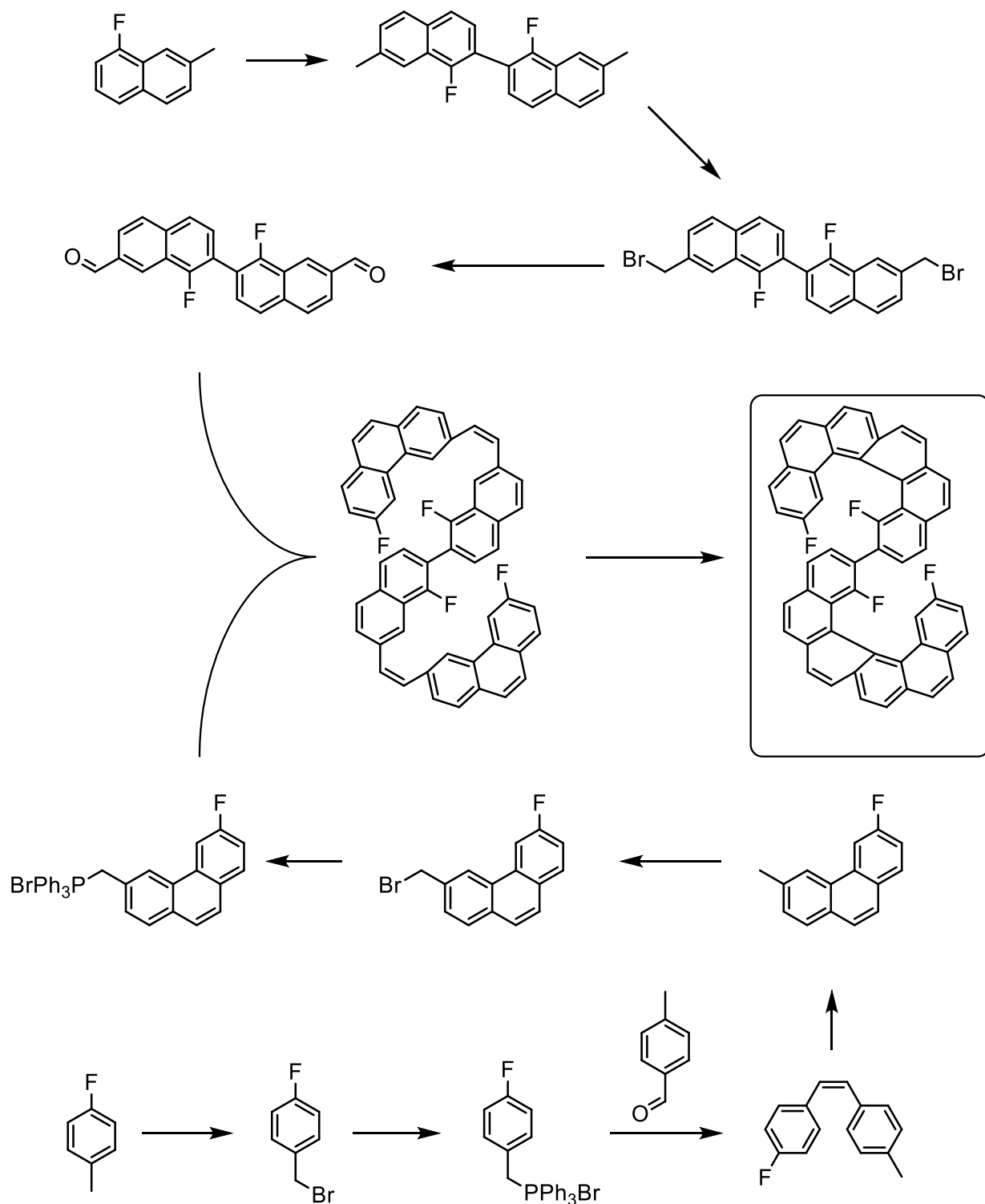
Reaction of 6,8,18,20-tetrafluorodiphenanthro[3,4-c:3',4'-l]chrysene

6,8,18,20-tetrafluorodiphenanthro[3,4-c:3',4'-l]chrysene (15 mg) was reacted on activated Al_2O_3 according to general procedure 4 at 200 °C for 1 d. After extraction with toluene 9,19,21-trifluorobenzo[no]benzo[5,6]phenanthro[3,4-b]naphtho[2,1,8,7-ghij]pleiadene (0.4 mg, 3 %) was found by mass-spectrometry.



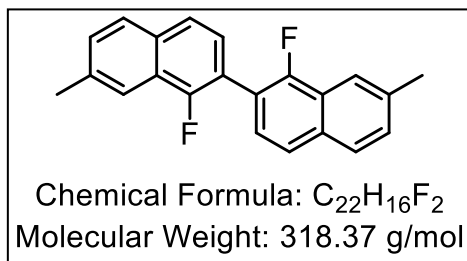
1H NMR (400 MHz, c_6d_6) δ 9.78 (s, 1H), 9.67 (s, 1H), 9.34 (d, $J = 9.0$ Hz, 1H), 8.40 (d, $J = 4.9$ Hz, 1H), 8.18 (s, 1H), 8.08 – 7.17 (m, 25H), 7.05 – 6.38 (m, 14H). **^{19}F NMR** (376 MHz, c_6d_6) δ -94.93 (t, $J = 11.5$ Hz), -104.91 – -105.67 (m), -111.84 (d, $J = 8.8$ Hz), -112.11 (q, $J = 9.0$ Hz), -112.40 (dd, $J = 18.7, 9.0$ Hz), -112.57 (q, $J = 8.6$ Hz), -115.41 (dd, $J = 11.4, 8.7$ Hz), -116.78 (s).

6.2.8. Synthesis of 12,12',14,14'-tetrafluoro-11,11'-bihexahelicene



Scheme 19: Synthetic route towards fluorinated precursor 12,12',14,14'-tetrafluoro-11,11'-bihexahelicene.

Synthesis of 1,1'-difluoro-7,7'-dimethyl-2,2'-binaphthalene

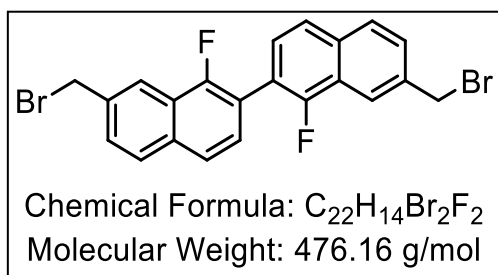


2,2,6,6-Tetramethylpiperidine (2.95 mL, 17.5 mmol, 1.6 equiv.) was added to THF (12 mL) at -78 °C under nitrogen atmosphere. Afterwards *n*-butyllithium (2.5 M in hexanes, 6.55 mL, 16.4 mmol, 1.5 equiv.) was added dropwise. After stirring for

30 min at -78 °C a solution of 1-fluoro-7-methylnaphthalene (1.75 g, 10.9 mmol, 1 equiv.) in THF (2 mL) was added dropwise and stirred for a further 30 min. CuBr₂ (2.44 g, 10.9 mmol, 1 equiv.) was added in one portion and the mixture was stirred for 45 min. Nitrobenzene (1.12 mL, 10.9 mmol, 1 equiv.) was added and the solution was allowed to reach rt over a period of 3 h. A sat. aqueous solution of NH₄Cl (4 x 100 mL) was added, phases were separated and the aqueous phase extracted with DCM (3 x 100 mL). The combined organic phases were dried over Na₂SO₄ and after filtrating the solvent was removed *in vacuo*. The product was purified by flash column chromatography on silica gel (*n*-hexane) and the resulting solid washed with methanol. The product was yielded as a white solid (952 mg, 55 %).

¹H NMR (400 MHz, chloroform-*d*) δ 8.00 (s, 1H), 7.82 (d, *J* = 8.4 Hz, 1H), 7.70 (d, *J* = 8.4 Hz, 1H), 7.59 – 7.48 (m, 1H), 7.42 (dd, *J* = 8.4, 1.6 Hz, 1H), 2.59 (s, 4H). **¹⁹F NMR** (377 MHz, chloroform-*d*) δ -124.81 (s).

Synthesis of 7,7'-bis(bromomethyl)-1,1'-difluoro-2,2'-binaphthalene

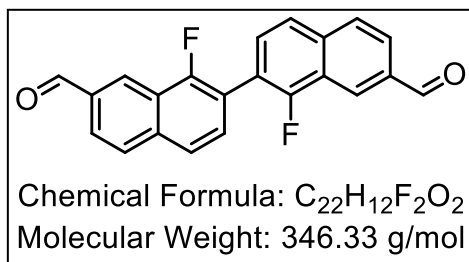


1,1'-difluoro-7,7'-dimethyl-2,2'-binaphthalene (504 mg, 1.58 mmol, 1 equiv.) and NBS (620 mg, 3.48 mmol, 2.4 equiv.) were reacted with DBPO (7.6 mg, 31.6 μmol, 0.02 equiv.) in fluorobenzene (25 mL) under reflux for 6 h. After cooling to rt, the

mixture was washed with water (3 x 50 mL) and dried over Na₂SO₄. After filtration and evaporation of the solvent, the crude product was purified by flash column chromatography on silica gel (*n*-hexane) and isolated as white solid (419 mg, 55 %).

¹H NMR (400 MHz, chloroform-*d*) δ 8.21 (s, 1H), 7.93 (d, *J* = 8.5 Hz, 1H), 7.76 (d, *J* = 8.5 Hz, 1H), 7.69 – 7.48 (m, 2H), 4.73 (s, 2H). **¹⁹F NMR** (377 MHz, chloroform-*d*) δ -123.50 (s).

Synthesis of 1,1'-difluoro-[2,2'-binaphthalene]-7,7'-dicarbaldehyde

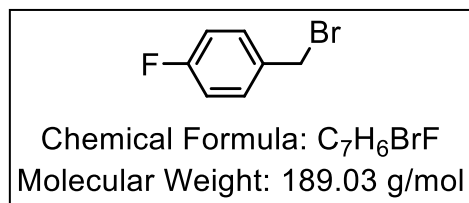


A chloroform solution (25 mL) of 7,7'-bis(bromomethyl)-1,1'-difluoro-2,2'-binaphthalene (525 mg, 1.10 mmol, 1 equiv.) and hexamethylenetetramine (464 mg, 3.31 mmol, 3 equiv.) was refluxed for 18 h. After cooling to rt the

solvent was removed *in vacuo*, a mixture of AcOH/H₂O (10 mL, 1:1 v:v) was added and stirred under reflux for 2 h. A sat. aqueous solution of NaHCO₃ (3 x 20 mL) was added, phases were separated and the aqueous phase extracted with DCM (3 x 20 mL). The combined organic phases were dried over Na₂SO₄ and after filtrating the solvent was removed *in vacuo*. The product was purified by flash column chromatography on silica gel (*n*-hexane/EtOAc 85:15 → 30:70) and isolated as yellow solid (84 mg, 22 %).

¹H NMR (400 MHz, chloroform-*d*) δ 10.23 (s, 1H), 8.73 (d, *J* = 1.5 Hz, 1H), 8.16 – 7.97 (m, 2H), 7.95 – 7.63 (m, 2H). **¹⁹F NMR** (377 MHz, chloroform-*d*) δ -121.18(s). **¹³C NMR** (101 MHz, cdcl₃) δ 191.74, 191.69, 134.73, 131.32, 128.74, 127.79, 126.92, 124.21, 123.92.

Synthesis of 1-(bromomethyl)-4-fluorobenzene

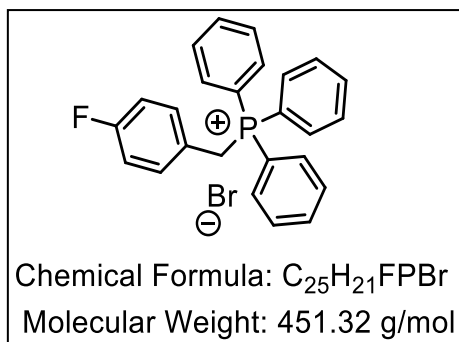


1-Fluoro-4-methylbenzene (10.0 g, 90.8 mmol, 1.0 equiv.) and NBS (17.7 g, 99.9 mmol, 1.1 equiv.) were reacted with DBPO (587 mg, 1.82 mmol, 0.02 equiv.) in fluorobenzene (200 mL) under reflux

for 24 h. The reaction mixture was filtered over silica gel (*n*-hexane) and the product was obtained as yellow oil (16.6 g, 97 %).

R_f = 0.56 (SiO₂, *n*-hexane). **¹H NMR** (400 MHz, chloroform-*d*) δ 7.66 – 7.56 (m, 2H), 7.33 – 7.20 (m, 2H), 4.71 (s, 2H). **¹⁹F NMR** (377 MHz, chloroform-*d*) δ -112.73 – -113.26 (m).

Synthesis of (4-fluorobenzyl)triphenyl-phosphonium bromide

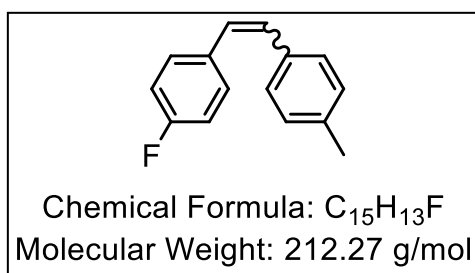


1-(Bromomethyl)-4-fluorobenzene (16.6 g, 87.8 mmol, 1 equiv.) and triphenylphosphine (30.0 g, 114 mmol, 1.3 equiv.) were reacted in toluene (250 mL) for 60 h under reflux. The suspension was filtered by suction filtration, the resulting solid was washed with toluene and dried *in vacuo*. The product was isolated as white solid (28.0 g, 73 %).

1H NMR (400 MHz, chloroform-*d*) δ 7.90 – 7.46 (m, 15H), 7.16 (dd, $J = 7.3, 3.6$ Hz, 2H), 6.90 – 6.72 (m, 2H), 5.54 (d, $J = 14.3$ Hz, 2H).

^{19}F NMR (377 MHz, chloroform-*d*) δ -112.97 (s). **^{31}P NMR** (162 MHz, chloroform-*d*) δ 23.32 (d, $J = 6.5$ Hz).

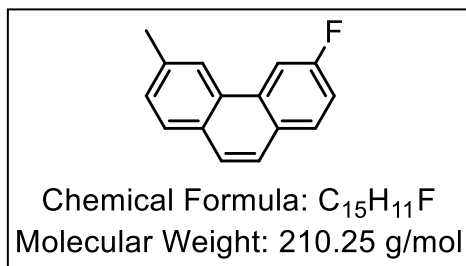
Synthesis of 1-fluoro-4-(4-methylstyryl)benzene



(4-Fluorobenzyl)triphenylphosphonium bromide (14.0 g, 32.0 mmol, 1 equiv.), 4-methylbenzaldehyde (4.15 mL, 35.2 mmol, 1.1 equiv.) and potassium *tert*-butoxide (3.95 g, 35.2 mmol, 1.1 equiv.) were reacted in *iso*-propanol (250 mL) for 24 h according to general procedure 2a. The mixture was filtrated through silica gel (*n*-hexane) and both *E*- and *Z*- isomer of 1-fluoro-4-(4-methylstyryl)benzene were obtained as white solid (4.4 g, 65 %).

$R_f = 0.45; 0.63$ (SiO_2 , *n*-hexane). **1H NMR** (400 MHz, chloroform-*d*) δ 7.47 (dd, $J = 8.8, 5.4$ Hz), 7.40 (d, $J = 8.2$ Hz), 7.24 – 7.10 (m), 7.09 – 6.99 (m), 6.96 – 6.88 (m), 6.53 (q, $J = 12.2$ Hz), 2.37 (s, 3H), 2.32 (s, 3H). **^{19}F NMR** (376 MHz, $cdCl_3$) δ -104.26 (tt, $J = 8.4, 5.4$ Hz), -113.25 – -115.65 (m). **^{13}C NMR** (101 MHz, $cdCl_3$) δ 144.62, 132.88, 132.79, 130.23, 130.12, 129.39, 129.20, 129.02, 127.84, 127.76, 127.15, 126.81, 126.47, 126.33, 115.80, 115.65, 115.58, 115.43, 77.31, 76.99, 76.67, 21.73, 21.22.

Synthesis of 3-fluoro-6-methylphenanthrene

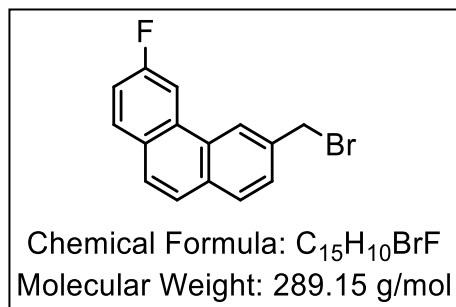


1-Fluoro-4-(4-methylstyryl)benzene (1.00 g, 4.71 mmol), iodine (1.32 g, 5.18 mmol, 1 equiv.) and propylene oxide (3.3 mL, 51.8 mmol, 10 equiv.) were reacted in cyclohexane for 8 h according to general procedure 3. The product was purified by

flash column chromatography on silica gel (*n*-hexane) and isolated as white solid (473 mg, 48 %).

R_f = 0.45 (SiO₂, *n*-hexane). **¹H NMR** (400 MHz, chloroform-*d*) δ 8.34 (s, 1H), 8.28 (dd, *J* = 11.2, 2.3 Hz, 1H), 7.85 (dd, *J* = 8.7, 6.0 Hz, 1H), 7.79 (d, *J* = 8.1 Hz, 1H), 7.66 (s, 2H), 7.46 (d, *J* = 9.2 Hz, 1H), 7.40 – 7.30 (m, 1H), 2.63 (s, 3H). **¹⁹F NMR** (377 MHz, chloroform-*d*) δ -113.80 – -114.03 (m). **¹³C NMR** (100 MHz, chloroform-*d*) δ 161.49 (d, *J* = 244.8 Hz), 136.40, 131.52 (d, *J* = 8.3 Hz), 130.48 (d, *J* = 9.0 Hz), 130.15, 129.76 (d, *J* = 4.3 Hz), 128.92, 128.45, 125.94 (d, *J* = 2.6 Hz), 125.33, 122.57, 115.44 (d, *J* = 23.8 Hz), 107.69 (d, *J* = 22.1 Hz), 22.08.

Synthesis of 3-(bromomethyl)-6-fluorophenanthrene



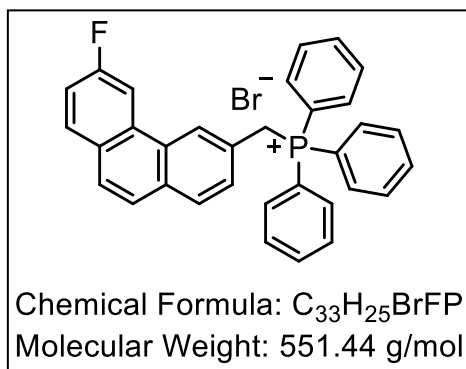
3-Fluoro-6-methylphenanthrene (350 mg, 1.66 mmol, 1 equiv.) and NBS (295 mg, 1.66 mmol, 1 equiv.) were reacted with DBPO (8.0 mg, 33.2 μmol, 0.02 equiv.) in fluorobenzene (10 mL) for 4 h under reflux. Water (3 x 20 mL) was added, phases were separated and the aqueous phase

extracted with DCM (3 x 20 mL). The combined organic phases were dried over Na₂SO₄ and after filtrating the solvent was removed *in vacuo*. The product was purified by flash column chromatography on silica gel (*n*-hexane) and isolated as white solid (151 mg, 31 %).

R_f = 0.56 (SiO₂, *n*-hexane). **¹H NMR** (400 MHz, chloroform-*d*) δ 8.55 (s, 1H), 8.29 (dd, *J* = 11.0, 2.6 Hz, 1H), 7.94 – 7.79 (m, 1H), 7.79 – 7.56 (m, 2H), 7.48 – 7.31 (m, 1H), 4.77 (s, 1H).

Synthesis of ((6-fluorophenanthren-3-yl)methyl)triphenylphosphonium bromide

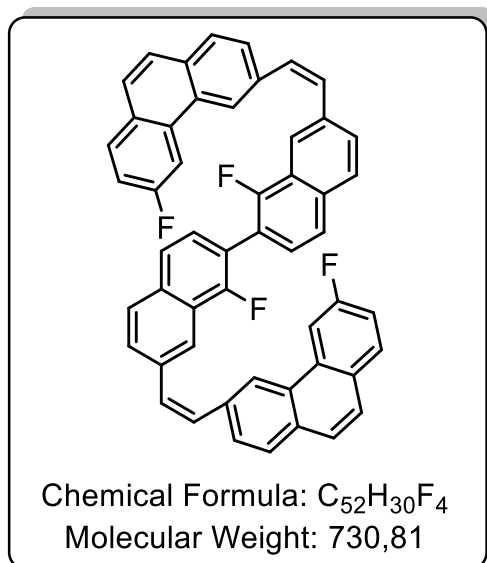
3-(Bromomethyl)-6-fluorophenanthrene (140 mg, 0.484 mmol, 1 equiv.) and triphenylphosphine (190 mg, 0.726 mmol, 1.5 equiv.) were reacted in toluene (10 mL)



for 16 h at 120 °C. After cooling to rt, the resulting precipitate was collected by suction filtration, washed with toluene (50 mL) and dried *in vacuo*. The product was obtained as white solid (236 mg, 88 %).

1H NMR (400 MHz, chloroform-*d*) δ 8.01 (d, J = 3.2 Hz, 1H), 7.89 – 7.70 (m, 10H), 7.70 – 7.54 (m, 10H), 7.48 (d, J = 8.9 Hz, 1H), 7.30 – 7.22 (m, 1H), 5.79 (d, J = 14.6 Hz, 2H). ^{19}F NMR (377 MHz, chloroform-*d*) δ -112.64 (d, J = 10.3 Hz). ^{31}P NMR (162 MHz, chloroform-*d*) δ 23.11 (s).

Synthesis of (6,6'-((1,1'-difluoro-[2,2'-binaphthalene]-7,7'-diyl)bis(ethene-2,1-diyl))bis(3-fluorophenanthrene)

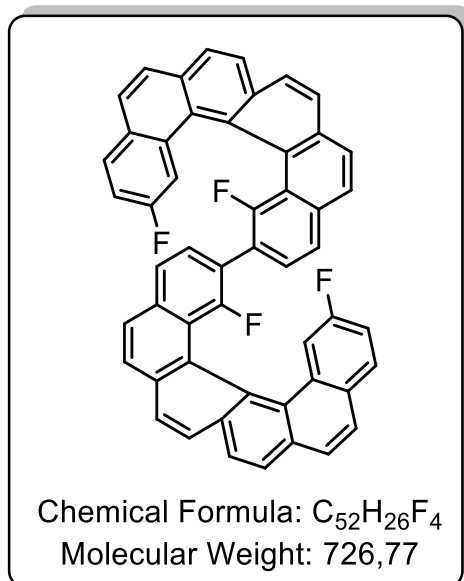


A solution of 1,1'-difluoro-[2,2'-binaphthalene]-7,7'-dicarbaldehyde (104 mg, 0.300 mmol, 1 equiv.), bromo((6-fluorophenanthren-3-yl)methyl)triphenylphosphine (364 mg, 0.661 mmol, 2.2 equiv.) in chloroform (10 mL) was reacted with an aqueous solution of KOH (50 %, 4 mL) for 18 h according to general procedure 2b. The (E) and (Z)-products were purified by flash column chromatography on silica gel (*n*-hexane: DCM 5:1) and isolated as a white solid (137 mg, 63 %).

1H NMR (400 MHz, chloroform-*d*) δ 8.57 (s, 1H), 8.41 (s, 1H), 8.34 – 8.15 (m, 1H), 8.10 (s), 8.03 – 6.97 (m), 5.21 (s, 1H), 4.94 (d, J = 3.3 Hz, 1H).

^{19}F NMR (377 MHz, chloroform-*d*) δ -113.19, -123.93.

Synthesis of 12,12',14,14'-tetrafluoro-11,11'-bihexahelicene



(6,6'-((1,1'-difluoro-[2,2'-binaphthalene]-7,7'-diyl)bis(ethene-2,1-diyl))bis(3-fluorophenanthrene) (200 mg, 273 μ mol), iodine (208 mg, 821 μ mol, 3 equiv.) and propylene oxide (383 mL, 5.47 mmol, 20 equiv.) were reacted in cyclohexane for 4 h according to general procedure 3. The product was purified by HPLC (PBr(semi), toluene:methanol 1:1) and isolated as yellow solid (11.3 mg, 6 %, t_R = 8 min).

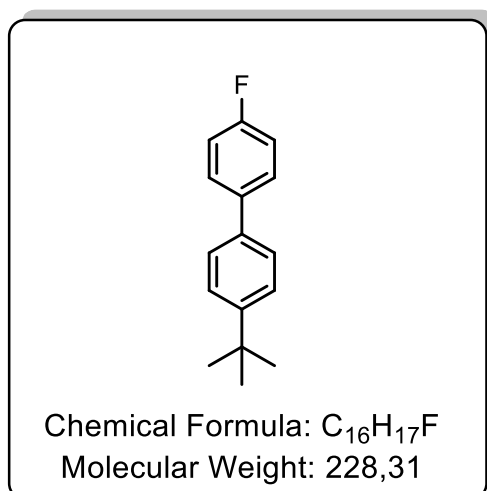
1H NMR (400 MHz, CD_2Cl_2) δ 9.04 (s, 1H), 8.45 (d, J = 11.4 Hz, 1H), 8.35 (d, J = 14.9 Hz, 1H), 8.25 (t, J = 7.8 Hz, 1H), 8.19 – 8.11 (m, 2H), 8.10 (d, J = 8.8 Hz, 2H), 7.98 – 7.76 (m, 6H), 7.72 – 7.53 (m, 2H), 7.50 – 7.32 (m, 1H), 7.28 – 6.95 (m, 9H).

^{19}F NMR (377 MHz, CD_2Cl_2) δ -114.20, -117.83.

6.3. Oxodefluorination of fluoroarenes

6.3.1. Synthesis of 2,8-bis(4-(tert-butyl)phenyl)dibenzo[b,d]furan

Synthesis of 4-(tert-butyl)-4'-fluoro-1,1'-biphenyl

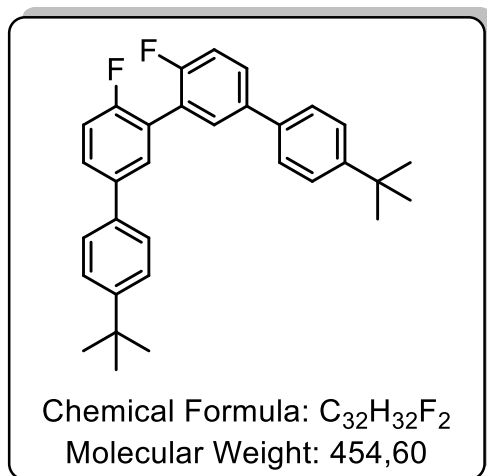


1-bromo-4-fluorobenzene (0.62 mL, 5.71 mmol, 1 equiv.), (4-(tert-butyl)phenyl)boronic acid (1.12 g, 6.29 mmol, 1.1 equiv.), Cs_2CO_3 (3.72 g, 11.4 mmol, 2 equiv.) were reacted in THF/ H_2O (24 mL, 5:1) with $Pd(PPh_3)_2Cl_2$ (80 mg, 115 μ mol, 0.02 equiv.) for 20 h under reflux. After cooling to rt, water was added, phases were separated and the aqueous layer extracted with DCM. The combined organic fractions were dried over

Na₂SO₄, filtrated and the solvent removed in vacuo. The crude product was purified by flash column chromatography on silica gel with *n*-hexane to afford the product as a white solid (1.17 g, 90 %).

¹H NMR (400 MHz, CDCl₃) δ 7.57 – 7.52 (m, 2H), 7.52 – 7.44 (m, 4H), 7.15 – 7.08 (m, 2H), 1.37 (s, 9H). **¹⁹F NMR** (376 MHz, CDCl₃) δ -116.23 – -116.40 (m). **¹³C NMR** (101 MHz, CDCl₃) δ 163.51, 161.07, 150.27, 137.32, 137.16, 137.13, 128.51, 128.43, 126.62, 125.74, 115.61, 115.39, 77.30, 76.98, 76.67, 34.51, 31.33.

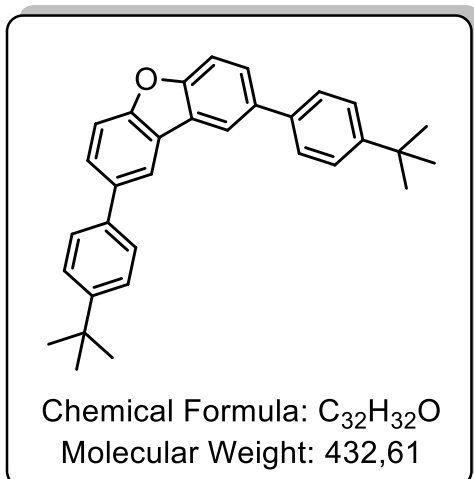
Synthesis of 4,4'''-di-tert-butyl-4',6''-difluoro-1,1':3',1'':3'',1'''-quaterphenyl



Under dry conditions, anhydrous THF (6mL) was cooled to -78°C. TMP (1.38 mL, 8.20 mmol, 1.6 equiv.) and *n*-Butyllithium (3.07 mL, 2.5 M in hexane, 7.69 mmol, 1.5 equiv.) was added und stirred for 30 min.. 4-(tert-butyl)-4'-fluoro-1,1'-biphenyl (1.17 g, 5.12mmol) was reacted with the solution for 30 min.. Afterwards copper(II) bromide (1.14 g, 5.12 mmol, 1 equiv.) was added and stirred for 45 min.. Lastly, nitrobenzene (0.525 mL, 5,12mmol, 1 equiv.) was reacted with the mixture for 3h at rt. The reaction was quenched with water (30 mL), DCM (30 mL) was added and the organic phase was separated. The organic phase was dried over Na₂SO₄, and the solvent removed in vacuo. Column chromatography (silica gel; *n*-hexane) yielded the product as a white solid (198 mg, 8%).

¹H NMR (400 MHz, CDCl₃) δ 7.65 – 7.62 (m, 2H), 7.61 – 7.56 (m, 2H), 7.55 – 7.50 (m, 4H), 7.50 – 7.44 (m, 4H), 7.23 (d, *J* = 8.8 Hz, 2H), 1.36 (s, 18H). **¹⁹F NMR** (376 MHz, CDCl₃) δ -117.54 – -117.75 (m). **¹³C NMR** (101 MHz, CDCl₃) δ 150.45, 137.03, 130.18, 130.16, 130.13, 128.30, 128.25, 128.21, 126.69, 125.77, 34.65, 31.32.

Synthesis of 2,8-bis(4-(tert-butyl)phenyl)dibenzo[b,d]furan

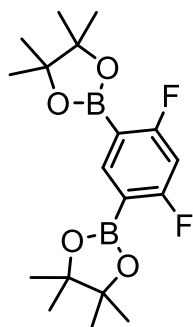


4,4''-di-tert-butyl-4',6''-difluoro-1,1':3',1'':3'',1'''-quaterphenyl (100 mg, 219 μ mol, 1 equiv.) was reacted with potassium tert-butoxide (148 mg, 1.32 mmol, 6 equiv.) in HMPA (5mL) at 120 °C for 3 h in the microwave. The mixture was directly purified by flash column chromatography (silica gel; *n*-hexane to *n*-hexane / ethyl acetate 1:1) to afford the product as a white solid (54.6 mg, 57 %).

¹H NMR (400 MHz, CDCl₃) δ 8.17 (d, *J* = 1.9 Hz, 2H), 7.72 – 7.68 (m, 2H), 7.63 (tt, *J* = 5.3, 2.7 Hz, 6H), 7.54 – 7.50 (m, 4H), 1.40 (s, 18H).

¹³C NMR (101 MHz, CDCl₃) δ 156.10, 150.07, 138.36, 136.31, 127.02, 126.61, 125.78, 124.76, 118.97, 111.77, 34.53, 31.38.

Synthesis of 2,2'-(4,6-difluoro-1,3-phenylene)bis(4,4,5,5-tetramethyl-1,3,2-dioxaborolane)



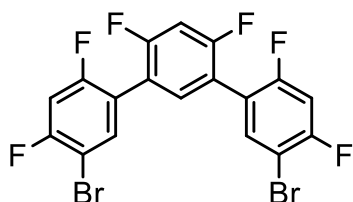
Chemical Formula: $C_{18}H_{26}B_2F_2O_4$
Molecular Weight: 366,02

Under nitrogen atmosphere, 1,5-dibromo-2,4-difluorobenzene (1.76 g, 6.47 mmol, 1 equiv.), bis(pinacolato)diboron (4.93 g, 19.4 mmol, 3 equiv.), potassium acetate (2.54 g, 25.9 mmol, 4 equiv.) were reacted in 1,4-dioxane (40 mL) with $Pd(dppf)Cl_2$ (98 mg, 129 μ mol, 0.02 equiv.) for 16 h under reflux. After cooling to rt, water was added, phases were separated and the aqueous

layer extracted with CH_2Cl_2 (3 x 50 mL). The combined organic fractions were dried over Na_2SO_4 , filtered and the solvent removed *in vacuo*. The product was purified by recrystallization in ethanol and isolated as a white solid (1.32 g 56 %).

1H NMR (400 MHz, $cdCl_3$) δ 8.13 (t, $J = 7.6$ Hz, 1H), 6.72 (t, $J = 9.7$ Hz, 1H), 1.48 (s, 4H), 1.35 (s, 20H). **^{19}F NMR** (376 MHz, $cdCl_3$) δ -94.12 – -94.27 (m). **^{13}C NMR** (101 MHz, $cdCl_3$) δ 145.92, 145.81, 145.71, 103.67, 103.40, 103.13, 83.92, 24.79.

Synthesis of 5,5''-dibromo-2,2'',4,4',4'',6'-hexafluoro-1,1':3',1''-terphenyl



Chemical Formula: $C_{18}H_6Br_2F_6$
Molecular Weight: 496,04

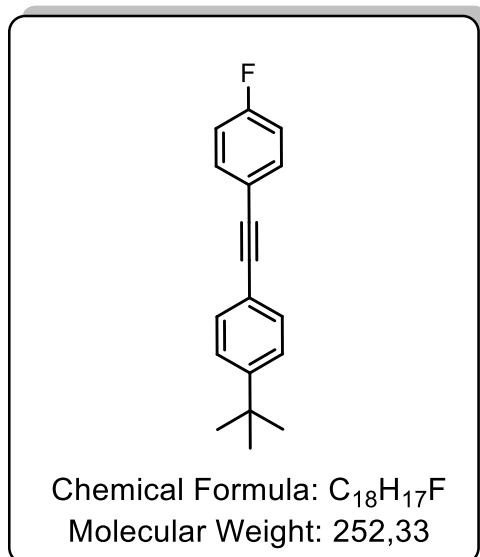
2,2'-(4,6-difluoro-1,3-phenylene)bis(4,4,5,5-tetramethyl-1,3,2-dioxaborolane) (528 mg, 1.44 mmol, 1 equiv.), 1,5-dibromo-2,4-difluorobenzene (1.57g, 5.77mmol, 4 equiv.) potassium carbonate (4 g, 49.1 mmol, 34 equiv.) were reacted in H_2O / 1,4-dioxane (15mL/ 30 mL) with $Pd(PPh_3)_2Cl_2$ (20.3 mg, 28.9 μ mol, 0.02

equiv.) for 3 h under reflux. After cooling to rt, water was added, phases were separated and the aqueous layer extracted with CH_2Cl_2 (3 x 50 mL). The combined organic fractions were dried over Na_2SO_4 , filtered and the solvent removed *in vacuo*. The crude product was purified by flash column chromatography on silica gel with *n*-hexane/DCM 2:1 to afford the product as a yellow solid (44.7 mg, 6 %).

1H NMR (400 MHz, $cdCl_3$) δ 7.66 – 7.51 (m, 2H), 7.41 – 7.27 (m, 3H), 7.10 – 6.90 (m, 1H). **^{19}F NMR** (376 MHz, $cdCl_3$) δ -83.55 – -83.91 (m), -89.41 – -89.68 (m), -101.67 (d,

$J = 8.0$ Hz), -102.37 – -102.59 (m), -102.87 – -103.04 (m), -109.14 – -111.23 (m), -115.04 – -115.24 (m), -121.23 – -121.63 (m), -134.87 (dd, $J = 14.0, 5.6$ Hz). ^{13}C NMR (101 MHz, CDCl_3) δ 134.70, 134.64, 134.57, 131.08, 130.85, 130.61, 130.38, 130.21, 128.00, 127.95, 127.90.

Synthesis of 1-(tert-butyl)-4-((4-fluorophenyl)ethynyl)benzene



1-ethynyl-2-fluorobenzene (254 mg, 2.11 mmol, 1.1 equiv.), 1-tert-butyl-4-iodo-benzene (0,37 mL, 1.92 mmol, 1 equiv.), Cs_2CO_3 (1.25 g, 3.84 mmol, 2 equiv.) and copper(I) iodide (37 mg, 0.192 mmol, 0.1 equiv.) were reacted in N-methylpyrrolidinone (6 mL) for 4 h at 195 °C in a microwave. The reaction mixture was cooled to rt and the solvent was removed in vacuo. The crude product was purified by flash column chromatography on silica gel with *n*-hexane to afford the product (187 mg, 39 %).

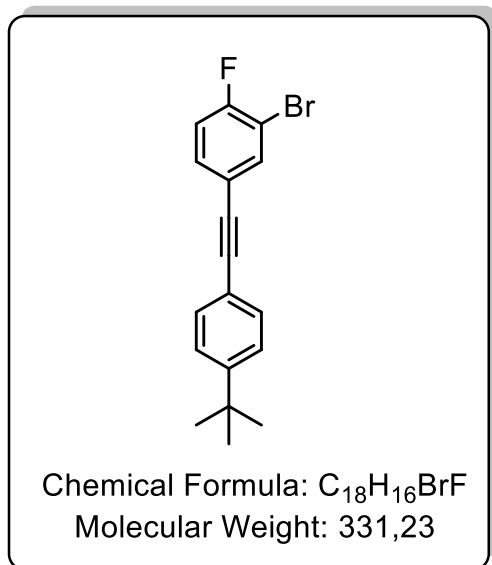
^1H NMR (500 MHz, CDCl_3) δ 7.55 – 7.44 (m, 4H), 7.39 (d, $J = 8.1$ Hz, 2H), 7.05 (t, $J = 8.6$ Hz, 2H), 1.35 (d, $J = 0.7$ Hz, 9H).

^{19}F NMR (470 MHz, CDCl_3) δ -110.97 – -111.96 (m).

^{13}C NMR (126 MHz, CDCl_3) δ 163.37, 161.39, 151.61, 133.44, 133.37, 131.28, 125.36, 120.06, 119.64, 119.61, 115.65, 115.47, 89.20, 89.19, 87.64, 34.79, 31.16.

Procedure was done according to literature.⁸⁷

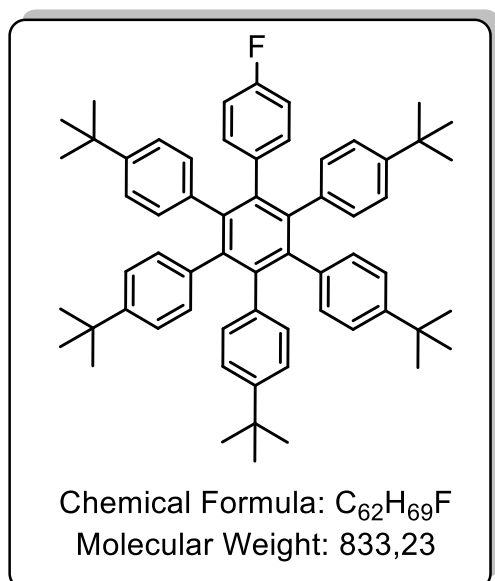
Synthesis of 2-bromo-4-((4-(tert-butyl)phenyl)ethynyl)-1-fluorobenzene



2-bromo-1-fluoro-4-iodobenzene (749 mmL, 3.66 mmol, 1.0 equiv.), 1-(tert-butyl)-4-ethynylbenzene (636 mg, 4.02 mmol, 1.1 equiv.) and Cs_2CO_3 (2.38 g, 7.31 mmol, 2 equiv.) were reacted with copper(I)iodide (69.6mg, 365 μ mol, 0.1 equiv.) N-methylpyrrolidinone (6 mL) for 4 h at 200 °C in a microwave. The reaction mixture was cooled to rt and the solvent was removed in vacuo. The crude product was purified by flash column chromatography on silica gel with *n*-hexane to afford the product (208 mg, 17 %)

1H NMR (400 MHz, $cdCl_3$) δ 7.69 (dd, J = 6.7, 2.1 Hz, 2H), 7.53 – 7.41 (m, 12H), 7.39 (ddd, J = 6.4, 4.0, 2.0 Hz, 9H), 7.11 – 7.03 (m, 3H), 1.34 (d, J = 0.8 Hz, 4H). **^{19}F NMR** (376 MHz, $cdCl_3$) δ -108.86 (ddd, J = 9.0, 6.8, 4.9 Hz). **^{13}C NMR** (101 MHz, $cdCl_3$) δ 163.28, 160.75, 152.06, 151.73, 136.45, 136.44, 132.80, 132.72, 131.46, 131.30, 126.93, 125.71, 125.34, 119.87, 119.80, 119.76, 119.65, 115.82, 115.60, 86.92, 81.23, 34.65, 31.57.

Synthesis of 4,4''-di-tert-butyl-3',4',5'-tris(4-(tert-butyl)phenyl)-6'-(4-fluorophenyl)-1,1':2',1''-terphenyl



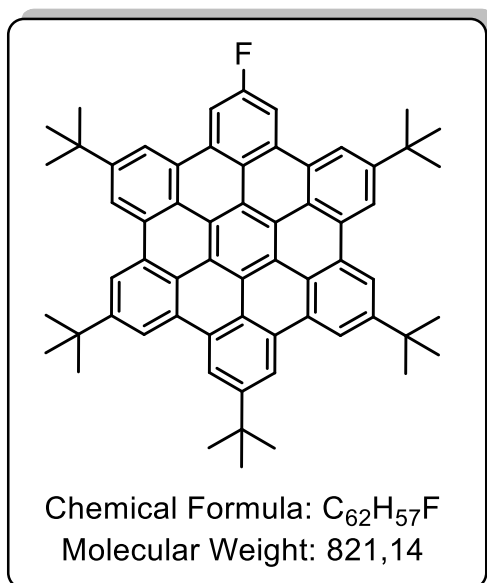
2,3,4,5-tetrakis(4-(tert-butyl)phenyl)cyclopenta-2,4-dien-1-one (400 mg, 656 μ mol, 1 equiv.), 1-(tert-butyl)-4-((4-fluorophenyl)ethynyl)benzene 166 mg, 657 μ mol, 1 equiv.) were reacted in biphenyl oxide (15 mL) for 4 d under reflux. After cooling to rt, methanol was added and phases were separated. The methanol fractions were dried over Na_2SO_4 , filtered and the solvent removed *in vacuo*. The crude product was purified by flash column chromatography on silica gel with *n*-hexane to afford the product as

a white solid (419 mg, 77 %).

1H NMR (400 MHz, $cdCl_3$) δ 6.82 (ddd, J = 14.0, 11.1, 7.0 Hz, 12H), 6.68 (dt, J = 9.6,

5.2 Hz, 10H), 6.54 (t, $J = 8.9$ Hz, 2H), 1.12 (d, $J = 8.8$ Hz, 45H). **^{19}F NMR** (376 MHz, cdcl_3) δ -118.34 (tt, $J = 9.0, 5.6$ Hz). **^{13}C NMR** (101 MHz, cdcl_3) δ 161.73, 159.31, 147.69, 147.45, 147.40, 140.66, 140.64, 140.26, 138.70, 137.80, 137.70, 137.03, 136.99, 133.03, 132.95, 131.05, 131.01, 130.99, 129.69, 123.26, 123.18, 123.04, 123.00, 118.86, 113.36, 113.15, 34.07, 34.02, 31.17.

Synthesis of 2,5,8,11,14-penta-tert-butyl-17-fluorohexa-benzo[bc,ef,hi,kl,no,qr]coronene



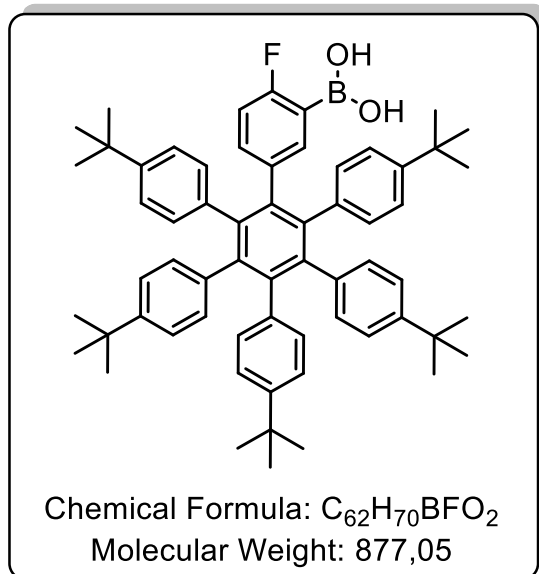
A mixture of 4,4''-di-tert-butyl-3',4',5'-tris(4-(tert-butyl)phenyl)-6'-(4-fluorophenyl)-1,1':2,1''-terphenyl (236 mg, 283 μmol , 1 equiv.) and DDQ (1.29g, 5.66 mmol, 20 equiv.) was degassed twice with argon. Anhydrous DCM (35 mL) was added and degassed again. The solution was cooled to 0°C and trifluoromethanesulfonic acid (497 μL , 5.66 mmol, 20 equiv.) was added slowly. The solution was stirred for 2 h and quenched with hydrogen carbonate solution (20 mL). The

phases were separated and the aqueous layer extracted with CH_2Cl_2 (2 x 20 mL). The combined organic fractions were dried over Na_2SO_4 , filtered and the solvent removed *in vacuo*. The crude product was purified by flash column chromatography on silica gel with *n*-hexane/DCM 1:1 to afford the product as a white solid (125 mg, 53 %).

^1H NMR (400 MHz, cdcl_3) δ 9.24 (d, $J = 12.0$ Hz, 4H), 9.15 (d, $J = 12.4$ Hz, 4H), 8.88 (s, 2H), 8.53 (d, $J = 10.2$ Hz, 2H), 1.87 (s, 7H), 1.85 (s, 19H), 1.78 (s, 19H). **^{19}F NMR** (376 MHz, cdcl_3) δ -113.79 (s). **^{13}C NMR** (101 MHz, cdcl_3) δ 152.44, 148.74, 130.33, 130.29, 130.11, 130.05, 129.36, 129.23, 123.62, 123.57, 123.53, 120.27, 119.42, 119.24, 119.19, 118.79, 118.77, 118.67, 114.53, 110.00, 107.92, 34.65, 32.04, 31.99.

This method was used according to Lungerich et al.¹¹⁷

Synthesis of (4''-(tert-butyl)-3',4',5',6'-tetrakis(4-(tert-butyl)phenyl)-4-fluoro-[1,1':2',1''-terphenyl]-3-yl)boronic acid



2,2,6,6-Tetramethylpiperidine (136 mL, 805 μ mol, 1.6 equiv.) was added to THF (3 mL) at -78 °C. Afterwards *n*-butyllithium (2.5 M in hexane, 302 mL, 754 μ mol, 1.5 equiv.) was added dropwise. After stirring for 30 min at 78 °C, a solution of 4,4''-di-tert-butyl-3',4',5'-tris(4-(tert-butyl)phenyl)-6''-(4-fluorophenyl)-1,1':2',1''-terphenyl (419 mg, 503 μ mol, 1 equiv.), in THF (3 mL) was added dropwise and stirred for 30 min. Trimethyl borate (286 mL, 2.51 mmol, 5 equiv.) was added

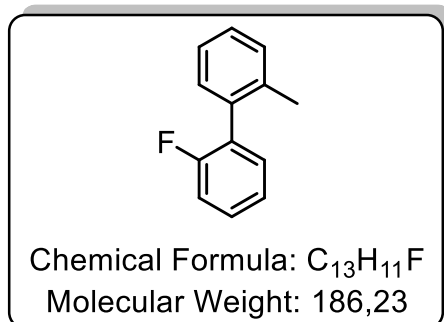
dropwise, the solution was allowed to warm to rt and stirred for 3 h. After quenching with HCl (1 M, 6 mL) and stirring for 10 min, water (30 mL) was added and the organic phase separated. The aqueous phase was extracted with DCM (2 x 25 mL). The combined organic phases were dried over Na_2SO_4 and after filtrating, the solvent was removed *in vacuo*. The crude product was purified by flash column chromatography on silica gel (*n*-hexanes \rightarrow *n*-hexanes/DCM 1:1 \rightarrow DCM \rightarrow DCM/EtOAc 20:1 \rightarrow DCM/EtOAc 10:1 \rightarrow DCM/EtOAc 5:1 \rightarrow DCM/EtOAc 1:1) to afford the product as a white solid (19 mg, 4 %).

1H NMR (500 MHz, $cdCl_3$) δ 6.86 (t, $J = 8.7$ Hz, 4H), 6.82 – 6.77 (m, 6H), 6.73 – 6.63 (m, 10H), 6.55 (dd, $J = 10.7, 8.5$ Hz, 1H), 6.50 (dd, $J = 8.7, 2.1$ Hz, 1H), 6.34 (ddd, $J = 8.4, 4.7, 2.1$ Hz, 1H), 4.59 (d, $J = 4.0$ Hz, 2H), 1.11 (d, $J = 15.1$ Hz, 45H). **^{19}F NMR** (470 MHz, $cdCl_3$) δ -145.45 – -145.57 (m). **^{13}C NMR** (126 MHz, $cdCl_3$) δ 149.79, 147.91, 147.70, 147.43, 147.38, 141.68, 141.57, 140.70, 140.58, 140.12, 138.48, 138.07, 138.04, 137.77, 137.76, 137.62, 130.97, 130.83, 124.40, 124.35, 123.34, 123.18, 123.02, 122.99, 120.47, 113.47, 113.33, 34.09, 34.02, 34.01, 31.17, 31.16.

6.4. Construction of zig-zag periphery by C_{sp^3} - C_{aryl} coupling *via* AmCFA

6.4.1. Reactions with small molecules

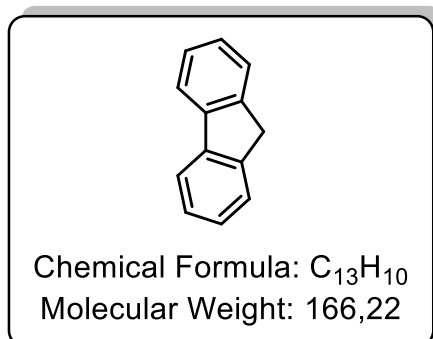
Synthesis of 2-fluoro-2'-methyl-1,1'-biphenyl



A 100 mL round bottom flask equipped with a magnetic stir bar and a condenser was charged with 2-bromotoluene (610 mg, 3.57 mmol), 2-fluorophenylboronic acid (500 mg, 3.57 mmol), K_2CO_3 (2.96 g, 21.4 mmol) and $Pd(PPh_3)_4$ (107 mg, 92 μ mol). The solids were suspended in 6:4/1 toluene/MeOH/H₂O (55 mL), degassed and the atmosphere was exchanged by argon. The mixture was brought to reflux for 16 h. The solvent was evaporated and the product was purified by silica gel column chromatography, eluting with cyclohexane yielding 2-fluoro-2'-methyl-1,1'-biphenyl as colorless oil in 68 % yield (450 mg, 2.42 mmol).

1H NMR (400 MHz, $CDCl_3$) δ 7.25 – 7.09 (m, 6H), 7.06 (td, J = 7.4, 1.2 Hz, 1H), 7.01 (ddd, J = 9.5, 8.2, 1.1 Hz, 1H), 2.10 (d, J = 1.2 Hz, 3H). **^{19}F NMR** (377 MHz, $CDCl_3$) δ -114.67 (s, 1F). **^{13}C NMR** (101 MHz, $CDCl_3$) δ 159.6 (d, J = 245.7 Hz), 136.6, 135.7, 131.5 (d, J = 3.7 Hz), 130.0, 129.9, 129.3 (d, J = 16.7 Hz), 129.0 (d, J = 8.0 Hz), 127.9, 125.6, 123.9 (d, J = 3.6 Hz), 115.5 (d, J = 22.5 Hz), 19.9 (d, J = 2.8 Hz).

Synthesis of 9H-fluorene



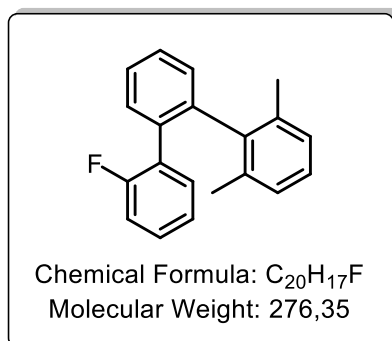
The compound was obtained according to the general procedure using 2-fluoro-2'-methyl 1,1'-biphenyl (20 mg) as a white solid (13.4 mg, 75 %). **1H NMR** (400 MHz, $CDCl_3$) δ 7.82 (d, J = 7.5 Hz, 2H), 7.58 (d, J = 7.4 Hz, 2H), 7.41 (t, J = 7.3 Hz, 2H), 7.33 (td, J = 7.4, 1.1 Hz, 2H), 3.93 (s, 2H). The spectroscopic data were consistent with previously

reported

Synthesis of 2-fluoro-2'-isopropyl-1,1'-biphenyl.¹⁰¹

A 100 mL round bottom flask equipped with a magnetic stir bar and a condenser was charged with 1-iodo-2-isopropylbenzene (500 mg, 2 mmol), 2-fluorophenylboronic acid (280 mg, 2.0 mmol), K_2CO_3 (1.1 g, 8.0 mmol) and $Pd(PPh_3)_4$ (84 mg, 72 μ mol). The solids were suspended in 3/1/0.3 toluene/MeOH/H₂O (18.5 mL), degassed and the atmosphere was exchanged by argon. The mixture was brought to reflux for 16 h. The solvent was evaporated and the product was purified by silica gel column chromatography, eluting with cyclohexane yielding 2-fluoro-2'-isopropyl-1,1'-biphenyl as orange solid in 16 % yield (70 mg, 0.32 mmol). **¹H NMR** (400 MHz, CDCl₃) δ 7.45 – 7.32 (m, 3H), 7.29 – 7.09 (m, 5H), 2.89 – 2.82 (m, 1H), 1.23 (d, J = 6.6 Hz, 3H), 1.11 (d, J = 6.7 Hz, 3H). **¹⁹F NMR** (376 MHz, CDCl₃) δ -114.35 (dt, J = 8.3, 6.3 Hz). **¹³C NMR** (101 MHz, CDCl₃) δ 159.7 (d, J = 245.0 Hz), 147.3, 134.4, 131.8 (d, J = 3.6 Hz), 130.1, 129.3 (d, J = 17.1 Hz), 128.9 (d, J = 7.9 Hz), 128.3, 125.4, 125.3, 123.8 (d, J = 3.8 Hz), 115.5, 30.2, 24.5, 23.4.

Synthesis of 2''-fluoro-2,6-dimethyl-1,1':2',1''-terphenyl

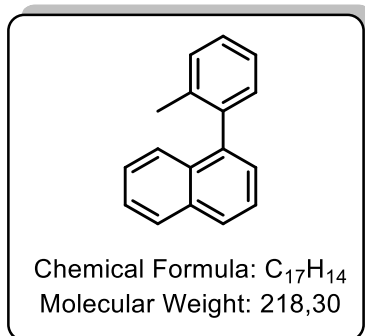


(2'-fluoro-[1,1'-biphenyl]-2-yl)boronic acid (100mg, 463 μ mol, 1 equiv.), 2-bromo-1,3-dimethylbenzene (62mL, 463 μ mol, 1 equiv.) and Cs_2CO_3 (302 mg, 926 μ mol, 2 equiv.) were reacted in THF/H₂O (12 mL, 5:1) with $Pd(PPh_3)_2Cl_2$ (27 mg, 23 μ mol, 0.05 equiv.) for 48 h under reflux. After cooling to rt water was added, phases were separated and the aqueous layer extracted with

DCM. The combined organic fractions were dried over Na_2SO_4 , filtrated and the solvent removed in vacuo. The crude product was purified by flash column chromatography on silica gel with *n*-hexane to afford the product as a mixture. The mixture was further purified by HPLC. The product was successfully isolated (22 mg, 17 %).

¹H NMR (500 MHz, CDCl₃) δ 7.49 – 7.43 (m, 3H), 7.26 – 7.23 (m, 1H), 7.14 (dddd, J = 8.2, 7.1, 5.1, 1.9 Hz, 1H), 7.04 (dd, J = 7.9, 7.1 Hz, 1H), 6.99 – 6.93 (m, 4H), 6.92 – 6.87 (m, 1H), 1.99 (s, 6H). **¹⁹F NMR** (470 MHz, CDCl₃) δ -115.50 – -115.65 (m).

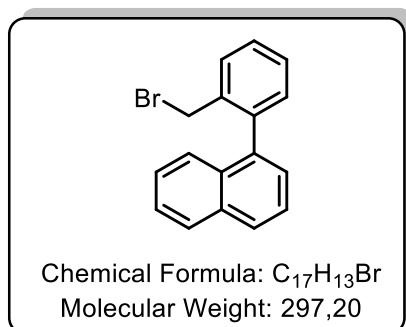
Synthesis of 1-(*o*-tolyl)naphthalene



1-Bromo-2-methylbenzene (2.71 g, 1.91 mL, 15.9 mmol, 1 equiv.), naphthalen-1-ylboronic acid (3.00 g, 17.4 mmol, 1.1 equiv.), Cs₂CO₃ (10.3 g, 31.7 mmol, 2 equiv.) were reacted in THF/H₂O (36 mL, 5:1) with Pd(PPh₃)₂Cl₂ (222 mg, 0.317 mmol, 0.02 equiv.) for 18 h under reflux. After cooling to rt water was added, phases were separated and the aqueous layer extracted with DCM. The combined organic fractions were dried over Na₂SO₄, filtrated and the solvent removed in vacuo. The crude product was purified by flash column chromatography on silica gel with *n*-hexane to afford the product as a white solid (2.45 g, 71 %).

R_f = 0.50 (SiO₂, *n*-hexane) **¹H NMR** (400 MHz, CDCl₃) δ 8.03 – 7.90 (m, *J* = 15.6, 8.2 Hz, 2H), 7.64 – 7.53 (m, *J* = 9.3, 4.7, 4.1 Hz, 3H), 7.49 – 7.33 (m, 6H), 2.13 (s, 3H). **¹³C NMR** (101 MHz, CDCl₃) δ 140.32, 139.88, 136.87, 133.64, 132.11, 130.45, 129.95, 128.29, 127.65, 127.51, 126.70, 126.19, 126.05, 125.79, 125.66, 125.45, 20.15.

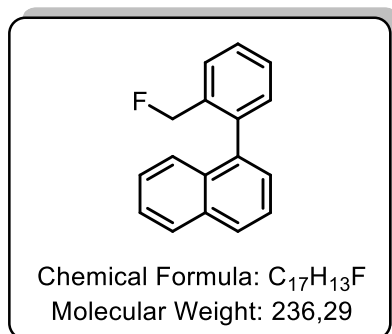
Synthesis of 1-(2-(bromomethyl)phenyl)naphthalene



1-(*o*-tolyl)naphthalene (1.00 g, 4.58 mmol, 1 equiv.), and *N*-bromosuccinimid (892 mg, 5.04 mmol, 1.1 equiv.) were reacted in DCM (40 mL) with benzoyl peroxide (55mg, 0,05 equiv.) for 6 h under reflux. After cooling to rt water was added, phases were separated and the aqueous layer extracted with DCM. The combined organic fractions were dried over Na₂SO₄, filtrated and the solvent removed in vacuo. The crude product was purified by flash column chromatography on silica gel with *n*-hexane to afford the product (1.12 g, 82 %).

R_f = 0.27 (SiO₂, *n*-hexane) **¹H NMR** (400 MHz, CDCl₃) δ 7.91 (d, *J* = 6.5 Hz, 2H), 7.70 – 7.60 (m, 1H), 7.60 – 7.52 (m, 1H), 7.51 – 7.43 (m, 3H), 7.43 – 7.32 (m, 3H), 7.32 – 7.24 (m, 1H), 4.39 – 4.29 (m, 1H), 4.19 – 4.09 (m, 1H). **¹³C NMR** (101 MHz, CDCl₃) δ 140.17, 137.38, 136.49, 133.56, 132.18, 131.16, 130.61, 130.35, 128.33, 128.30, 128.24, 128.10, 127.16, 126.18, 125.91, 125.21, 31.77.

Synthesis of 1-(2-(fluoromethyl)phenyl)naphthalene

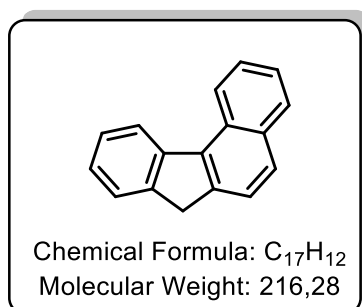


1-(2-(bromomethyl)phenyl)naphthalene (250 mg, 0,841 mmol, 1 equiv.) and Tetra-*n*-butylammonium fluoride (550 mg, 2.10 mmol, 2.5 equiv.) were reacted in acetonitrile for 21 h at 80 °C. After cooling to rt water was added, phases were separated and the aqueous layer extracted with DCM. The combined organic fractions were dried over Na₂SO₄, filtrated and the solvent

removed in vacuo. The crude product was purified by flash column chromatography on silica gel with *n*-hexane/DCM 8:2 to afford the product (68 mg, 34%).

R_f = 0.53 (SiO₂, *n*-hexane/DCM 8:2) **¹H NMR** (400 MHz, CDCl₃) δ 7.94 – 7.89 (m, 2H), 7.65 (d, *J* = 7.4 Hz, 1H), 7.56 – 7.43 (m, 5H), 7.43 – 7.32 (m, 3H), 5.13 (s, 1H), 5.03 (s, 1H). **¹⁹F NMR** (376 MHz, CDCl₃) δ 29.54 (t, *J* = 47.7 Hz). **¹³C NMR** (101 MHz, CDCl₃) δ 139.42, 139.39, 137.37, 135.15, 134.99, 133.51, 132.09, 130.77, 128.43, 128.39, 128.28, 128.23, 128.04, 127.96, 127.15, 126.24, 125.91, 125.78, 125.18, 83.32, 81.67.

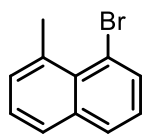
Synthesis of 7H-benzo[*c*]fluorene



1-(2-(fluoromethyl)phenyl)naphthalene (13 mg, 55,0 umol) was reacted on activated Al₂O₃ for 24 h at 200°C according to general procedure 4. Only 7H-benzo[*c*]fluorene (2.7 mg, 23 %) could be isolated by flash column chromatography on silica gel (*n*-hexane).

¹H NMR (400 MHz, CDCl₃) δ 8.78 (d, *J* = 8.5 Hz, 1H), 8.41 (d, *J* = 7.8 Hz, 1H), 7.97 (d, *J* = 8.2 Hz, 1H), 7.83 (d, *J* = 8.3 Hz, 1H), 7.70 (d, *J* = 8.2 Hz, 1H), 7.68 – 7.62 (m, 2H), 7.57 – 7.47 (m, 2H), 7.36 (td, *J* = 7.4, 0.9 Hz, 1H), 4.03 (s, 2H). **¹³C NMR** (101 MHz, CDCl₃) δ 142.80, 137.83, 133.40, 129.14, 129.00, 128.18, 127.66, 126.86, 126.44, 125.72, 125.26, 124.95, 124.83, 123.68, 123.23, 122.85, 31.57.

Synthesis of 1-bromo-8-methylnaphthalene



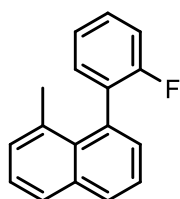
Chemical Formula: C₁₁H₉Br
Molecular Weight: 221,10

A solution of 1,8-dibromonaphthalene (1.00 g, 3.5 mmol) in THF (20 mL) was cooled to 0°C. Methyllithium (2.26 mL, 1.6 M in hexane, 3.67 mmol) was added slowly and after 30 min. methyl iodide (0.87 mL, 14.0 mmol) was added dropwise. The reaction mixture stirred for 3 h at 20°C. The reaction was quenched with brine (50 mL), the organic phase separated, dried over Na₂SO₄, and the solvent removed in vacuo. Column chromatography (silica gel; *n*-hexane) gave 1-bromo-8-methylnaphthalene (520 mg, 67 %) as white solid.

¹H NMR (400 MHz, CDCl₃) δ 7.83 (dd, *J* = 7.4, 1.2 Hz, 1H), 7.78 (dd, *J* = 8.1, 0.8 Hz, 1H), 7.73 – 7.68 (m, 1H), 7.37 – 7.32 (m, 2H), 7.21 (t, *J* = 7.8 Hz, 1H), 3.14 (s, 3H).

Procedure was done according to literature.¹¹⁸

Synthesis of 1-(2-fluorophenyl)-8-methylnaphthalene



Chemical Formula: C₁₇H₁₃F
Molecular Weight: 236,29

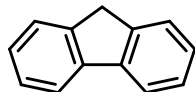
1-bromo-8-methylnaphthalene (520 mg, 2.35 mmol), (2-fluorophenyl)boronic acid (362 mg, 2.59 mmol, 1.1 equiv.), Cs₂CO₃ (1.53 g, 4,70 mmol, 2 equiv.) were reacted in THF/H₂O (12 mL, 5:1) with Pd(PPh₃)₂Cl₂ (33 mg, 47.0 μmol, 0.02 equiv.) for 24 h under reflux. After cooling to rt water was added, phases were separated and the aqueous layer extracted with DCM. The combined organic fractions were dried over Na₂SO₄, filtrated and the solvent removed in vacuo. The crude product was purified by flash column chromatography on silica gel with *n*-hexane to afford the product as a solid (394 g, 71 %).

¹H NMR (400 MHz, CDCl₃) δ 7.95 – 7.91 (m, 1H), 7.82 (d, *J* = 8.1 Hz, 1H), 7.52 – 7.48 (m, 1H), 7.43 – 7.33 (m, 4H), 7.28 (d, *J* = 7.0 Hz, 1H), 7.26 – 7.12 (m, 2H), 2.14 (s, 3H). **¹⁹F NMR** (376 MHz, CDCl₃) δ -114.31 – -114.41 (m). **¹³C NMR** (101 MHz, CDCl₃) δ 161.19, 158.76, 134.98, 134.91, 131.92, 131.89, 129.86, 129.76, 129.69, 129.14, 129.07, 127.66, 125.53, 124.37, 123.49, 123.45, 115.29, 115.07, 23.66.

Reaction of 1-benzyl-2-fluorobenzene

1-benzyl-2-fluorobenzene (127 mg, 682 μmol) was reacted on activated $\gamma\text{-Al}_2\text{O}_3$ (10 g) for 168 h at 200 °C according to the general procedure 4. After extraction of alumina with toluene and methanol, 9H-fluorene (3.6 mg, 3 %) and 2-benzylphenol (27.8 mg, 22 %) were isolated by flash column chromatography on silica gel with hexane/ethylacetat 10:1.

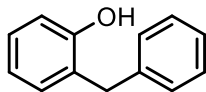
9H-fluorene:



Chemical Formula: $\text{C}_{13}\text{H}_{10}$
Molecular Weight: 166,22

$^1\text{H NMR}$ (400 MHz, CDCl_3) δ 7.80 (d, $J = 7.5$ Hz, 2H), 7.54 (t, $J = 8.3$ Hz, 2H), 7.38 (dd, $J = 7.7, 7.2$ Hz, 2H), 7.34 – 7.23 (m, 2H), 3.91 (s, 2H). **$^{13}\text{C NMR}$** (101 MHz, CDCl_3) δ 143.18, 141.67, 126.68, 126.66, 124.98, 119.83, 36.90.

2-benzylphenol:

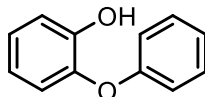


Chemical Formula: $\text{C}_{13}\text{H}_{12}\text{O}$
Molecular Weight: 184,24

$^1\text{H NMR}$ (400 MHz, CDCl_3) δ 7.35 – 7.28 (m, 2H), 7.27 – 7.18 (m, 3H), 7.16 (dd, $J = 11.5, 4.4$ Hz, 2H), 6.95 – 6.88 (m, 1H), 6.80 (d, $J = 8.3$ Hz, 1H), 4.69 (d, $J = 34.8$ Hz, 1H), 4.02 (s, $J = 9.8$ Hz, 2H). **$^{13}\text{C NMR}$** (101 MHz, CDCl_3) δ 153.69, 139.85, 130.98, 128.68, 128.63, 127.83, 126.98, 126.35,

120.97, 115.73, 36.34.

Reaction of 1-fluoro-2-phenoxybenzene



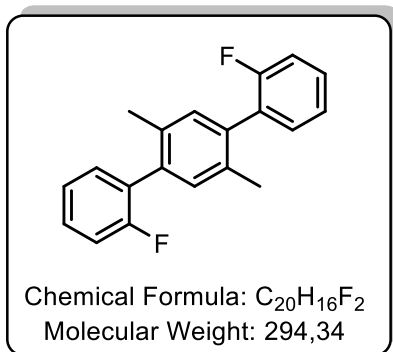
Chemical Formula: $\text{C}_{12}\text{H}_{10}\text{O}_2$
Molecular Weight: 186,21

1-fluoro-2-phenoxybenzene (60 mg, 319 μmol) was reacted on activated $\gamma\text{-Al}_2\text{O}_3$ (10 g) for 168 h at 200 °C according to the general procedure 4. After extraction of alumina with toluene, no product was isolated. After extraction of alumina with methanol and flash column

chromatography on silica gel with *n*-hexane/ethylacetat 10:1 2-phenoxyphenol was isolated (23 mg, 38 %).

$^1\text{H NMR}$ (400 MHz, CDCl_3) δ 7.40 – 7.31 (m, 2H), 7.16 – 7.10 (m, 1H), 7.09 – 7.00 (m, 4H), 6.92 – 6.80 (m, 2H), 5.58 (s, 1H). **$^{13}\text{C NMR}$** (101 MHz, CDCl_3) δ 156.75, 147.49, 143.46, 129.86, 124.75, 123.59, 120.61, 118.85, 117.98, 116.16.

Synthesis of 2,2''-difluoro-2',5'-dimethyl-1,1':4',1''-terphenyl



1,4-dibromo-2,5-dimethylbenzene (200 mg, 758 μ mol), (2-fluorophenyl)boronic acid (234 mg, 1.67 mmol, 2.2 equiv.), Cs₂CO₃ (987 mg, 3.03 mmol, 4 equiv.) were reacted in THF/H₂O (12 mL, 5:1) with Pd(PPh₃)₂Cl₂ (24 mg, 38 μ mol, 0.05 equiv.) for 72 h under reflux. After cooling to rt water was added, phases were separated and the aqueous layer extracted with DCM. The

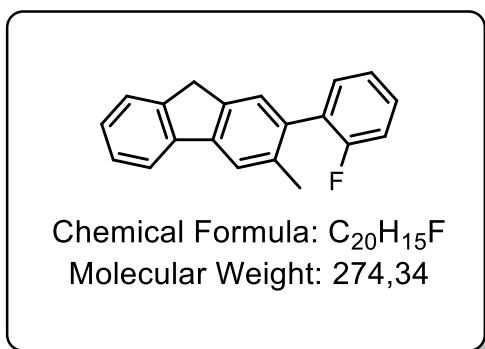
combined organic fractions were dried over Na₂SO₄, filtrated and the solvent removed in vacuo. The crude product was purified by flash column chromatography on silica gel with *n*-hexane/DCM 5:1 to afford the product (174 mg, 78 %).

R_f = 0.44(SiO₂, *n*-hexane/DCM 5:1) **¹H NMR** (400 MHz, CD₂Cl₂) δ 7.44 – 7.36 (m, 2H), 7.34 (td, *J* = 7.5, 1.9 Hz, 2H), 7.26 (td, *J* = 7.5, 1.1 Hz, 2H), 7.22 – 7.14 (m, 4H), 2.20 (s, 6H). **¹⁹F NMR** (376 MHz, CD₂Cl₂) δ -115.62 (ddd, *J* = 22.2, 9.5, 5.0 Hz). **¹³C NMR** (101 MHz, CD₂Cl₂) δ 160.87, 158.44, 135.37, 133.81, 131.59, 131.55, 131.52, 129.15, 129.07, 128.94, 128.78, 124.07, 124.03, 115.47, 115.25, 19.04, 19.02.

Reaction of 2,2''-difluoro-2',5'-dimethyl-1,1':4',1''-terphenyl

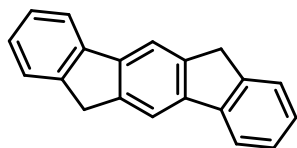
2,2''-difluoro-2',5'-dimethyl-1,1':4',1''-terphenyl(9 mg) was reacted on activated γ -Al₂O₃ (1.8 g) in *o*-DCB (4 mL) for 20 h at 220°C. After extraction of alumina with toluene all products formed were isolated by preparative HPLC (Methanol/toluene 70:30).

2-(2-fluorophenyl)-3-methyl-9H-fluorene



¹H NMR (400 MHz, CDCl₃) δ 7.80 (d, *J* = 7.6 Hz, 1H), 7.71 (s, 1H), 7.53 (dd, *J* = 10.8, 5.9 Hz, 2H), 7.43 – 7.28 (m, 6H), 7.19 (ddd, *J* = 26.3, 12.7, 4.8 Hz, 3H), 3.90 (s, 2H), 2.30 (s, 3H).

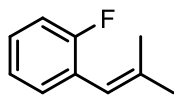
6,12-dihydroindeno[1,2-b]fluorene



Chemical Formula: C₂₀H₁₄
Molecular Weight: 254,33

¹H NMR (400 MHz, CDCl₃) δ 7.95 (s, 1H), 7.81 (d, *J* = 7.6 Hz, 1H), 7.56 (d, *J* = 7.4 Hz, 1H), 7.39 (t, *J* = 7.4 Hz, 1H), 7.30 (td, *J* = 7.4, 1.1 Hz, 1H), 3.98 (s, 2H).

Synthesis of 1-fluoro-2-(2-methylprop-1-en-1-yl)benzene



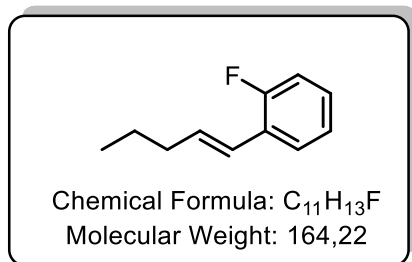
Chemical Formula: C₁₀H₁₁F
Molecular Weight: 150,20

A solution of (isopropyl)triphenyl-phosphonium iodide (5.22 g, 12.1 mmol, 1.5 equiv.) in THF (20 mL) was cooled to 0°C. *N*-BuLi (7.55 mL, 1.6 M, 12.1 mmol, 1.5 equiv.) was added slowly and after 30 min. 2-fluorobenzaldehyde (0.85 mL, 8.06 mmol, 1 equiv.)

was added. The solution was warmed to room temperature and stirred for 72 h. The reaction was quenched with water, phases were separated and the aqueous layer extracted with DCM. The combined organic fractions were dried over Na₂SO₄, filtrated and the solvent removed in vacuo. The crude product was purified by flash column chromatography on silica gel with *n*-hexane to afford 1-fluoro-2-(2-methylprop-1-en-1-yl)benzene (939 mg, 78 %).

¹H NMR (400 MHz, CDCl₃) δ 7.27 – 7.14 (m, 2H), 7.12 – 6.99 (m, 2H), 6.24 (s, 1H), 1.94 (d, *J* = 1.4 Hz, 3H), 1.80 (s, 3H). **¹⁹F NMR** (376 MHz, CDCl₃) δ -115.54 – -115.70 (m). **¹³C NMR** (101 MHz, CDCl₃) δ 161.32, 158.88, 137.87, 137.86, 130.80, 130.78, 130.74, 127.67, 127.59, 126.30, 126.15, 123.41, 123.37, 117.73, 117.70, 115.30, 115.08, 77.30, 76.98, 76.66, 31.58, 26.43.

Synthesis of 1-fluoro-2-(pent-1-en-1-yl)benzene

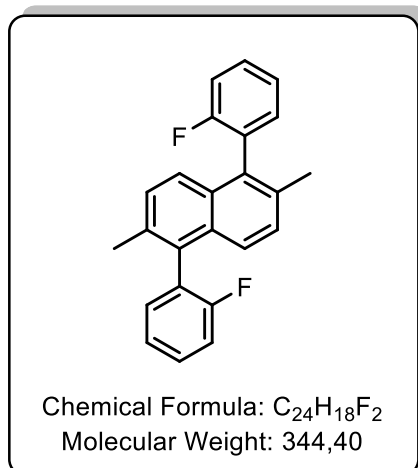


A solution of (butyl)triphenyl-phosphonium bromide (4.83 g, 12.1 mmol, 1.5 equiv.) in THF (20 mL) was cooled to 0°C. N-BuLi (7.55 mL, 1.6 M, 12.1 mmol, 1.5 equiv.) was added slowly and after 30 min. 2-fluorobenzaldehyde (0.85 mL, 8.06 mmol, 1 equiv.) was added. The solution was warmed to room temperature and stirred for 24 h. The reaction was quenched with water, phases were separated and the aqueous layer extracted with DCM. The combined organic fractions were dried over Na₂SO₄, filtrated and the solvent removed in vacuo. The crude product was purified by flash column chromatography on silica gel with *n*-hexane to afford 1-fluoro-2-(pent-1-en-1-yl)benzene (716 mg, 54 %).

E+Z-Isomer:

¹H NMR (400 MHz, CDCl₃) δ 7.29 (td, *J* = 7.6, 1.7 Hz, 1H), 7.10 – 6.97 (m, 3H), 6.44 (dd, *J* = 11.6, 1.2 Hz, 1H), 5.80 (dt, *J* = 11.6, 7.3 Hz, 1H), 2.22 – 2.18 (m, 2H), 1.46 (ddd, *J* = 14.7, 7.4, 4.0 Hz, 2H), 0.93 (t, *J* = 7.4 Hz, 3H). **¹H NMR** (400 MHz, CDCl₃) δ 7.43 (td, *J* = 7.7, 1.8 Hz, 1H), 7.25 – 7.11 (m, 3H), 6.53 (t, *J* = 11.9 Hz, 1H), 6.30 (dt, *J* = 16.0, 6.9 Hz, 1H), 2.26 – 2.22 (m, 2H), 1.57 – 1.50 (m, 2H), 0.97 (t, *J* = 7.4 Hz, 3H). **¹⁹F NMR** (376 MHz, CDCl₃) δ -115.46 – -115.60 (m), -119.08 (ddd, *J* = 10.9, 7.7, 5.2 Hz). **¹³C NMR** (101 MHz, CDCl₃) δ 161.32, 161.14, 158.87, 158.67, 135.01, 135.00, 133.66, 133.62, 130.50, 130.46, 128.25, 128.17, 127.91, 127.82, 126.98, 126.94, 125.68, 125.56, 125.43, 125.28, 123.93, 123.89, 123.44, 123.40, 122.22, 122.19, 121.38, 121.35, 115.65, 115.43, 115.38, 115.16, 35.47, 30.82, 30.81, 22.82, 22.42, 13.77, 13.68.

Synthesis of 1,5-bis(2-fluorophenyl)-2,6-dimethylnaphthalene



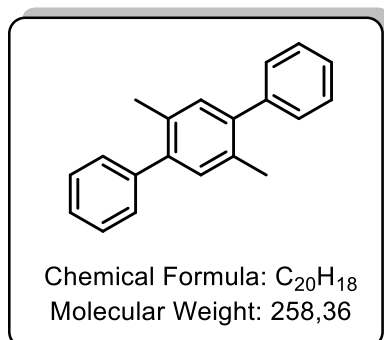
1,5-dibromo-2,6-dimethylnaphthalene* (100 mg, 318 μ mol, 1 equiv.), (2-fluorophenyl)boronic acid (98 mg, 701 μ mol, 2.2 equiv.) and K₂CO₃ (220mg, 1.59 mmol, 5 equiv.) were reacted in THF/H₂O (12 mL, 5:1) with Pd(PPh₃)₄ (8 mg, 16.0 μ mol, 0.05 equiv.) for 48 h under reflux. After cooling to rt water was added, phases were separated and the aqueous layer extracted with DCM. The combined organic fractions were dried over Na₂SO₄, filtrated and the solvent

removed in vacuo. The crude product was purified by flash column chromatography on silica gel with *n*-hexane/DCM 9:1 to afford 1,5-bis(2-fluorophenyl)-2,6-dimethylnaphthalene (60.6 mg,

¹H NMR (400 MHz, CDCl₃) δ 7.51 – 7.43 (m, 2H), 7.38 (dd, *J* = 8.6, 3.5 Hz, 2H), 7.29 (ddd, *J* = 22.5, 12.6, 6.2 Hz, 8H), 2.24 (s, 6H). **¹⁹F NMR** (376 MHz, CDCl₃) δ -114.11 (ddd, *J* = 175.3, 11.4, 4.7 Hz). **¹³C NMR** (101 MHz, CDCl₃) δ 161.45, 159.02, 133.29, 132.55, 132.51, 132.47, 132.43, 131.58, 131.52, 131.26, 131.21, 129.39, 129.32, 128.66, 127.10, 126.93, 125.53, 124.18, 124.14, 124.11, 124.08, 115.98, 115.89, 115.75, 115.67, 20.29.

*1,5-dibromo-2,6-dimethylnaphthalene was synthesized by Vladimir Akhmetov.

Synthesis of 2',5'-dimethyl-1,1':4',1''-terphenyl



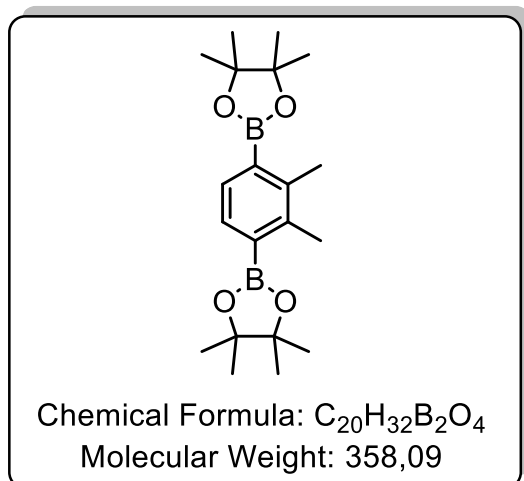
1,4-dibromo-2,5-dimethylbenzene (1.00 g, 3.79 mmol, 1 equiv.), phenylboronic acid (1.02g, 8.33 mmol, 2.2 equiv.) and K₂CO₃ (4.94 g, 15.5 mmol, 4 equiv.) were reacted in THF/H₂O (24 mL, 5:1) with Pd(PPh₃)₂Cl₂ (53 mg, 75.8 μ mol, 0.02 equiv.) for 18 h under reflux. After cooling to rt, water was added, phases were separated and the aqueous layer extracted with DCM. The combined

organic fractions were dried over Na₂SO₄, filtrated and the solvent removed in vacuo. The crude product was purified by flash column chromatography on silica gel with *n*-hexane. The product was isolated as a white solid (585 mg, 60 %).

¹H NMR (400 MHz, CDCl₃) δ 7.50 – 7.35 (m, 6H), 7.20 (s, 6H), 2.32 (s, 6H). **¹³C NMR**

(101 MHz, CDCl₃) δ 141.73, 140.85, 132.58, 131.84, 129.24, 128.08, 126.76, 19.92.

Synthesis of 2,2'-(2,3-dimethyl-1,4-phenylene)bis(4,4,5,5-tetramethyl-1,3,2-dioxaborolane)



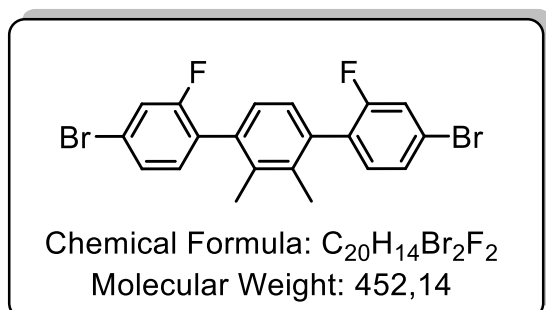
1,4-dibromo-2,3-dimethylbenzene (500 mg, 1.89 mmol, 1 equiv.), 4,4,4',4',5,5,5',5'-octamethyl-2,2'-bi(1,3,2-dioxaborolane) (1.44 g, 5.68 mmol, 3 equiv.), potassium acetate (0.744 g, 7.58 mmol, 4 equiv.) were reacted in 1,4-dioxane (20 mL) with Pd(dppf)Cl₂ for 24 h under reflux. After cooling to rt water was added, phases were separated and the aqueous layer extracted with DCM. The

combined organic fractions were dried over Na₂SO₄, filtrated and the solvent removed in vacuo. The crude product was purified by flash column chromatography on silica gel (*n*-hexane to *n*-hexane: EtOAc 1:1) to afford 2,2'-(2,3-dimethyl-1,4-phenylene)bis(4,4,5,5-tetramethyl-1,3,2-dioxaborolane) as a white solid (467 mg, 69 %).

¹H NMR (400 MHz, cdcl₃) δ 7.53 (s, 2H), 2.45 (s, 6H), 1.33 (s, 12H), 1.25 (s, 12H).

¹³C NMR (101 MHz, cdcl₃) δ 142.55, 132.04, 83.43, 24.99, 24.81, 18.84.

Synthesis of 4,4''-dibromo-2,2''-difluoro-2',3'-dimethyl-1,1':4',1''-terphenyl



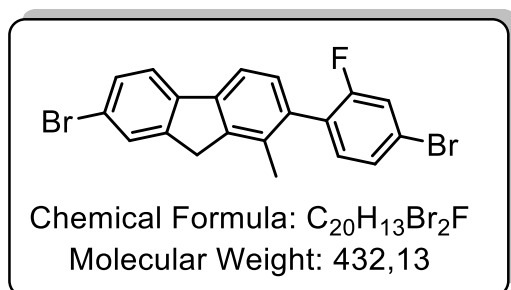
2,2'-(2,3-dimethyl-1,4-phenylene)bis(4,4,5,5-tetramethyl-1,3,2-dioxaborolane) (467 mg, 1.30 mmol, 1 equiv.), 4-bromo-2-fluoro-1-iodobenzene (1.02 g, 3.39 mmol, 2.6 equiv.) and Cs₂CO₃ (1,70g, 5,22mmol, 4 equiv.) were reacted in

THF/H₂O (12 mL, 5:1) with Pd(PPh₃)₂Cl₂ (40 mg, 65.0 μmol, 0.05 equiv.) for 3 h under reflux according to general procedure 1. After cooling to rt water was added, phases were separated and the aqueous layer extracted with DCM. The combined organic

fractions were dried over Na₂SO₄, filtrated and the solvent removed in vacuo. The crude product was purified by flash column chromatography on silica gel with *n*-hexane to afford 4,4''-dibromo-2,2''-difluoro-2',3'-dimethyl-1,1':4',1''-terphenyl as a white solid (228 mg, 39 %).

¹H NMR (500 MHz, cdcl₃) δ 7.40 (ddd, *J* = 11.4, 5.6, 1.1 Hz, 4H), 7.20 (t, *J* = 7.9 Hz, 2H), 7.14 (s, 2H), 2.21 (d, *J* = 1.6 Hz, 6H). **¹⁹F NMR** (470 MHz, cdcl₃) δ -90.68 (t, *J* = 7.1 Hz), -111.09 (d, *J* = 255.1 Hz). **¹³C NMR** (126 MHz, cdcl₃) δ 160.50, 158.51, 135.69, 134.91, 132.64, 128.94, 128.80, 127.43, 127.41, 127.31, 121.51, 121.44, 119.31, 119.11, 31.65.

Reaction of 4,4''-dibromo-2,2''-difluoro-2',3'-dimethyl-1,1':4',1''-terphenyl on Al₂O₃

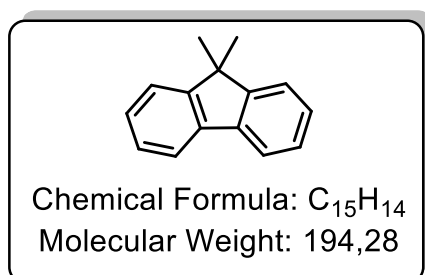


4,4''-dibromo-2,2''-difluoro-2',3'-dimethyl-1,1':4',1''-terphenyl was reacted on activated Al₂O₃ according to general procedure 4 at 190°C for 4 d. After washing with toluene, starting material and 7-bromo-2-(4-bromo-2-fluorophenyl)-1-methyl-9H-fluorene was found

by ¹H-NMR analysis.

¹H NMR (400 MHz, cdcl₃) δ 7.68 (dd, *J* = 19.1, 8.1 Hz, 2H), 7.51 (d, *J* = 8.4 Hz, 1H), 7.36 (t, *J* = 7.9 Hz, 1H), 7.29 – 7.11 (m, 4H), 3.84 (s, 2H), 2.24 (s, 3H).

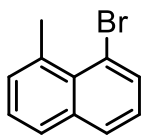
Synthesis of 9,9-dimethyl-9H-fluorene



2-fluoro-2'-isopropyl-1,1'-biphenyl (20 mg) was reacted on activated Al₂O₃ according to general procedure 4 at 190 °C for 24 h. After washing with toluene, the product was isolated without further purification as a white solid (8 mg, 40 %).

¹H NMR (400 MHz, cdcl₃) δ 7.76 – 7.70 (m, 2H), 7.44 (dt, *J* = 7.9, 3.5 Hz, 2H), 7.38 – 7.28 (m, 4H), 1.49 (s, 6H).

Synthesis of 1-bromo-8-methylnaphthalene

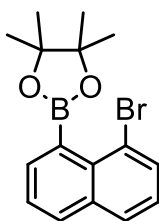


Chemical Formula: C₁₁H₉Br
Molecular Weight: 221,10

1,8-dibromonaphthalene (10.0 g, 35.0 mmol, 1 equiv.) was dissolved in THF (100 mL) and degassed three times. The solution was cooled to 0°C and methyllithium (8.71 mL, 139 mmol, 4 equiv.) was added slowly. After stirring for 45 min., iodomethane (23.0 mL, 1.6 M, 36.7 mmol, 1.05 equiv.) was added. After 3 h, the reaction was quenched by adding water (50 mL), phases were separated and the aqueous layer extracted with DCM. The combined organic fractions were dried over Na₂SO₄, filtrated and the solvent removed in vacuo. The crude product was purified by flash column chromatography on silica gel with *n*-hexane to afford 1-bromo-8-methylnaphthalene (4.00 g, 52 %).

¹H NMR (400 MHz, cdcl₃) δ 7.97 – 7.72 (m, 3H), 7.40 (dd, *J* = 7.1, 6.0 Hz, 2H), 7.24 (dd, *J* = 17.0, 9.2 Hz, 1H), 3.23 (s, 3H). **¹³C NMR** (101 MHz, cdcl₃) δ 136.68, 135.38, 133.46, 131.36, 131.07, 129.40, 128.22, 126.01, 125.65, 120.07, 26.31.

Synthesis of 2-(8-bromonaphthalen-1-yl)-4,4,5,5-tetramethyl-1,3,2-dioxaborolane

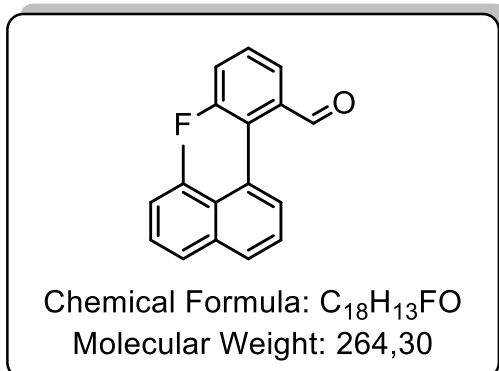


Chemical Formula: C₁₆H₁₈BBrO₂
Molecular Weight: 333,03

1-bromo-8-methylnaphthalene (1.00 g, 4.52 mmol, 1 equiv.), B₂pin₂ (1.72 g, 6.78 mmol, 1.5 equiv.), KOAc (887 mg, 9.05 mmol, 2 equiv.) were reacted in 1,4-dioxane (35 mL) with Pd(dppf)Cl₂ for 24 h under reflux. After cooling to rt water was added, phases were separated and the aqueous layer extracted with DCM. The combined organic fractions were dried over Na₂SO₄, filtrated and the solvent removed in vacuo. The crude product was purified by flash column chromatography on silica gel (*n*-hexane to *n*-hexane: EtOAc 1:1) to afford 2-(8-bromonaphthalen-1-yl)-4,4,5,5-tetramethyl-1,3,2-dioxaborolane (460 mg, 38 %).

¹H NMR (400 MHz, cdcl₃) δ 8.15 (d, *J* = 8.3 Hz, 1H), 7.96 – 7.88 (m, 1H), 7.78 (ddd, *J* = 7.5, 5.5, 4.2 Hz, 1H), 7.60 – 7.50 (m, 1H), 7.43 (ddd, *J* = 11.4, 7.8, 5.5 Hz, 2H), 2.91 (s, 3H), 1.49 (d, *J* = 5.5 Hz, 12H). **¹³C NMR** (101 MHz, cdcl₃) δ 135.69, 135.31, 134.90, 133.97, 133.91, 132.58, 132.20, 130.81, 128.62, 127.92, 127.80, 127.35, 126.56, 125.88, 125.85, 125.45, 125.42, 124.61, 124.43, 84.19, 25.00, 24.93, 24.74, 22.79.

Synthesis of 3-fluoro-2-(8-methylnaphthalen-1-yl)benzaldehyde

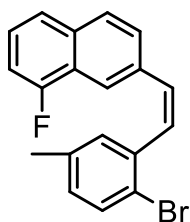


1-bromo-8-methylnaphthalene (100 mg, 452 μ mol, 1 equiv.), 3-fluoro-2-(4,4,5,5-tetramethyl-1,3,2-dioxaborolan-2-yl)benzaldehyde (113 mg, 452 μ mol, 1 equiv.) and potassium carbonate (125 mg, 904.6 μ mol, 2 equiv.) were reacted in toluene/methanol/water (10 mL/2 mL/1 mL) mixture with Pd(PPh₃)₄ under reflux for 24 h. After cooling to rt water was added, phases were

separated and the aqueous layer extracted with DCM. The combined organic fractions were dried over Na₂SO₄, filtrated and the solvent removed in vacuo. The crude product was purified by flash column chromatography on silica gel (*n*-hexane to *n*-hexane: EtOAc 9:1) to afford 3-fluoro-2-(8-methylnaphthalen-1-yl)benzaldehyde as a white solid (35.3 mg, 29 %).

¹H NMR (400 MHz, cdcl₃) δ 9.62 (s, 1H), 8.00 – 7.95 (m, 1H), 7.88 – 7.80 (m, 2H), 7.58 – 7.47 (m, 2H), 7.45 – 7.36 (m, 2H), 7.32 – 7.24 (m, 2H), 2.04 (s, 3H). **¹⁹F NMR** (376 MHz, cdcl₃) δ -113.19 (dd, *J* = 8.6, 5.2 Hz). **¹³C NMR** (101 MHz, cdcl₃) δ 190.88, 190.84, 161.31, 158.87, 142.09, 136.50, 135.88, 135.79, 135.69, 134.83, 134.66, 134.22, 132.10, 131.86, 130.78, 130.66, 130.34, 129.69, 129.54, 129.38, 129.30, 128.74, 127.99, 127.59, 126.02, 125.40, 124.21, 123.90, 122.63, 122.59, 120.66, 120.43, 23.54.

Synthesis of (E) and (Z)-7-(2-bromo-5-methylstyryl)-1-fluoronaphthalene



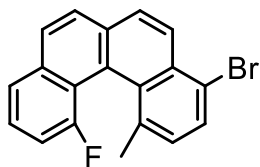
Chemical Formula: C₁₉H₁₄BrF
Molecular Weight: 341,22

A solution of 2-bromo-5-methylbenzaldehyde (1.80 g, 9.04 mmol, 1 equiv.) and [(8-fluoro-2-naphthalenyl)methyl]triphenylphosphonium bromide (6.38 g, 13.6 mmol, 1.5 equiv.) in CHCl₃ (100 mL) was reacted with an aqueous solution of KOH (50 %, 30 mL) for 18 h according to general procedure 2b. The (E) and (Z)-product was purified by flash column chromatography on silica

gel (*n*-hexanes) and isolated as white solid (2.55 g, 83 %).

¹H NMR (400 MHz, CDCl₃) δ 8.03 (s, 1H), 7.65 – 7.60 (m, 1H), 7.56 (dd, *J* = 8.0, 6.2 Hz, 2H), 7.41 – 7.31 (m, 2H), 7.15 (dd, *J* = 11.7, 4.0 Hz, 1H), 7.11 (d, *J* = 1.7 Hz, 1H), 6.98 (dd, *J* = 8.1, 2.0 Hz, 1H), 6.93 – 6.76 (m, 2H), 2.15 (s, 3H). **¹⁹F NMR** (376 MHz, CDCl₃) δ -122.73 (dd, *J* = 10.6, 5.4 Hz), -123.02 (dd, *J* = 11.3, 4.6 Hz). **¹³C NMR** (101 MHz, CDCl₃) δ 160.24, 160.11, 157.73, 157.61, 137.56, 137.53, 137.40, 137.00, 136.57, 135.11, 135.09, 134.62, 134.61, 134.10, 134.06, 132.88, 132.57, 131.40, 130.93, 130.48, 130.13, 129.90, 128.45, 128.14, 128.10, 127.66, 127.65, 127.38, 127.10, 127.06, 125.88, 125.81, 125.73, 124.55, 123.84, 123.68, 123.59, 123.55, 123.43, 123.39, 121.17, 121.12, 120.58, 119.77, 119.72, 110.16, 109.96, 109.81, 109.61, 20.77.

Synthesis of 4-bromo-12-fluoro-1-methylbenzo[*c*]phenanthrene



Chemical Formula: C₁₉H₁₂BrF
Molecular Weight: 339,21

(Z)-7-(2-bromo-5-methylstyryl)-1-

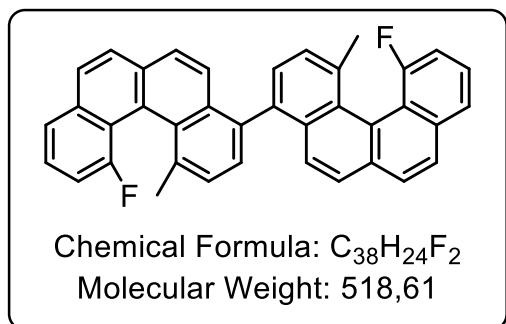
fluoronaphthalene (2.56 g, 7.49 mmol, 1 equiv.), iodine (2.09 g, 8.24 mmol, 1.1 equiv.) and propylene oxide (5.24 mL, 74.9 mmol, 10 equiv.) were reacted in cyclohexane (800 mL) for 10 h according to general procedure 3. The product was purified according to general procedure 3 and

further by flash column chromatography on silica gel (*n*-hexanes). The product was isolated as a white solid (1.36 g, 54 %).

¹H NMR (400 MHz, CDCl₃) δ 8.41 (d, *J* = 8.7 Hz, 1H), 7.90 (dd, *J* = 17.4, 8.1 Hz, 2H), 7.86 – 7.76 (m, 3H), 7.57 (tt, *J* = 14.1, 6.9 Hz, 1H), 7.34 – 7.21 (m, 2H), 2.30 (s, *J* =

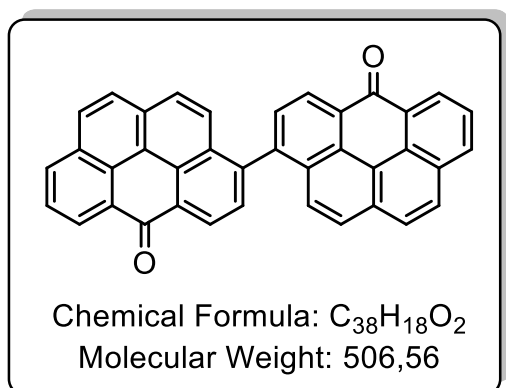
23.7 Hz, 3H). **¹⁹F NMR** (376 MHz, CDCl₃) δ -105.25 – -105.66 (m). **¹³C NMR** (101 MHz, CDCl₃) δ 160.40, 157.88, 137.33, 137.27, 134.07, 134.02, 132.70, 132.45, 131.54, 129.96, 128.21, 127.37, 127.33, 126.79, 126.63, 126.54, 126.46, 123.61, 123.58, 122.44, 122.42, 120.87, 120.74, 119.30, 111.66, 111.43, 22.38, 22.29.

Synthesis of 12,12'-difluoro-1,1'-dimethyl-4,4'-bibenzo[*c*]phenanthrene



4-bromo-12-fluoro-1-methylbenzo[*c*]phenanthrene (114 mg, 336 μmol) was dissolved in toluene (4 mL) and tert-butyllithium (0.24 mL, 403 μmol, 1.2 equiv.) was added. The reaction was catalyzed by Dichloro-[1,3-bis-(2,6-di-3-pentylphenyl)-imidazol-2-ylidene](3-chloropyridyl)-palladium(II) (5.3 mg, 6.72 μmol, 0.02 equiv.). After stirring for 2h at rt, the reaction was quenched by methanol. The solvent was removed in vacuo and the product was purified by flash column chromatography on silica gel with *n*-hexane/DCM 8:2. The resulting yellow oil was frozen with benzene and dried in vacuo, yielding a yellow powder (15 mg, 17 %). **¹H NMR** (400 MHz, CDCl₃) δ 8.05 – 7.49 (m, 16H), 7.31 (ddd, *J* = 11.0, 9.3, 5.1 Hz, 2H), 2.49 – 2.44 (m, 6H). **¹³C NMR** (101 MHz, CDCl₃) δ 160.61, 158.07, 135.58, 135.49, 135.33, 134.00, 133.05, 132.66, 132.08, 127.71, 127.48, 127.20, 127.01, 126.73, 126.18, 124.89, 123.47, 111.47, 111.24, 22.62, 22.54. **¹⁹F NMR** (376 MHz, cdcl₃) δ -105.08 (s), -105.23 (s).

Synthesis of 6H,6'H-[3,3'-bibenzo[*cd*]pyrene]-6,6'-dione

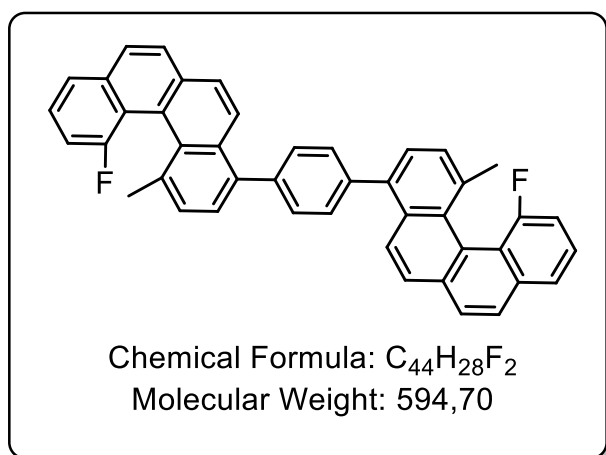


12,12'-difluoro-1,1'-dimethyl-4,4'-bibenzo[*c*]phenanthrene (19.5 mg) was reacted on Al₂O₃ according to general procedure 4 at 190 °C for 1 d. After extraction with toluene and methanol, it was purified by flash column chromatography on silica gel with *n*-hexane:EtOAc 9:1. The product (8.7 mg, 45 %) was isolated from the remaining starting material (6.7 mg, 34 %). As the product was still not clean enough for easy identification, the

product was again purified by flash column chromatography on silica gel (*n*-hexane→*n*-hexane:EtOAc 9:1).

¹H NMR (500 MHz, cdcl₃) δ 9.07 (d, *J* = 7.5 Hz, 1H), 8.97 (dd, *J* = 7.5, 1.2 Hz, 1H), 8.39 (d, *J* = 7.0 Hz, 1H), 8.18 (d, *J* = 7.3 Hz, 1H), 7.98 (dt, *J* = 20.9, 7.6 Hz, 3H), 7.86 (d, *J* = 9.0 Hz, 1H), 7.69 (d, *J* = 9.0 Hz, 1H). **¹³C NMR** (126 MHz, cdcl₃) δ 184.26, 135.57, 135.27, 134.78, 132.06, 131.40, 129.47, 129.14, 129.07, 128.64, 127.54, 127.10, 127.02, 126.92.

Synthesis of 1,4-bis(12-fluoro-1-methylbenzo[*c*]phenanthren-4-yl)benzene

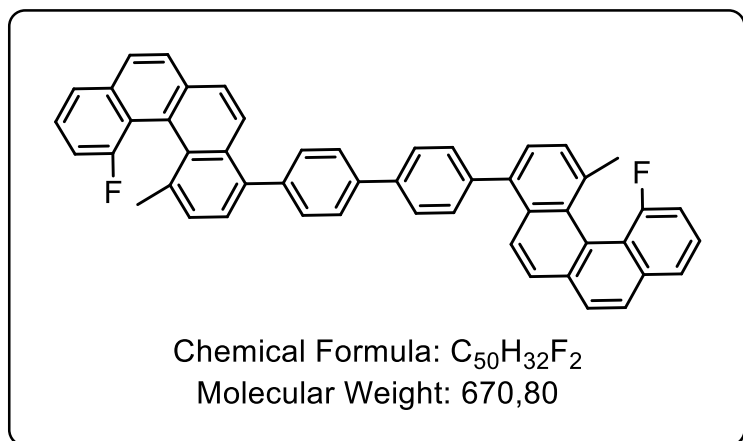


4-bromo-12-fluoro-1-methylbenzo[*c*]phenanthrene (30 mg, 88.4 μmol, 3 equiv.), 1,4-phenylenediboronic acid (5 mg, 30 μmol, 1equiv.) and Cs₂CO₃ (70 mg, 215 μmol, 7.3 equiv.) was dissolved in THF/H₂O (2.5 mL/0.5 mL). The mixture was reacted with Pd(PPh₃)₄ (5 mg, 4.31 μmol, 0.14 equiv.) for 96 h under reflux. After

cooling to rt, water was added, phases were separated and the aqueous layer extracted with DCM. The combined organic fractions were dried over Na₂SO₄, filtrated and the solvent removed in vacuo. The crude product was purified by flash column chromatography on silica gel with *n*-hexane:DCM 5:1. The product was isolated as a yellow solid (10.0 mg, 34 %).

¹H NMR (400 MHz, CDCl₃) δ 8.26 – 8.14 (m, 1H), 8.01 – 7.84 (m, 3H), 7.80 – 7.54 (m, 6H), 7.33 – 7.28 (m, 1H), 2.41 (d, *J* = 1.5 Hz, 3H). **¹⁹F NMR** (376 MHz, CDCl₃) δ -105.17 – -105.70 (m). **¹³C NMR** (101 MHz, CDCl₃) δ 160.56, 158.04, 140.01, 137.08, 136.62, 133.99, 133.94, 132.15, 131.28, 130.75, 127.47, 126.98, 126.85, 126.80, 126.23, 126.14, 124.94, 123.53, 123.50, 122.55, 111.46, 111.23, 22.56, 22.47.

Synthesis of 4,4'-bis(12-fluoro-1-methylbenzo[c]phenanthren-4-yl)-1,1'-biphenyl



4-bromo-12-fluoro-1-methylbenzo[c]phenanthrene (30 mg, 88.4 μ mol, 3 equiv.), [1,1'-biphenyl]-4,4'-diyldiboronic acid (7.1 mg, 29.5 μ mol, 1 equiv.) and Cs_2CO_3 (70 mg, 215 μ mol, 7.3 equiv.) was dissolved in THF/ H_2O (2.5 mL/0.5 mL). The

mixture was reacted with $Pd(PPh_3)_4$ (5 mg, 4.31 μ mol, 0.14 equiv.) for 24 h under reflux. After cooling to rt, water was added, phases were separated and the aqueous layer extracted with DCM. The combined organic fractions were dried over Na_2SO_4 , filtrated and the solvent removed in vacuo. The crude product was purified by flash column chromatography on silica gel with *n*-hexane:DCM 5:1. The product was isolated as a yellow solid (11.7 mg, 59 %). Further purification by HPLC (DCM/MeOH 1:1) resulted in the same yellow solid.

1H NMR (400 MHz, $CDCl_3$) δ 8.11 (d, J = 8.7 Hz, 2H), 7.96 (dd, J = 8.5, 1.7 Hz, 2H), 7.93 – 7.81 (m, 8H), 7.72 (dd, J = 8.5, 3.7 Hz, 6H), 7.69 – 7.63 (m, 2H), 7.59 (td, J = 7.9, 4.8 Hz, 2H), 7.53 (d, J = 7.4 Hz, 2H), 7.33 – 7.27 (m, 2H), 2.40 (d, J = 1.3 Hz, 6H).

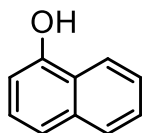
^{19}F NMR (376 MHz, $CDCl_3$) δ -105.08 – -106.80 (m). **^{13}C NMR** (101 MHz, $CDCl_3$) δ 160.55, 158.03, 140.25, 139.62, 137.18, 137.12, 136.42, 133.98, 133.94, 132.14, 131.66, 131.63, 131.31, 131.24, 127.44, 127.00, 126.87, 126.82, 126.79, 126.22, 126.13, 124.93, 123.52, 123.49, 122.53, 121.26, 121.14, 111.45, 111.22, 22.64.

6.5. Screening the reactivity of different functional groups on Al₂O₃

General procedure 5

The oxide was activated by annealing at 400 °C for 4 h in air. Afterwards, it was activated by annealing at 400 °C under vacuum (10-2 mbar) for 18 h. After cooling to room temperature an ampule was filled with the compound and the previously activated oxide (5 g). The ampule was put under vacuum and sealed by melting the glass ampule. After reacting for 24 h at 200 °C the ampule was opened and products extracted with toluol (100 mL) and methanol (100 mL). After removing the solvent in vacuo the residue was examined by ¹H-NMR spectroscopy.

Synthesis of naphthalen-1-ol



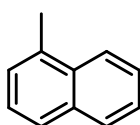
Chemical Formula: C₁₀H₈O
Molecular Weight: 144,17

1-fluoronaphthalene (140 mg) reacted on Al₂O₃ according to general procedure 5. After washing with methanol, naphthalen-1-ol was extracted and identified by ¹H-NMR.

¹H NMR (400 MHz, cdcl₃) δ 8.27 – 8.13 (m, 1H), 7.88 – 7.79 (m, 1H), 7.56 – 7.42 (m, 3H), 7.32 (dd,

J = 9.4, 6.3 Hz, 1H), 6.82 (dd, J = 7.4, 0.8 Hz, 1H), 5.31 (s, 1H).

Synthesis of 1-methylnaphthalene

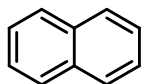


Chemical Formula: C₁₁H₁₀
Molecular Weight: 142,20

1-naphthaldehyde (105 mg) reacted on Al₂O₃ according to general procedure 5. After washing with toluene, 1-methylnaphthalene was extracted and identified by ¹H-NMR.

¹H NMR (400 MHz, cdcl₃) δ 8.01 (dd, J = 8.8, 4.9 Hz, 1H), 7.87 – 7.81 (m, 1H), 7.71 (d, J = 8.0 Hz, 1H), 7.50 (tdd, J = 14.4, 6.7, 1.4 Hz, 2H), 7.41 – 7.34 (m, 1H), 7.32 (d, J = 6.8 Hz, 1H), 2.70 (s, 3H).

Synthesis of naphthalene

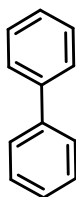


Chemical Formula: C₁₀H₈
Molecular Weight: 128,17

naphthalen-1-ylboronic acid (84 mg) reacted on Al₂O₃ according to general procedure 5. After washing with toluene, naphthalene was extracted and identified by ¹H-NMR.

¹H NMR (400 MHz, cdcl₃) δ 7.92 – 7.84 (m, 4H), 7.56 – 7.48 (m, 4H).

Synthesis of 1,1'-biphenyl

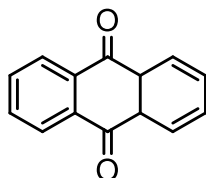


Chemical Formula: C₁₂H₁₀
Molecular Weight: 154,21

[1,1'-biphenyl]-2-ylboronic acid (65 mg) reacted on Al₂O₃ according to general procedure 5. After washing with toluene, 1,1'-biphenyl was extracted and identified by ¹H-NMR.

¹H NMR (400 MHz, cdcl₃) δ 7.62 (dt, J = 3.2, 1.9 Hz, 4H), 7.51 – 7.44 (m, 4H), 7.40 – 7.34 (m, 2H).

Synthesis of 4a,9a-dihydroanthracene-9,10-dione

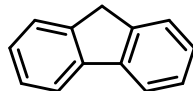


Chemical Formula: C₁₄H₁₀O₂
Molecular Weight: 210,23

Anthracene (92 mg) reacted on Al₂O₃ according to general procedure 5. After washing with methanol, 4a,9a-dihydroanthracene-9,10-dione was extracted and identified by ¹H-NMR.

¹H NMR (400 MHz, cdcl₃) δ 8.36 – 8.30 (m, 4H), 7.49 – 7.44 (m, 4H).

Synthesis of 9H-fluorene

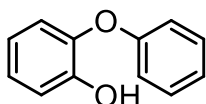


Chemical Formula: C₁₃H₁₀
Molecular Weight: 166,22

1-benzyl-2-fluorobenzene (99 mg) reacted on Al₂O₃ according to general procedure 5. After washing with toluene, 9H-fluorene was extracted and identified by ¹H-NMR.

¹H NMR (400 MHz, cdcl₃) δ 7.80 (d, J = 7.5 Hz, 1H), 7.56 (d, J = 7.4 Hz, 1H), 7.41 – 7.36 (m, 1H), 7.34 – 7.27 (m, 6H), 3.92 (s, 1H).

Synthesis of 2-phenoxyphenol

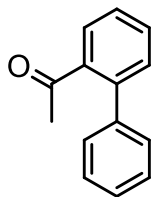


Chemical Formula: C₁₂H₁₀O₂
Molecular Weight: 186,21

1-fluoro-2-phenoxybenzene (60 mg) reacted on Al₂O₃ according to general procedure 5 for 7d. After washing with methanol, 2-phenoxyphenol was extracted and identified by ¹H-NMR. The product was purified by flash column chromatography on silica gel with *n*-hexane:ethylacetat 9:1 to afford the product as a white solid (23 mg, 38 %).

¹H NMR (400 MHz, cdcl₃) δ 7.35 (dd, J = 8.6, 7.5 Hz, 2H), 7.13 (t, J = 7.4 Hz, 1H), 7.08 – 7.00 (m, 4H), 6.92 – 6.81 (m, 2H), 5.58 (s, 1H). **¹³C NMR** (101 MHz, cdcl₃) δ 156.75, 147.49, 143.46, 129.86, 124.75, 123.59, 120.61, 118.85, 117.98, 116.16.

Synthesis of 1-([1,1'-biphenyl]-2-yl)ethan-1-one

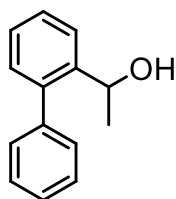


Chemical Formula: C₁₄H₁₂O
Molecular Weight: 196,25

1-(2-bromophenyl)ethan-1-one (676 μL, 5.02 mmol, 1 equiv.), phenylboronic acid (674 mg, 5.53 mmol, 1.1 equiv.) Cs₂CO₃ (3.27 g, 10.0 mmol, 2 equiv.) were reacted in THF/H₂O (12 mL, 5:1) with Pd(PPh₃)₂Cl₂ (75 mg, 100 μmol, 0.02 equiv.) for 20 h under reflux according to general procedure 1. After cooling to rt, water was added, phases were separated and the aqueous layer extracted with DCM. The combined organic fractions were dried over Na₂SO₄, filtrated and the solvent removed in vacuo. The crude product was purified by flash column chromatography on silica gel with *n*-hexane:ethylacetat 9:1 to afford the product as a white solid.

¹H NMR (400 MHz, cdcl₃) δ 7.58 – 7.55 (m, 1H), 7.53 – 7.47 (m, 1H), 7.45 – 7.37 (m, 5H), 7.34 (ddd, J = 8.8, 4.9, 2.4 Hz, 2H), 2.01 (s, 3H). **¹³C NMR** (101 MHz, cdcl₃) δ 204.70, 140.91, 140.74, 140.51, 130.71, 130.24, 128.85, 128.68, 127.88, 127.45, 30.42.

Synthesis of 1-([1,1'-biphenyl]-2-yl)ethan-1-ol



Chemical Formula: C₁₄H₁₄O
Molecular Weight: 198,27

1-([1,1'-biphenyl]-2-yl)ethan-1-one (104 mg) reacted on Al₂O₃ according to general procedure 5. After washing with toluene and methanol, 1-([1,1'-biphenyl]-2-yl)ethan-1-ol was extracted and identified by ¹H-NMR.

¹H NMR (400 MHz, cdcl₃) δ 7.84 – 7.78 (m, 4H), 7.59 – 7.53 (m, 3H), 7.51 – 7.45 (m, 2H), 3.99 (q,

J = 7.5 Hz, 1H), 3.27 (d, J = 4.2 Hz, 1H), 1.58 (d, J = 7.5 Hz, 3H).

Synthesis of 2-(difluoromethyl)-1,1'-biphenyl



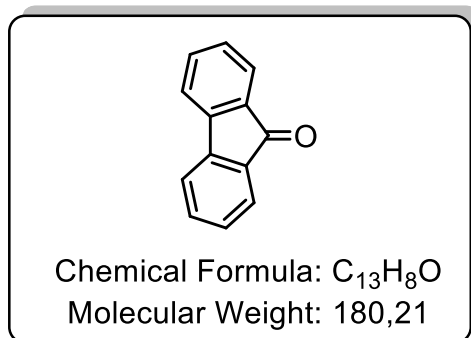
Chemical Formula: C₁₃H₁₀F₂
Molecular Weight: 204,22

[1,1'-biphenyl]-2-carbaldehyde (200 mg, 1.10 mmol), N,N-diethyl-1,1,1-trifluoro-λ⁴-sulfanamine (435 mL, 3.29 mmol, 3 equiv.) were reacted in dichloromethane (2 mL) at rt for 18 h. Water and more dichloromethane was added, phases were separated and the aqueous layer extracted with DCM. The combined organic fractions were dried

over Na₂SO₄, filtrated and the solvent removed in vacuo. The crude product was purified by flash column chromatography on silica gel with *n*-hexane to afford the product as a solid (80.6 mg, 36%).

¹H NMR (400 MHz, cdcl₃) δ 7.80 (dt, J = 8.2, 3.6 Hz, 1H), 7.58 – 7.33 (m, 8H), 6.56 (t, J = 54.9 Hz, 1H). **¹⁹F NMR** (376 MHz, cdcl₃) δ -107.35 (s), -107.49 (s). **¹³C NMR** (101 MHz, cdcl₃) δ 141.44, 141.37, 141.31, 138.64, 131.95, 131.73, 131.51, 130.44, 130.42, 130.40, 130.19, 129.43, 129.43, 129.42, 128.39, 127.85, 127.83, 127.82, 125.63, 125.58, 125.53, 115.46, 113.11, 110.77.

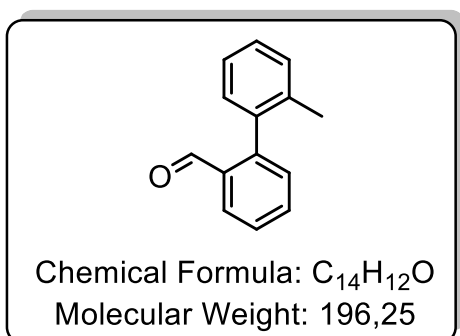
Synthesis of 9H-fluoren-9-one



2-(difluoromethyl)-1,1'-biphenyl (60 mg) reacted on Al₂O₃ according to general procedure 5 at 100°C. After washing with toluene, 9H-fluoren-9-one was extracted and identified by ¹H-NMR.

¹H NMR (400 MHz, cdcl₃) δ 7.66 (dd, J = 7.4, 0.8 Hz, 1H), 7.55 – 7.46 (m, 2H), 7.30 (td, J = 7.3, 1.3 Hz, 1H).

Synthesis of 2'-methyl-[1,1'-biphenyl]-2-carbaldehyde

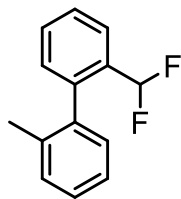


2-bromobenzaldehyde (1,25mL, 10,81mmol, 1 equiv.), o-tolylboronic acid (1,62g, 11,89mmol, 1.1 equiv.) and Cs₂CO₃ (7,04g, 21,62mmol, 2 equiv.) were reacted in THF/H₂O (46 mL, 5:1) with Pd(PPh₃)₂Cl₂ (150 mg, 200 μmol, 0.02 equiv.) for 20 h under reflux according to general procedure 1.

After cooling to rt, water was added, phases were separated and the aqueous layer extracted with DCM. The combined organic fractions were dried over Na₂SO₄, filtrated and the solvent removed in vacuo. The crude product was purified by flash column chromatography on silica gel with *n*-hexane to afford the product as a yellow oil (1.52 g, 71 %).

¹H NMR (400 MHz, cdcl₃) δ 9.77 (d, J = 0.7 Hz, 1H), 8.05 (td, J = 8.2, 1.3 Hz, 1H), 7.69 – 7.58 (m, 1H), 7.53 – 7.46 (m, 1H), 7.40 – 7.23 (m, 4H), 7.23 – 7.15 (m, 1H), 2.11 (s, 4H). **¹³C NMR** (101 MHz, cdcl₃) δ 192.21, 191.74, 145.66, 137.49, 136.15, 135.30, 133.88, 133.85, 133.70, 131.10, 130.75, 130.18, 130.08, 129.86, 128.28, 127.90, 127.81, 127.33, 127.08, 125.68, 20.30.

Synthesis of 2-(difluoromethyl)-2'-methyl-1,1'-biphenyl



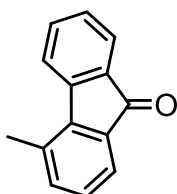
Chemical Formula: C₁₄H₁₂F₂
Molecular Weight: 218,25

2'-methyl-[1,1'-biphenyl]-2-carbaldehyde (200 mg, 1.02 mmol, 1 equiv.), N,N-diethyl-1,1,1-trifluoro- λ^4 -sulfanamine (492 mg, 3.06 mmol, 3 equiv.) were reacted in dichloromethane (2 mL) at rt for 18 h. Water and more dichloromethane was added, phases were separated and the aqueous layer extracted with DCM. The combined organic

fractions were dried over Na₂SO₄, filtrated and the solvent removed in vacuo. The crude product was purified by flash column chromatography on silica gel with *n*-hexane to afford the product as a solid (119 mg, 54 %)

¹H NMR (400 MHz, cdcl₃) δ 7.81 – 7.73 (m, 1H), 7.54 – 7.46 (m, 2H), 7.37 – 7.20 (m, 4H), 7.18 – 7.12 (m, 1H), 6.31 (t, J = 55.3 Hz, 1H), 2.08 (s, 3H). **¹⁹F NMR** (376 MHz, cdcl₃) δ -108.44 (dd, J = 304.3, 55.2 Hz), -110.93 (dd, J = 304.3, 55.4 Hz). **¹³C NMR** (101 MHz, cdcl₃) δ 140.78, 140.72, 140.65, 138.00, 136.15, 132.43, 132.21, 131.99, 130.33, 130.31, 130.29, 130.08, 129.91, 129.68, 128.13, 127.82, 127.81, 125.54, 125.42, 125.37, 125.32, 115.41, 113.06, 110.71, 20.01, 20.01.

Synthesis of 4-methyl-9H-fluoren-9-one



Chemical Formula: C₁₄H₁₀O
Molecular Weight: 194,23

2-(difluoromethyl)-2'-methyl-1,1'-biphenyl (35 mg) reacted on Al₂O₃ according to general procedure 5 at 100°C. After washing with toluene, 4-methyl-9H-fluoren-9-one was extracted and identified by ¹H-NMR.

¹H NMR (400 MHz, cdcl₃) δ 7.69 (d, J = 7.3 Hz, 1H), 7.64 (d, J = 7.6 Hz, 1H), 7.54 (d, J = 7.3 Hz, 1H), 7.52 – 7.46 (m, 1H), 7.32 – 7.27 (m, 1H), 7.21 – 7.17 (m, 2H), 2.61 (s, 3H).

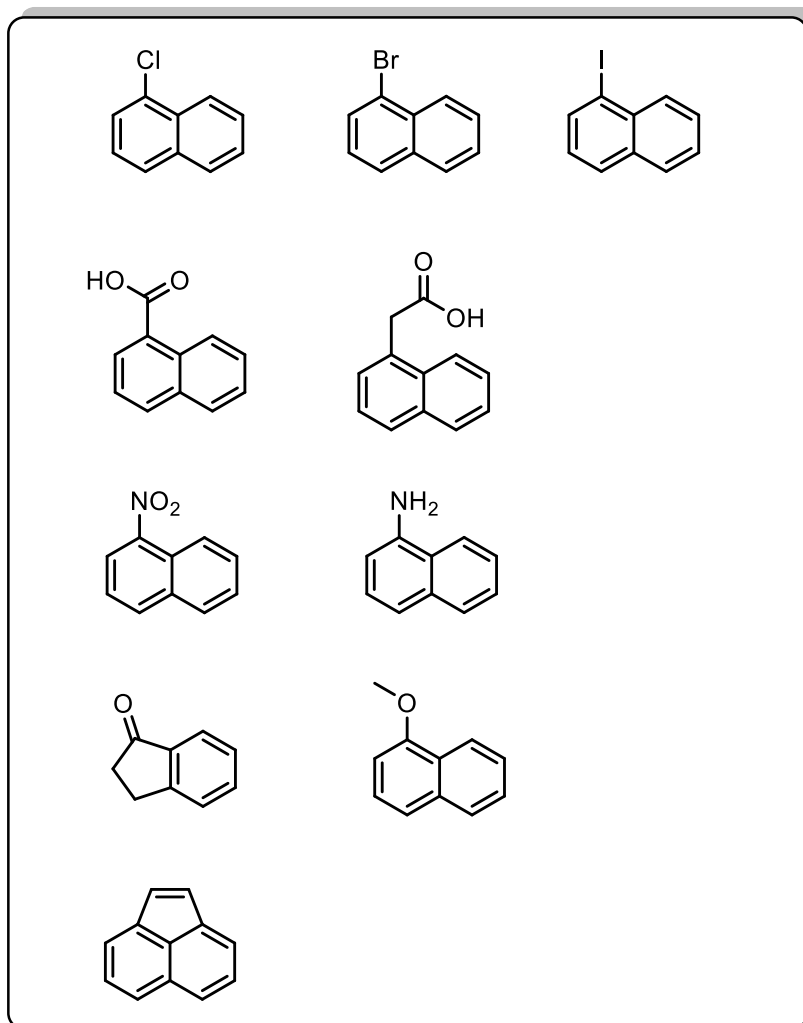
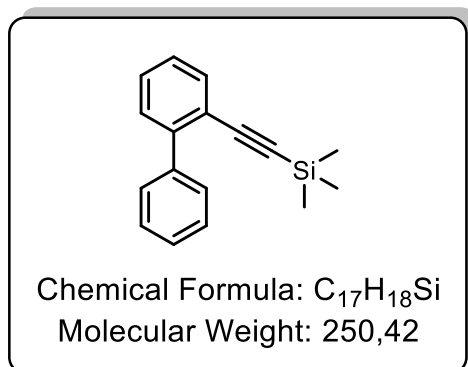


Figure 6.3: molecules, which showed no reaction on Al_2O_3 .

6.6. Screening the reactivity of 2-ethynyl-1,1'-biphenyl on different metal oxides

Synthesis of [1,1'-biphenyl]-2-ylethynyl)trimethylsilane

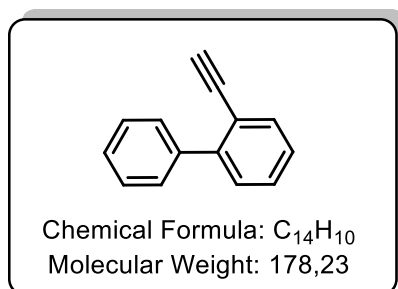


2-iodo-1,1'-biphenyl (2.52 mL, 14.3 mmol, 1 equiv.), triethylamine (5.94 mL, 42.8 mmol, 3 equiv.), ethynyltrimethylsilane (2.44 mL, 17.1 mmol, 1.2 equiv.), copper(I) iodide (109 mg, 571 μmol, 0.04 equiv.) were reacted in THF (25 mL) with Pd(PPh₃)₂Cl₂ (400 mg, 571 μmol, 0.04 equiv.) for 20 h at rt. After water was added, phases were

separated and the aqueous layer extracted with DCM. The combined organic fractions were dried over Na₂SO₄, filtrated and the solvent removed *in vacuo*. The crude product was purified by flash column chromatography on silica gel with n-hexane to afford the product (1.65 g, 45 %).

¹H NMR (400 MHz, CDCl₃) δ 7.68 – 7.60 (m, 3H), 7.47 – 7.35 (m, 5H), 7.33 – 7.28 (m, 1H), 0.18 (s, 9H).

Synthesis of 2-ethynyl-1,1'-biphenyl



[1,1'-biphenyl]-2-ylethynyl)trimethylsilane (1.65 g, 6.59 mmol) and K₂CO₃ (2.73 g, 19.8 mmol, 3 equiv.) were reacted in methanol (20 mL) at rt for 48 h. After water was added, phases were separated and the aqueous layer extracted with DCM. The combined organic fractions were dried over Na₂SO₄, filtrated and the

solvent removed *in vacuo*. The crude product was purified by flash column chromatography on silica gel with n-hexane to afford the product as yellow oil (1.05 g, 90 %).

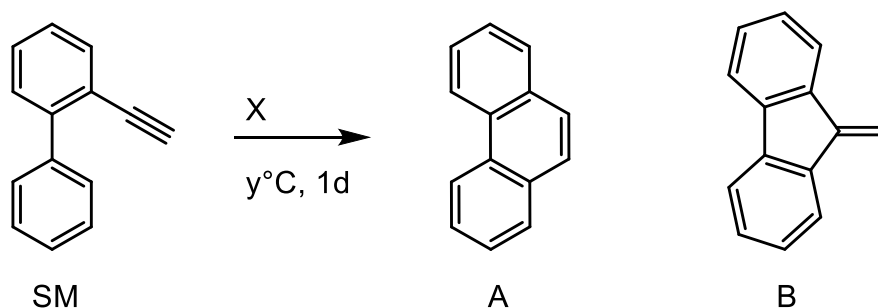
¹H NMR (400 MHz, CDCl₃) δ 7.64 – 7.57 (m, 3H), 7.46 – 7.35 (m, 5H), 7.34 – 7.28 (m, 1H), 3.03 (s, 1H).

General Procedure 6

An ampule was filled with 2-ethynyl-1,1'-biphenyl and the oxide (10 g). The ampule was put under vacuum and sealed by melting the glass ampule. After reacting for 18 h at 90 °C the ampule was opened and products extracted with toluol (100 mL) and methanol (100 mL).

General Procedure 7

The oxide was activated by annealing at 400 °C for 4 h in air. Afterwards, it was activated by annealing at 400 °C under vacuum (10-2 mbar) for 16 h. After cooling to room temperature an ampule was filled with 2-ethynyl-1,1'-biphenyl and the previously activated oxide (10 g). The ampule was put under vacuum and sealed by melting the glass ampule. After reacting for 18 h at 90°C, 200°C or 400°C the ampule was opened and products extracted with toluol (100 mL) and methanol (100 mL).



Scheme 21: Reaction of **SM** on different metal oxides (*X*) under different temperatures (*y*).

Surface material	90 °C General Procedure 6	90 °C General Procedure 7	200°C General Procedure 7	400°C General Procedure 7
Al ₂ O ₃	-	A	A	
TiO ₂ anatase	SM	SM	SM	
TiO ₂ rutil	SM	SM	SM	
SiO ₂	SM	SM	-	
α-Fe ₂ O ₃	SM	SM	-	
Ga ₂ O ₃	SM	SM, A, B*	A	
MgO	SM	SM	-	
ZrO ₂	SM	A, B	-	
Nb ₂ O ₅	B	SM	-	
In ₂ O ₃	SM	SM	A	
Ce ₂ O ₃	SM	SM	-	
MoS ₂	-	SM, A	-	
Zr20	SM, A*, B	A		A
Si5	SM	B*		A*, B
Si30	SM, B*	B		
Mg5	SM	SM		SM
Mg30	SM	SM		SM
Ce20	SM	SM		SM*, A

Table 6: Experimental results of different metal oxides with biphenyl acetylene (**SM**)

*Small amount

- no product or starting material was found after extraction with toluene and methanol

Reaction on Zr20

Reaction of 2-ethynyl-1,1'-biphenyl (50 mg) on 2 g Puralox SCFa-190 Zr20 ($\text{Al}_2\text{O}_3 / \text{ZrO}_2 = 80 / 20$).

Reaction on Si5

Reaction of 2-ethynyl-1,1'-biphenyl (50 mg) on 2 g SIRAL 5 ($\text{Al}_2\text{O}_3 / \text{SiO}_2 = 95 / 5$).

Reaction on Si30

Reaction of 2-ethynyl-1,1'-biphenyl (50 mg) on 2 g SIRAL 30 ($\text{Al}_2\text{O}_3 / \text{SiO}_2 = 70 / 30$).

Reaction on Mg30

Reaction of 2-ethynyl-1,1'-biphenyl (50 mg) on 2 g PURAL MG30 ($\text{Al}_2\text{O}_3 / \text{MgO} = 70 / 30$).

Reaction on Ce20

Reaction of 2-ethynyl-1,1'-biphenyl (50 mg) on 2 g Puralox SCFa-160/Ce20 ($\text{Al}_2\text{O}_3 / \text{CeO}_2 = 80 / 20$).

Reaction on Mg5

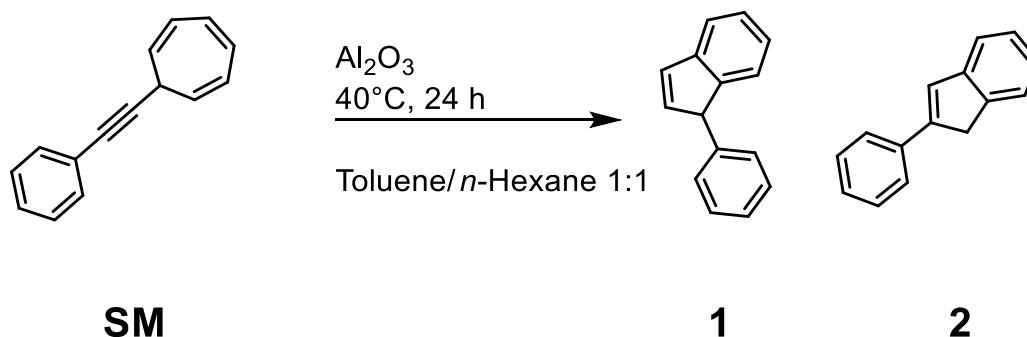
Reaction of 2-ethynyl-1,1'-biphenyl (50 mg) on 2 g PURAL MG5 ($\text{Al}_2\text{O}_3 / \text{MgO} = 95 / 5$).

The reactions were done according to Table 6 at 90, 200 and 400 °C with general procedure 6 and 7 with different surface material.

Phenanthrene (**A**): The $^1\text{H-NMR}$ data was consistent with literature and could be identified by duplet at 8.76 ppm.⁷³

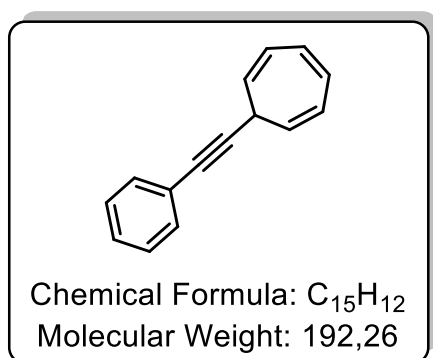
9-Methylene-9H-fluorene (**B**): The $^1\text{H-NMR}$ data was consistent with literature and could be identified by singlet at 6.08 ppm.¹¹⁹

6.7. Investigation for the soft pi-Lewis acidity of different alumina's terminations



Scheme 22: Reaction of 7-(phenylethynyl)cyclohepta-1,3,5-triene (**SM**) on different Al_2O_3 .

Synthesis of 7-(phenylethynyl)cyclohepta-1,3,5-triene



$n\text{-BuLi}$ (2.5 M in hexane, 1.1 mL, 2.70 mmol, 1.1 equiv.) was added slowly to a solution of ethynylbenzene (269 mmL, 2,45mmol) in THF (15 mL) at -78°C . After 45 min., cyclohepta-2,4,6-trien-1-ylum tetrafluoroborate (445 mg, 2.45 mmol) was added and the mixture was warmed to r.t.. After 18 h, water was added, phases were separated and the aqueous layer extracted with DCM. The combined organic fractions were dried over Na_2SO_4 , filtrated and the solvent removed *in vacuo*. The crude product was purified by flash column chromatography on silica gel (*n*-hexane) to afford the desired product as a colorless oil (462 mg, 98 %). $^1\text{H NMR}$ (400 MHz, cdcl_3) δ 7.49 (d, $J = 3.6$ Hz, 2H), 7.32 (d, $J = 2.4$ Hz, 3H), 6.76 – 6.64 (m, 2H), 6.23 (dd, $J = 7.4, 3.8$ Hz, 2H), 5.46 (dd, $J = 8.7, 5.5$ Hz, 2H), 2.80 – 2.66 (m, 1H). $^{13}\text{C NMR}$ (101 MHz, cdcl_3) δ 132.11, 131.70, 131.00, 128.20, 127.86, 124.74, 123.50, 123.20, 91.02, 80.61.

General Procedure 11

Different aluminum oxides (Table 4) were activated by annealing at 400 °C for 6 h in air. Afterwards, it was heated at 400 °C under vacuum (10-2 mbar) for 16 h. It was cooled to room temperature. 5 μ L 7-(phenylethynyl)cyclohepta-1,3,5-triene (**SM**) reacted in distilled *n*-hexane/dry toluene (0.25mL/0.25mL) on different activated alumina (50-70 mg) under inert conditions (Ar). The mixture was diluted and filtered before injection into HPLC.

Experiment	Sample	Alumina	SA [m ² /g]	comment	Ratio SM/1/2 [%]
0	0	γ -alumina, commercial		Our normal alumina	15/5/80
1.1(rt)	1	γ -alumina rods	75		50/40/10
1.2(40 °C)	1	γ -alumina rods	75		5/15/80
1.3(40 °C)	1	γ -alumina rods	75		5/15/80
2.1	2	γ -alumina platelet	72		10/85/5
2.2	2	γ -alumina platelet	72		80/5/15
3.1	3	γ -alumina hexagonal	70-75		5/15/80
3.2	3	γ -alumina hexagonal	70-75		80/1/14
4.1	4	0.1 weight% Rhodium/ γ -alumina			5/45/50
4.2	4	0.1 weight% Rhodium/ γ -alumina			30/60/10
5.1	5	0.05 weight% Palladium/ γ -alumina			10/85/5
5.2	5	0.05 weight% Palladium/ γ -alumina			60/5/35
6.1	6	pure theta-alumina	75	has very little OH groups on the surface	20/60/20
6.2	6	pure theta-alumina	75	has very little OH groups on the surface	80/0/20
7.1	7	pure theta-alumina	75	is covered with OH groups	80/19/1
7.2	7	pure theta-alumina	75	is covered with OH groups	60/0/40
8.1	8	1 weight% Lanthanum/ γ -alumina			5/15/80

8.2	8	1 weight% Lanthanum/ γ -alumina			20/30/50
9.1	9	gamma-alumina, commercial	200		5/90/5
9.2	9	γ -alumina, commercial	200		20/30/50
10.1	10	γ -alumina, commercial	90		10/85/5
10.2	10	γ -alumina, commercial	90		95/0/5
11.1	11	α -alumina nanosheets	20	recipe and made by MIT	85/0/15
11.2	11	α -alumina nanosheets	20	recipe and made by MIT	95/0/5

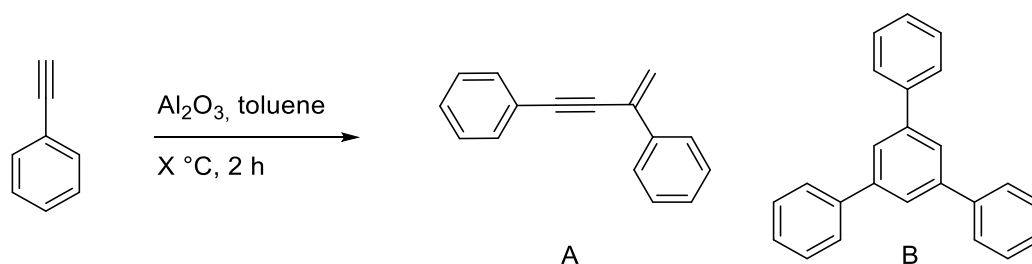
Table 7: Characteristic of different Al_2O_3 samples used in reaction of 7-(phenylethynyl)cyclohepta-1,3,5-triene (**SM**) and approximate conversion using HPLC Contour view and spectra as reference.

Samples from Table 7 were reacted according to general procedure 11 at 40 °C, except experiment 1.1, which was done at room temperature.

6.8. Homodimerization of terminal Alkyne- Model molecule with different temperatures

General procedure 8- Al₂O₃-Mediated dimerization in Microwave

γ -Al₂O₃ was activated by annealing at 400 °C for 4 h in air. Afterwards, it was activated by annealing at 400 °C under vacuum (10-2 mbar) for 16 h. After cooling to room temperature an ampule was filled with the compound (100 mg), the previously activated oxide (2 g) and toluene (4 mL). The ampule was closed and stirred for 2-48 h at different temperatures in the microwave. After washing with toluene, dichloromethane and methanol, solvent was evaporated via vacuo and the residue was analyzed by ¹H-NMR spectroscopy.



Scheme 23: AmCFA of phenylacetylene at different temperatures.

Temperature [°C]	Reaction time	Ratio of A/B [%]
20	2d	68:32
40	2h	88:12
60	2h	94:6
60	6h	83:17
90	2h	0:100
120	2h	9:91
150	2h	19:81

Table 8: Results of AmCFA of phenylacetylene under varying temperatures.

General Procedure 9- Al₂O₃ with induced defects -Mediated dimerization in dry

conditions

Aluminum oxide doped with different metals, was activated by annealing at 400 °C for 6 h in air. Afterwards, it was heated at 400 °C under vacuum (10-2 mbar) for 16 h. After cooling to room temperature, phenylacetylene was added under argon atmosphere. The tube containing the obtained mixture was sealed under vacuum and heated at 90 °C for 1 d. After cooling to room temperature, products were extracted with dichloromethane. Yields were determined by ¹H-NMR analysis.

Reaction on Mg30

After reaction according to general procedure 9 on PURAL MG30 (Al₂O₃ / MgO = 70 / 30), the trimer (4 %), the head-to-tail dimer (51 %) and the Z-head-to-head dimer (45 %) were found by ¹H-NMR.

Calculation of yield: $x = \text{Integral of trimer} / 3$ $y = \text{Integral of dimer} / 2$

$\text{Yield(Trimer)} = x / (x + y_1 + y_2)$

$\text{Yield(Dimer 1)} = y_1 / (x + y_1 + y_2)$

Reaction on Si30

After reaction according to general procedure 9 on SIRAL 30 (Al₂O₃ / SiO₂ = 70 / 30), only trimer was found by ¹H-NMR.

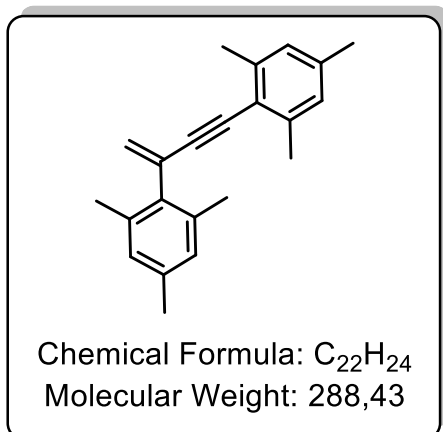
Reaction on Ce20

After reaction according to general procedure 9 on Puralox SCFa-160/Ce20 (Al₂O₃ / CeO₂ = 80 / 20), the trimer (15 %), the E-head-to-head dimer (47 %) and the Z-head-to-head dimer (38 %) were found by ¹H-NMR.

Reaction on Ce20

After reaction according to general procedure 8 at 120°C in toluene for 5 h on Puralox SCFa-160/Ce20 (Al₂O₃ / CeO₂ = 80 / 20), the trimer (23 %) and the Z-head-to-head dimer (77 %) were found by ¹H-NMR.

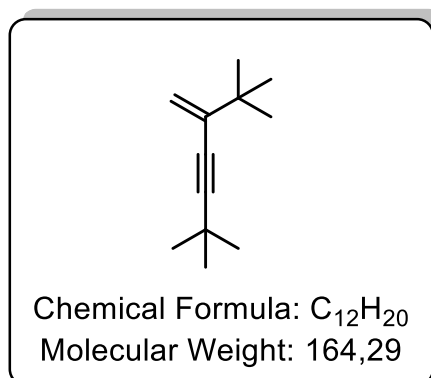
Dimerization of 2-ethynyl-1,3,5-trimethylbenzene



2-ethynyl-1,3,5-trimethylbenzene was reacted according to general procedure 8 at 120 °C for 2 h. The Dimer has been isolated.

1H NMR (400 MHz, $cdCl_3$) δ 6.88 (s, 2H), 6.82 (s, 2H), 5.88 (d, $J = 2.1$ Hz, 1H), 5.30 (d, $J = 2.1$ Hz, 1H), 2.33 (d, $J = 10.0$ Hz, 12H), 2.27 (d, $J = 12.6$ Hz, 6H).

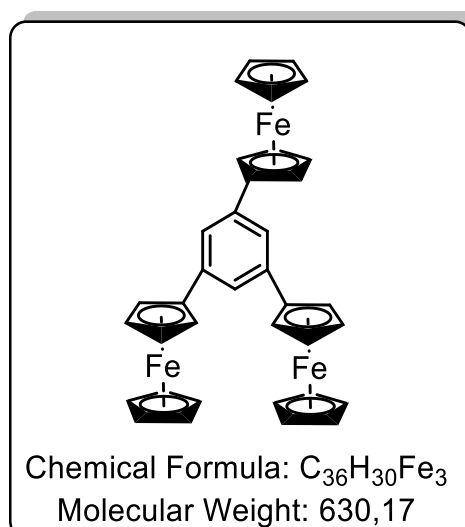
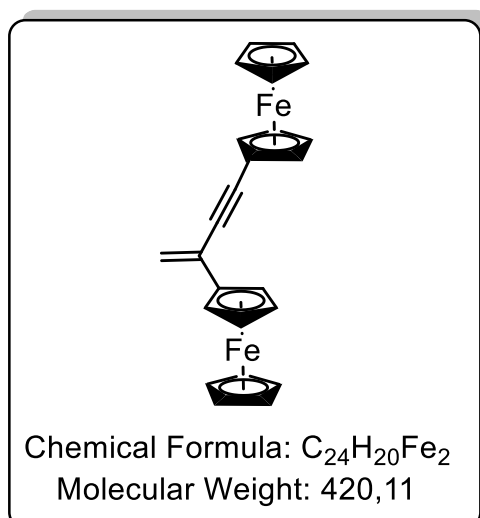
Dimerization of 3,3-dimethylbut-1-yne



3,3-dimethylbut-1-yne was reacted according to general procedure 8 at 60 and 120 °C for 4 h. The Dimer has been isolated.

1H NMR (400 MHz, $cdCl_3$) δ 5.34 (s, 1H), 5.12 (s, 1H), 1.25 (s, 18H).

Reaction of ferrocene acetylene



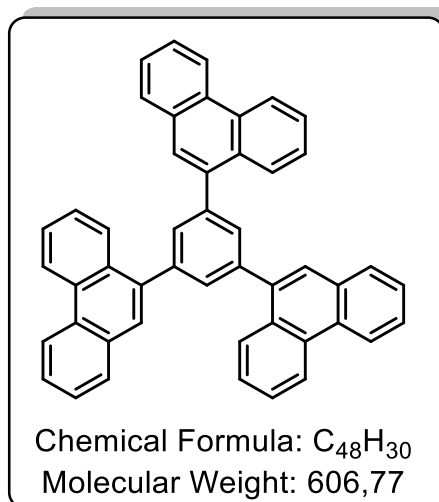
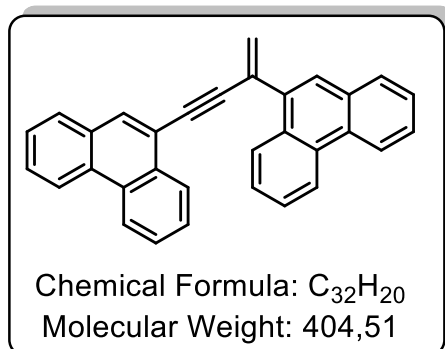
Ferrocene acetylene was reacted according to general procedure 8 at 60 °C for 4 h. The dimer and trimer has been identified by 1H NMR spectrum.

Dimer: 1H NMR (400 MHz, $cdCl_3$) δ 5.54 (s, 1H), 5.40 (s, 1H), 4.57 – 4.51 (m, 4H), 4.31

– 4.19 (m, 14H).

Trimer: $^1\text{H NMR}$ (400 MHz, cdCl_3) δ 7.44 (s, 3H), 4.79 – 4.62 (m, 6H), 4.57 – 4.03 (m, 21H).

Reaction of 9-ethynylphenanthrene



9-ethynylphenanthrene was reacted according to general procedure 8 at 120 °C for 4 h. The ratio of dimer and trimer was 1.9:1.

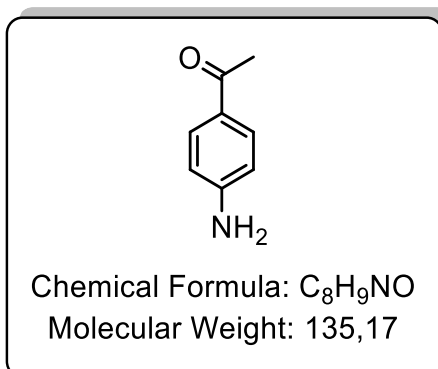
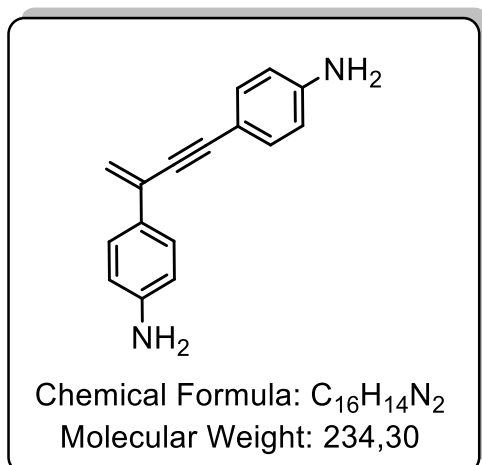
9-ethynylphenanthrene was reacted according to general procedure 8 at 60 °C for 4 h. The ratio of dimer and trimer was 1:6.6.

The dimer and trimer have been identified by $^1\text{H NMR}$ spectrum

Dimer: $^1\text{H NMR}$ (400 MHz, cdCl_3) δ 8.83 – 7.48 (m, 18H), 6.24 (d, $J = 1.8$ Hz, 1H), 5.96 (d, $J = 1.8$ Hz, 1H).

Trimer: $^1\text{H NMR}$ (400 MHz, cdCl_3) δ 8.72 – 8.62 (m, 7H), 8.53 – 8.44 (m, 3H), **8.07** (s, 3H), 7.86 (dt, $J = 6.9, 3.5$ Hz, 4H), 7.75 – 7.56 (m, 13H).

Reaction of 4-ethynylaniline



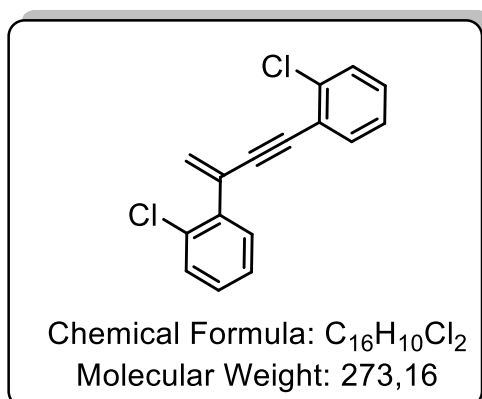
4-ethynylaniline was reacted according to general procedure 8 at 120 °C. The dimer was found by ¹H-NMR spectrum in low yield. The main product was 1-(4-aminophenyl)ethan-1-one.

Dimer: **¹H NMR** (400 MHz, cdcl₃) δ 7.76 (d, *J* = 2.1 Hz, 1H), 7.28 (d, *J* = 8.6 Hz, 2H), 7.15 (d, *J* = 8.5 Hz, 3H), 6.61 – 6.55 (m, 2H), 5.68 (s, 1H), 5.18 (s, 1H), 4.09 (s, 3H).

1-(4-aminophenyl)ethan-1-one: **¹H NMR** (400 MHz, cdcl₃) δ 7.79 (t, *J* = 9.1 Hz, 2H), 6.68 – 6.59 (m, 2H), 4.17 (s, 2H), 2.50 (s, *J* = 4.9 Hz, 3H).

4-ethynylaniline was reacted according to general procedure 10 at 40 °C. Only the dimer was found by ¹H-NMR spectrum.

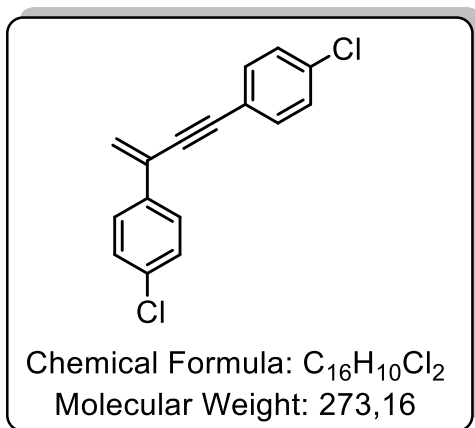
Dimerization of 1-chloro-2-ethynylbenzene



1-chloro-2-ethynylbenzene was reacted according to general procedure 4 at 40 °C for 1 d. The Dimer has been isolated.

¹H NMR (400 MHz, cdcl₃) δ 7.53 – 7.35 (m, 4H), 7.32 – 7.17 (m, 4H), 6.03 (d, *J* = 1.4 Hz, 1H), 5.81 (d, *J* = 1.4 Hz, 1H).

Dimerization of 1-chloro-4-ethynylbenzene

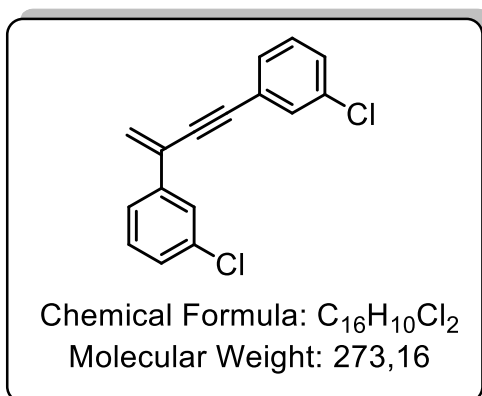


121.33, 121.25, 89.89, 88.91.

1-chloro-4-ethynylbenzene was reacted according to general procedure 4 at 40 °C. The dimer has been isolated.

1H NMR (400 MHz, $CDCl_3$) δ 7.64 – 7.61 (m, 2H), 7.46 – 7.43 (m, 2H), 7.37 – 7.31 (m, 4H), 5.97 (s, 1H), 5.77 (s, 1H). **^{13}C NMR** (101 MHz, $CDCl_3$) δ 135.56, 135.44, 134.62, 134.33, 132.82, 129.88, 129.43, 128.79, 128.71, 128.56, 128.47, 127.33,

Dimerization of 1-chloro-3-ethynylbenzene

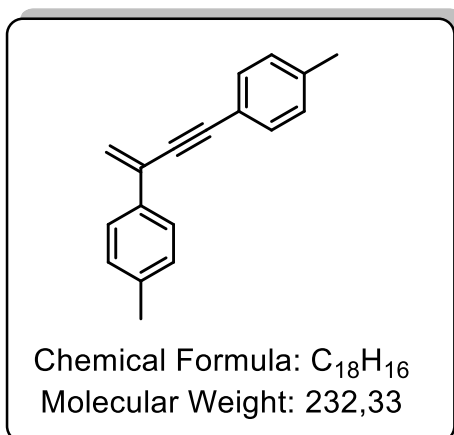


122.09, 85.82, 82.94.

1-chloro-3-ethynylbenzene was reacted according to general procedure 4 at 40 °C. The dimer has been isolated.

1H NMR (400 MHz, $CDCl_3$) δ 7.68 (s, 1H), 7.62 – 7.51 (m, 2H), 7.44 – 7.28 (m, 5H), 6.01 (s, 1H), 5.81 (s, 1H). **^{13}C NMR** (101 MHz, $cdcl_3$) δ 131.49, 130.87, 130.71, 129.71, 129.56, 129.47, 129.43, 129.33, 129.07, 128.76, 128.39, 126.21, 124.16,

Dimerization of 1-ethynyl-4-methylbenzene

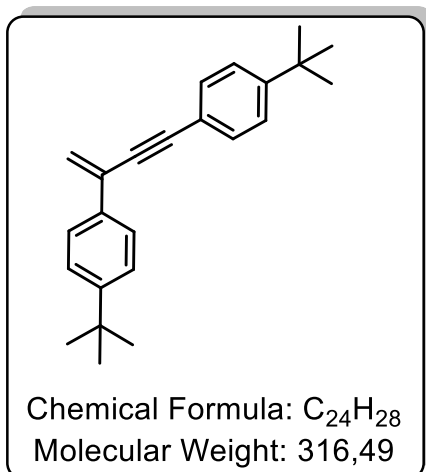


120.20, 119.15, 90.69, 88.05, 41,35.

1-ethynyl-4-methylbenzene was reacted according to general procedure 4 at 40 °C. The dimer has been isolated.

1H NMR (400 MHz, $CDCl_3$) δ 7.66 – 7.60 (m, 2H), 7.46 – 7.41 (m, 2H), 7.21 – 7.13 (m, 4H), 5.92 (d, J = 1.1 Hz, 1H), 5.69 (d, J = 1.0 Hz, 1H), 2.38 (s, 6H). **^{13}C NMR** (101 MHz, $CDCl_3$) δ 138.32, 138.05, 134.67, 131.50, 130.64, 128.98, 128.96, 125.97,

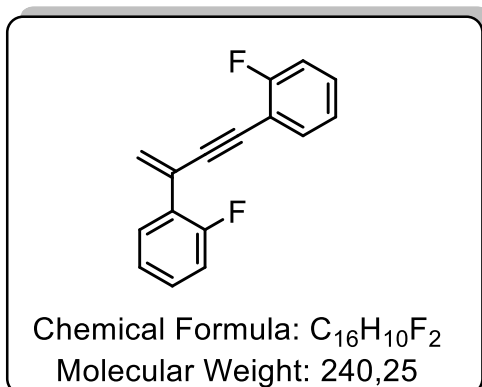
Dimerization of 1-(tert-butyl)-4-ethynylbenzene



1-(tert-butyl)-4-ethynylbenzene was reacted according to general procedure 4 at 40 °C. The dimer has been isolated.

¹H NMR (400 MHz, cdcl₃) δ 7.67 (d, *J* = 8.6 Hz, 2H), 7.47 (d, *J* = 8.5 Hz, 2H), 7.39 (dd, *J* = 14.5, 8.5 Hz, 4H), 5.93 (s, 1H), 5.70 (s, 1H), 1.45 (s, 18H). **¹³C NMR** (101 MHz, cdcl₃) δ 151.51, 151.32, 131.35, 130.59, 125.81, 125.22, 125.21, 119.31, 90.67, 88.08, 77.21, 76.89, 76.57, 41.35, 34.63.

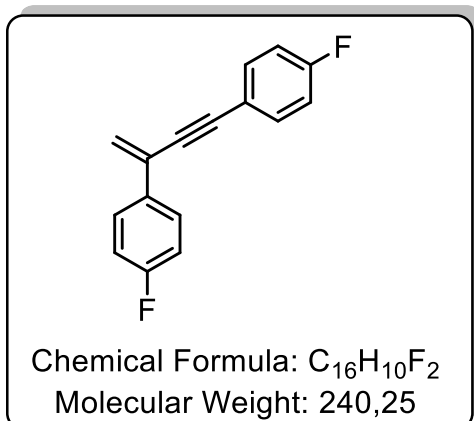
Dimerization of 1-ethynyl-2-fluorobenzene



1-ethynyl-2-fluorobenzene was reacted according to general procedure 4 at 40 °C. The dimer has been isolated.

¹H NMR (400 MHz, CDCl₃) δ 7.75 (td, *J* = 7.9, 1.8 Hz, 1H), 7.53 – 7.46 (m, 1H), 7.35 – 7.27 (m, 2H), 7.17 (td, *J* = 7.6, 1.3 Hz, 1H), 7.15 – 7.06 (m, 3H), 6.14 (s, 1H), 6.05 – 6.02 (m, 1H). **¹⁹F NMR** (376 MHz, CDCl₃) δ -109.61 – -109.85 (m), -114.32 – -114.56 (m). **¹³C NMR** (101 MHz, CDCl₃) δ 133.38, 130.42, 130.09, 130.01, 129.58, 129.49, 126.69, 126.59, 126.33, 123.97, 123.85, 121.85, 119.32, 116.22, 115.99, 115.56, 115.35.

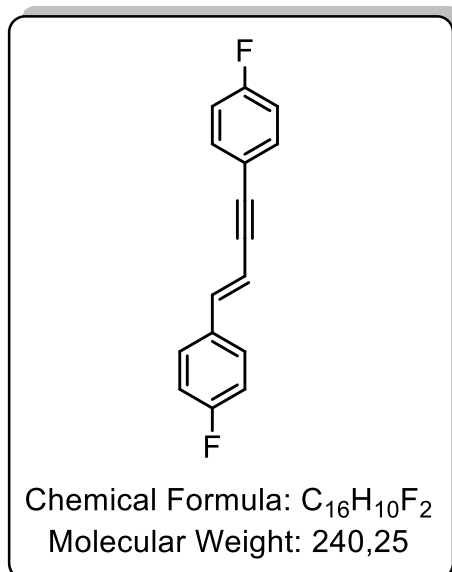
Dimerization of 1-ethynyl-4-fluorobenzene



1-ethynyl-4-fluorobenzene was reacted according to general procedure 4 at 40 °C. The dimer has been isolated.

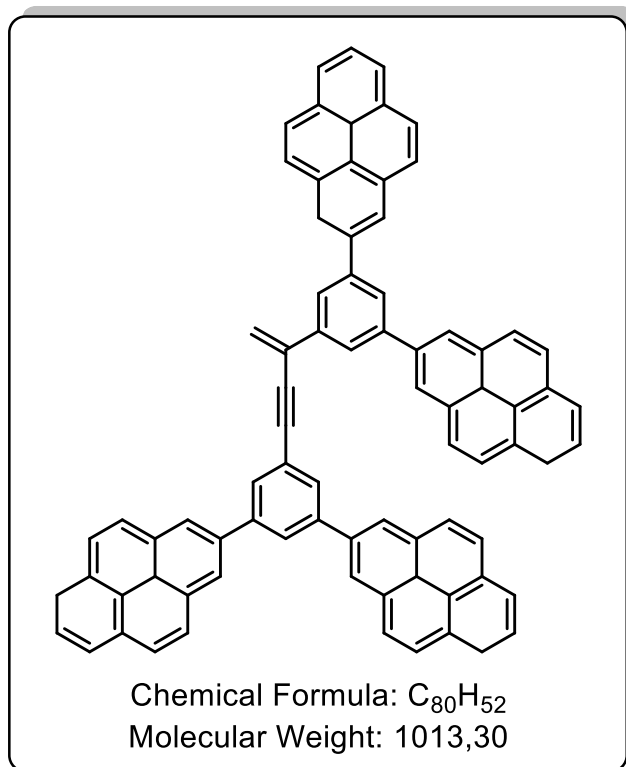
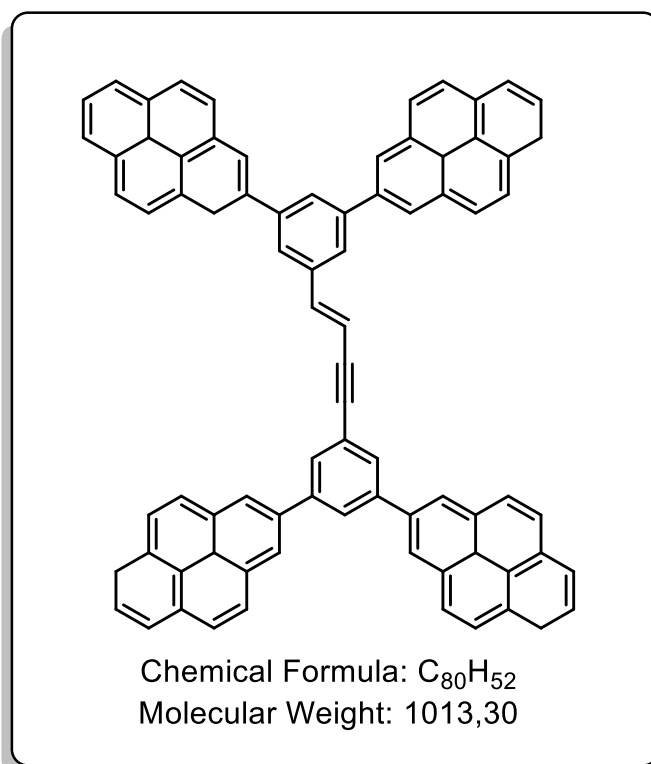
¹H NMR (400 MHz, CDCl₃) δ 7.72 – 7.63 (m, 2H), 7.59 – 7.45 (m, 2H), 7.12 – 7.00 (m, 4H), 5.91 (s, 1H), 5.72 (s, 1H). **¹⁹F NMR** (376 MHz, CDCl₃) δ -110.45 – -110.68 (m), -113.64 – -113.81 (m).

Reaction according to general procedure 8 at 120 °C for 4 h yielded the head-to-head dimer. Reaction according to general procedure 8 at 60 °C for 4 h was unsuccessful.



¹H NMR (400 MHz, cdcl₃) δ 7.14 – 7.06 (m, 1H), 7.06 – 6.98 (m, 1H), 6.95 – 6.70 (m, 6H), 3.61 – 3.43 (m, 1H), 3.02 (dd, *J* = 5.7, 3.1 Hz, 1H). **¹⁹F NMR** (376 MHz, cdcl₃) δ -110.67 (tt, *J* = 8.6, 5.4 Hz), -114.98 (tt, *J* = 8.7, 5.7 Hz), -116.25 (tt, *J* = 8.7, 5.5 Hz), -116.43 (tt, *J* = 8.7, 5.6 Hz).

Dimerization of 7,7'-(5-ethynyl-1,3-phenylene)bis(1,5a1-dihydropyrene)



7,7'-(5-ethynyl-1,3-phenylene)bis(1,5a1-dihydropyrene) was reacted according to general procedure 4 at 40 °C for 1 d. Very small amount of dimer was found by ¹H-NMR spectrometry.

Head-to-head dimer: **¹H NMR** (400 MHz, cdcl₃) δ 6.82 (dd, *J* = 17.6, 10.9 Hz, 2H),

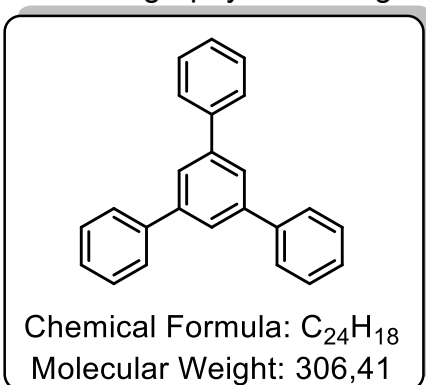
Head-to-tail dimer: $^1\text{H NMR}$ (400 MHz, cdCl_3) δ 5.84 (dd, $J = 17.6, 0.9$ Hz, 1H), 5.34 (dd, $J = 10.9, 0.8$ Hz, 1H).

Aromatic proton could not be assigned and purification by column chromatography was unsuccessful.

Reaction of phenylacetylene with 1,3,5-triethynylbenzene

1,3,5-triethynylbenzene (11.2 mg, 74.6 μmol , 1 equiv.) and phenylacetylene (22.8 mg, 224 μmol , 3 equiv.) were reacted on Al_2O_3 according to general procedure 8 at 120 $^\circ\text{C}$ for 18 h.

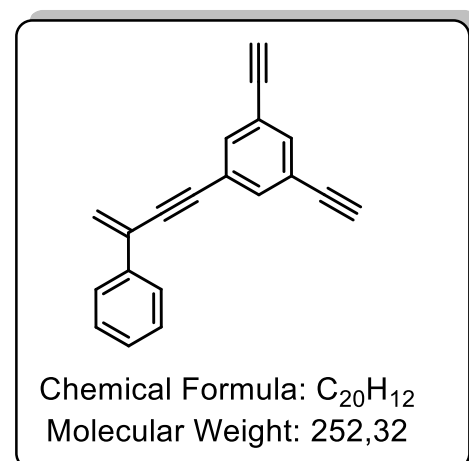
The trimer 5'-phenyl-1,1':3',1''-terphenyl was formed and isolated by flash column chromatography on silica gel with *n*-hexane.



$^1\text{H NMR}$ (400 MHz, cdCl_3) δ 7.79 (s, 1H), 7.71 (dt, $J = 3.2, 1.8$ Hz, 2H), 7.51 – 7.46 (m, 2H), 7.42 – 7.37 (m, 1H). $^{13}\text{C NMR}$ (101 MHz, cdCl_3) δ 142.33, 141.15, 128.78, 127.48, 127.31, 125.14.

1,3,5-triethynylbenzene (21.9 mg, 146 μmol , 1 equiv.) and phenylacetylene (47.7 mg, 467 μmol , 3.2 equiv.) were reacted on Al_2O_3 according to general procedure 4 at 40 $^\circ\text{C}$ for 3 d.

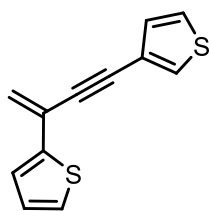
The dimer 1,3-diethynyl-5-(3-phenylbut-3-en-1-yn-1-yl)benzene was formed and



isolated by flash column chromatography on silica gel with *n*-hexane.

$^1\text{H NMR}$ (400 MHz, cdCl_3) δ 7.68 (ddd, $J = 12.1, 7.2, 1.5$ Hz, 2H), 7.61 (d, $J = 1.5$ Hz, 1H), 7.59 – 7.50 (m, 1H), 7.43 – 7.29 (m, 4H), 6.01 (d, $J = 0.8$ Hz, 1H), 5.77 (d, $J = 0.7$ Hz, 1H), 3.14 – 3.08 (m, 2H). $^{13}\text{C NMR}$ (101 MHz, cdCl_3) δ 135.14, 131.69, 128.45, 126.00, 121.52, 81.72, 78.52, 77.17, 76.73.

Dimerization of 3-ethynylthiophene



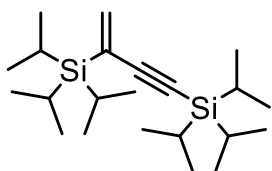
Chemical Formula: $C_{12}H_8S_2$
Molecular Weight: 216,32

3-ethynylthiophene was reacted according to general procedure 4 at 40 °C for 1 d. The dimer has been isolated.

1H NMR (400 MHz, $cdCl_3$) δ 7.58 – 7.48 (m, 1H), 7.36 – 7.28 (m, 4H), 7.21 – 7.15 (m, 1H), 5.85 (s, 1H), 5.65 (s, 1H).

Dimerization of ethynyltriisopropylsilane

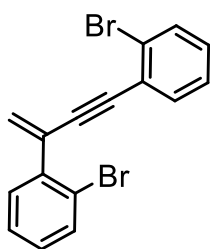
Ethynyltriisopropylsilane was reacted according to general procedure 4 at 40 °C for 3 d. The dimer has been found by 1H -NMR spectroscopy but could not be isolated.



Chemical Formula: $C_{22}H_{44}Si_2$
Molecular Weight: 364,76

1H NMR (400 MHz, $cdCl_3$) δ 6.37 (d, J = 19.6 Hz, 1H), 6.04 (d, J = 19.6 Hz, 1H), 1.25 (s, 6H), 1.09 (d, J = 2.0 Hz, 36H).

Dimerization of 1-bromo-2-ethynylbenzene



Chemical Formula: $C_{16}H_{10}Br_2$
Molecular Weight: 362,06

1-bromo-2-ethynylbenzene was reacted according to general procedure 4 at 40 °C for 3 d. The dimer has been isolated.

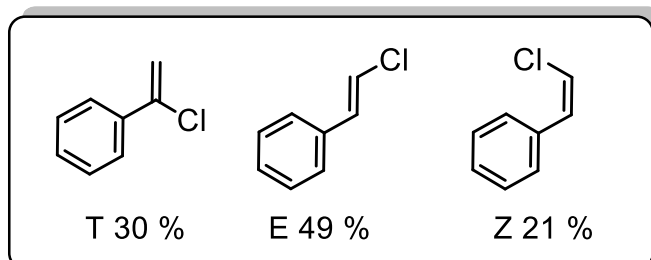
1H NMR (400 MHz, $cdCl_3$) δ 7.59 – 7.47 (m, 1H), 7.38 (d, J = 8.4 Hz, 1H), 5.98 (s, 1H), 5.78 (s, 1H).

6.9. Hydrochlorination of terminal Alkynes on $\gamma\text{-Al}_2\text{O}_3$

General procedure 10

Aluminum oxide was activated by annealing at 400 °C for 6 h in air. Afterwards, it was heated at 400 °C under vacuum (10-2 mbar) for 16 h. After cooling to room temperature, the oxide (2 g) and phenylacetylene-derivate (70 mg) was added to a two-neck flask under argon atmosphere. 12 mL dry toluene was added as a solvent and the reaction was started by flowing HCl-gas into the solution. The HCl-gas was prepared by adding HCl (3 mL) slowly to CaCl_2 and after heating with heatgun, transferred it through a plug of CaCl_2 . No additional Ar was necessary to transfer the gas into the solution. The addition of Ar was counterproductive after starting the reaction. After 1h, the oxide was washed with toluene and methanol. The combined toluene fractions were reduced in vacuo and analysed by $^1\text{H-NMR}$.

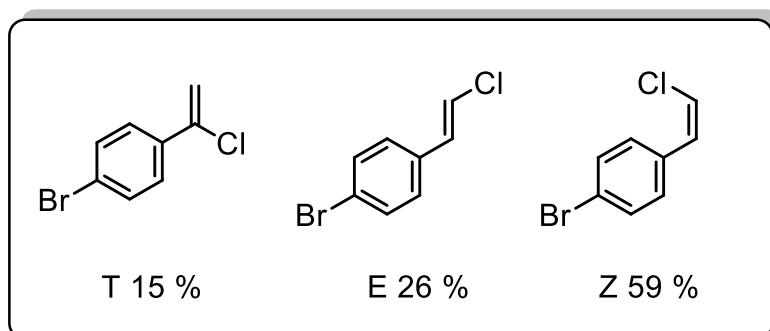
Chlorination of phenylacetylene



Phenylacetylene was reacted on activated Al_2O_3 under HCl-gas according to general procedure 10. The three different (chlorovinyl)benzene were found

after reaction by $^1\text{H-NMR}$. Further purification by flash column chromatography was unsuccessful.

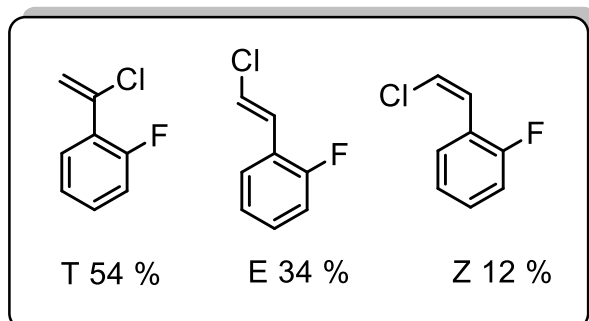
Chlorination of 1-bromo-4-ethynylbenzene



1-Bromo-4-ethynylbenzene was reacted on activated Al_2O_3 under HCl-gas according to general procedure 10. The three different 1-bromo-4-

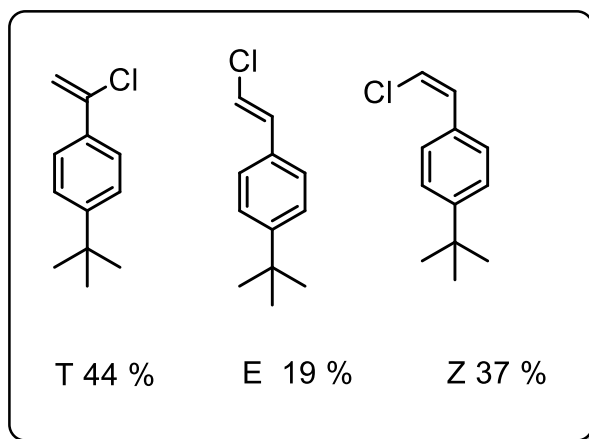
(chlorovinyl)benzene were found after reaction by $^1\text{H-NMR}$.

Chlorination of 1-ethynyl-2-fluorobenzene



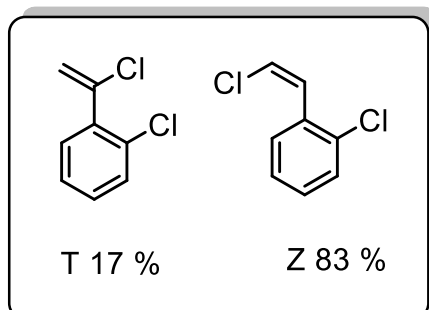
1-ethynyl-2-fluorobenzene was reacted on activated Al_2O_3 under HCl-gas according to general procedure 10. The three different 1-(chlorovinyl)-2-fluorobenzene were found after reaction by $^1\text{H-NMR}$.

Chlorination of 1-(tert-butyl)-4-ethynylbenzene



1-(tert-butyl)-4-ethynylbenzene was reacted on activated Al_2O_3 under HCl-gas according to general procedure 10. The three different 1-(tert-butyl)-4-(chlorovinyl)benzene were found after reaction by $^1\text{H-NMR}$.

Chlorination of 1-chloro-2-ethynylbenzene



1-chloro-2-ethynylbenzene was reacted on activated Al_2O_3 under HCl-gas according to general procedure 10. 1-chloro-2-(1-chlorovinyl)benzene (T) and (Z)-1-chloro-2-(2-chlorovinyl)benzene were found after reaction by $^1\text{H-NMR}$.

7. BIBLIOGRAPHY

- (1) NobelPrize.org. The Nobel Prize in Chemistry 1996.
<https://www.nobelprize.org/prizes/chemistry/1996/curl/biographical/> (accessed Jan 11, 2023).
- (2) NobelPrize.org. The Nobel Prize in Physics 2010.
<https://www.nobelprize.org/prizes/physics/2010/summary/> (accessed Jan 11, 2023).
- (3) Novoselov, K. S.; Geim, A. K.; Morozov, S. V.; Jiang, D.; Zhang, Y.; Dubonos, S. V.; Grigorieva, I. V.; Firsov, A. A. *Science (New York, N.Y.)* **2004**, *306*, 666–669.
- (4) a) *Zur Theorie der phasenumwandlungen II*, 1937; b) *Quelques propriétés typiques des corps solides*, 1935;
- (5) Sur, U. K. *International Journal of Electrochemistry* **2012**, *2012*, 1–12.
- (6) Rodgers, P. *Nanoscience and technology: A collection of reviews from Nature journals*; World Scientific, 2009.
- (7) Kuzmenko, A. B.; van Heumen, E.; Carbone, F.; van der Marel, D. *Phys. Rev. Lett.* **2008**, *100*, 117401.
- (8) Balandin, A. A.; Ghosh, S.; Bao, W.; Calizo, I.; Teweldebrhan, D.; Miao, F.; Lau, C. N. *Nano letters* **2008**, *8*, 902–907.
- (9) Lee, C.; Wei, X.; Kysar, J. W.; Hone, J. *Science (New York, N.Y.)* **2008**, *321*, 385–388.
- (10) Wu, J.; Pisula, W.; Müllen, K. *Chem. Rev.* **2007**, *107*, 718–747.
- (11) Meric, I.; Han, M. Y.; Young, A. F.; Ozyilmaz, B.; Kim, P.; Shepard, K. L. *Nat. Nanotechnol.* **2008**, *3*, 654–659.
- (12) Lee, C.; Wei, X.; Kysar, J. W.; Hone, J. *Science* **2008**, *321*, 385–388.
- (13) a) Ivanov, E.; Kotsilkova, R.; Xia, H.; Chen, Y.; Donato, R.; Donato, K.; Godoy, A.; Di Maio, R.; Silvestre, C.; Cimmino, S.; Angelov, V. *Applied Sciences* **2019**, *9*, 1209; b) Balandin, A. A. *Nature Mater* **2011**, *10*, 569–581;
- (14) Lin, Y.-M.; Dimitrakopoulos, C.; Jenkins, K. A.; Farmer, D. B.; Chiu, H.-Y.; Grill, A.; Avouris, P. *Science (New York, N.Y.)* **2010**, *327*, 662.
- (15) Wang, X.; Zhi, L.; Müllen, K. *Nano letters* **2008**, *8*, 323–327.
- (16) a) Kim, K.; Choi, J.-Y.; Kim, T.; Cho, S.-H.; Chung, H.-J. *Nature* **2011**, *479*, 338–344; b) Wojciech Pisula; Klaus Müllen. *Pure and Applied Chemistry* **1351**, 2203–2224; c) Akinwande, D.; Tao, L.; Yu, Q.; Lou, X.; Peng, P.; Kuzum, D. *IEEE Nanotechnology Mag.* **2015**, *9*, 6–14;
- (17) Huang, L.; Zhang, M.; Li, C.; Shi, G. *The journal of physical chemistry letters* **2015**, *6*, 2806–2815.
- (18) Zhu, S.; Li, T. *ACS nano* **2014**, *8*, 2864–2872.
- (19) a) Varghese, S. S.; Lonkar, S.; Singh, K. K.; Swaminathan, S.; Abdala, A. *Sensors and Actuators B: Chemical* **2015**, *218*, 160–183; b) Boland, C. S.; Khan, U.; Backes, C.; O'Neill, A.; McCauley, J.; Duane, S.; Shanker, R.; Liu, Y.; Jurewicz, I.; Dalton, A. B.; Coleman, J. N. *ACS nano* **2014**, *8*, 8819–8830; c) Green, N. S.; Norton, M. L. *Analytica Chimica Acta* **2015**, *853*, 127–142;
- (20) Wojciech Pisula; Klaus Müllen. *Pure and Applied Chemistry* **1351**, 2203–2224.
- (21) Müller, M.; Kübel, C.; Morgenroth, F.; Iyer, V. S.; Müllen, K. *Carbon* **1998**, *36*, 827–831.
- (22) Klärner, G.; Müller, M.; Morgenroth, F.; Wehmeier, M.; Soczka-Guth, T.; Müllen, K.

- Synthetic Metals* **1997**, *84*, 297–301.
- (23) Ai, Q.; Jarolimek, K.; Mazza, S.; Anthony, J. E.; Risko, C. *Chem. Mater.* **2018**, *30*, 947–957.
- (24) a) Anthony, J. E. *Angewandte Chemie International Edition* **2008**, *47*, 452–483; b) Anthony, J. E. *Chem. Rev.* **2006**, *106*, 5028–5048; c) Sun, Z.; Ye, Q.; Chi, C.; Wu, J. *Chem. Soc. Rev.* **2012**, *41*, 7857–7889; d) Hu, X.; Wang, W.; Wang, D.; Zheng, Y. *J. Mater. Chem. C* **2018**, *6*, 11232–11242; e) Mei, J.; Diao, Y.; Appleton, A. L.; Fang, L.; Bao, Z. *J. Am. Chem. Soc.* **2013**, *135*, 6724–6746; f) Wang, C.; Dong, H.; Hu, W.; Liu, Y.; Zhu, D. *Chem. Rev.* **2012**, *112*, 2208–2267;
- (25) a) Muhammad, S.; Nakano, M.; Al-Sehemi, A. G.; Kitagawa, Y.; Irfan, A.; Chaudhry, A. R.; Kishi, R.; Ito, S.; Yoneda, K.; Fukuda, K. *Nanoscale* **2016**, *8*, 17998–18020; b) Ni, Y.; Wu, J. *Tetrahedron Letters* **2016**, *57*, 5426–5434; c) Nakano, M.; Champagne, B. *J. Phys. Chem. Lett.* **2015**, *6*, 3236–3256;
- (26) a) Mishra, A.; Bäuerle, P. *Angewandte Chemie International Edition* **2012**, *51*, 2020–2067; b) Aumaitre, C.; Morin, J.-F. *The Chemical Record* **2019**, *19*, 1142–1154; c) Kaur, N.; Singh, M.; Pathak, D.; Wagner, T.; Nunzi, J. M. *Synthetic Metals* **2014**, *190*, 20–26;
- (27) a) Itoh, T. *Chem. Rev.* **2012**, *112*, 4541–4568; b) Lee, J.-H.; Chen, C.-H.; Lee, P.-H.; Lin, H.-Y.; Leung, M.; Chiu, T.-L.; Lin, C.-F. *J. Mater. Chem. C* **2019**, *7*, 5874–5888; c) Lee, J.-H.; Chen, C.-H.; Lee, P.-H.; Lin, H.-Y.; Leung, M.; Chiu, T.-L.; Lin, C.-F. *J. Mater. Chem. C* **2019**, *7*, 5874–5888;
- (28) Wöhrle, T.; Wurzbach, I.; Kirres, J.; Kostidou, A.; Kapernaum, N.; Litterscheidt, J.; Haenle, J. C.; Staffeld, P.; Baro, A.; Giesselmann, F.; Laschat, S. *Chem. Rev.* **2016**, *116*, 1139–1241.
- (29) a) Krishnapriya, K. C.; Musser, A. J.; Patil, S. *ACS Energy Lett.* **2019**, *4*, 192–202; b) Casanova, D. *Chem. Rev.* **2018**, *118*, 7164–7207; c) Smith, M. B.; Michl, J. *Chem. Rev.* **2010**, *110*, 6891–6936;
- (30) Plakhotnik, T.; Donley, E. A.; Wild, U. P. *Annual Review of Physical Chemistry* **1997**, *48*, 181–212.
- (31) Zazyev, O. V. *Rep. Prog. Phys.* **2010**, *73*, 56501.
- (32) a) Kumar, S.; Kumar, Y.; Keshri, S.; Mukhopadhyay, P. *Magnetochemistry* **2016**, *2*, 42; b) Mishra, S.; Beyer, D.; Berger, R.; Liu, J.; Gröning, O.; Urgel, J. I.; Müllen, K.; Ruffieux, P.; Feng, X.; Fasel, R. *J. Am. Chem. Soc.* **2020**, *142*, 1147–1152;
- (33) Scott, L. T.; Boorum, M. M.; McMahan, B. J.; Hagen, S.; Mack, J.; Blank, J.; Wegner, H.; Meijere, A. de. *Science (New York, N.Y.)* **2002**, *295*, 1500–1503.
- (34) Frank B. Mallory; Clelia W. Mallory. Photocyclization of Stilbenes and Related Molecules. In *Organic Reactions*; John Wiley & Sons, Ltd, 2005, pp 1–456.
- (35) Pascual, S.; Mendoza, P. de; Echavarren, A. M. *Org. Biomol. Chem.* **2007**, *5*, 2727–2734.
- (36) Alberico, D.; Scott, M. E.; Lautens, M. *Chem. Rev.* **2007**, *107*, 174–238.
- (37) King, B. T.; Kroulík, J.; Robertson, C. R.; Rempala, P.; Hilton, C. L.; Korinek, J. D.; Gortari, L. M. *The Journal of organic chemistry* **2007**, *72*, 2279–2288.
- (38) Müller, M.; Iyer, V. S.; Kübel, C.; Enkelmann, V.; Müllen, K. *Angewandte Chemie International Edition* **1997**, *36*, 1607–1610.
- (39) Morgenroth, F.; Kübel, C.; Müller, M.; Wiesler, U. M.; Berresheim, A. J.; Wagner, M.; Müllen, K. *Carbon* **1998**, *36*, 833–837.
- (40) Morgenroth, F.; Müllen, K. *Tetrahedron* **1997**, *53*, 15349–15366.
- (41) Stabel, A.; Herwig, P.; Müllen, K.; Rabe, J. P. *Angewandte Chemie International Edition* **1995**, *34*, 1609–1611.
- (42) a) Sakamoto, J.; van Heijst, J.; Lukin, O.; Schlüter, A. D. *Angewandte Chemie International Edition* **2009**, *48*, 1030–1069; b) Simpson, C. D.; Brand, J. D.; Berresheim,

- A. J.; Przybilla, L.; Räder, H. J.; Müllen, K. *Chemistry – A European Journal* **2002**, *8*, 1424–1429;
- (43) Danz, M.; Tonner, R.; Hilt, G. *Chem. Commun.* **2012**, *48*, 377–379.
- (44) Amsharov, K. Y.; Kabdulov, M. A.; Jansen, M. *Angewandte Chemie International Edition* **2012**, *51*, 4594–4597.
- (45) Amii, H.; Uneyama, K. *Chem. Rev.* **2009**, *109*, 2119–2183.
- (46) O'Hagan, D. *Chem. Soc. Rev.* **2008**, *37*, 308–319.
- (47) Amsharov, K. Y.; Jansen, M. *The Journal of organic chemistry* **2008**, *73*, 2931–2934.
- (48) Kabdulov, M. A.; Amsharov, K. Y.; Jansen, M. *Tetrahedron* **2010**, *66*, 8587–8593.
- (49) Amsharov, K. Y.; Kabdulov, M. A.; Jansen, M. *Chemistry – A European Journal* **2010**, *16*, 5868–5871.
- (50) Pascual, S.; Mendoza, P. de; Echavarren, A. M. *Org. Biomol. Chem.* **2007**, *5*, 2727–2734.
- (51) a) Douvris, C.; Ozerov, O. V. *Science (New York, N.Y.)* **2008**, *321*, 1188–1190; b) Allemann, O.; Duttwyler, S.; Romanato, P.; Baldrige, K. K.; Siegel, J. S. *Science (New York, N.Y.)* **2011**, *332*, 574–577;
- (52) Amsharov, K. Y.; Merz, P. *The Journal of organic chemistry* **2012**, *77*, 5445–5448.
- (53) Steiner, A.-K.; Amsharov, K. Y. *Angewandte Chemie International Edition* **2017**, *56*, 14732–14736.
- (54) Amsharov, K. *Phys. Status Solidi B* **2016**, *253*, 2473–2477.
- (55) Vicarelli, L.; Heerema, S. J.; Dekker, C.; Zandbergen, H. W. *ACS nano* **2015**, *9*, 3428–3435.
- (56) Narita, A.; Wang, X.-Y.; Feng, X.; Müllen, K. *Chem. Soc. Rev.* **2015**, *44*, 6616–6643.
- (57) King, B. T. *Nat. Chem.* **2013**, *5*, 730–731.
- (58) a) Wang, X.; Yu, S.; Lou, Z.; Zeng, Q.; Yang, M. *Phys. Chem. Chem. Phys.* **2015**, *17*, 17864–17871; b) Öttl, S.; Huber, S. E.; Kimeswenger, S.; Probst, M. *A&A* **2014**, *568*, A95;
- (59) Papaianina, O.; Akhmetov, V. A.; Goryunkov, A. A.; Hampel, F.; Heinemann, F. W.; Amsharov, K. Y. *Angewandte Chemie International Edition* **2017**, *56*, 4834–4838.
- (60) Jessup, P. J.; Reiss, J. A. *Tetrahedron Letters* **1975**, *16*, 1453–1456.
- (61) Yamamoto, K.; Harada, T.; Nakazaki, M.; Naka, T.; Kai, Y.; Harada, S.; Kasai, N. *J. Am. Chem. Soc.* **1983**, *105*, 7171–7172.
- (62) Mughal, E. U.; Kuck, D. *Chem. Commun.* **2012**, *48*, 8880–8882.
- (63) Kawai, K.; Kato, K.; Peng, L.; Segawa, Y.; Scott, L. T.; Itami, K. *Organic Letters* **2018**, *20*, 1932–1935.
- (64) Miao, Q. *The Chemical Record* **2015**, *15*, 1156–1159.
- (65) Márquez, I. R.; Castro-Fernández, S.; Millán, A.; Campaña, A. G. *Chem. Commun.* **2018**, *54*, 6705–6718.
- (66) Ruffieux, P.; Wang, S.; Yang, B.; Sánchez-Sánchez, C.; Liu, J.; Dienel, T.; Talirz, L.; Shinde, P.; Pignedoli, C. A.; Passerone, D.; Dumlaff, T.; Feng, X.; Müllen, K.; Fasel, R. *Nature* **2016**, *531*, 489–492.
- (67) Mishra, S.; Beyer, D.; Eimre, K.; Kezilebieke, S.; Berger, R.; Gröning, O.; Pignedoli, C. A.; Müllen, K.; Liljeroth, P.; Ruffieux, P.; Feng, X.; Fasel, R. *Nat. Nanotechnol.* **2020**, *15*, 22–28.
- (68) a) Salvi, N.; Belpassi, L.; Tarantelli, F. *Chemistry – A European Journal* **2010**, *16*, 7231–7240; b) Kubas, G. J. *Journal of Organometallic Chemistry* **2001**, *635*, 37–68; c) Chatt, J.; Duncanson, L. A. *J. Chem. Soc.* **1953**, 2939;
- (69) a) Dorel, R.; Echavarren, A. M. *Chem. Rev.* **2015**, *115*, 9028–9072; b) Hashmi, A. S. K. *Chem. Rev.* **2007**, *107*, 3180–3211;
- (70) Fürstner, A.; Davies, P. W. *Angewandte Chemie (International ed. in English)* **2007**, *46*,

3410–3449.

- (71) Leyva-Pérez, A.; Corma, A. *Angewandte Chemie International Edition* **2012**, *51*, 614–635.
- (72) Gorin, D. J.; Toste, F. D. *Nature* **2007**, *446*, 395–403.
- (73) Akhmetov, V.; Feofanov, M.; Sharapa, D. I.; Amsharov, K. **2021**, *143*, 15420–15426.
- (74) a) Fürstner, A.; Mamane, V. *The Journal of organic chemistry* **2002**, *67*, 6264–6267; b) Mamane, V.; Hannen, P.; Fürstner, A. *Chemistry (Weinheim an der Bergstrasse, Germany)* **2004**, *10*, 4556–4575;
- (75) Akhmetov, V.; Förtsch, A.; Feofanov, M.; Troyanov, S.; Amsharov, K. *Org. Chem. Front.* **2020**, *7*, 1271–1275.
- (76) a) Yamamoto, K.; Harada, T.; Nakazaki, M.; Naka, T.; Kai, Y.; Harada, S.; Kasai, N. *J. Am. Chem. Soc.* **1983**, *105*, 7171–7172; b) *Dehydrogenation of heterohelicenes by a Scholl type reaction*, 1975; c) Jessup, P. J.; Reiss, J. A. *Aust. J. Chem.* **1976**, *29*, 173; d) Kato, K.; Segawa, Y.; Scott, L. T.; Itami, K. *Chemistry – An Asian Journal* **2015**, *10*, 1635–1639; e) Kawasumi, K.; Zhang, Q.; Segawa, Y.; Scott, L. T.; Itami, K. *Nature Chem* **2013**, *5*, 739–744;
- (77) Steiner, A.-K.; Amsharov, K. Y. *Angewandte Chemie International Edition* **2017**, *56*, 14732–14736.
- (78) Miyaura, N.; Suzuki, A. *J. Chem. Soc., Chem. Commun.* **1979**, 866.
- (79) Miyaura, N.; Suzuki, A. *Chem. Rev.* **1995**, *95*, 2457–2483.
- (80) Akhmetov, V.; Feofanov, M.; Troyanov, S.; Amsharov, K. *Chemistry – A European Journal* **2019**, *25*, 7607–7612.
- (81) a) Cheung, K. Y.; Xu, X.; Miao, Q. *J. Am. Chem. Soc.* **2015**, *137*, 3910–3914; b) Pun, S. H.; Chan, C. K.; Luo, J.; Liu, Z.; Miao, Q. *Angewandte Chemie International Edition* **2018**, *57*, 1581–1586;
- (82) Nishio, M. *Phys. Chem. Chem. Phys.* **2011**, *13*, 13873–13900.
- (83) Vladimir, A.; Mikhail, F.; Amsharov, K. *RSC Advances* **2020**, *10*, 10879–10882.
- (84) Cai, Z.; Awais, M. A.; Zhang, N.; Yu, L. *Chem* **2018**, *4*, 2538–2570.
- (85) a) Feofanov, M.; Akhmetov, V.; Takayama, R.; Amsharov, K. *Angewandte Chemie* **2021**, *133*, 5259–5263; b) Peng, L.; Zhang, X.; Ma, J.; Zhong, Z.; Zhang, Z.; Zhang, Y.; Wang, J. *Sci. China Ser. B-Chem.* **2009**, *52*, 1622–1630; c) Marshall, J. A.; DuBay, W. J. *J. Am. Chem. Soc.* **1992**, *114*, 1450–1456; d) Tsuji, H.; Nakamura, E. *Accounts of chemical research* **2017**, *50*, 396–406;
- (86) Hill, J. P.; Jin, W.; Kosaka, A.; Fukushima, T.; Ichihara, H.; Shimomura, T.; Ito, K.; Hashizume, T.; Ishii, N.; Aida, T. *Science* **2004**, *304*, 1481–1483.
- (87) He, H.; Wu, Y.-J. *Tetrahedron Letters* **2004**, *45*, 3237–3239.
- (88) a) Kratzer, A.; Englert, J. M.; Lungerich, D.; Heinemann, F. W.; Jux, N.; Hirsch, A. *Faraday discussions* **2014**, *173*, 297–310; b) Ammon, F.; Sauer, S. T.; Lippert, R.; Lungerich, D.; Reger, D.; Hampel, F.; Jux, N. *Org. Chem. Front.* **2017**, *4*, 861–870; c) Reger, D.; Schöll, K.; Hampel, F.; Maid, H.; Jux, N. *Chemistry – A European Journal* **2021**, *27*, 1984–1989;
- (89) a) Kubo, T. *The Chemical Record* **2015**, *15*, 218–232; b) Sun, Z.; Wu, J. *J. Mater. Chem.* **2012**, *22*, 4151–4160;
- (90) a) Bullard, Z.; Girão, E. C.; Owens, J. R.; Shelton, W. A.; Meunier, V. *Sci Rep* **2015**, *5*, 7634; b) Slota, M.; Keerthi, A.; Myers, W. K.; Tretyakov, E.; Baumgarten, M.; Ardavan, A.; Sadeghi, H.; Lambert, C. J.; Narita, A.; Müllen, K.; Bogani, L. *Nature* **2018**, *557*, 691–695;
- (91) a) Das, A.; Müller, T.; Plasser, F.; Lischka, H. *The journal of physical chemistry. A* **2016**, *120*, 1625–1636; b) Liu, J.; Feng, X. *Angewandte Chemie International Edition* **2020**, *59*, 23386–23401;

- (92) a) Liu, J.; Feng, X. *Angewandte Chemie International Edition* **2020**, *59*, 23386–23401; b) Song, S.; Su, J.; Telychko, M.; Li, J.; Li, G.; Li, Y.; Su, C.; Wu, J.; Lu, J. *Chem. Soc. Rev.* **2021**, *50*, 3238–3262;
- (93) Mishra, S.; Beyer, D.; Eimre, K.; Ortiz, R.; Fernández - Rossier, J.; Berger, R.; Gröning, O.; Pignedoli, C. A.; Fasel, R.; Feng, X.; Ruffieux, P. *Angew. Chem.* **2020**, *132*, 12139–12145.
- (94) Mishra, S.; Yao, X.; Chen, Q.; Eimre, K.; Gröning, O.; Ortiz, R.; Di Giovannantonio, M.; Sancho-García, J. C.; Fernández-Rossier, J.; Pignedoli, C. A.; Müllen, K.; Ruffieux, P.; Narita, A.; Fasel, R. *Nat. Chem.* **2021**, *13*, 581–586.
- (95) Trauzettel, B.; Bulaev, D. V.; Loss, D.; Burkard, G. *Nature Phys* **2007**, *3*, 192–196.
- (96) a) Mistry, A.; Moreton, B.; Schuler, B.; Mohn, F. *Chemistry – A European Journal* **2015**, *21*, 2011–2018; b) Pavliček, N.; Mistry, A.; Majzik, Z.; Moll, N.; Meyer, G.; Fox, D. J.; Gross, L. *Nat. Nanotechnol.* **2017**, *12*, 308–311;
- (97) Mistry, A.; Moreton, B.; Schuler, B.; Mohn, F.; Meyer, G.; Gross, L.; Williams, A.; Scott, P.; Costantini, G.; Fox, D. J. *Chemistry – A European Journal* **2015**, *21*, 2011–2018.
- (98) Holt, C. J.; Wentworth, K. J.; Johnson, R. P. *Angewandte Chemie International Edition* **2019**, *58*, 15793–15796.
- (99) Sun, K.; Fang, Y.; Chi, L. *ACS Materials Lett.* **2021**, *3*, 56–63.
- (100) a) Kolmer, M.; Zuzak, R.; Steiner, A. K.; Zajac, L.; Engelund, M.; Godlewski, S.; Szymonski, M.; Amsharov, K. *Science* **2019**, *363*, 57–60; b) Guo, C.; Wang, Y.; Kittelmann, M.; Kantorovitch, L.; Kühnle, A.; Floris, A. *J. Phys. Chem. C* **2017**, *121*, 10053–10062; c) Kolmer, M.; Ahmad Zebari, A. A.; Prauzner-Bechcicki, J. S.; Piskorz, W.; Zasada, F.; Godlewski, S.; Such, B.; Sojka, Z.; Szymonski, M. *Angewandte Chemie International Edition* **2013**, *52*, 10300–10303; d) Kolmer, M.; Zuzak, R.; Ahmad Zebari, A. A.; Godlewski, S.; Prauzner-Bechcicki, J. S.; Piskorz, W.; Zasada, F.; Sojka, Z.; Bléger, D.; Hecht, S.; Szymonski, M. *Chem. Commun.* **2015**, *51*, 11276–11279; e) Vasseur, G.; Abadia, M.; Miccio, L. A.; Brede, J.; Garcia-Lekue, A.; Oteyza, D. G. de; Rogero, C.; Lobo-Checa, J.; Ortega, J. E. *J. Am. Chem. Soc.* **2016**, *138*, 5685–5692;
- (101) Feofanov, M.; Förtsch, A.; Amsharov, K.; Akhmetov, V. *Chem. Commun.* **2021**, *57*, 12325–12328.
- (102) a) Shao, B.; Bagdasarian, A. L.; Popov, S.; Nelson, H. M. *Science* **2017**, *355*, 1403–1407; b) Allemann, O.; Baldrige, K. K.; Siegel, J. S. *Org. Chem. Front.* **2015**, *2*, 1018–1021; c) Allemann, O.; Duttwyler, S.; Romanato, P.; Baldrige, K. K.; Siegel, J. S. *Science* **2011**, *332*, 574–577;
- (103) Xu, L.; Yang, W.; Zhang, L.; Miao, M.; Yang, Z.; Xu, X.; Ren, H. *The Journal of organic chemistry* **2014**, *79*, 9206–9221.
- (104) Papaianina, O.; Amsharov, K. Y. *Chem. Commun.* **2016**, *52*, 1505–1508.
- (105) Vogel, A. Anthraquinone. In *Ullmann's encyclopedia of industrial chemistry*; Bohnet, M.; Ullmann, F., Eds.; Wiley-VCH: Weinheim, 2003, p 781.
- (106) Feofanov, M.; Akhmetov, V.; Amsharov, K. *Phys. Status Solidi B* **2020**, *257*, 2000296.
- (107) 0271.SAS-BR-Inorganics_Siral_Siralox_WEB.
http://www.sasolgermany.de/fileadmin/doc/alumina/0271.SAS-BR-Inorganics_Siral_Siralox_WEB.pdf (accessed Jan 6, 2023).
- (108) McGonigal, P. R.; de León, C.; Wang, Y.; Homs, A.; Solorio-Alvarado, C. R.; Echavarren, A. M. *Angew. Chem.* **2012**, *124*, 13270–13273.
- (109) a) Dorel, R.; Echavarren, A. M. *The Journal of organic chemistry* **2015**, *80*, 7321–7332; b) Jiménez-Núñez, E.; Echavarren, A. M. *Chem. Rev.* **2008**, *108*, 3326–3350;
- (110) Tian, J.; Chen, Y.; Vayer, M.; Djurovic, A.; Guillot, R.; Guermazi, R.; Dagorne, S.; Bour, C.; Gandon, V. *Chemistry – A European Journal* **2020**, *26*, 12831–12838.
- (111) Arnold, W. A.; Roberts, A. L. *Environ. Sci. Technol.* **1998**, *32*, 3017–3025.

- (112) Arnold, W. A.; Roberts, A. L. *Environ. Sci. Technol.* **2000**, *34*, 1794–1805.
- (113) Wehrmeier, A.; Lenoir, D.; Sidhu, S. S.; Taylor, P. H.; Rubey, W. A.; Kettrup, A.; Dellinger, B. *Environ. Sci. Technol.* **1998**, *32*, 2741–2748.
- (114) López, N.; Gómez-Segura, J.; Marín, R. P.; Pérez-Ramírez, J. *Journal of Catalysis* **2008**, *255*, 29–39.
- (115) a) Taylor, P. H.; Wehrmeier, A.; Sidhu, S. S.; Lenoir, D.; Schramm, K. W.; Kettrup, A. *Chemosphere* **2000**, *40*, 1297–1303; b) *Role of copper species in chlorination and condensation reactions of acetylene*, 1998;
- (116) a) Lee, F. S. C.; Rowland, F. S. *The Journal of Physical Chemistry* **1977**, *81*, 684–685; b) Zhang, H.; Shen, Y.; Liu, W.; He, Z.; Fu, J.; Cai, Z.; Jiang, G. *Environmental pollution (Barking, Essex : 1987)* **2019**, *253*, 831–840; c) Gao, Y.; Alecu, I. M.; Hsieh, P.-C.; McLeod, A.; McLeod, C.; Jones, M.; Marshall, P. *Proceedings of the Combustion Institute* **2007**, *31*, 193–200;
- (117) Lungerich, D.; Reger, D.; Hölzel, H.; Riedel, R.; Martin, M. M. J. C.; Hampel, F.; Jux, N. *Angewandte Chemie International Edition* **2016**, *55*, 5602–5605.
- (118) Miles, W. H.; Robinson, M. J.; Lessard, S. G.; Thamattoor, D. M. *The Journal of organic chemistry* **2016**, *81*, 10791–10801.
- (119) Eakins, G. L.; Cooper, M. W.; Gerasimchuk, N. N.; Phillips, T. J.; Breyfogle, B. E.; Stearman, C. J. *Can. J. Chem.* **2013**, *91*, 1059–1071.

8. APPENDIX

8.1 Folding of Fluorinated Oligoarylenes into Non-alternant PAHs with Various Topological Shapes

8.1.1. Synthesis of 1,16-dehydrohexahelicene

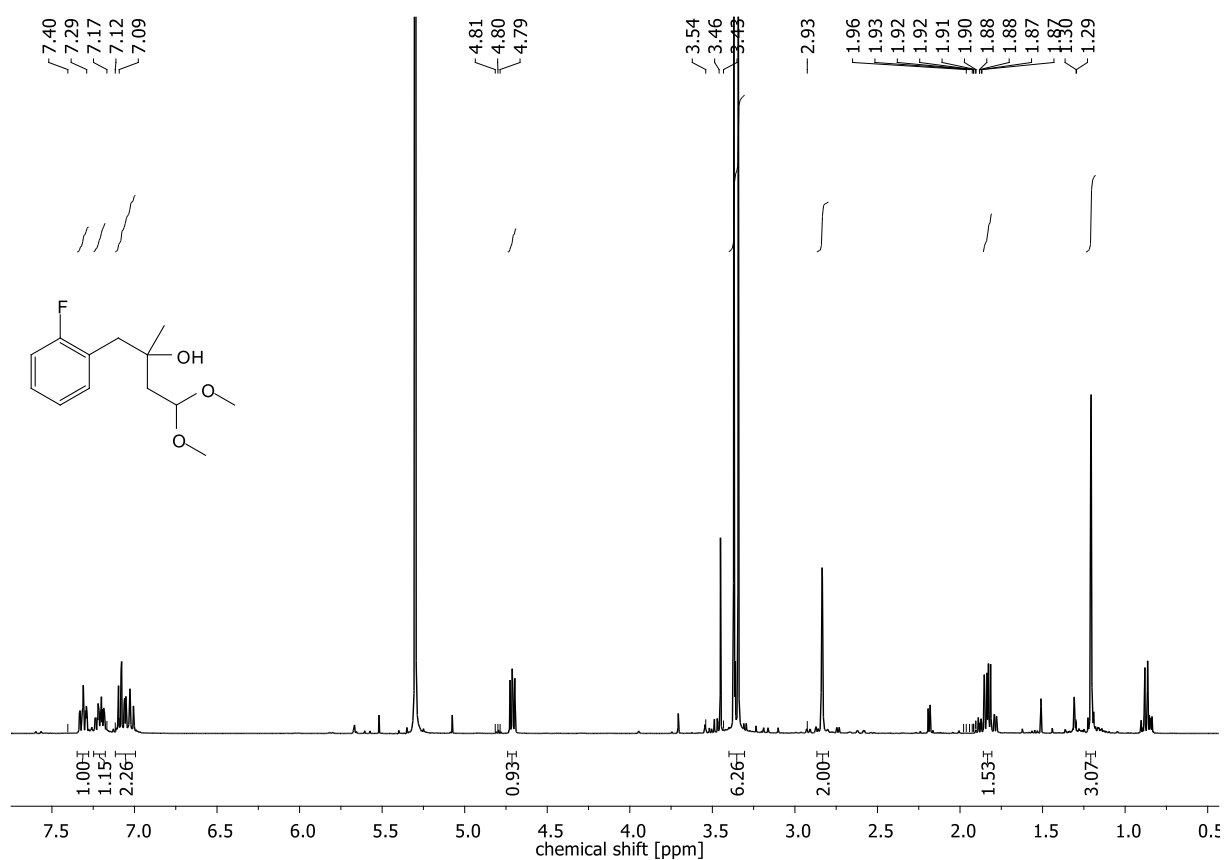


Figure 8.1: ¹H-NMR spectrum of 1-(2-fluorophenyl)-4,4-dimethoxy-2-methylbutan-2-ol.

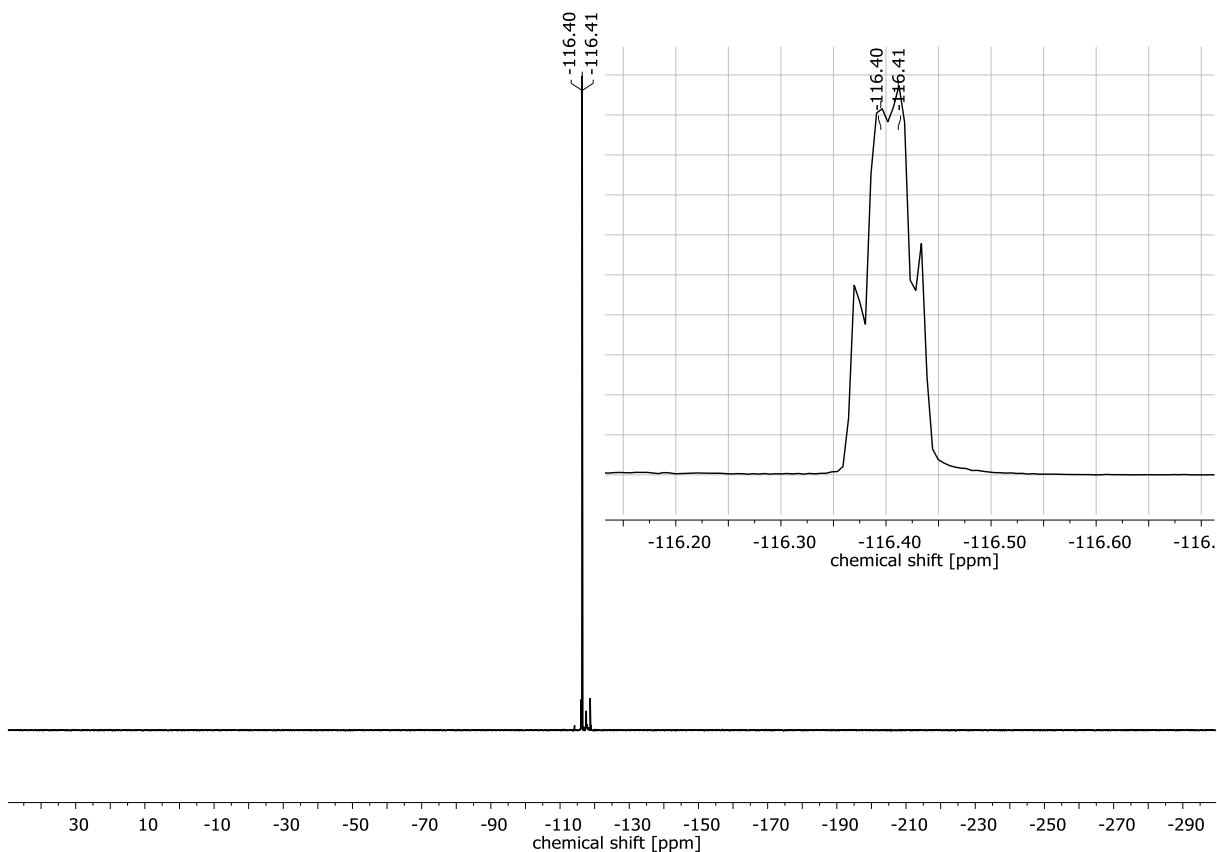


Figure 8.2: ^{19}F -NMR spectrum of 1-(2-fluorophenyl)-4,4-dimethoxy-2-methylbutan-2-ol.

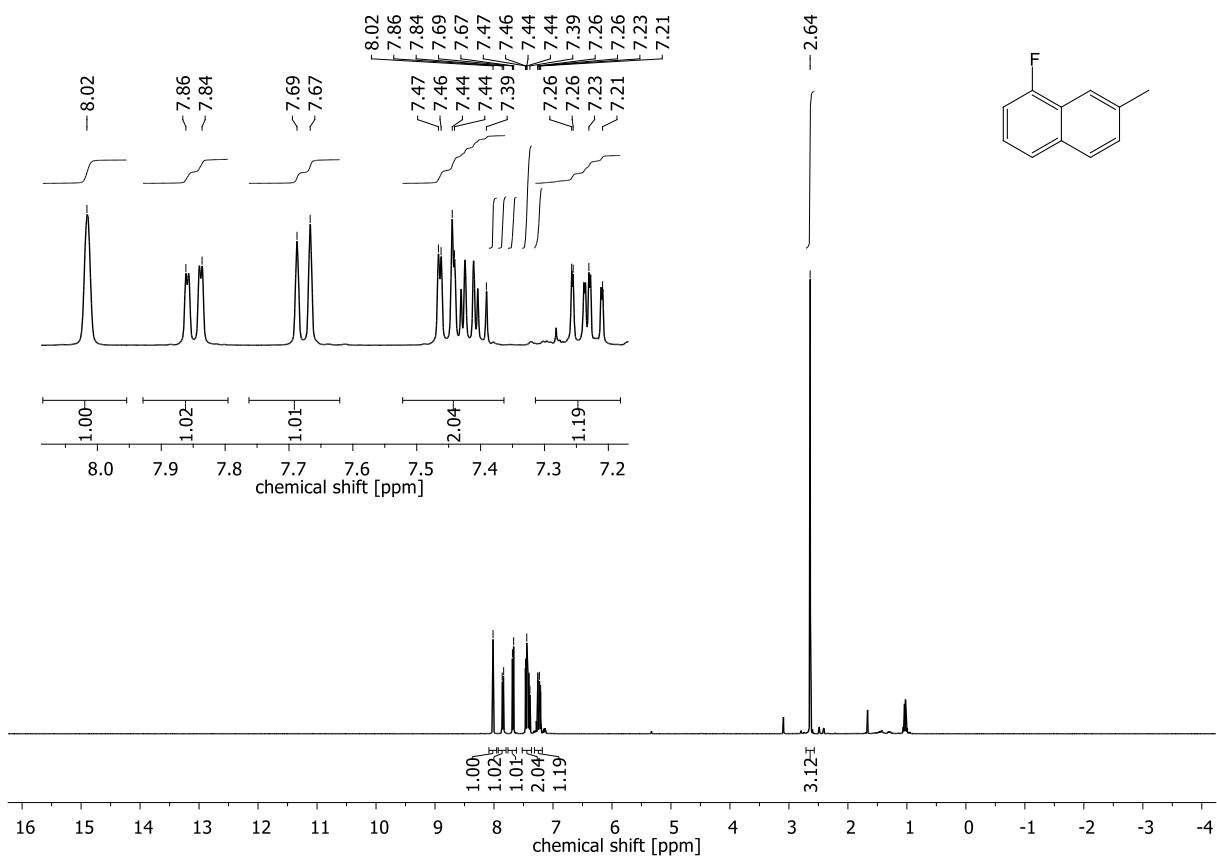


Figure 8.3: ^1H -NMR spectrum of 1-fluoro-7-methylnaphthalene.

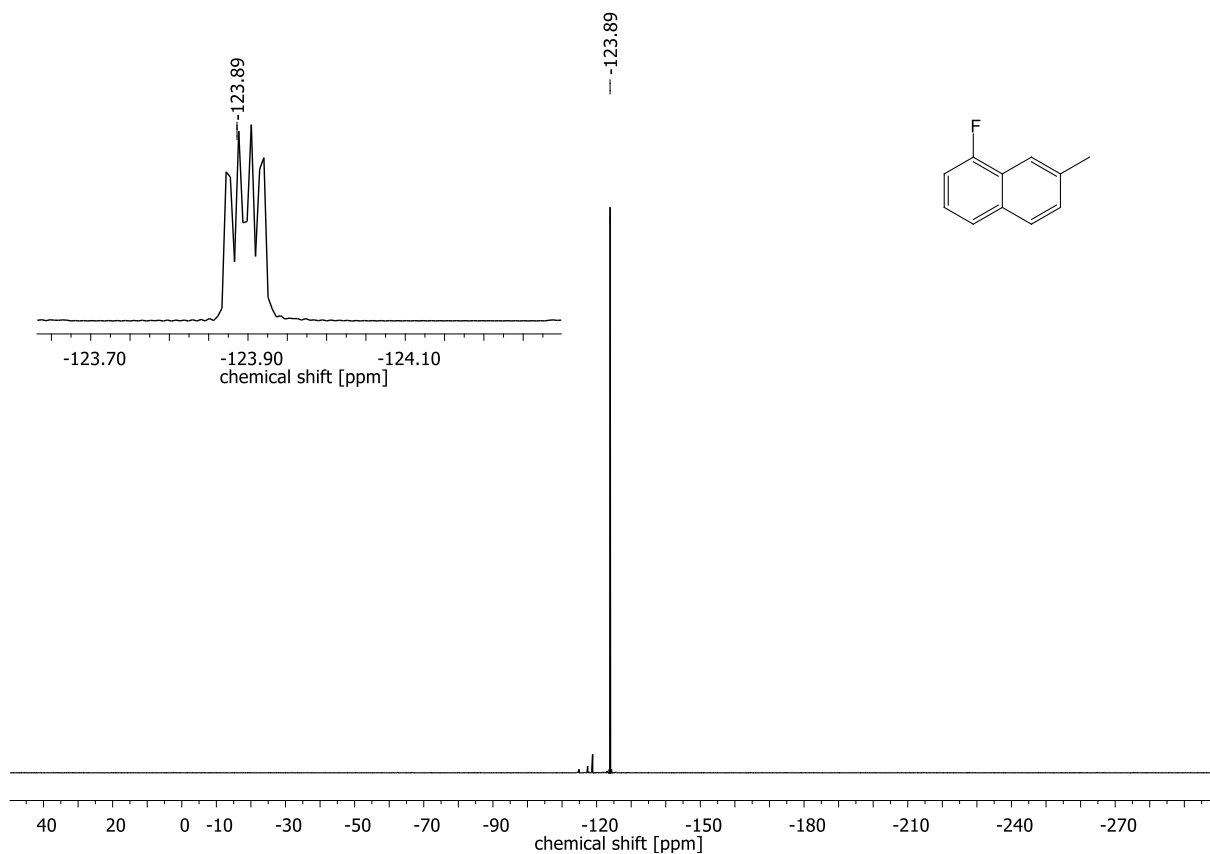


Figure 8.4: ^{19}F -NMR spectrum of 1-fluoro-7-methylnaphthalene.

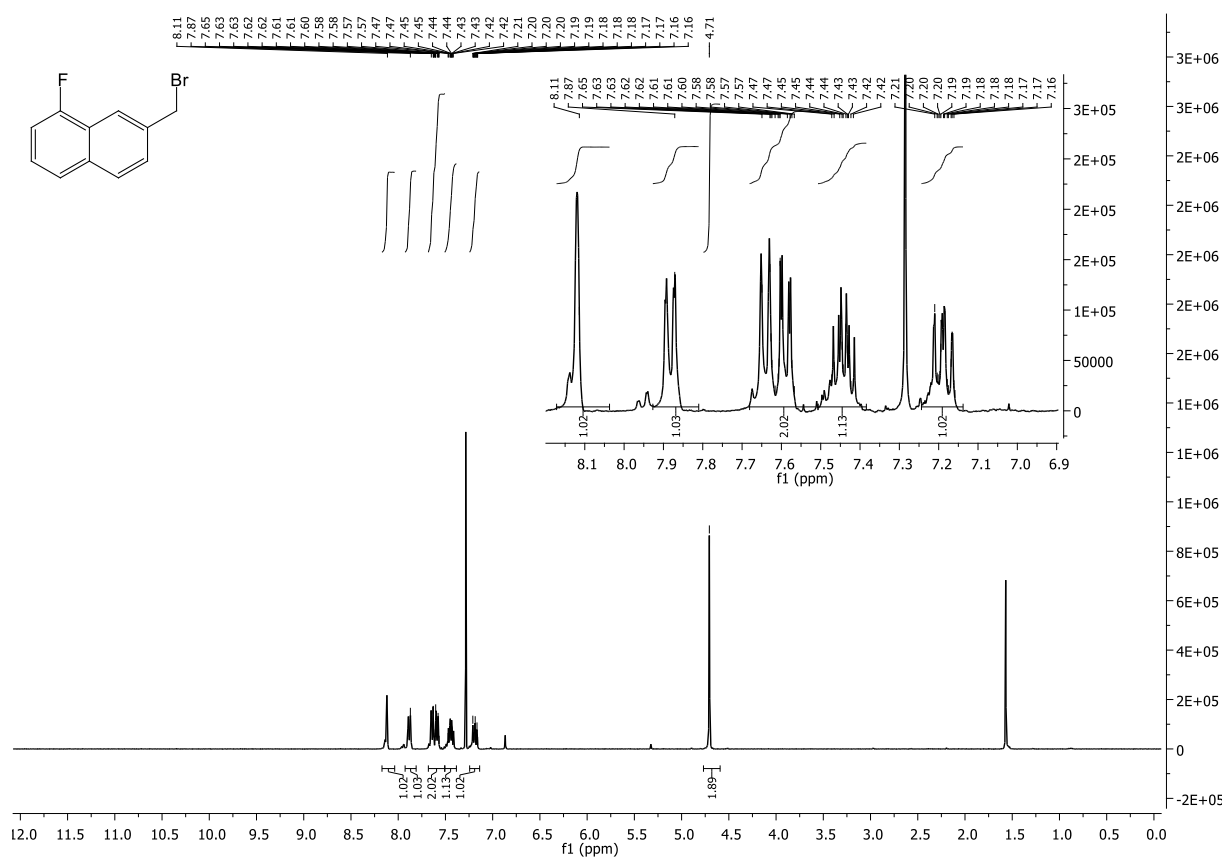


Figure 8.5: ^1H -NMR spectrum of 7-(bromomethyl)-1-fluoronaphthalene.

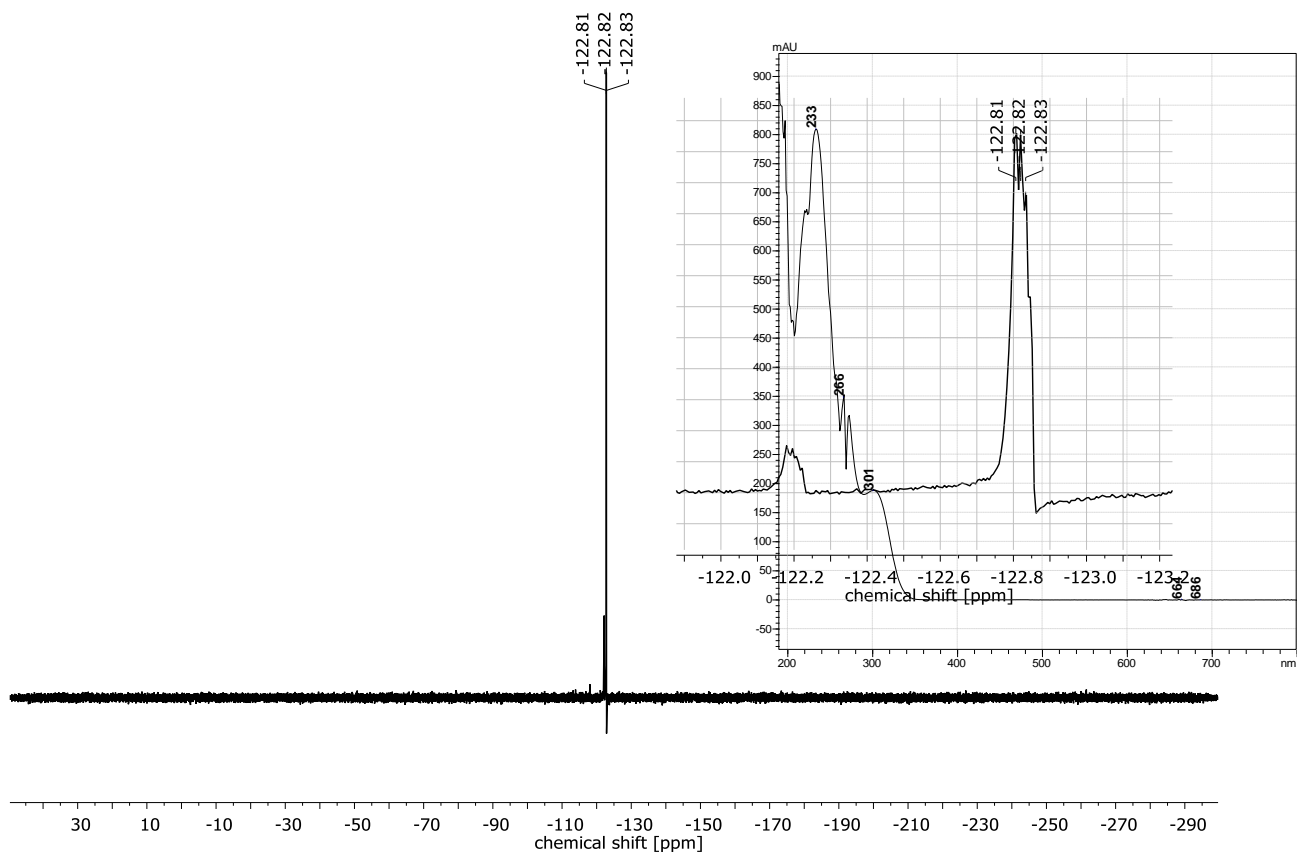


Figure 8.6: ^{19}F -NMR spectrum of 7-(bromomethyl)-1-fluoronaphthalene.

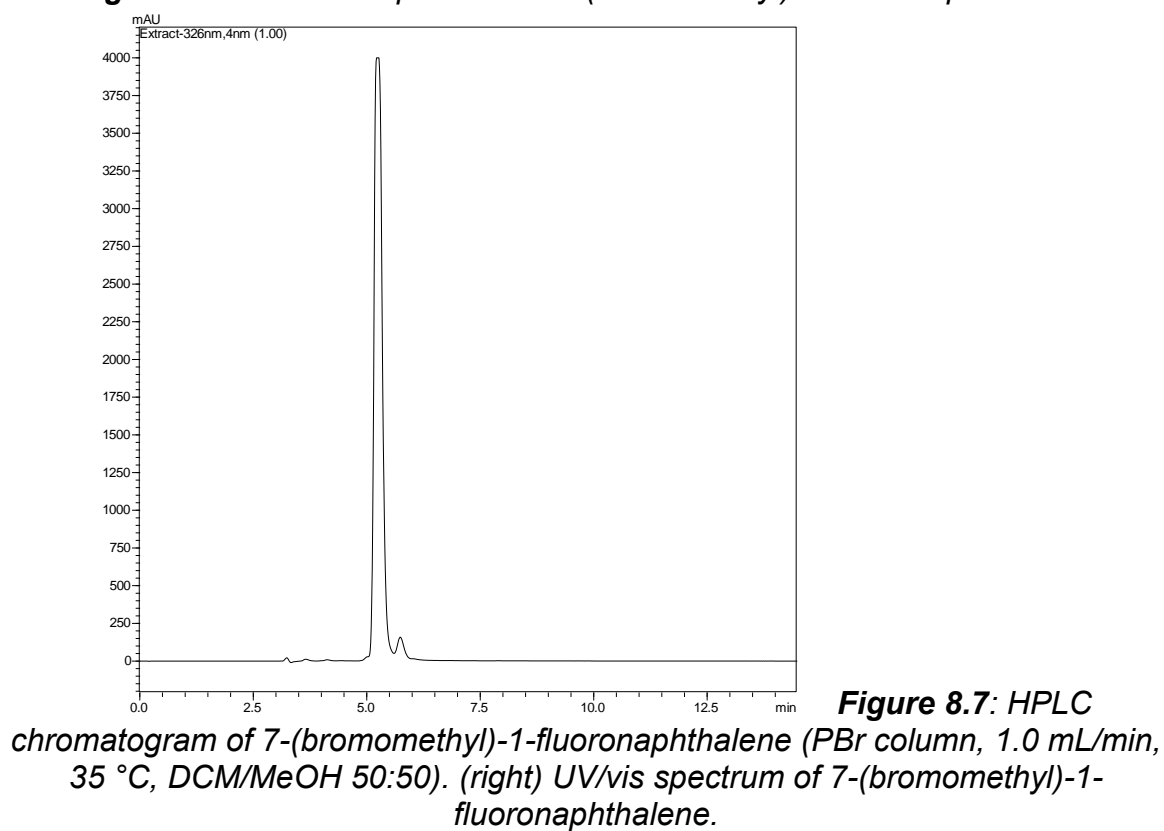


Figure 8.7: HPLC chromatogram of 7-(bromomethyl)-1-fluoronaphthalene (PBr column, 1.0 mL/min, 35 °C, DCM/MeOH 50:50). (right) UV/vis spectrum of 7-(bromomethyl)-1-fluoronaphthalene.

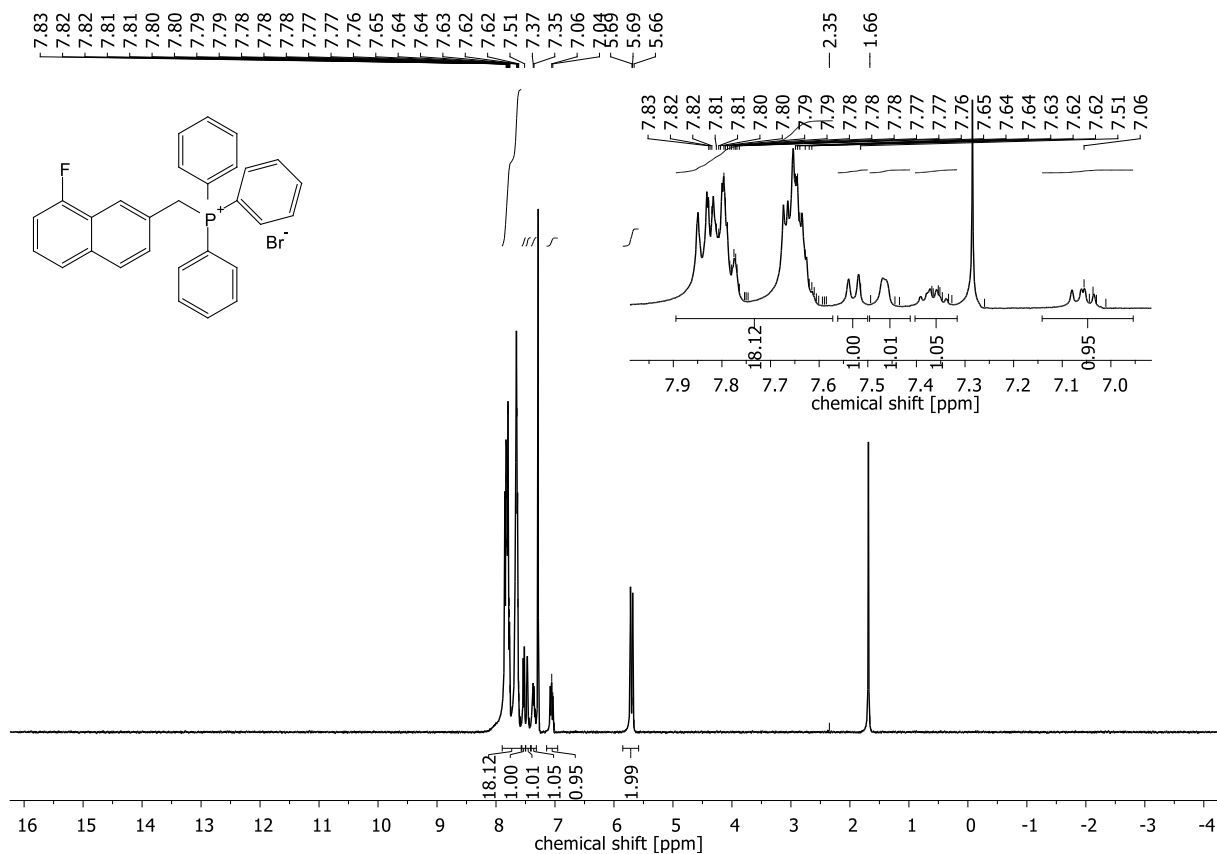


Figure 8.8: $^1\text{H-NMR}$ spectrum of [(8-fluoro-2-naphthalenyl)methyl]triphenylphosphonium bromide.

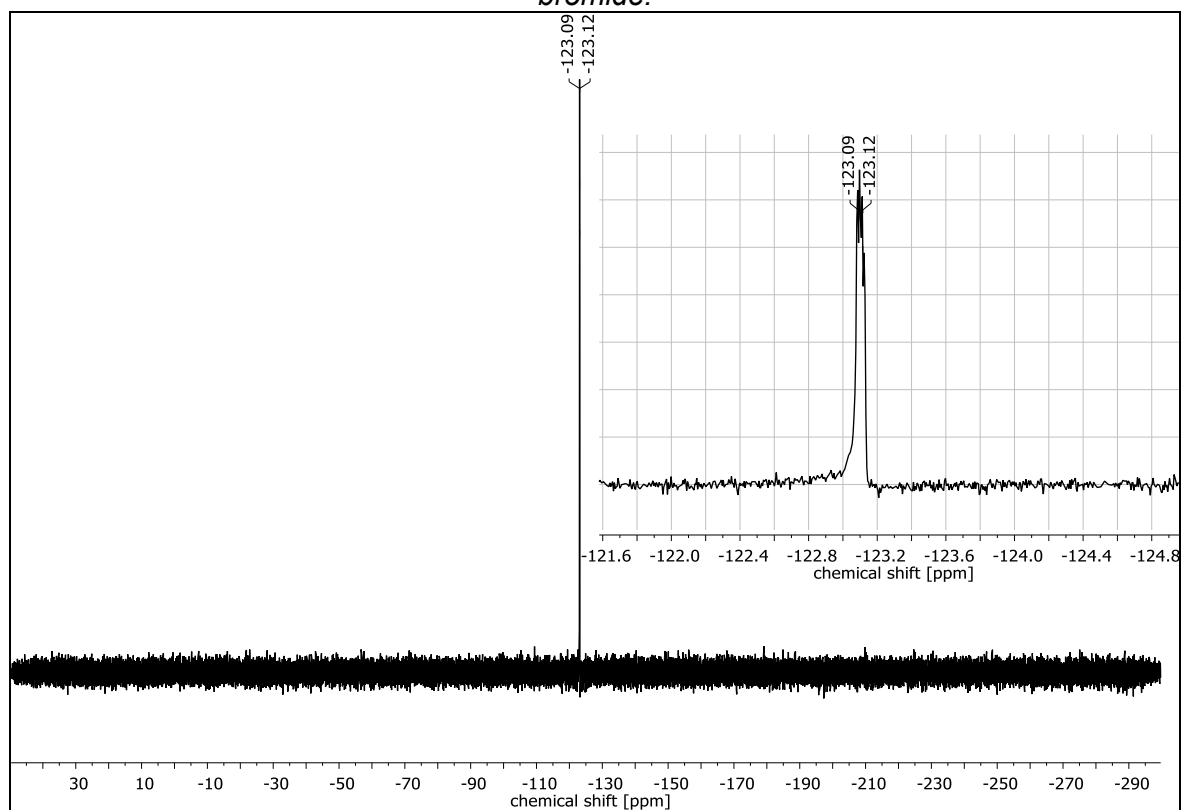


Figure 8.9: $^{13}\text{C-NMR}$ spectrum of [(8-fluoro-2-naphthalenyl)methyl]triphenylphosphonium bromide.

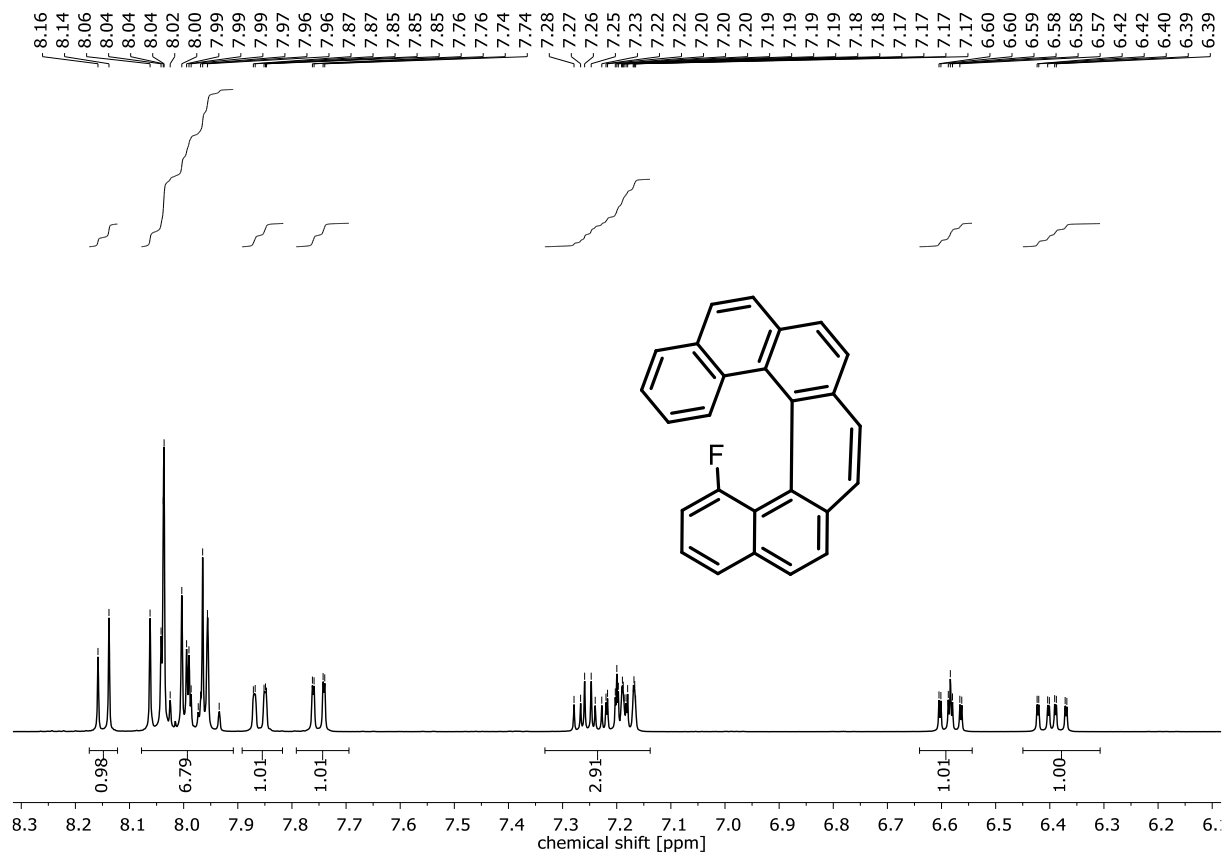


Figure 8.10: $^1\text{H-NMR}$ spectrum of 12-fluorohexahelicene.

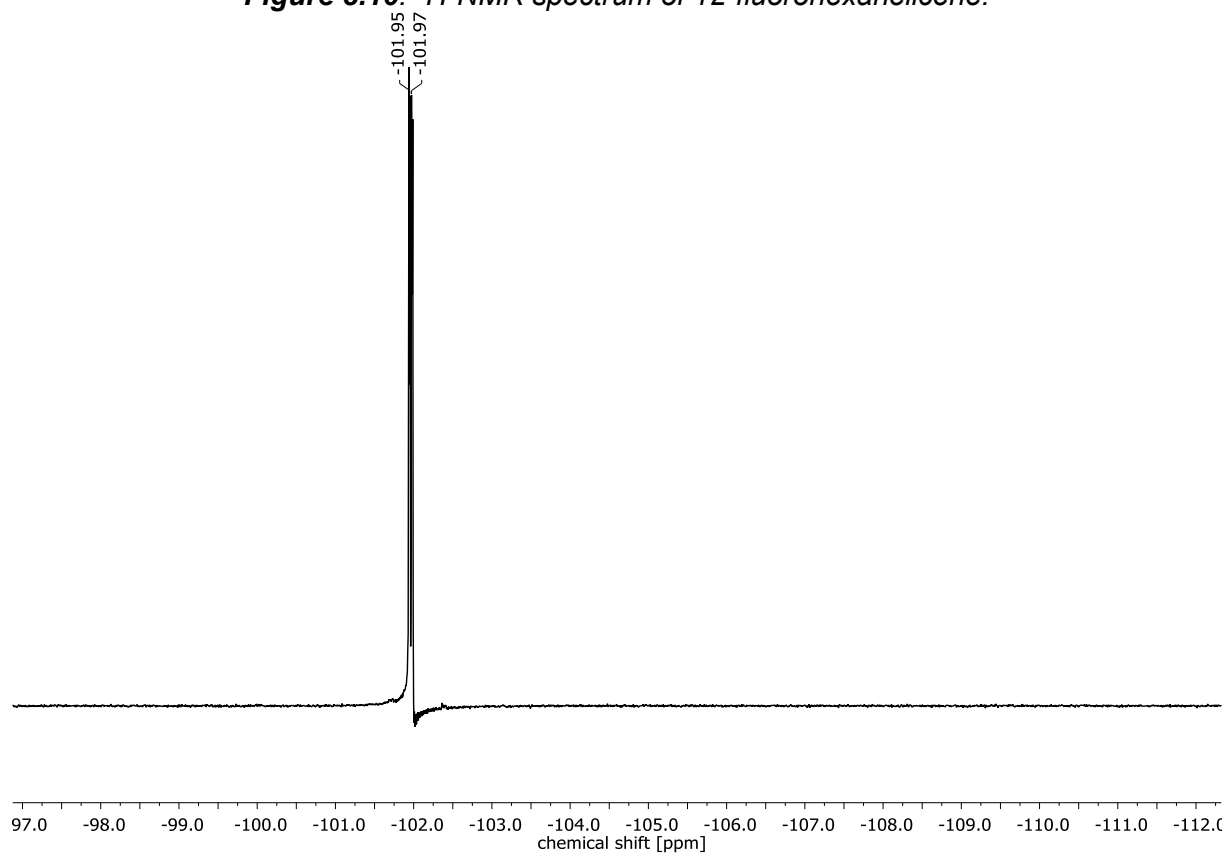


Figure 8.11: $^{19}\text{F-NMR}$ spectrum of 12-fluorohexahelicene.

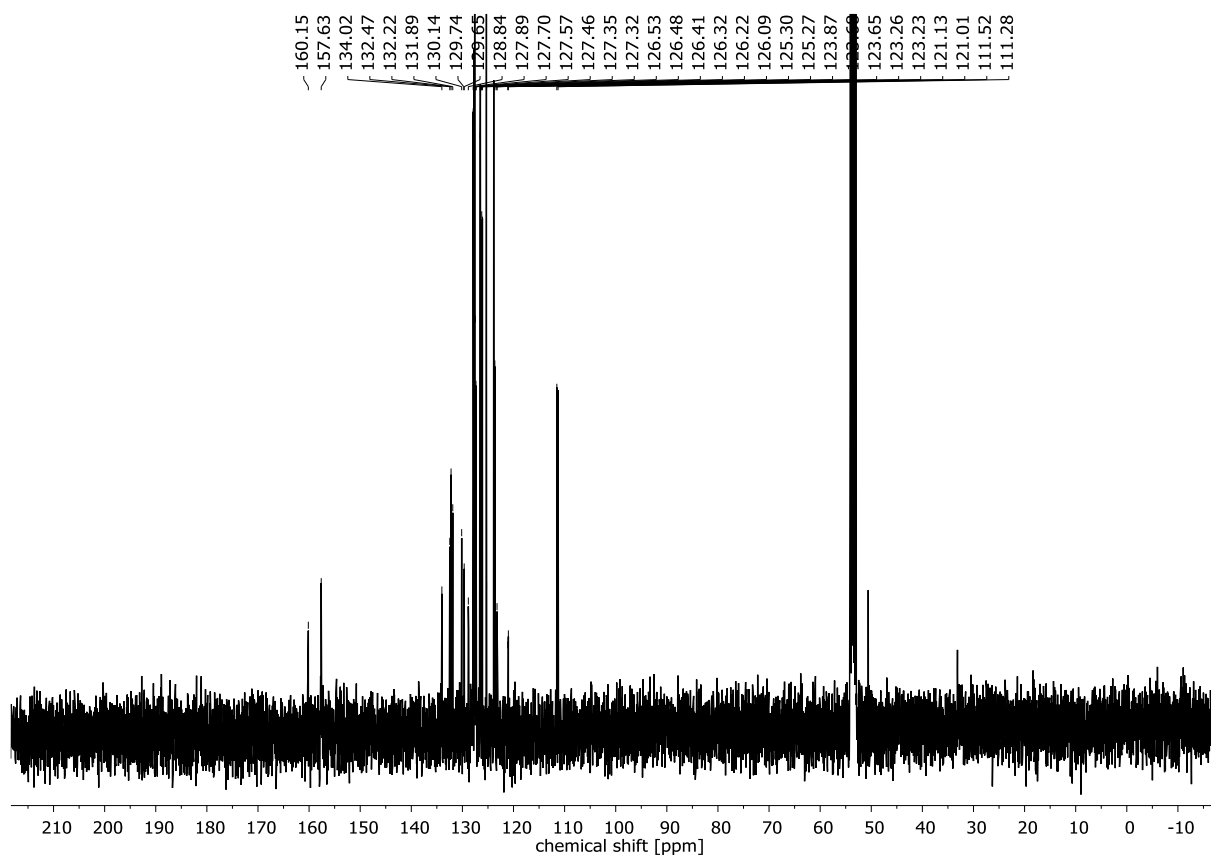


Figure 8.12: ^{13}C -NMR spectrum of 12-fluorohexahelicene.

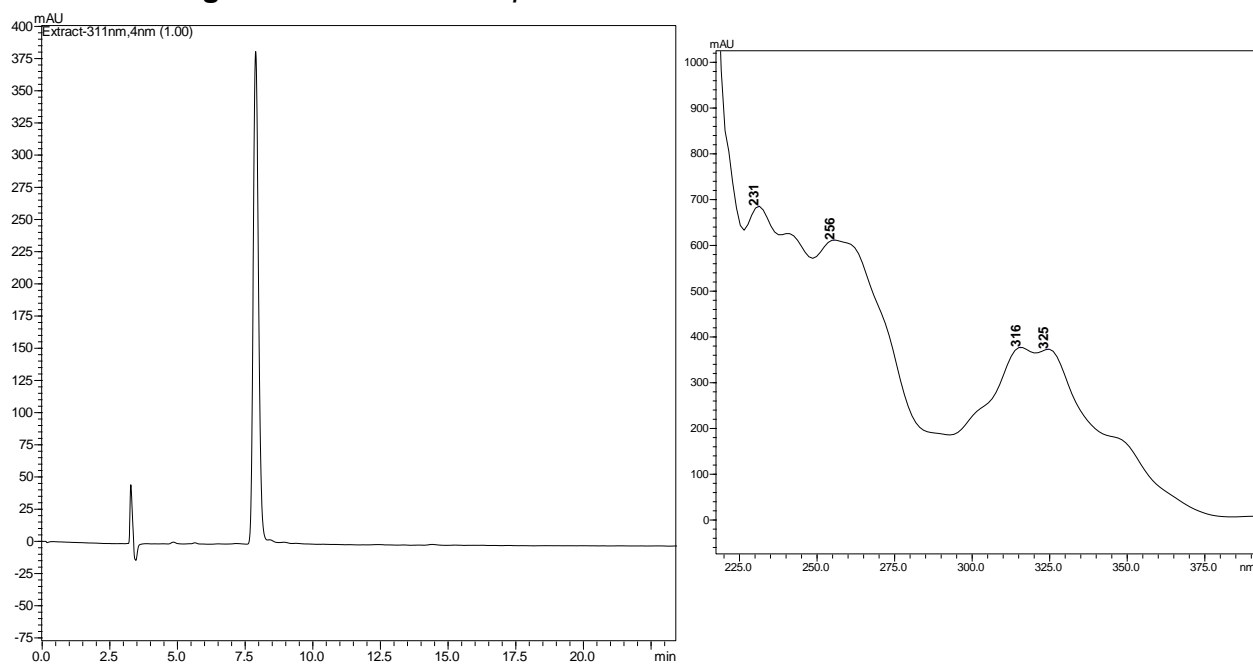


Figure 8.13: HPLC chromatogram of 12-fluorohexahelicene (PBr column, 1.0 mL/min, 35 °C, DCM/MeOH 30:70). (right) UV/vis spectrum of 12-fluorohexahelicene

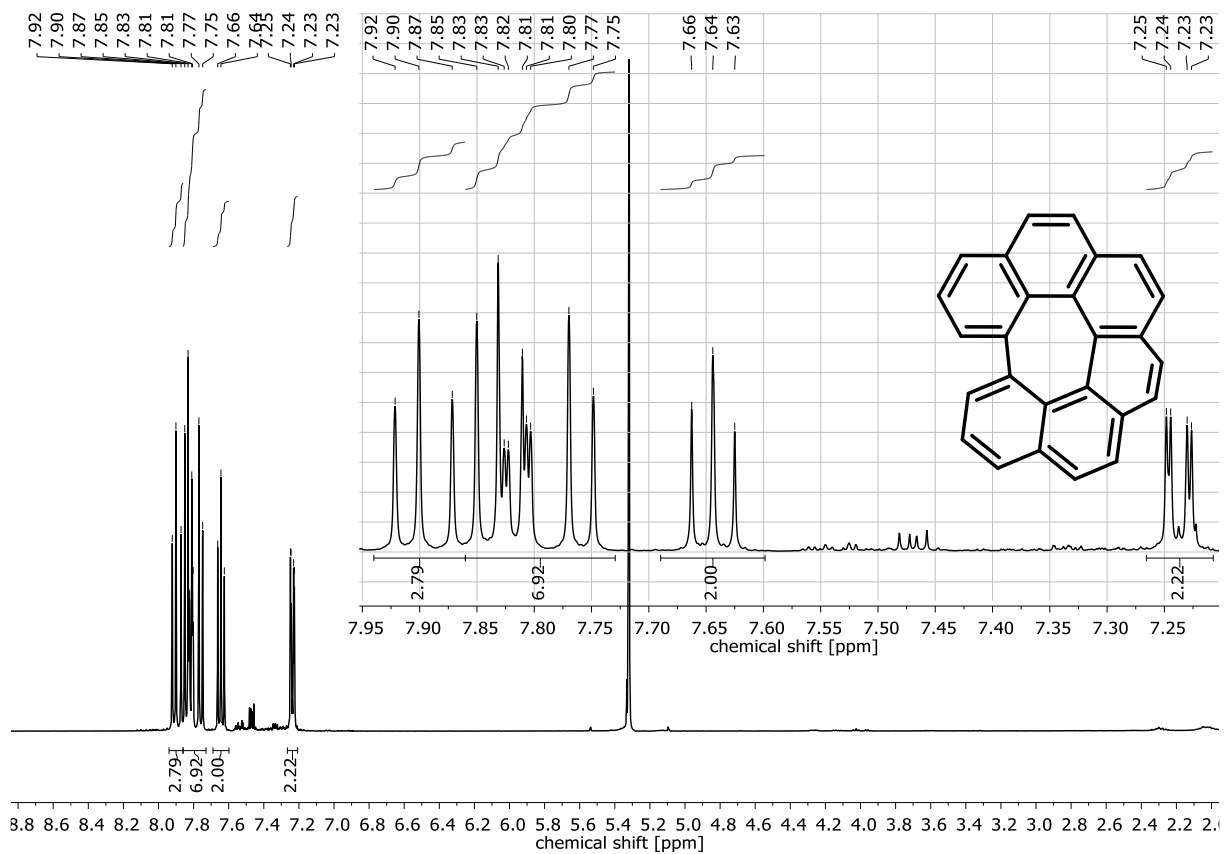


Figure 8.14 $^1\text{H-NMR}$ spectrum of benzo[no]naphtho[2,1,8,7-g hij]pleiadene.

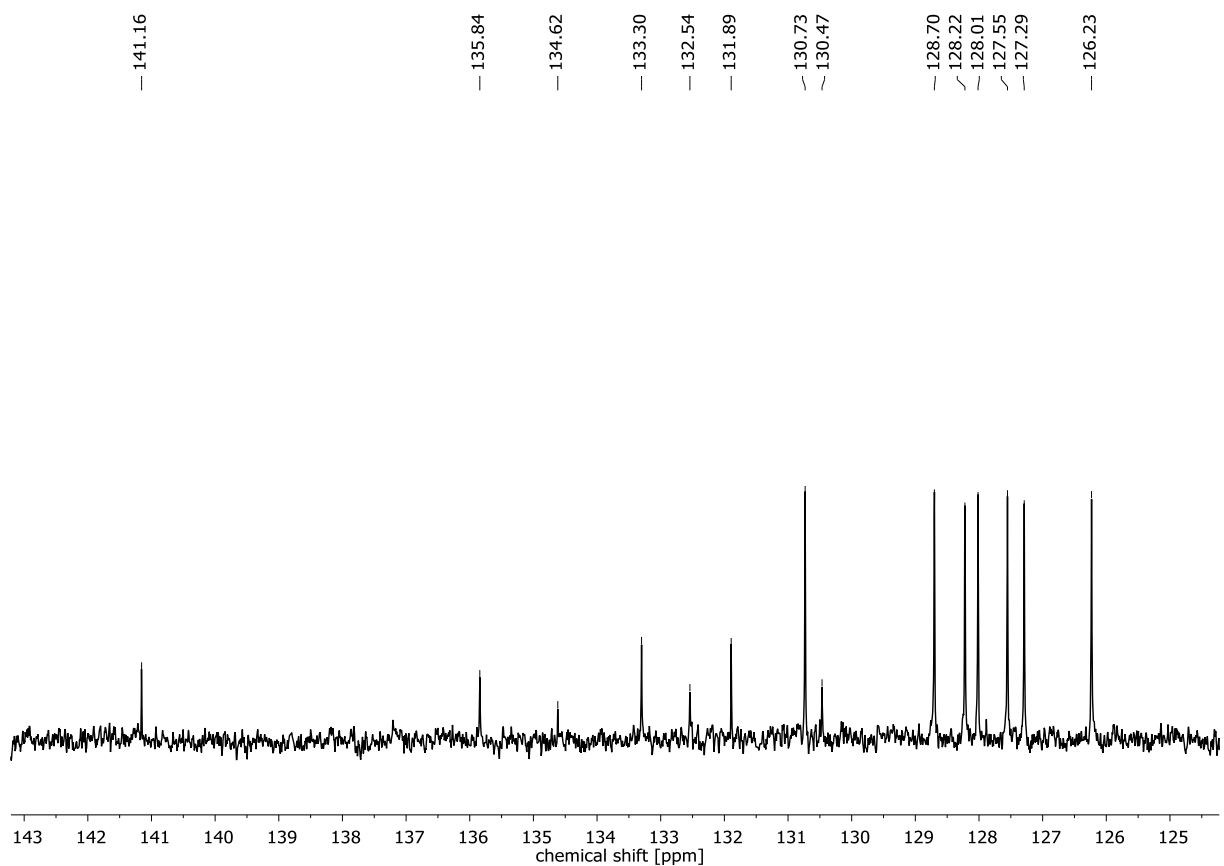


Figure 8.15: $^{13}\text{C-NMR}$ spectrum of benzo[no]naphtho[2,1,8,7-g hij]pleiadene.

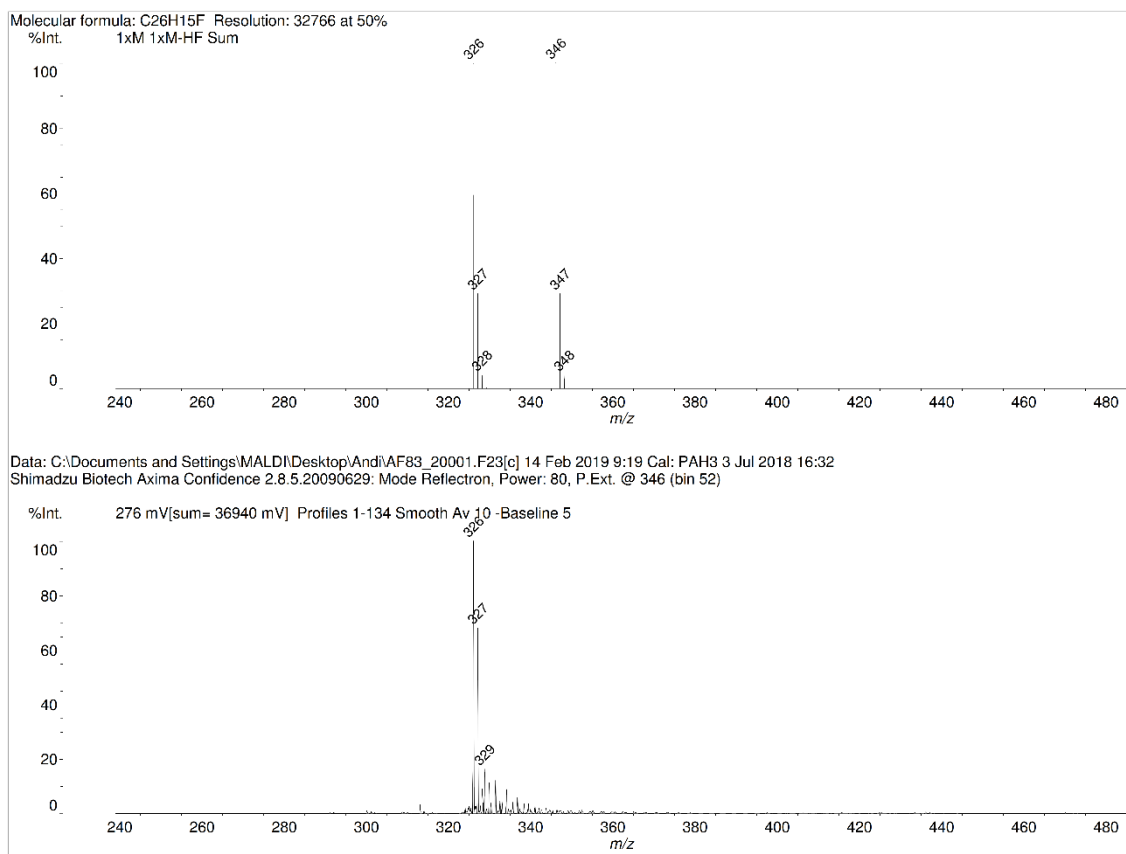


Figure 8.16: LDI MS spectrum of *benzo[no]naphtho[2,1,8,7-ghij]pleiadene*.

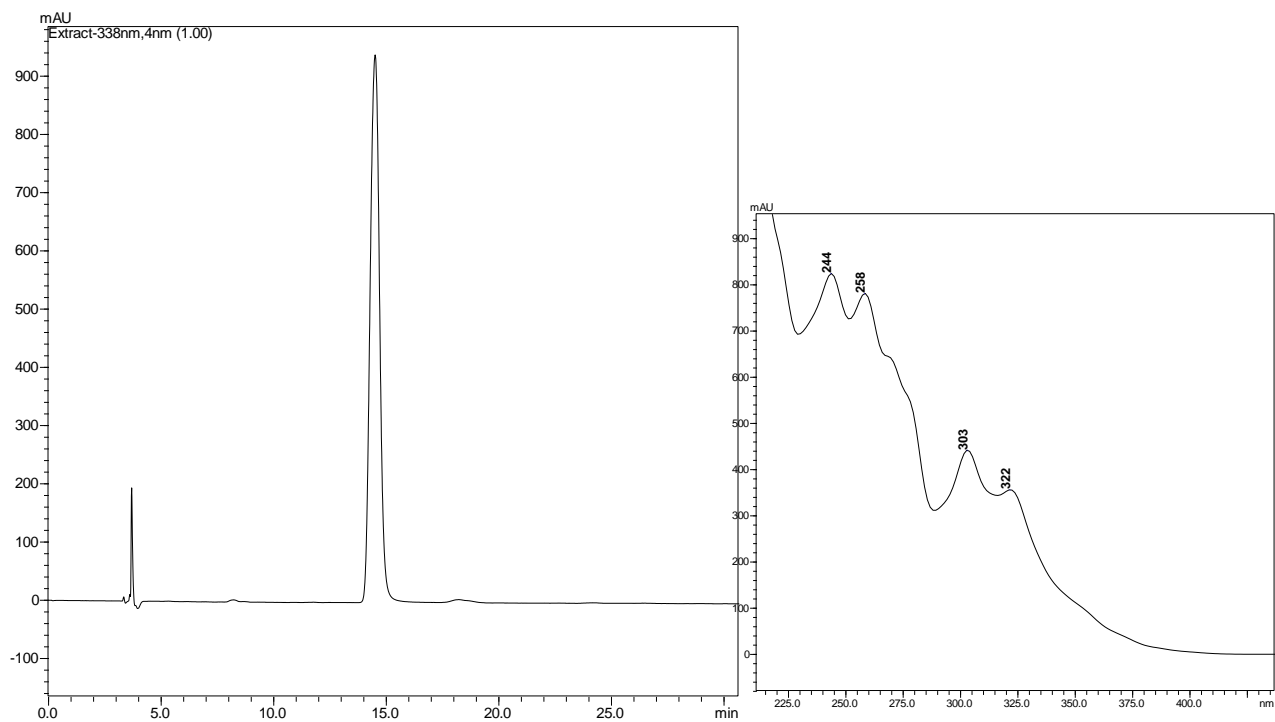


Figure 8.17: HPLC chromatogram of *benzo[no]naphtho[2,1,8,7-ghij]pleiadene* (PBr column, 1.0 mL/min, 35°C, DCM/MeOH 30:70). (right) UV/vis spectrum of *benzo[no]naphtho[2,1,8,7-ghij]pleiadene*.

8.1.2. Synthesis of dibenzo[e,gh]dibenzo[4,5:6,7]pleiaden[2,1,12-pqa]pleiadene

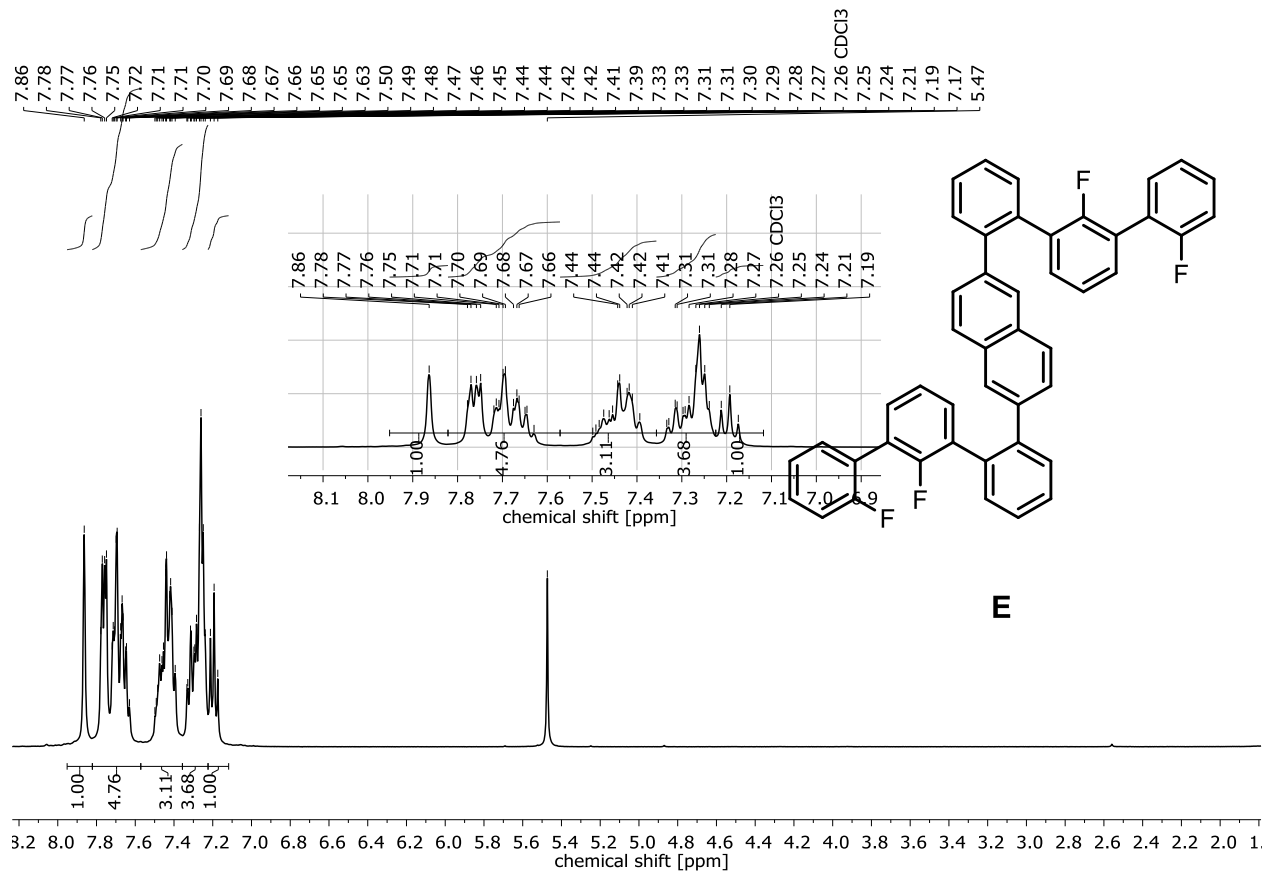


Figure 8.18: $^1\text{H-NMR}$ spectrum of 2,6-bis(2',2''-difluoro-[1,1':3',1''-terphenyl])-2-yl)naphthalene.

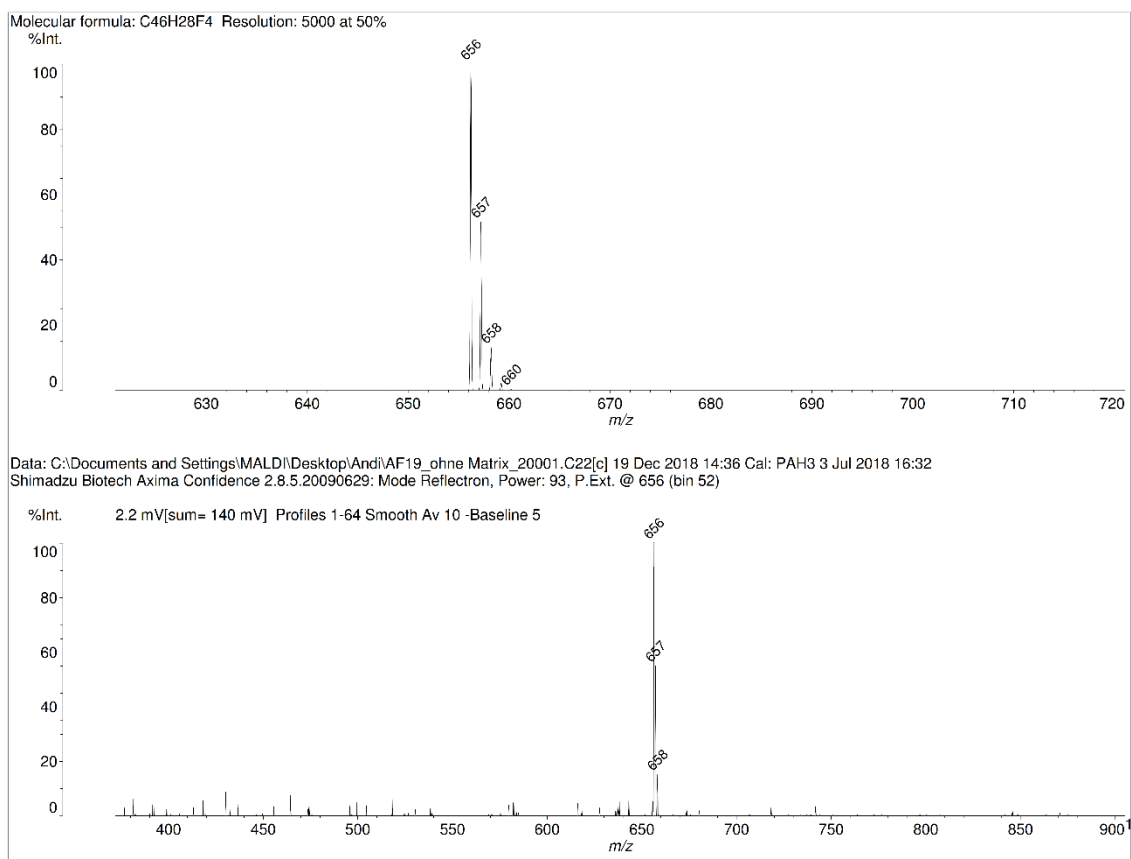


Figure 8.21: LDI MS spectrum of 2,6-bis(2',2''-difluoro-[1,1':3,1''-terphenyl]-2-yl)naphthalene.

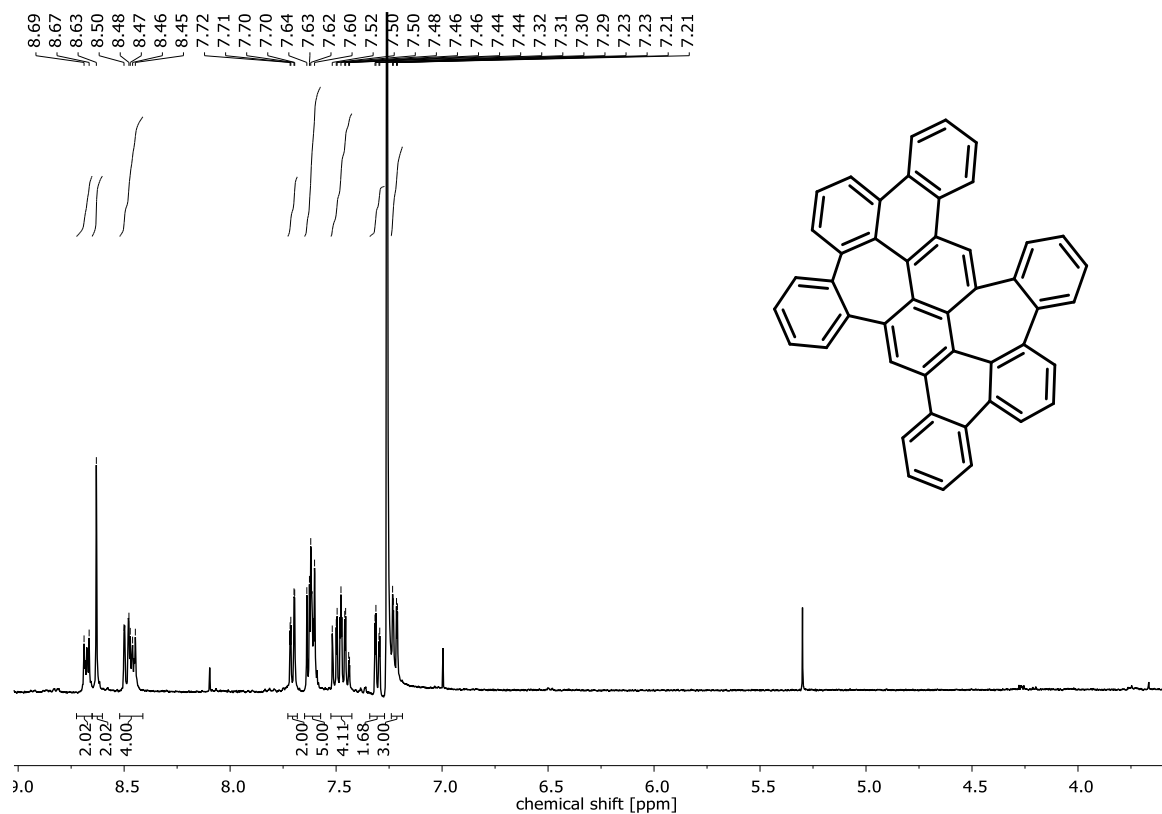


Figure 8.22: ¹H-NMR spectrum of dibenzo[e,gh]dibenzo[4,5:6,7]pleiadeno[2,1,12-pqa]pleiadene.

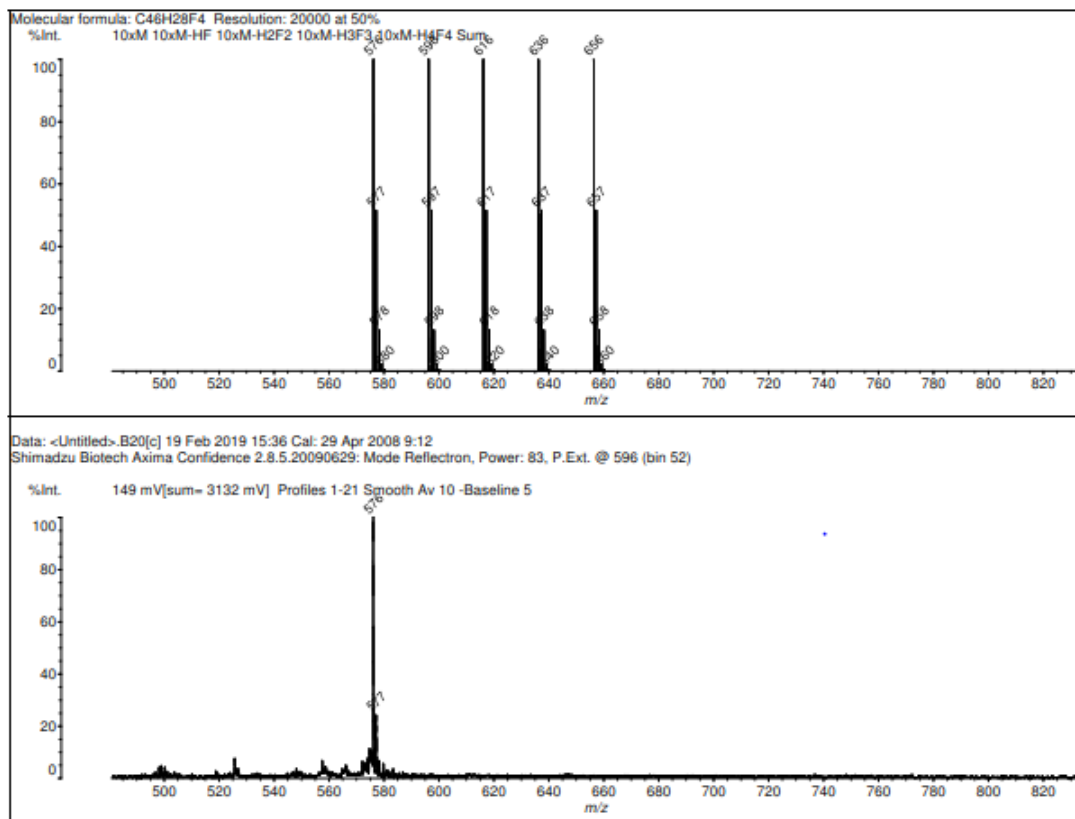


Figure 8.23: LDI MS spectrum of dibenzo[e,gh]dibenzo[4,5:6,7]pleiadeno[2,1,12-pqa]pleiadene.

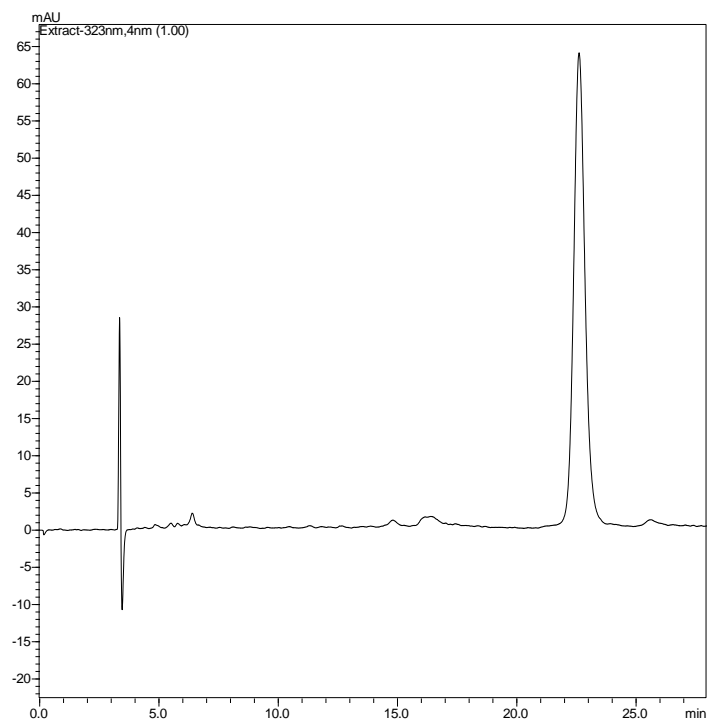


Figure 8.24: HPLC chromatogram of dibenzo[e,gh]dibenzo[4,5:6,7]pleiadeno[2,1,12-pqa]pleiadene (PBr column, 1.0 mL/min, 35°C DCM/MeOH 30/70).

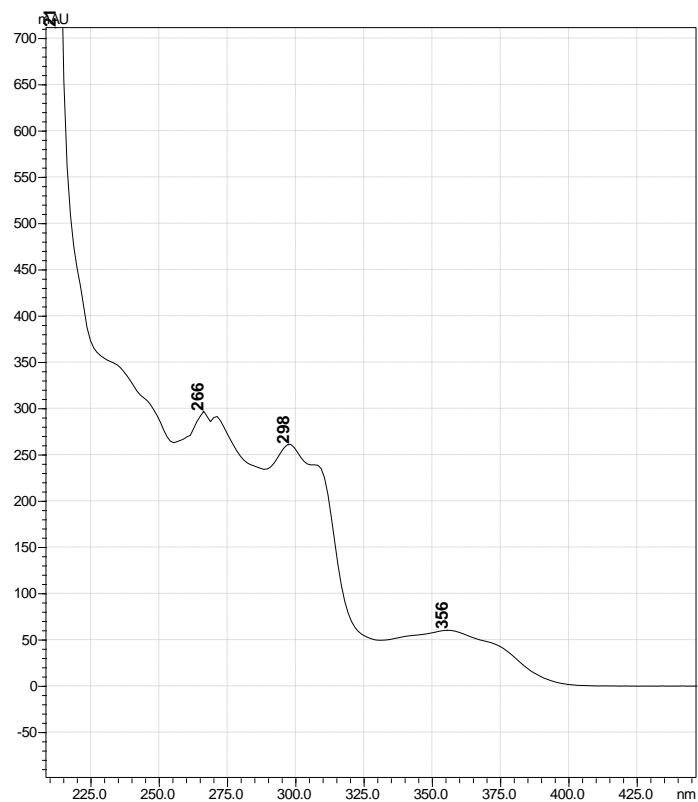


Figure 8.25: UV-vis spectrum of dibenzo[e,gh]dibenzo[4,5:6,7]pleiadeno[2,1,12-pq]pleiadene.

8.1.3 Synthesis of tribenzo[b,gh,pq]pleiadene

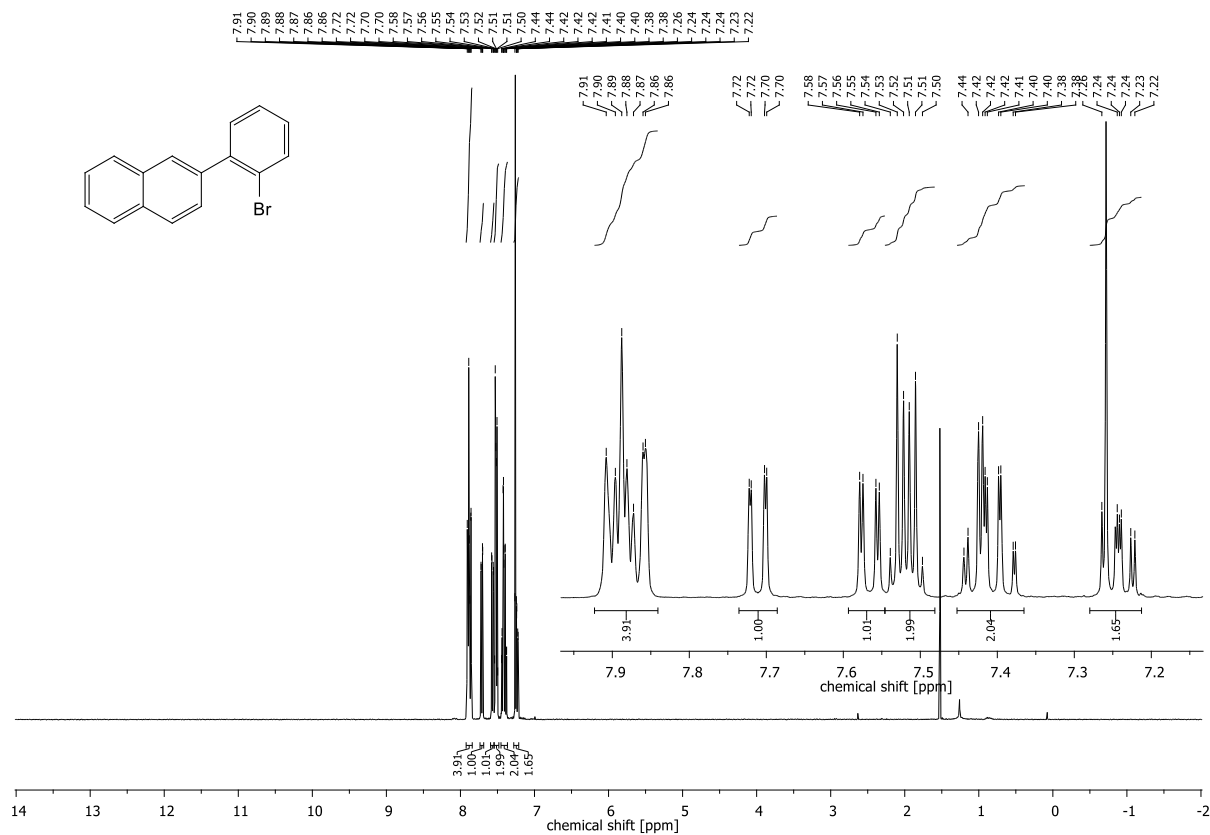


Figure 8.26: $^1\text{H-NMR}$ spectrum of 2-(2-bromophenyl)naphthalene.

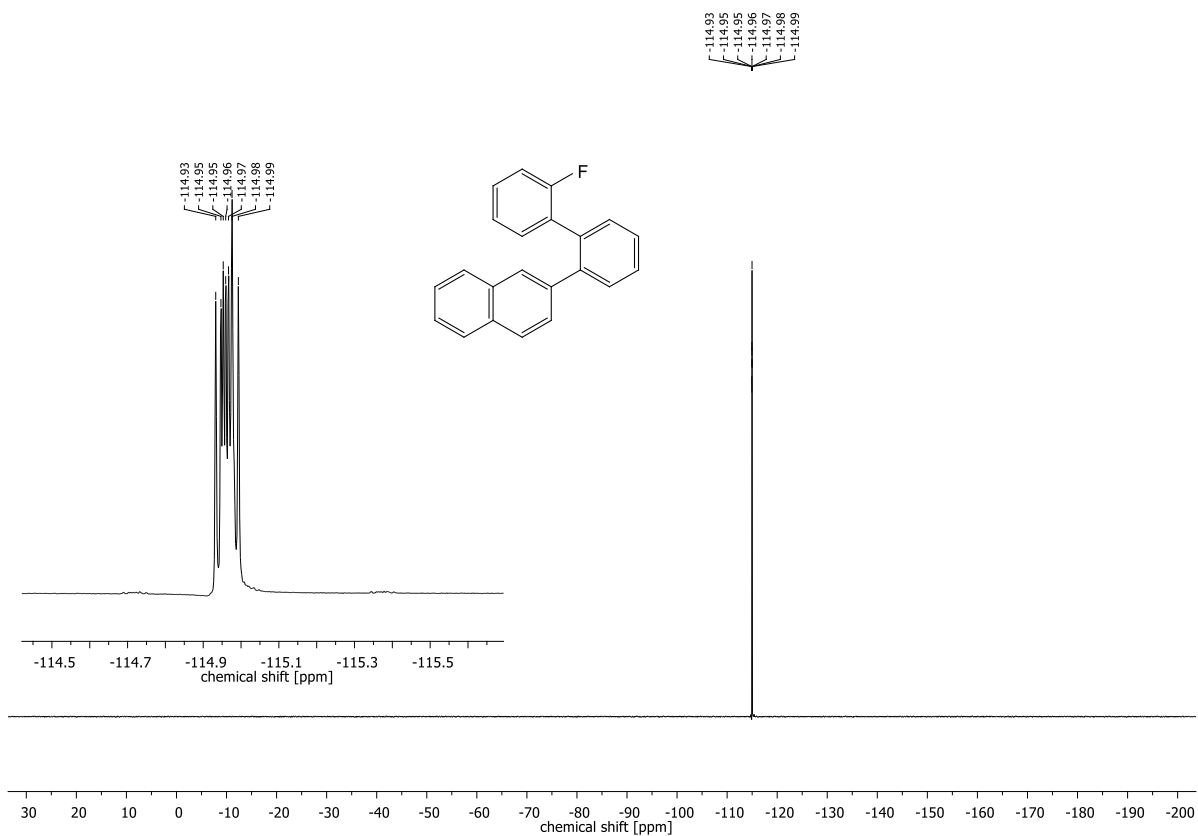


Figure 8.29: ¹⁹F-NMR spectrum of 2-(2'-fluoro-[1,1'-biphenyl]-2-yl)naphthalene.

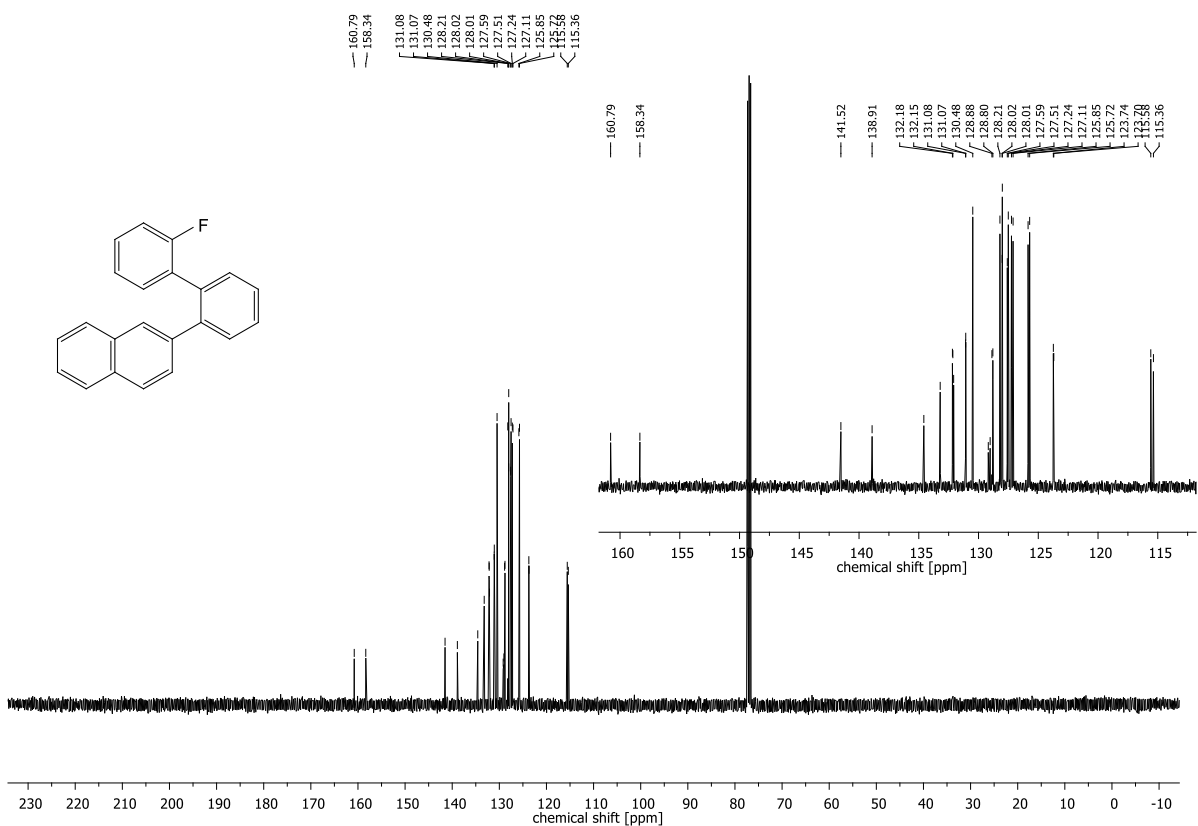


Figure 8.30: ¹³C-NMR spectrum of 2-(2'-fluoro-[1,1'-biphenyl]-2-yl)naphthalene.

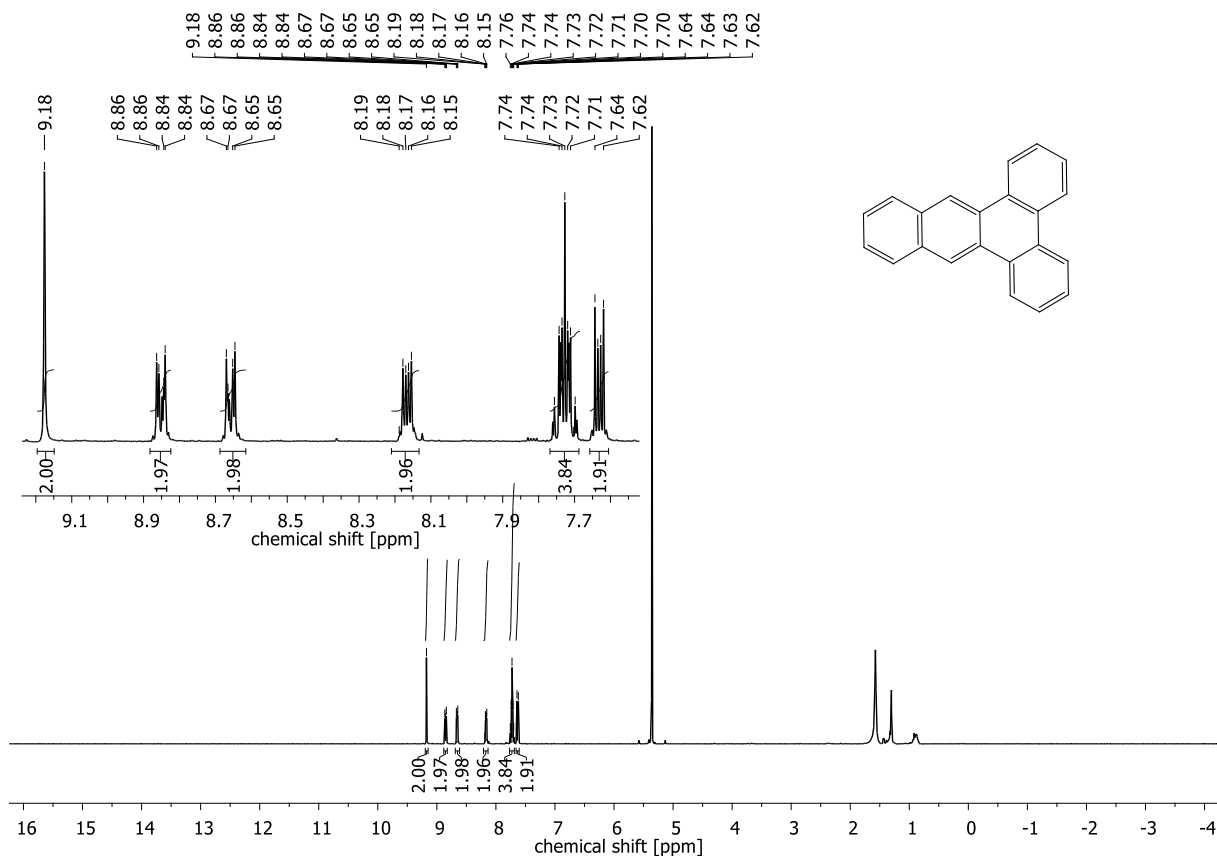


Figure 8.33: ¹H-NMR spectrum of benzo[f]tetraphene.

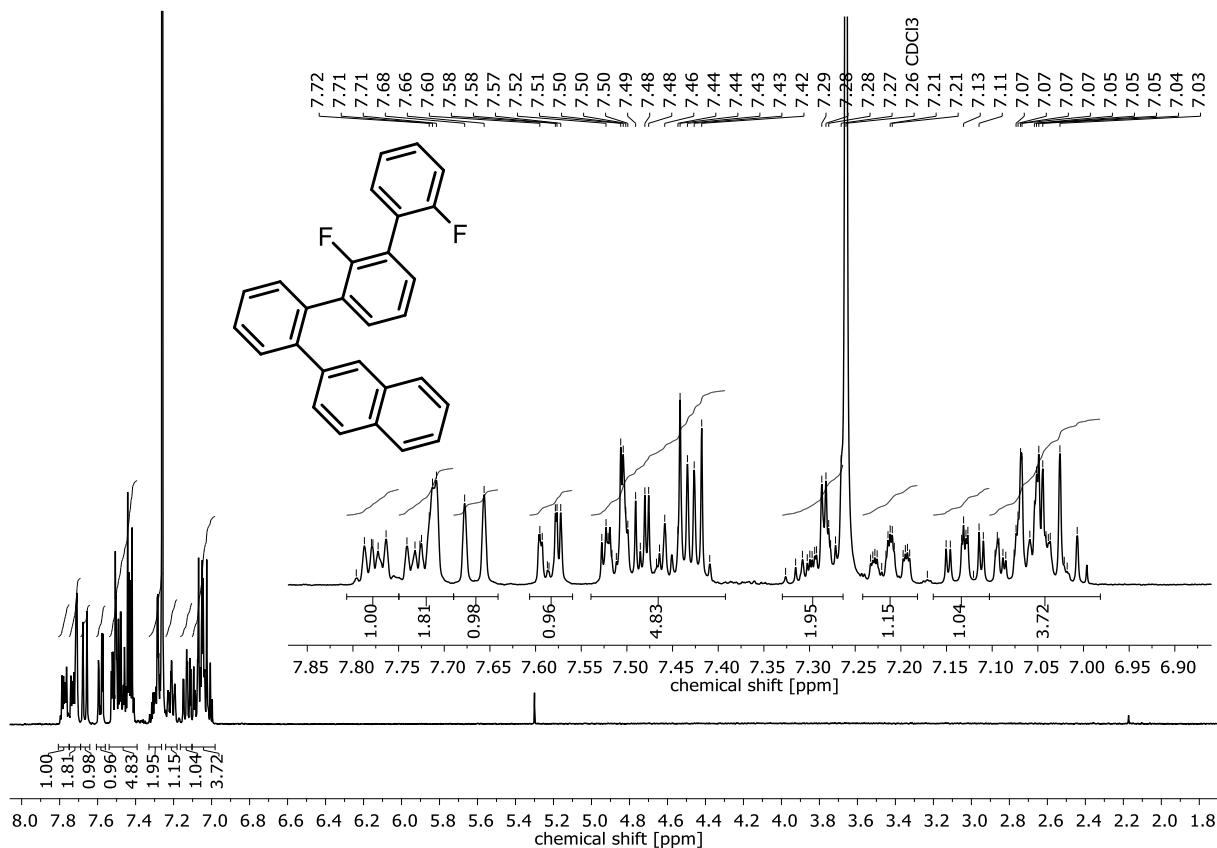


Figure 8.34: ¹H-NMR spectrum of 2-(2',2''-difluoro-[1,1':3,1''-terphenyl]-2-yl)naphthalene.

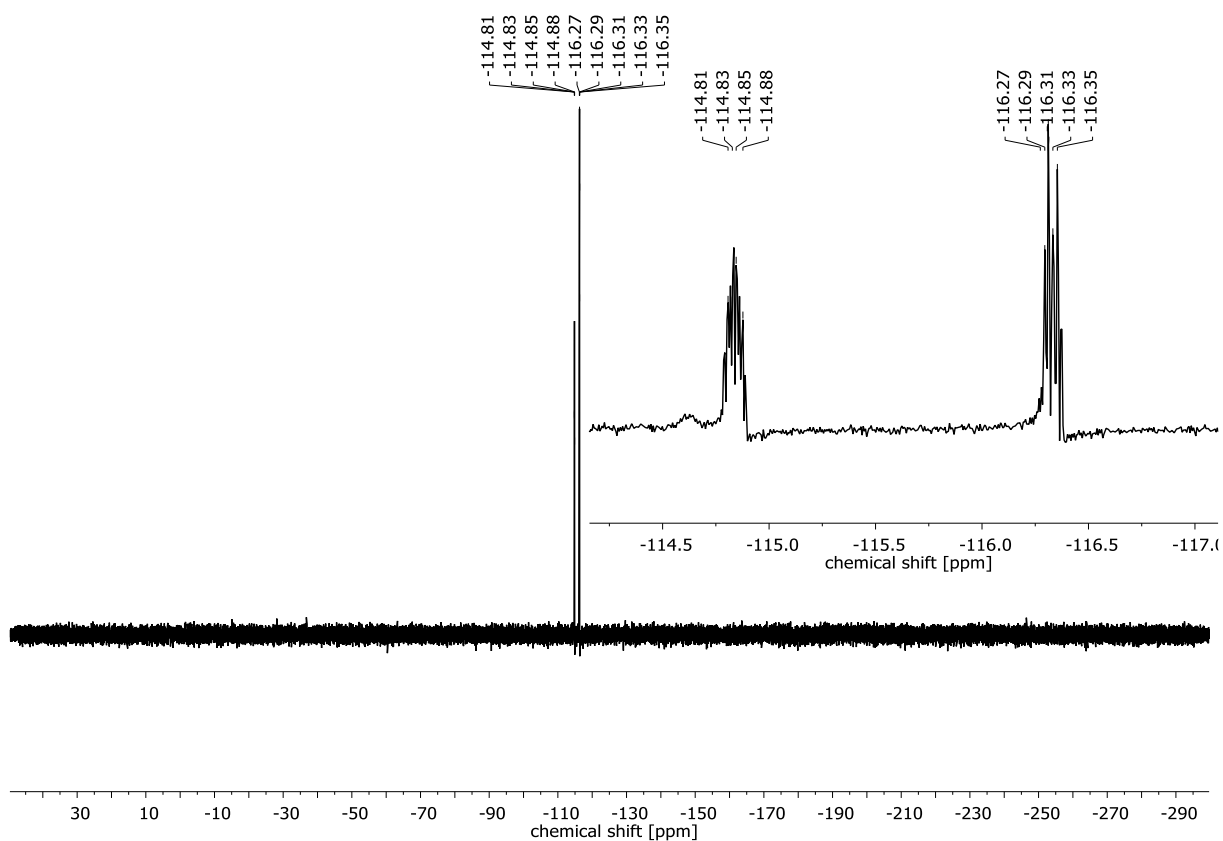


Figure 8.35: ^{19}F -NMR spectrum of 2-(2',2''-difluoro-[1,1':3',1''-terphenyl]-2-yl)naphthalene.

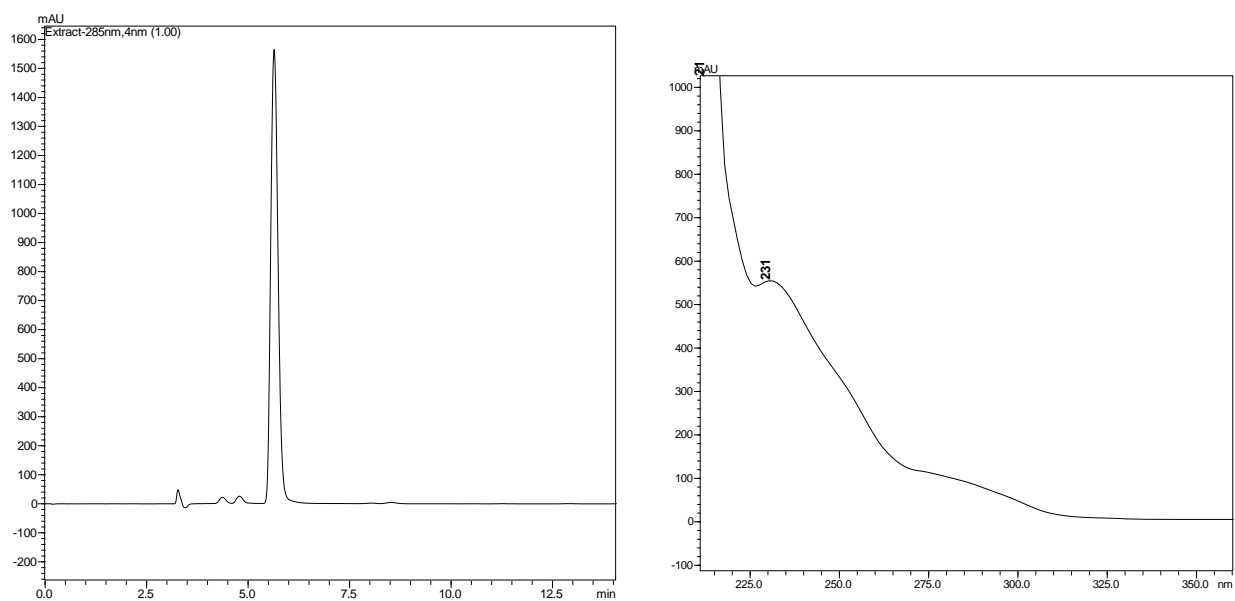


Figure 8.36: HPLC chromatogram of 2-(2',2''-difluoro-[1,1':3',1''-terphenyl]-2-yl)naphthalene (PBr column, 1.0 mL/min, 35°C DCM/MeOH 20/80) (left). UV/vis spectrum of 2-(2',2''-difluoro-[1,1':3',1''-terphenyl]-2-yl)naphthalene. (right).

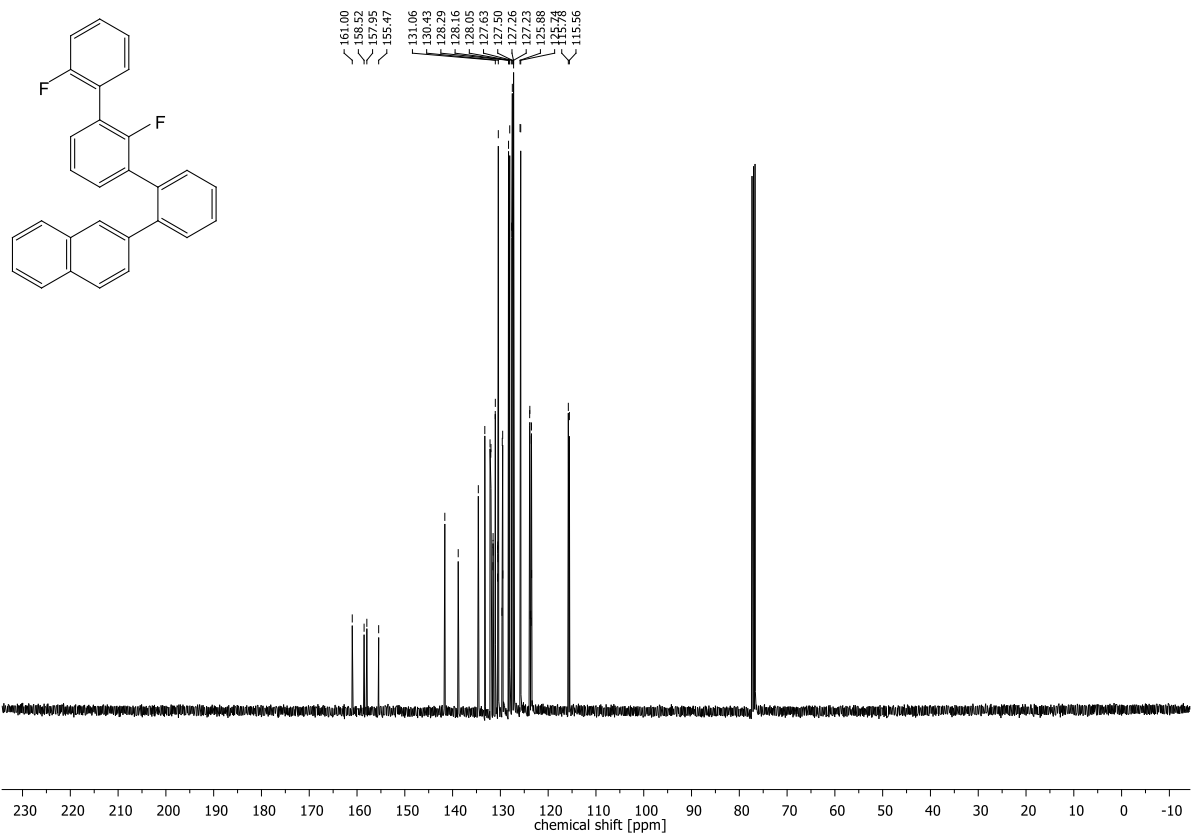


Figure 8.37: $^{13}\text{C-NMR}$ spectrum of 2-(2',2''-difluoro-[1,1':3',1''-terphenyl]-2-yl)naphthalene.

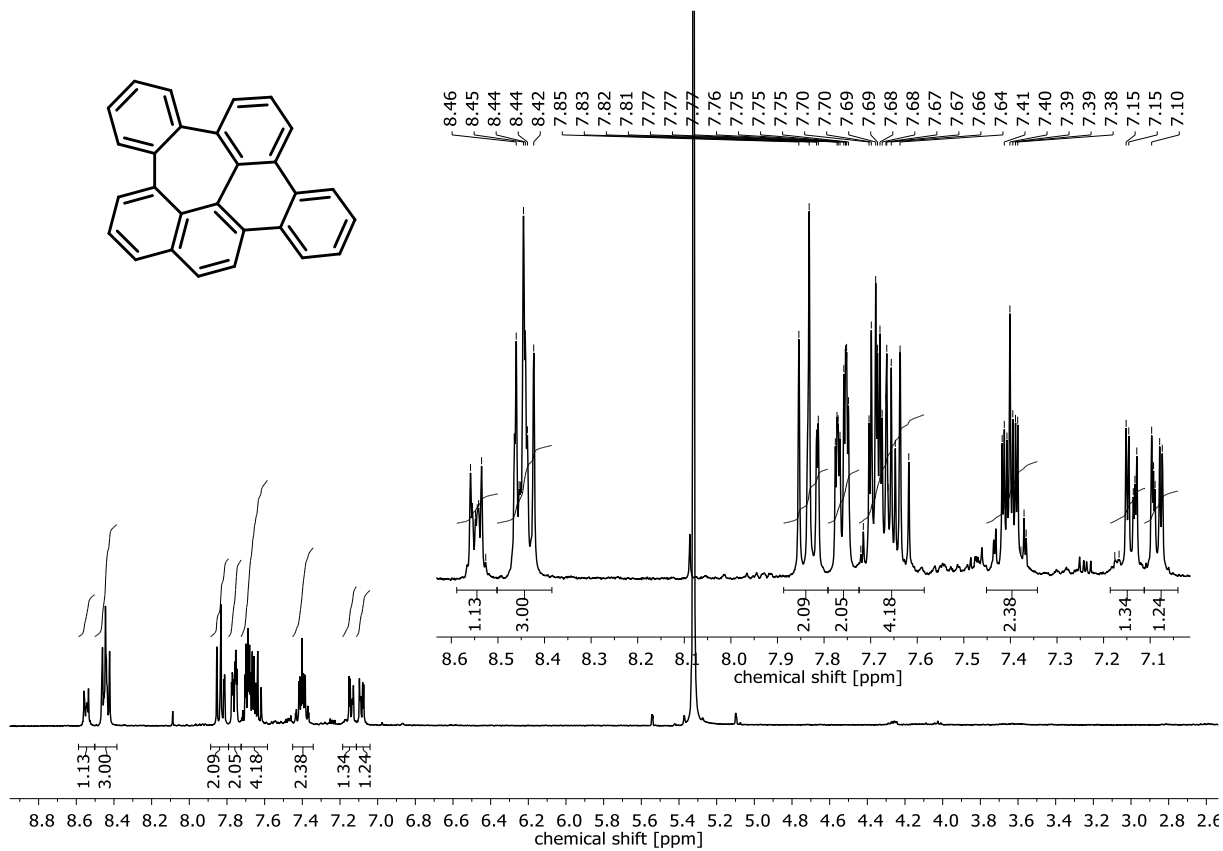


Figure 8.38: $^1\text{H-NMR}$ spectrum of tribenzo[b,gh,pq]pleiadene.

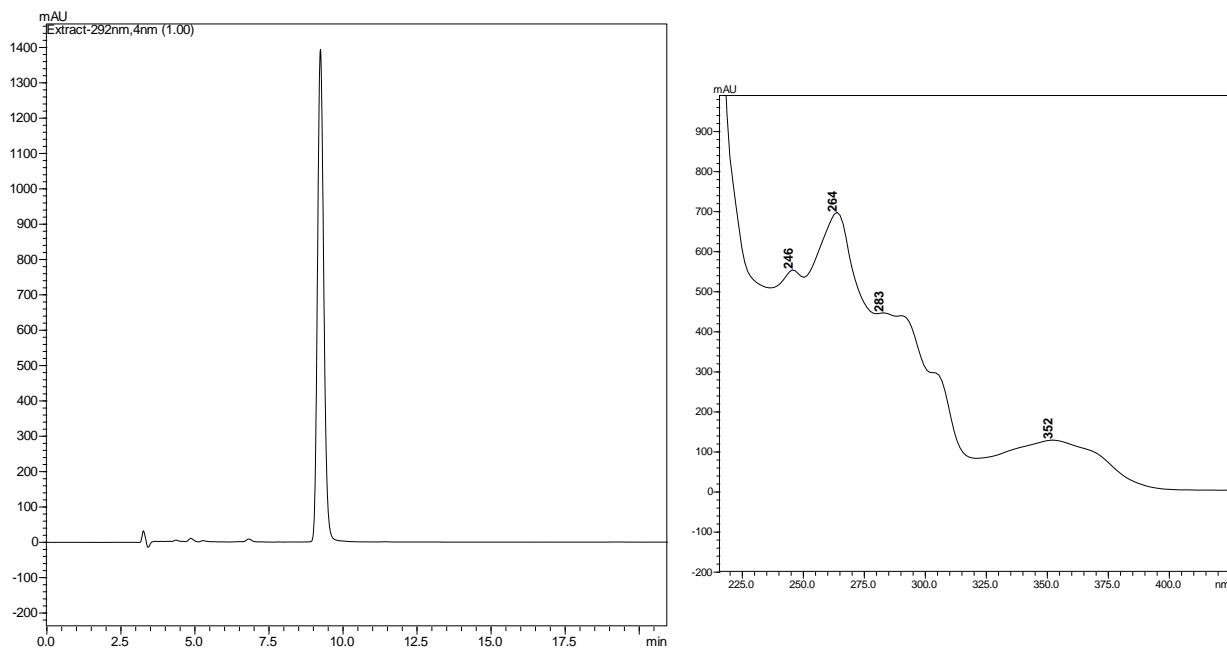


Figure 8.39: HPLC chromatogram of tribenzo[*b,gh,pq*]pleiadene (PBr 1.0ml/min 35°C DCM/MeOH 40:60,) (left). UV/vis spectrum of tribenzo[*b,gh,pq*]pleiadene. (right).

8.1.4 Synthesis of 14-methyldibenzo[*gh,pq*]pleiadene

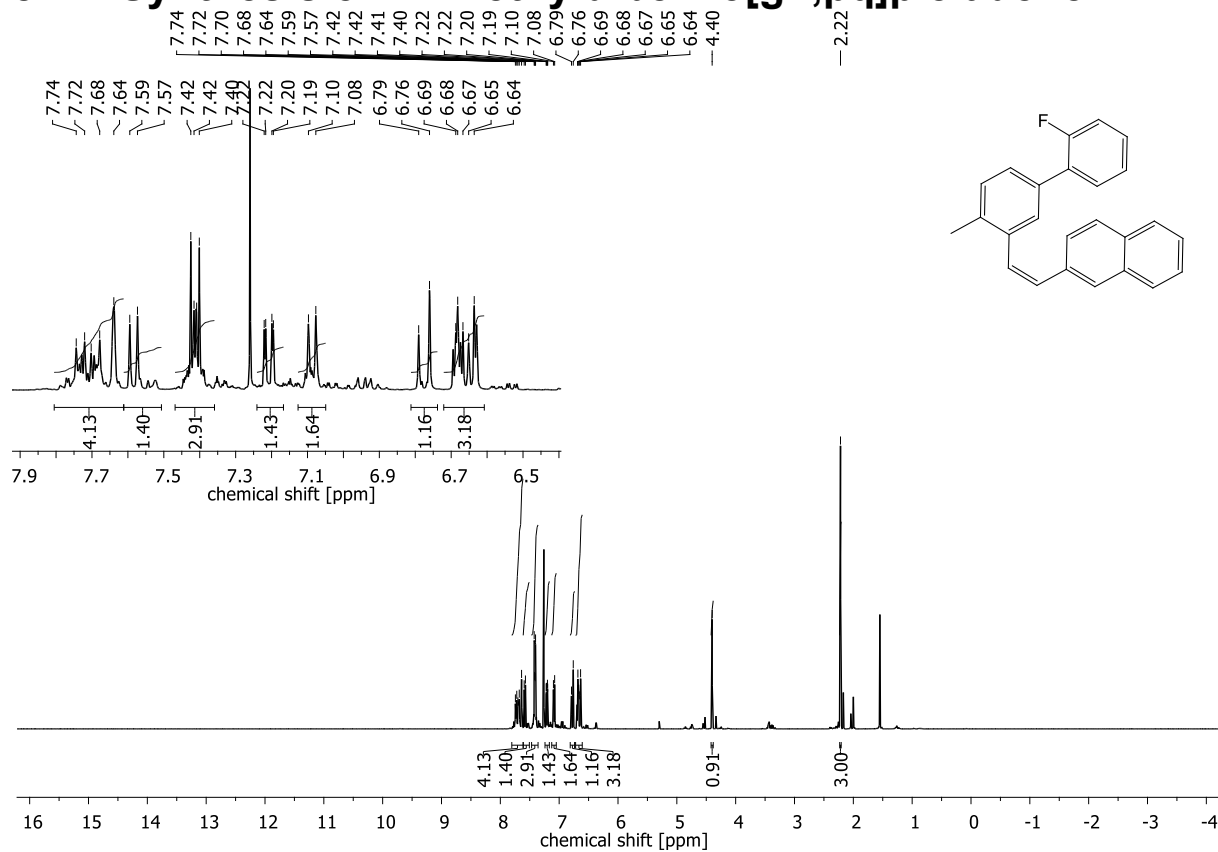


Figure 8.40: $^1\text{H-NMR}$ spectrum of 2-(2-(2'-fluoro-4-methyl-[1,1'-biphenyl]-3-yl)vinyl)naphthalene.

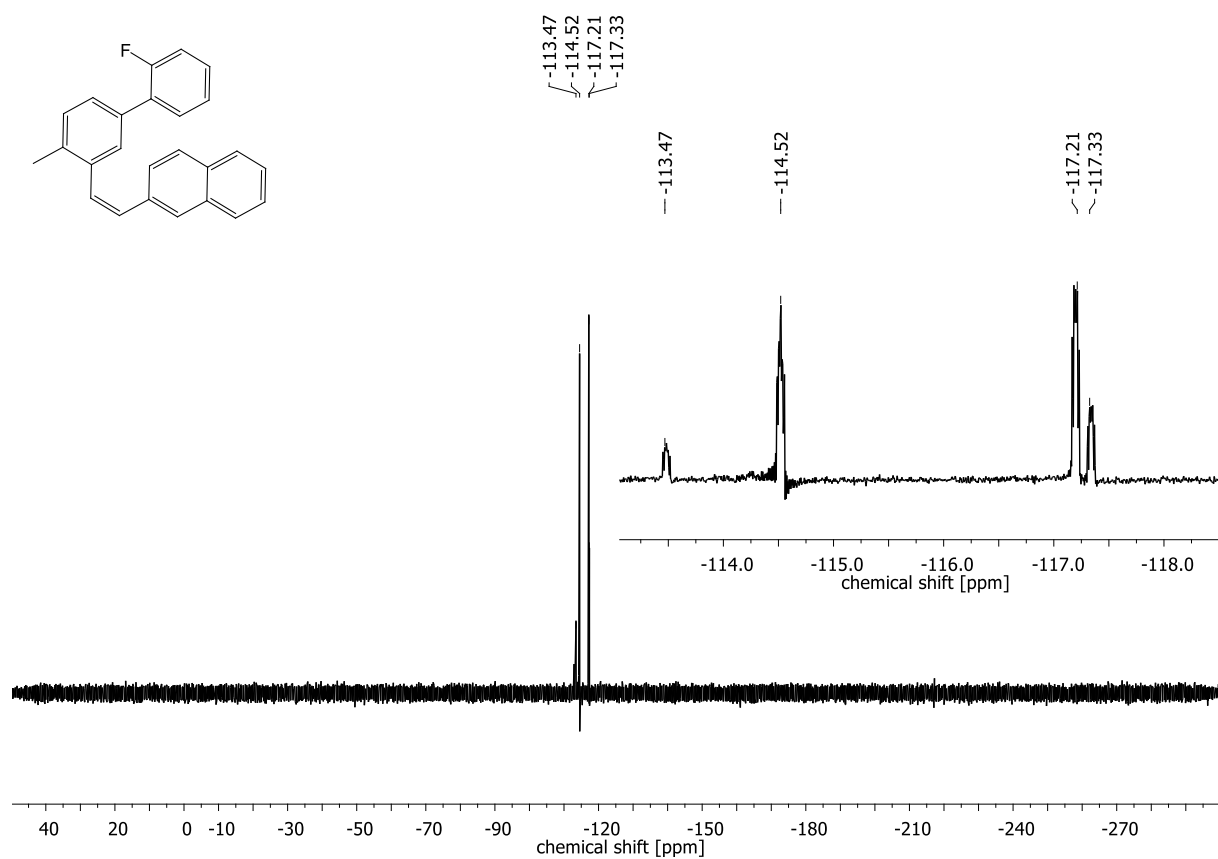


Figure 8.41: ^{19}F -NMR spectrum of 2-(2-(2'-fluoro-4-methyl-[1,1'-biphenyl]-3-yl)vinyl)naphthalene.

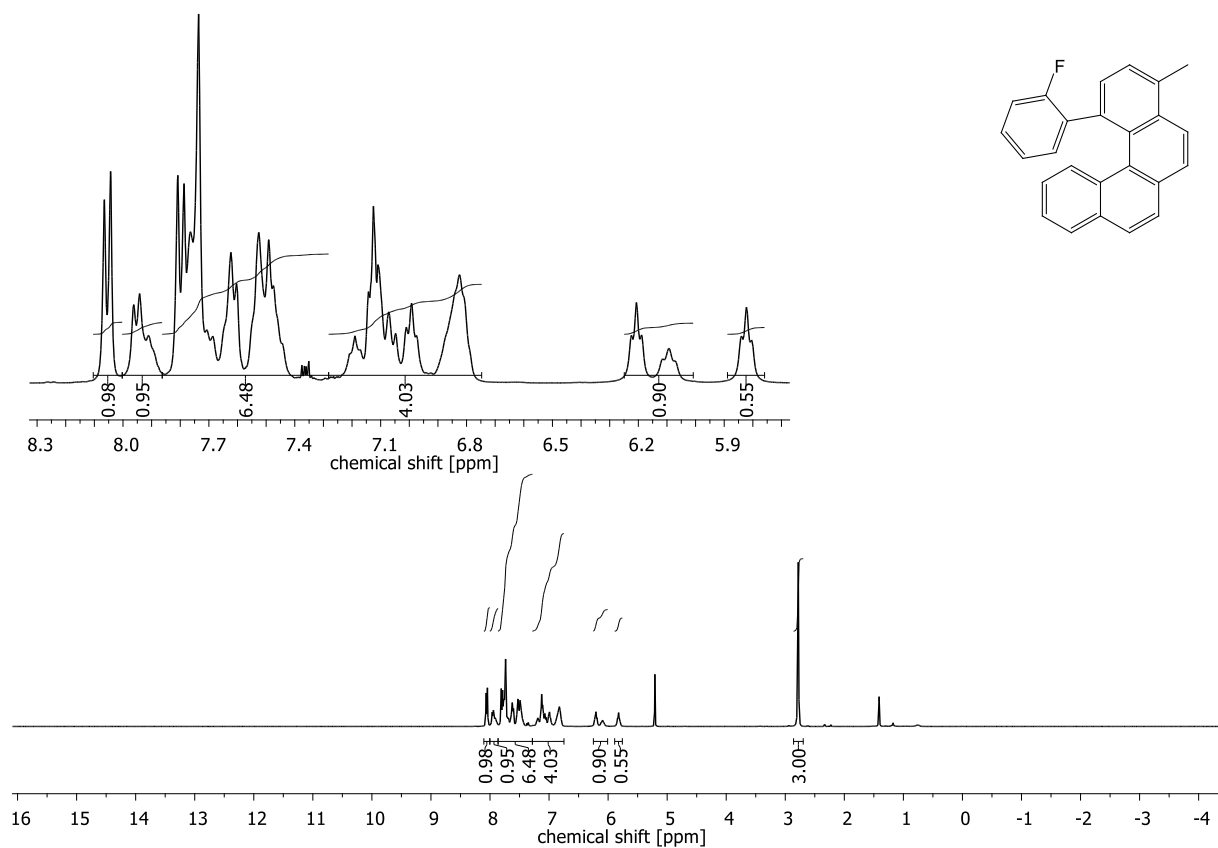


Figure 8.42: ^1H -NMR spectrum of 1-(2-fluorophenyl)-4-methylbenzo[c]phenanthrene.

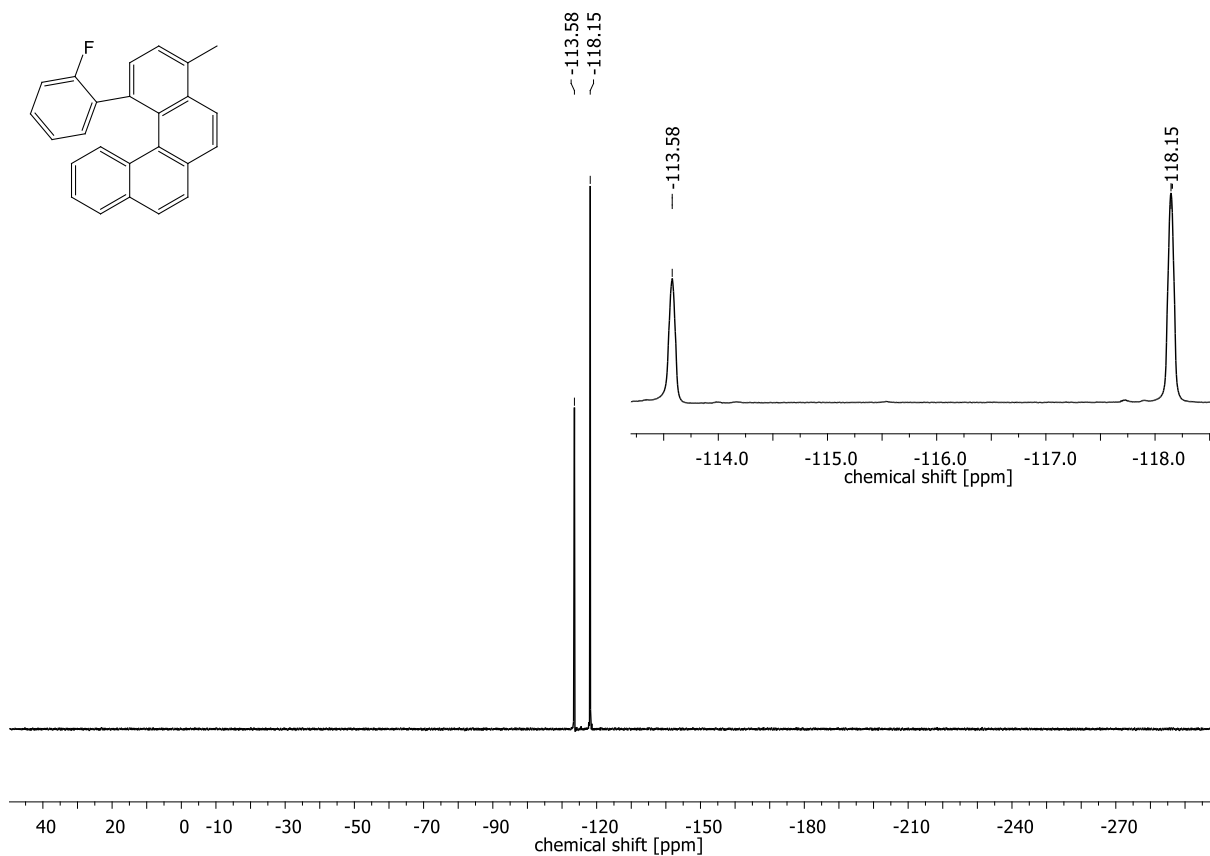


Figure 8.43: ^{19}F -NMR spectrum of 1-(2-fluorophenyl)-4-methylbenzo[*c*]phenanthrene.

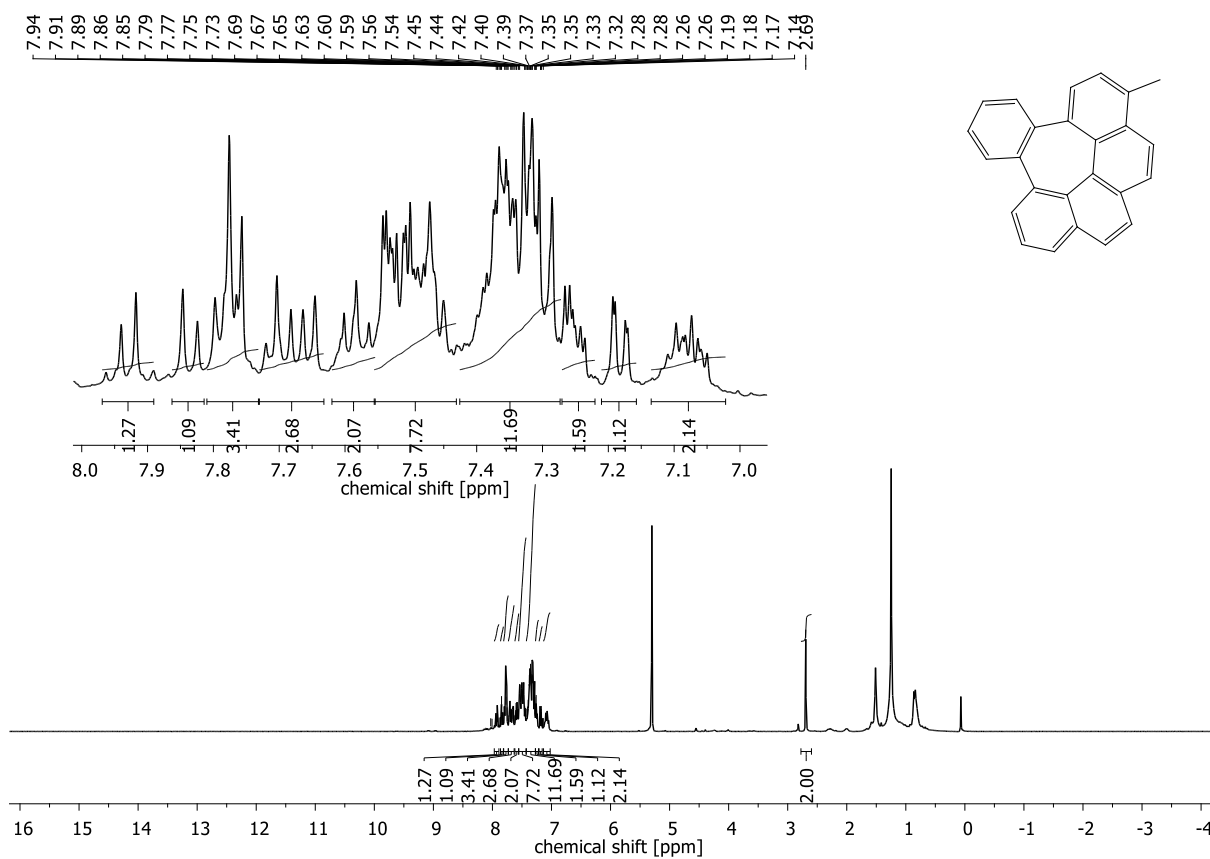


Figure 8.44: ^1H -NMR spectrum of 14-methyldibenzo[*gh,pq*]pleiadene.

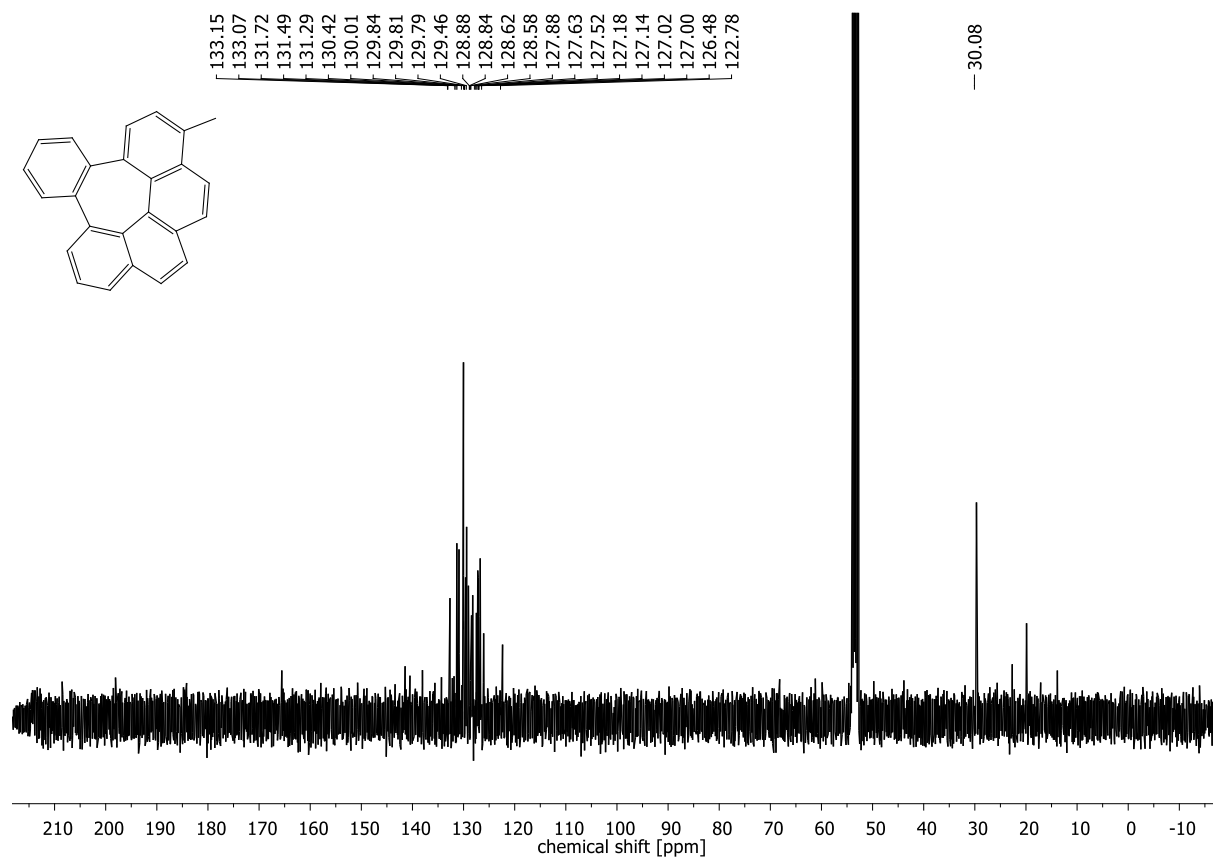


Figure 8.45: $^1\text{H-NMR}$ spectrum of 14-methyldibenzo[gh,pq]pleiadene.

8.1.5. Synthesis of 7-helicene-derivates and their opening on Al₂O₃

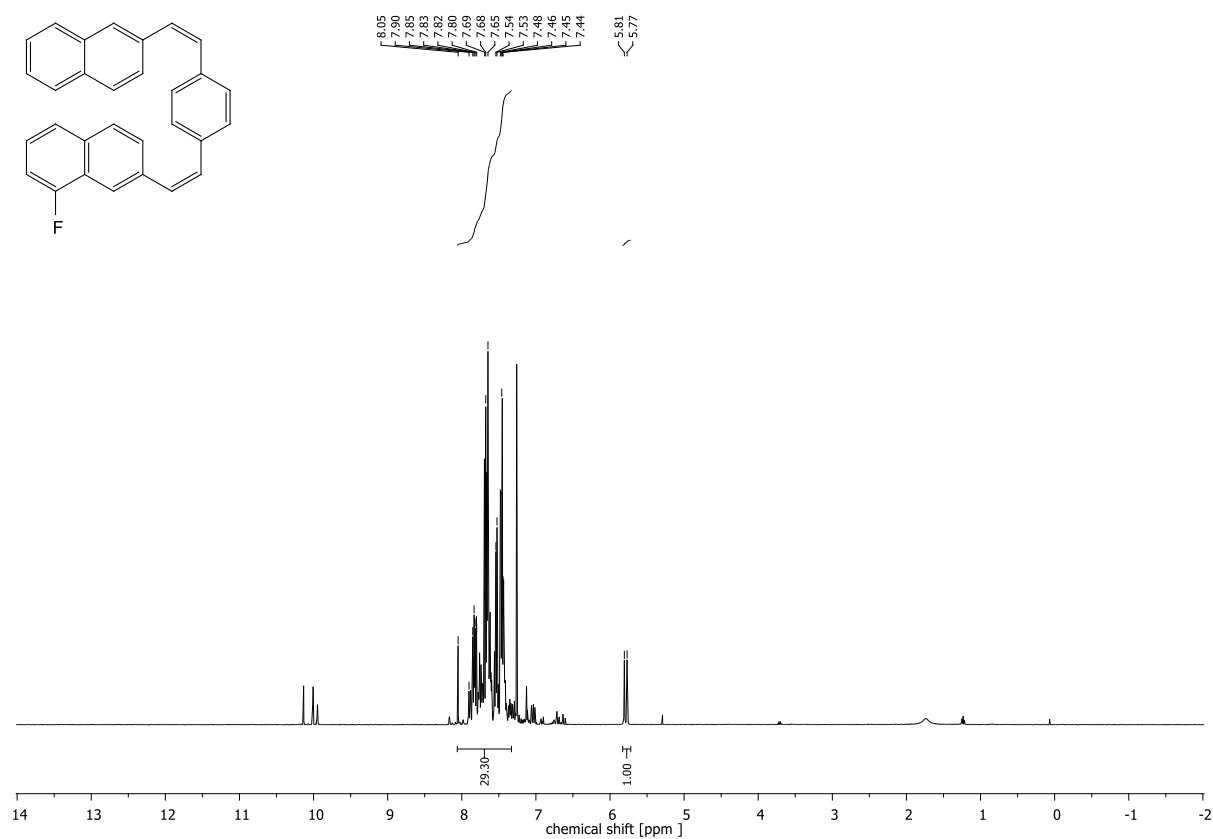


Figure 8.46: ¹H-NMR spectrum of 1-fluoro-7-(-4-(-2-(naphthalen-2-yl)vinyl)styryl)naphthalene.

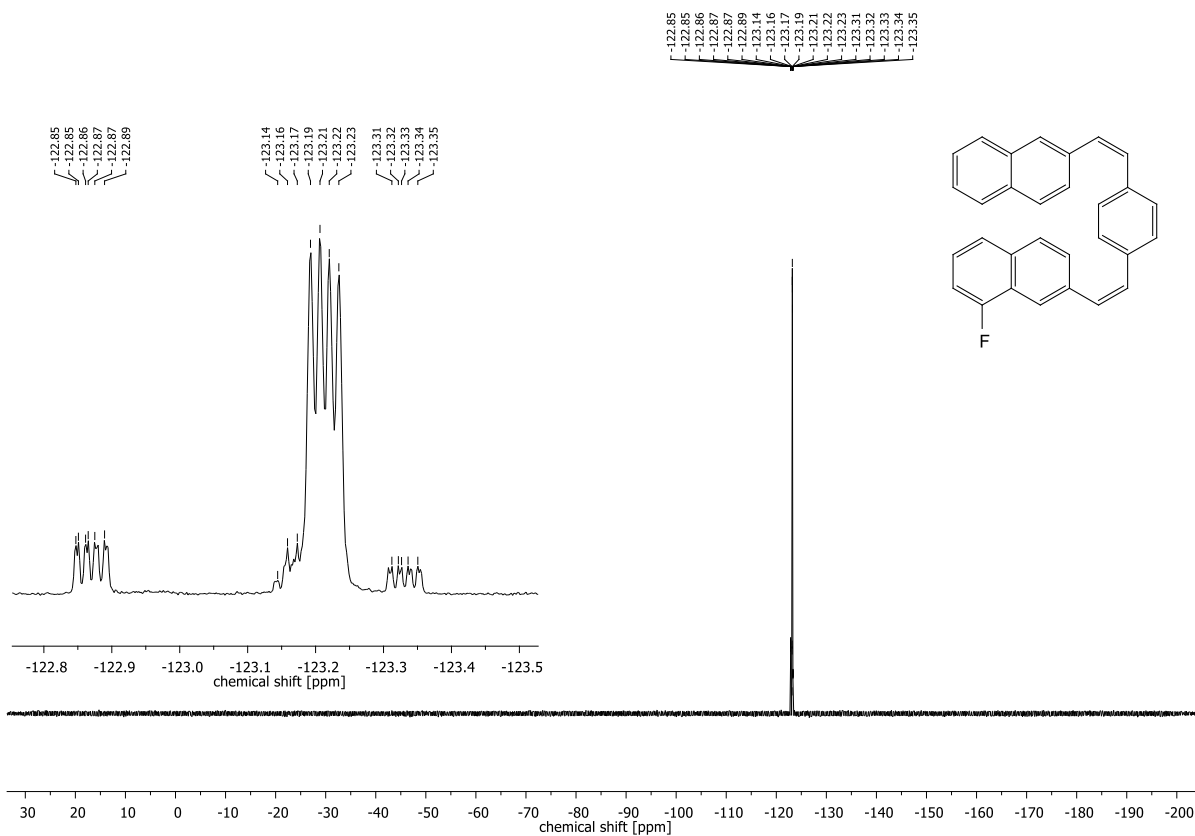


Figure 8.47: ^{19}F -NMR spectrum of 1-fluoro-7-(4-(2-(naphthalen-2-yl)vinyl)styryl)naphthalene.

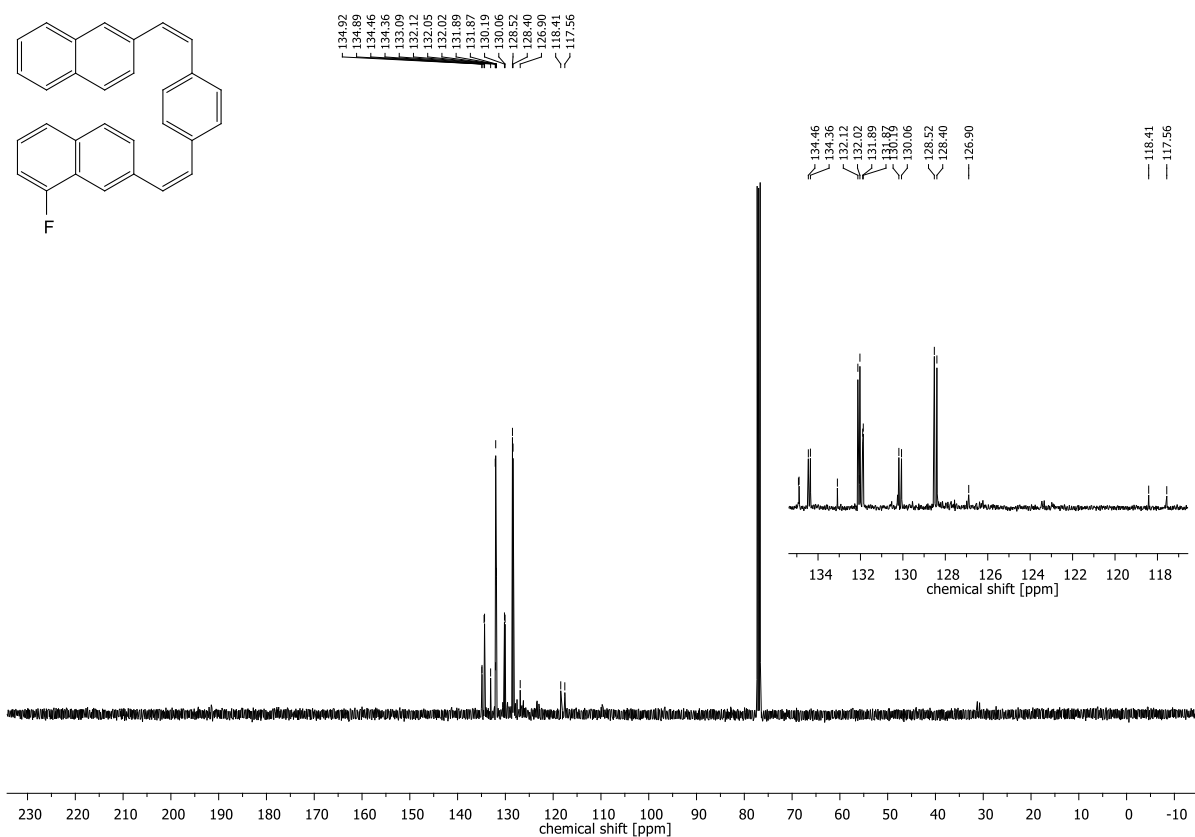


Figure 8.48: ^{13}C -NMR spectrum of 1-fluoro-7-(4-(2-(naphthalen-2-yl)vinyl)styryl)naphthalene.

Datafile Name: AF222_9h_1.lcd
Sample Name: AF222
Sample ID: AF222

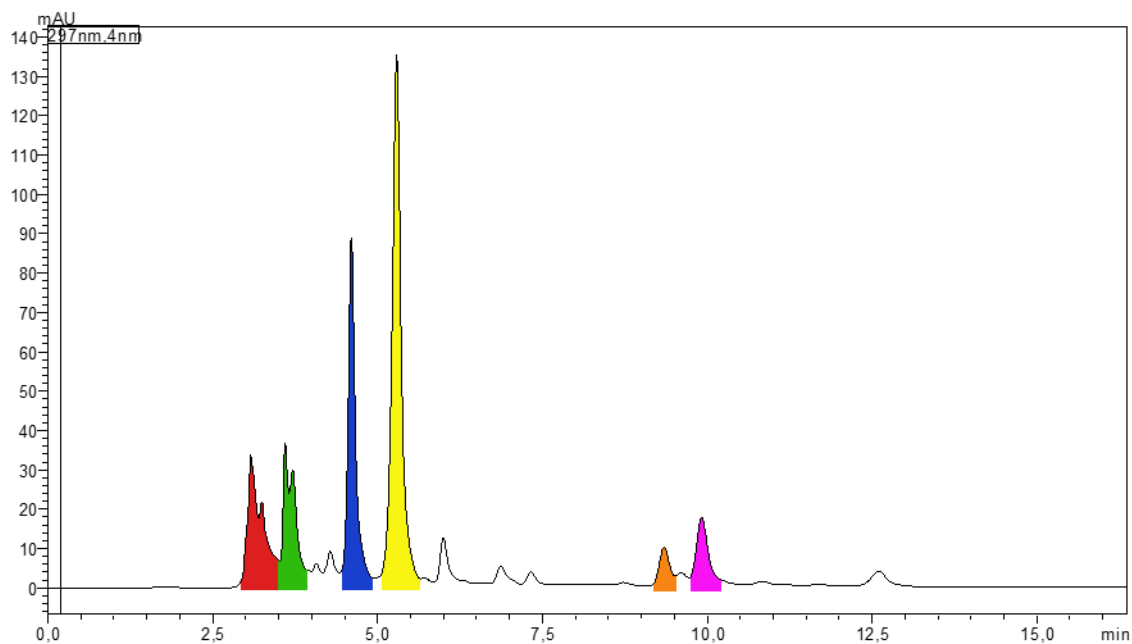


Figure 8.49: HPLC-spectrum of 1-fluorobenzo[1,2-c:4,3-c']diphenanthrene Fraktion 1 (red), 2 (green), 3 (blue), 4 (yellow), 5 (orange) and 6 (purple).

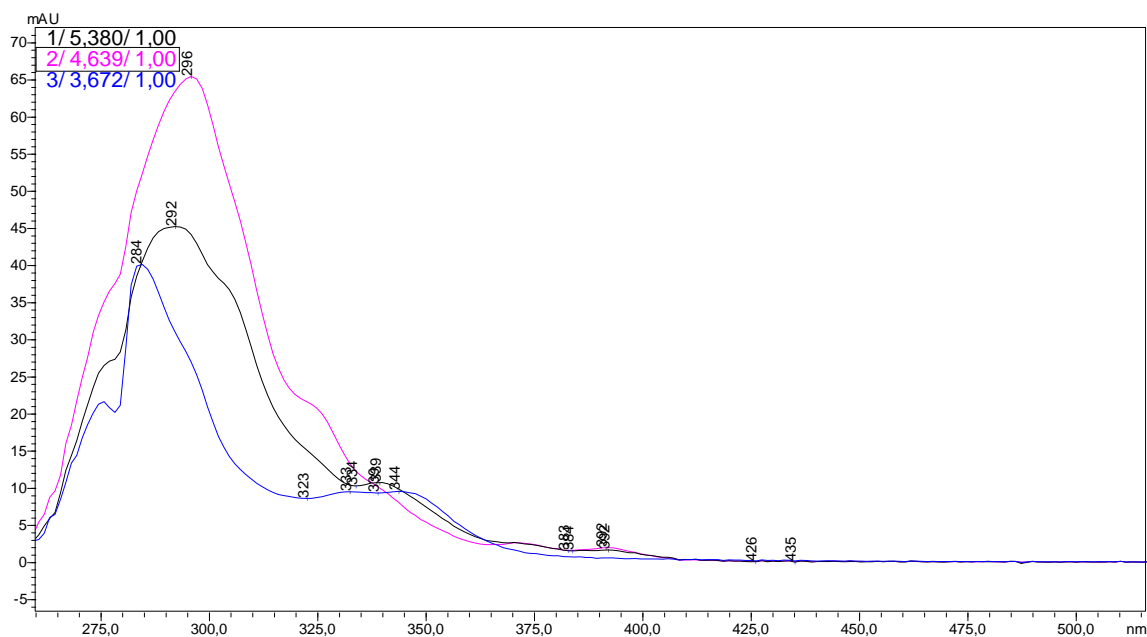


Figure 8.50: UV-Vis spectrum of 1-fluorobenzo[1,2-c:4,3-c']diphenanthrene Fraktion 2 (black) 3 (purple) and 4 (blue).

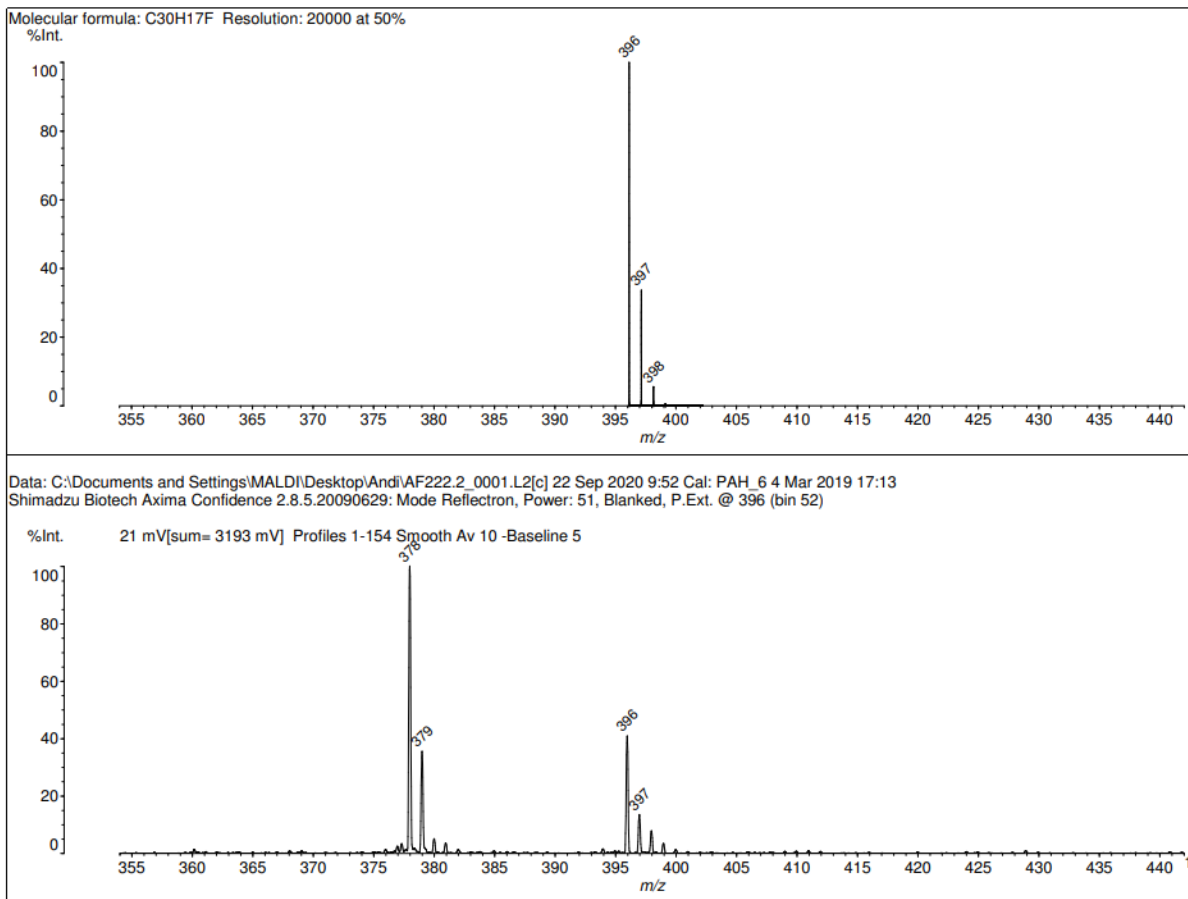


Figure 8.51: MS spectrum of 1-fluorobenzo[1,2-c:4,3-c']diphenanthrene fraktion 2.

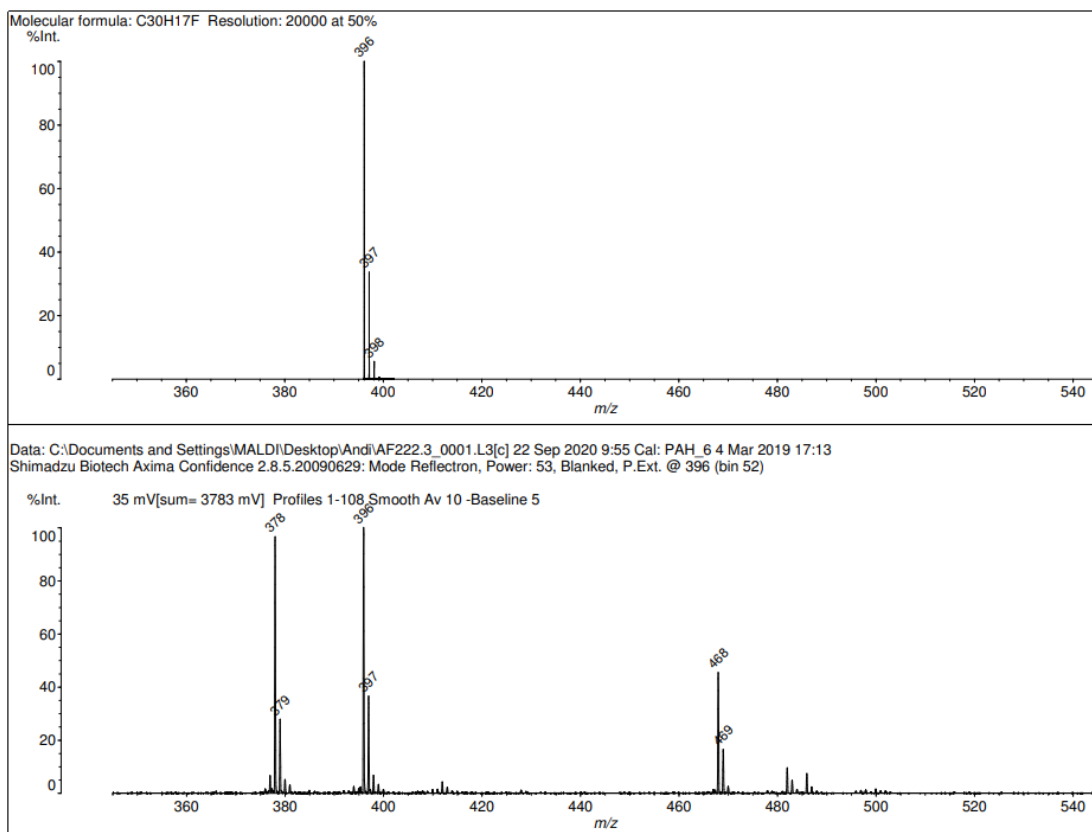


Figure 8.52: MS spectrum of 1-fluorobenzo[1,2-c:4,3-c']diphenanthrene fraktion 3.

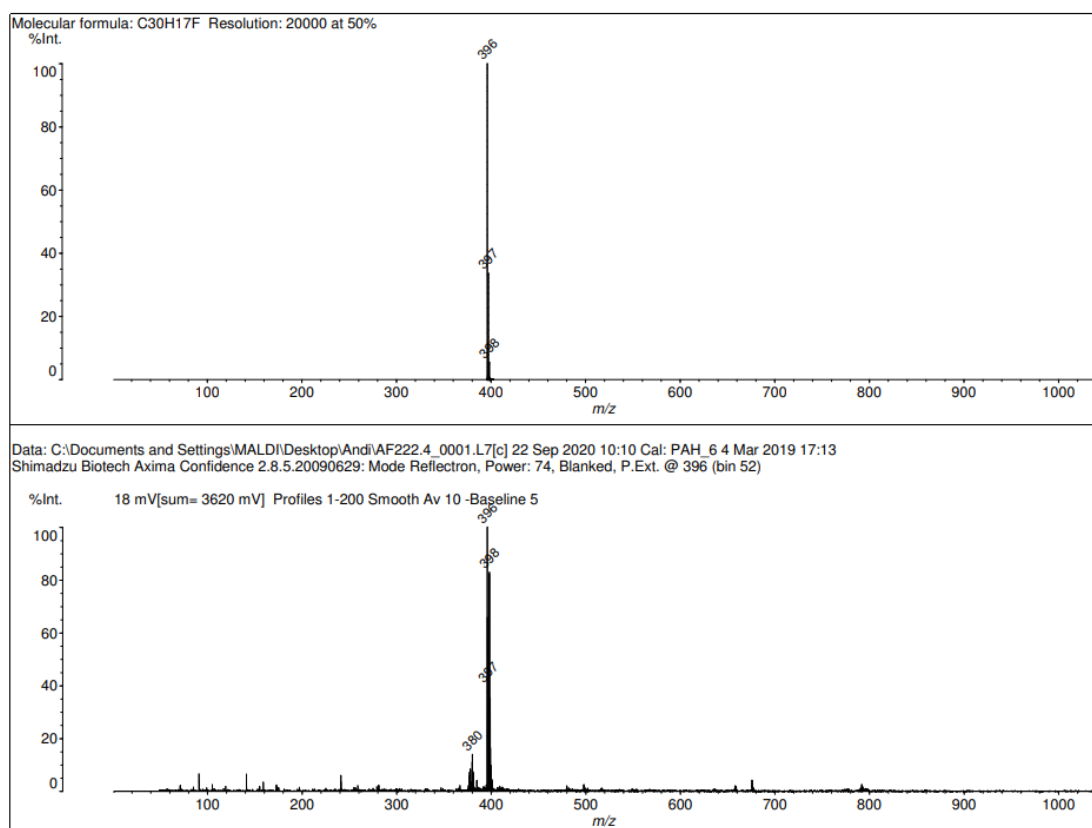


Figure 8.53: MS spectrum of 1-fluorobenzo[1,2-c:4,3-c']diphenanthrene fraktion 4.

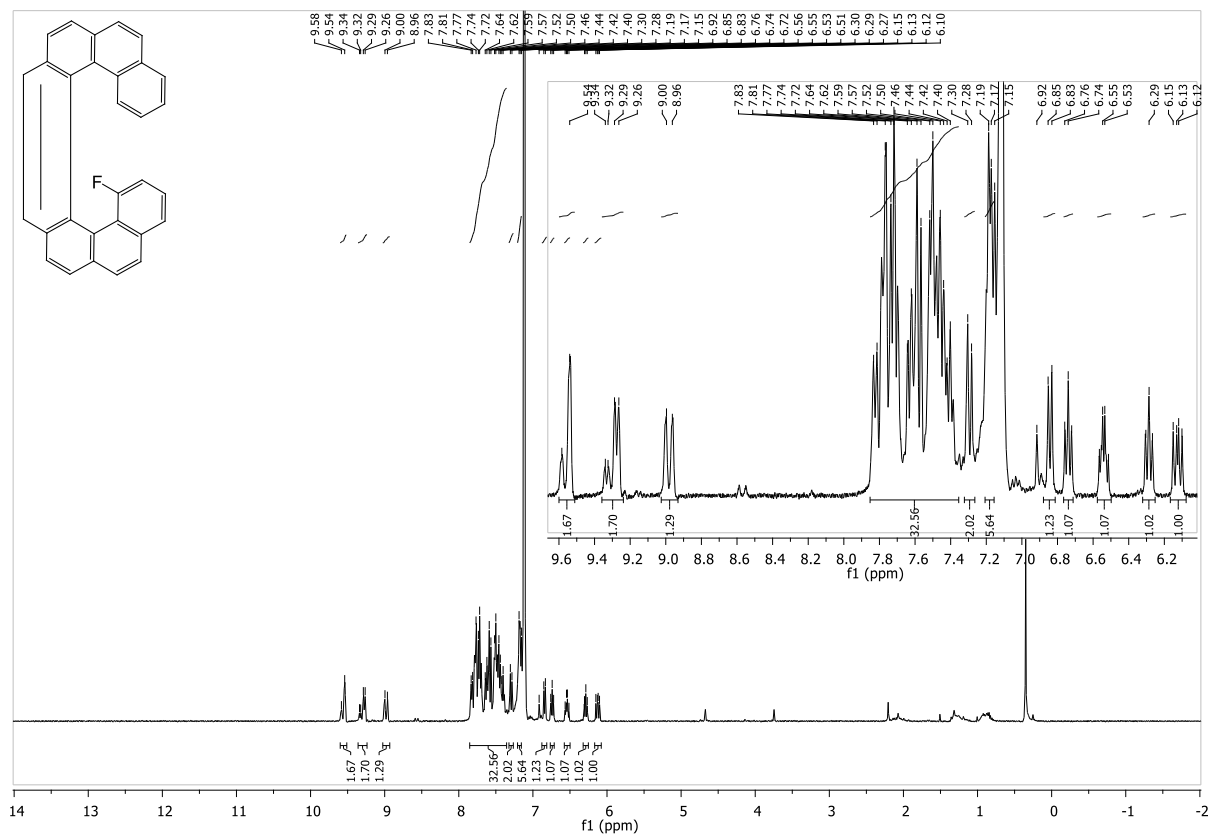


Figure 8.54: ¹H-NMR spectrum of 1-fluorobenzo[1,2-c:4,3-c']diphenanthrene fraktion 3.

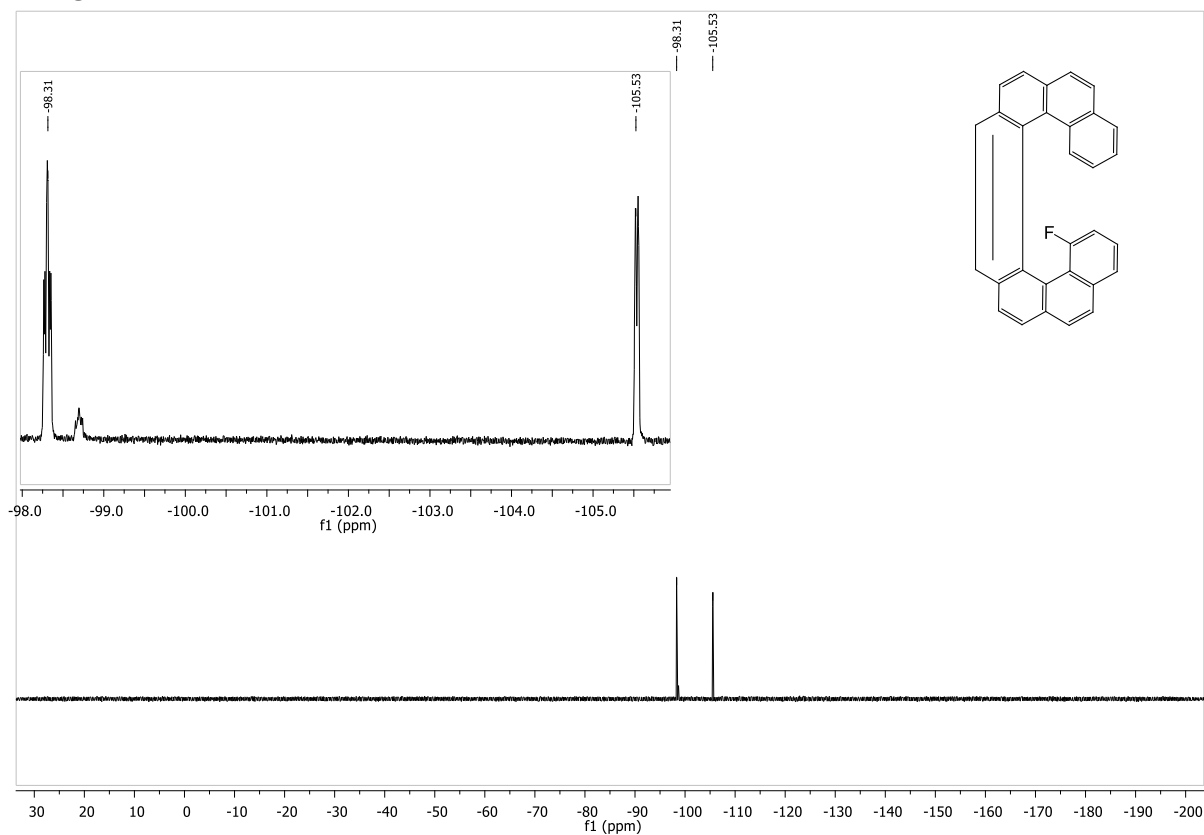


Figure 8.55: ¹⁹F-NMR spectrum of 1-fluorobenzo[1,2-c:4,3-c']diphenanthrene fraktion 3.

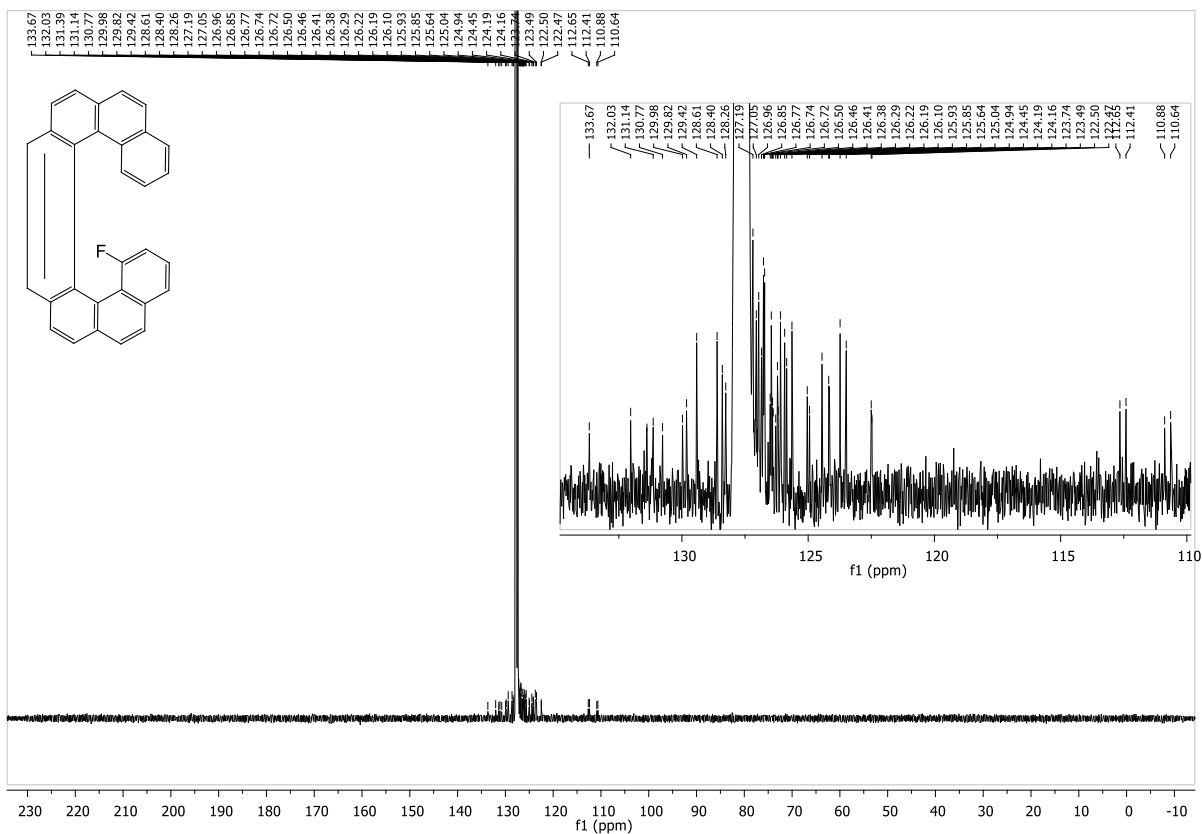


Figure 8.56: ¹³C-NMR spectrum of 1-fluorobenzo[1,2-c:4,3-c']diphenanthrene fraktion 3.

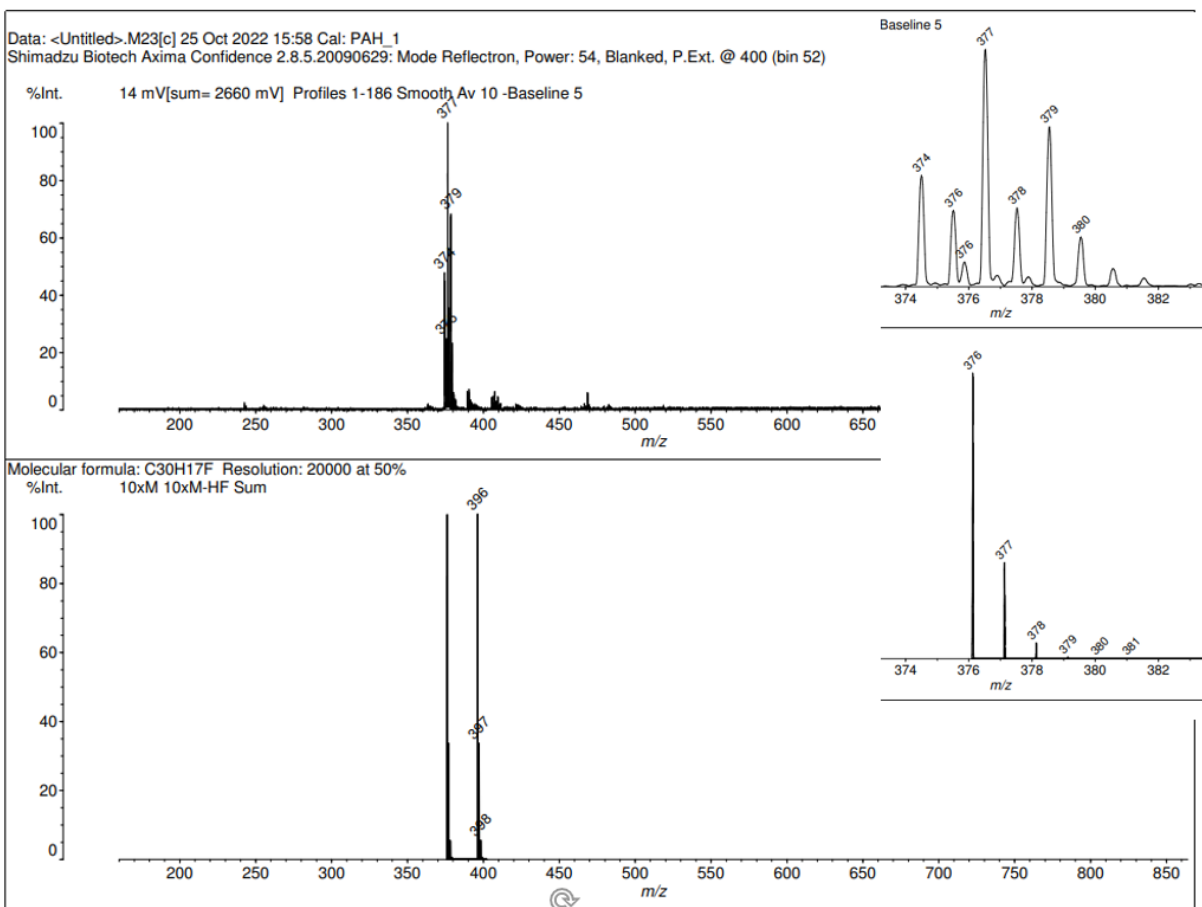


Figure 8.57: MS-spectrum of tribenzo[def,jkl,pqr]tetraphenylene.

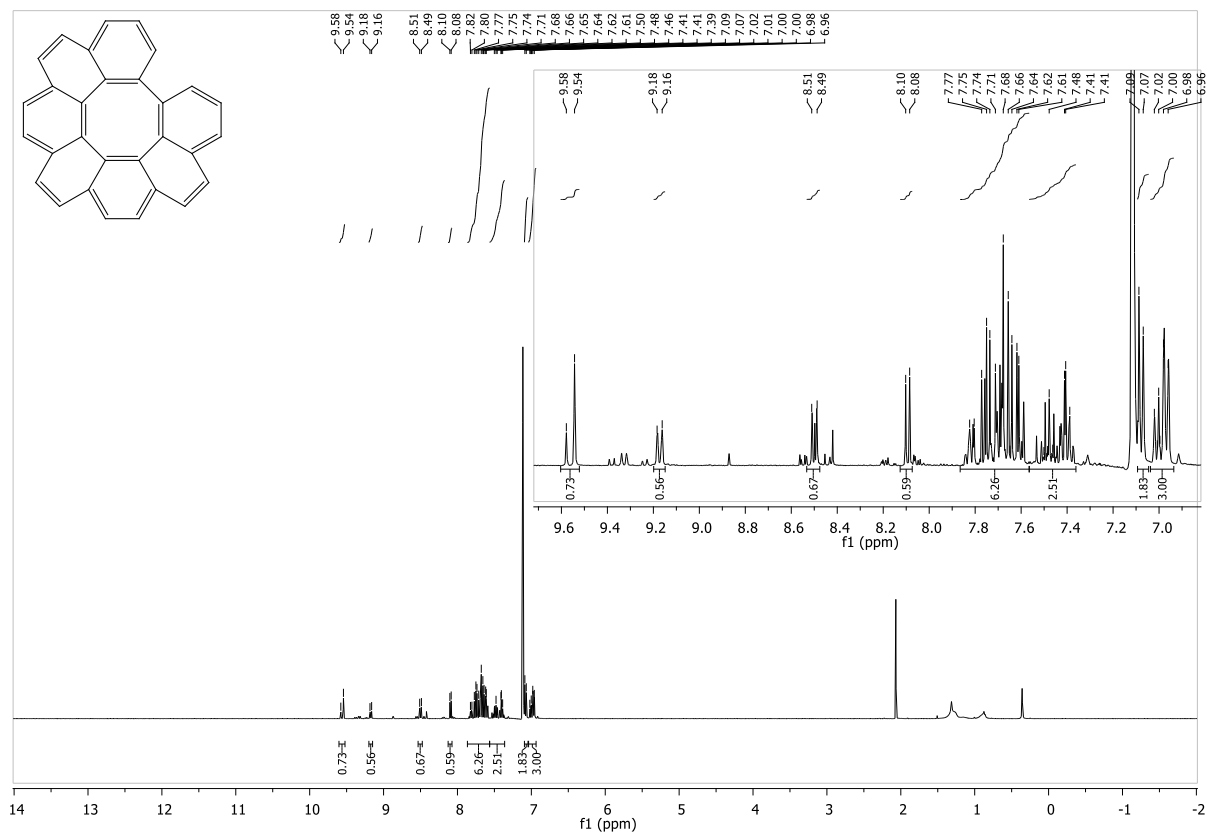


Figure 8.58: $^1\text{H-NMR}$ spectrum of tribenzo[def,jkl,pqr]tetraphenylene.

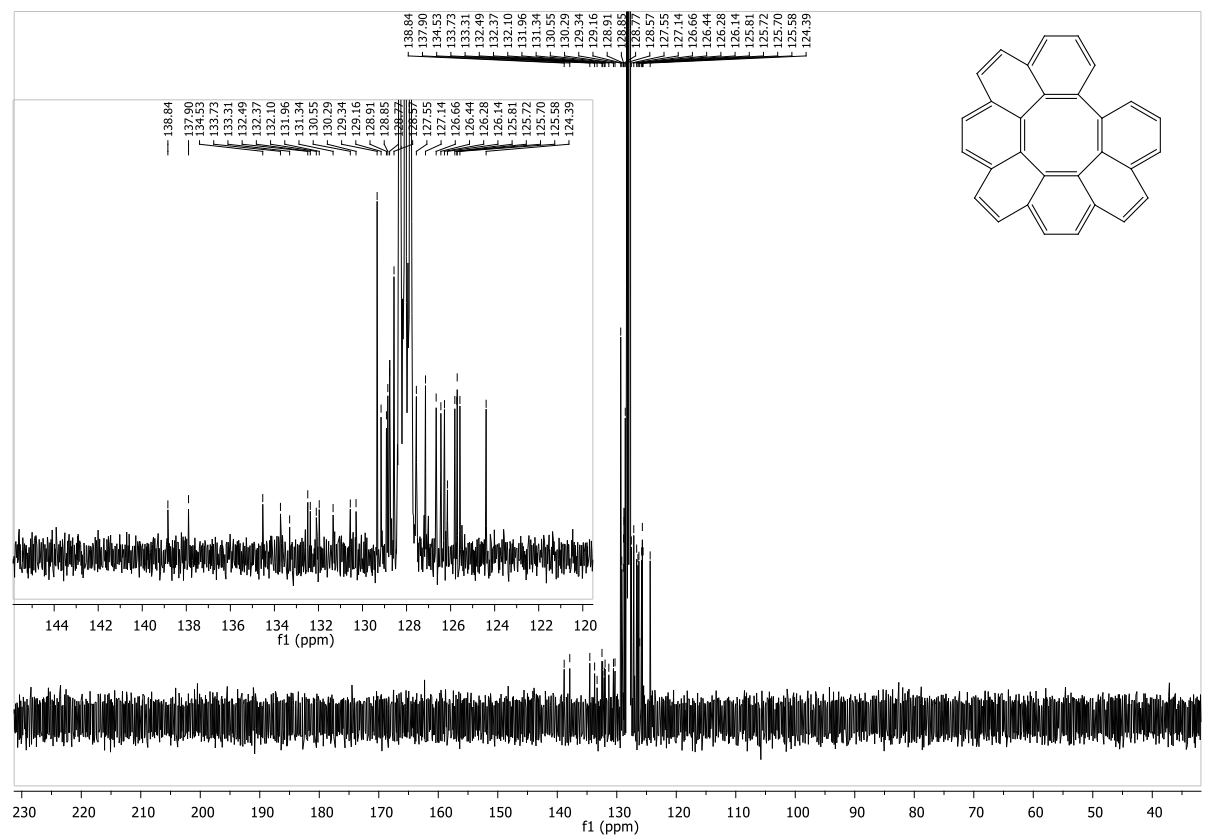


Figure 8.59: $^{13}\text{C-NMR}$ spectrum of tribenzo[def,jkl,pqr]tetraphenylene.

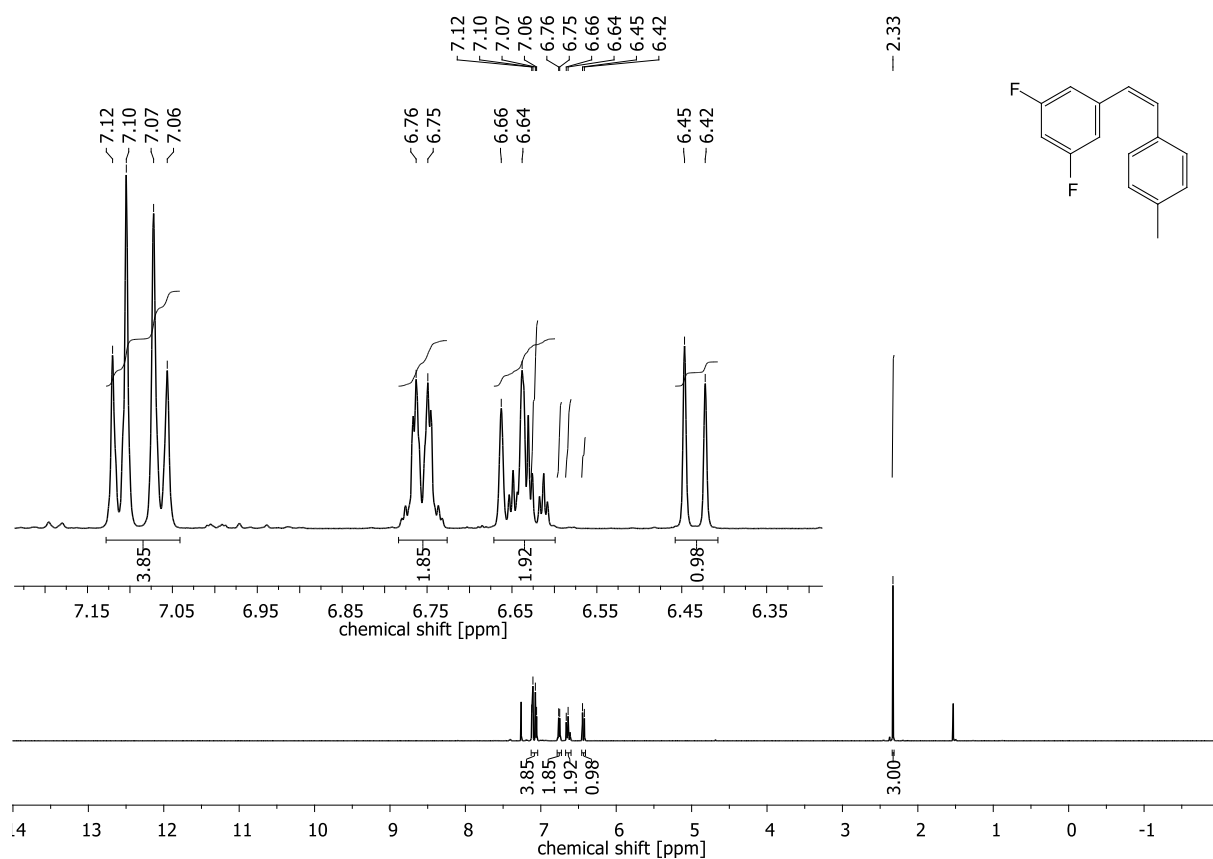


Figure 8.60: ¹H-NMR spectrum of 1,3-difluoro-5-(4-methylstyryl)benzene (liquid).

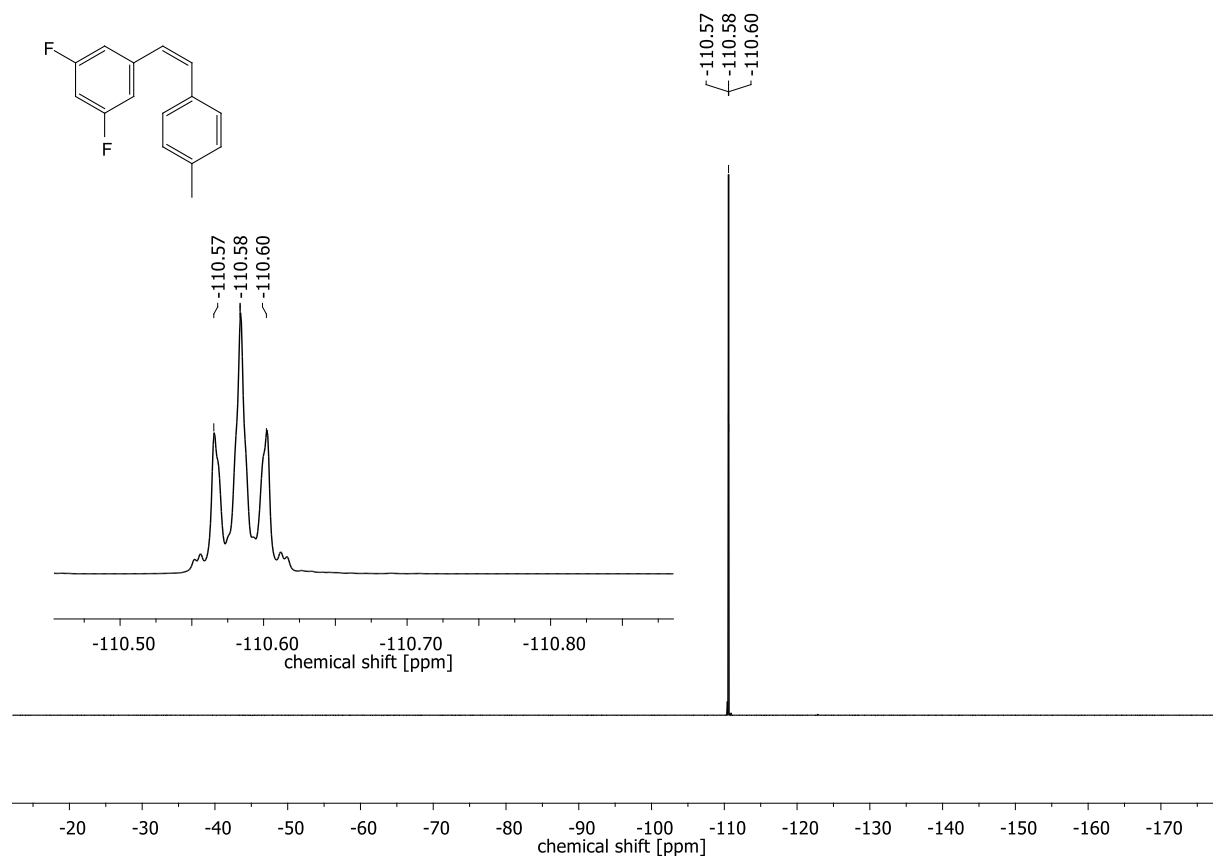


Figure 8.61: ¹⁹F-NMR spectrum of 1,3-difluoro-5-(4-methylstyryl)benzene (liquid).

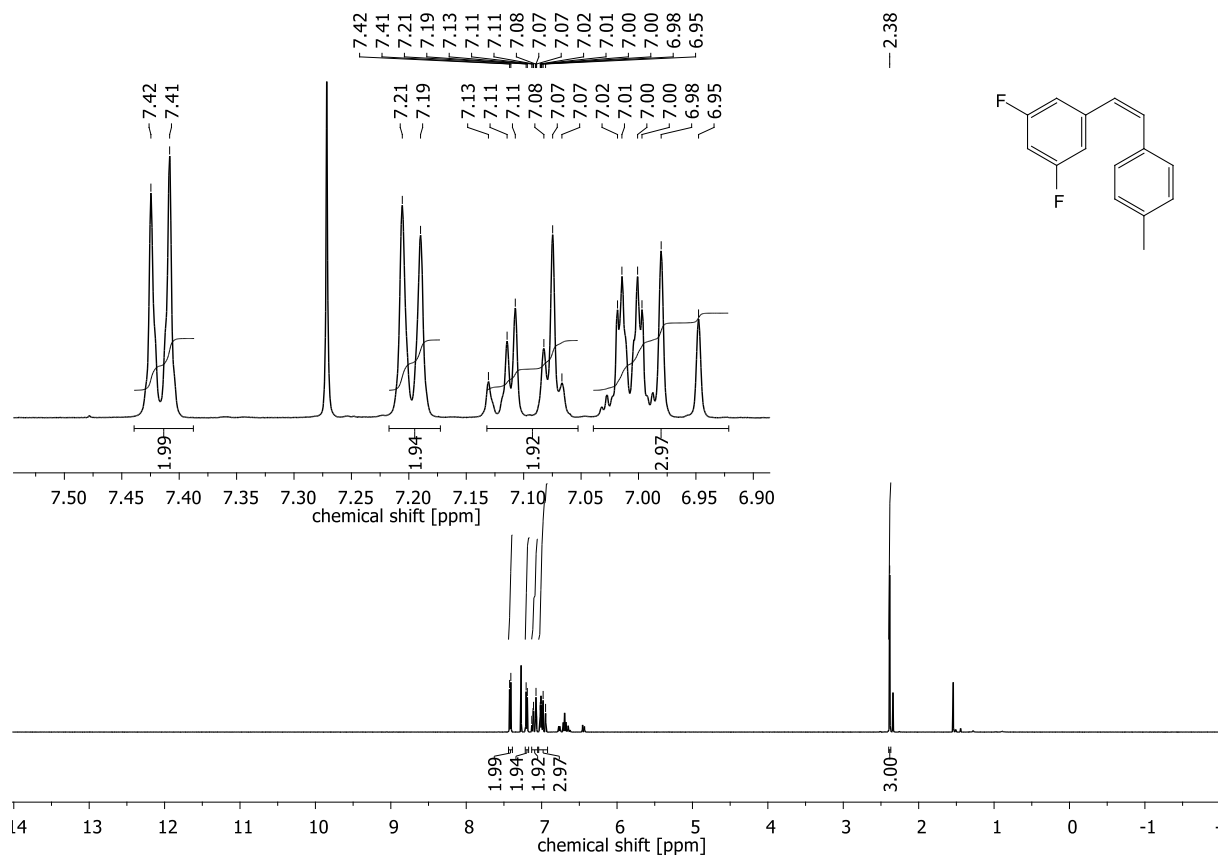


Figure 8.62: ¹H-NMR spectrum of 1,3-difluoro-5-(4-methylstyryl)benzene (solid).

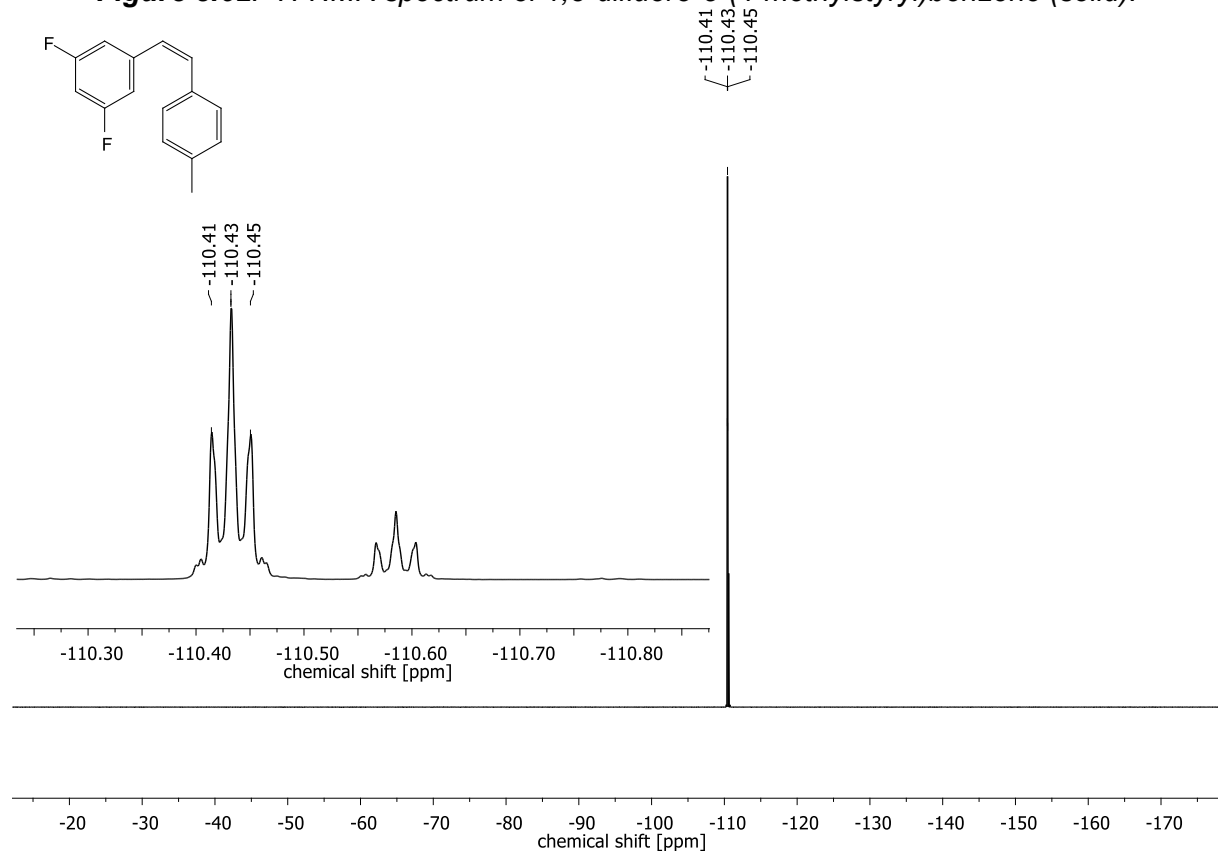


Figure 8.63: ¹⁹F-NMR spectrum of 1,3-difluoro-5-(4-methylstyryl)benzene (solid).

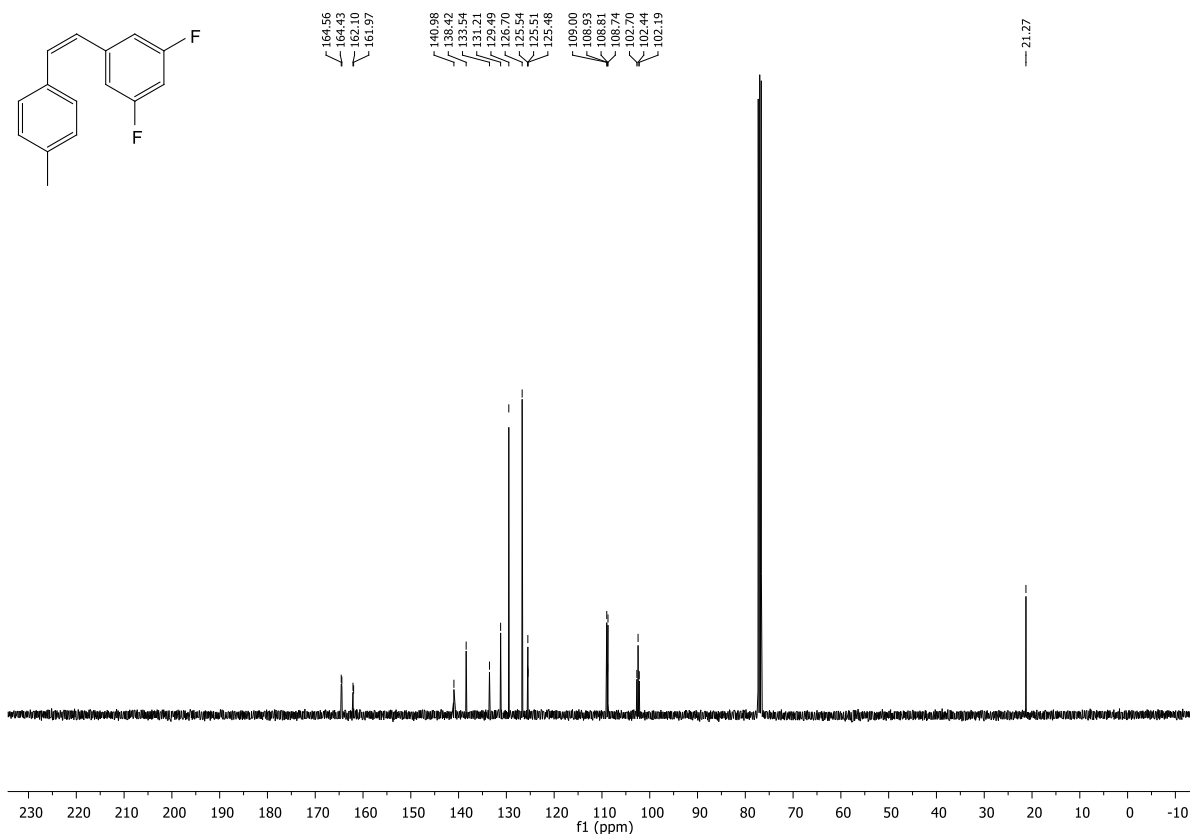


Figure 8.64: $^{13}\text{C-NMR}$ spectrum of 1,3-difluoro-5-(4-methylstyryl)benzene.

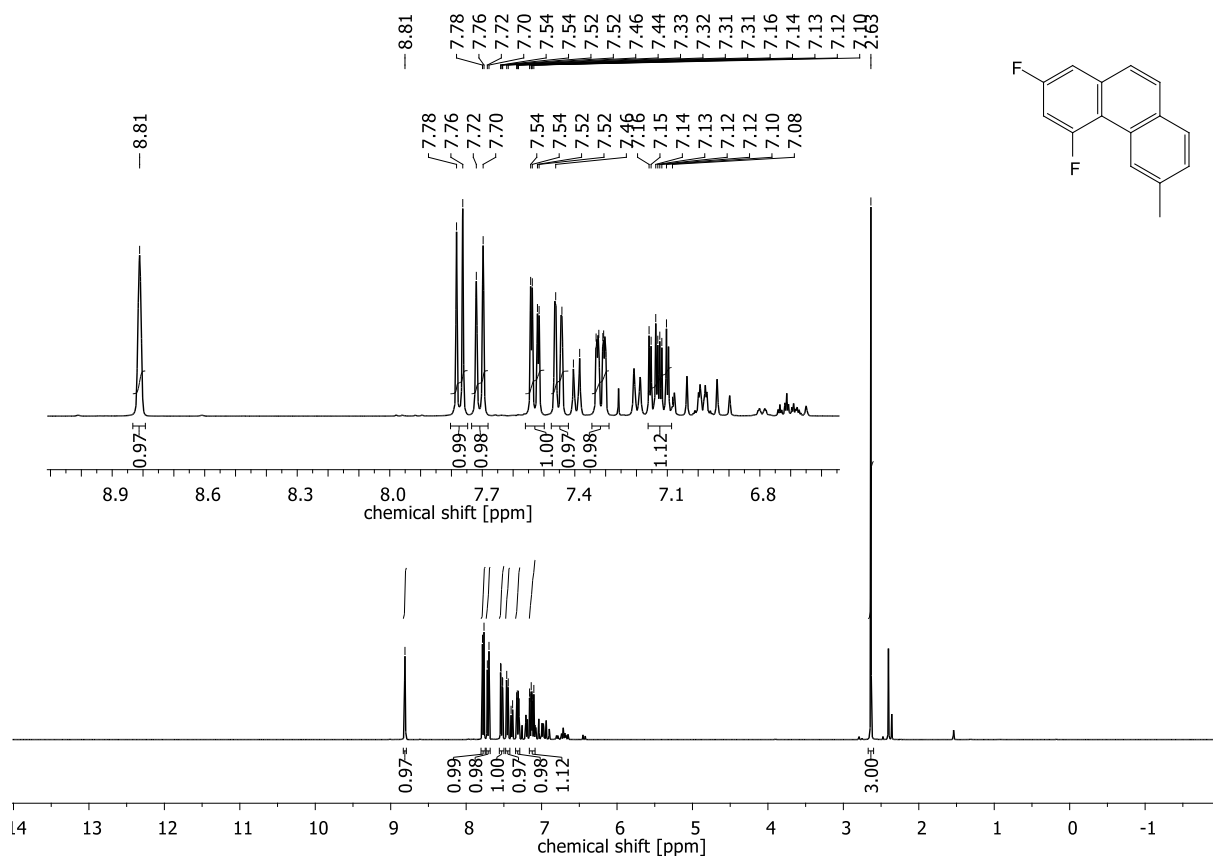


Figure 8.65: $^1\text{H-NMR}$ spectrum of 2,4-difluoro-6-methylphenanthrene.

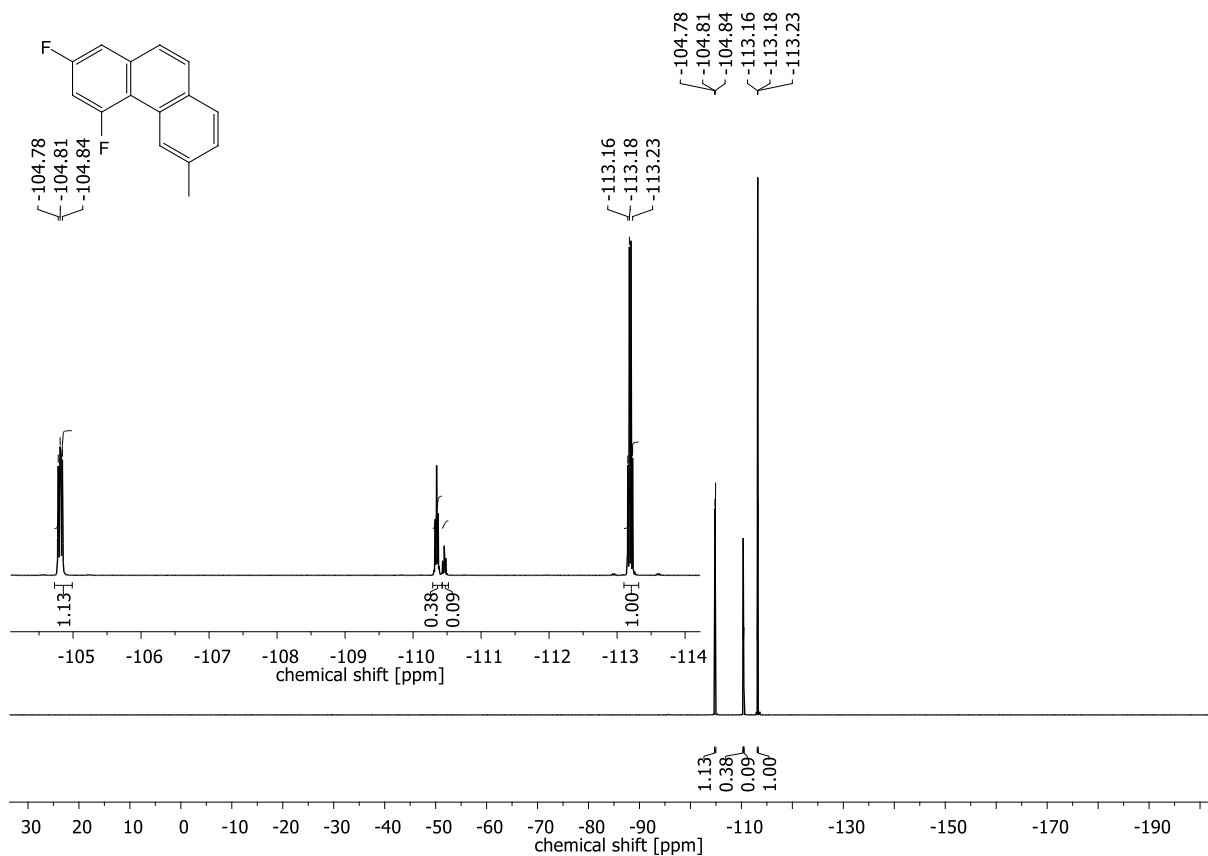


Figure 8.66: ^{19}F -NMR spectrum of 2,4-difluoro-6-methylphenanthrene.

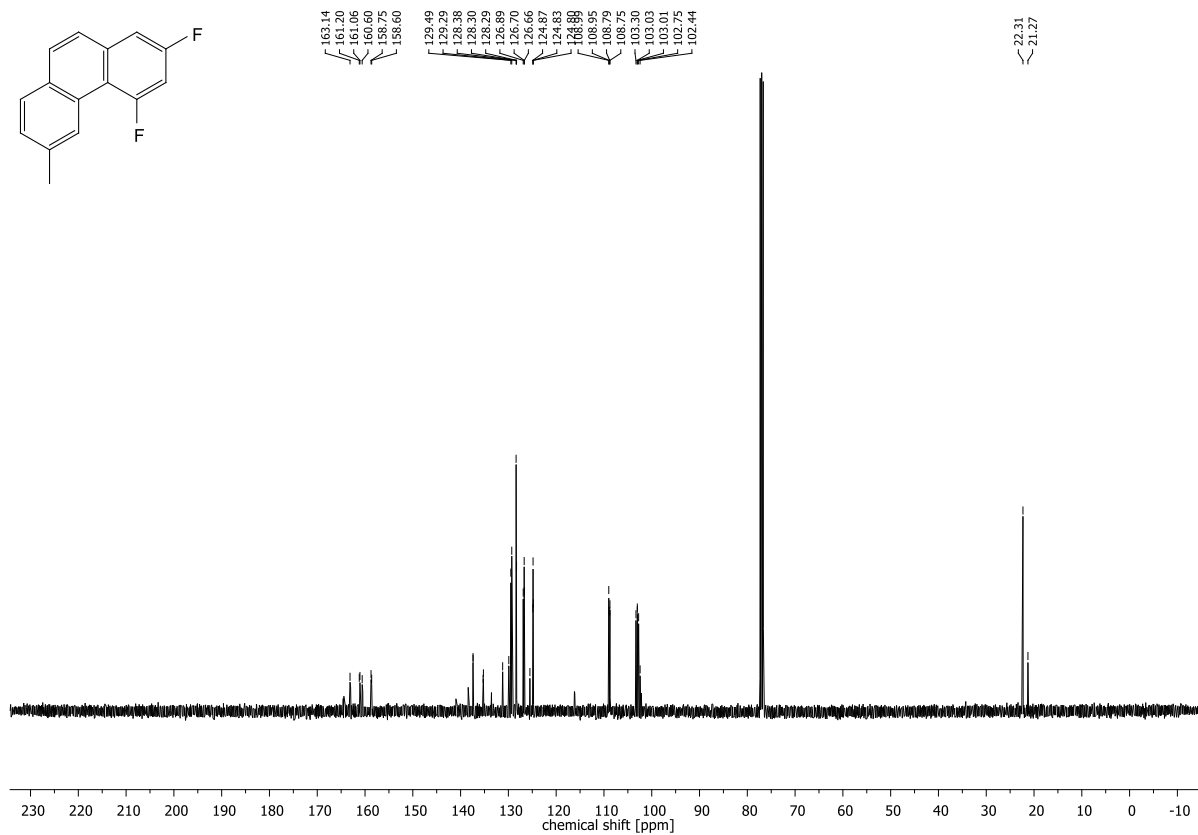


Figure 8.67: ^{13}C -NMR spectrum of 2,4-difluoro-6-methylphenanthrene.

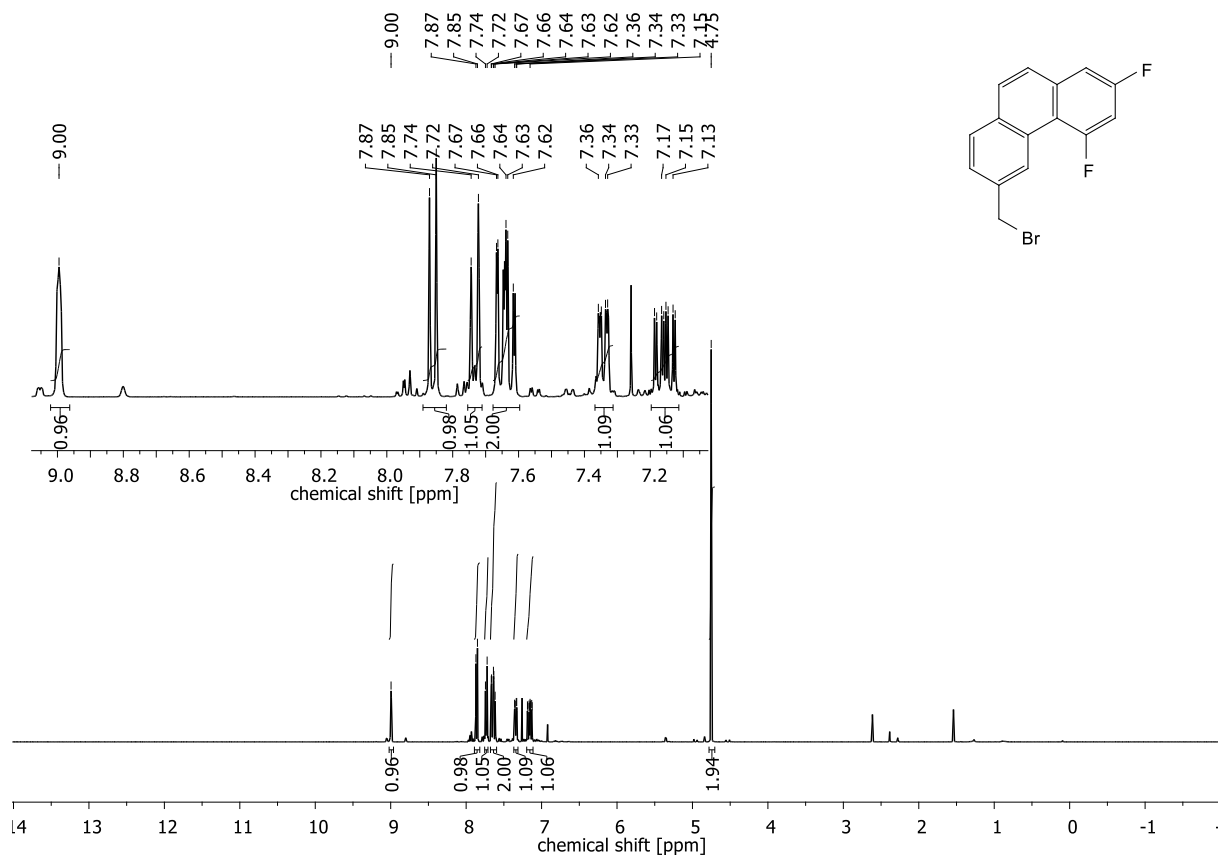


Figure 8.68: ¹H-NMR spectrum of 6-(bromomethyl)-2,4-difluorophenanthrene.

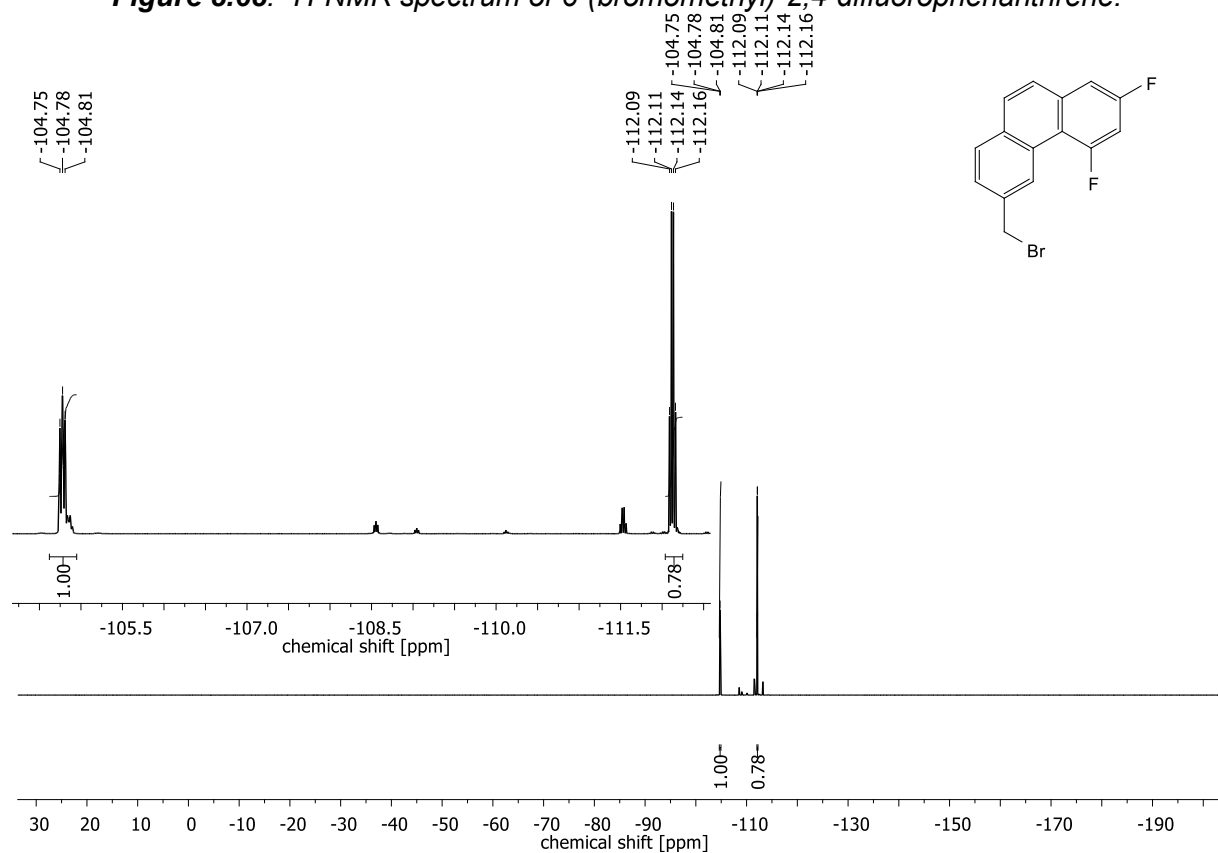


Figure 8.69: ¹⁹F-NMR spectrum of 6-(bromomethyl)-2,4-difluorophenanthrene.

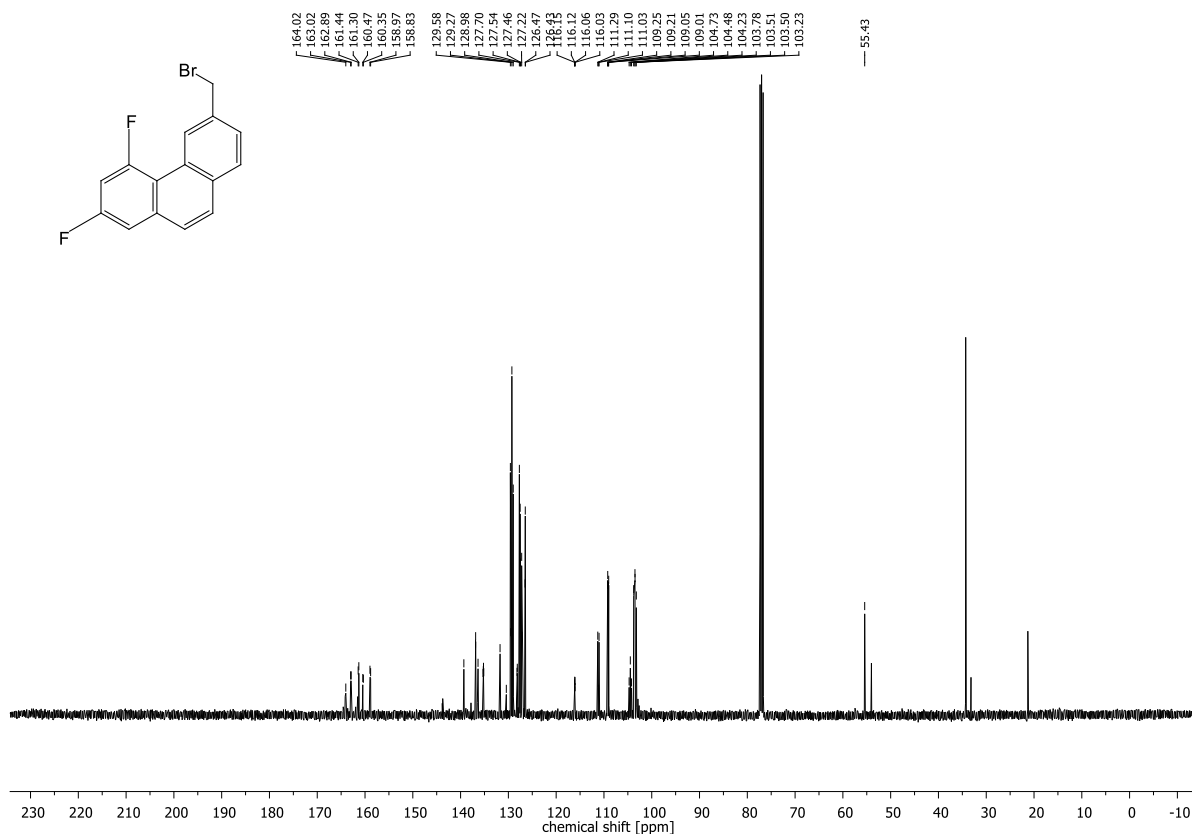


Figure 8.70: ¹³C-NMR spectrum of 6-(bromomethyl)-2,4-difluorophenanthrene.

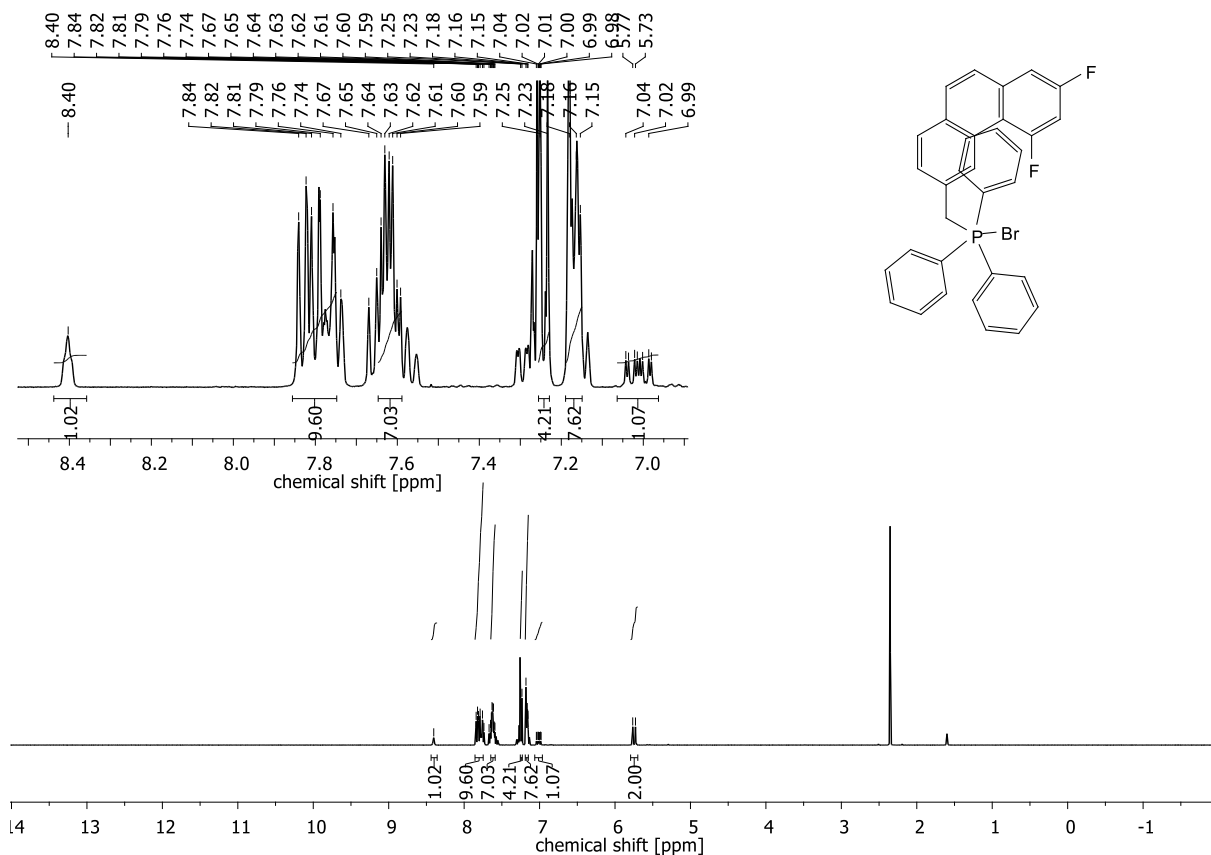


Figure 8.71: ¹H-NMR spectrum of bromo((5,7-difluorophenanthren-3-yl)methyl)triphenyl-λ⁵-phosphane.

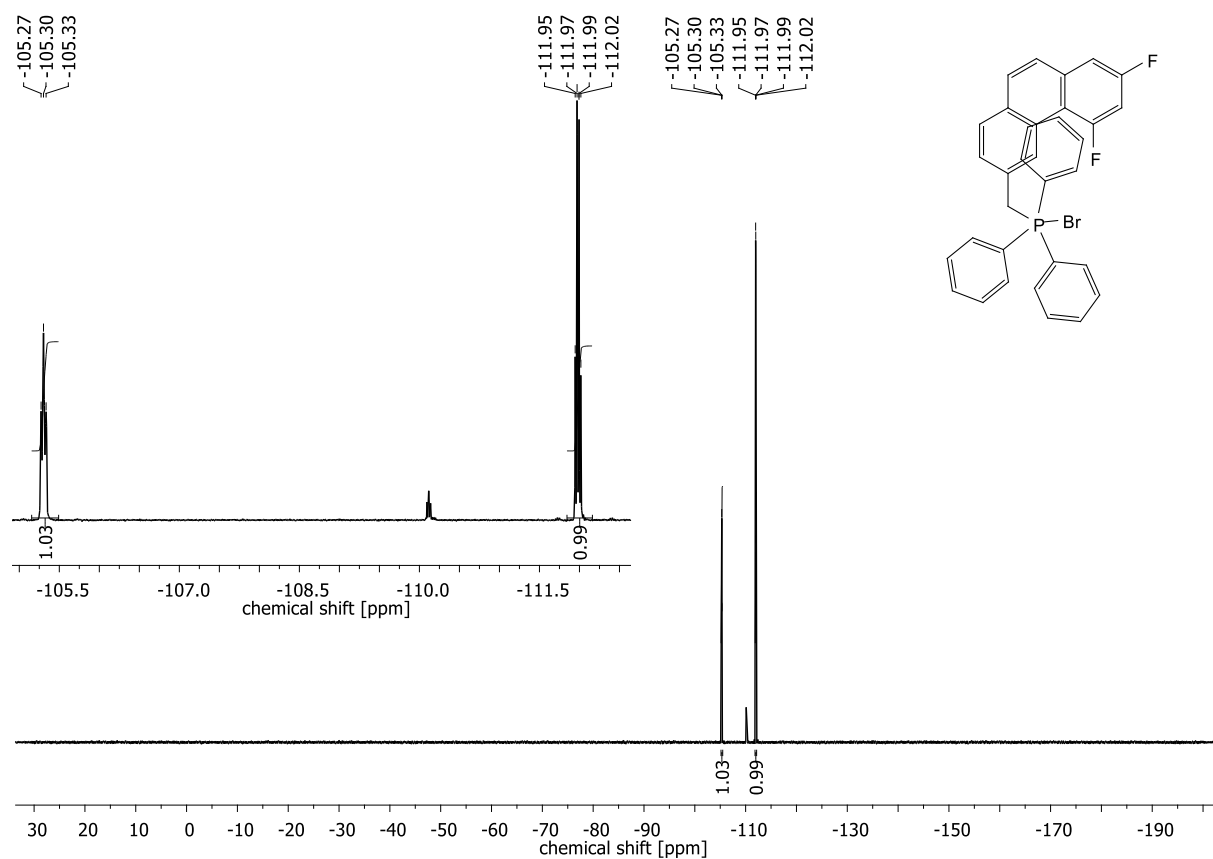


Figure 8.72: ^{19}F -NMR spectrum of bromo((5,7-difluorophenanthren-3-yl)methyl)triphenyl- λ 5-phosphane.

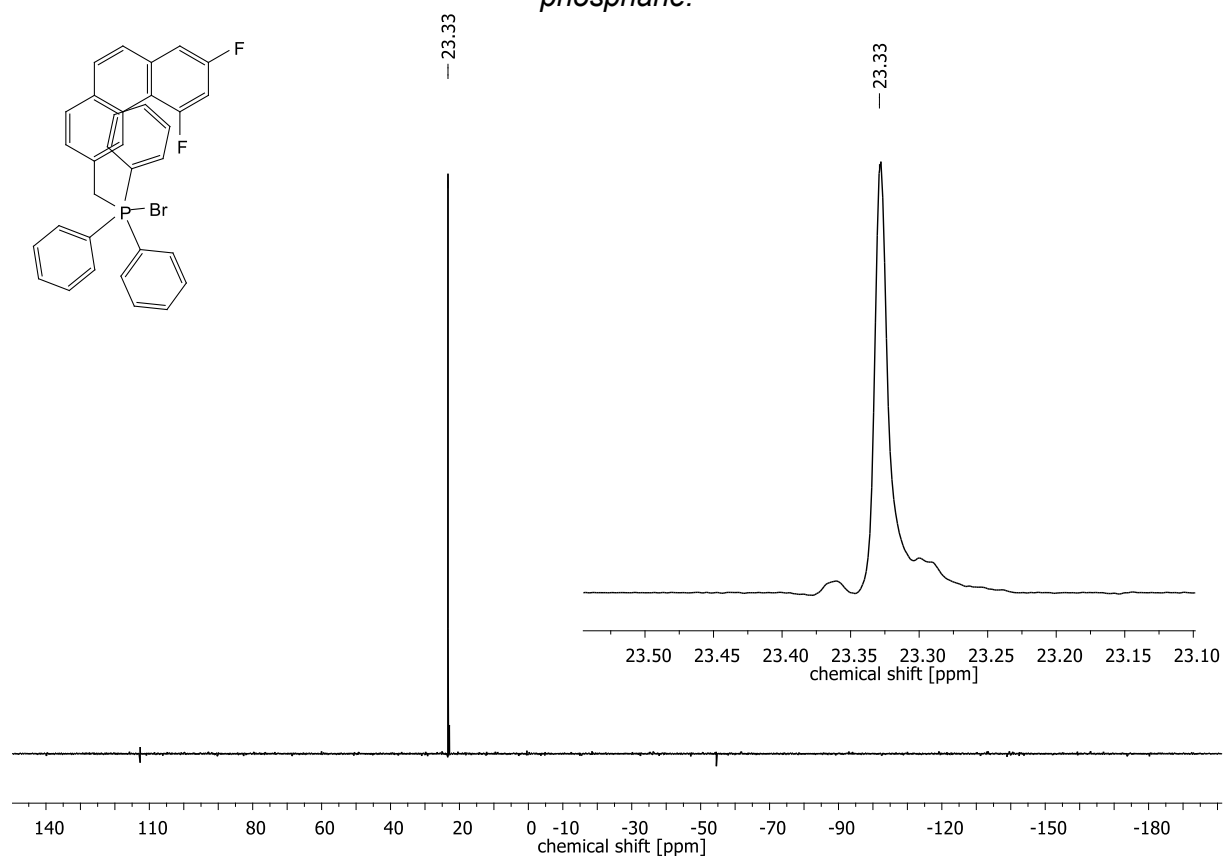


Figure 8.73: ^{31}P -NMR spectrum of bromo((5,7-difluorophenanthren-3-yl)methyl)triphenyl- λ 5-phosphane.

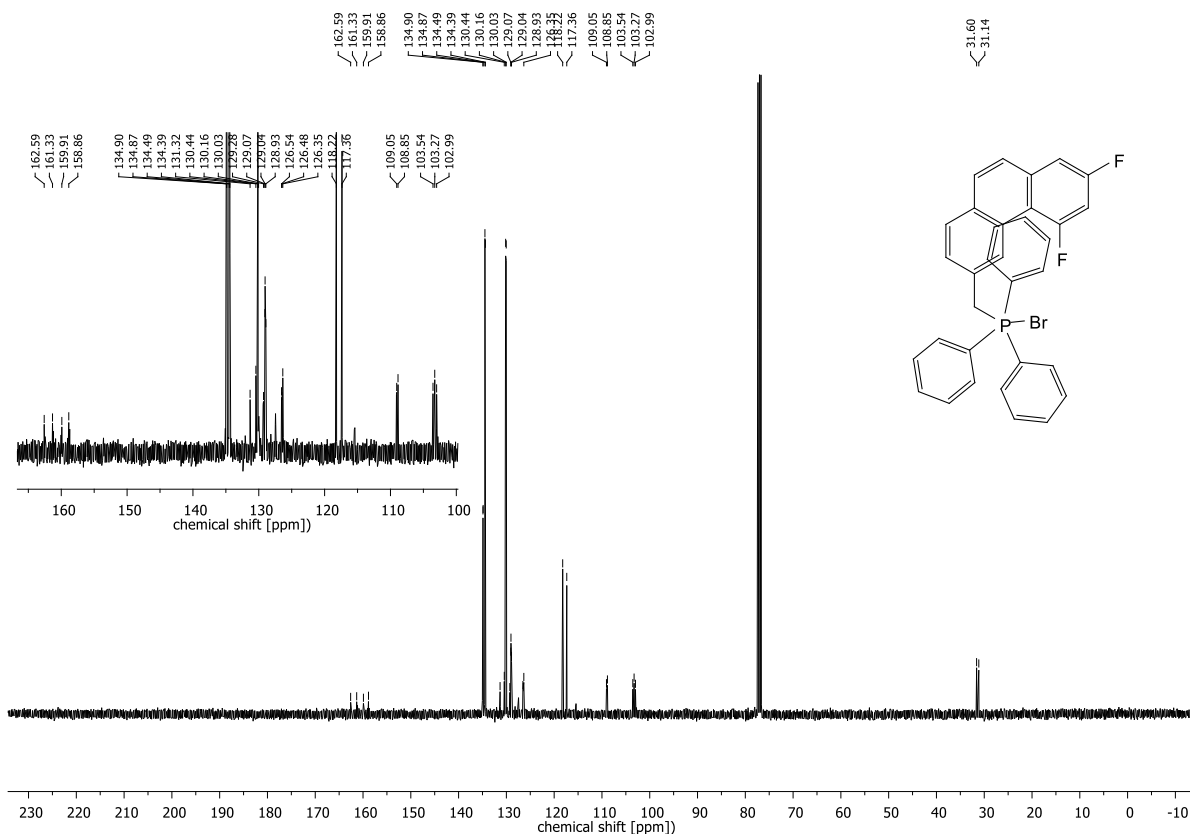


Figure 8.74: ^{13}C -NMR spectrum of bromo((5,7-difluorophenanthren-3-yl)methyl)triphenyl- λ^5 -phosphane.

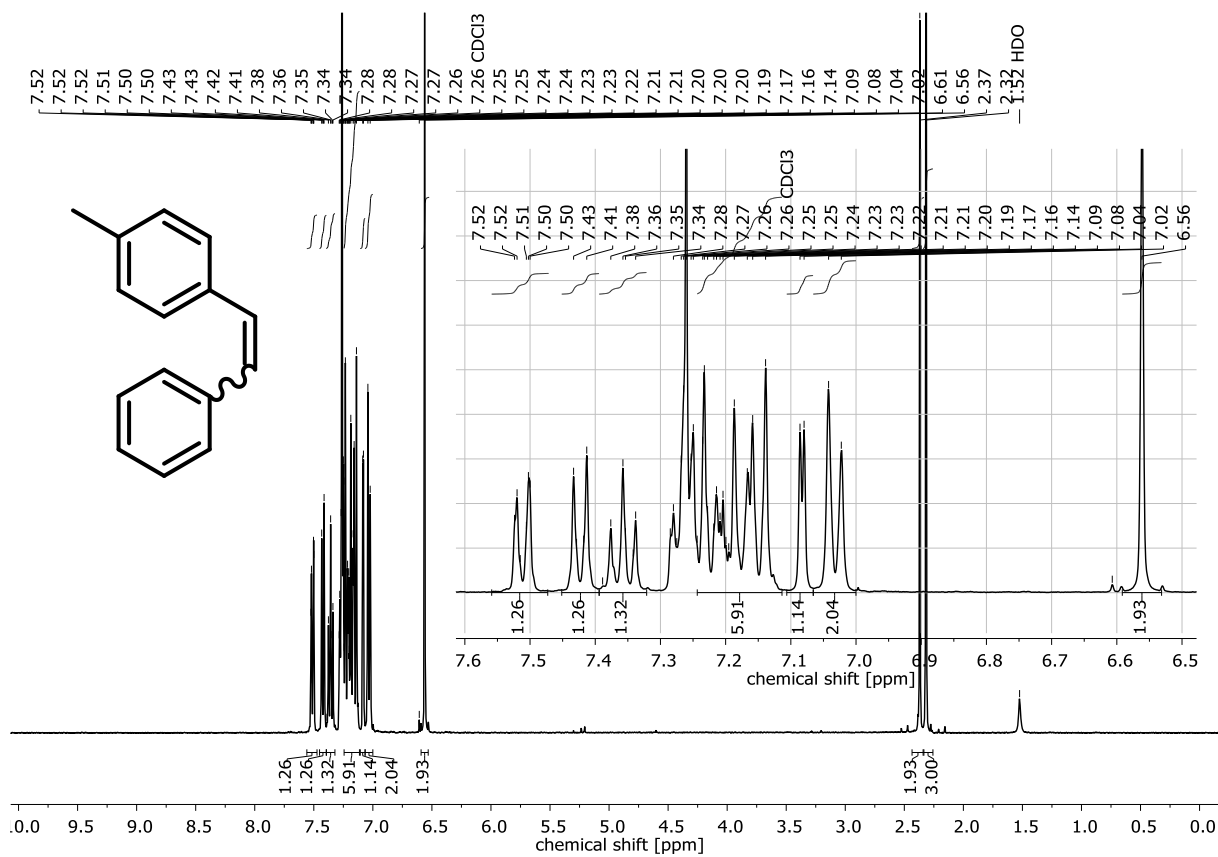


Figure 8.75: ^1H -NMR spectrum of 1-methyl-4-styrylbenzene.

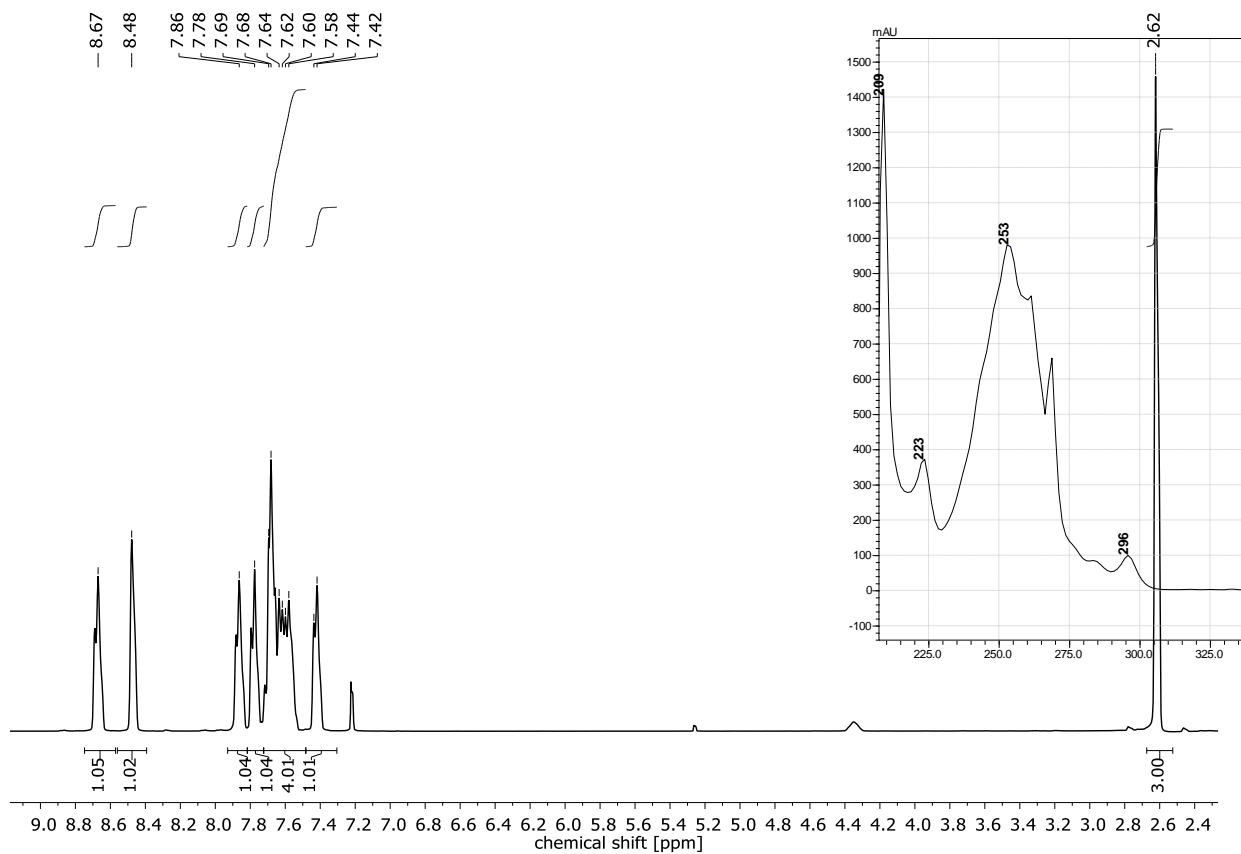


Figure 8.76: $^1\text{H-NMR}$ spectrum of 3-methylphenanthrene.

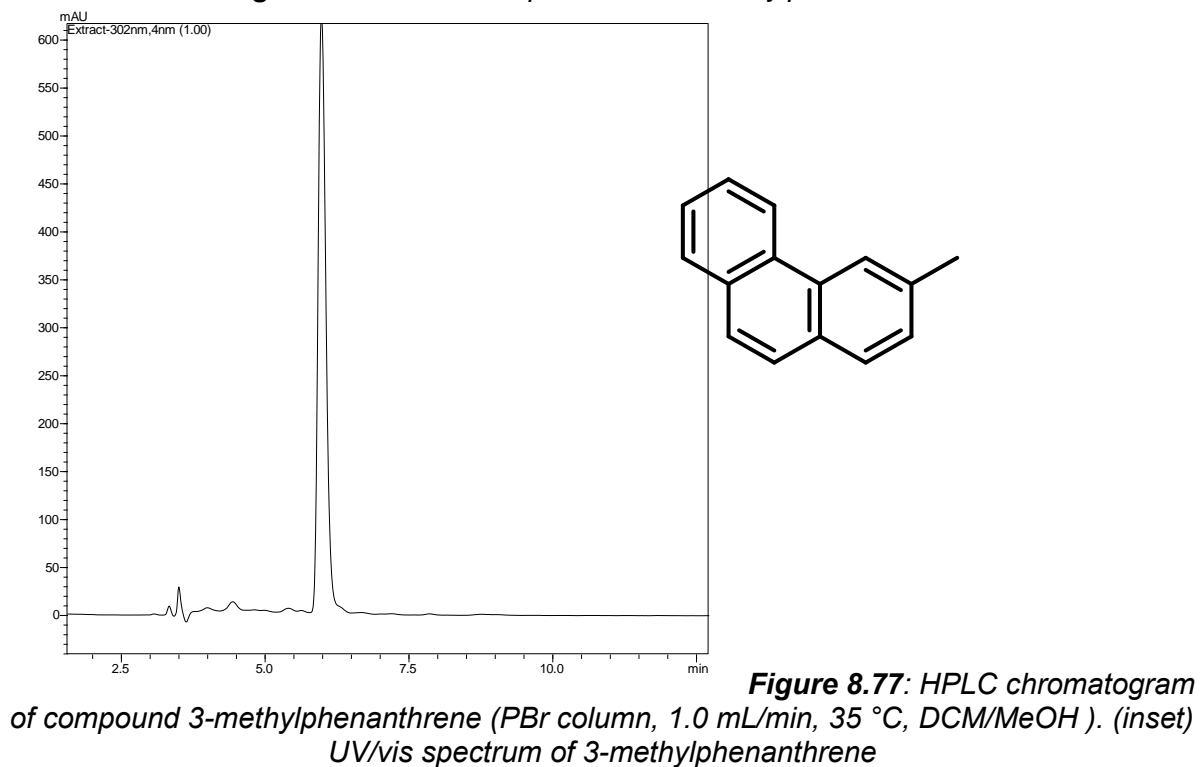


Figure 8.77: HPLC chromatogram of compound 3-methylphenanthrene (PBr column, 1.0 mL/min, 35 °C, DCM/MeOH). (inset) UV/vis spectrum of 3-methylphenanthrene

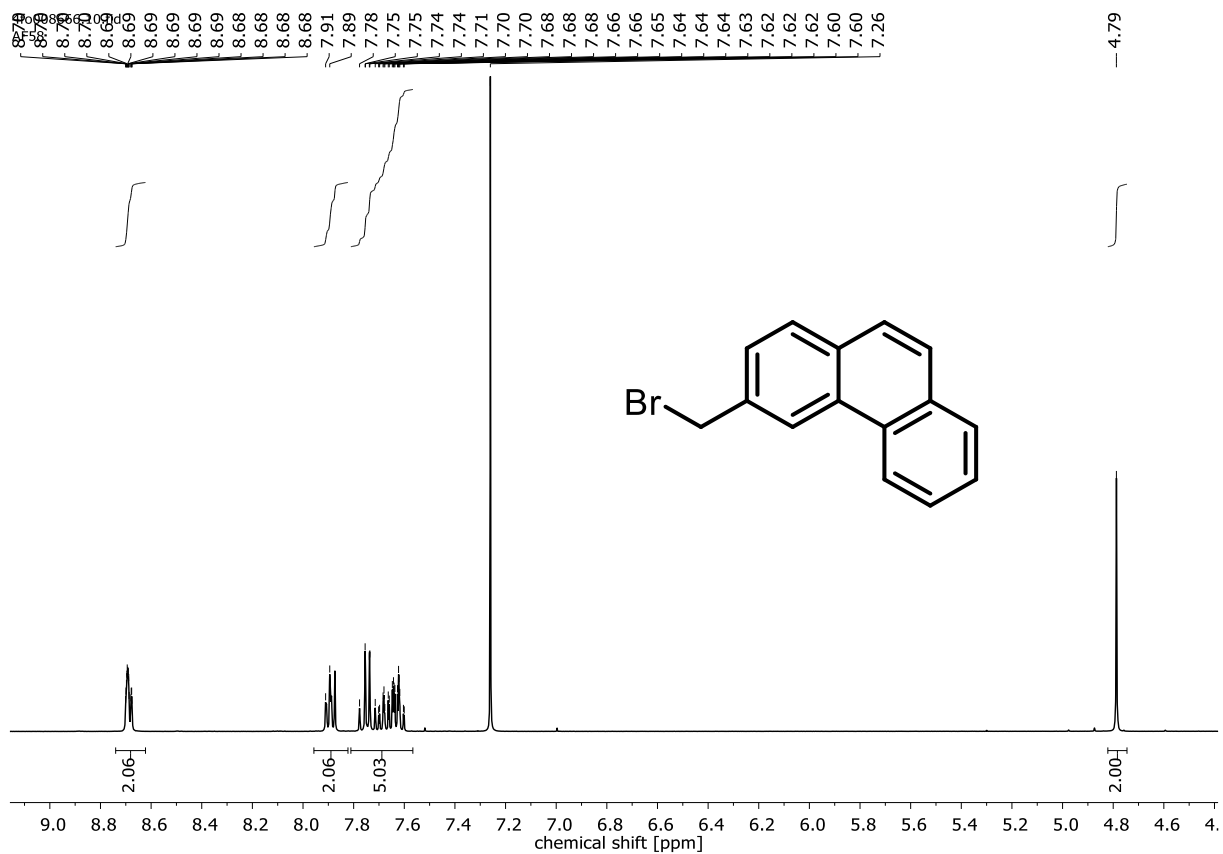


Figure 8.78: $^1\text{H-NMR}$ spectrum of 3-(bromomethyl)phenanthrene.

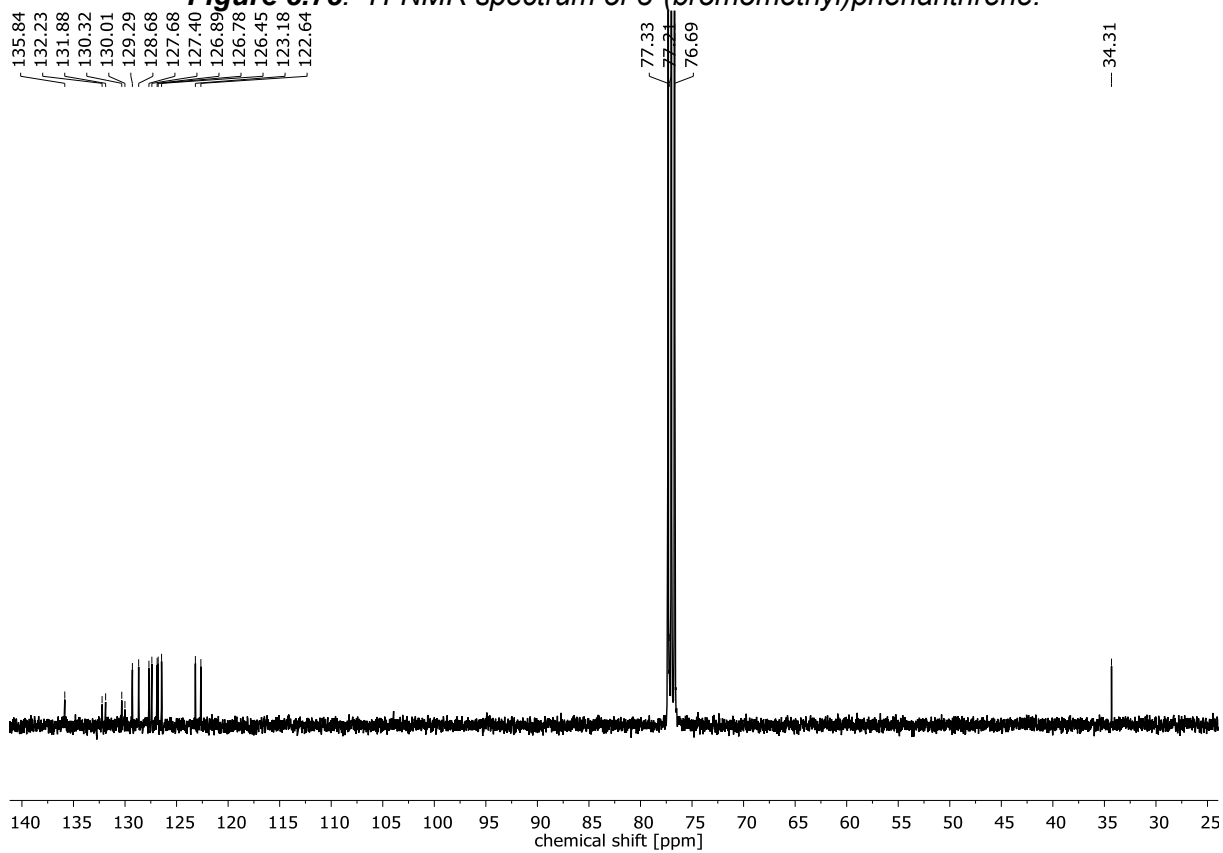


Figure 8.79: $^{13}\text{C-NMR}$ spectrum of 3-(bromomethyl)phenanthrene.



Figure 8.80: $^1\text{H-NMR}$ spectrum of phenanthrene-3-carbaldehyde.

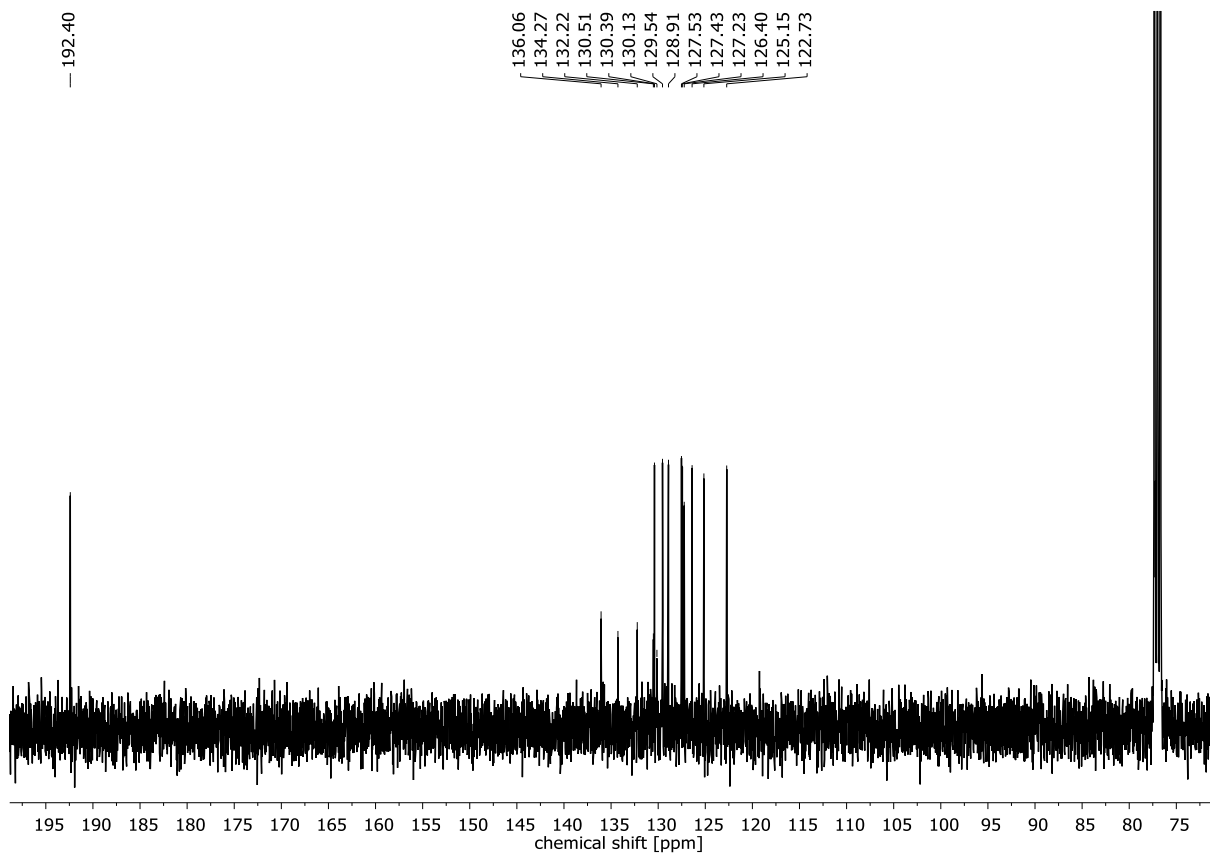


Figure 8.81: $^{13}\text{C-NMR}$ spectrum of phenanthrene-3-carbaldehyde.

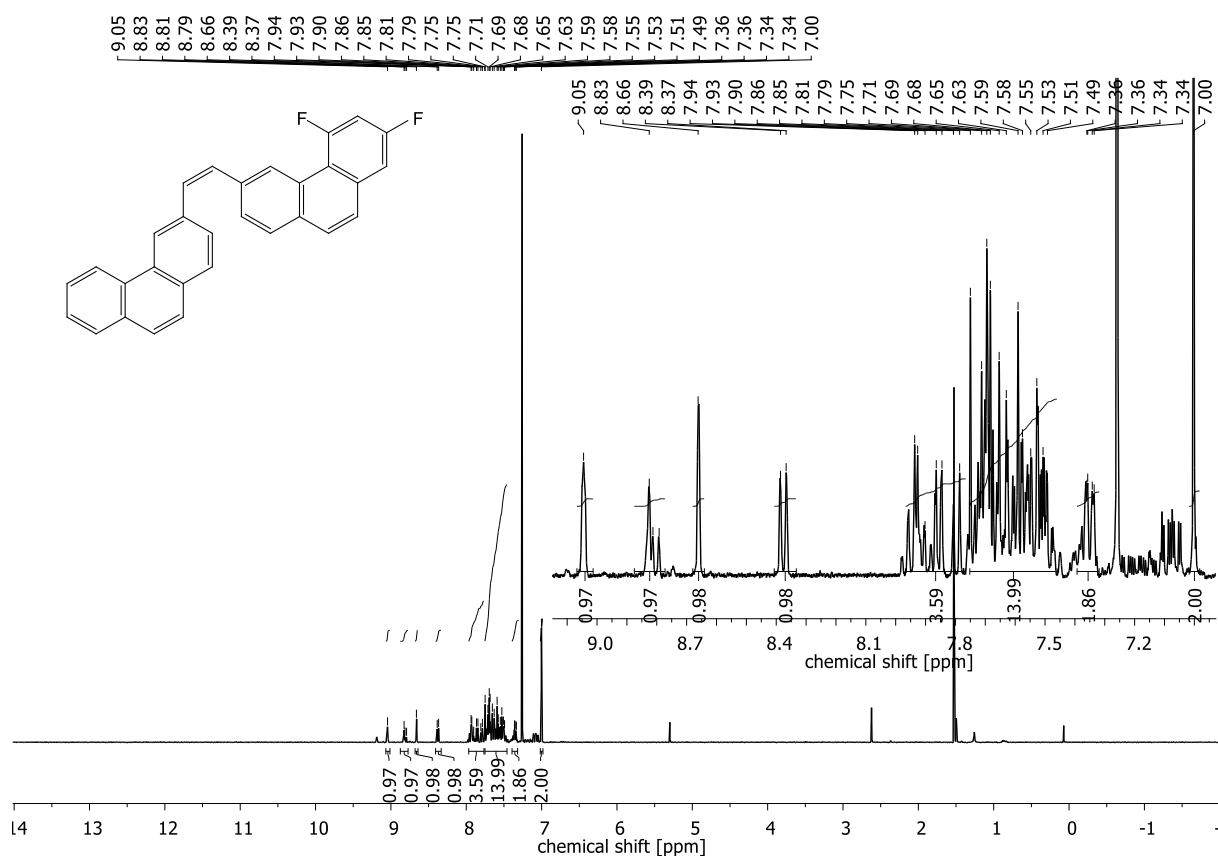


Figure 8.82: $^1\text{H-NMR}$ spectrum of 2,4-difluoro-6-(2-(phenanthren-3-yl)vinyl)phenanthrene.

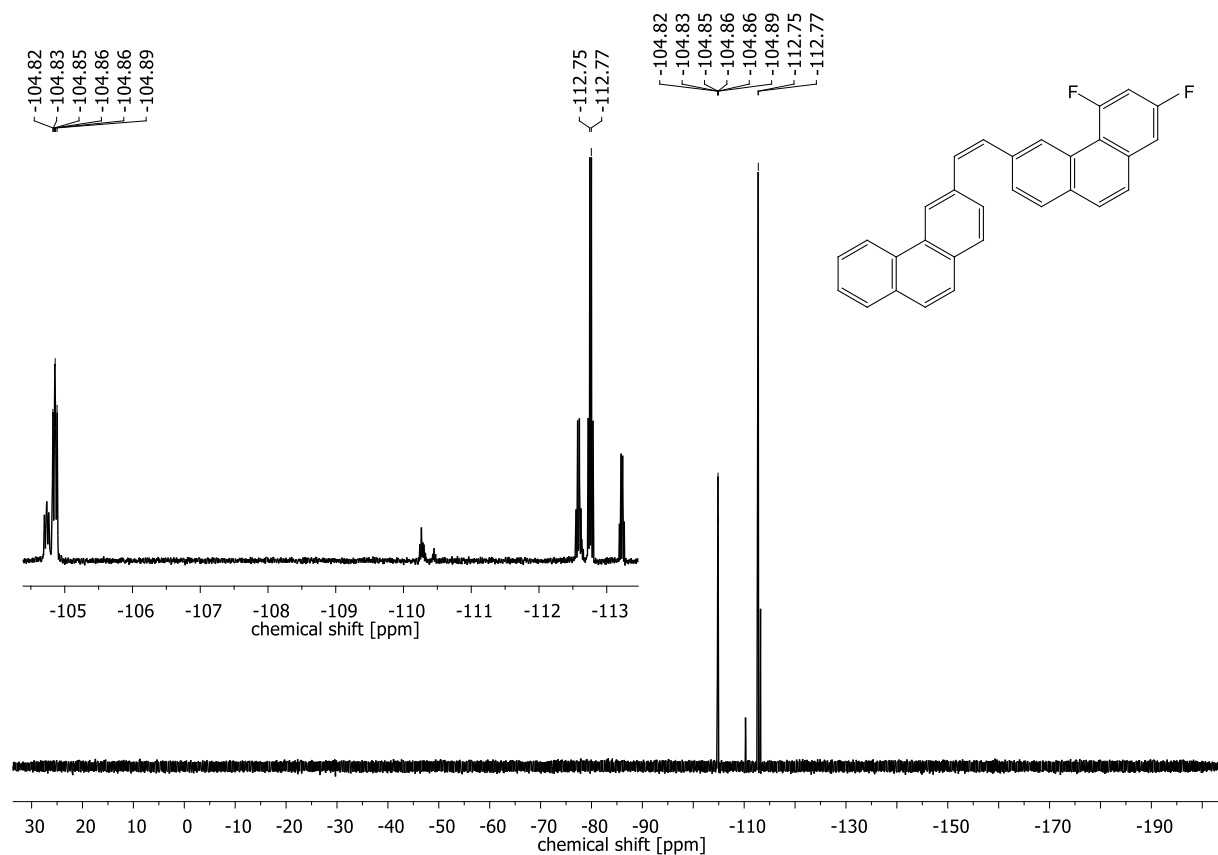


Figure 8.83: $^{19}\text{F-NMR}$ spectrum of 2,4-difluoro-6-(2-(phenanthren-3-yl)vinyl)phenanthrene.

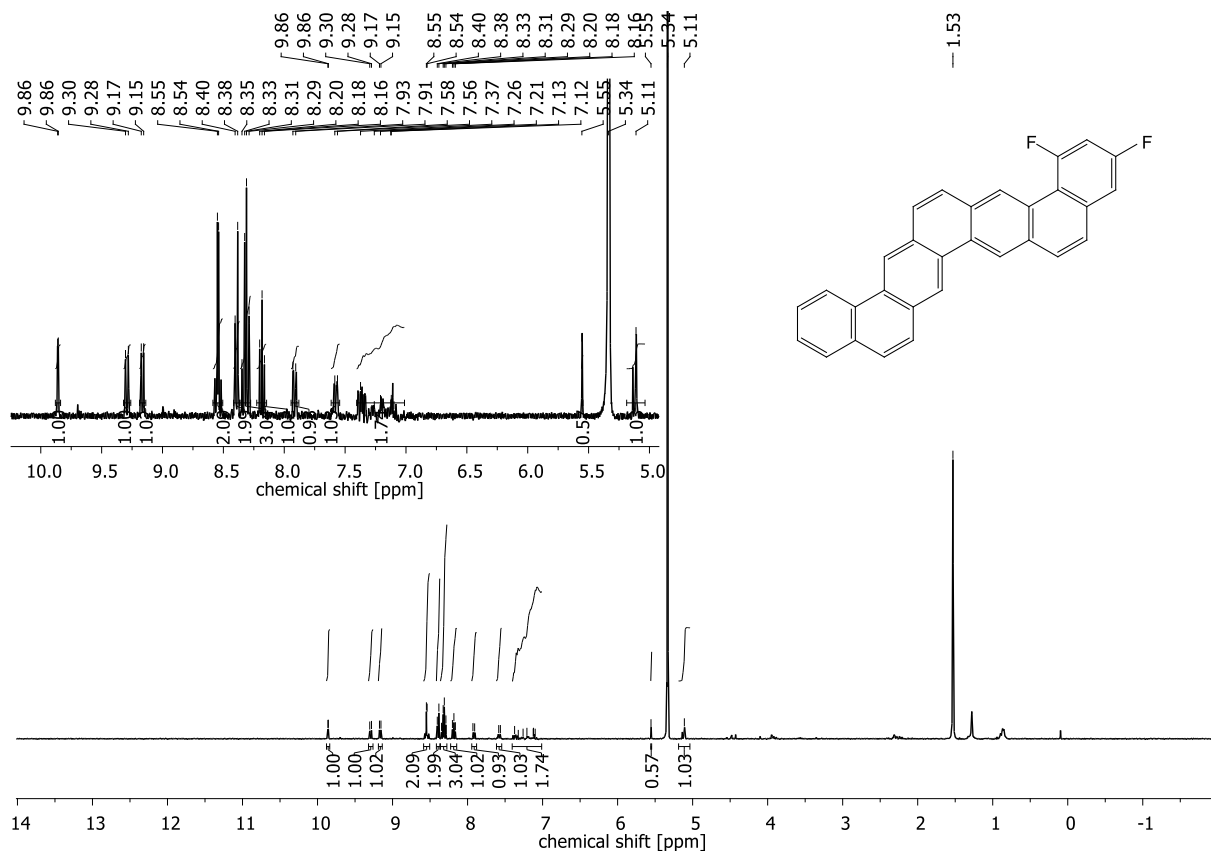


Figure 8.84: ¹H-NMR spectrum of 2,4-difluorodibenzo[*c,m*]pentaphene fraction 4.

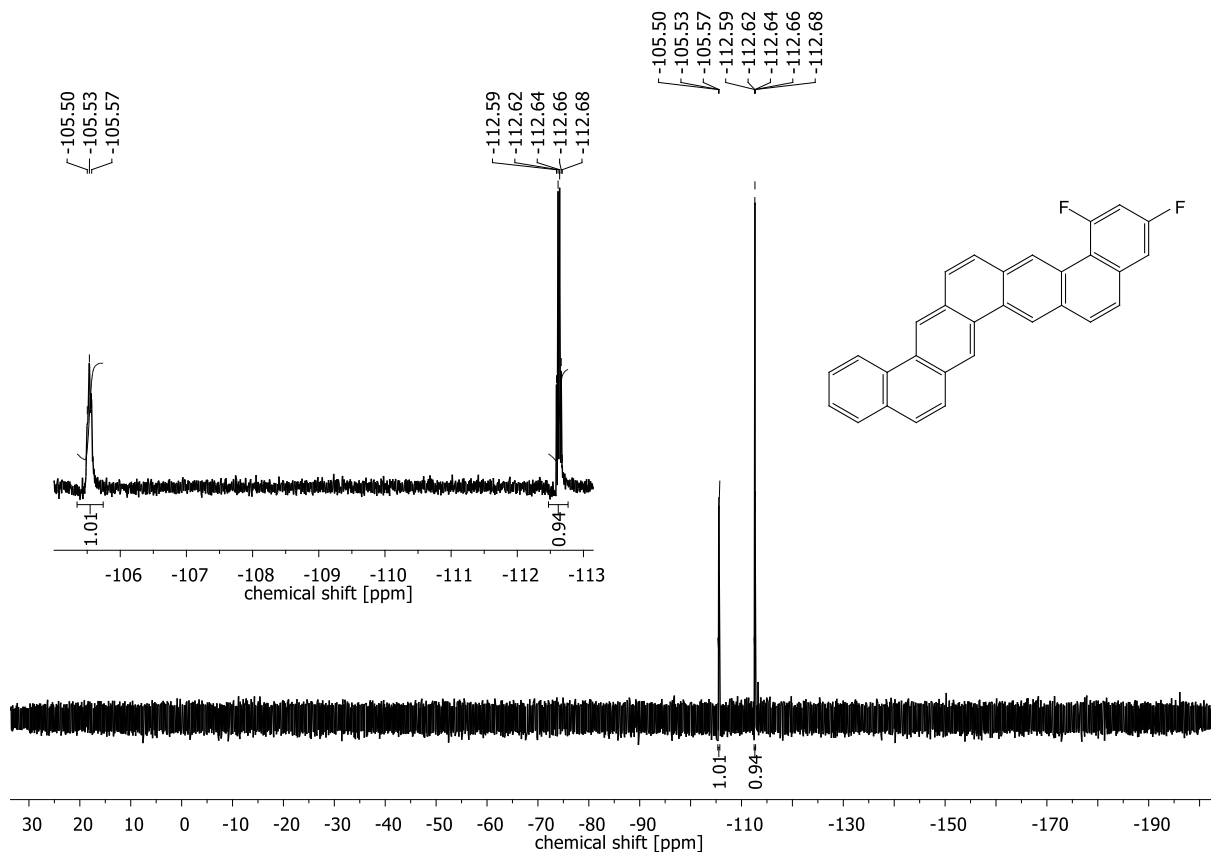


Figure 8.85: ¹³C-NMR spectrum of 2,4-difluorodibenzo[*c,m*]pentaphene fraction 4.

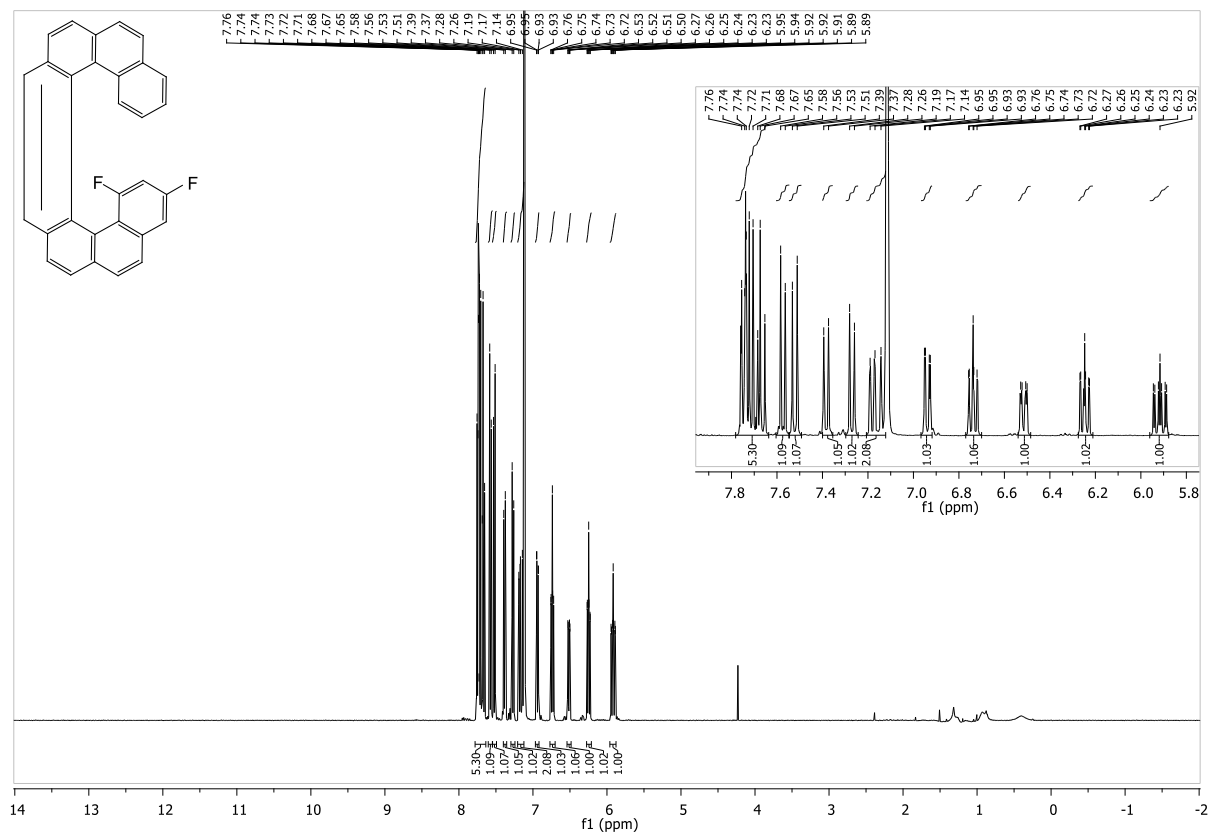


Figure 8.86: ¹H-NMR spectrum of 1,3-difluorobenzo[1,2-c:4,3-c']diphenanthrene fraction 5.

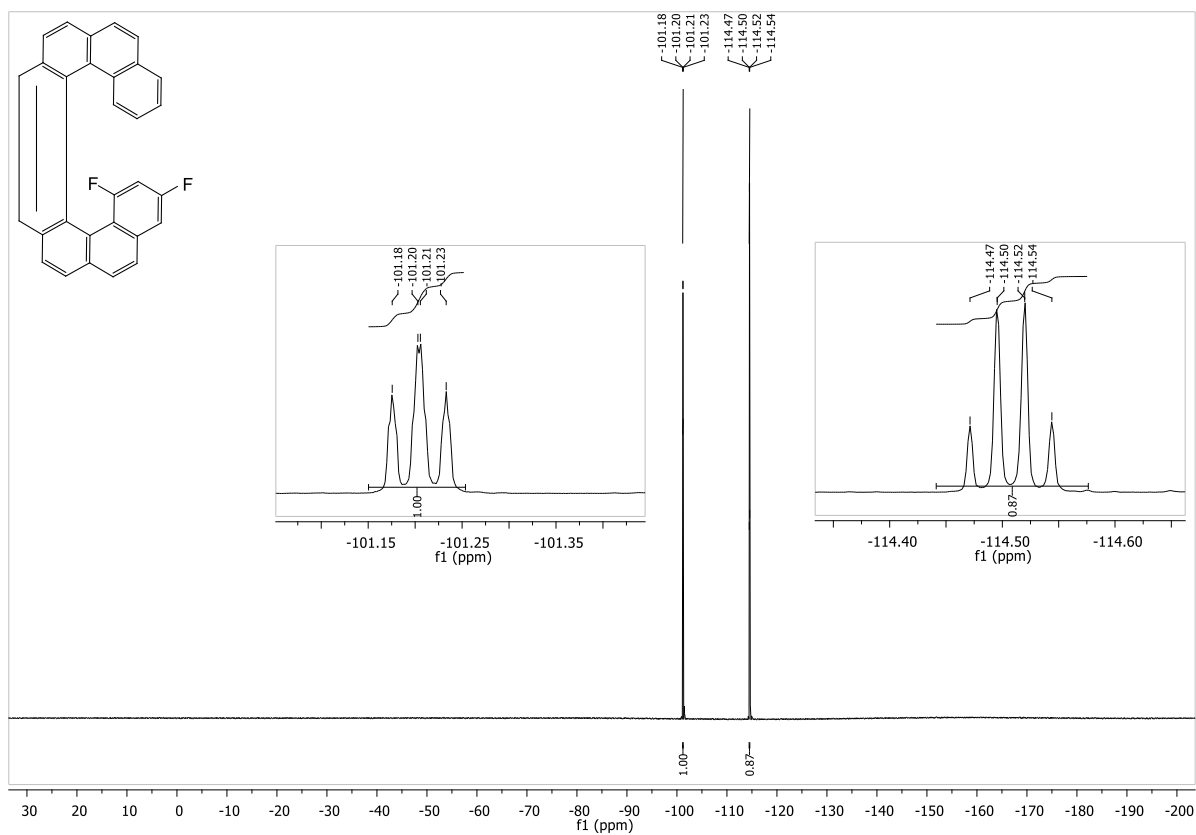


Figure 8.87: ¹⁹F-NMR spectrum of 1,3-difluorobenzo[1,2-c:4,3-c']diphenanthrene fraction 5.

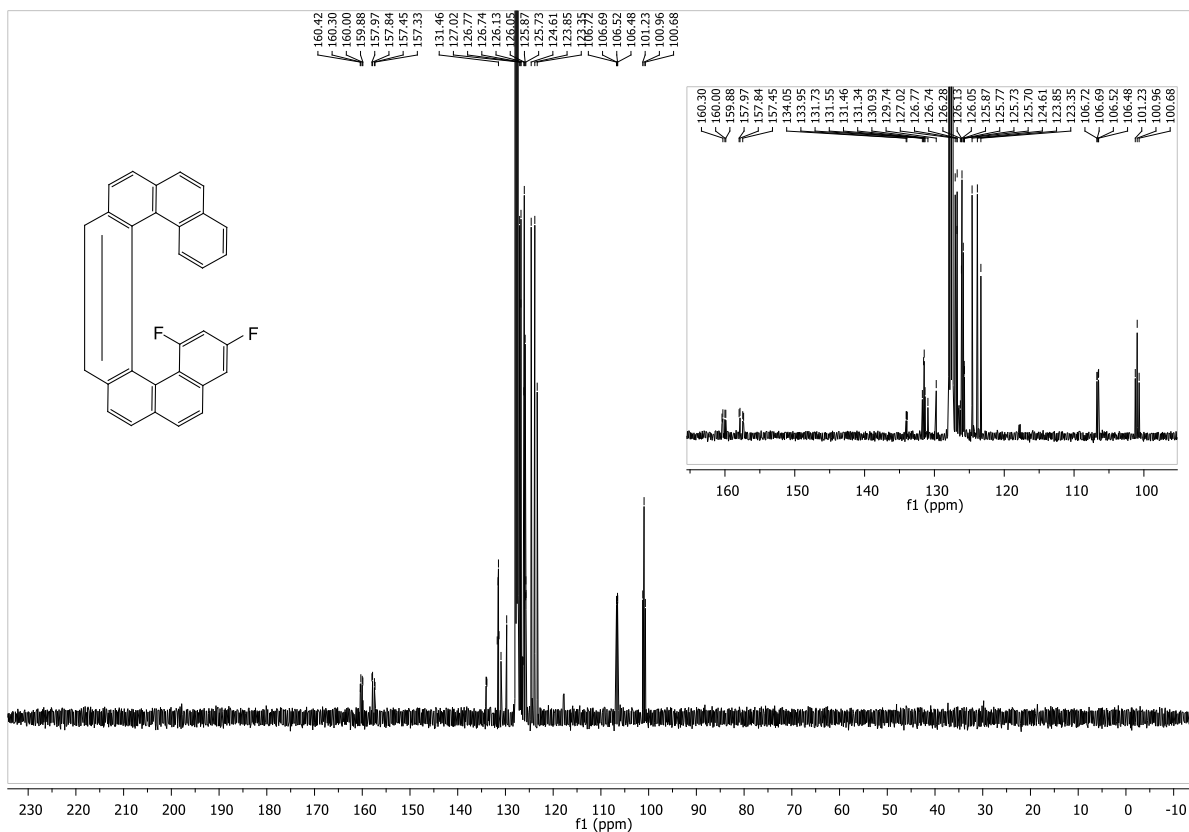


Figure 8.88: ¹³C-NMR spectrum of 1,3-difluorobenzo[1,2-c:4,3-c']diphenanthrene fraction 5

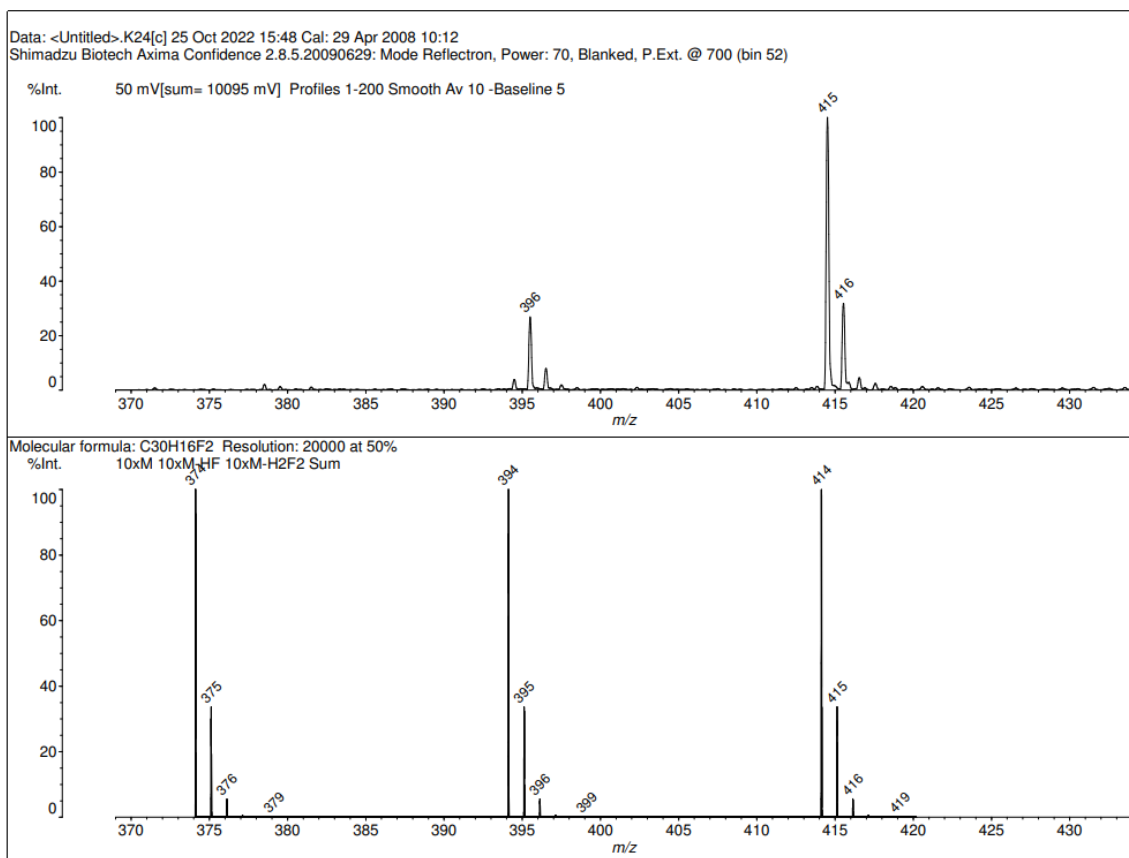


Figure 8.89: LDI MS spectrum of fraction 5 of 2,4-difluoro-6-(2-(phenanthren-3-

yl)vinyl)phenanthrene after reaction on Al₂O₃.

8.1.6. Synthesis and reaction of 6,8,18,20-tetrafluorodiphenanthro[3,4-c:3',4'-l]chrysene

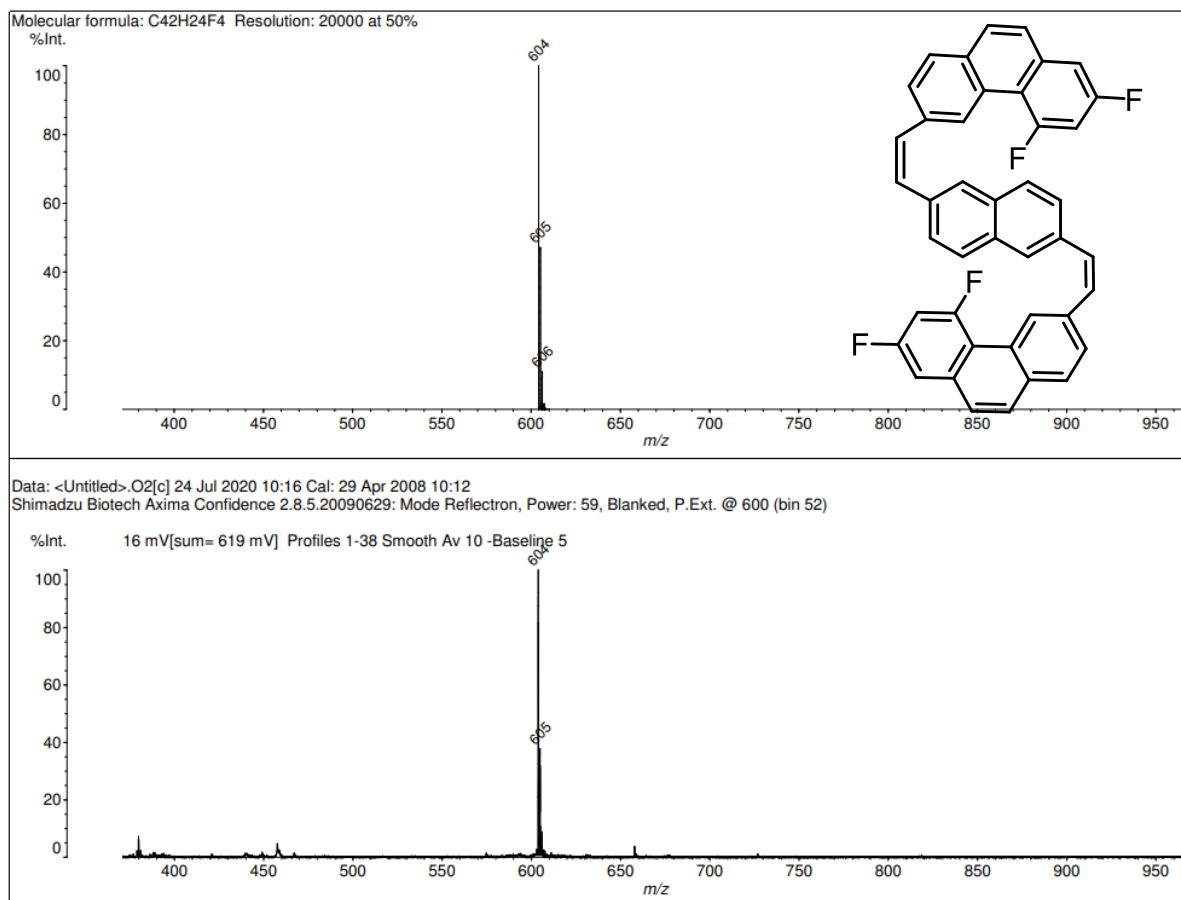


Figure 8.90: LDI MS-Spectrum of 2,6-bis(2-(5,7-difluorophenanthren-3-yl)vinyl)naphthalene.

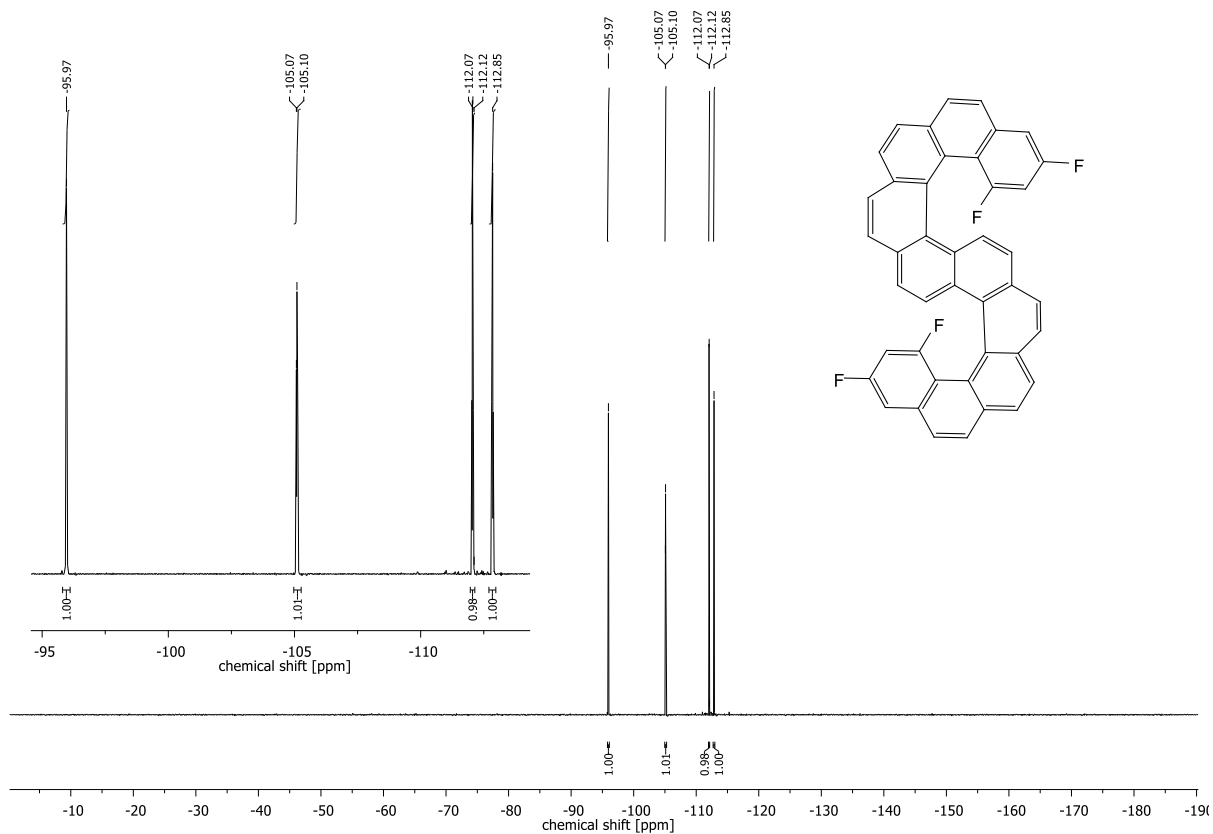


Figure 8.95: ^{19}F -NMR spectrum of 6,8,18,20-tetrafluorodiphenanthro[3,4-c:3',4'-l]chrysene fraction 3.

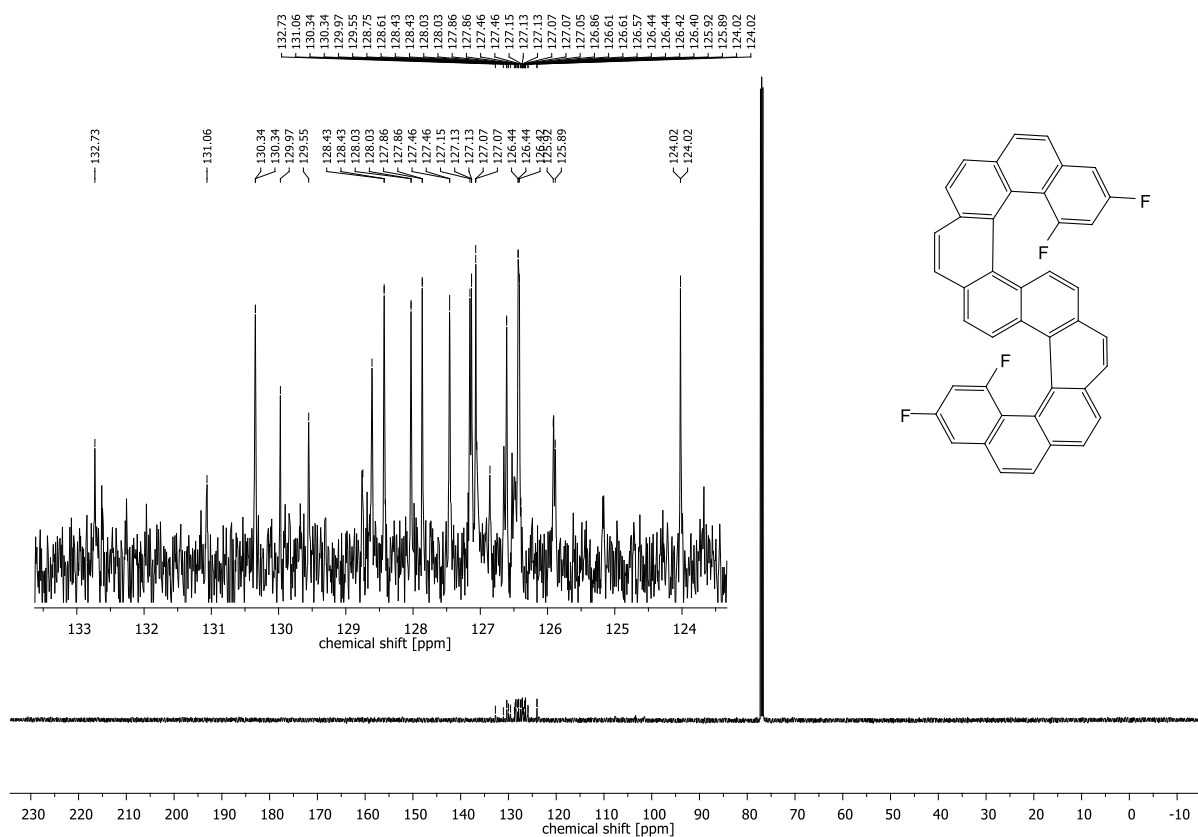


Figure 8.96: ^{13}C -NMR spectrum of 6,8,18,20-tetrafluorodiphenanthro[3,4-c:3',4'-l]chrysene fraction 3.

trifluorobenzo[ghi]naphtho[1',2':5,6]phenanthro[4,3-a]perylene.

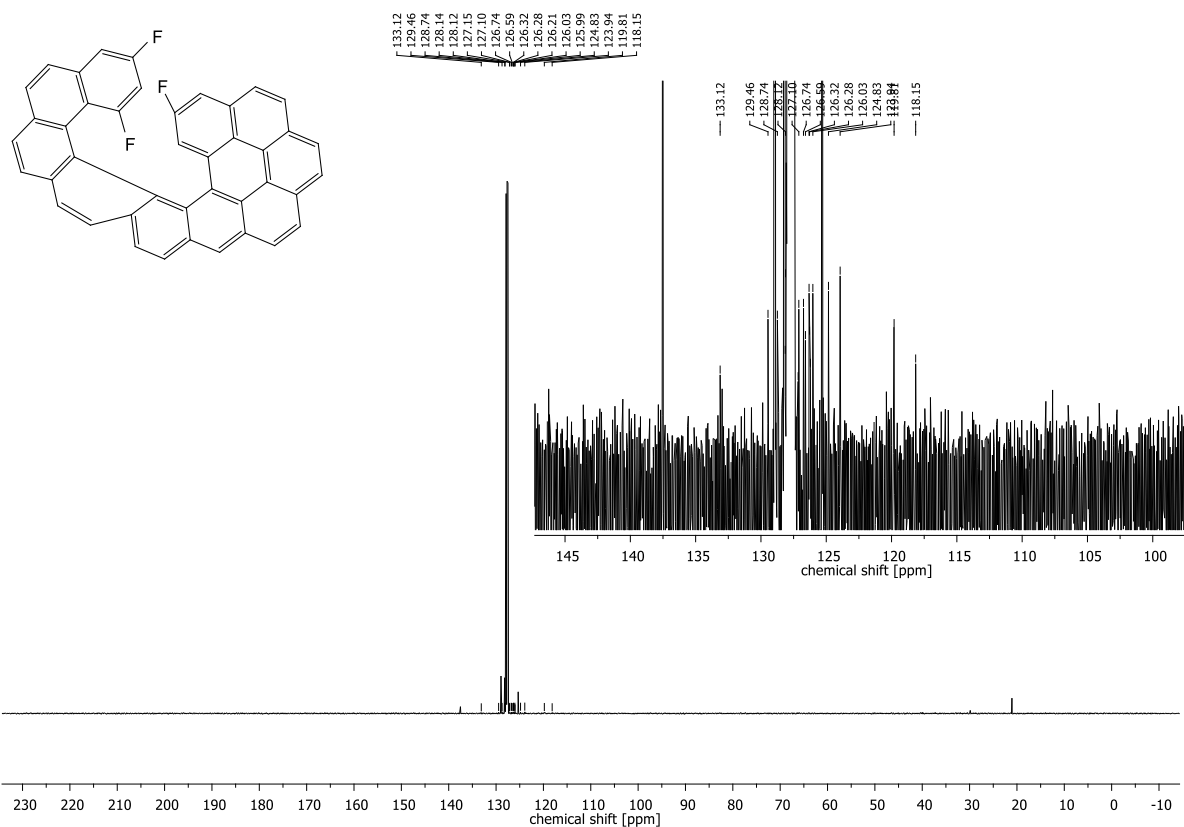
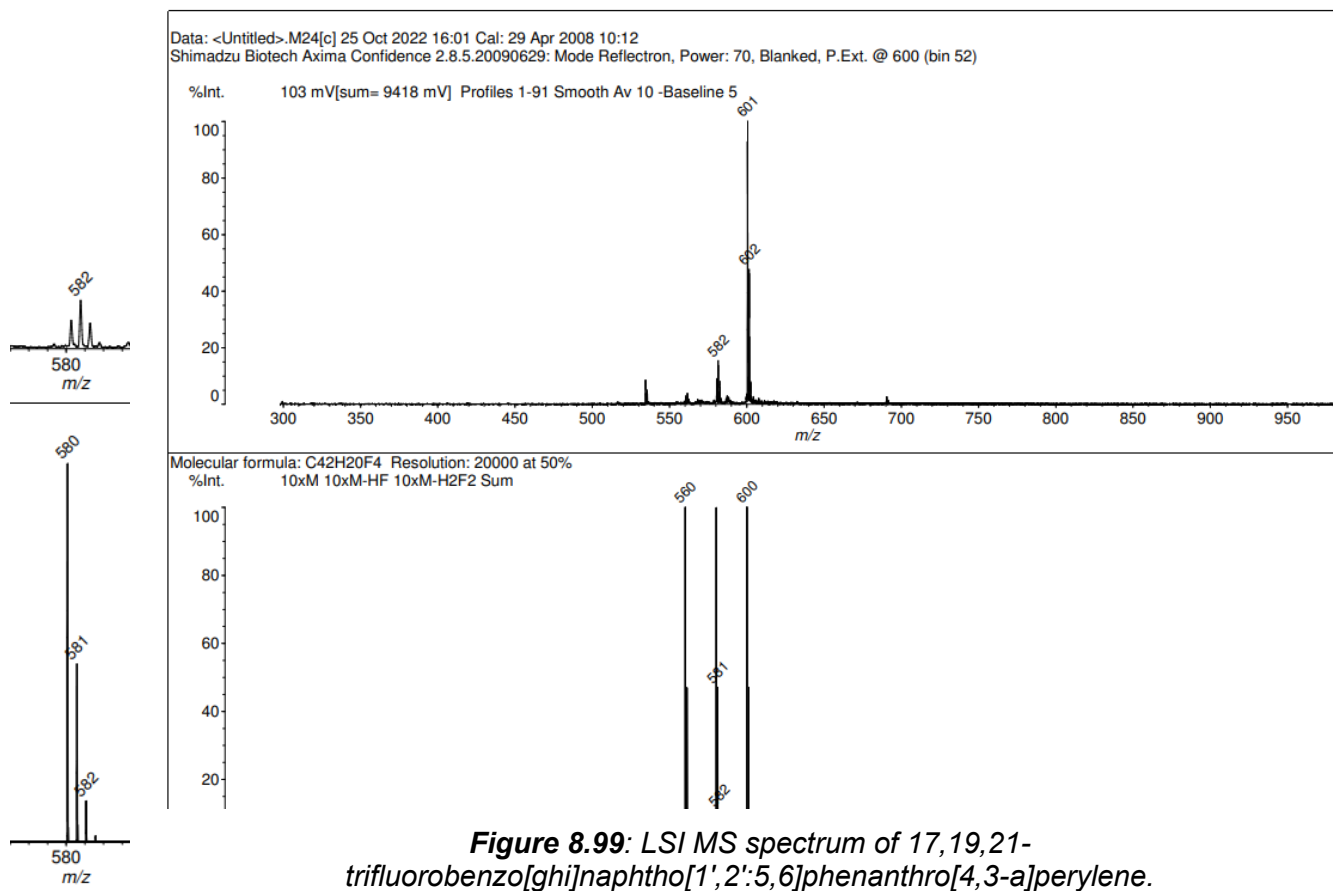


Figure 8.100: $^{13}\text{C-NMR}$ spectrum of 17,19,21-



trifluorobenzo[ghi]naphtho[1',2':5,6]phenanthro[4,3-a]perylene.

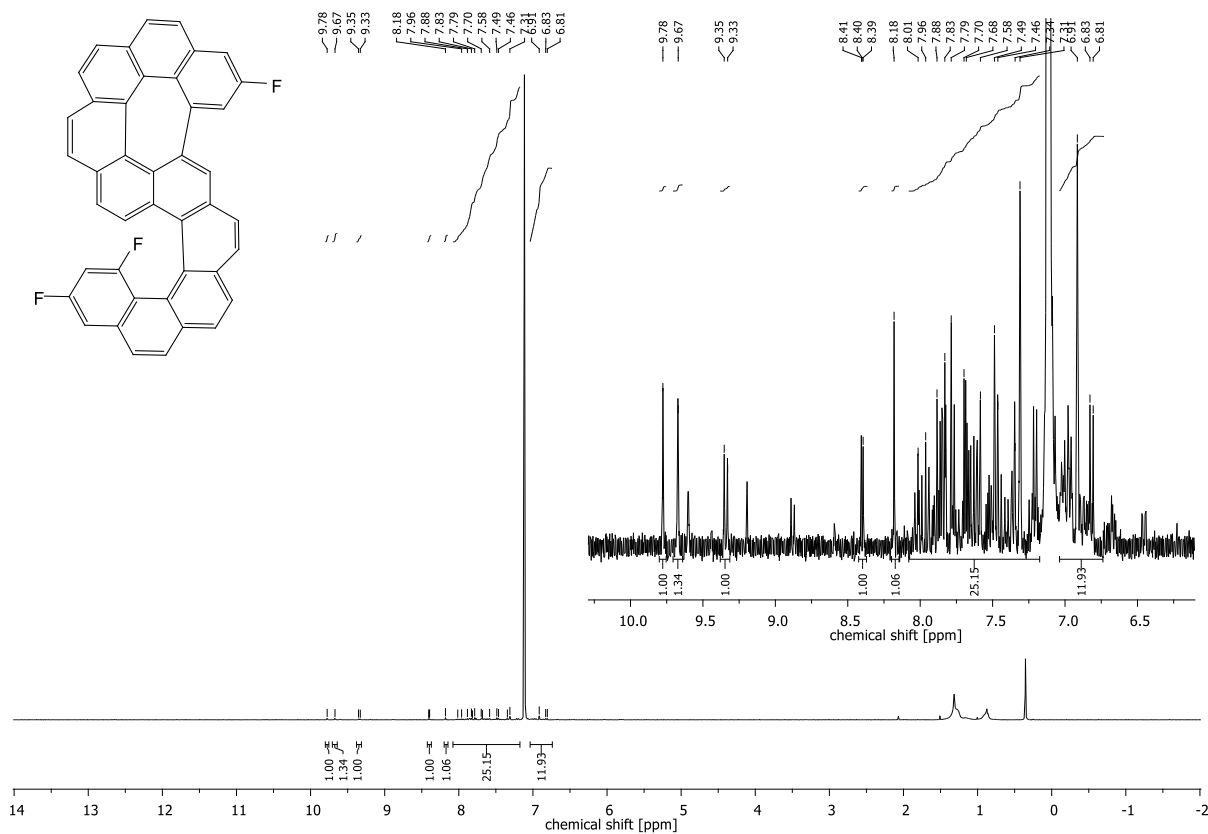


Figure 8.101: $^1\text{H-NMR}$ spectrum of 9,19,21-trifluorobenzo[no]benzo[5,6]phenanthro[3,4-b]naphtho[2,1,8,7-ghij]pleiadene.

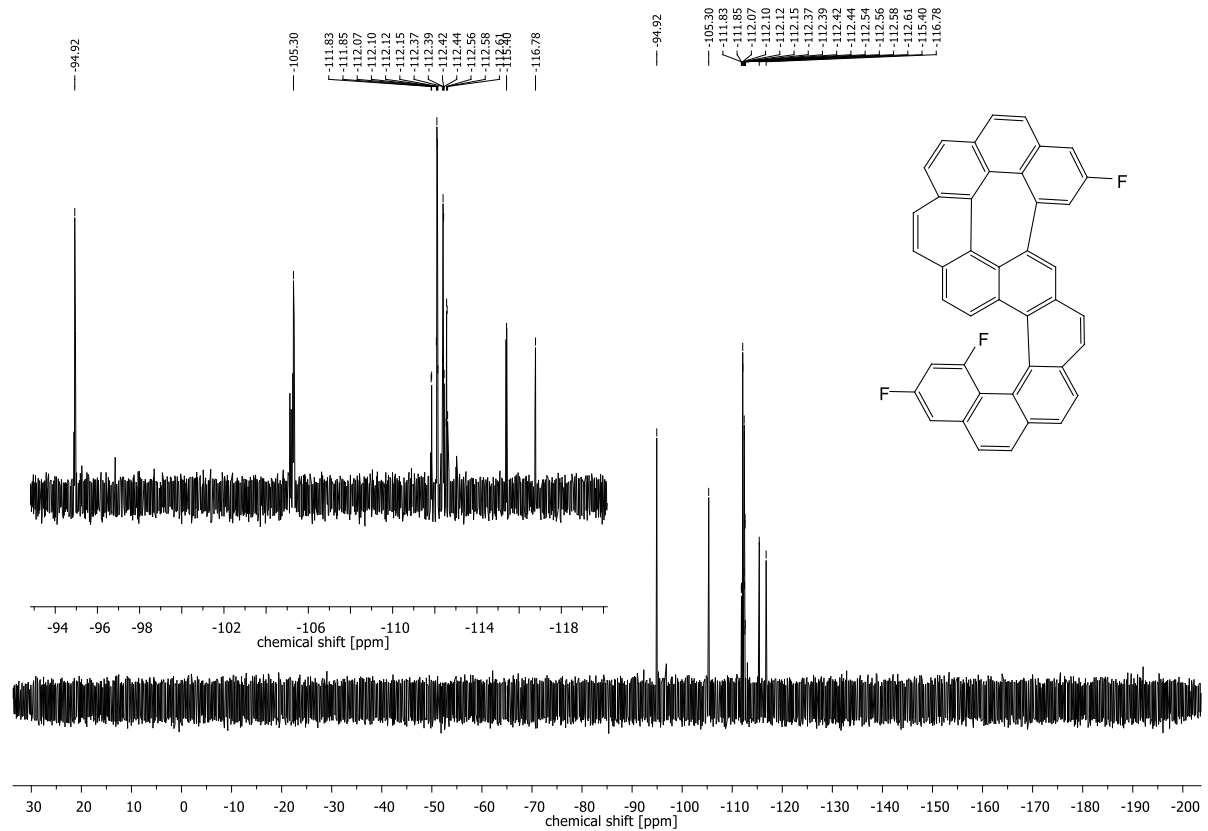


Figure 8.102: $^{19}\text{F-NMR}$ spectrum of 9,19,21-trifluorobenzo[no]benzo[5,6]phenanthro[3,4-b]naphtho[2,1,8,7-ghij]pleiadene.

b]naphtho[2,1,8,7-ghij]pleiadene.

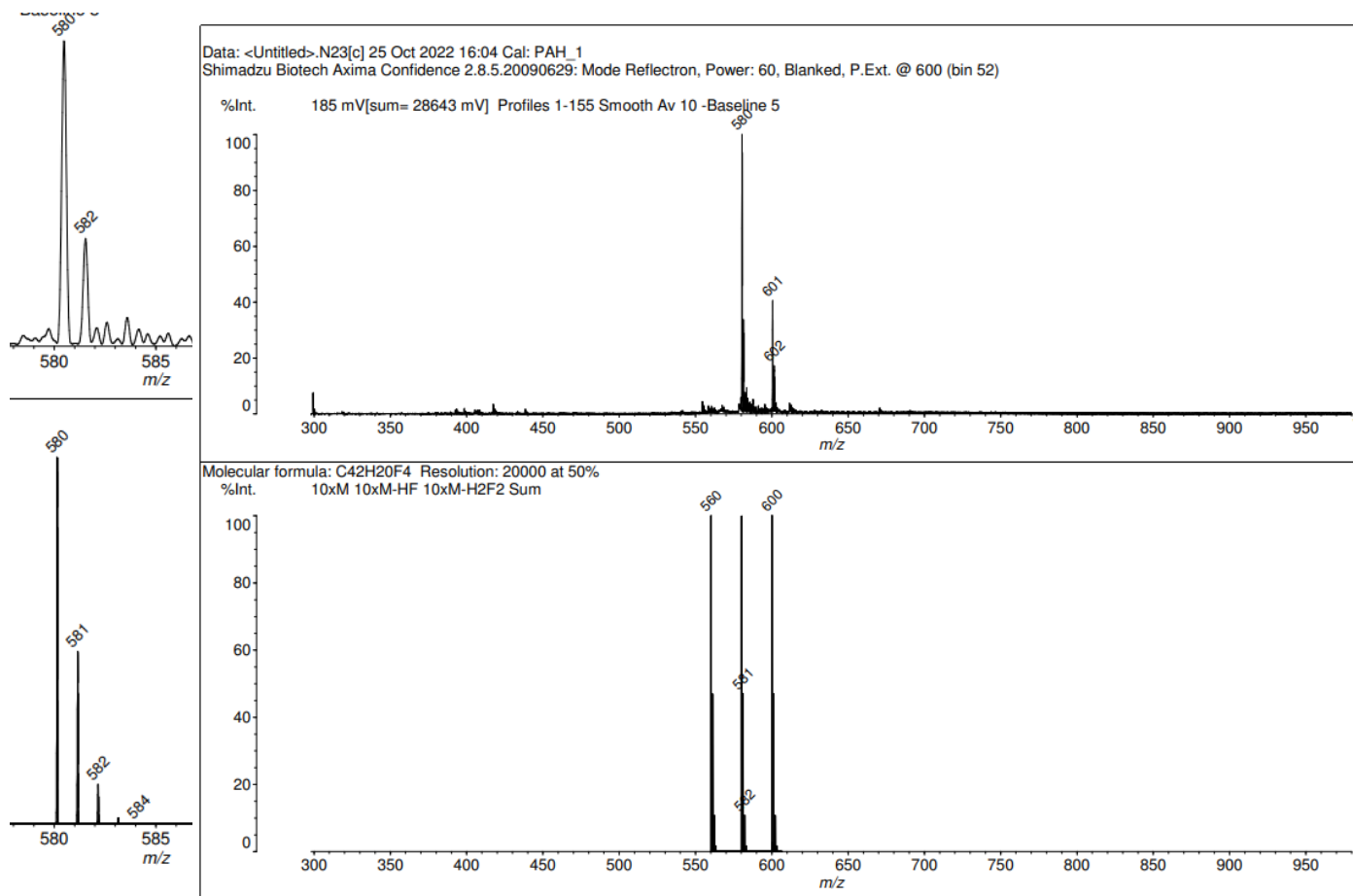


Figure 8.103: LSI MS spectrum of 9,19,21-trifluorobenzo[no]benzo[5,6]phenanthro[3,4-*b*]naphtho[2,1,8,7-ghij]pleiadene.

8.1.7. Synthesis of 12,12',14,14'-tetrafluoro-11,11'-bihexahelicene

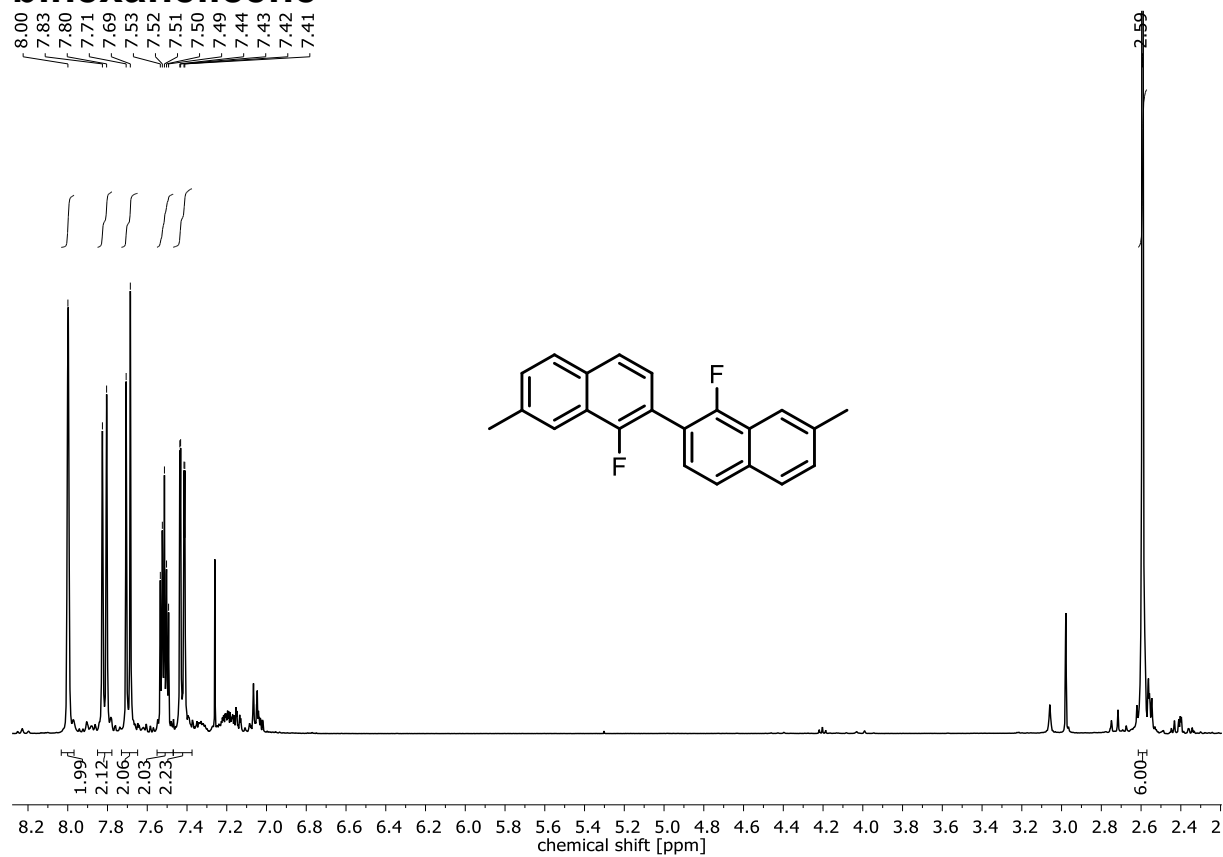


Figure 8.104: $^1\text{H-NMR}$ spectrum of 1,1'-difluoro-7,7'-dimethyl-2,2'-binaphthalene.

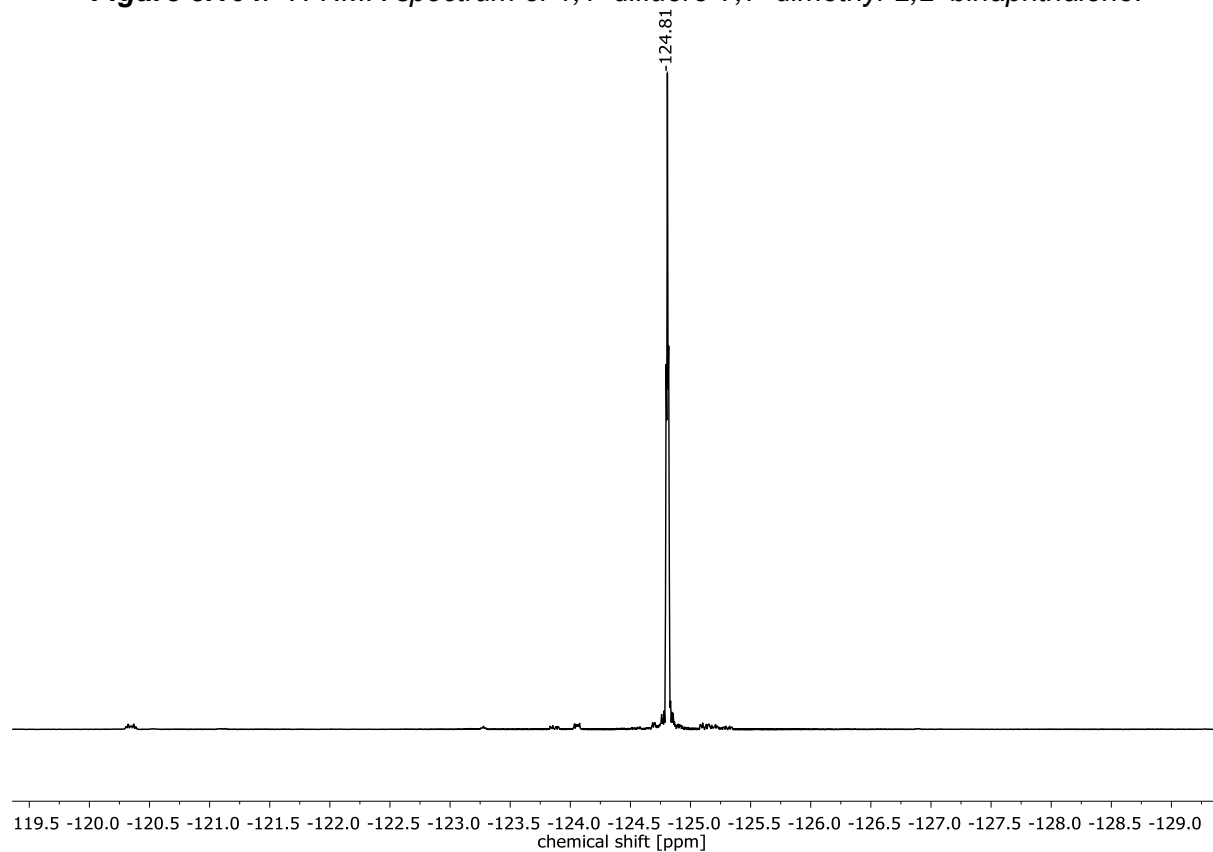


Figure 8.105: ^{19}F -NMR spectrum of 1,1'-difluoro-7,7'-dimethyl-2,2'-binaphthalene.

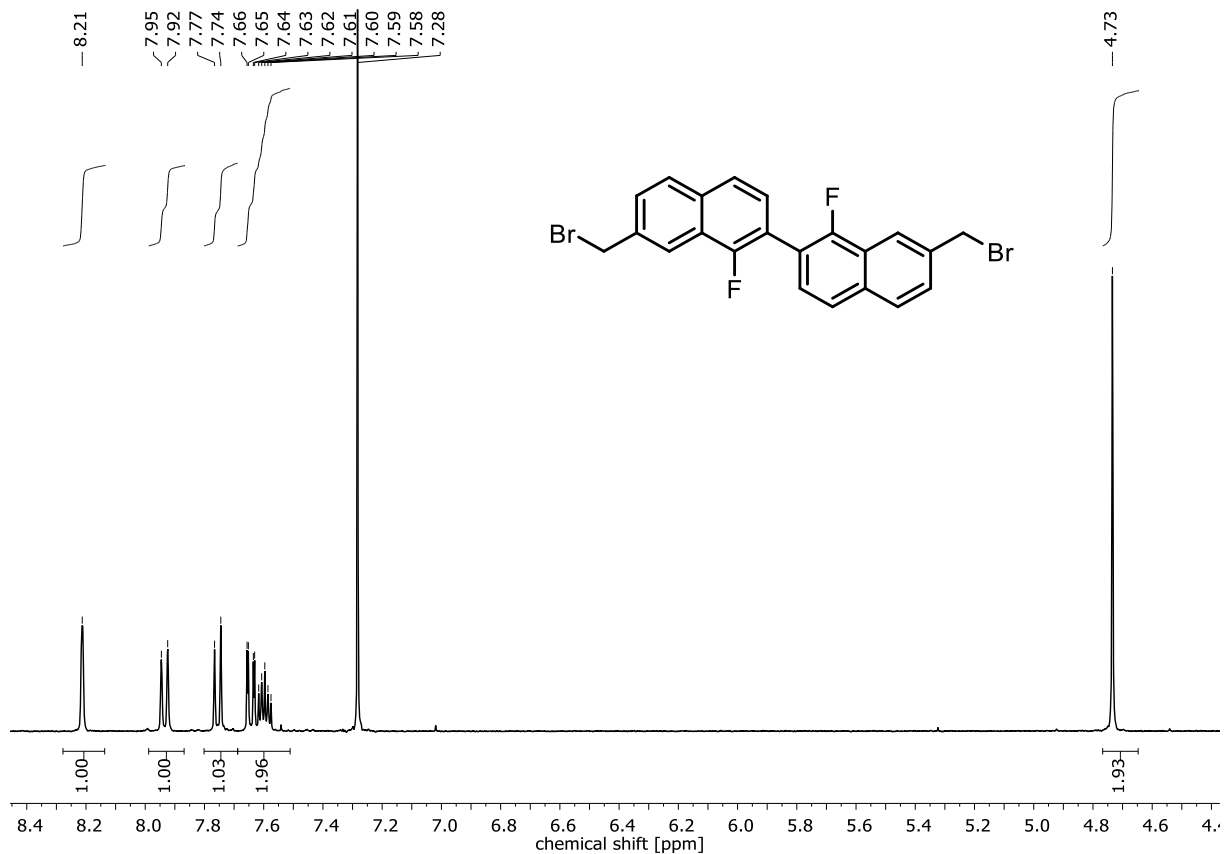


Figure 8.106: ^1H -NMR spectrum of 7,7'-bis(bromomethyl)-1,1'-difluoro-2,2'-binaphthalene.

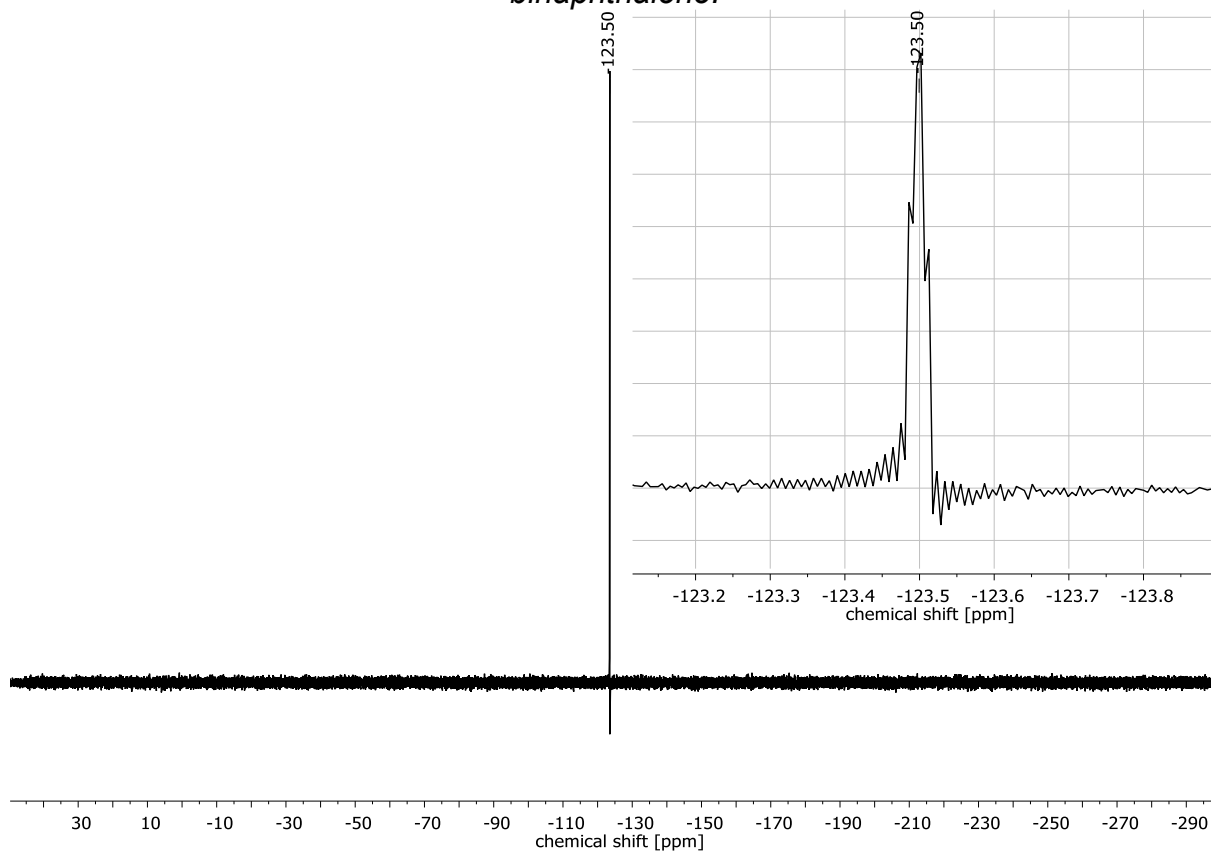


Figure 8.107: ^{19}F -NMR spectrum of 7,7'-bis(bromomethyl)-1,1'-difluoro-2,2'-

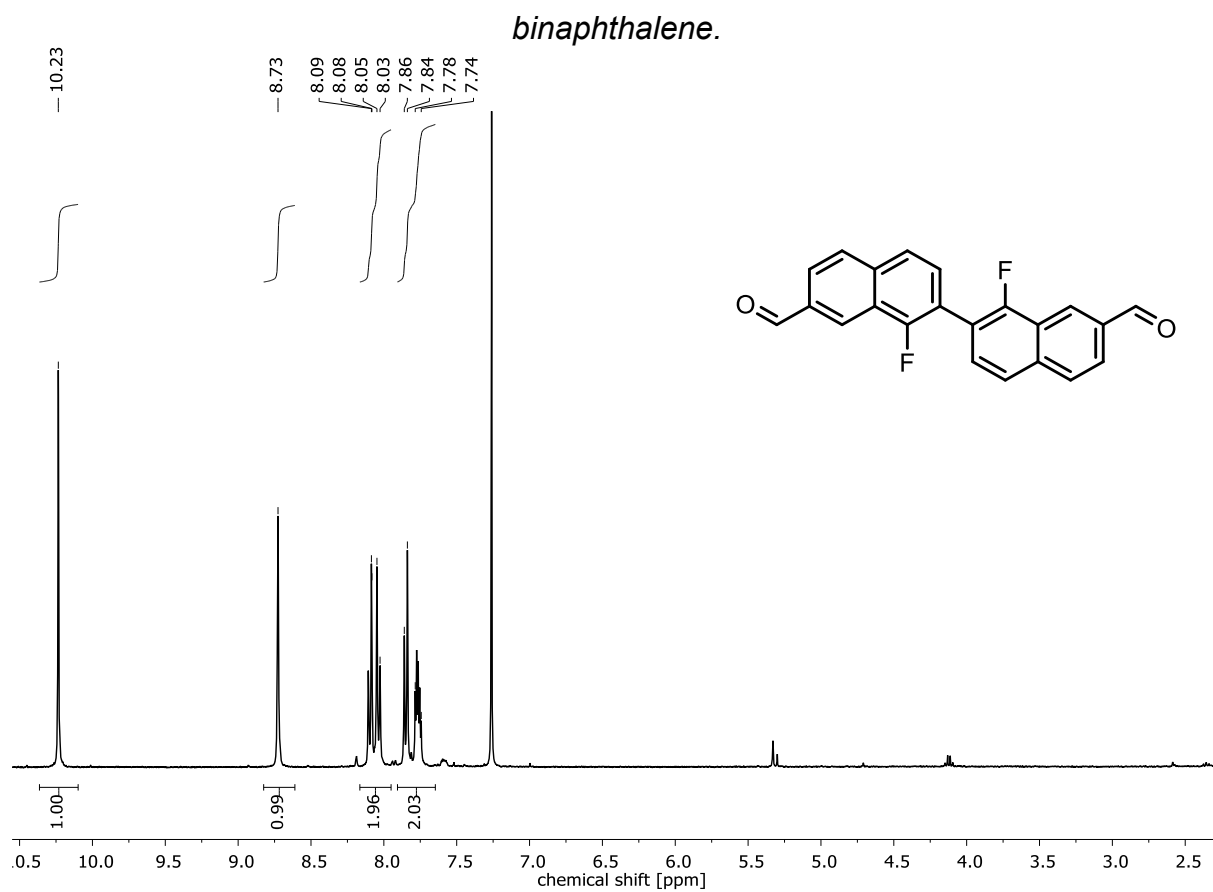


Figure 8.108: $^1\text{H-NMR}$ spectrum of 1,1'-difluoro-[2,2'-binaphthalene]-7,7'-dicarbaldehyde.

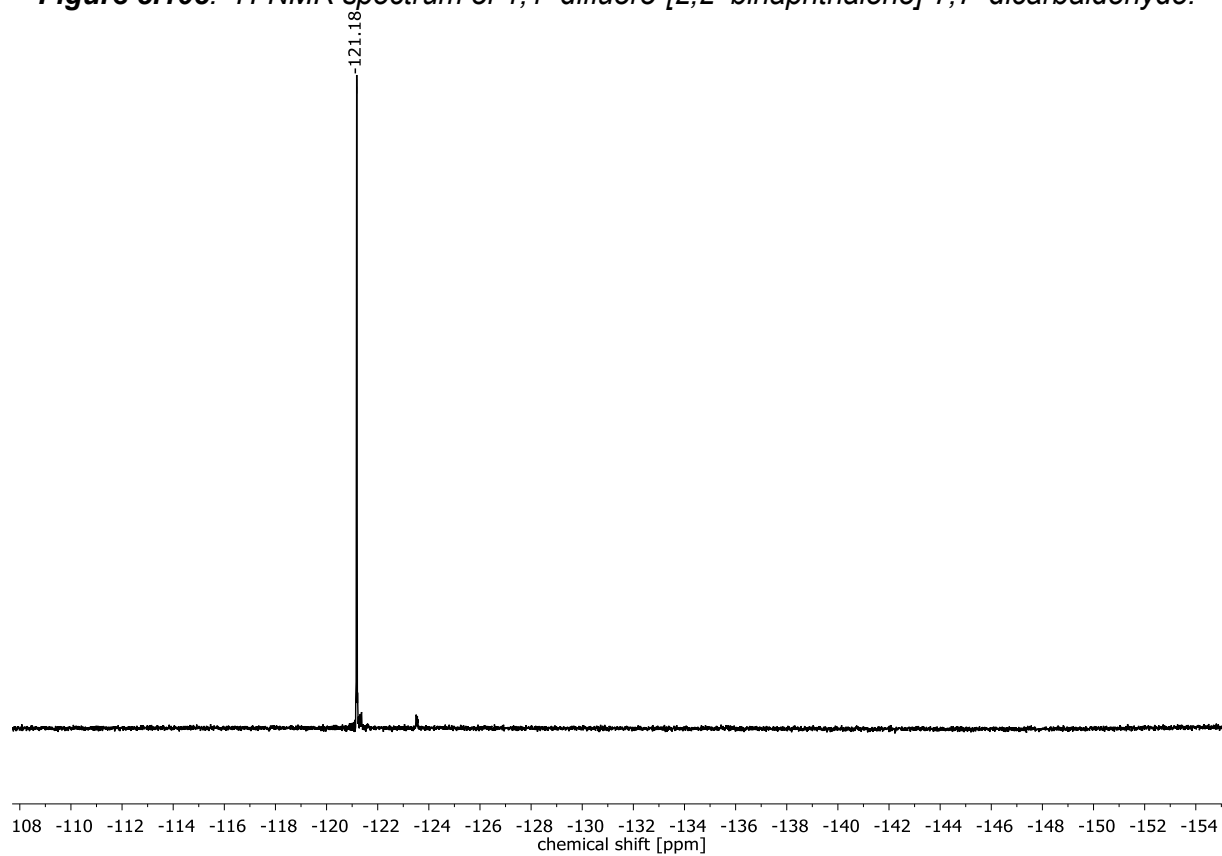


Figure 8.109: ^{19}F -NMR spectrum of 1,1'-difluoro-[2,2'-binaphthalene]-7,7'-dicarbaldehyde.

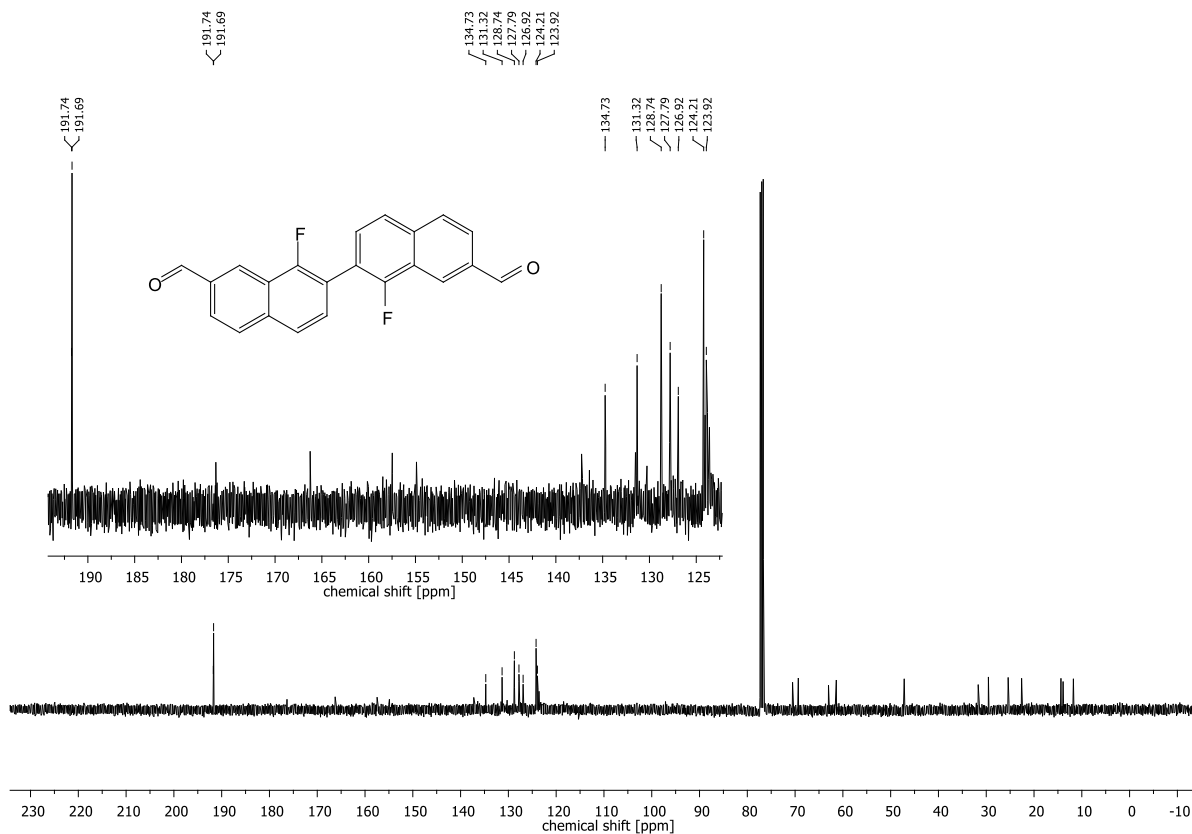


Figure 8.110: ^{13}C -NMR spectrum of 1,1'-difluoro-[2,2'-binaphthalene]-7,7'-dicarbaldehyde

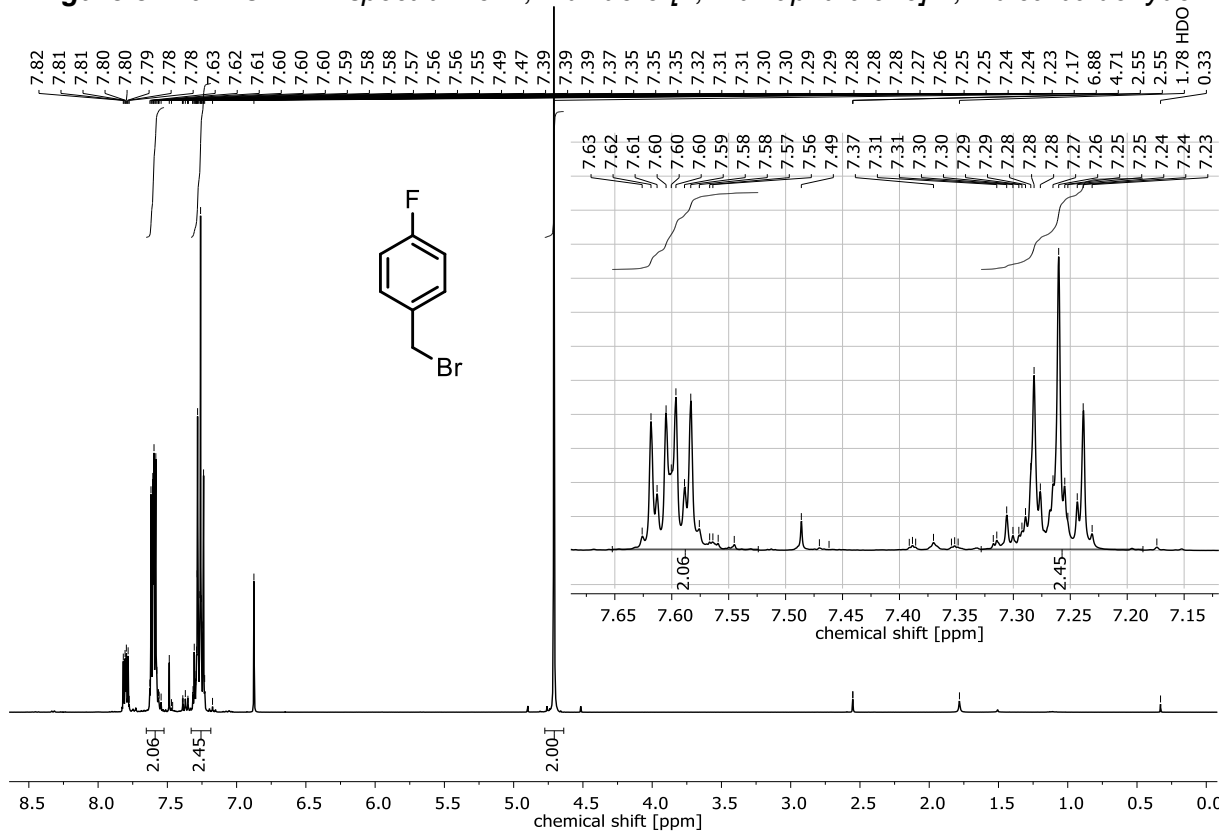
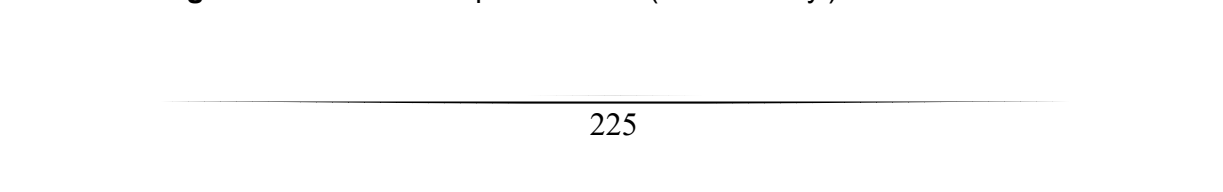


Figure 8.111: ^1H -NMR spectrum of 1-(bromomethyl)-4-fluorobenzene.



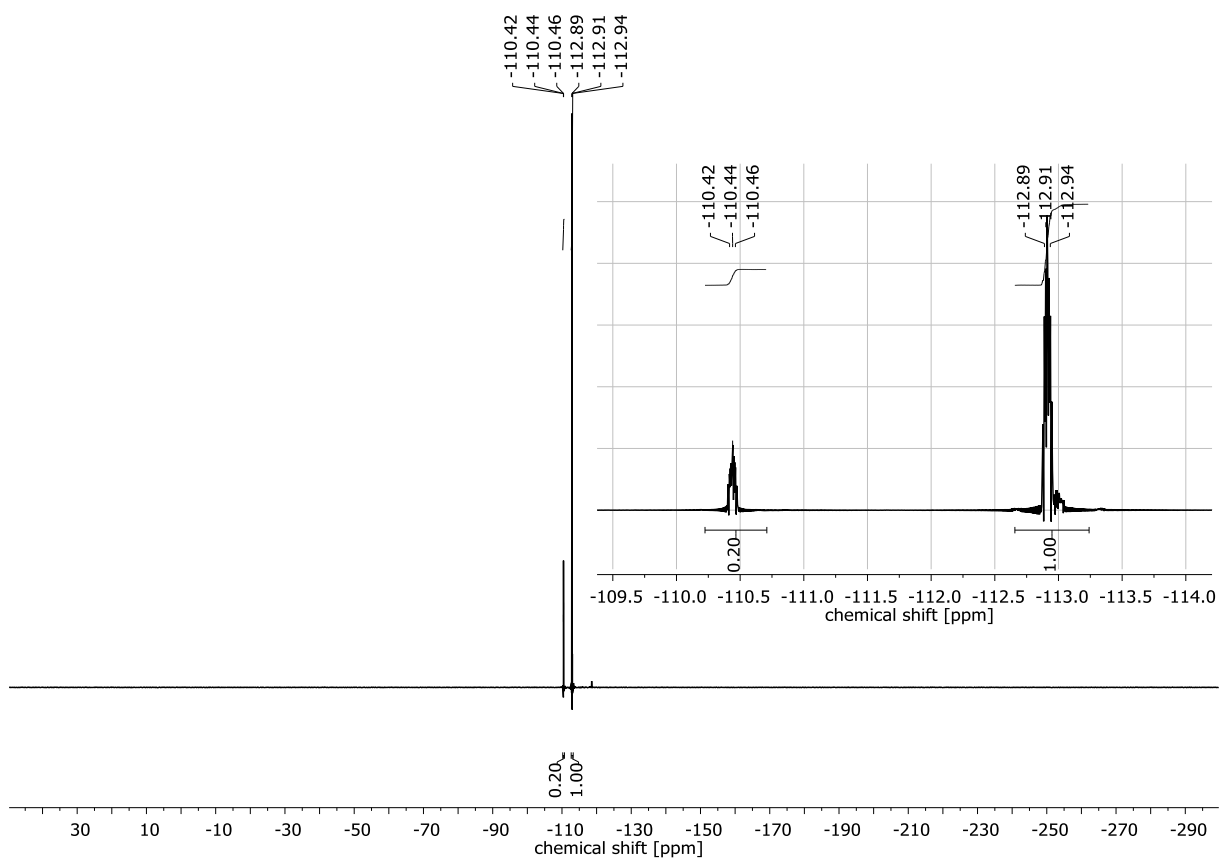


Figure 8.112: ^{19}F -NMR spectrum of 1-(bromomethyl)-4-fluorobenzene.

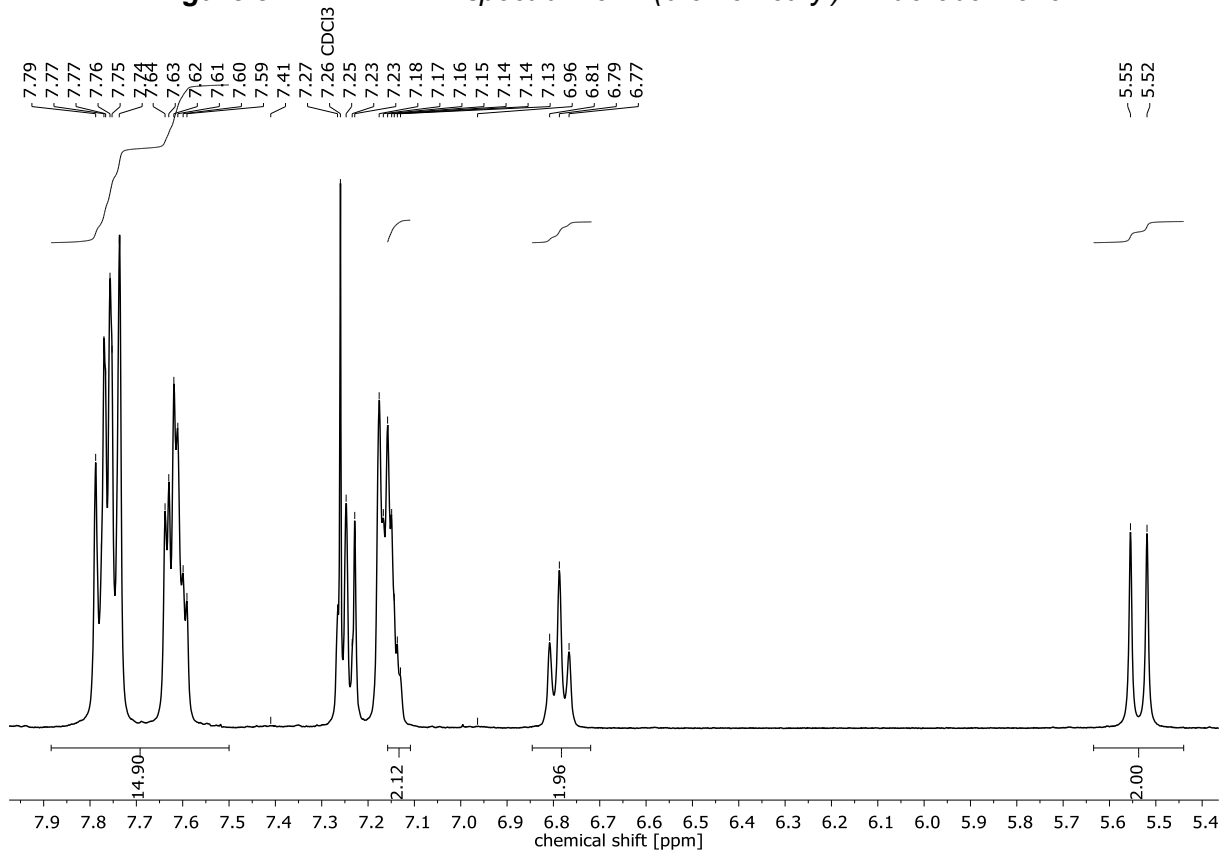


Figure 8.113: ^1H -NMR spectrum of (4-fluorobenzyl)triphenylphosphonium bromide.

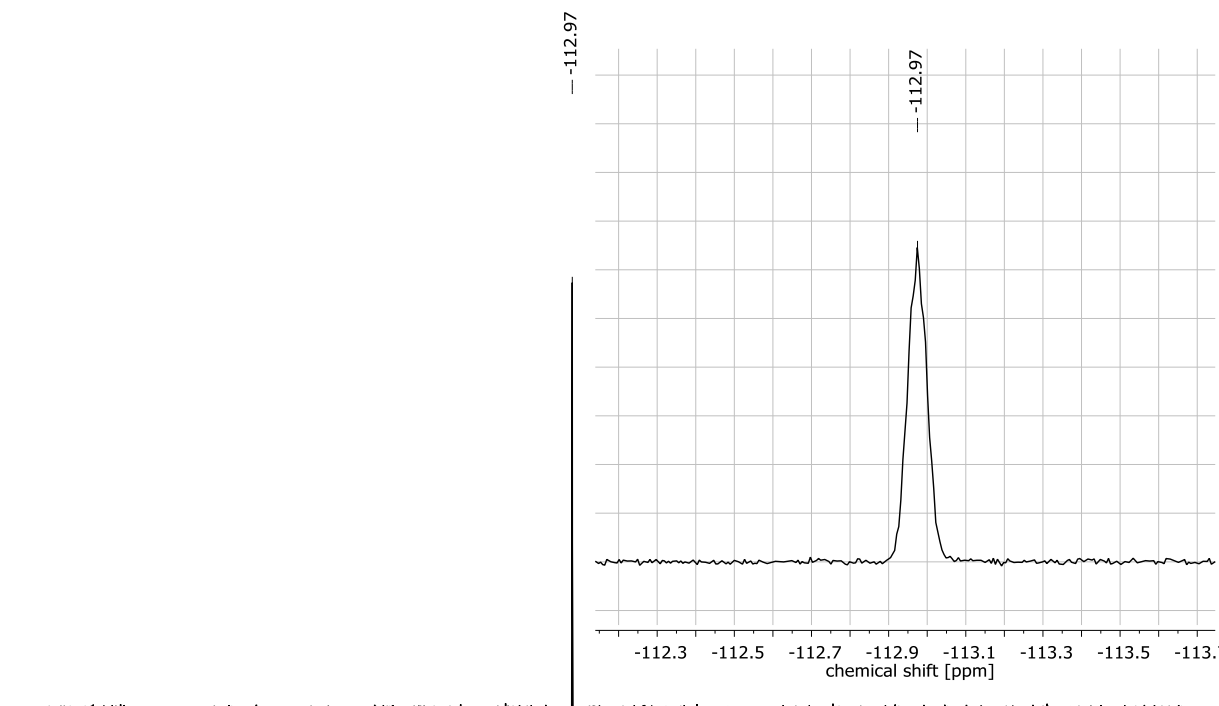


Figure 8.114: ^{19}F -NMR spectrum of (4-fluorobenzyl)triphenylphosphonium bromide.

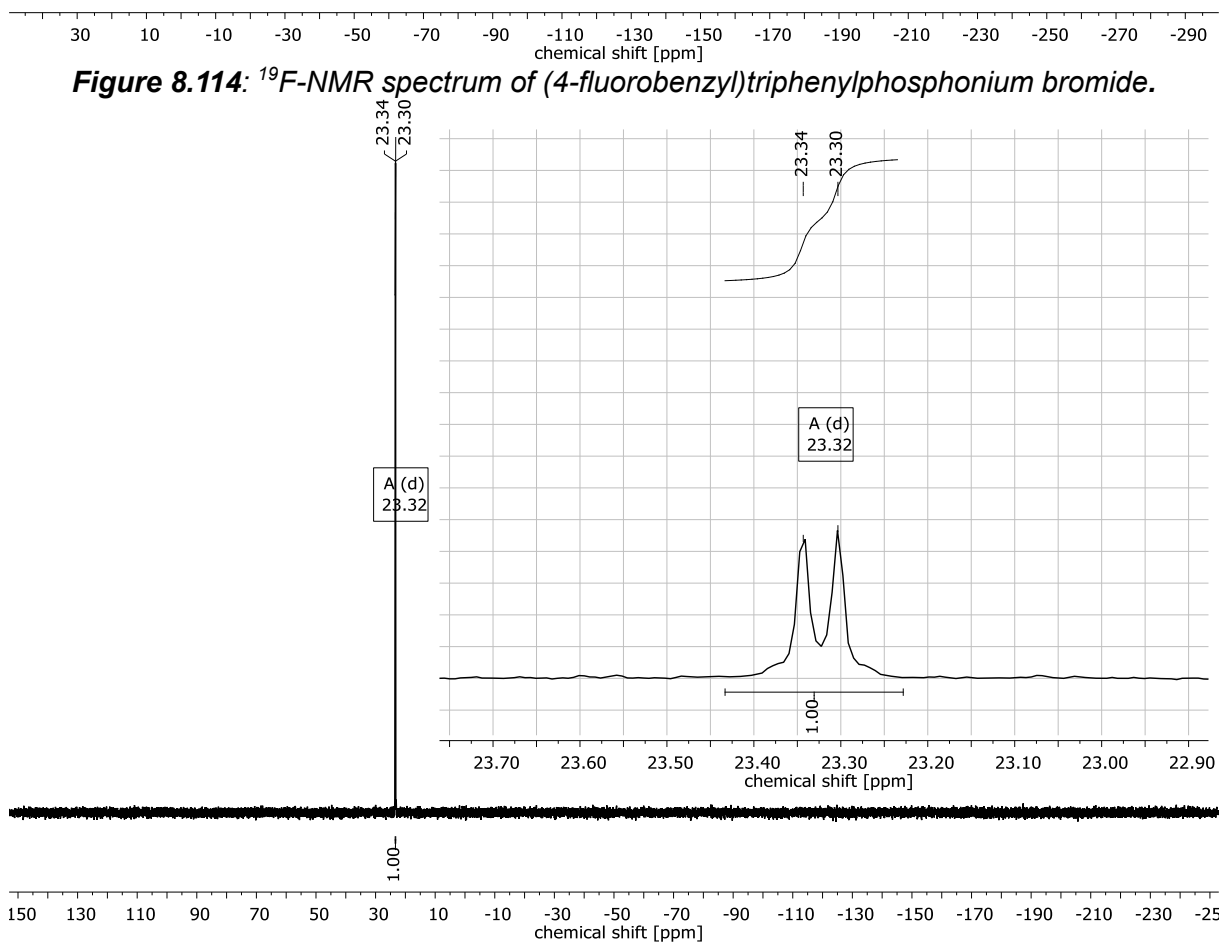


Figure 8.115: ^{31}P -NMR spectrum of (4-fluorobenzyl)triphenylphosphonium bromide.

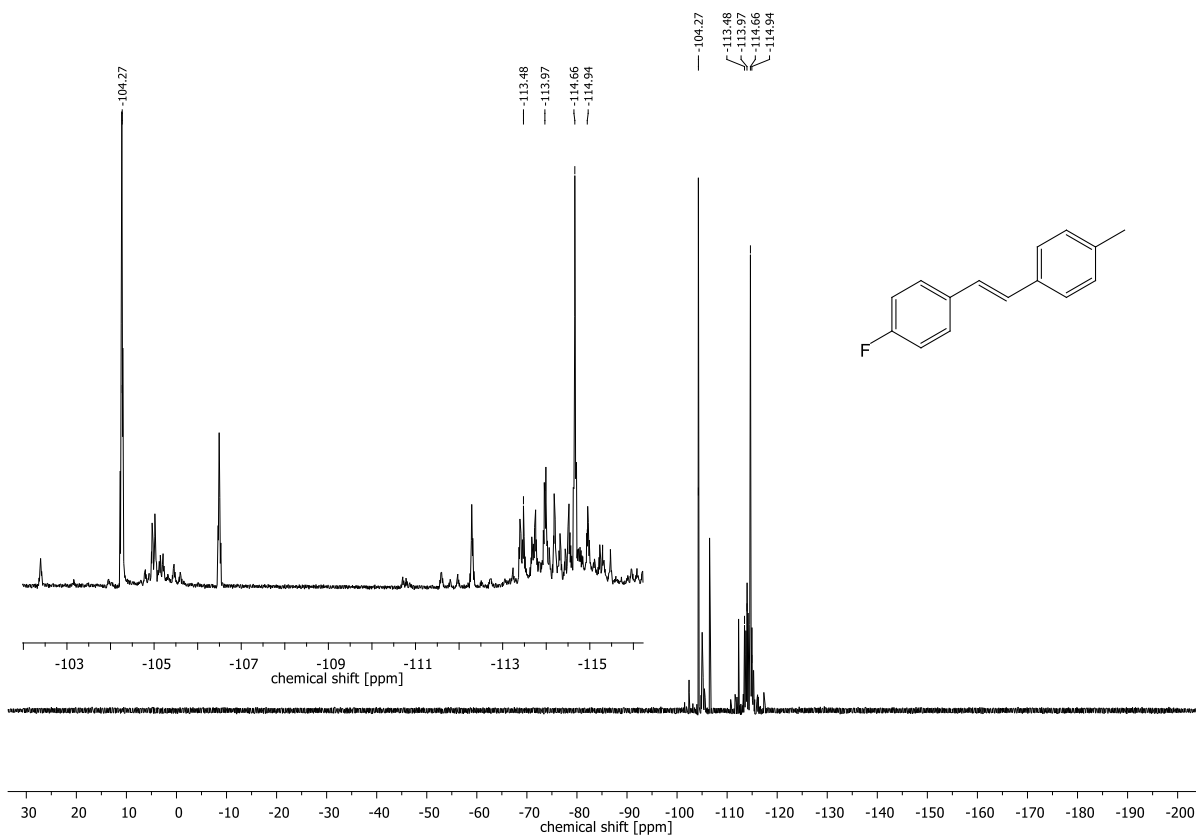
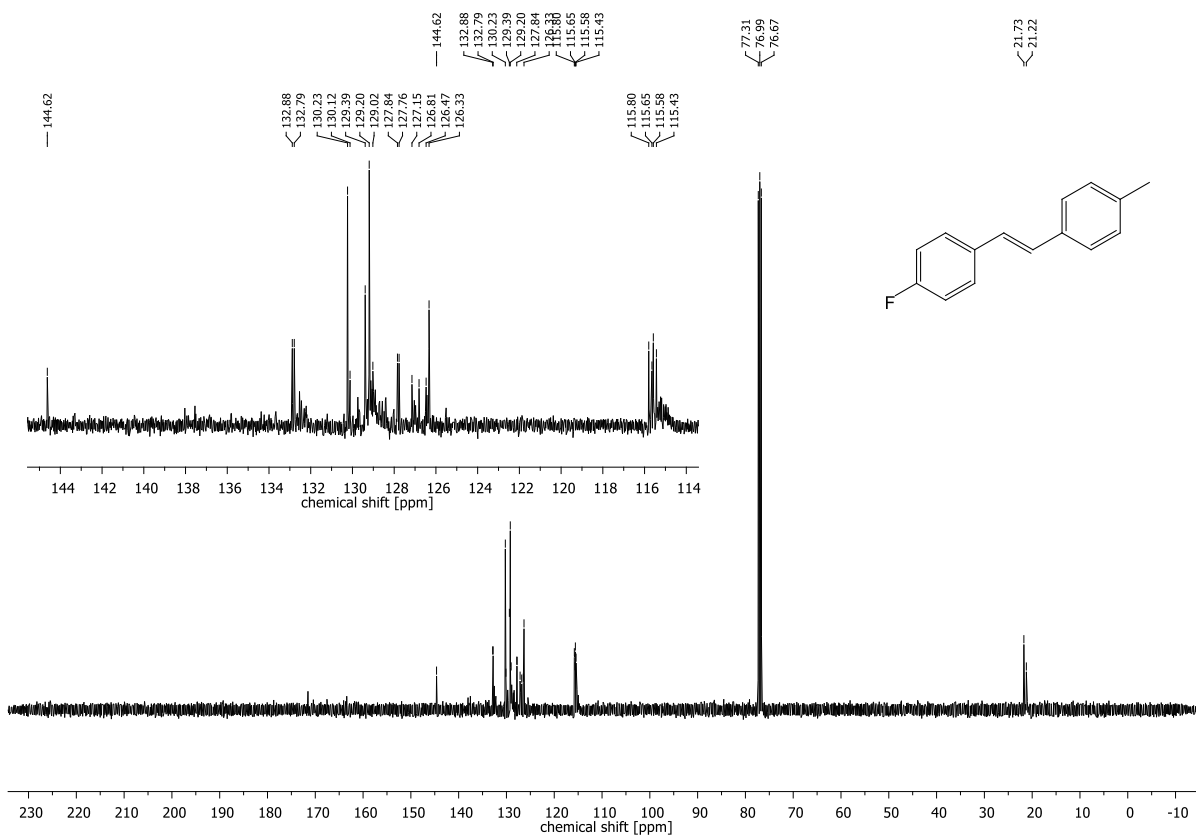


Figure 8.118: ^{19}F -NMR spectrum of 1-fluoro-4-(4-methylstyryl)benzene.



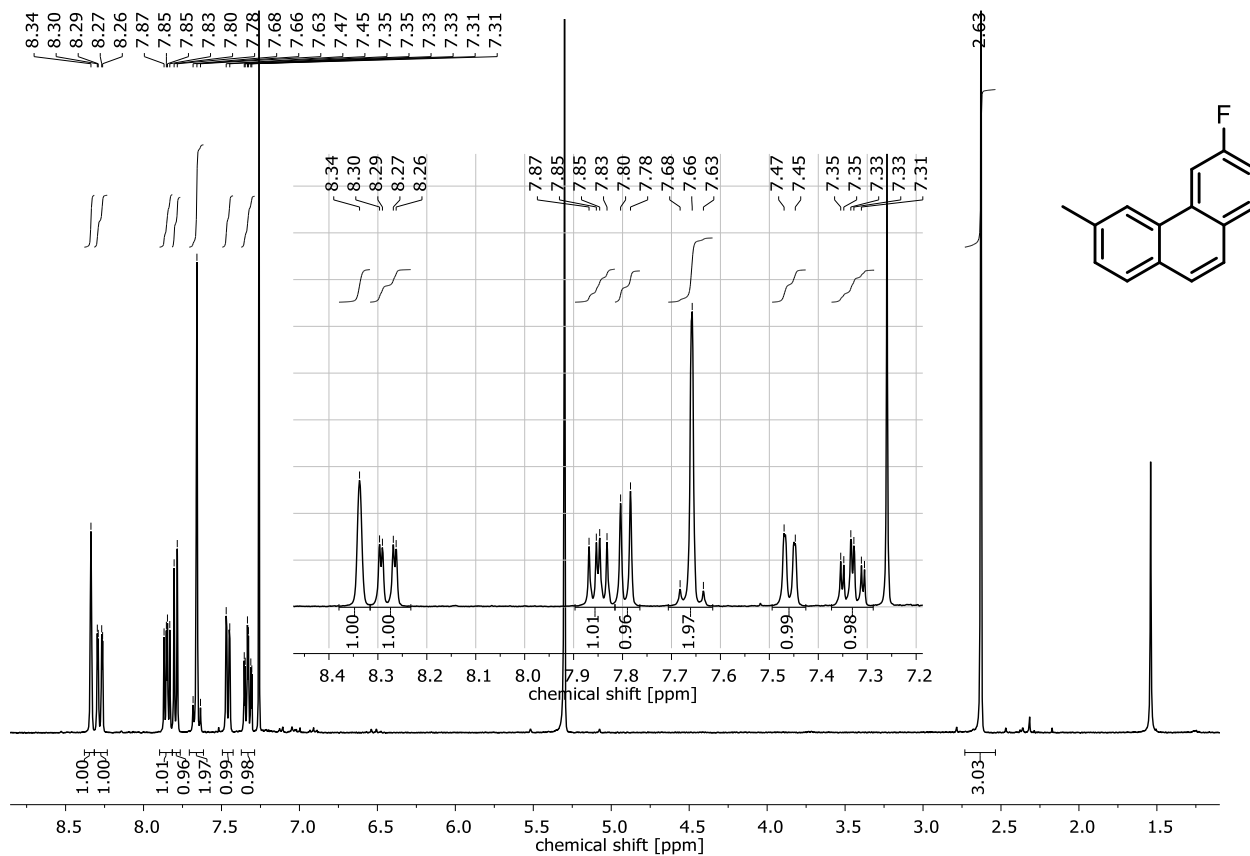


Figure 8.120: ¹H-NMR spectrum of 3-fluoro-6-methylphenanthrene.

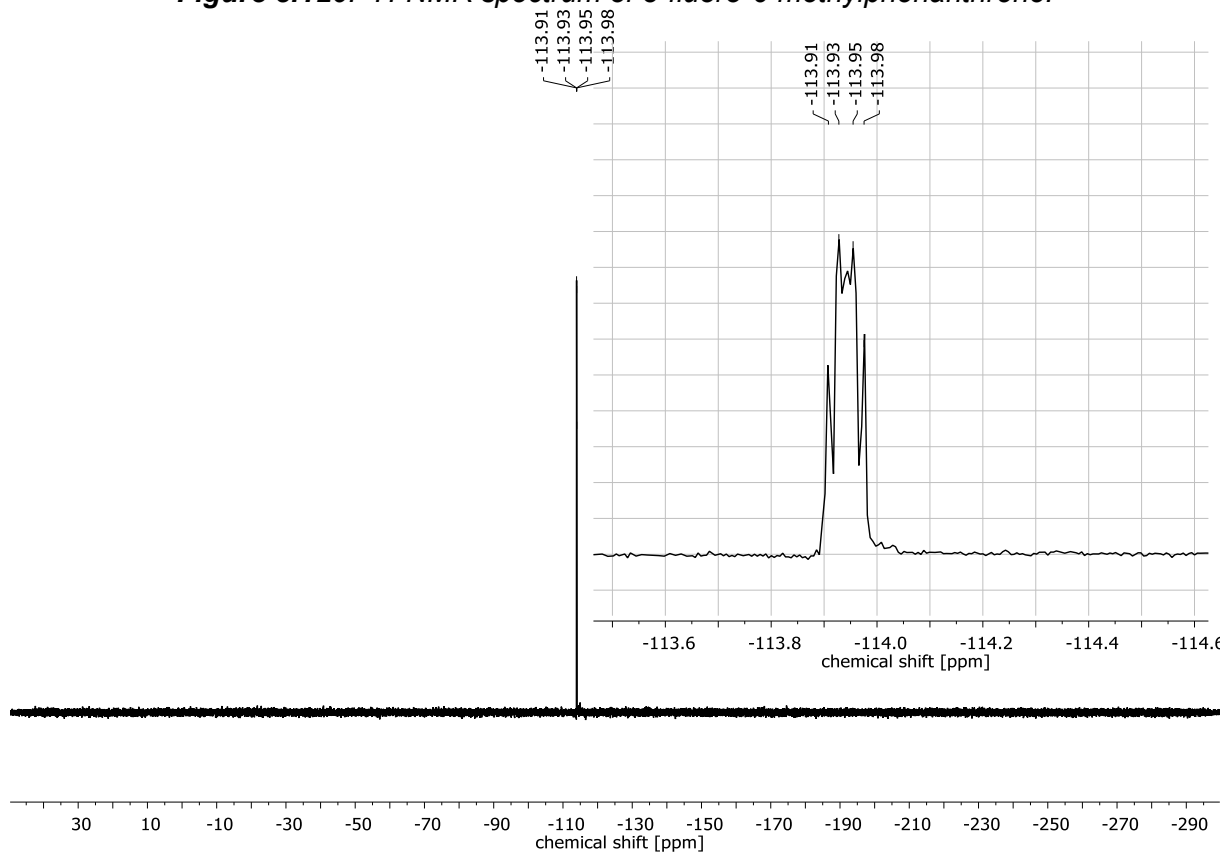


Figure 8.121: ¹⁹F-NMR spectrum of 3-fluoro-6-methylphenanthrene.

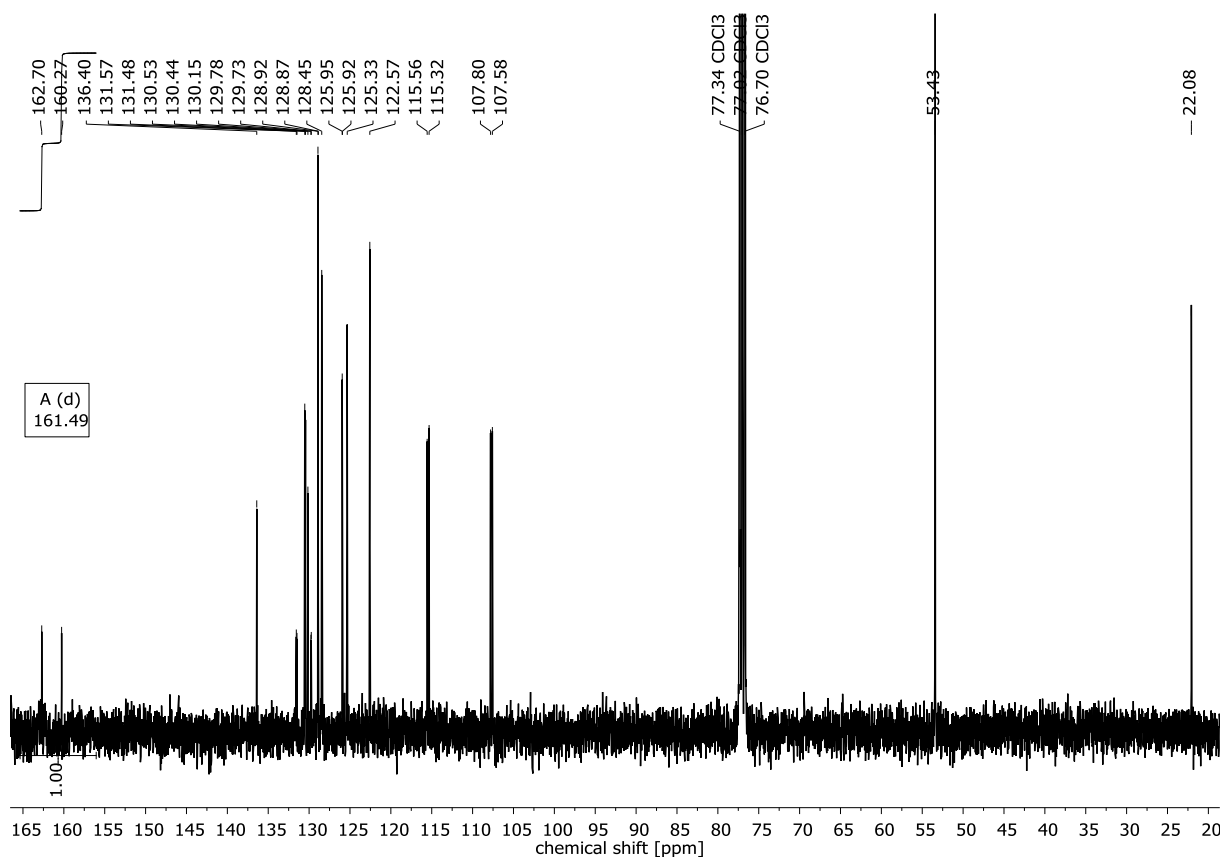


Figure 8.122: ^{13}C -NMR spectrum of 3-fluoro-6-methylphenanthrene.

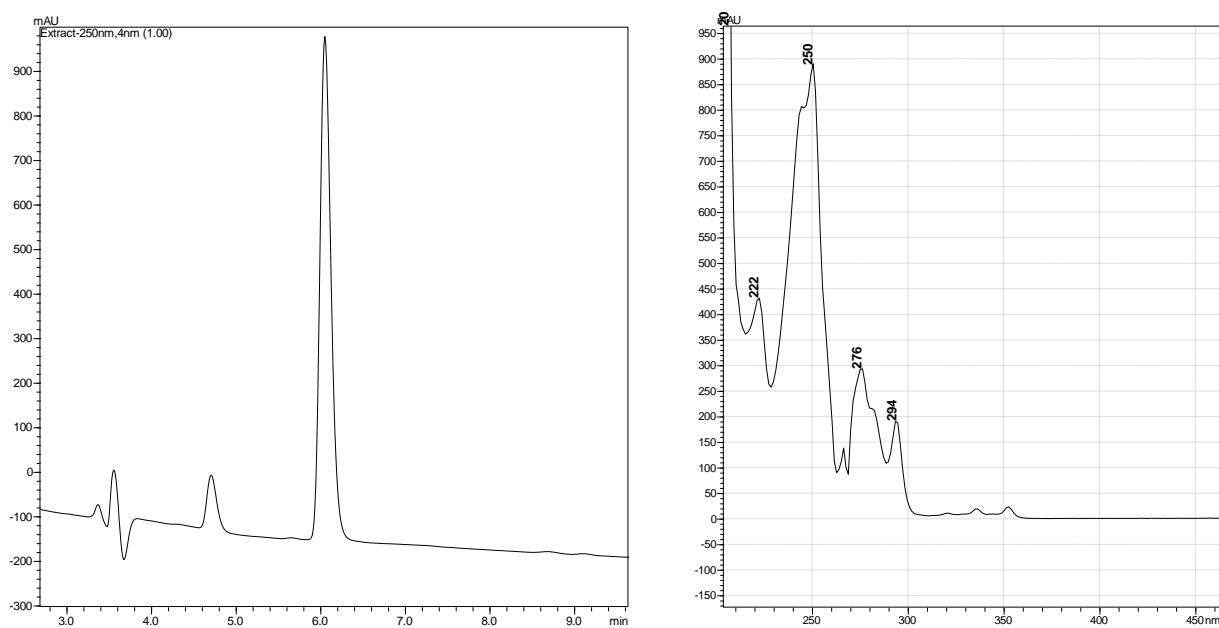


Figure 8.123: HPLC chromatogram of 3-fluoro-6-methylphenanthrene (PBr column, 1.0 mL/min, 35°C MeOH/DCM 70/30). (right) UV/vis spectrum of 3-fluoro-6-methylphenanthrene.

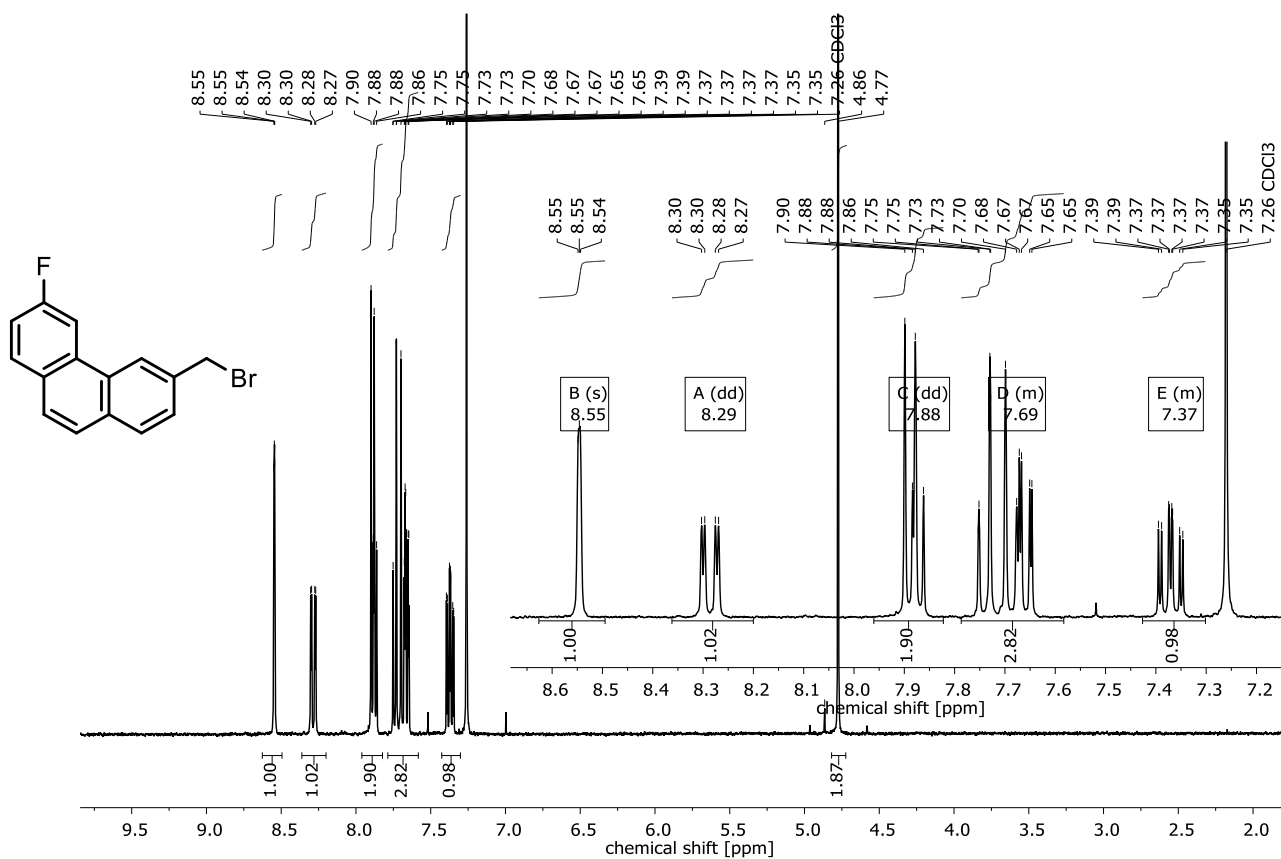


Figure 8.124: ¹H-NMR spectrum of 3-(bromomethyl)-6-fluorophenanthrene.

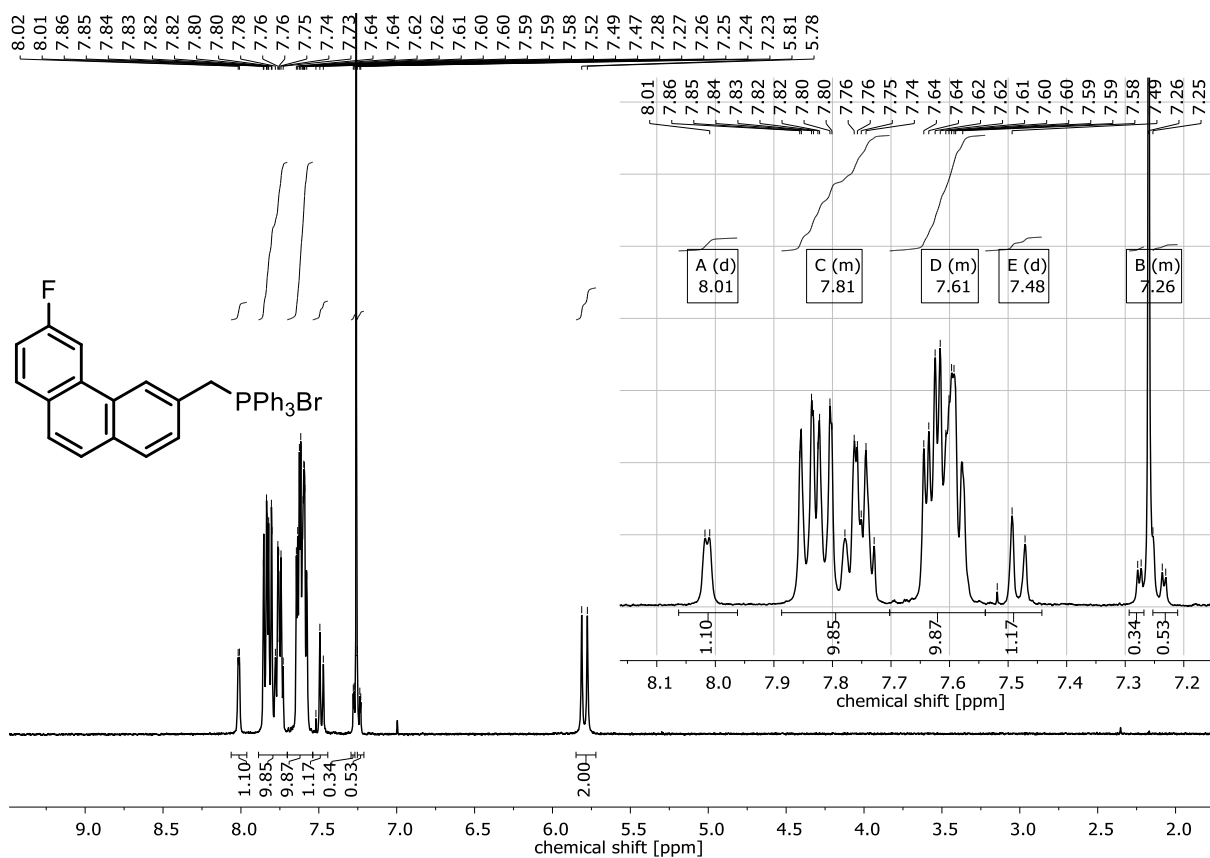


Figure 8.125: ¹H-NMR spectrum of bromo((6-fluorophenanthren-3-yl)methyl)triphenyl-15-

phosphane.

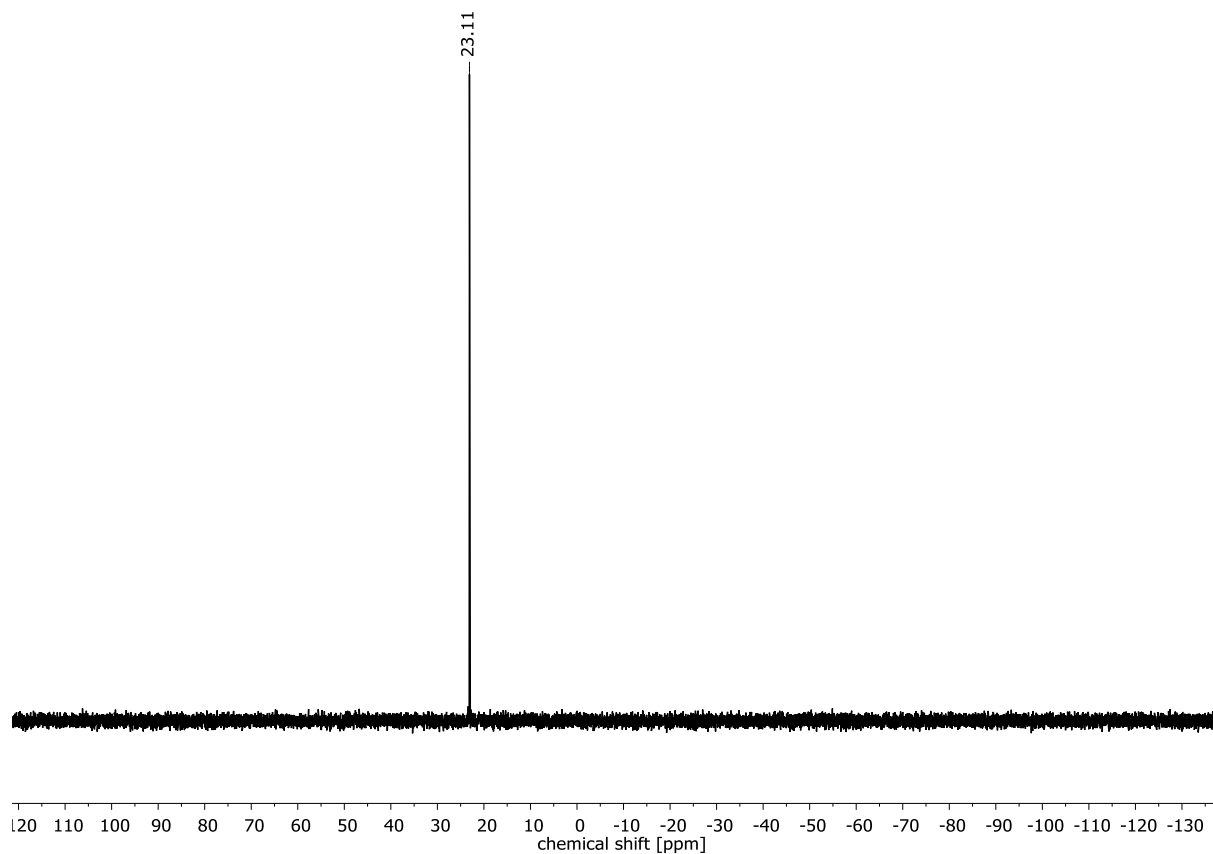


Figure 8.126: ^{31}P -NMR spectrum of bromo((6-fluorophenanthren-3-yl)methyl)triphenyl-15-

phosphane.

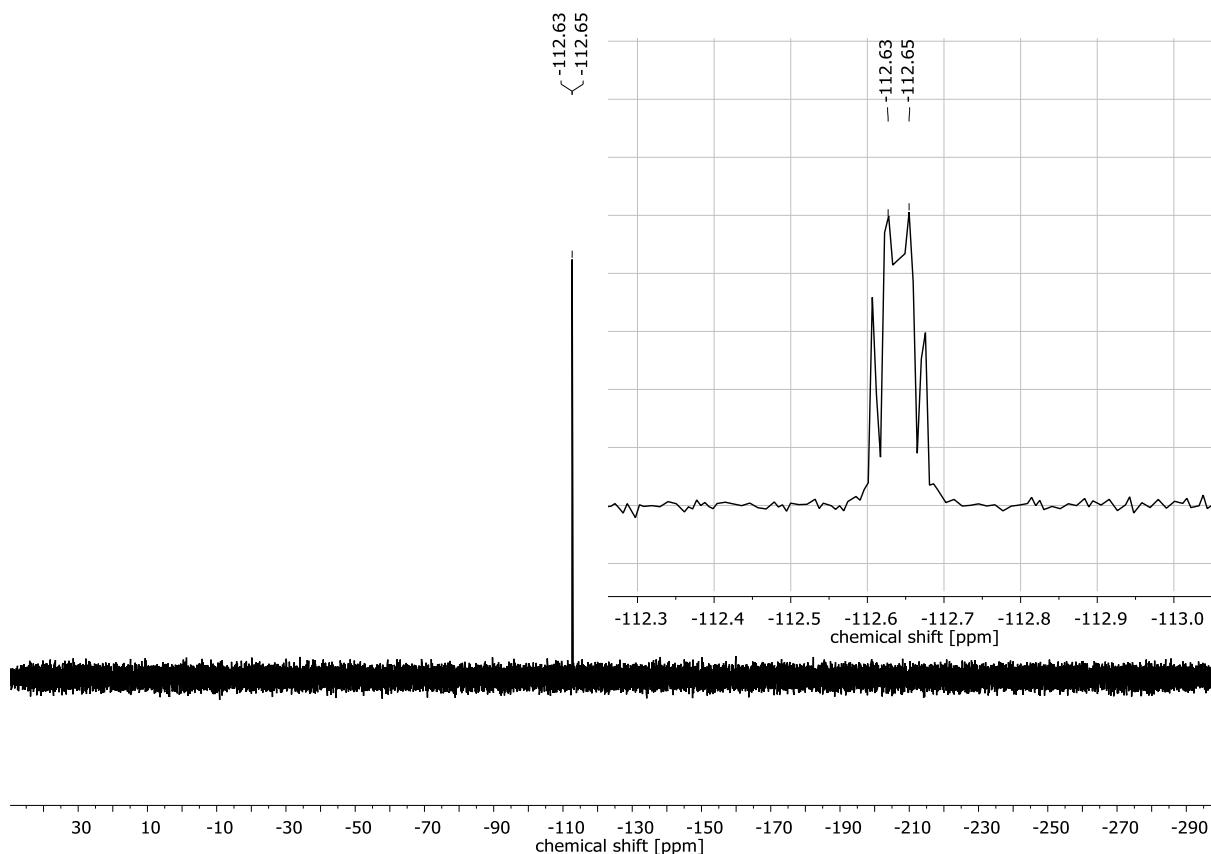


Figure 8.127: ^{19}F -NMR spectrum of bromo((6-fluorophenanthren-3-yl)methyl)triphenyl-15-phosphane.

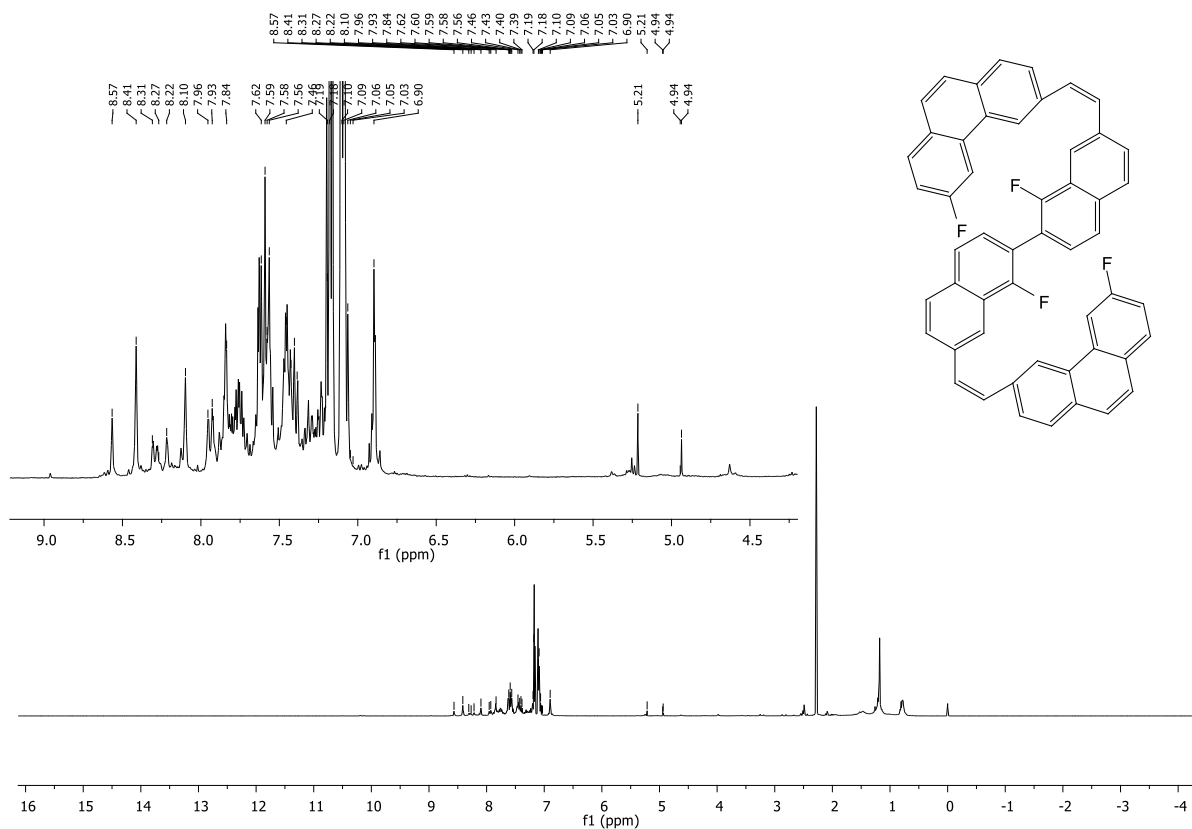


Figure 8.128: ¹H-NMR spectrum of (6,6'-((1,1'-difluoro-[2,2'-binaphthalene]-7,7'-diyl)bis(ethene-2,1-diyl))bis(3-fluorophenanthrene).

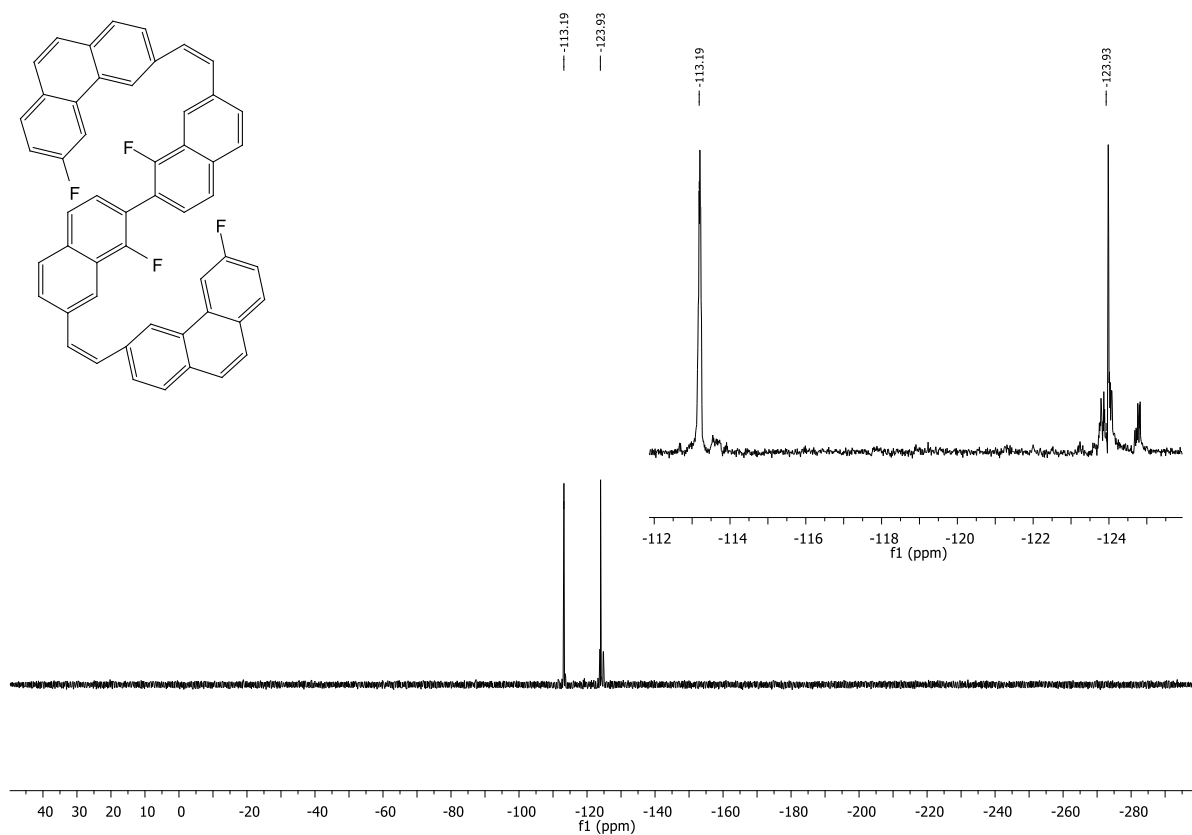


Figure 8.129: ¹⁹F-NMR spectrum of (6,6'-((1,1'-difluoro-[2,2'-binaphthalene]-7,7'-diyl)bis(ethene-2,1-diyl))bis(3-fluorophenanthrene).

8.1.8 Synthesis of 1-(2,3-difluorophenyl)-8-(2-fluorophenyl)phenanthrene

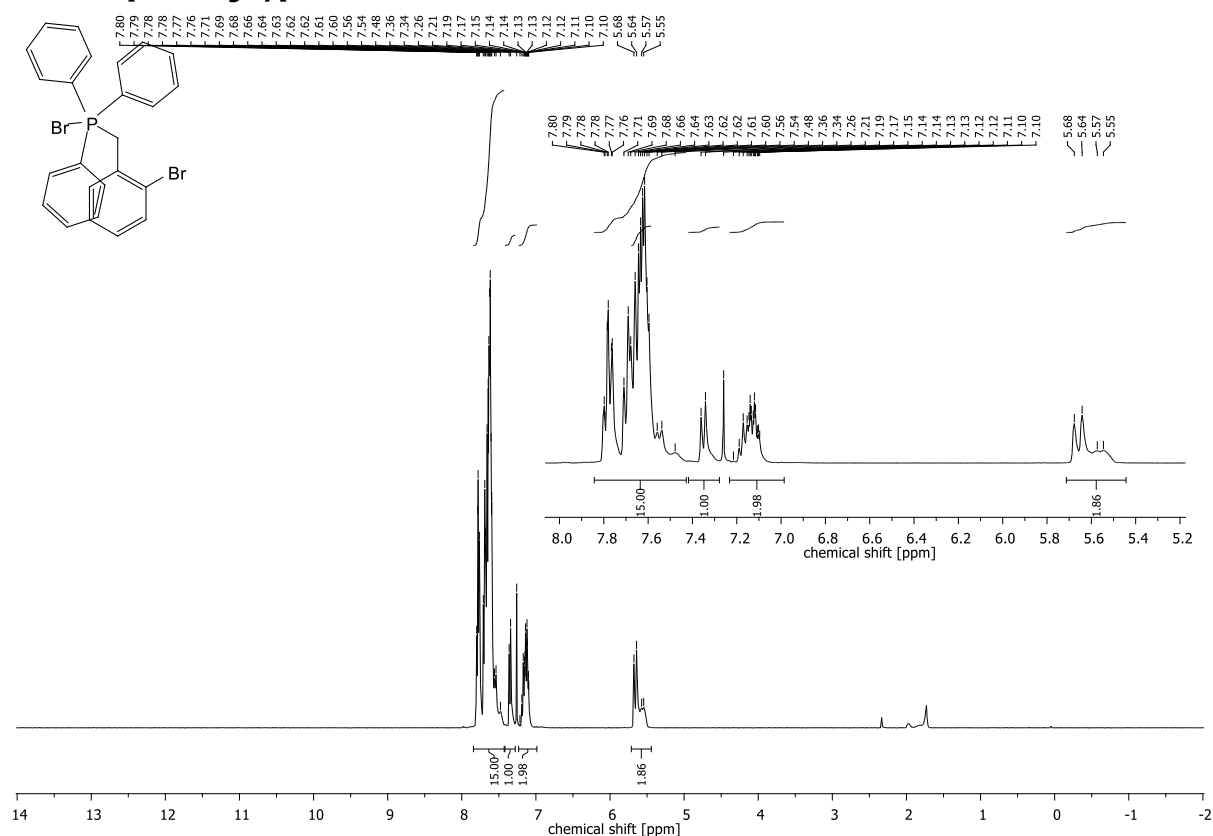


Figure 8.132: $^1\text{H-NMR}$ spectrum of bromo(2-bromobenzyl)triphenyl-15-phosphane.

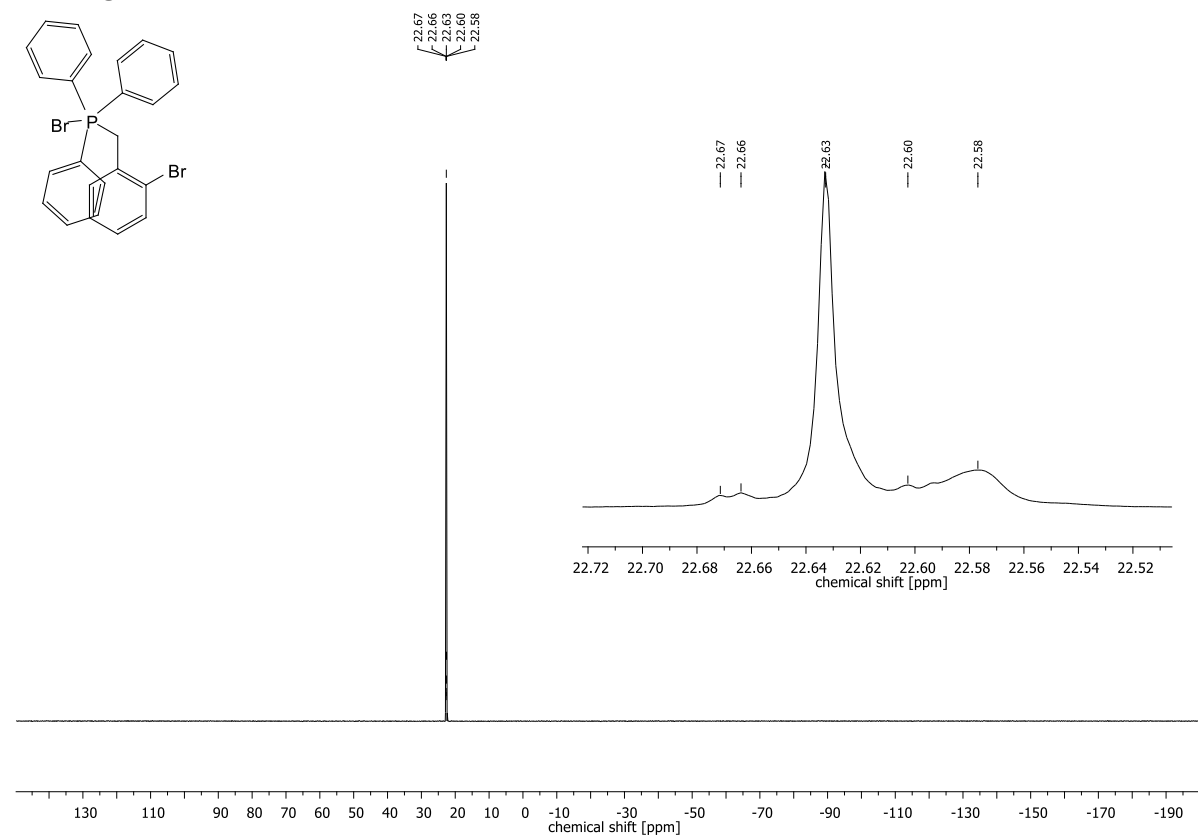


Figure 8.133: ^{31}P -NMR spectrum of bromo(2-bromobenzyl)triphenyl-1 λ -phosphane.

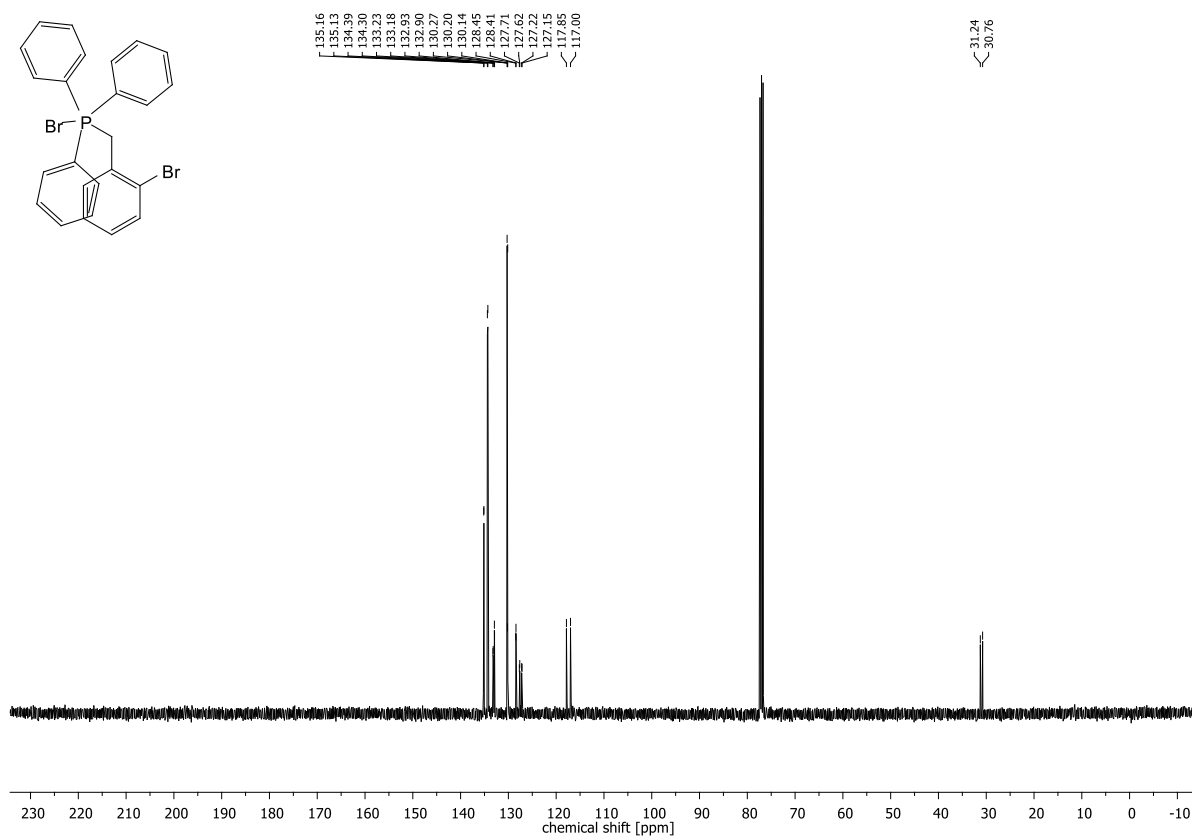


Figure 8.134: ^{13}C -NMR spectrum of bromo(2-bromobenzyl)triphenyl-1 λ -phosphane.

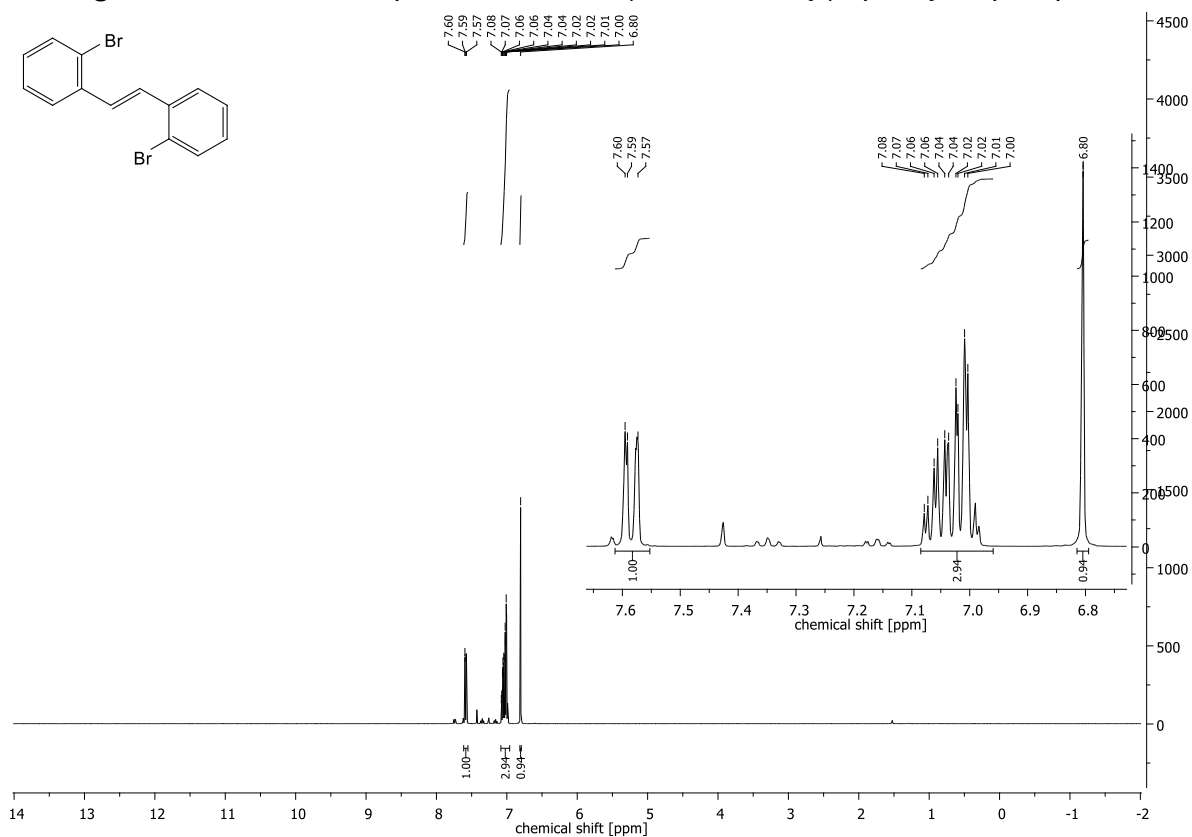
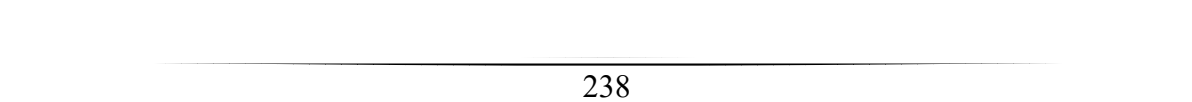


Figure 8.135: ^1H -NMR spectrum of 1,2-bis(2-bromophenyl)ethene.



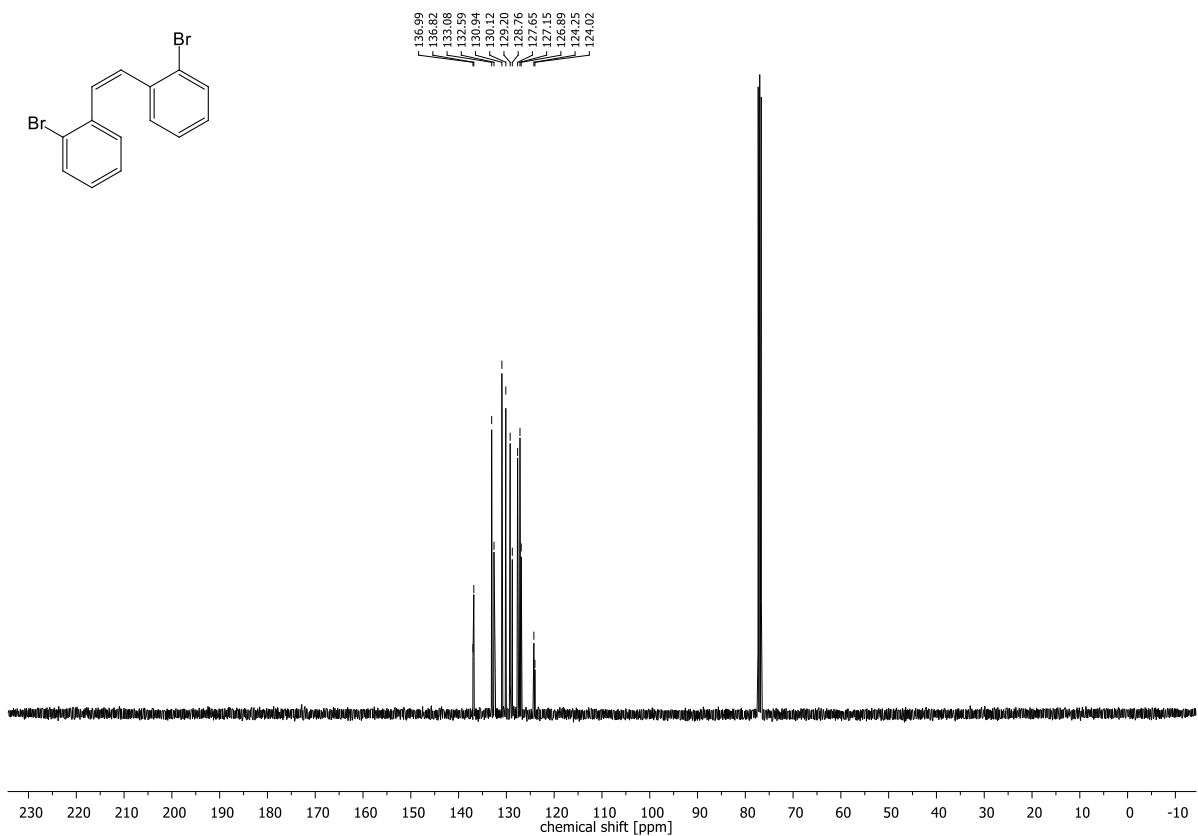


Figure 8.136: $^{13}\text{C-NMR}$ spectrum of 1,2-bis(2-bromophenyl)ethene.

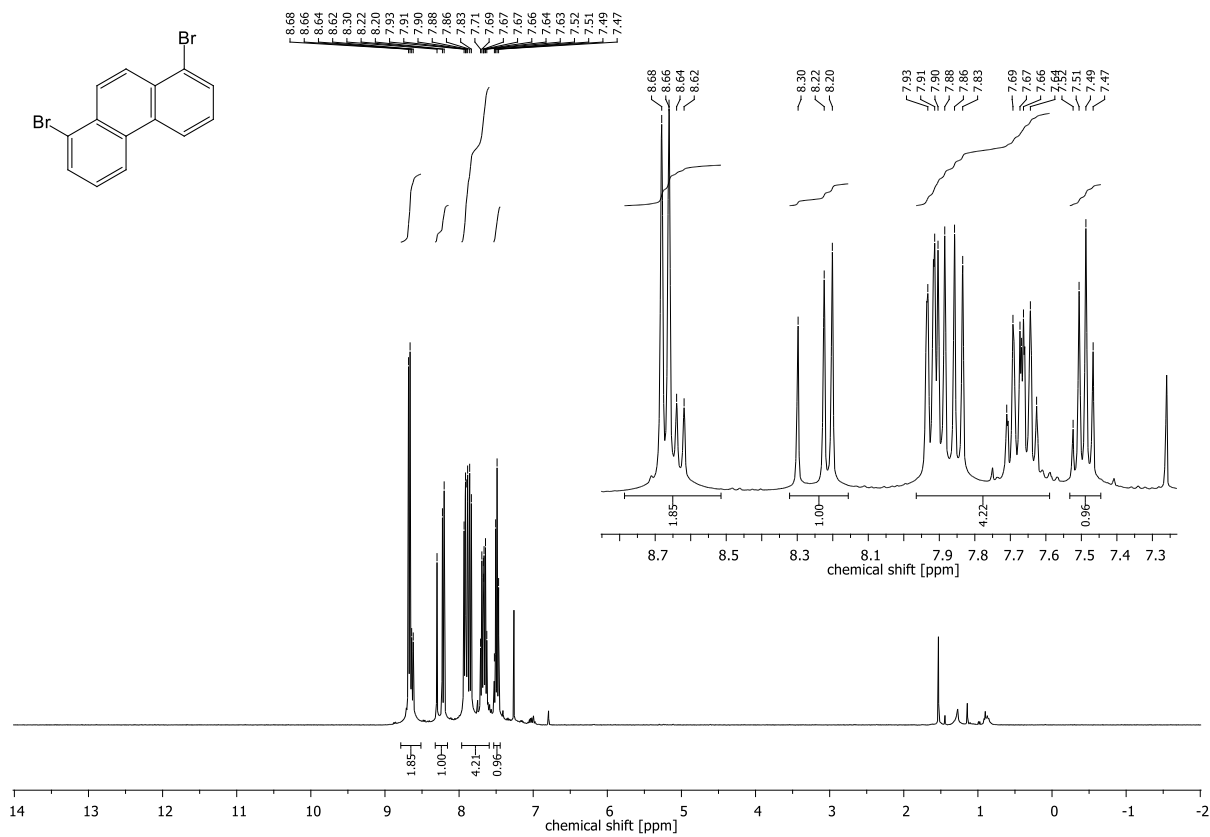


Figure 8.137: $^1\text{H-NMR}$ spectrum of 1,8-dibromophenanthrene.

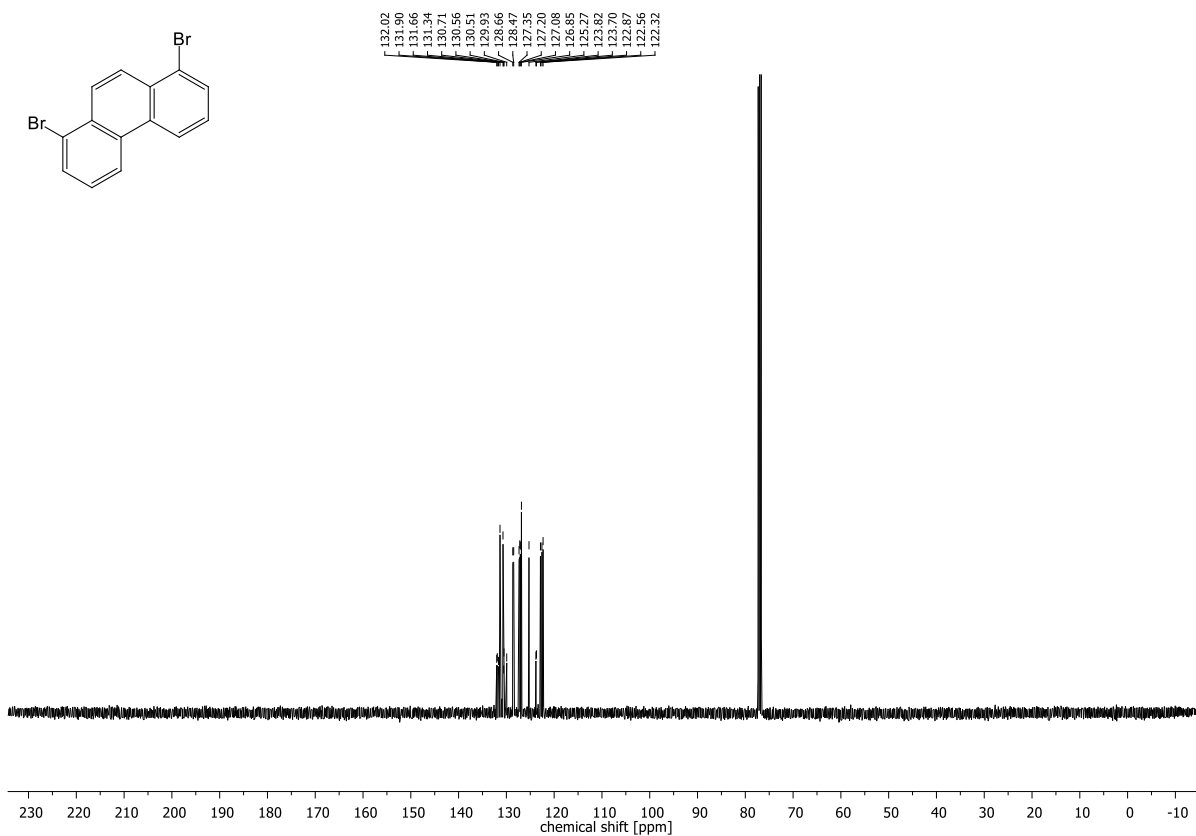


Figure 8.138: ^{13}C -NMR spectrum of 1,8-dibromophenanthrene.

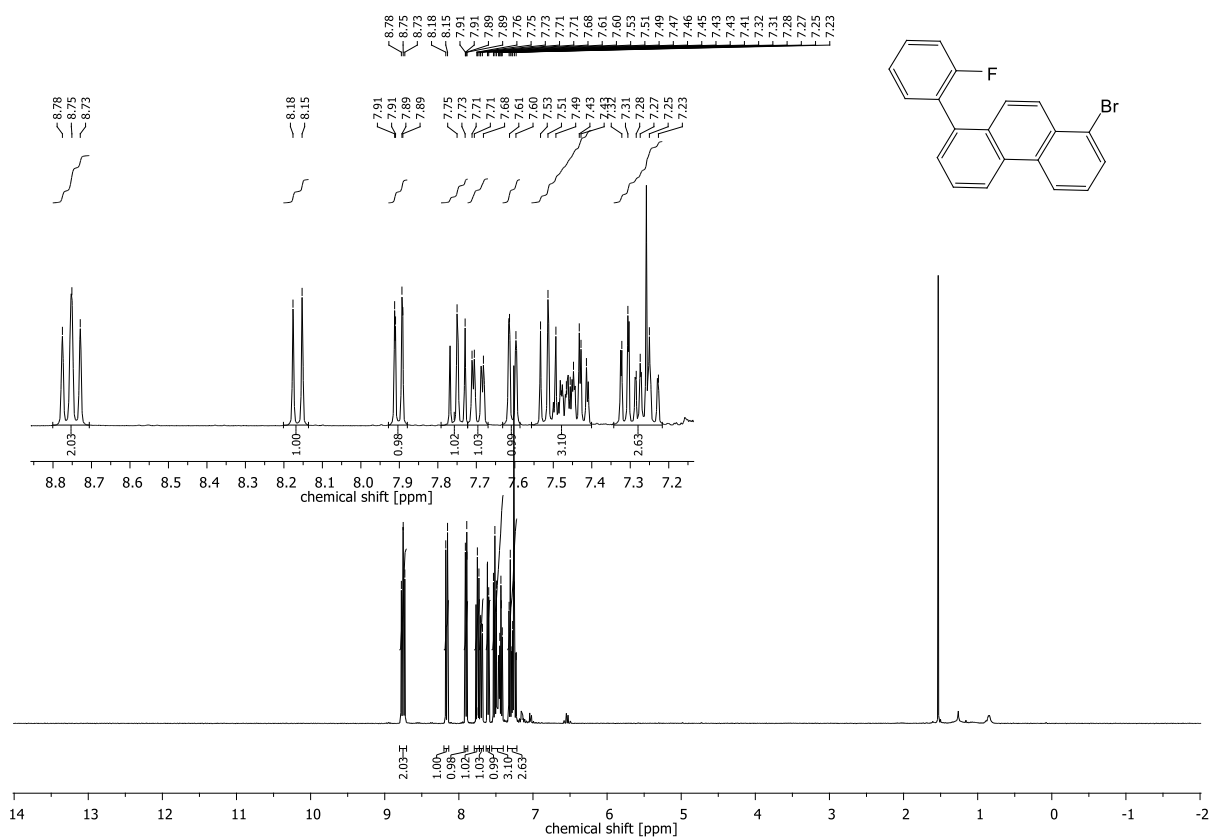


Figure 8.139: ^1H -NMR spectrum of 1-bromo-8-(2-fluorophenyl)phenanthrene.

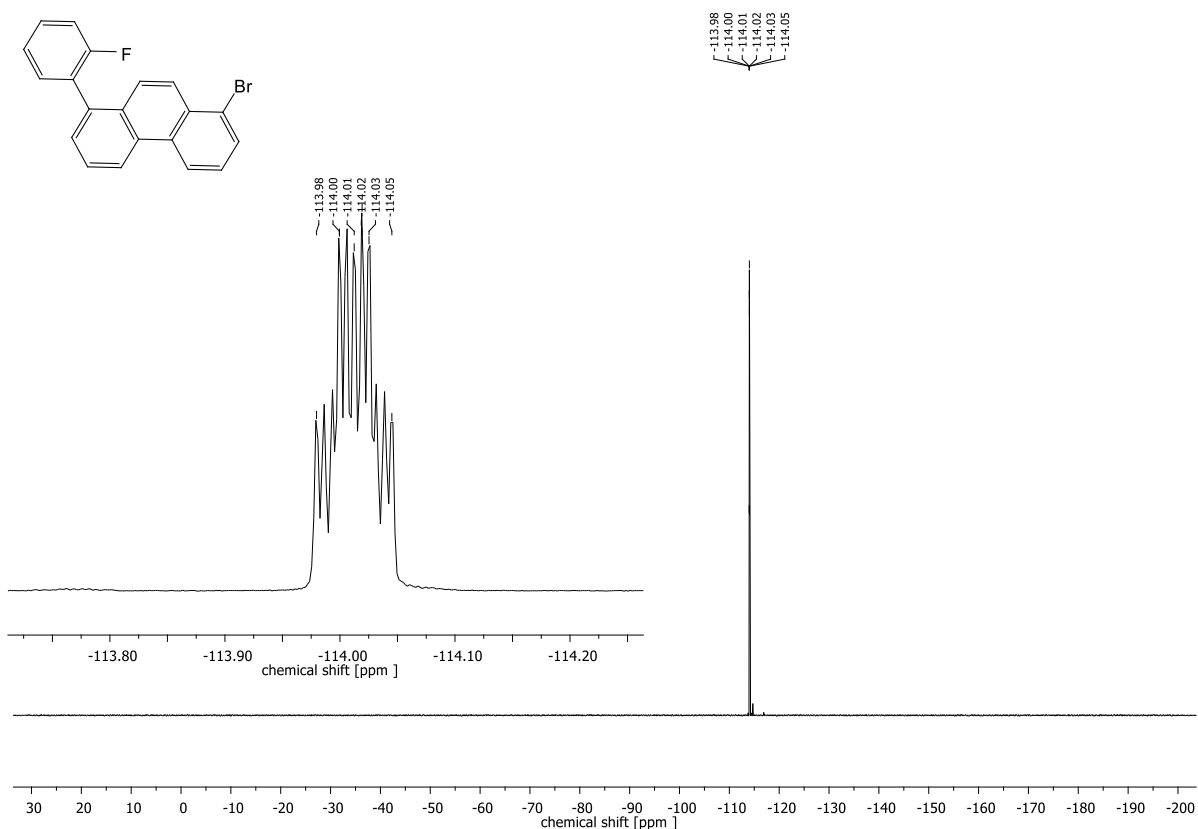


Figure 8.140: ^{19}F -NMR spectrum of 1-bromo-8-(2-fluorophenyl)phenanthrene.

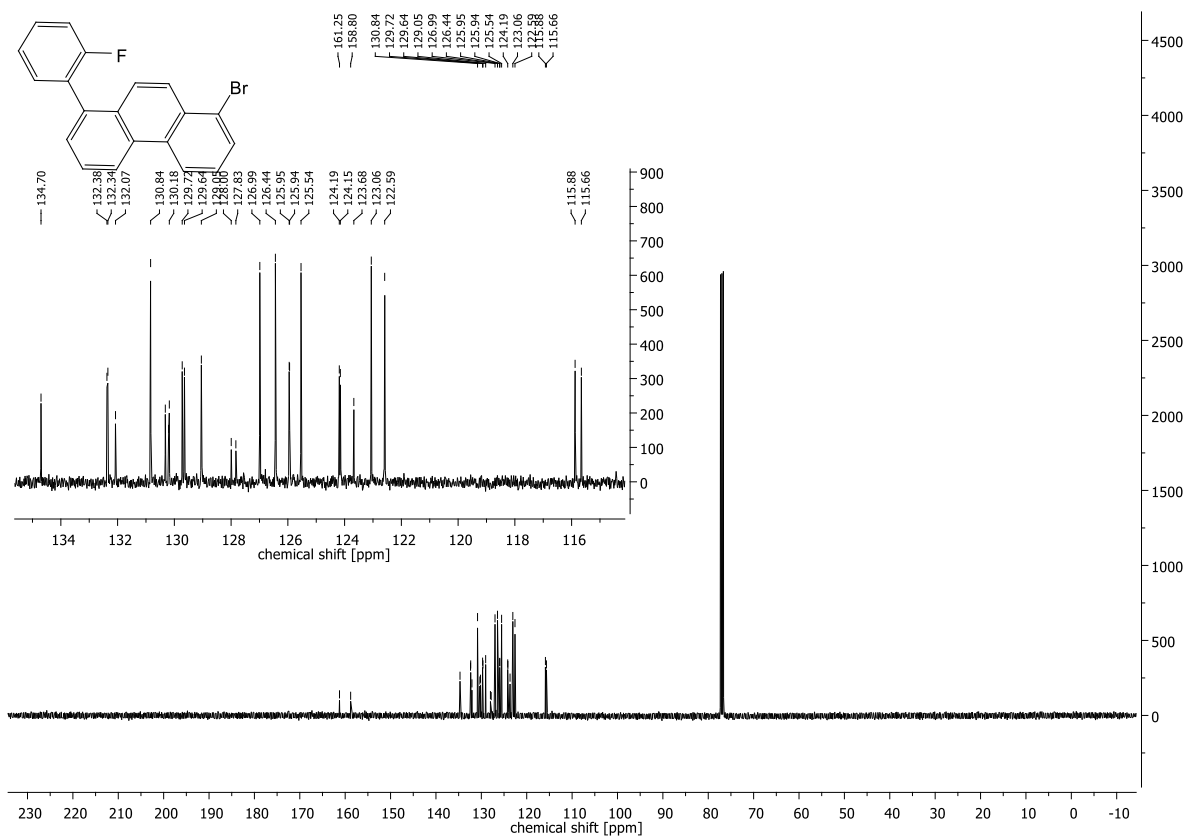


Figure 8.141: ^{13}C -NMR spectrum of 1-bromo-8-(2-fluorophenyl)phenanthrene.

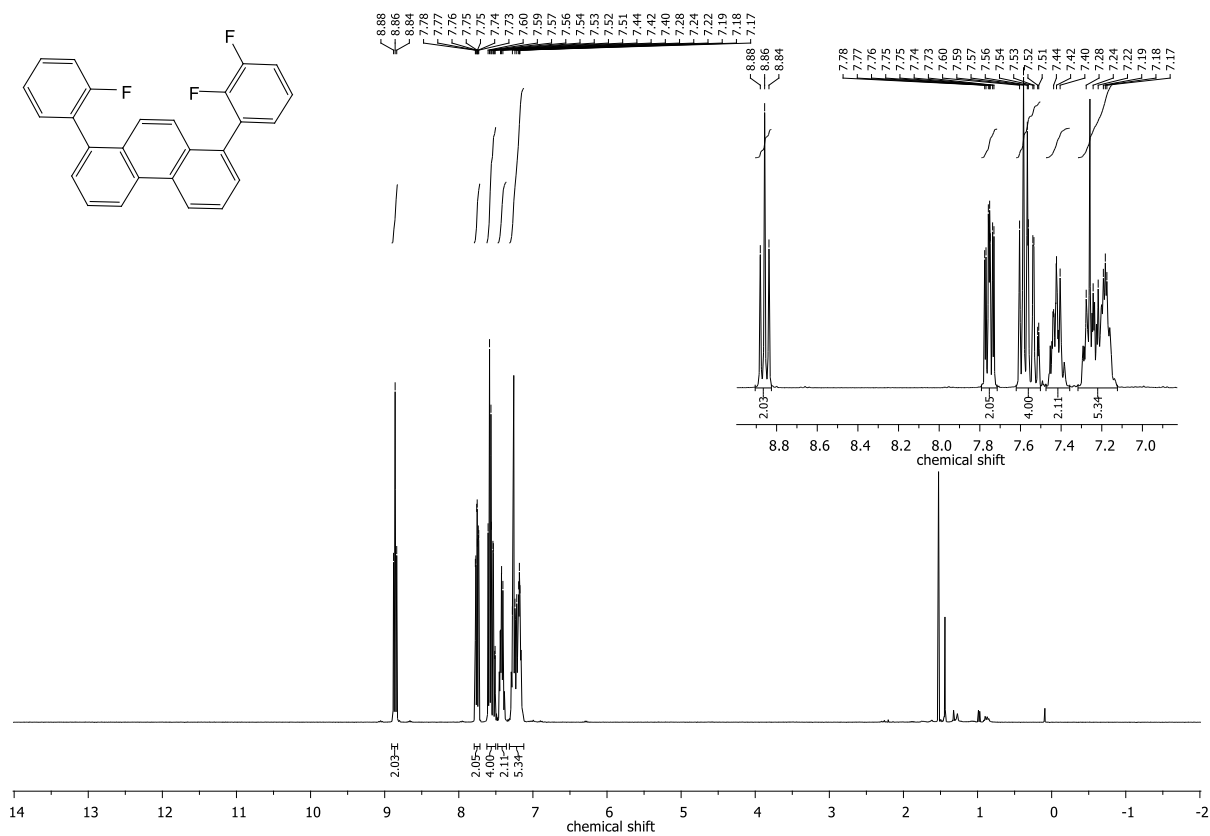


Figure 8.142: $^1\text{H-NMR}$ spectrum of 1-(2,3-difluorophenyl)-8-(2-fluorophenyl)phenanthrene.

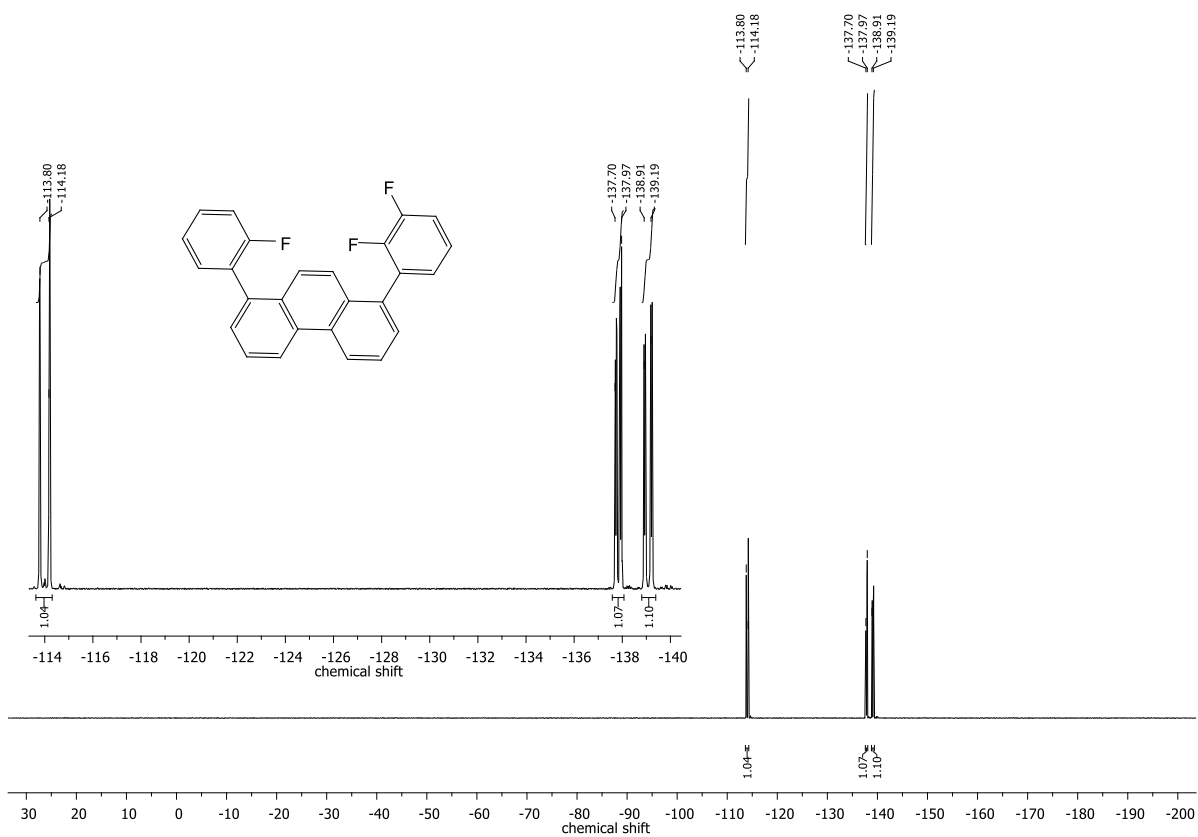


Figure 8.143: $^{19}\text{F-NMR}$ spectrum of 1-(2,3-difluorophenyl)-8-(2-fluorophenyl)phenanthrene.

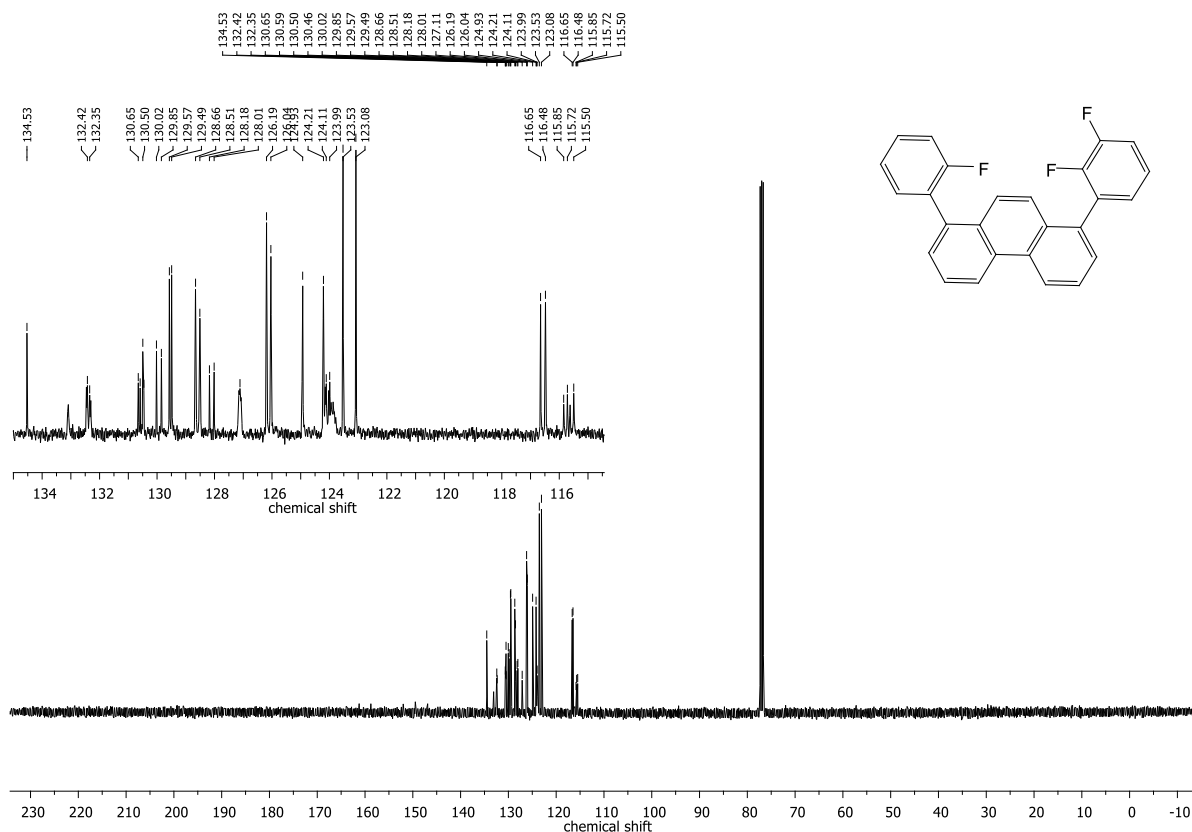


Figure 8.144: ^{13}C -NMR spectrum of 1-(2,3-difluorophenyl)-8-(2-fluorophenyl)phenanthrene.

8.2. Oxodefluorination of fluoroarenes

8.2.1. Synthesis of 2,8-bis(4-(tert-butyl)phenyl)dibenzo[b,d]furan

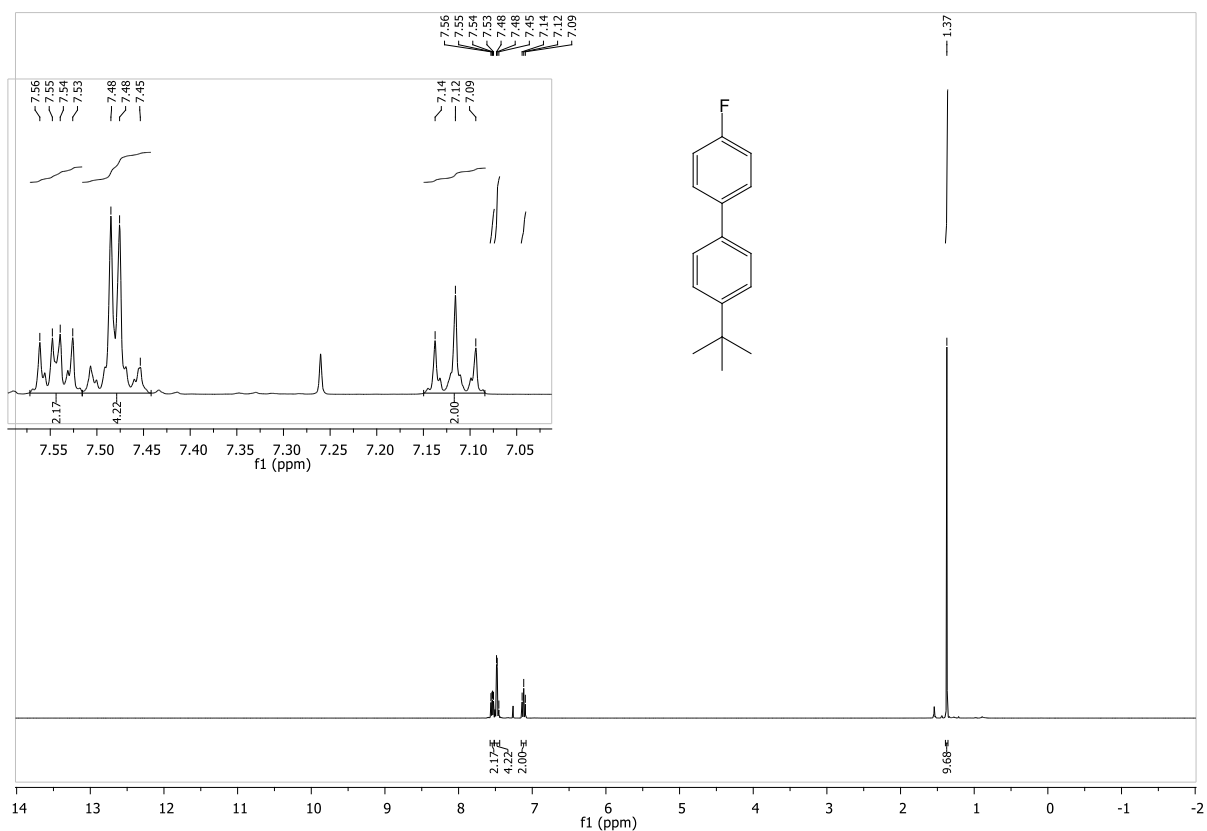


Figure 8.145: ¹H-NMR spectrum of 4-(tert-butyl)-4'-fluoro-1,1'-biphenyl.

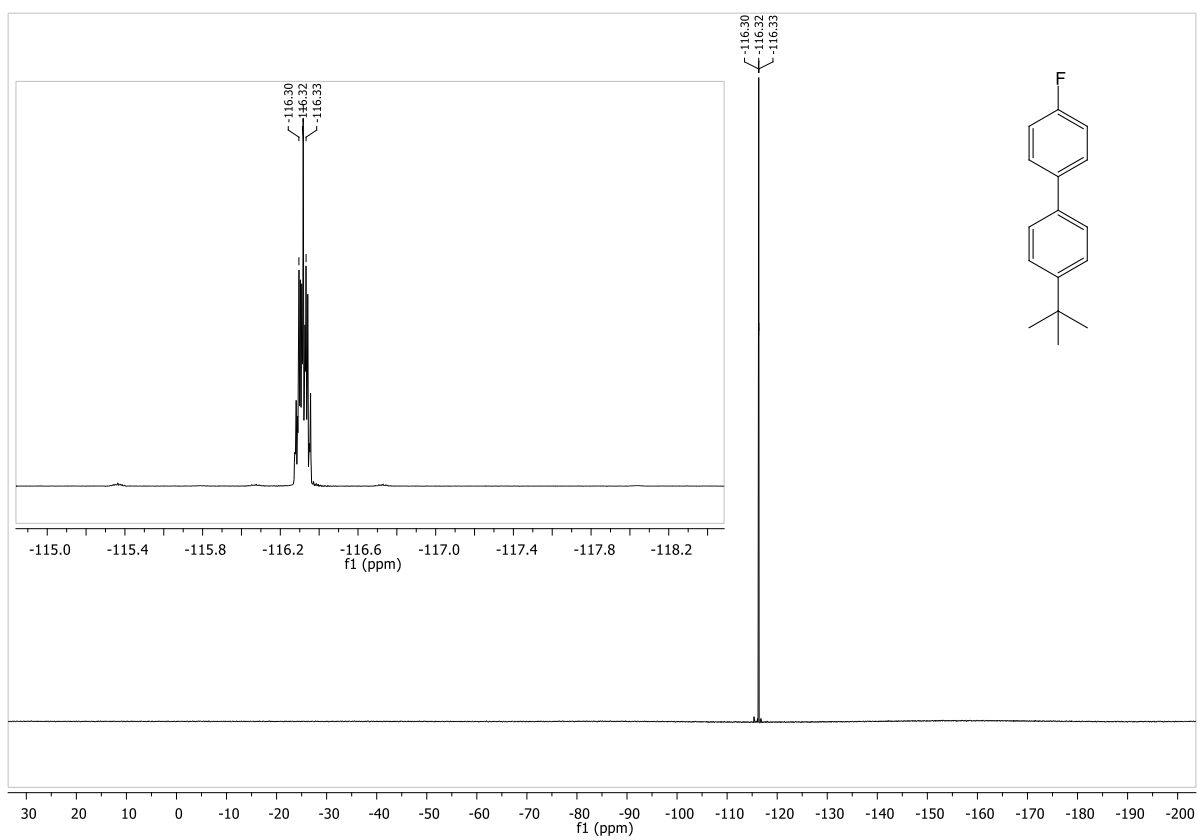


Figure 8.146: ¹⁹F-NMR spectrum of 4-(tert-butyl)-4'-fluoro-1,1'-biphenyl.

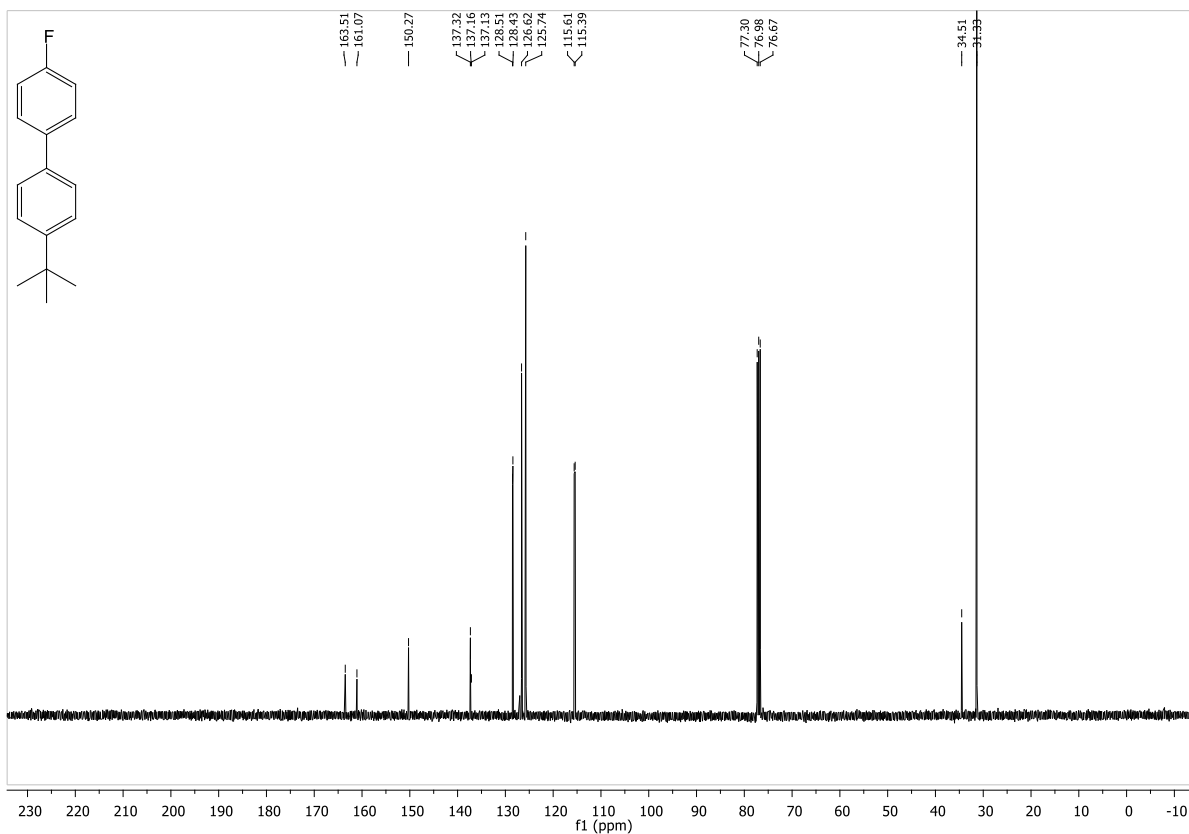


Figure 8.147: ¹³C-NMR spectrum of 4-(tert-butyl)-4'-fluoro-1,1'-biphenyl.

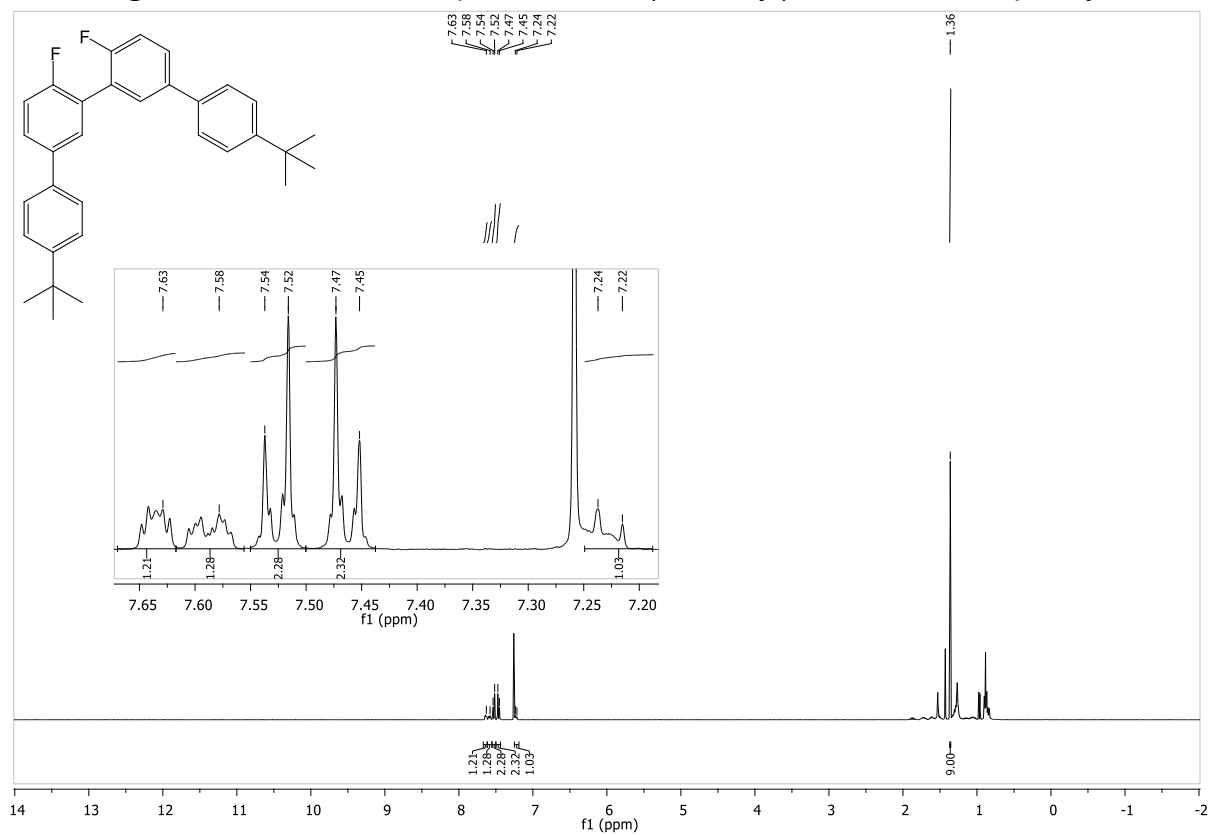


Figure 8.148: ¹H-NMR spectrum of 4,4''-di-tert-butyl-4',6''-difluoro-1,1':3,1'':3'',1'''-biphenyl.

quaterphenyl.

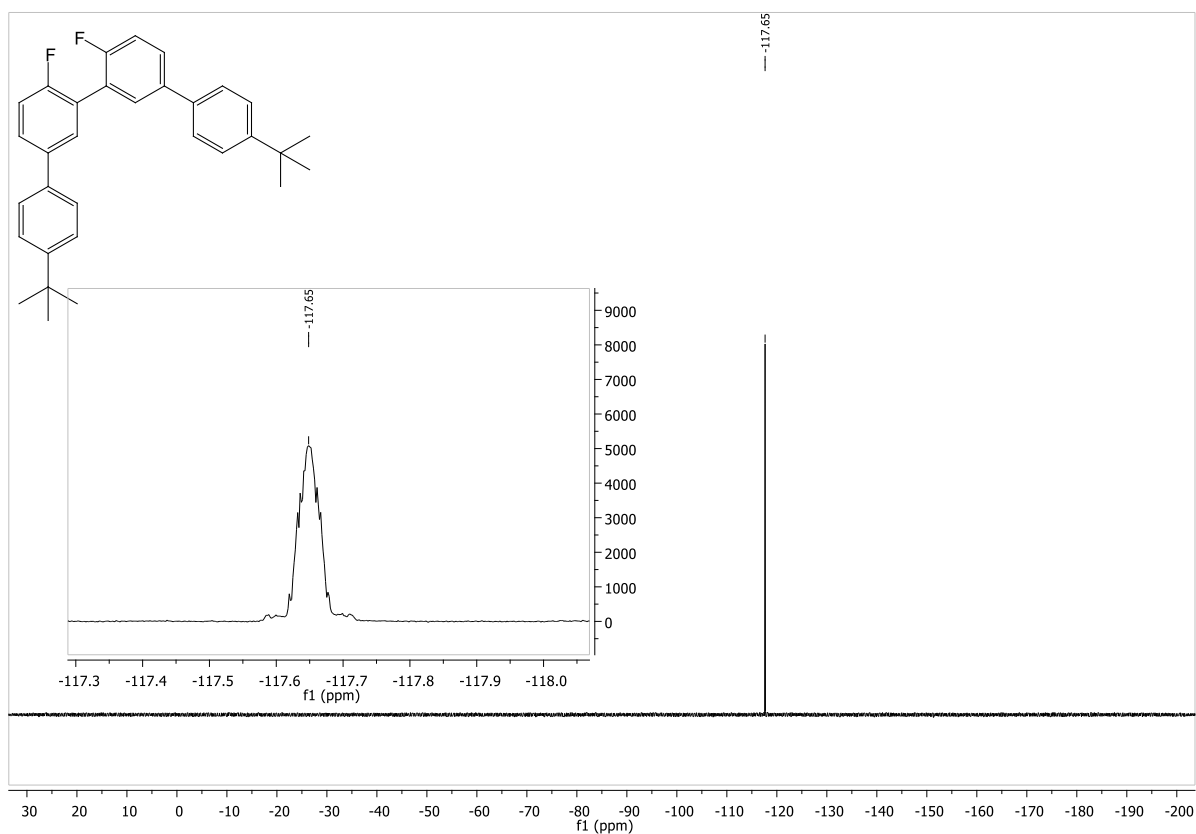


Figure 8.149: ^{19}F -NMR spectrum of 4,4''-di-tert-butyl-4',6''-difluoro-1,1':3,1':3'',1'''-

quaterphenyl.

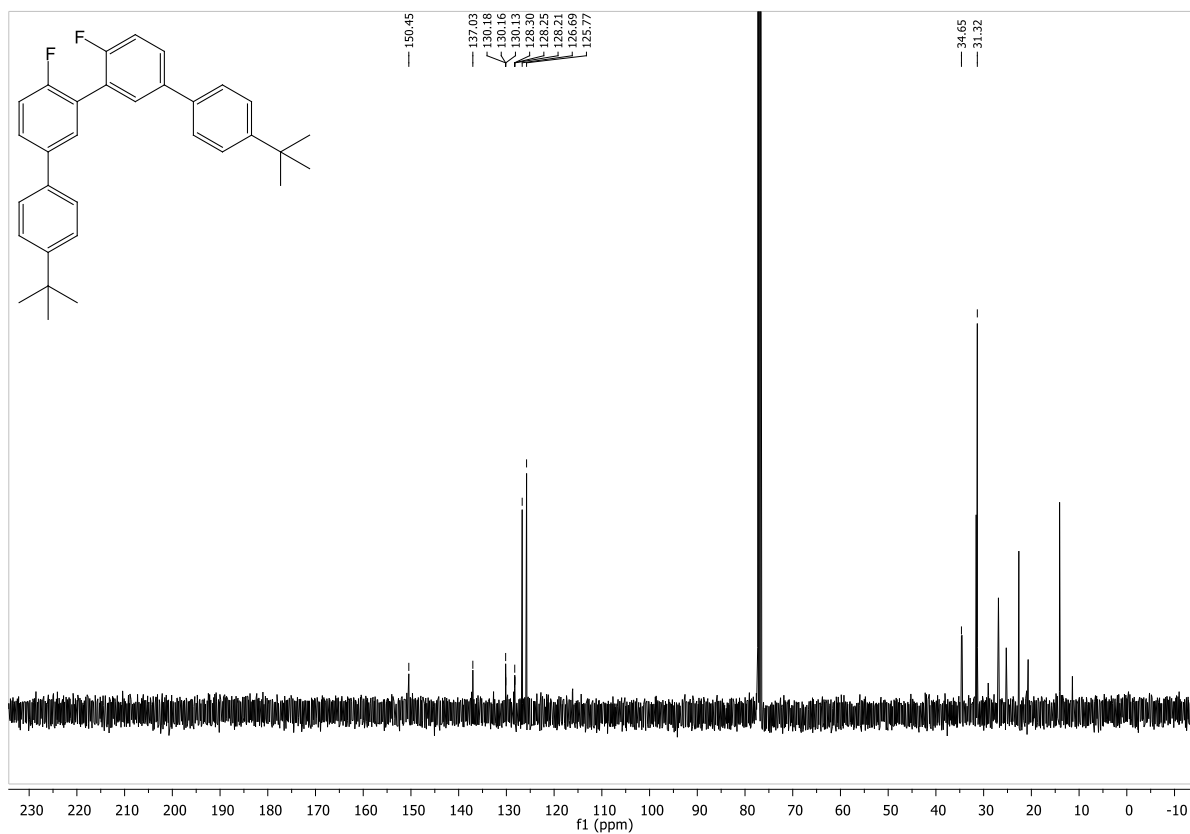


Figure 8.150: ¹³C-NMR spectrum of 4,4''-di-tert-butyl-4',6''-difluoro-1,1':3',1'':3'',1'''-quaterphenyl.

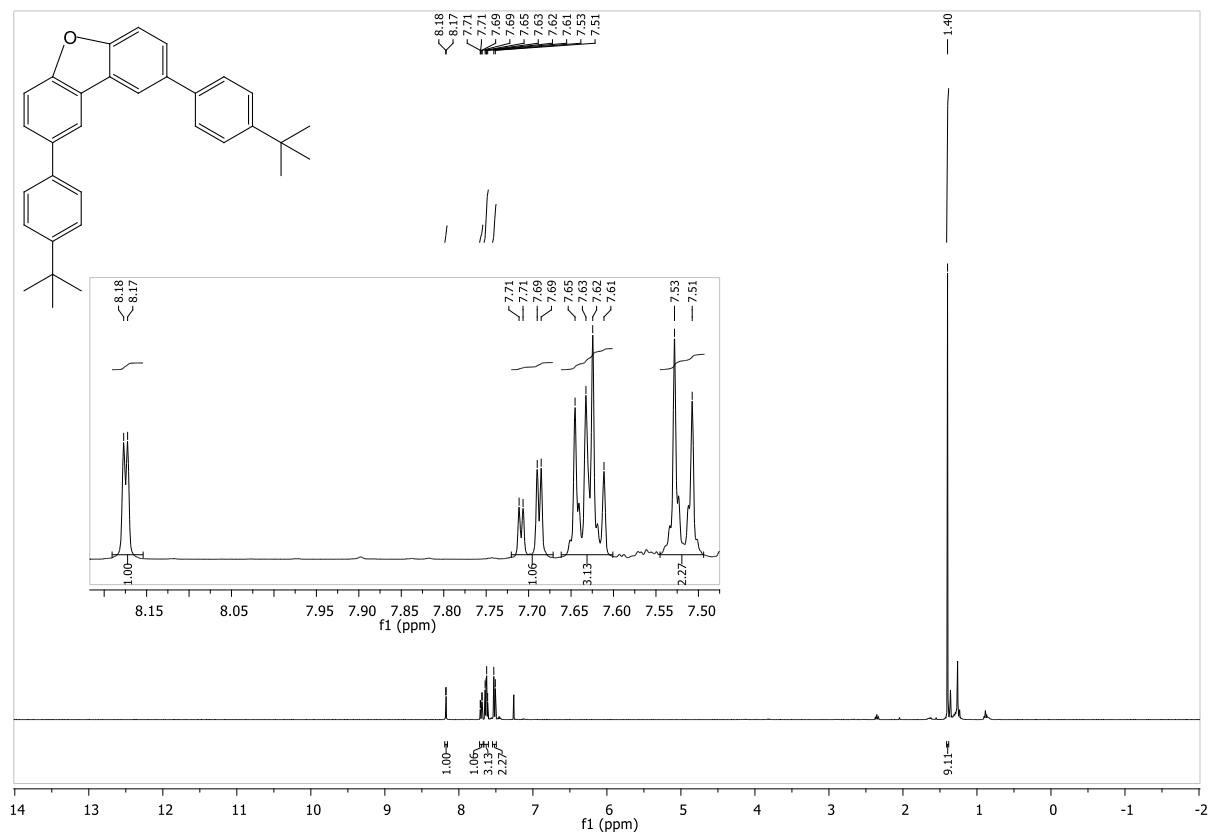


Figure 8.151: $^1\text{H-NMR}$ spectrum of 2,8-bis(4-(tert-butyl)phenyl)dibenzo[b,d]furan.

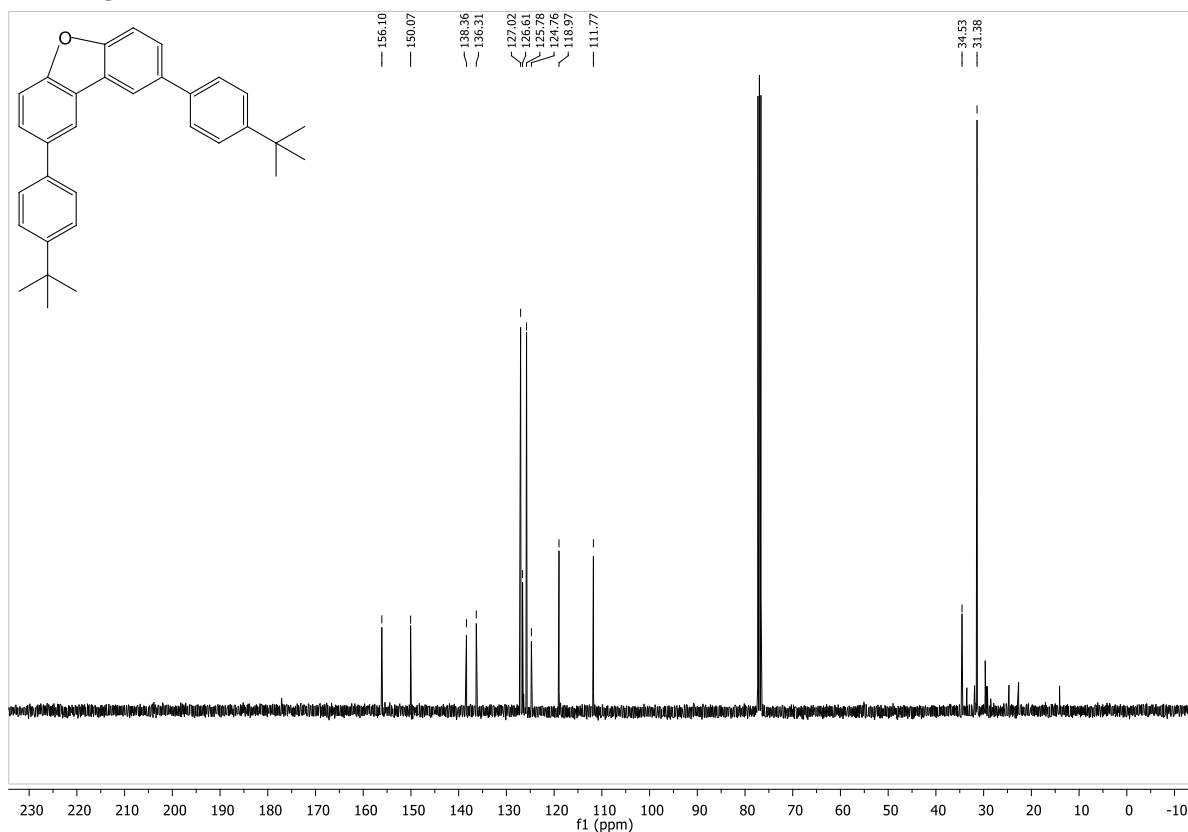


Figure 8.152: $^{13}\text{C-NMR}$ spectrum of 2,8-bis(4-(tert-butyl)phenyl)dibenzo[b,d]furan.

8.2.2. Synthesis of „smallest“ nanographene with bridge

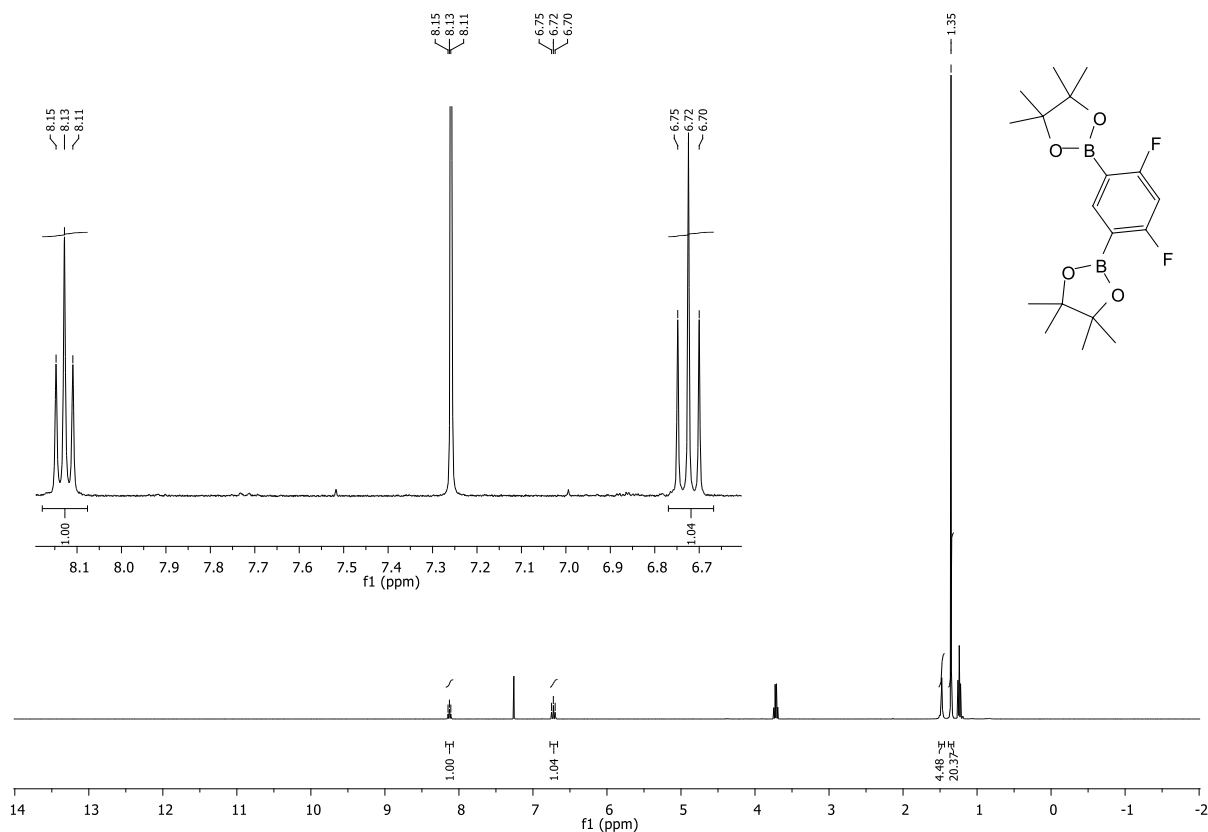


Figure 8.153: $^1\text{H-NMR}$ spectrum of 2,2'-(4,6-difluoro-1,3-phenylene)bis(4,4,5,5-tetramethyl-1,3,2-dioxaborolane).

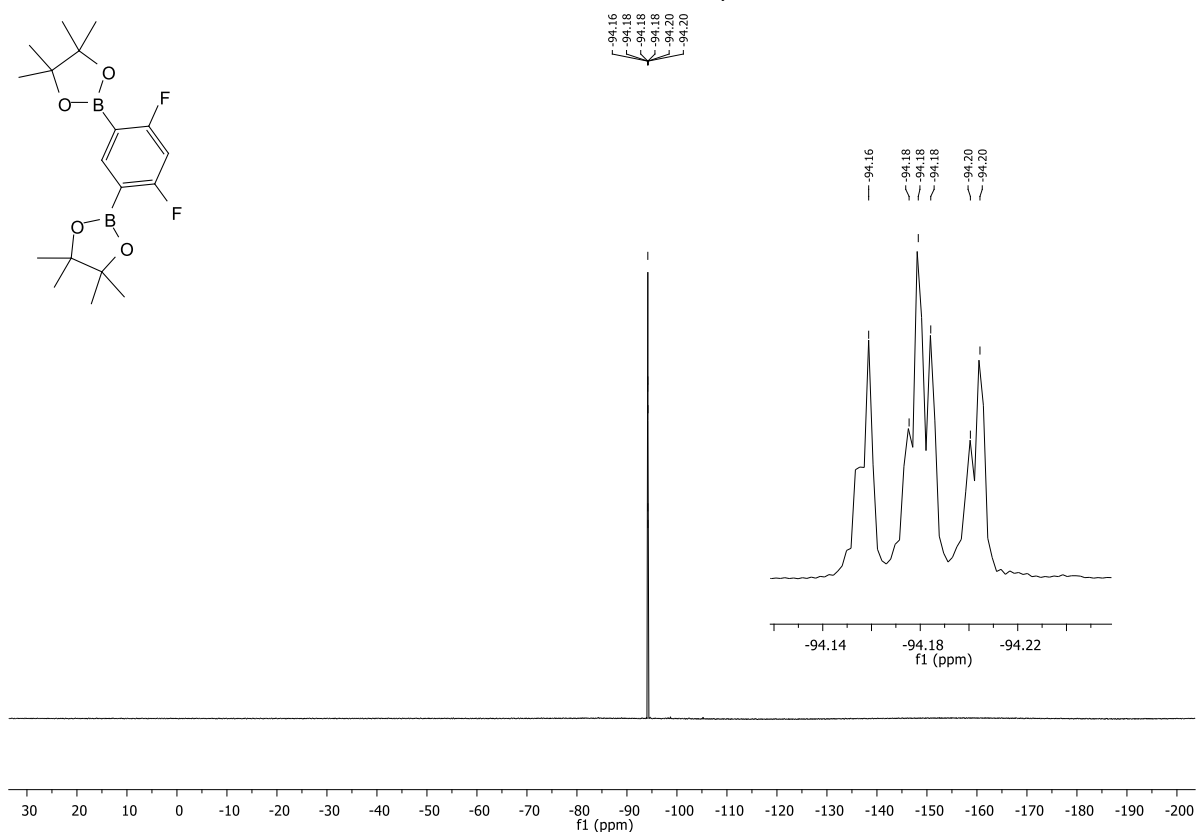


Figure 8.154: $^{19}\text{F-NMR}$ spectrum of 2,2'-(4,6-difluoro-1,3-phenylene)bis(4,4,5,5-tetramethyl-1,3,2-dioxaborolane).

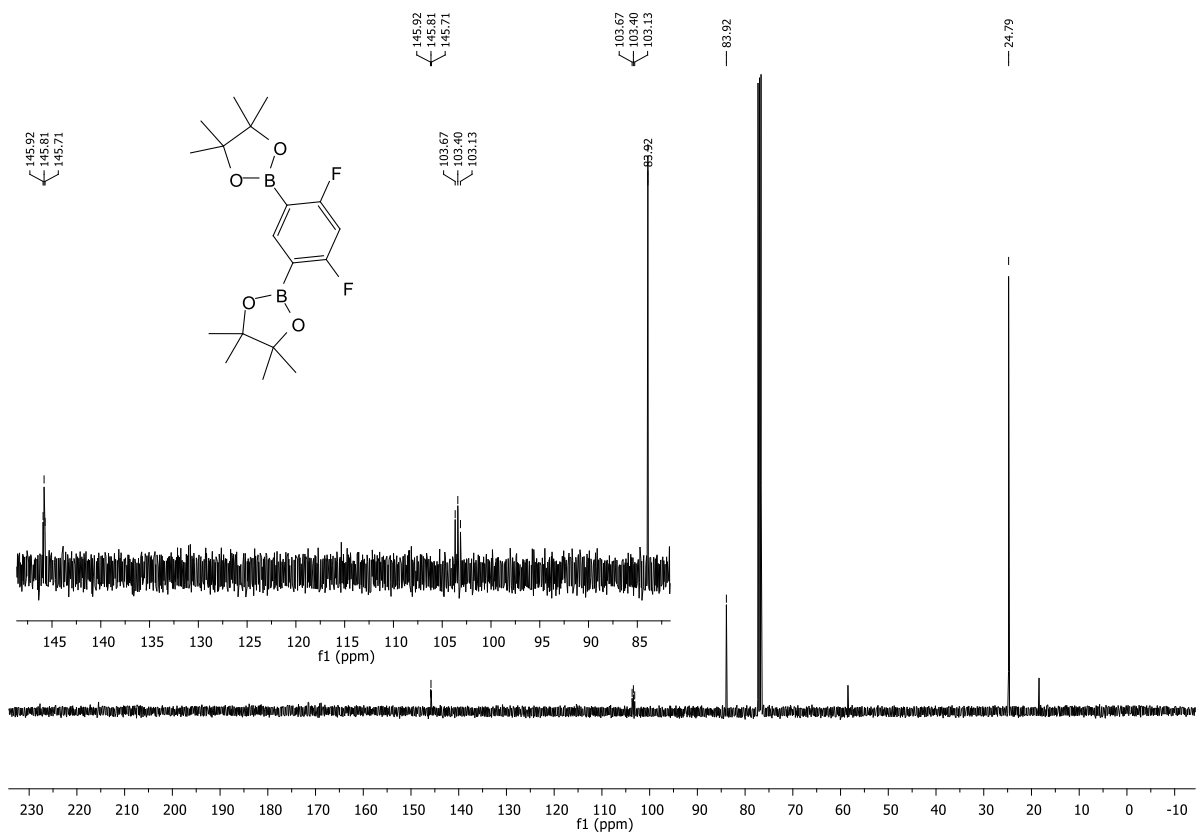


Figure 8.155: ^{13}C -NMR spectrum of 2,2'-(4,6-difluoro-1,3-phenylene)bis(4,4,5,5-tetramethyl-1,3,2-dioxaborolane).

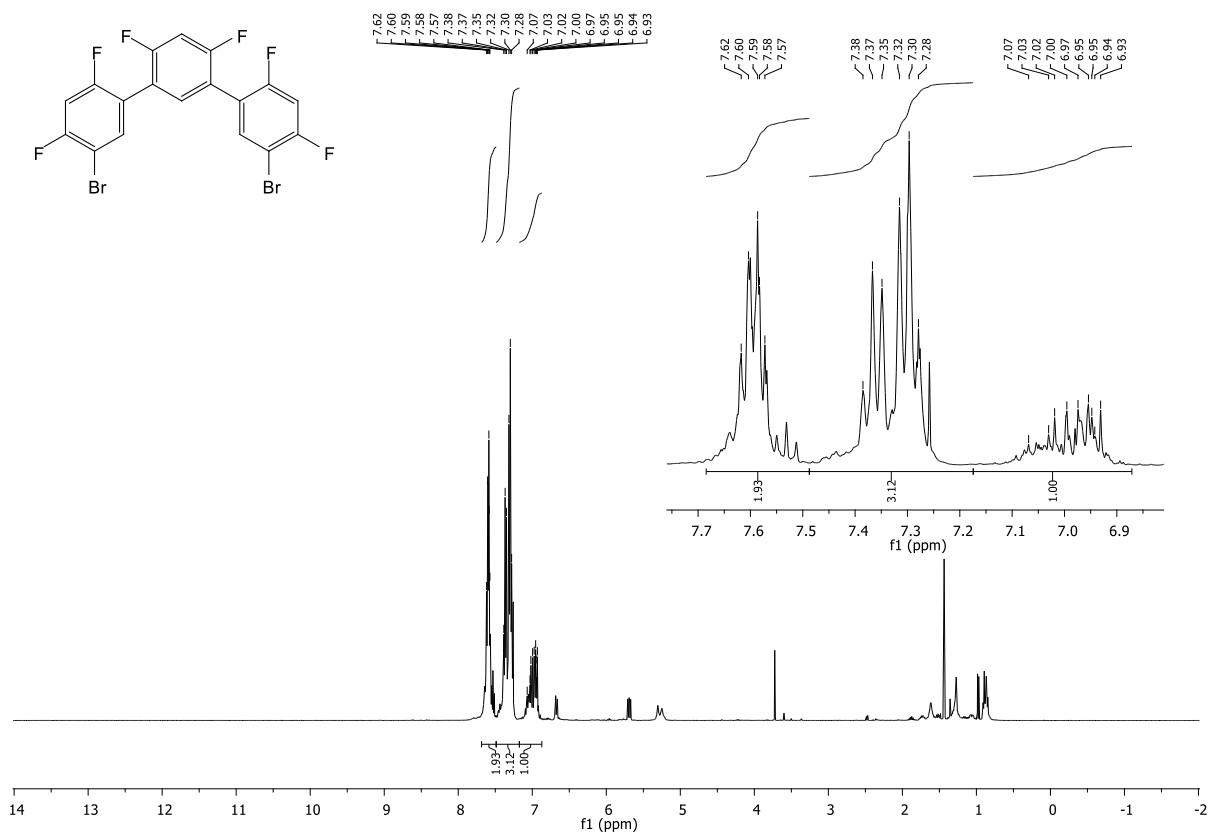


Figure 8.156: $^1\text{H-NMR}$ spectrum of 5,5''-dibromo-2,2'',4,4',4'',6'-hexafluoro-1,1':3',1''-terphenyl.

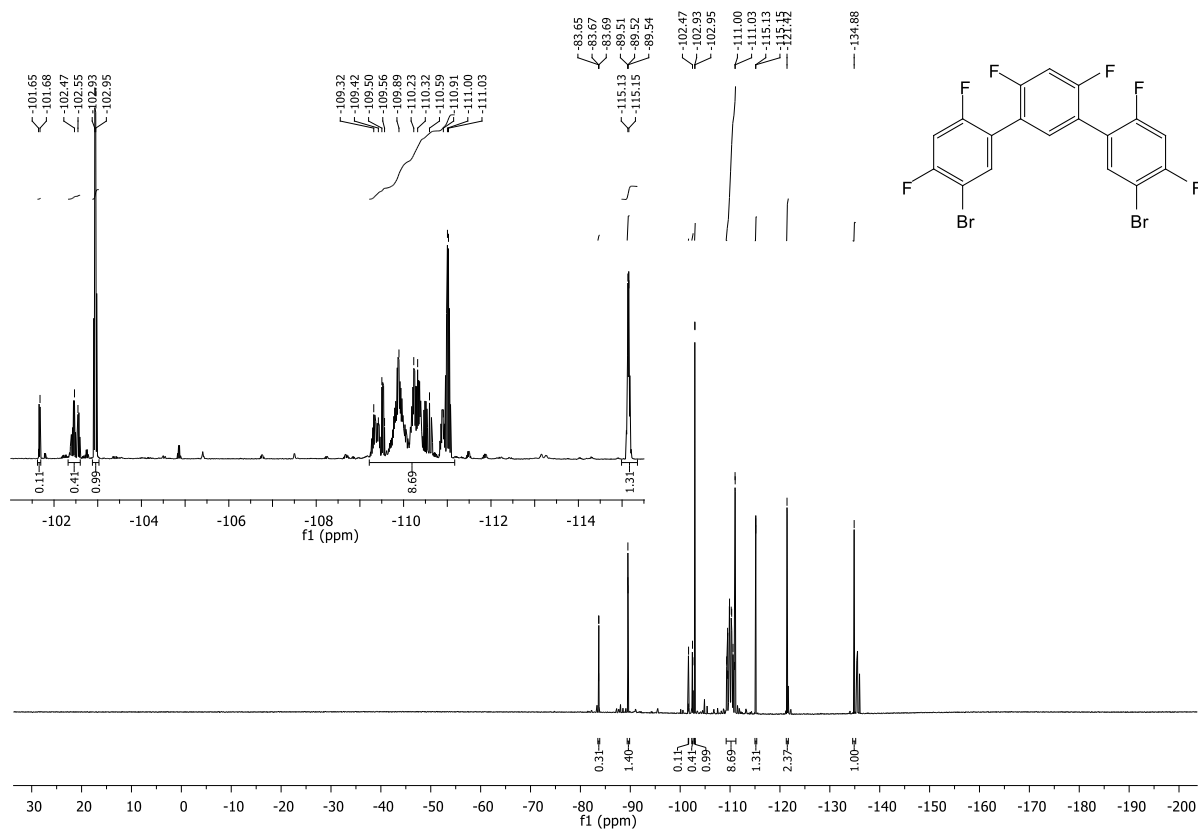


Figure 8.157: $^{19}\text{F-NMR}$ spectrum of 5,5''-dibromo-2,2'',4,4',4'',6'-hexafluoro-1,1':3',1''-terphenyl.

terphenyl.

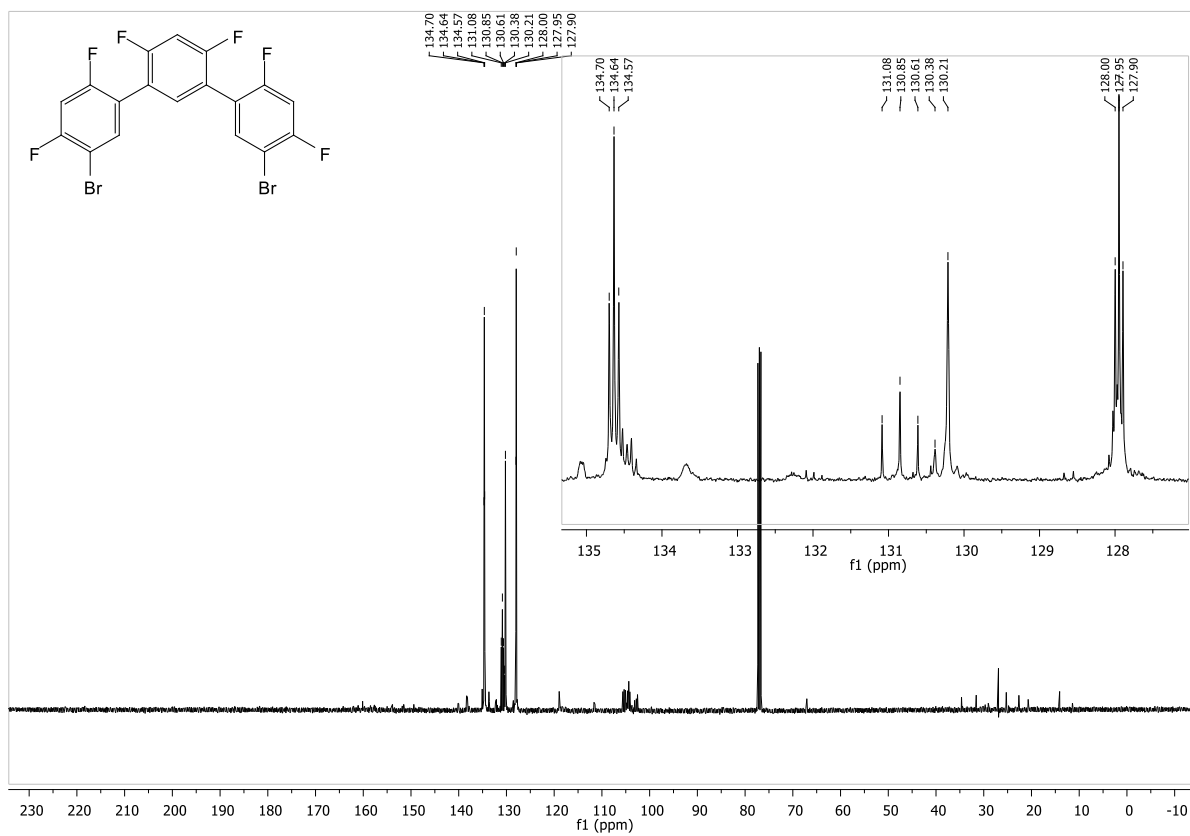


Figure 8.158: ^{13}C -NMR spectrum of 5,5''-dibromo-2,2'',4,4'',4'',6'-hexafluoro-1,1':3',1''-terphenyl.

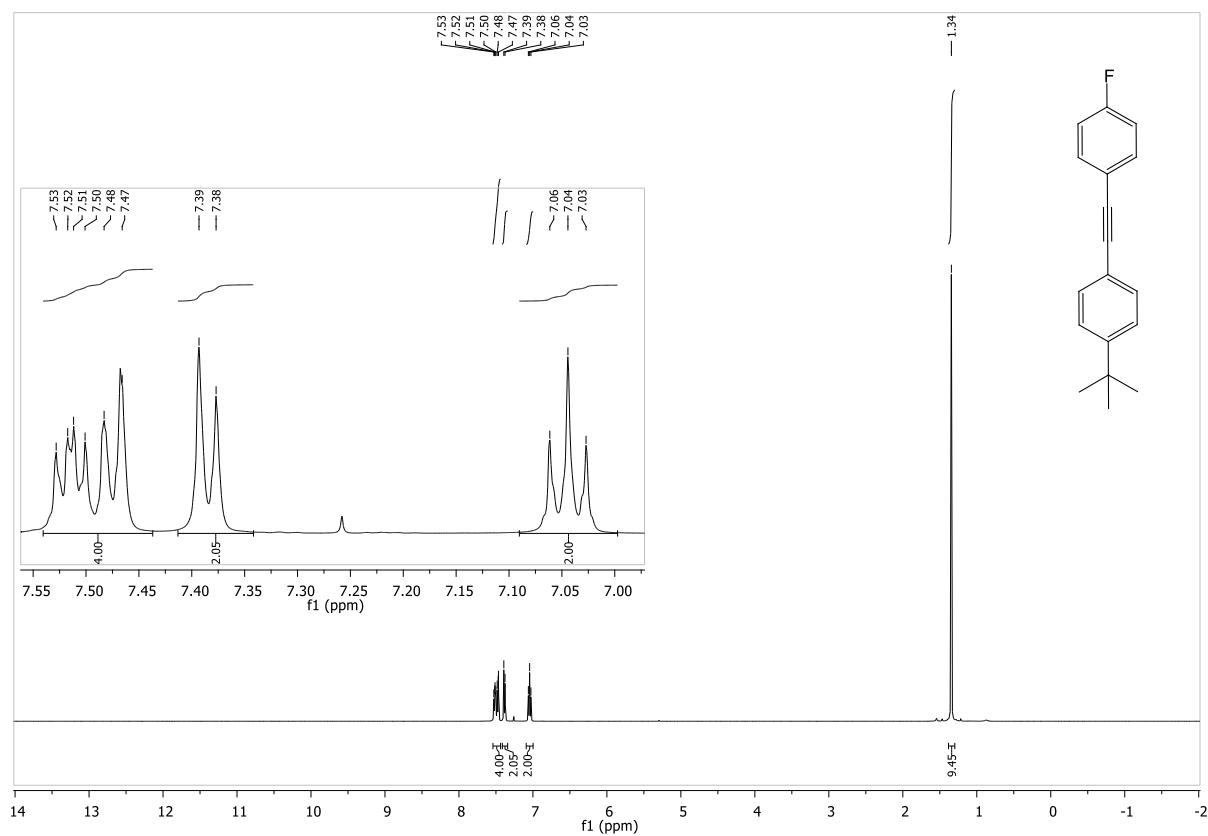


Figure 8.159: ¹H-NMR spectrum of 1-(tert-butyl)-4-((4-fluorophenyl)ethynyl)benzene.

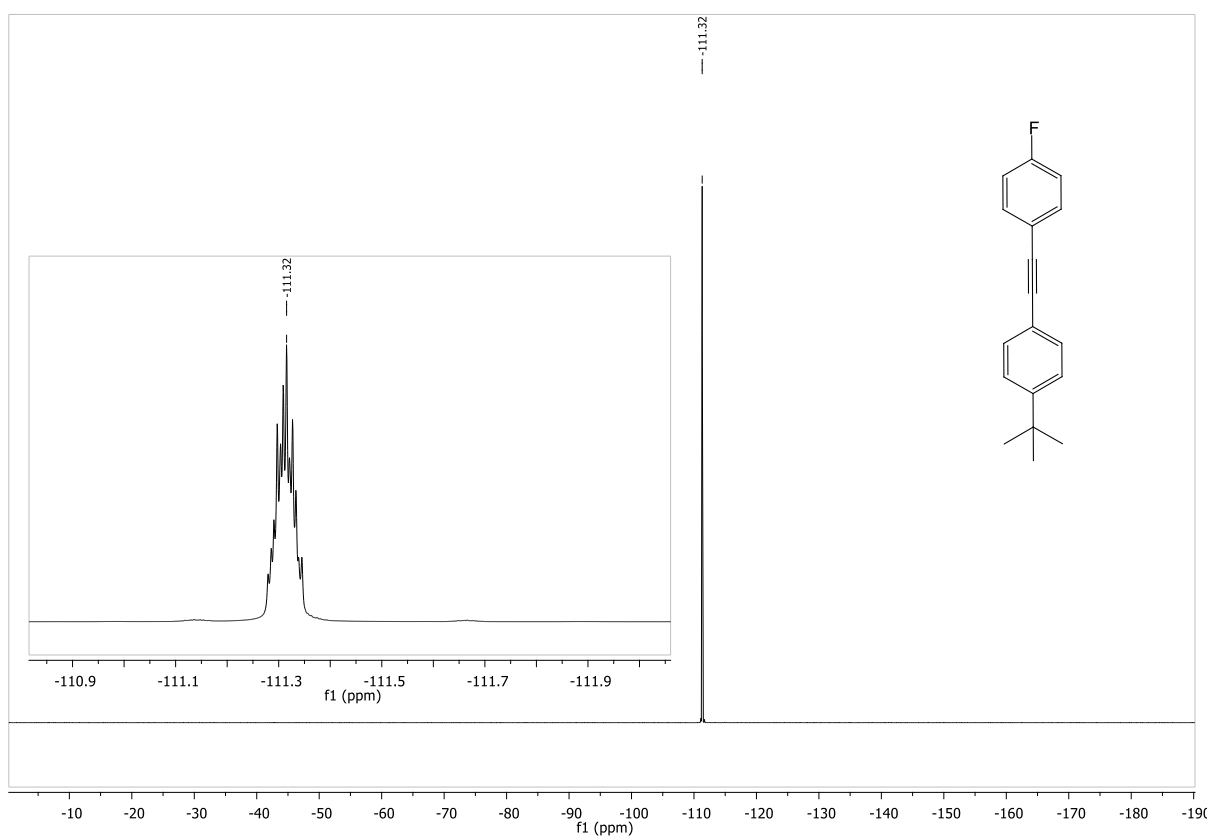


Figure 8.160: ¹⁹F-NMR spectrum of 1-(tert-butyl)-4-((4-fluorophenyl)ethynyl)benzene.

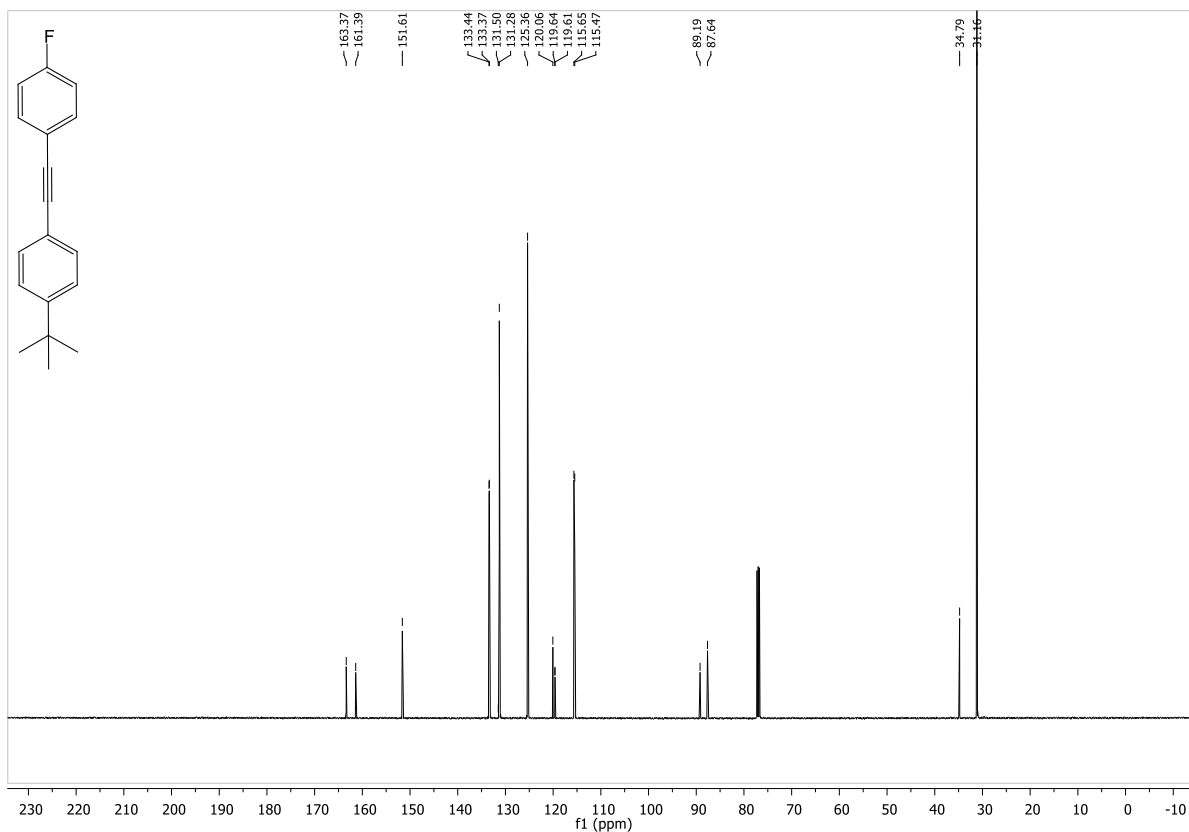


Figure 8.161: $^{13}\text{C-NMR}$ spectrum of 1-(tert-butyl)-4-((4-fluorophenyl)ethynyl)benzene.

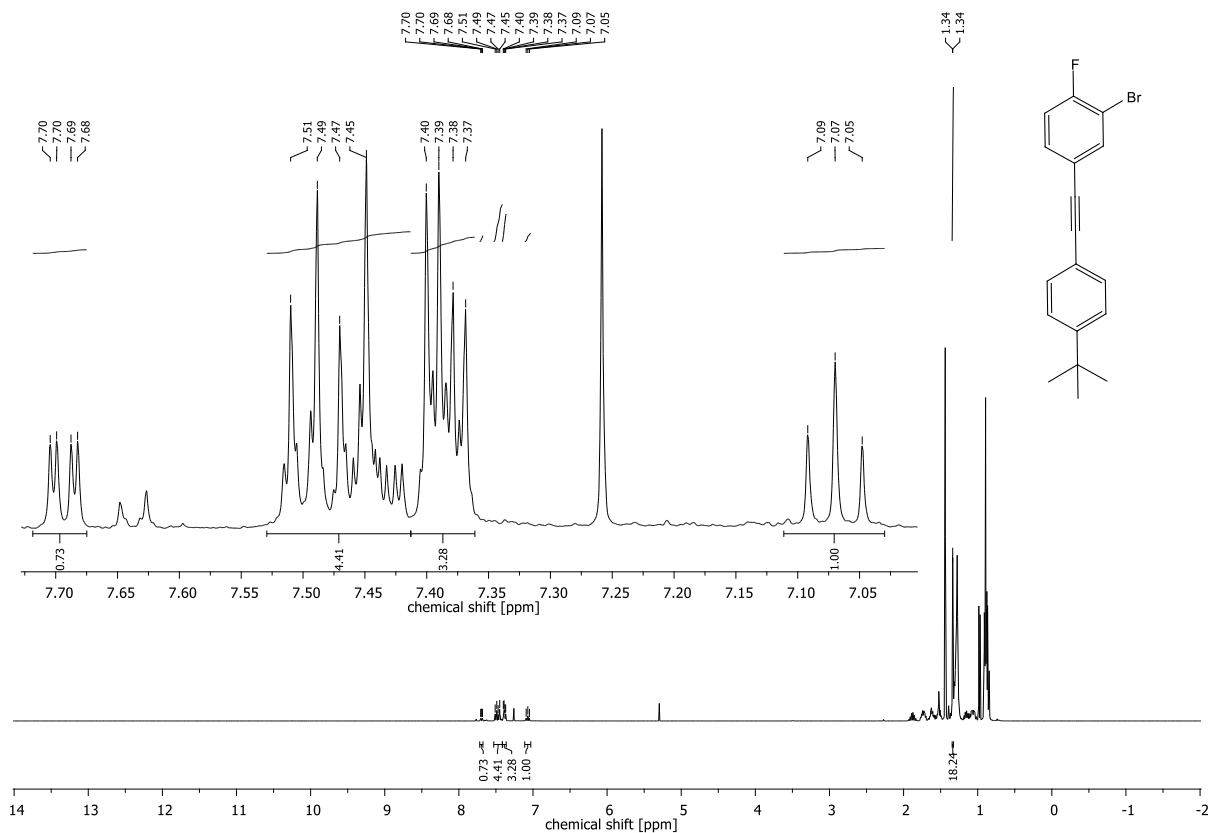


Figure 8.162: $^1\text{H-NMR}$ spectrum of 2-bromo-4-((4-(tert-butyl)phenyl)ethynyl)-1-fluorobenzene.

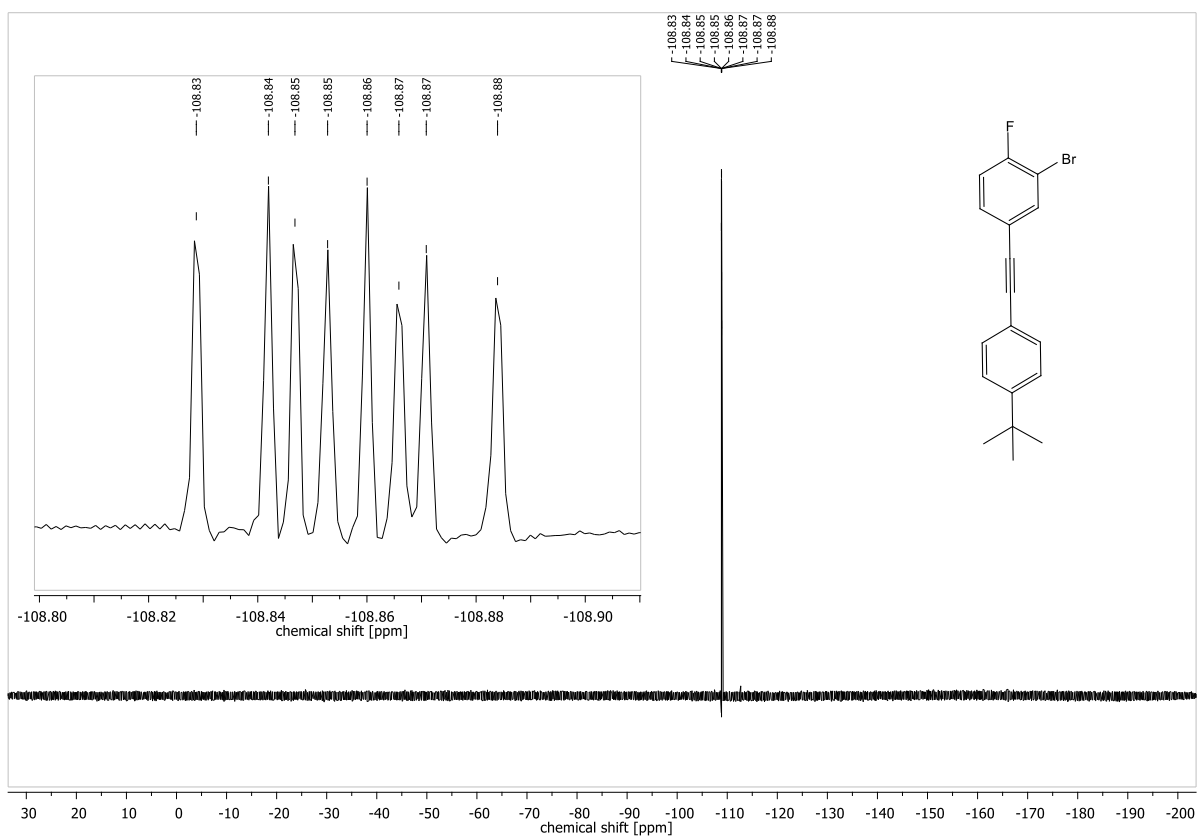


Figure 8.163: ^{19}F -NMR spectrum of 2-bromo-4-((4-(tert-butyl)phenyl)ethynyl)-1-fluorobenzene.

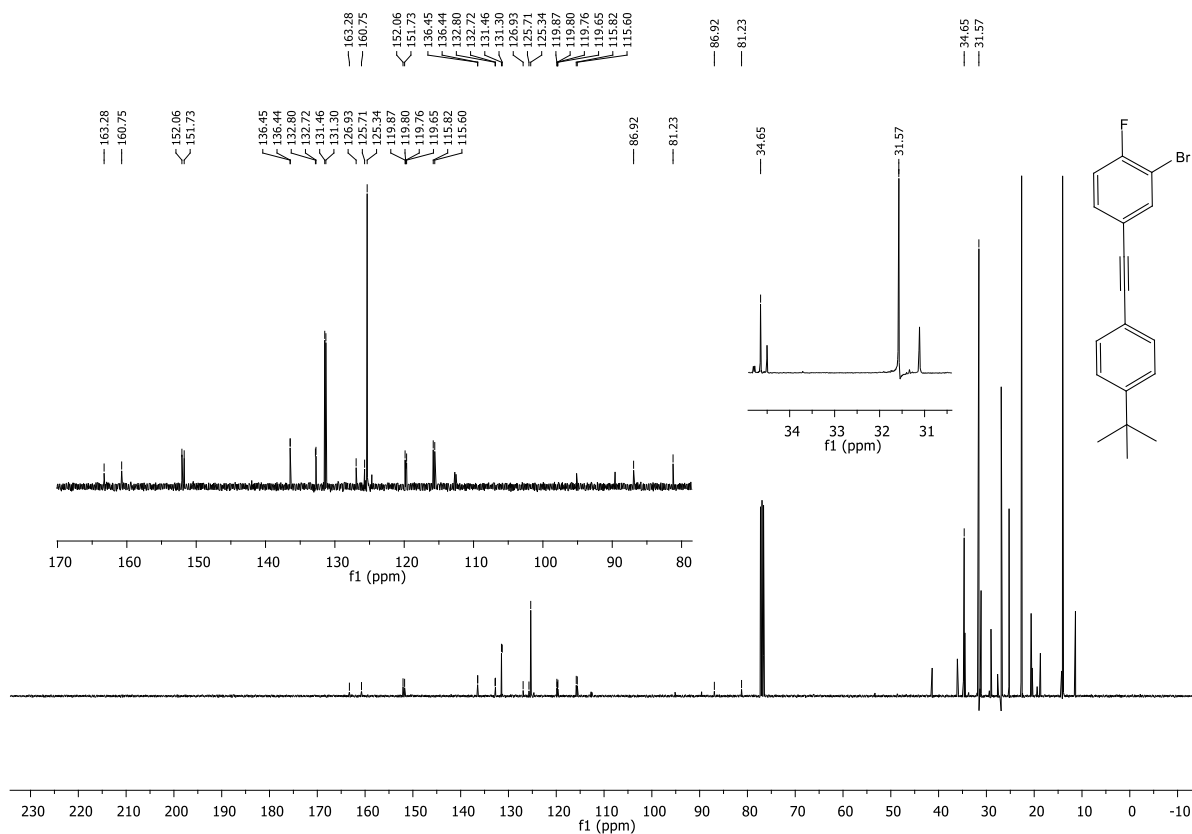


Figure 8.164: ^{13}C -NMR spectrum of 2-bromo-4-((4-(tert-butyl)phenyl)ethynyl)-1-fluorobenzene.

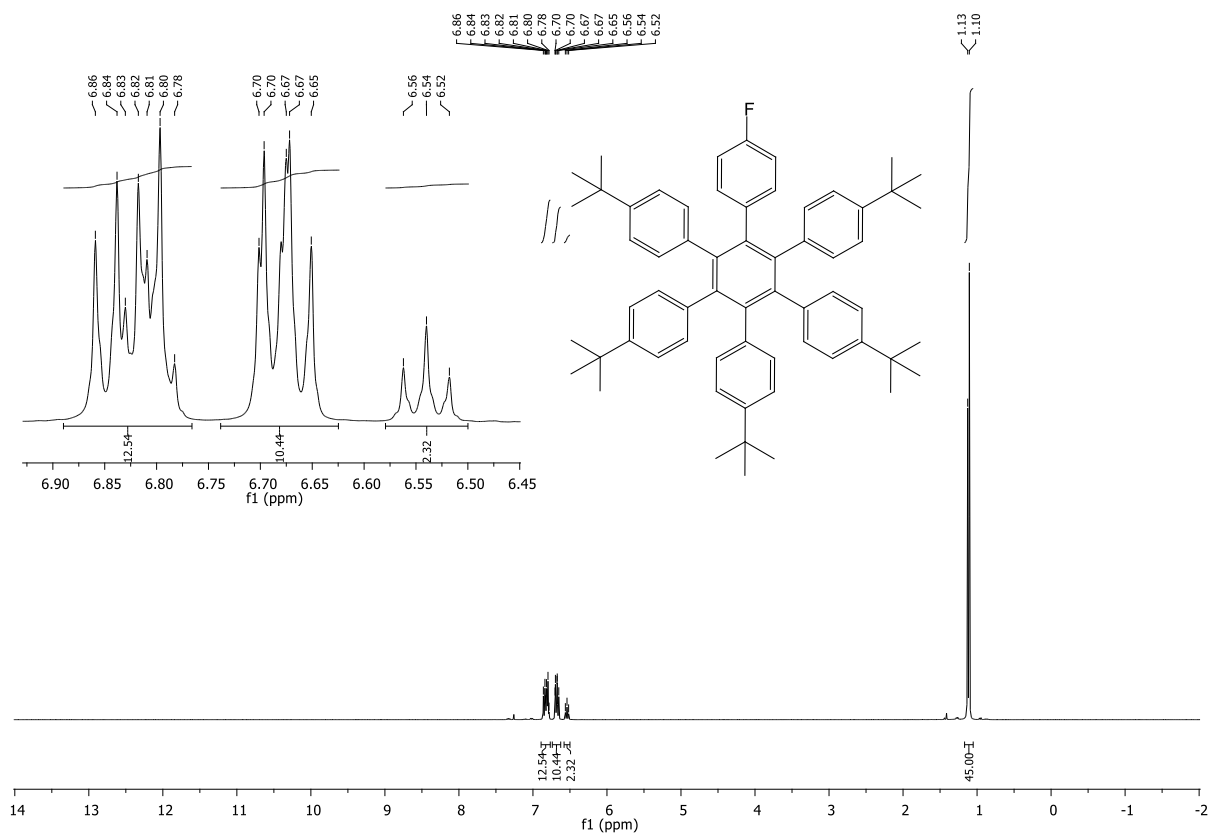


Figure 8.165: ^1H -NMR spectrum of 4,4''-di-tert-butyl-3',4',5'-tris(4-(tert-butyl)phenyl)-6'-(4-fluorophenyl)-1,1':2,1''-terphenyl.

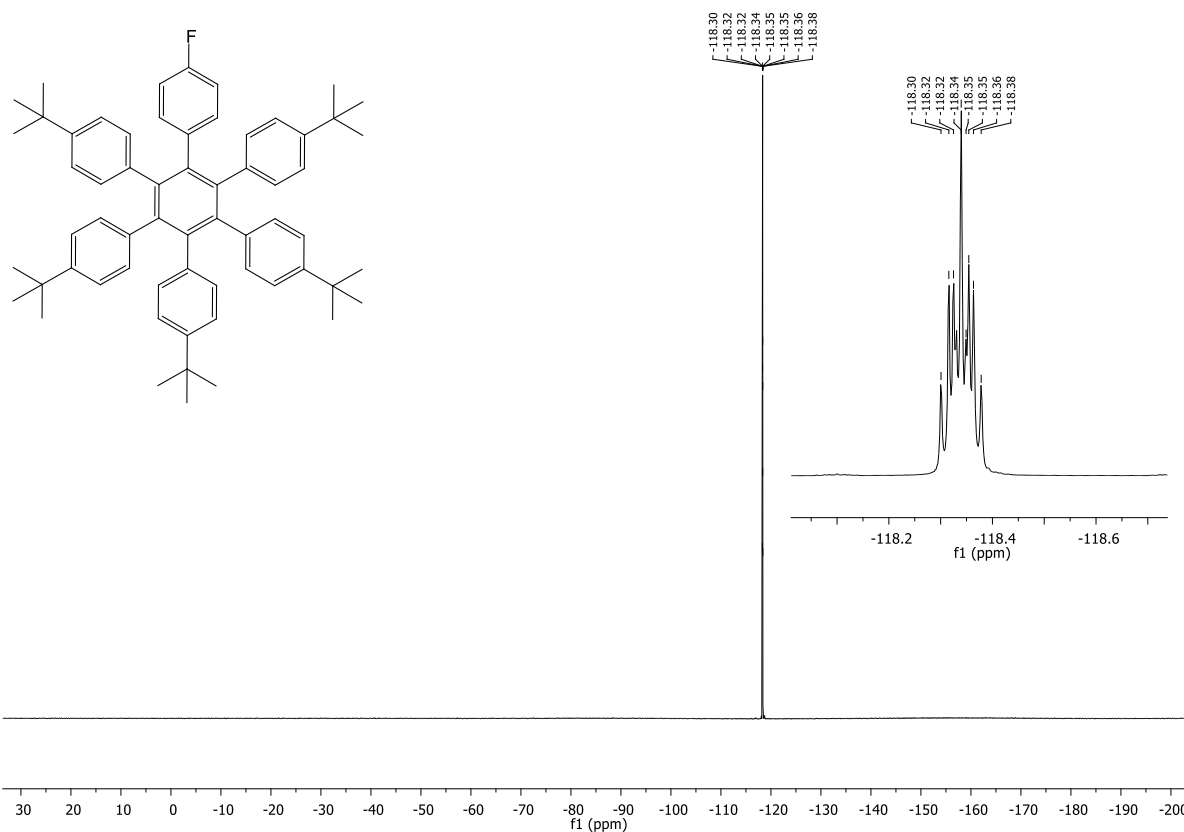


Figure 8.166: ^{19}F -NMR spectrum of 4,4''-di-tert-butyl-3',4',5'-tris(4-(tert-butyl)phenyl)-6'-(4-fluorophenyl)-1,1':2',1''-terphenyl.

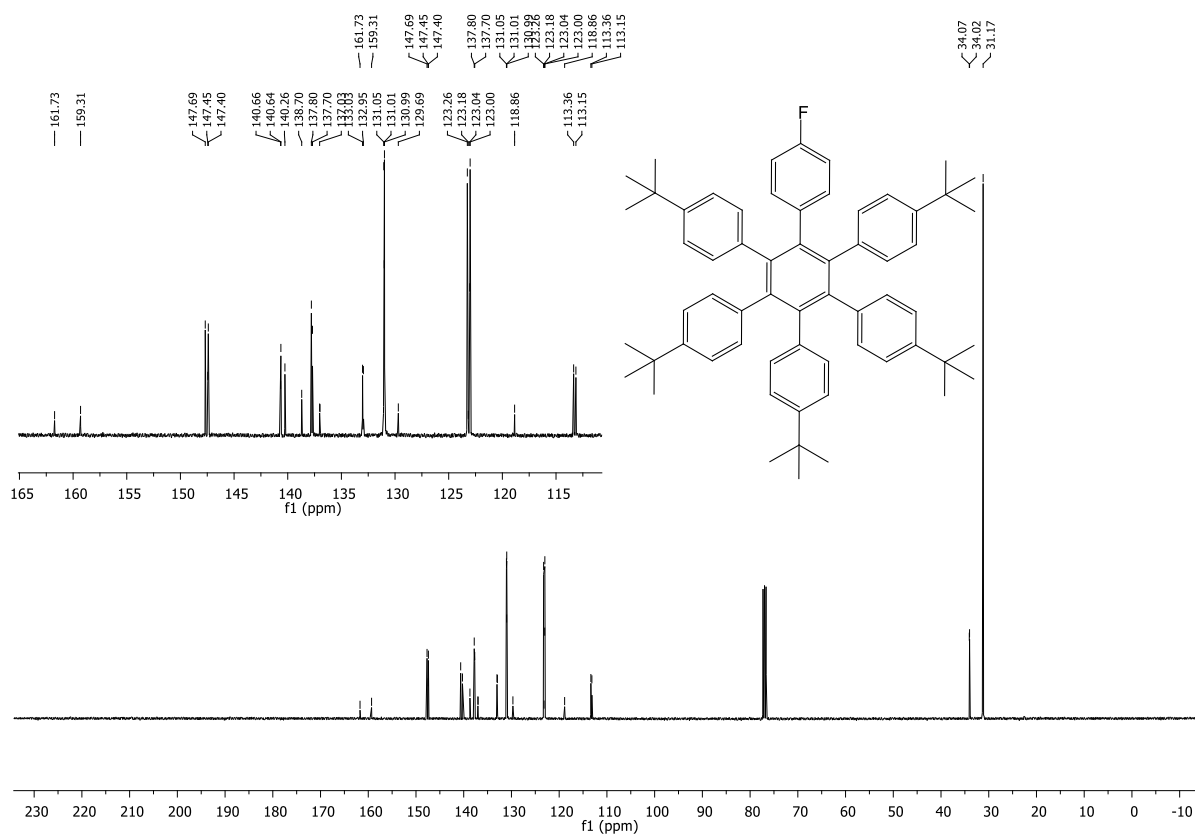


Figure 8.167: ^{13}C -NMR spectrum of 4,4''-di-tert-butyl-3',4',5'-tris(4-(tert-butyl)phenyl)-6'-(4-fluorophenyl)-1,1':2',1''-terphenyl.

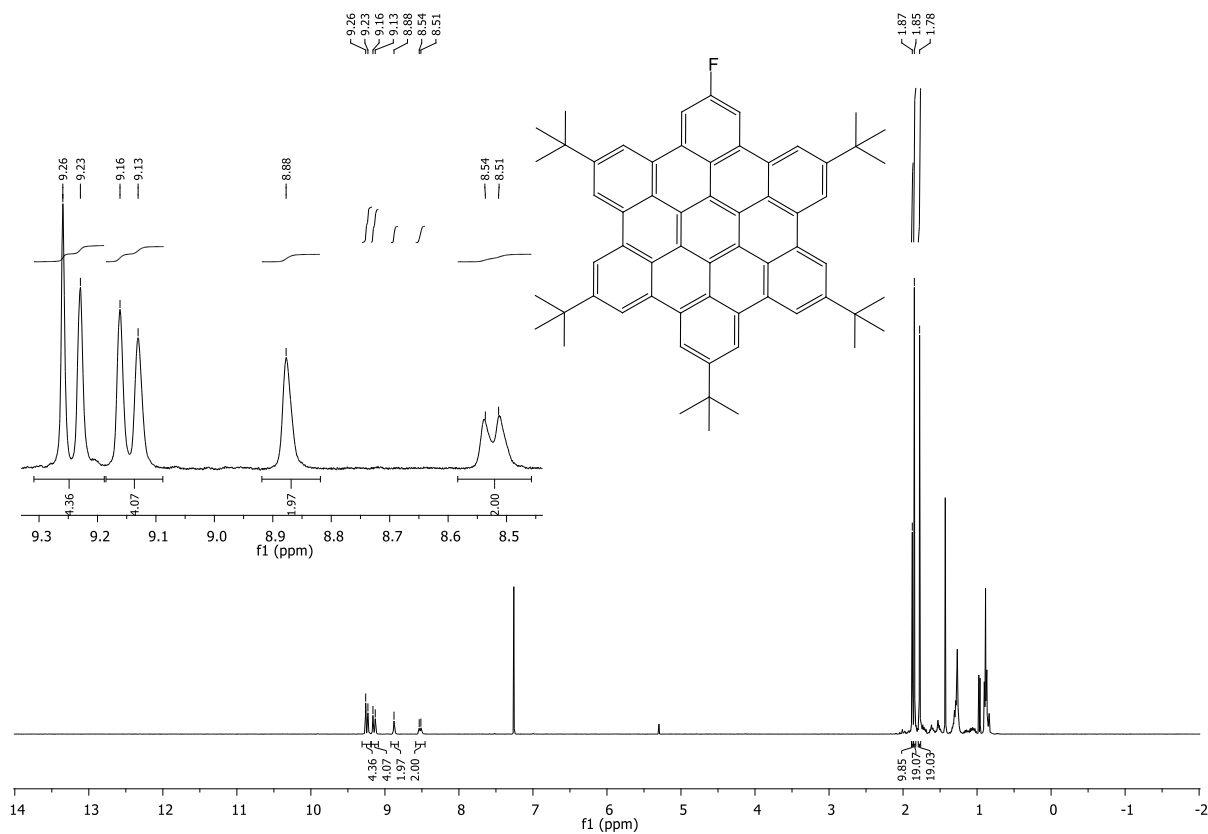


Figure 8.168: $^1\text{H-NMR}$ spectrum of 2,5,8,11,14-penta-tert-butyl-17-fluorohexabenzob[bc,ef,hi,kl,no,qr]coronene.

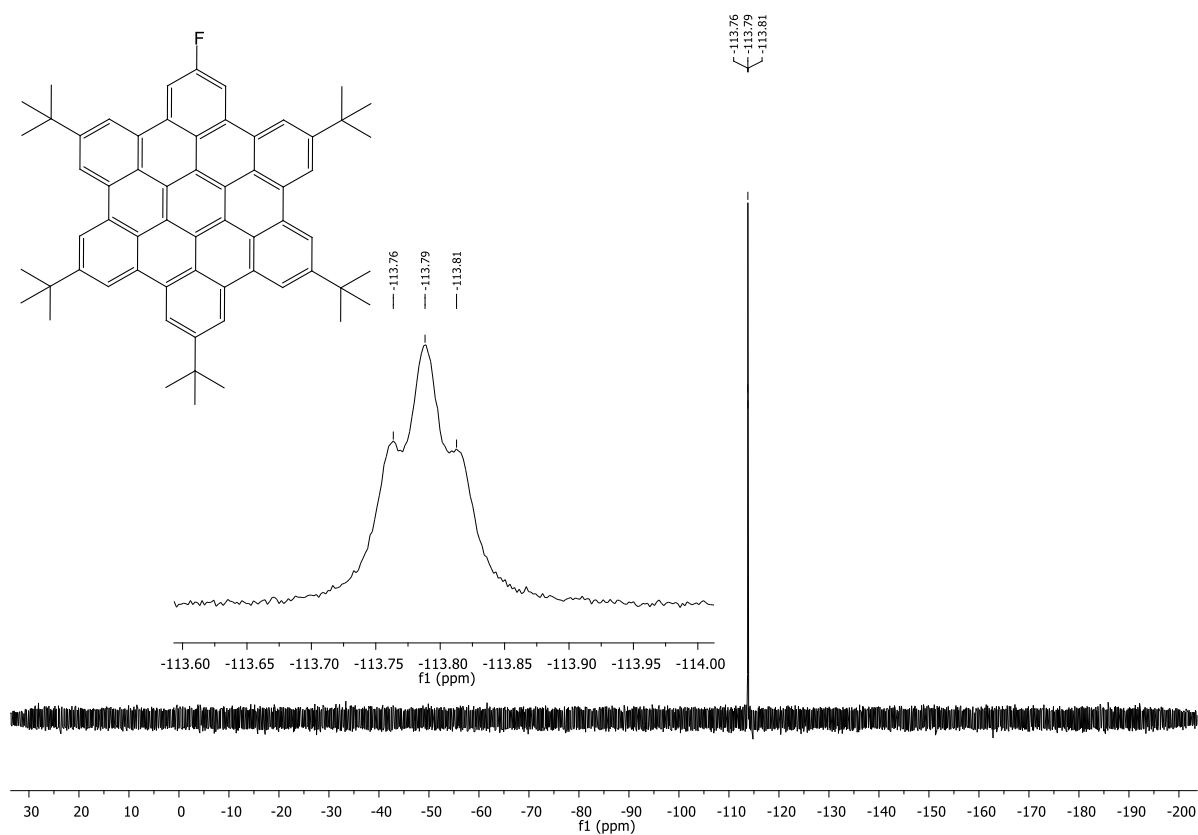


Figure 8.169: $^{19}\text{F-NMR}$ spectrum of 2,5,8,11,14-penta-tert-butyl-17-fluorohexabenzob[bc,ef,hi,kl,no,qr]coronene.

8.3. Construction of zig-zag periphery by Csp³-Caryl coupling via AmCFA

8.3.1. Reactions with small molecules

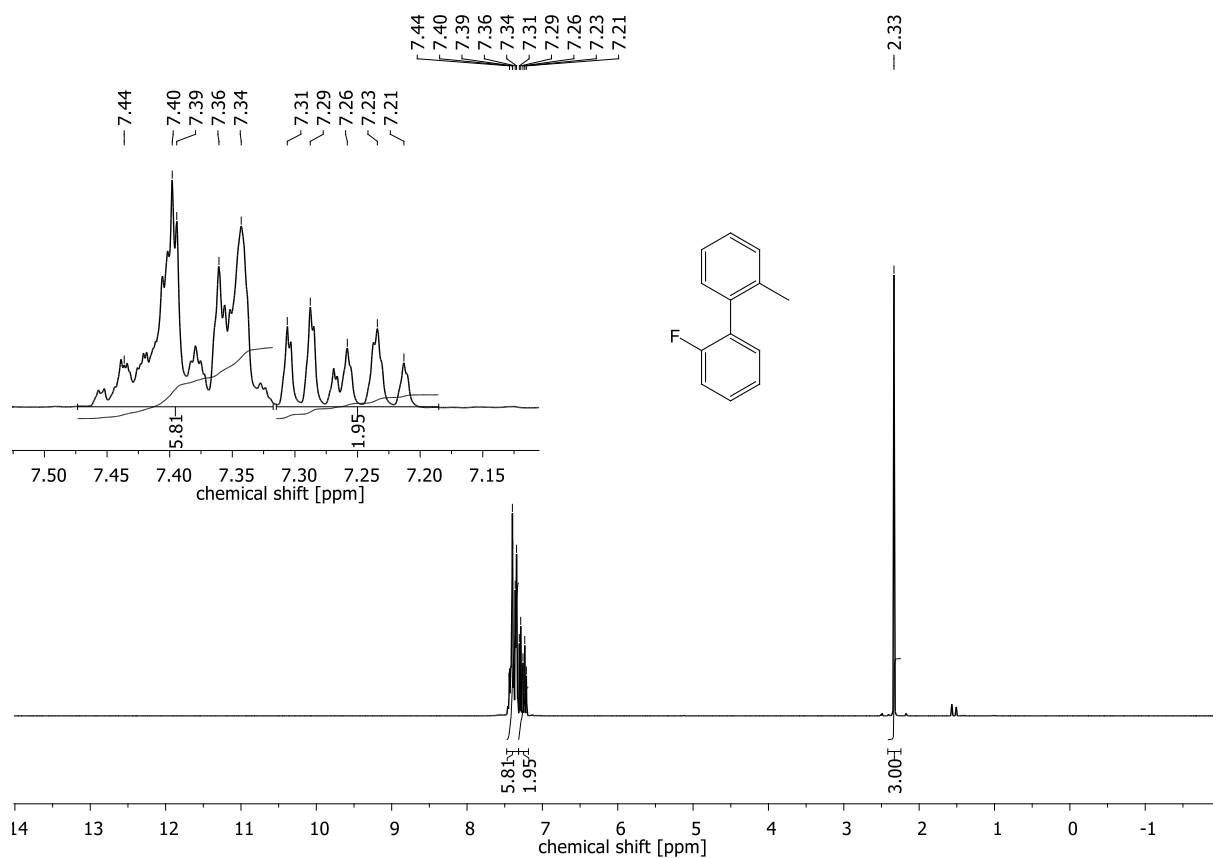


Figure 8.174: ¹H-NMR spectrum of 2-fluoro-2'-methyl-1,1'-biphenyl.

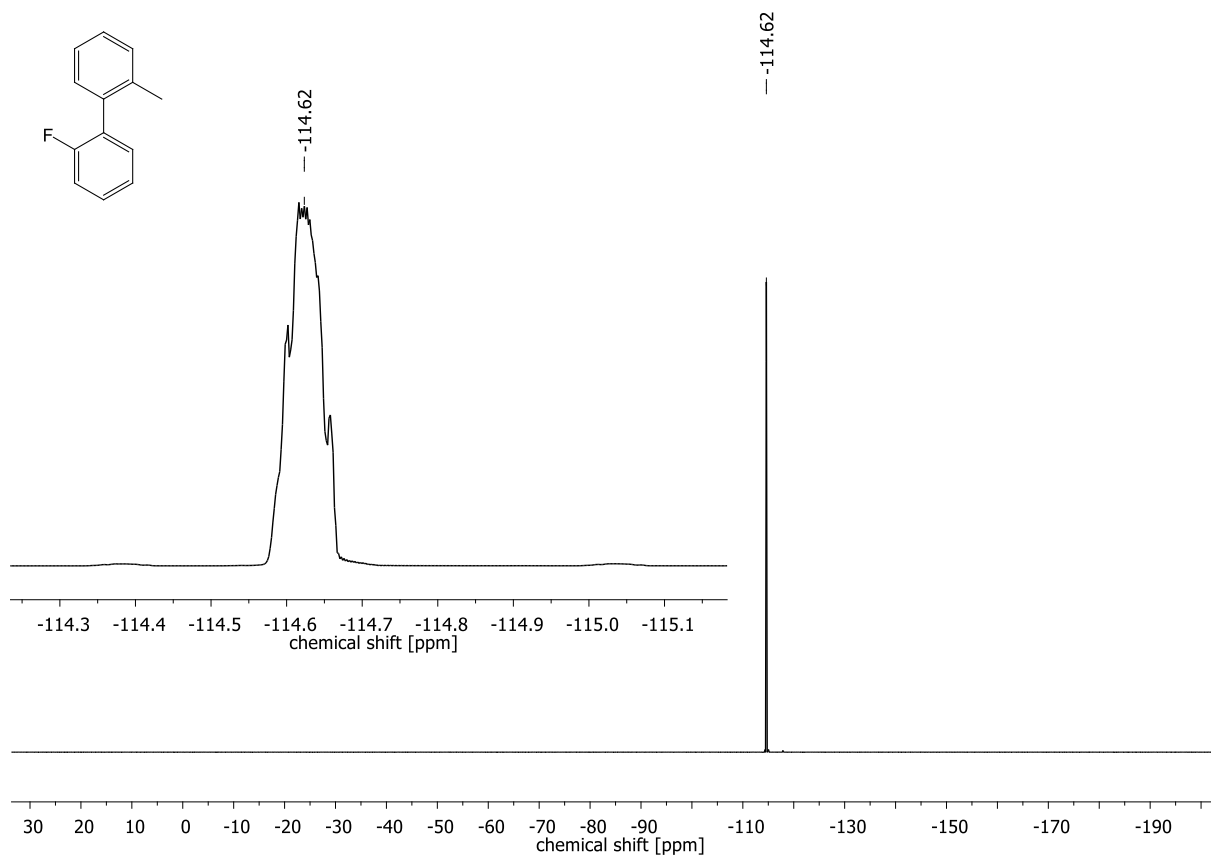


Figure 8.175: ^{19}F -NMR spectrum of 2-fluoro-2-methyl-1,1'-biphenyl.

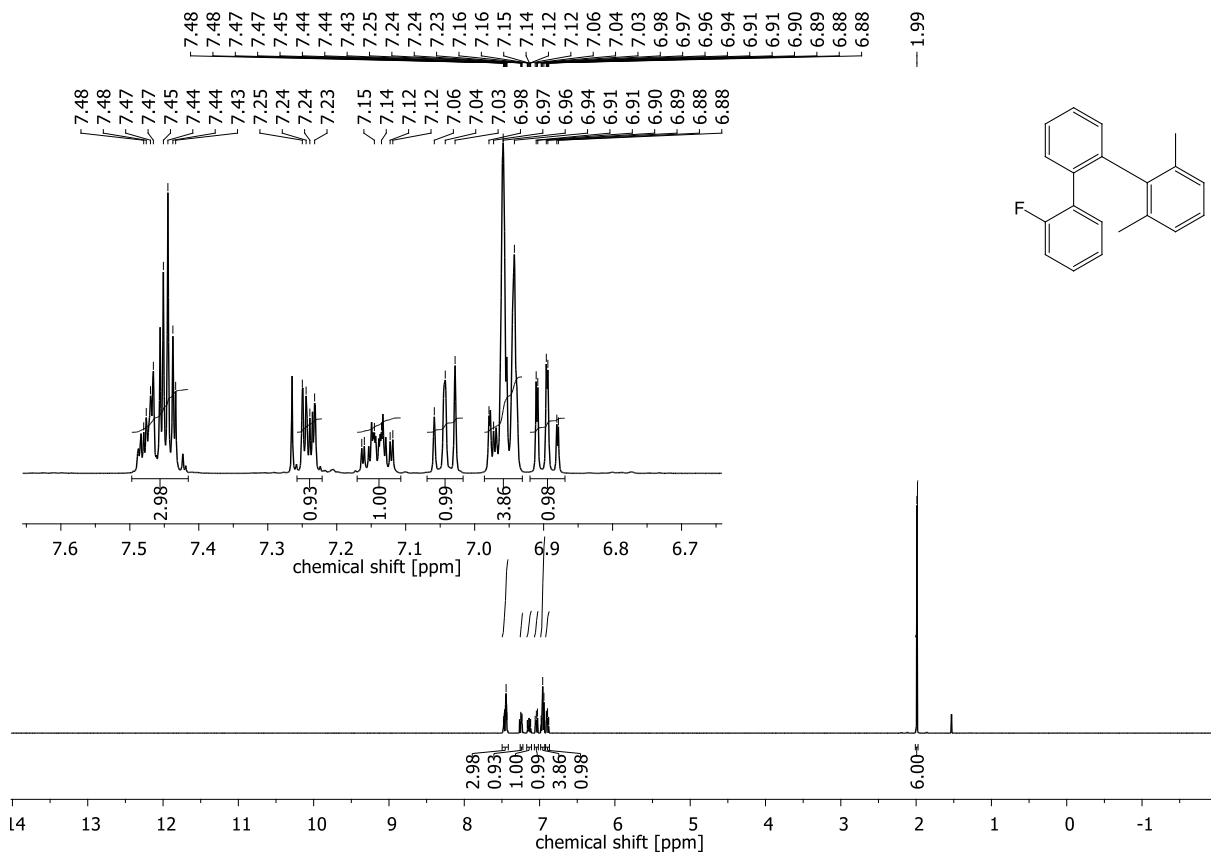


Figure 8.176: ^1H -NMR spectrum of 2''-fluoro-2,6-dimethyl-1,1':2',1''-terphenyl.

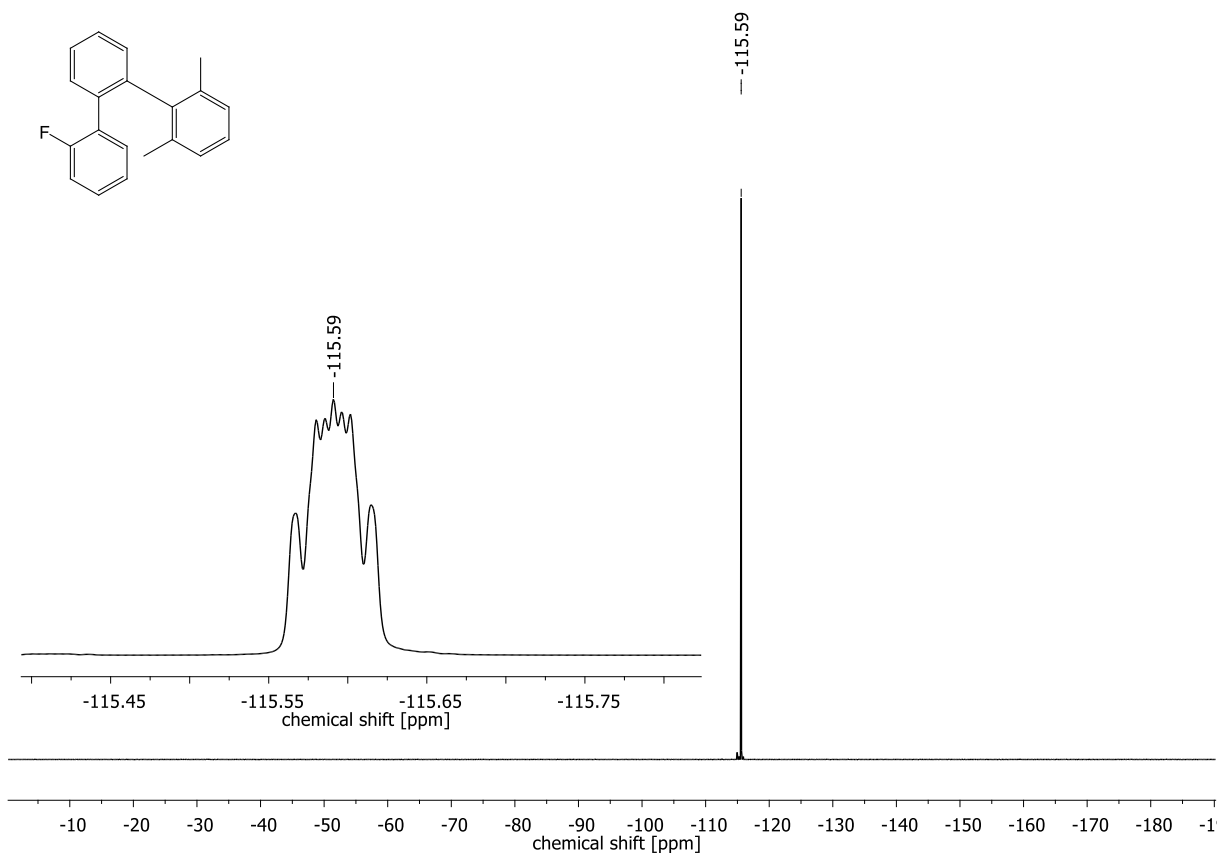


Figure 8.177: ^{19}F -NMR spectrum of 2''-fluoro-2,6-dimethyl-1,1':2',1''-terphenyl.

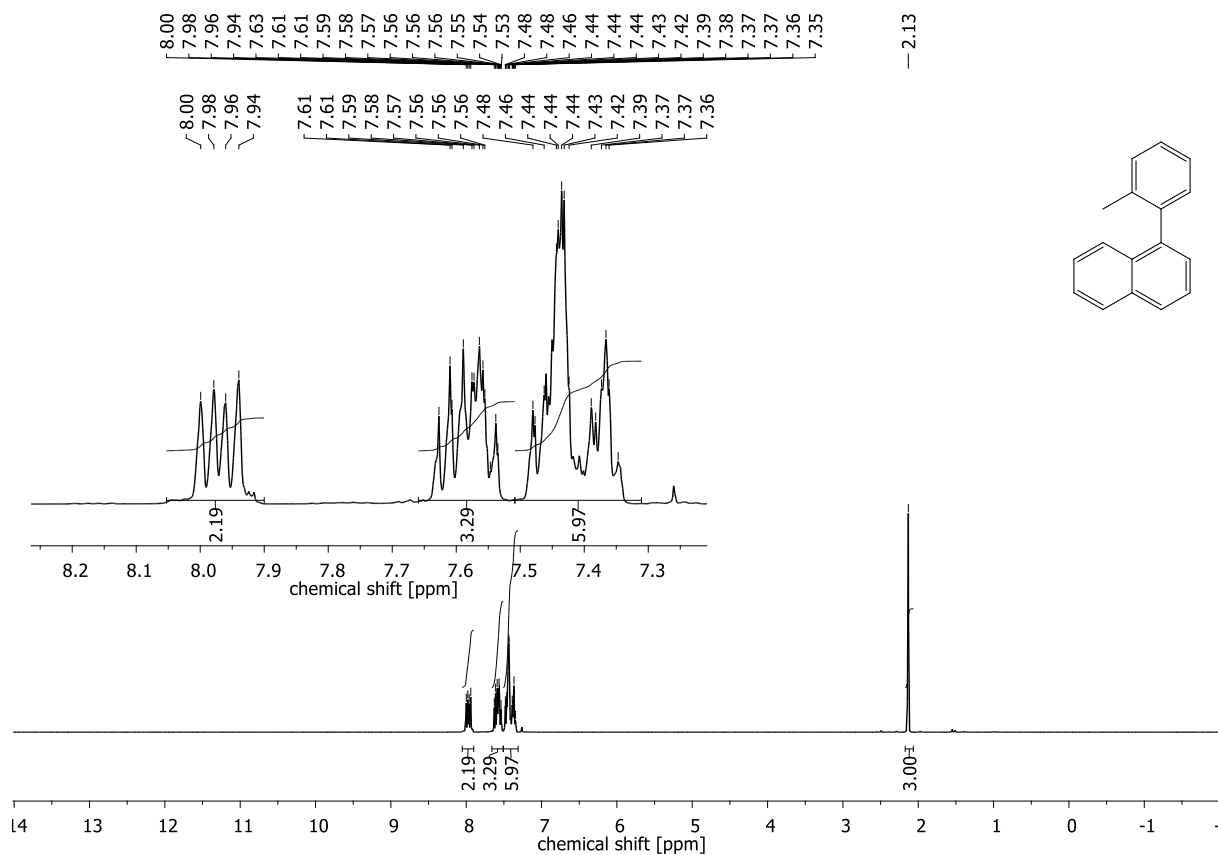


Figure 8.178: ^1H -NMR spectrum of 1-(o-tolyl)naphthalene.

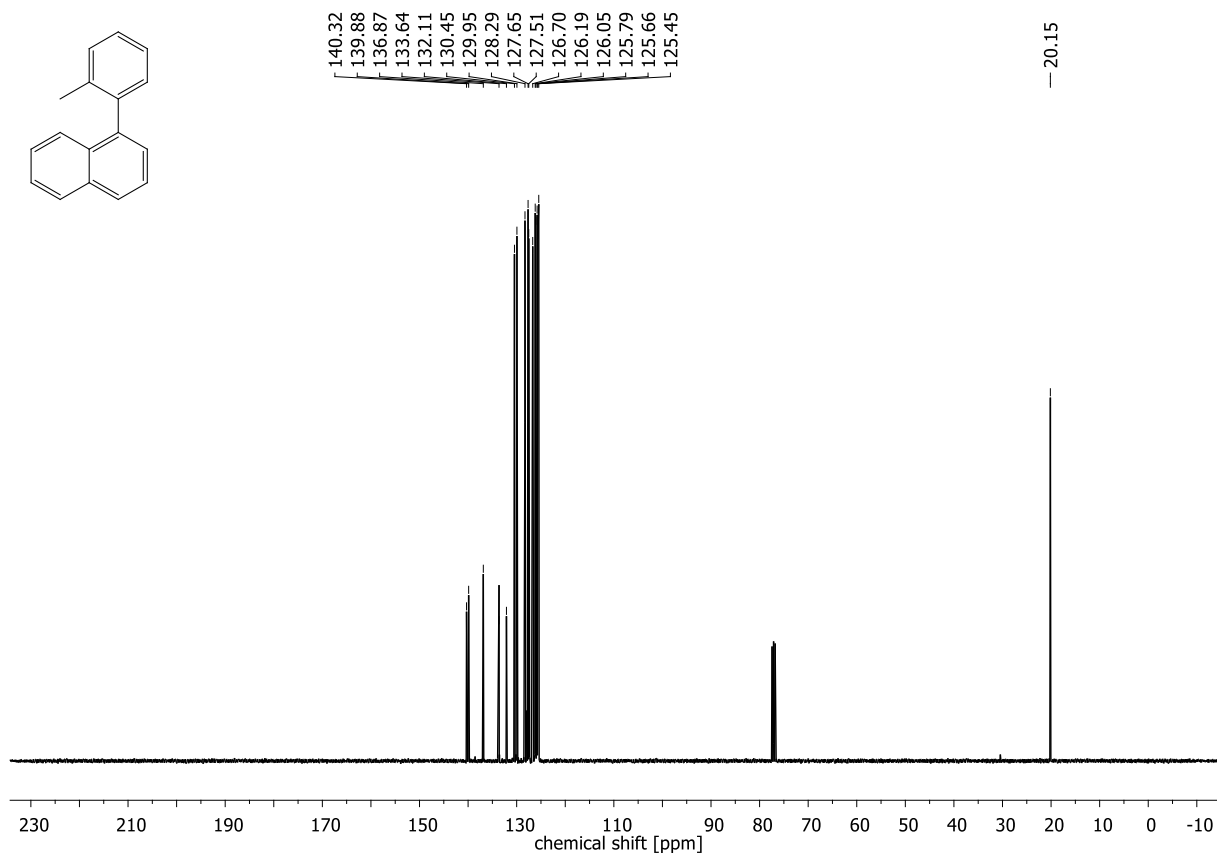


Figure 8.179: $^{13}\text{C-NMR}$ spectrum of 1-(*o*-tolyl)naphthalene.

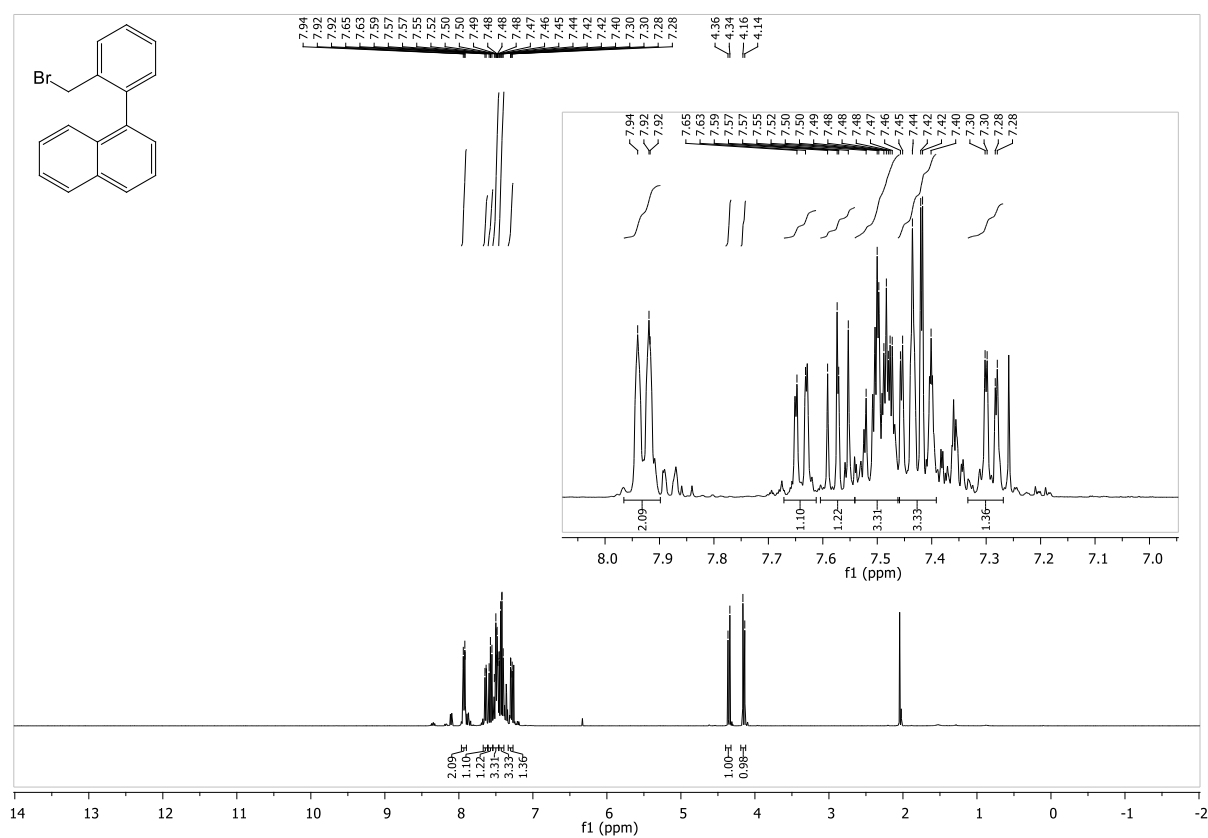


Figure 8.180: $^1\text{H-NMR}$ spectrum of 1-(2-(bromomethyl)phenyl)naphthalene.

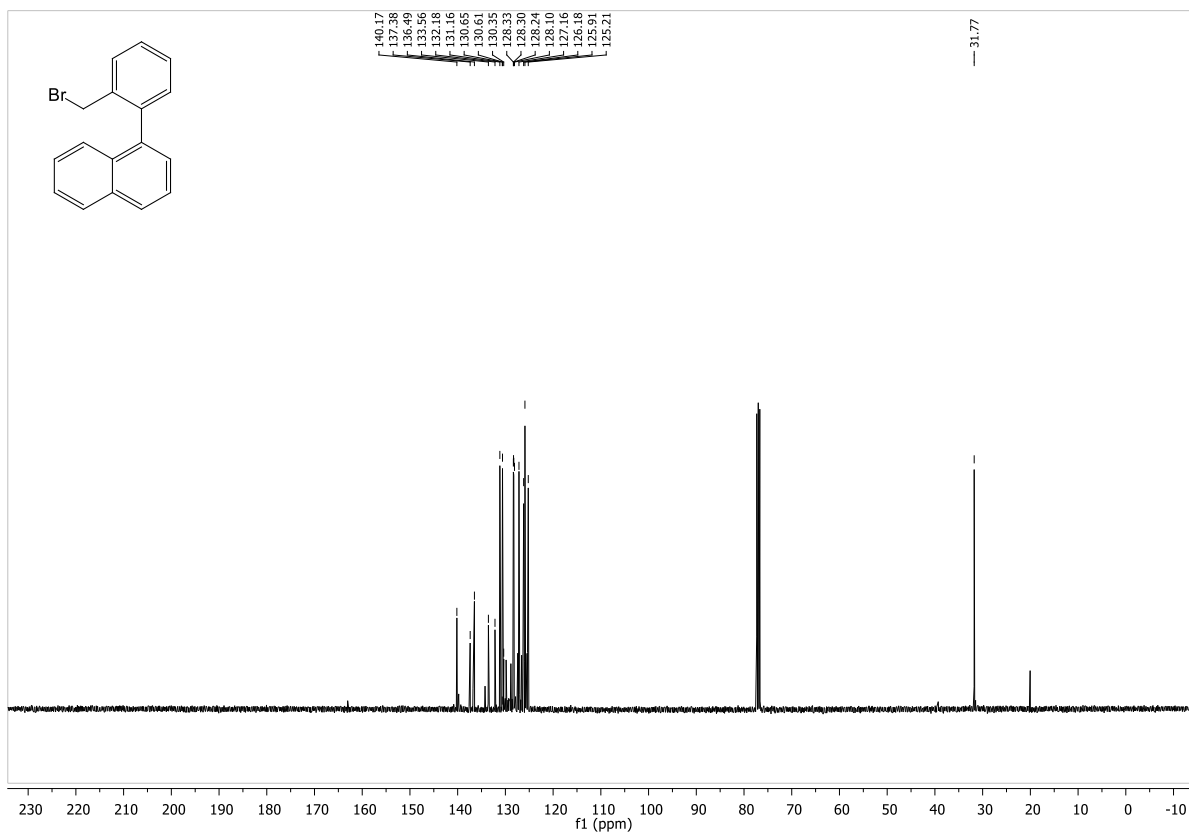


Figure 8.181: $^{13}\text{C-NMR}$ spectrum of 1-(2-(bromomethyl)phenyl)naphthalene.

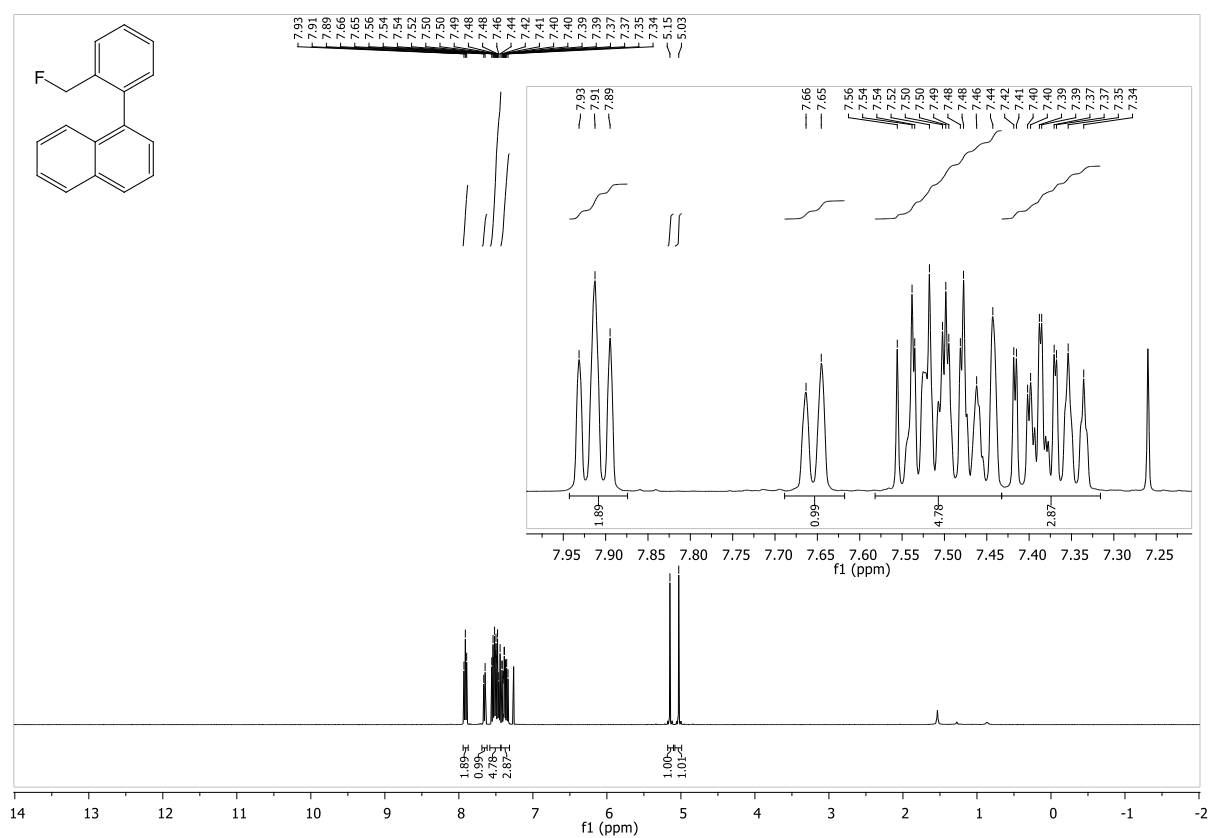


Figure 8.182: $^1\text{H-NMR}$ spectrum of 1-(2-(fluoromethyl)phenyl)naphthalene.

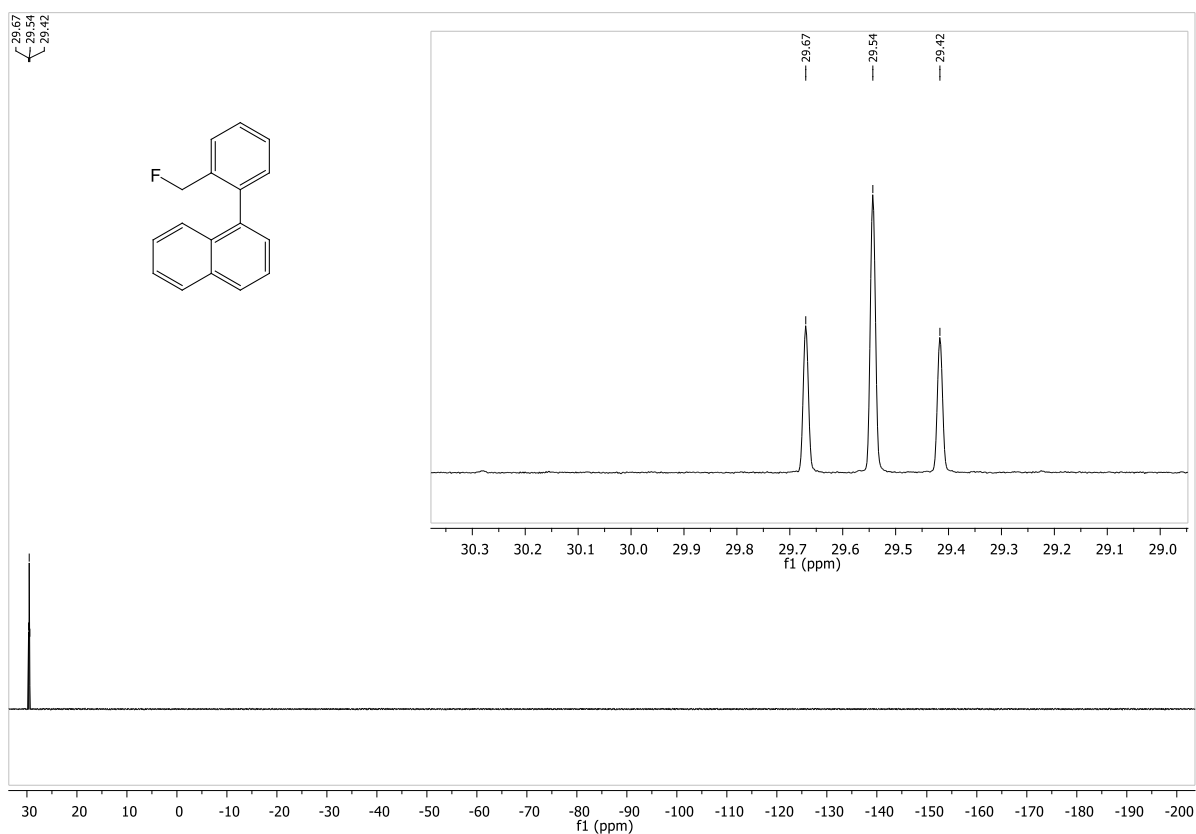


Figure 8.183: ^{19}F -NMR spectrum of 1-(2-(fluoromethyl)phenyl)naphthalene.

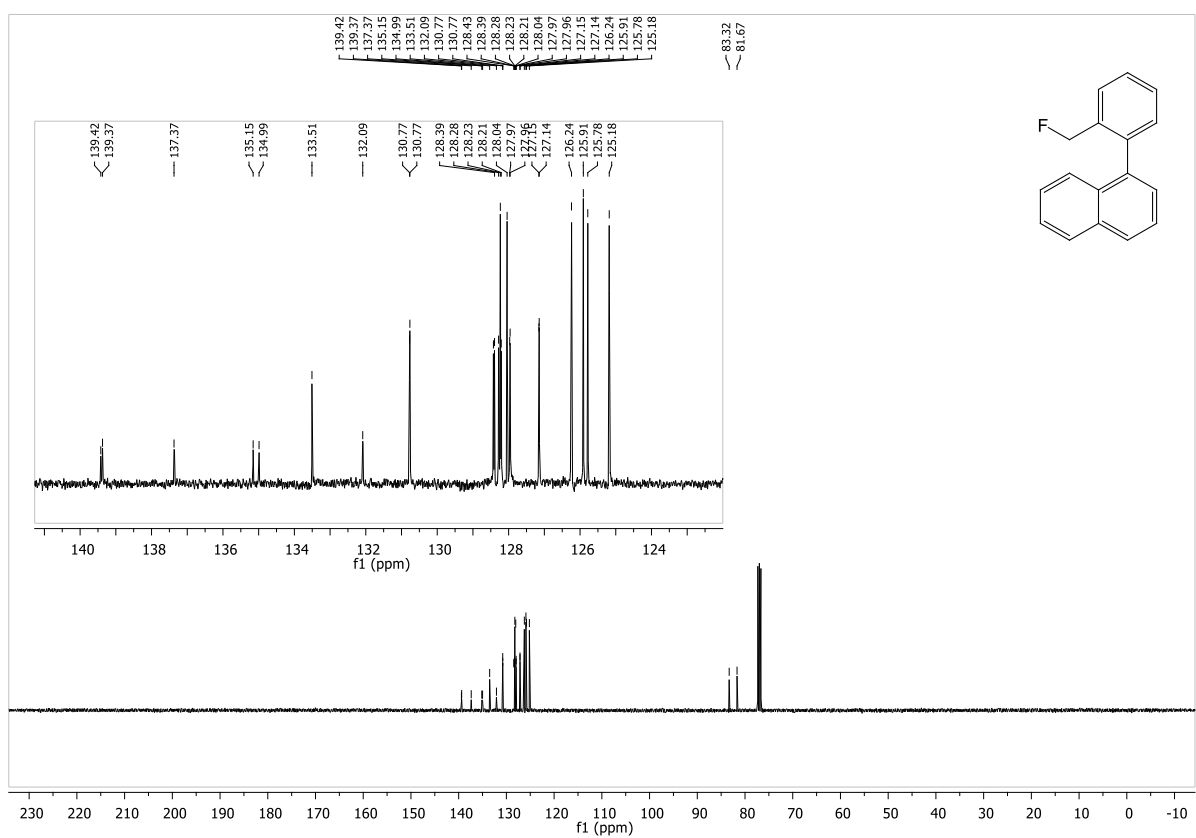


Figure 8.184: ^{13}C -NMR spectrum of 1-(2-(fluoromethyl)phenyl)naphthalene.

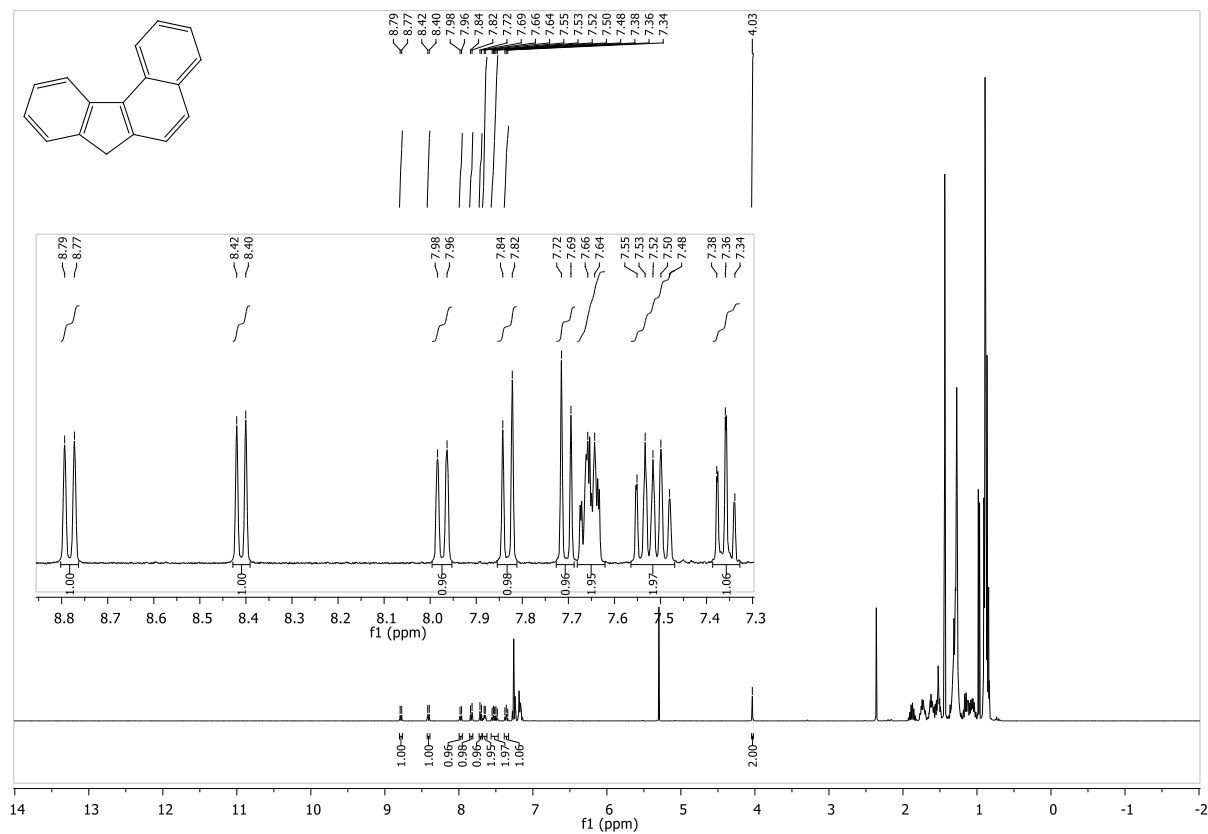


Figure 8.185: ¹H-NMR spectrum of 7H-benzo[c]fluorene.

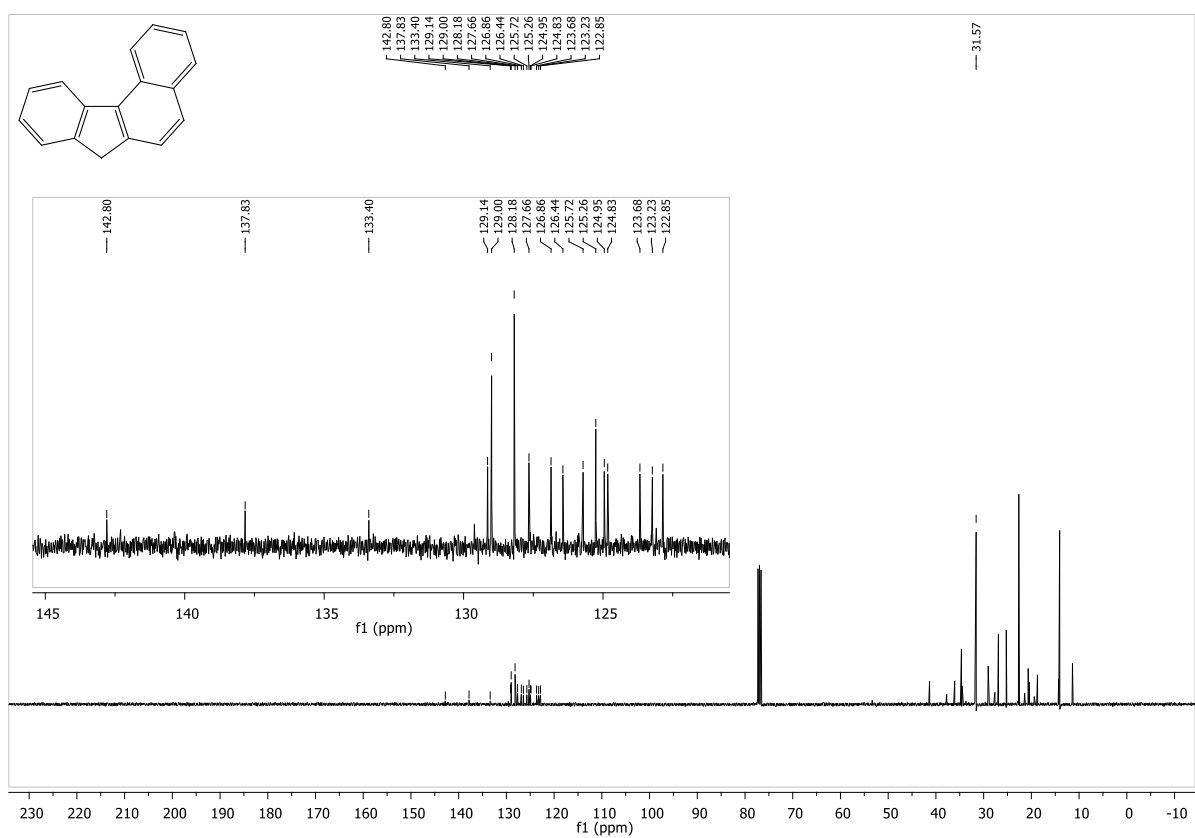


Figure 8.186: ¹³C-NMR spectrum of 7H-benzo[c]fluorene.

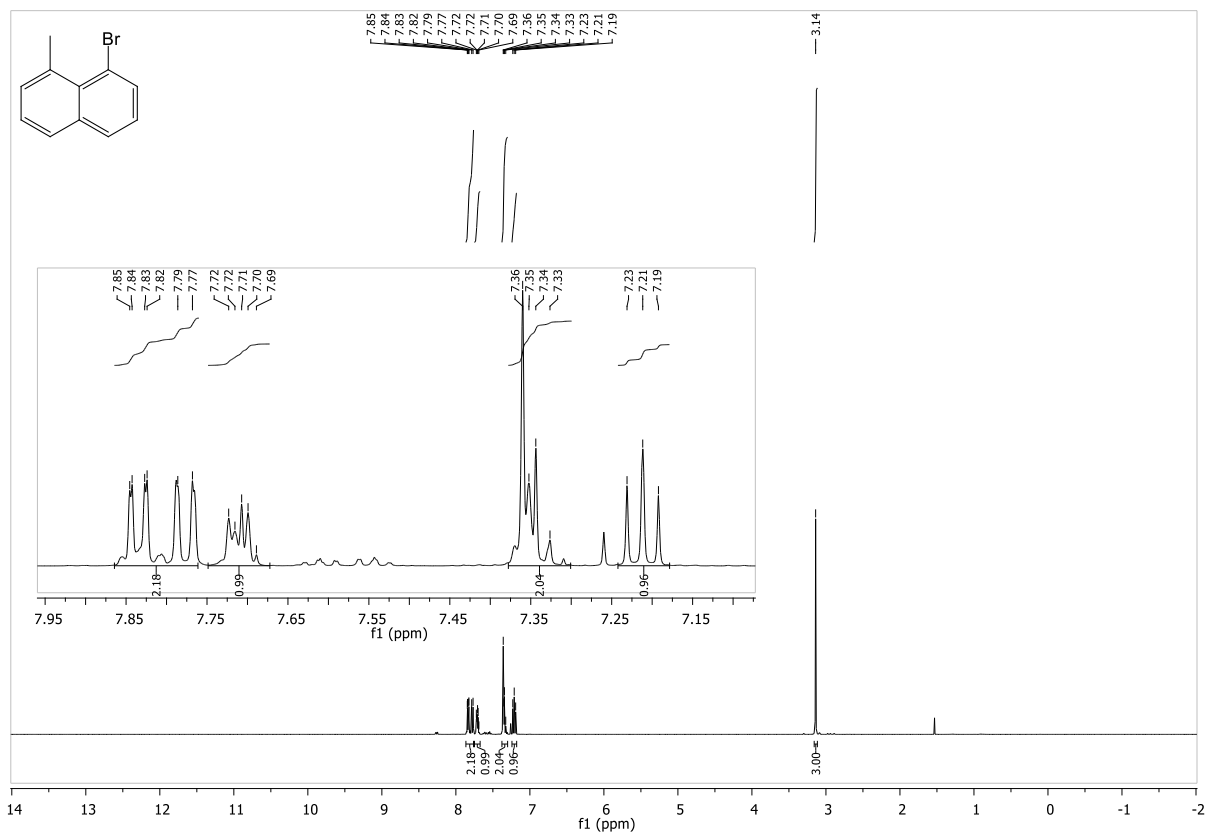


Figure 8.187: ¹H-NMR spectrum of 1-bromo-8-methylnaphthalene.

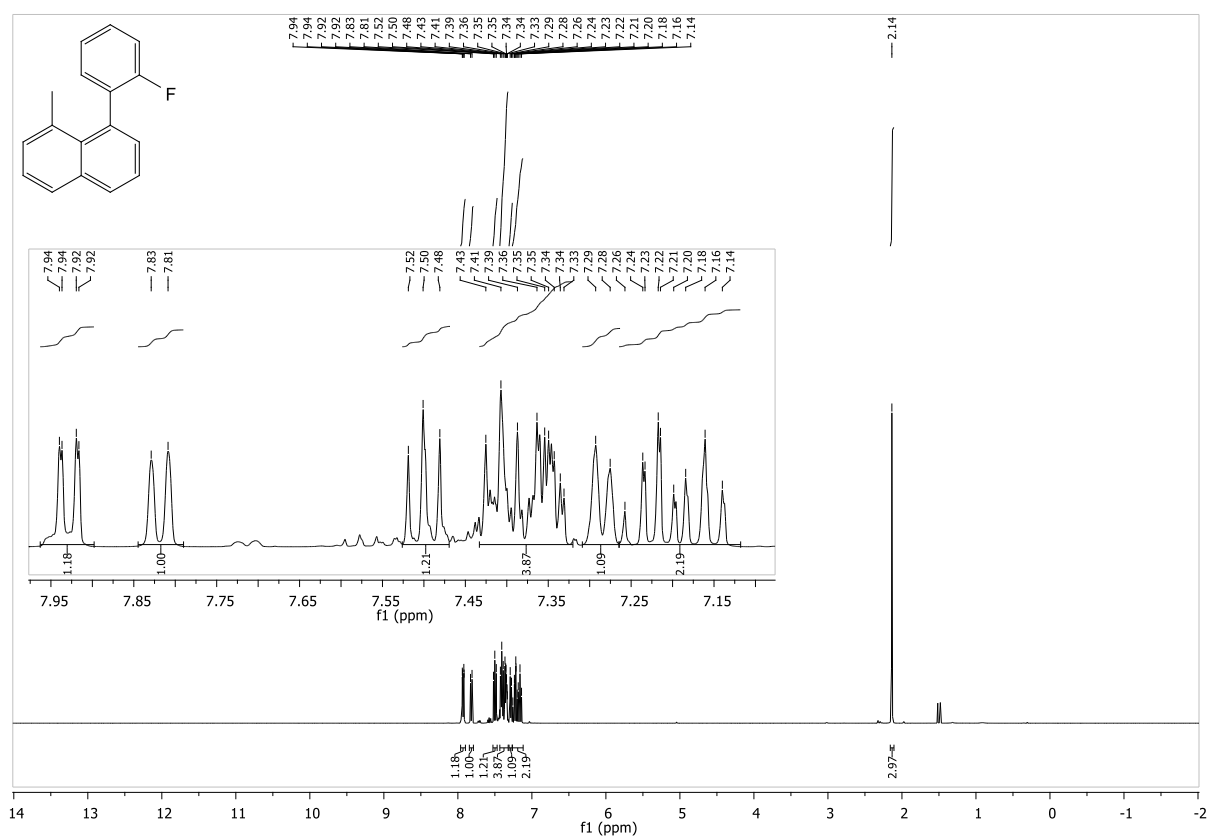


Figure 8.188: ¹H-NMR spectrum of 1-(2-fluorophenyl)-8-methylnaphthalene.

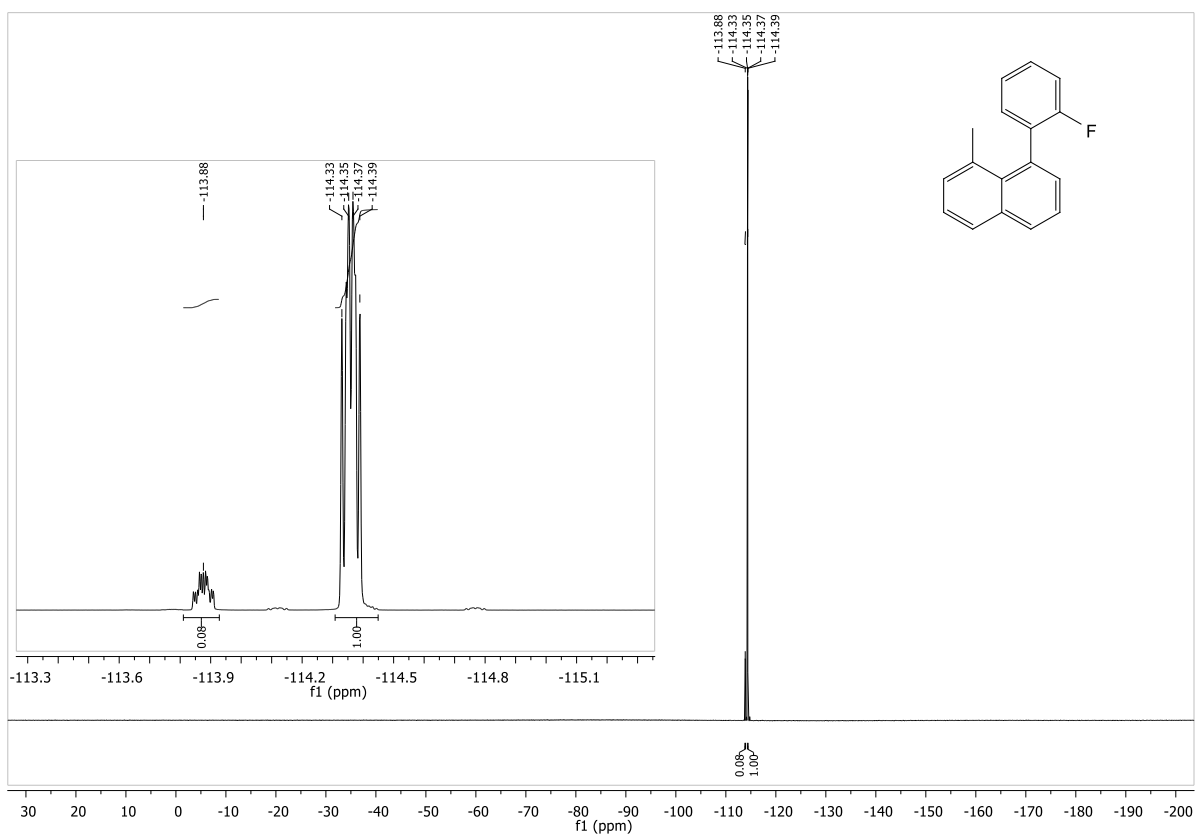


Figure 8.189: ^{19}F -NMR spectrum of 1-(2-fluorophenyl)-8-methylnaphthalene.

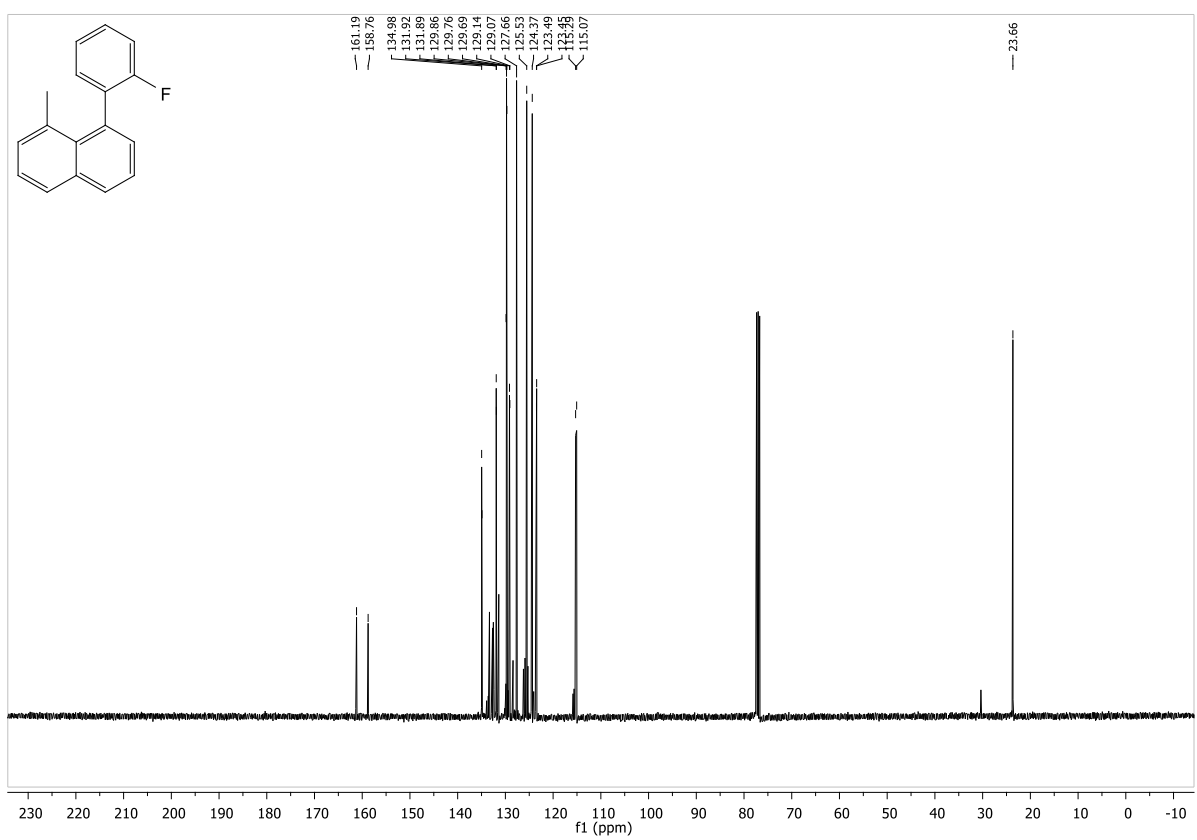


Figure 8.190: ^{13}C -NMR spectrum of 1-(2-fluorophenyl)-8-methylnaphthalene.

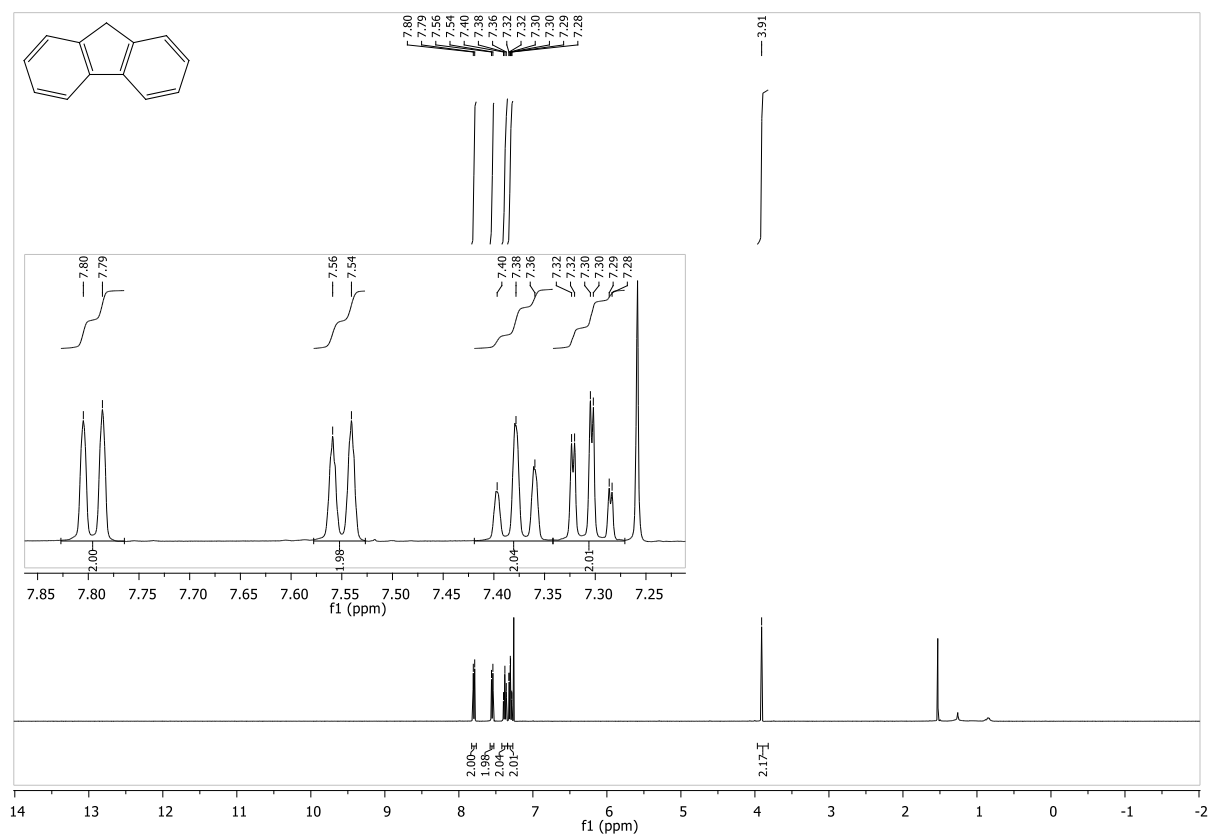


Figure 8.191: ¹H-NMR spectrum of 9H-fluorene.

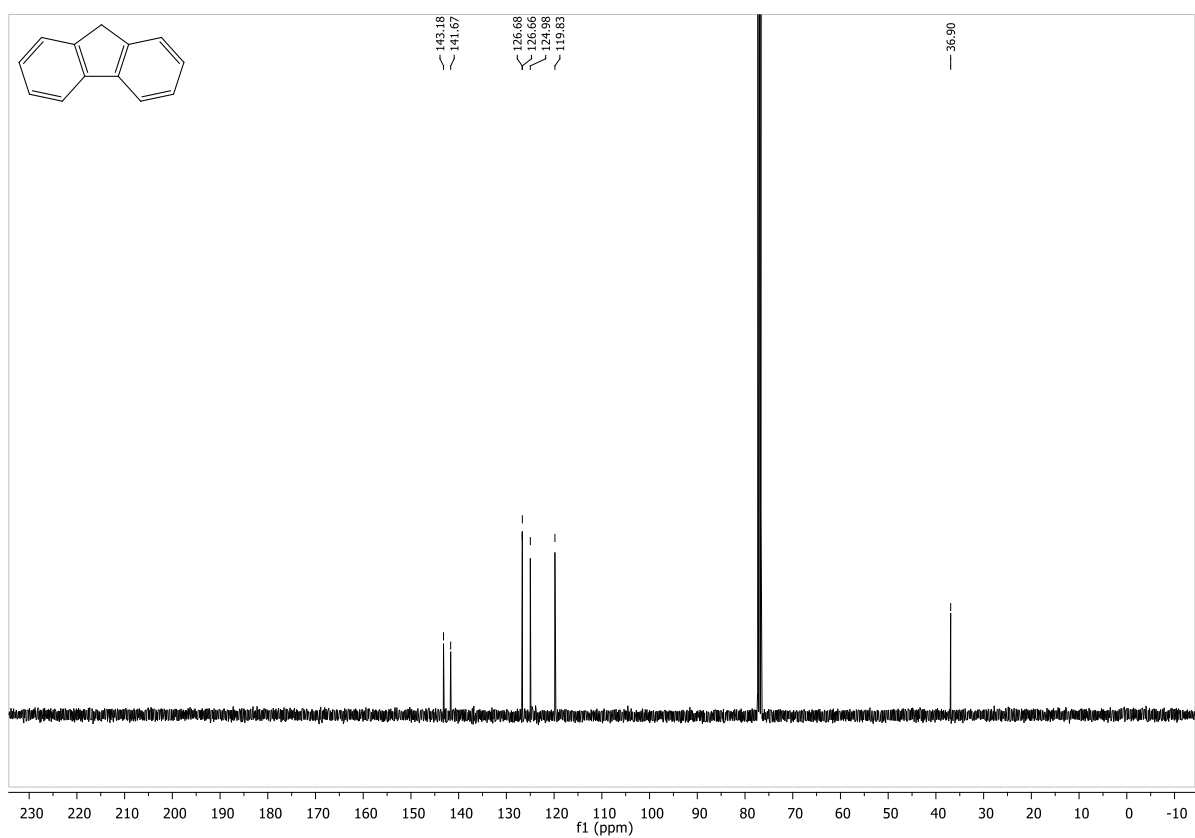


Figure 8.192: ¹³C-NMR spectrum of 9H-fluorene.

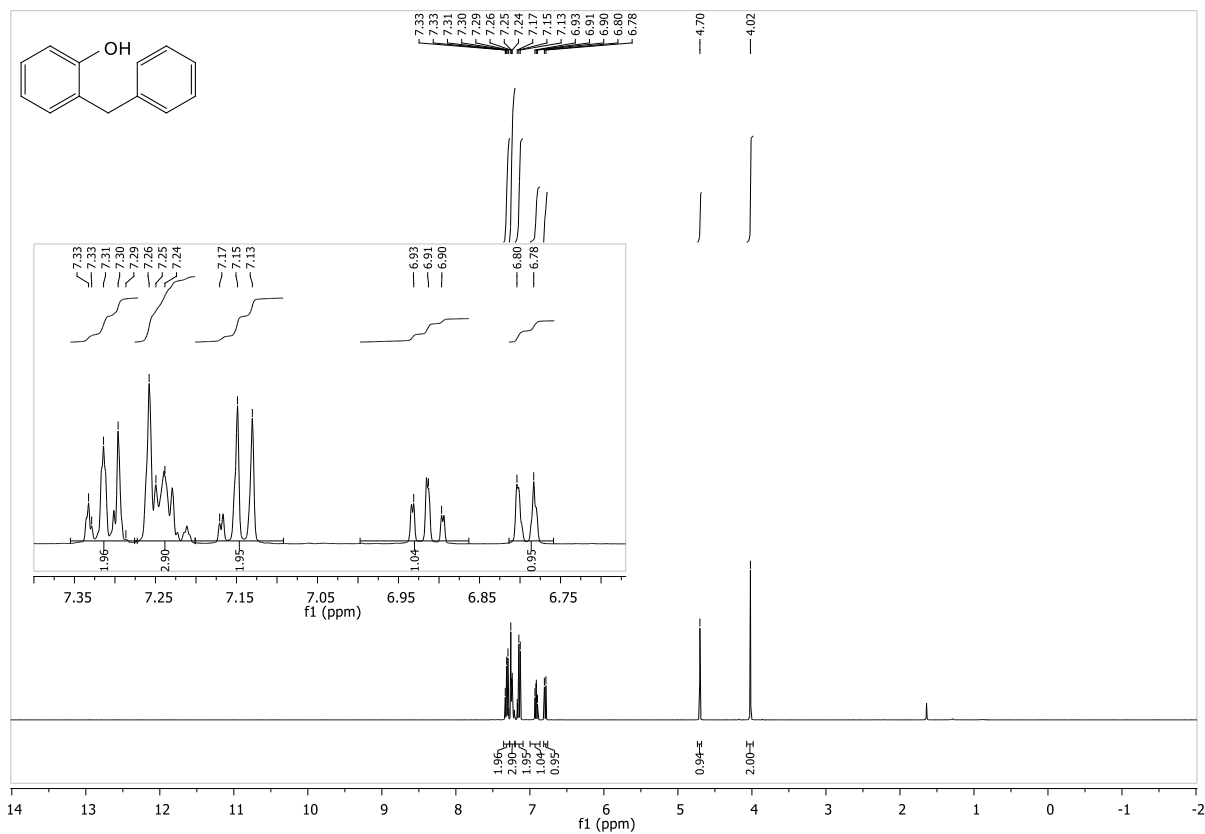


Figure 8.193: $^1\text{H-NMR}$ spectrum of 2-benzylphenol.

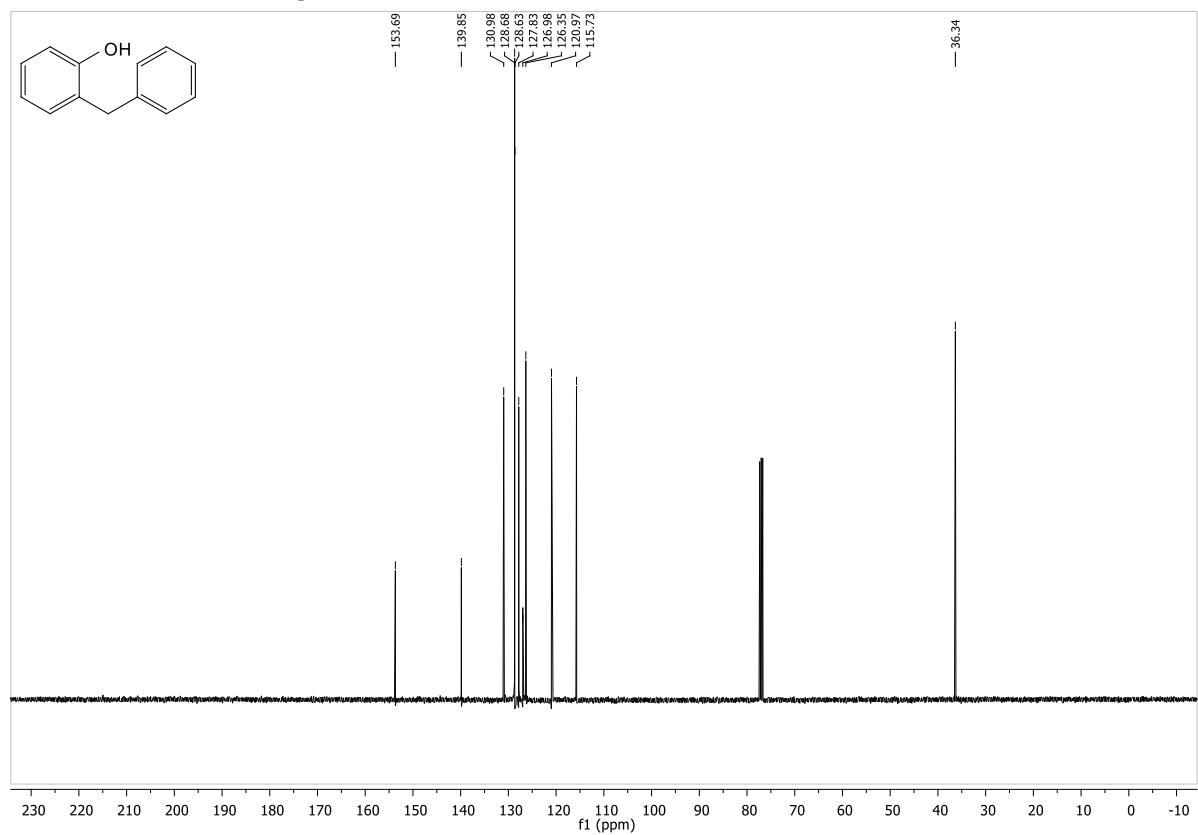


Figure 8.194: $^{13}\text{C-NMR}$ spectrum of 2-benzylphenol.

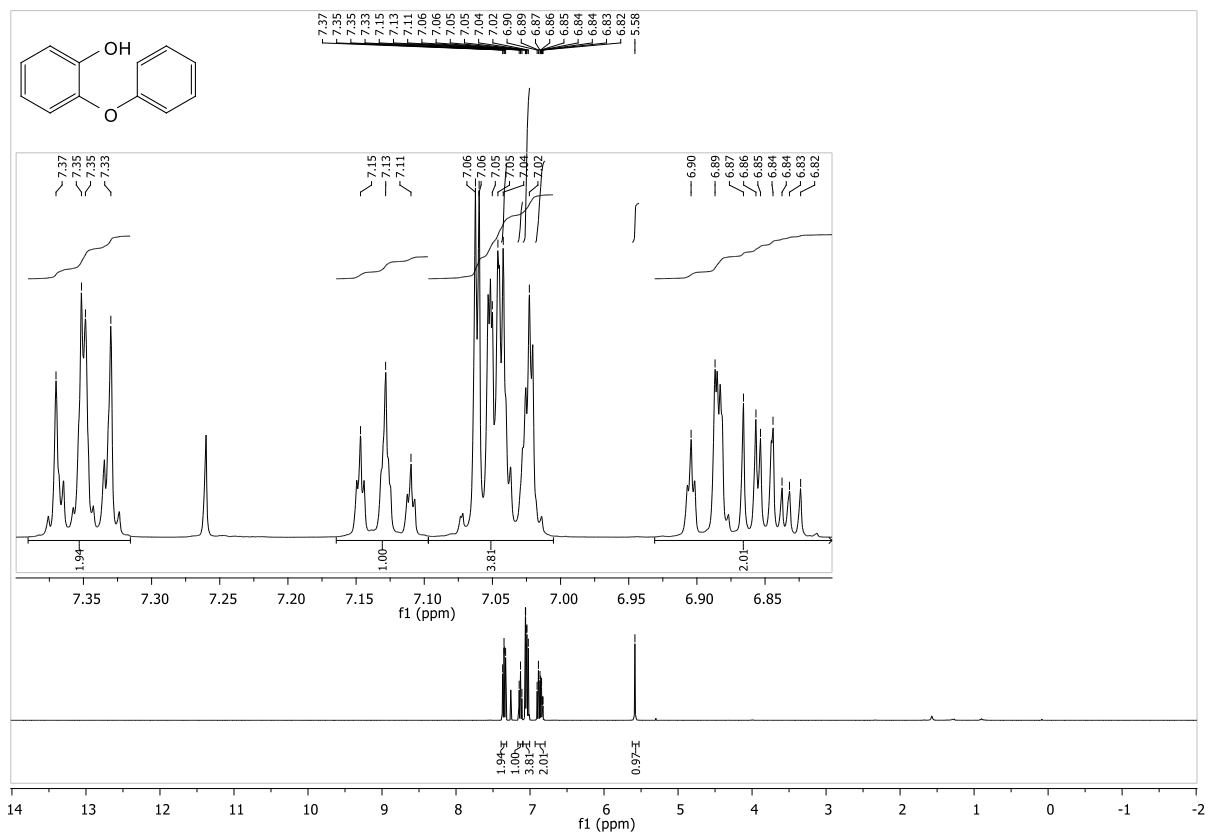


Figure 8.195: ¹H-NMR spectrum of 2-phenoxyphenol.

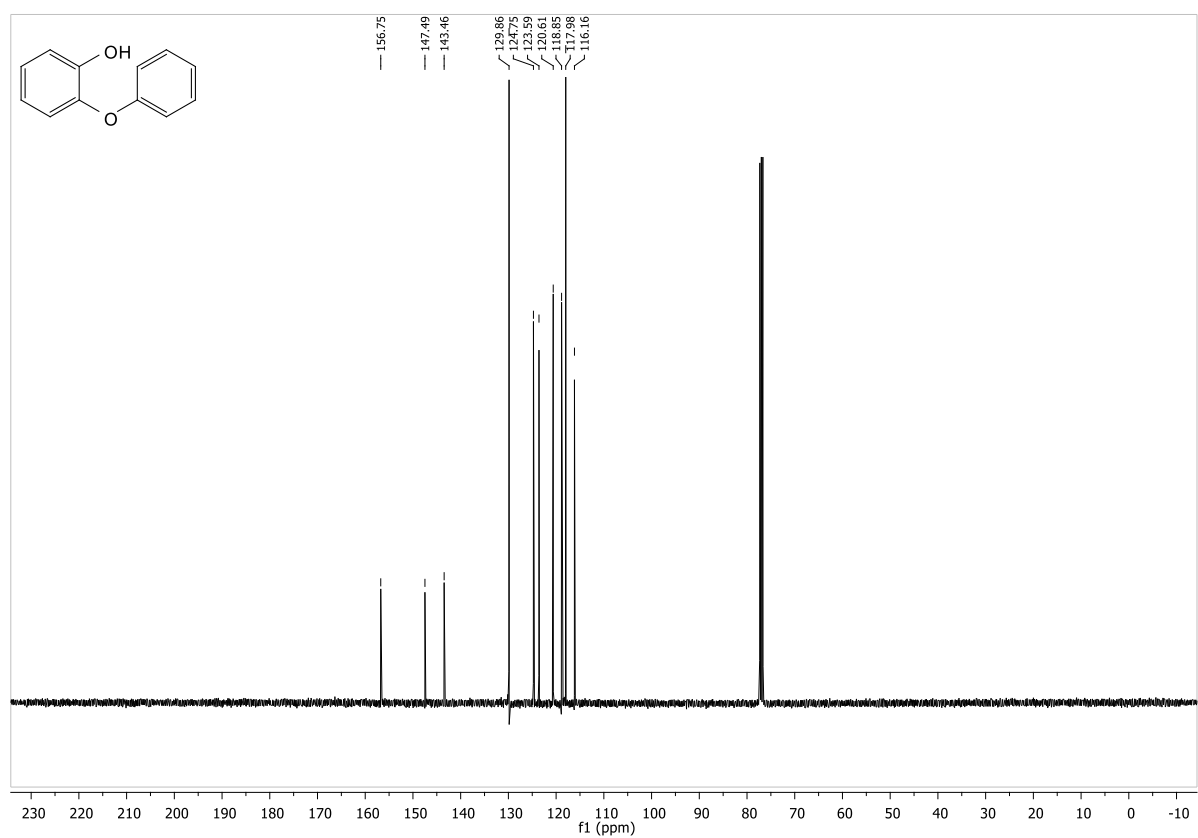


Figure 8.196: ¹³C-NMR spectrum of 2-phenoxyphenol.

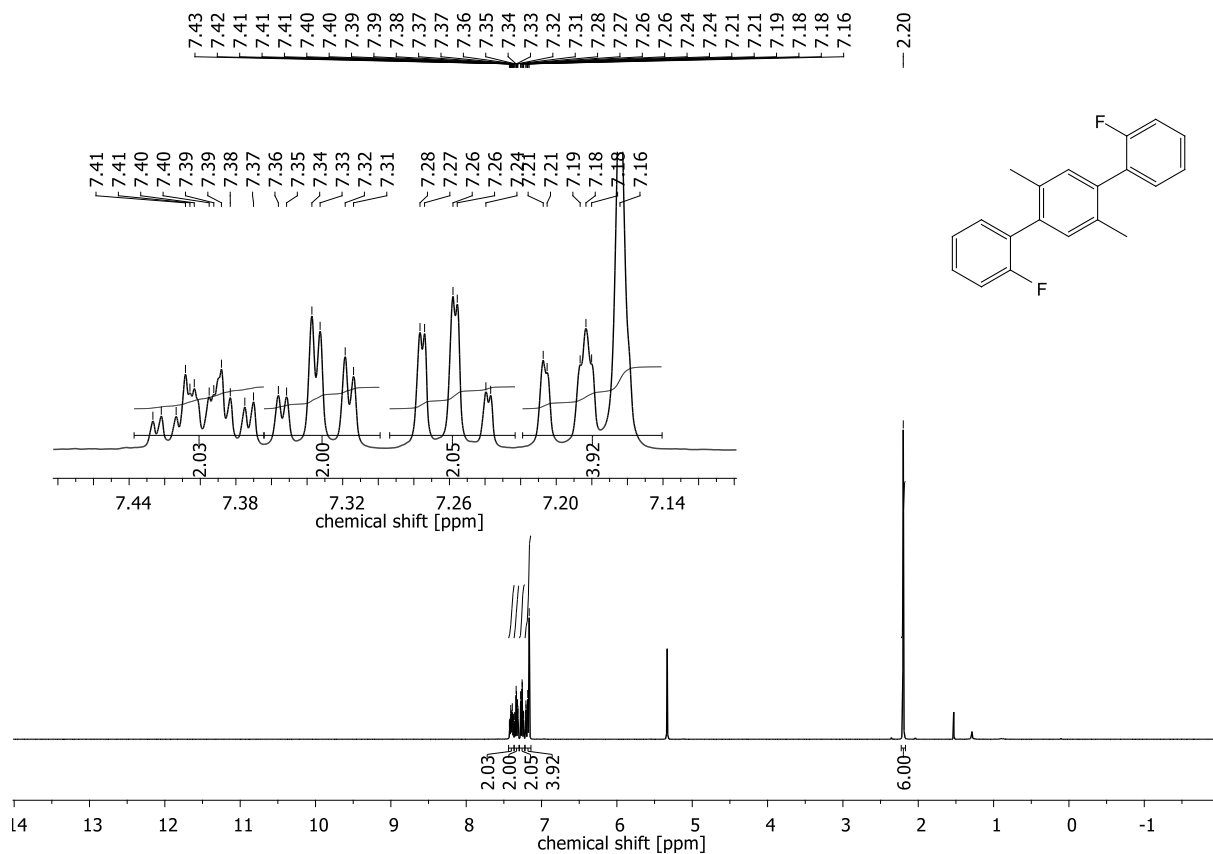


Figure 8.197: ¹H-NMR spectrum of 2,2''-difluoro-2',5'-dimethyl-1,1':4',1''-terphenyl.

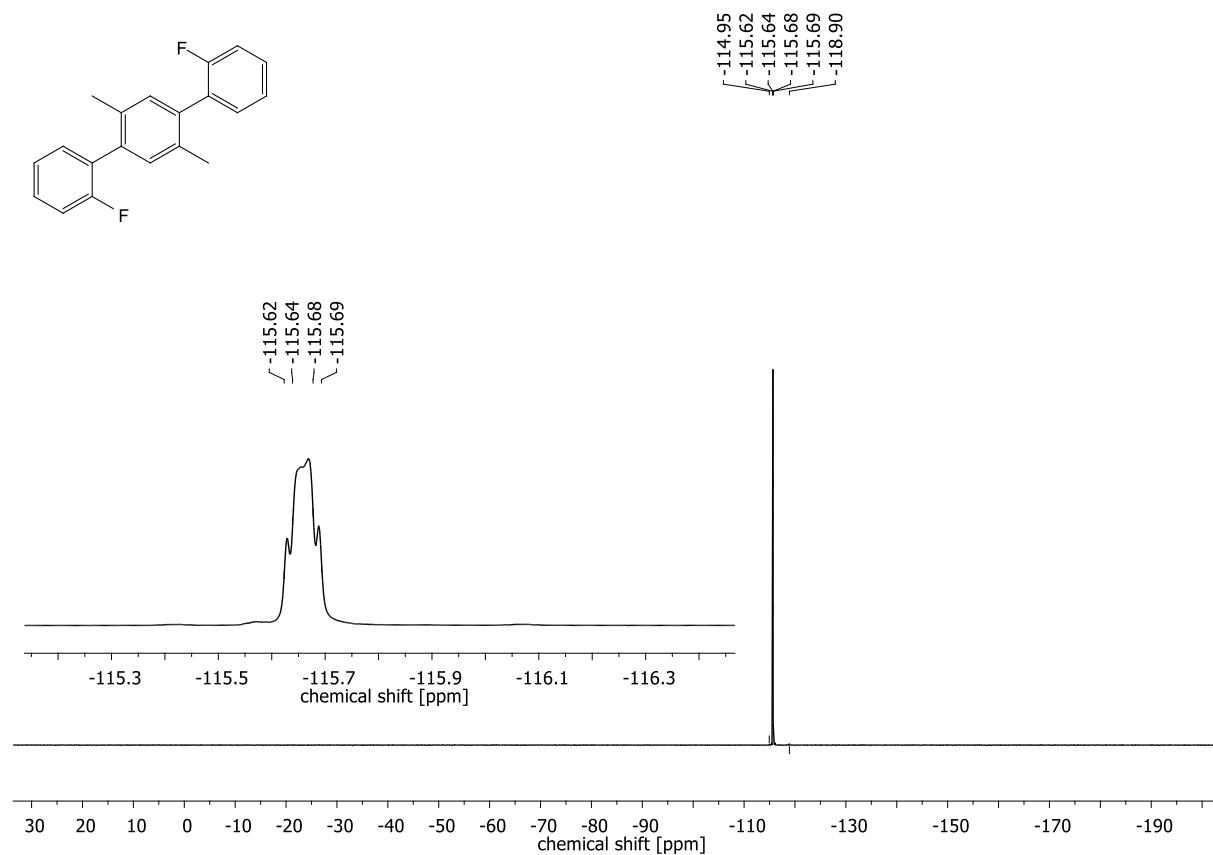


Figure 8.198: ¹⁹F-NMR spectrum of 2,2''-difluoro-2',5'-dimethyl-1,1':4',1''-terphenyl.

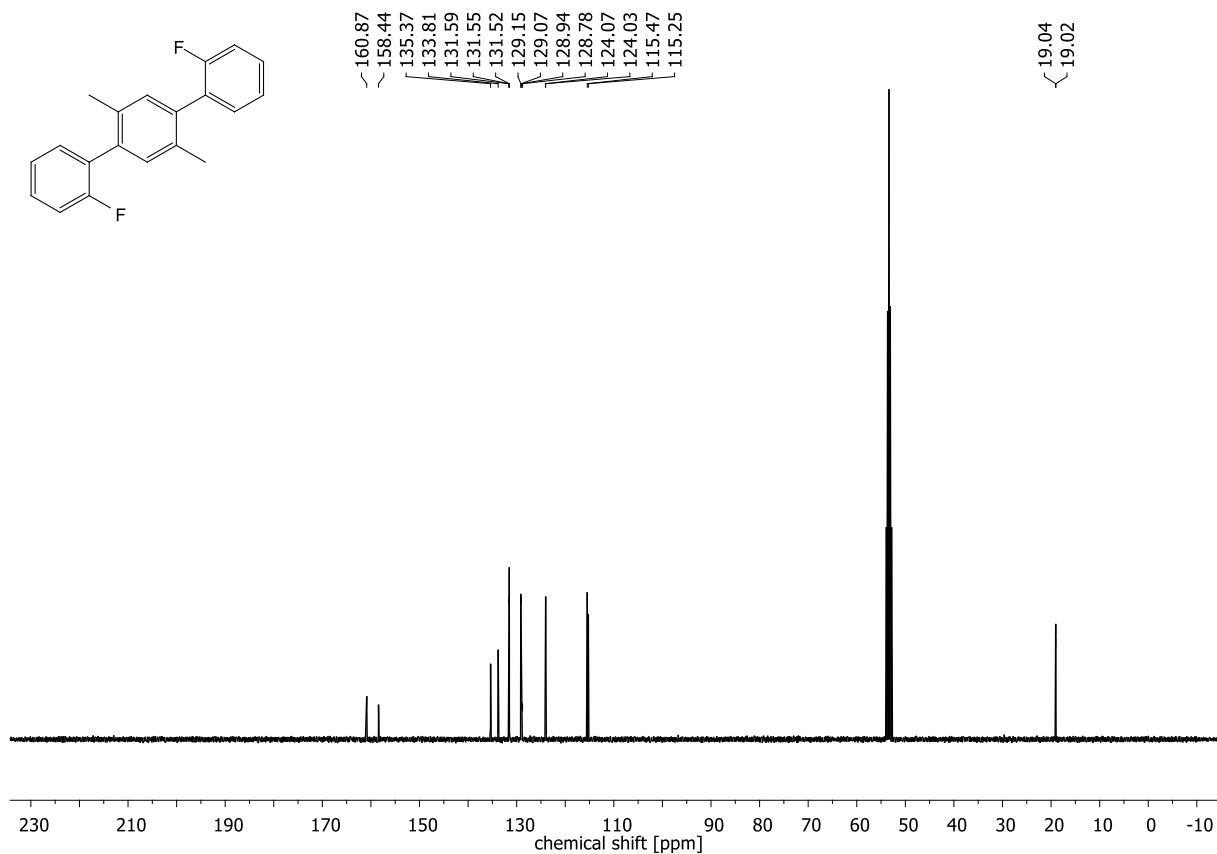


Figure 8.199: $^{13}\text{C-NMR}$ spectrum of 2,2''-difluoro-2',5'-dimethyl-1,1':4',1''-terphenyl.

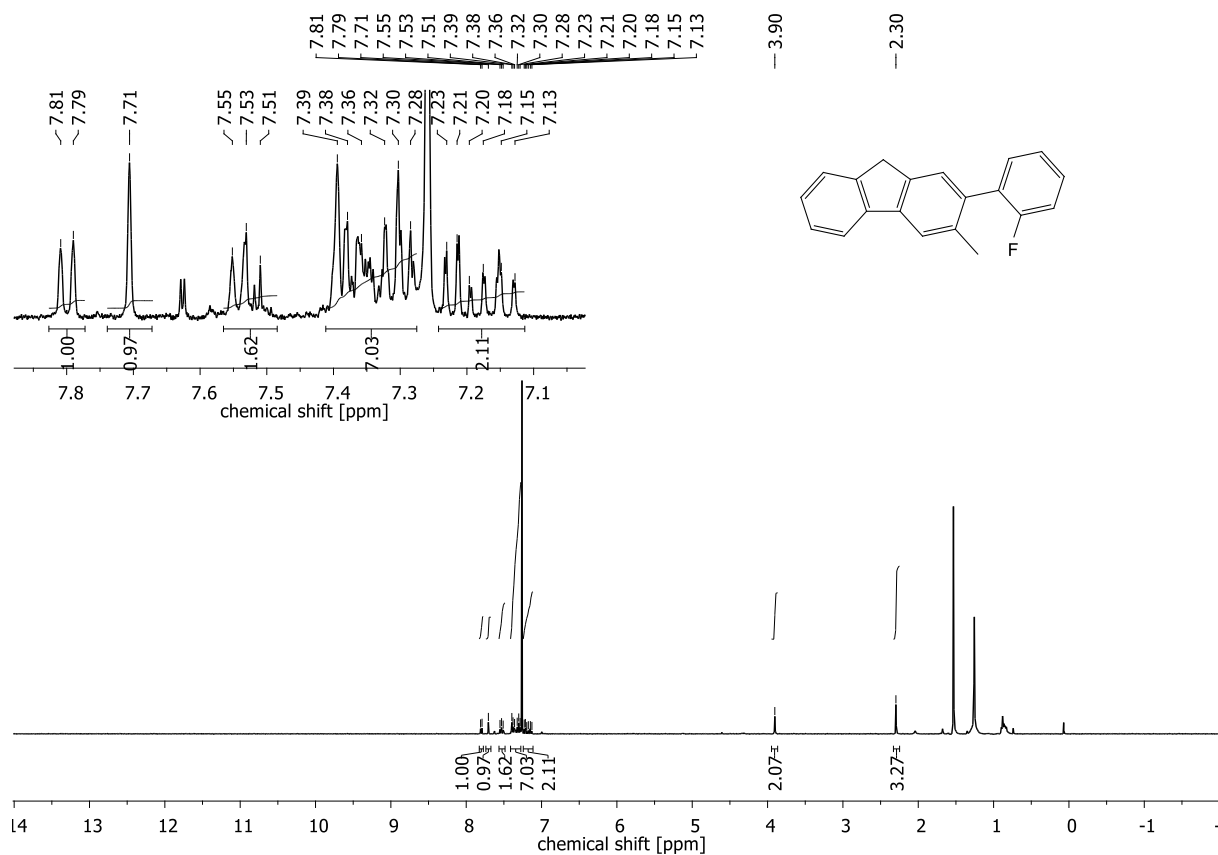


Figure 8.200: $^1\text{H-NMR}$ spectrum of 2-(2-fluorophenyl)-3-methyl-9H-fluorene.

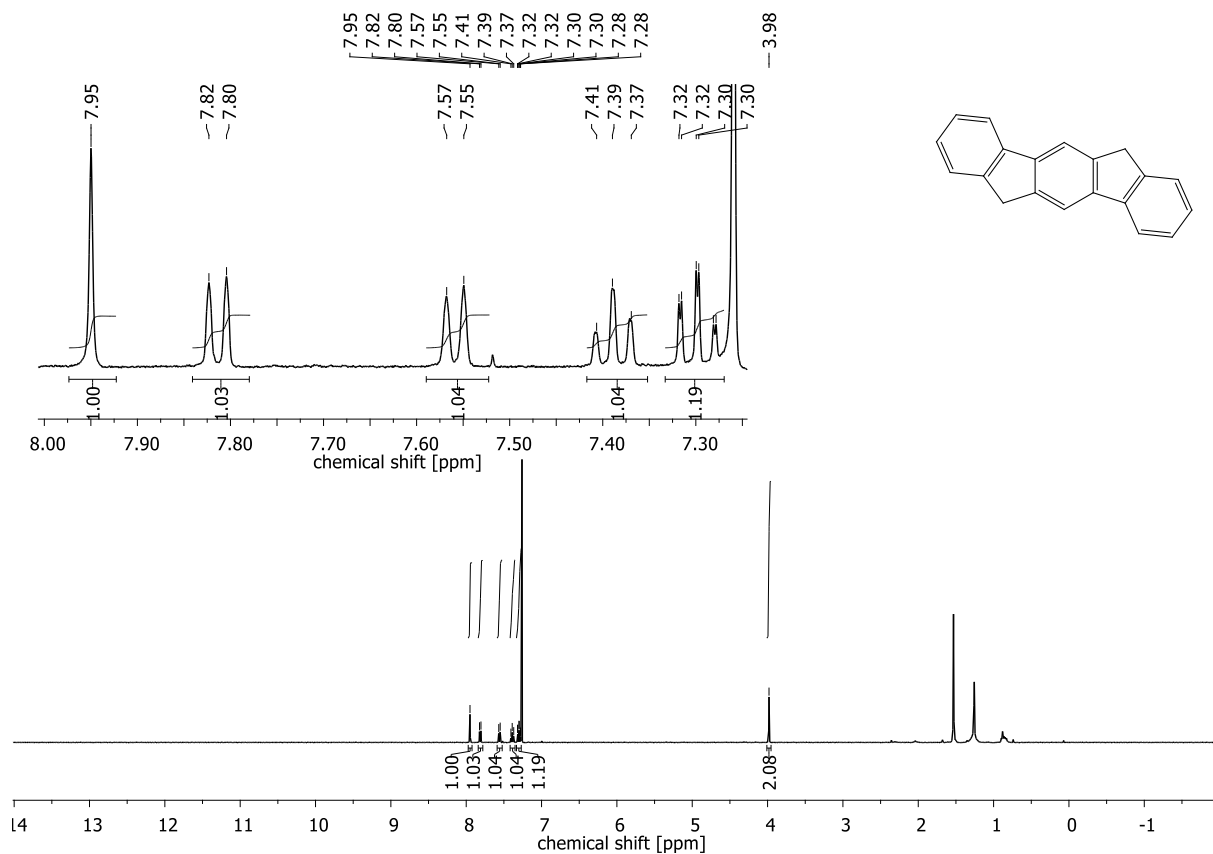


Figure 8.201: $^1\text{H-NMR}$ spectrum of 6,12-dihydroindeno[1,2-b]fluorene.

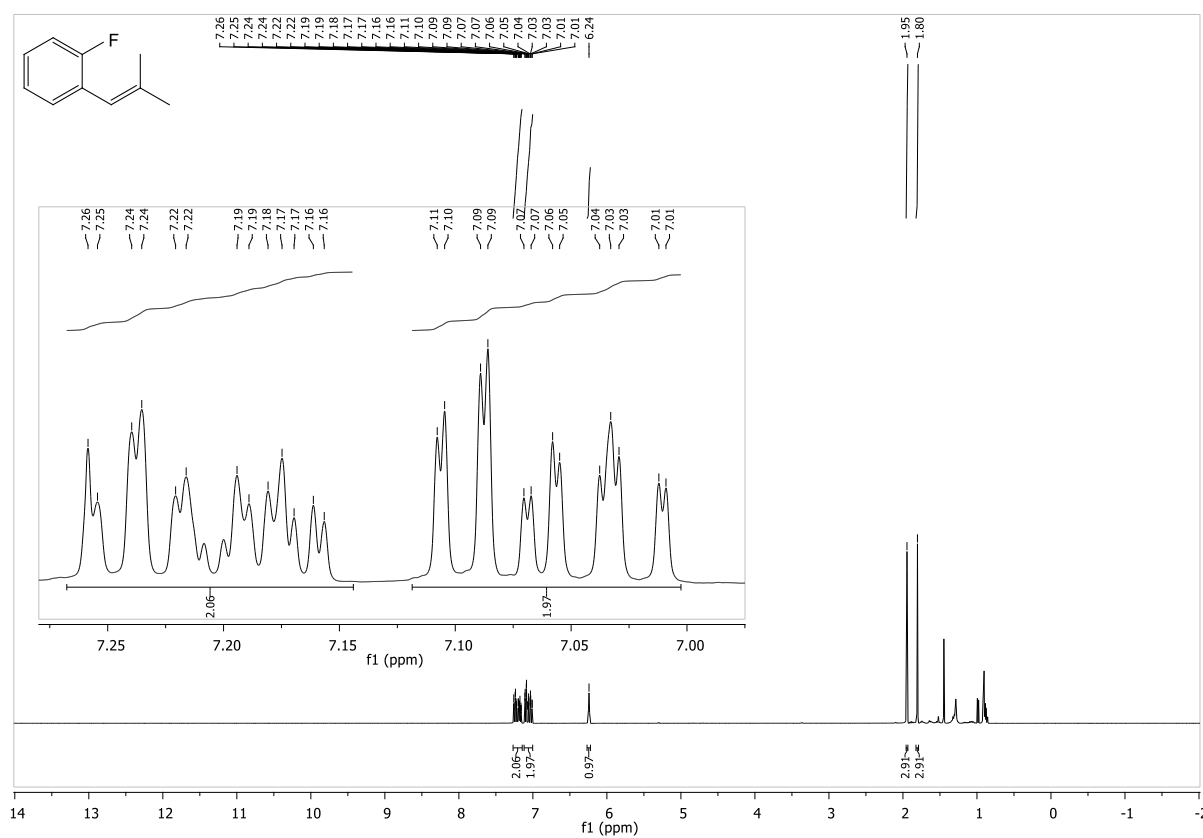


Figure 8.202: $^1\text{H-NMR}$ spectrum of 1-fluoro-2-(2-methylprop-1-en-1-yl)benzene.

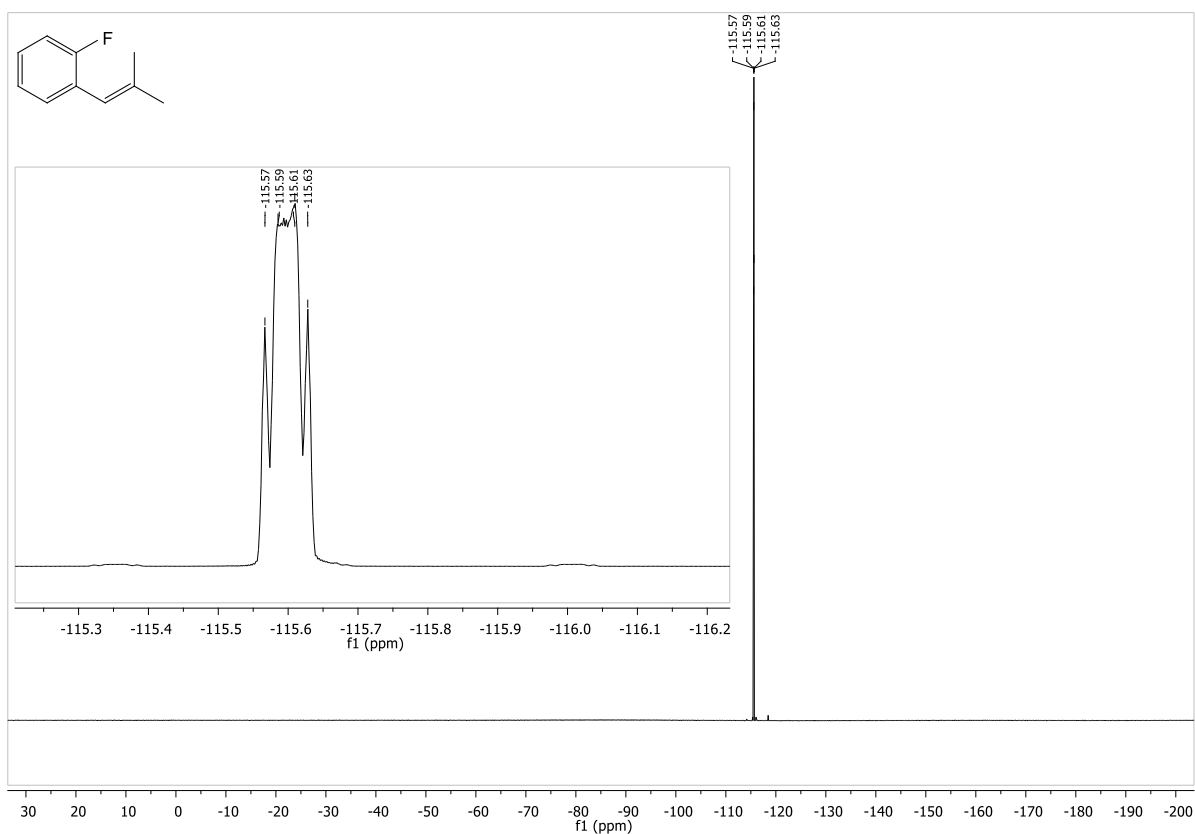


Figure 8.203: ^{19}F -NMR spectrum of 1-fluoro-2-(2-methylprop-1-en-1-yl)benzene.

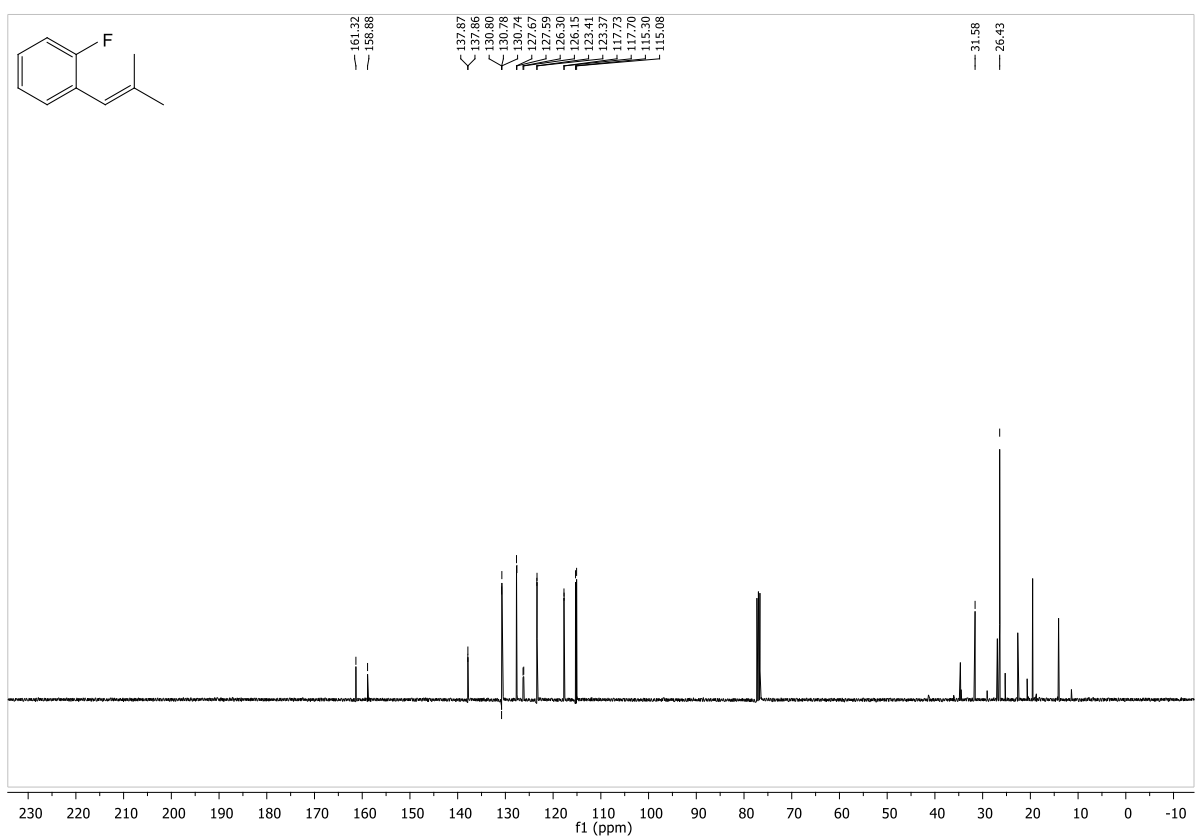


Figure 8.204: ^{13}C -NMR spectrum of 1-fluoro-2-(2-methylprop-1-en-1-yl)benzene.

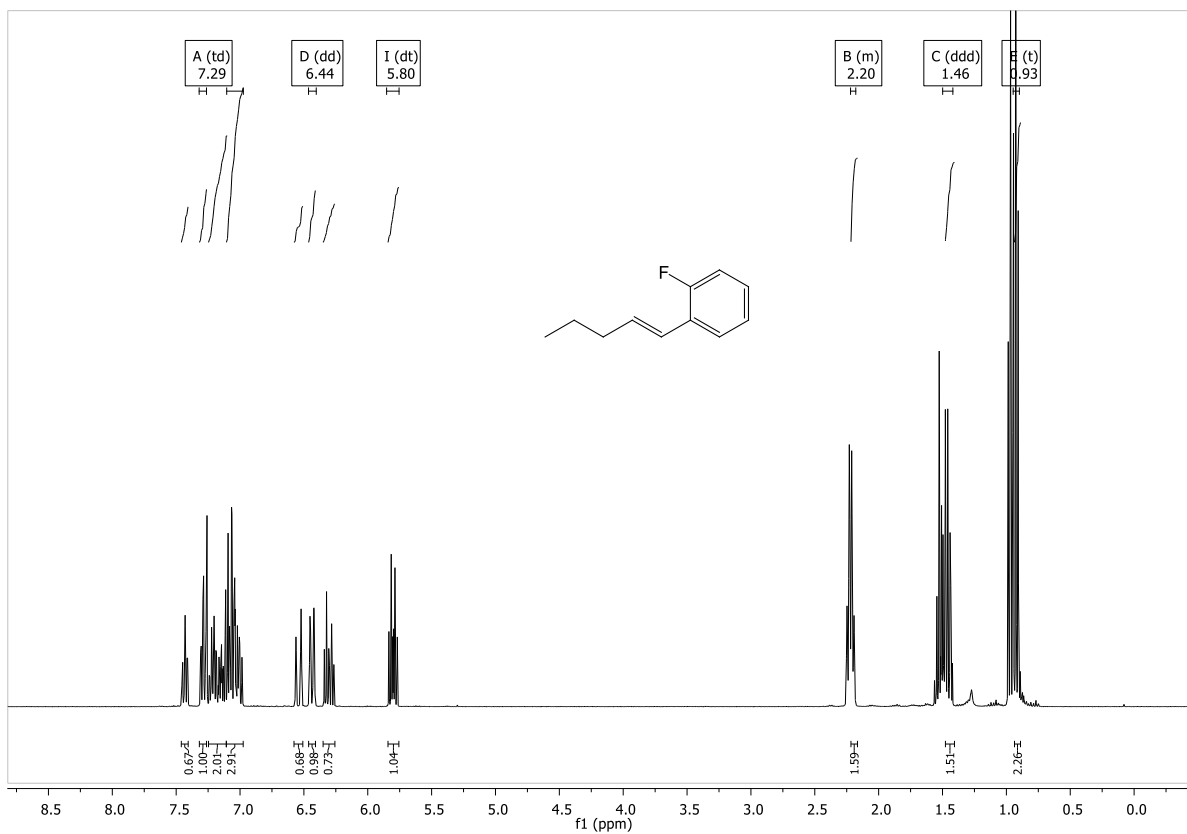


Figure 8.205: $^1\text{H-NMR}$ spectrum of 1-fluoro-2-(pent-1-en-1-yl)benzene.

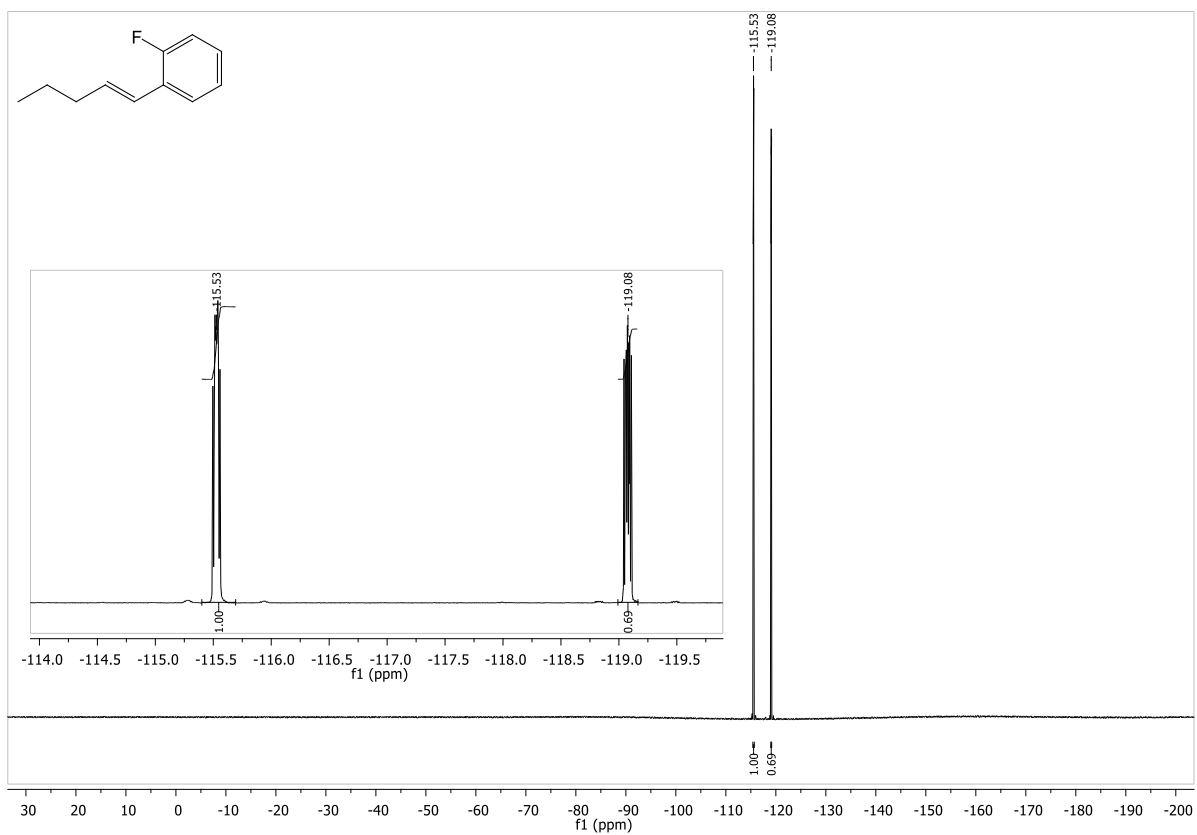


Figure 8.206: $^{19}\text{F-NMR}$ spectrum of 1-fluoro-2-(pent-1-en-1-yl)benzene.

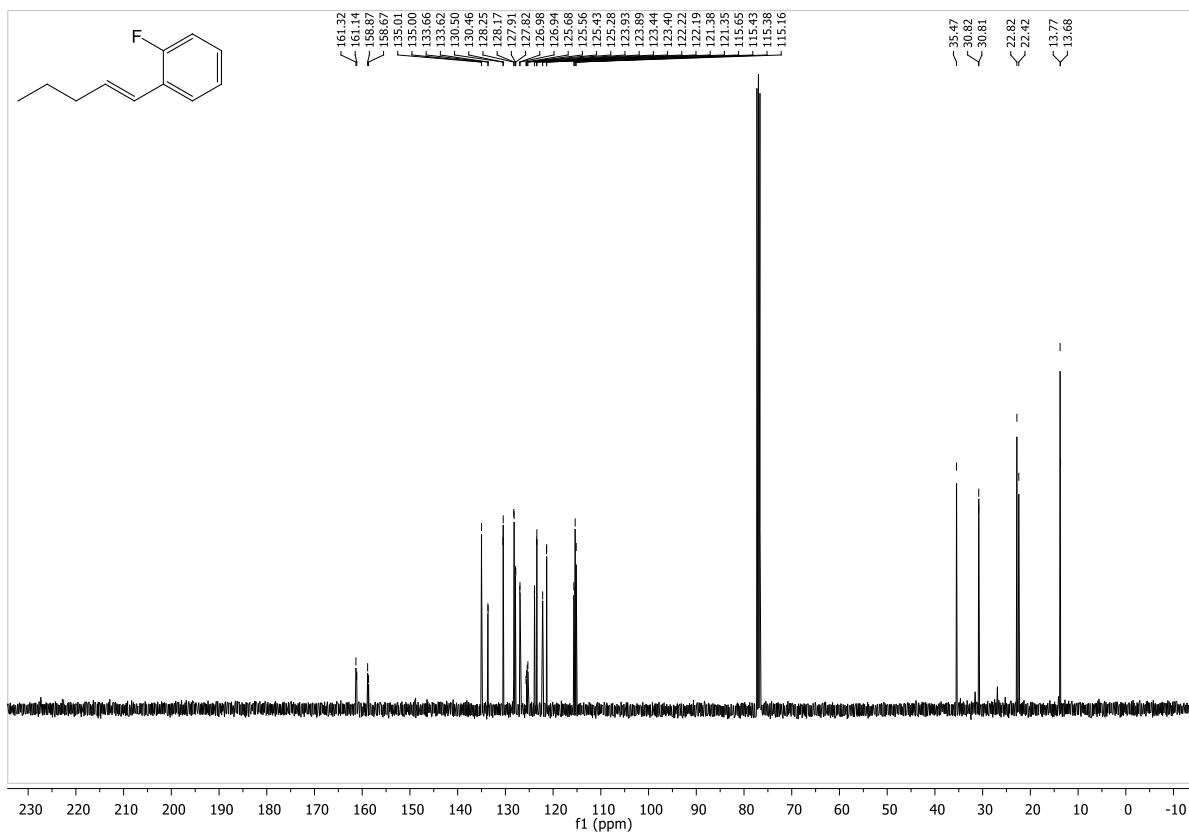


Figure 8.207: ^{13}C -NMR spectrum of 1-fluoro-2-(pent-1-en-1-yl)benzene.

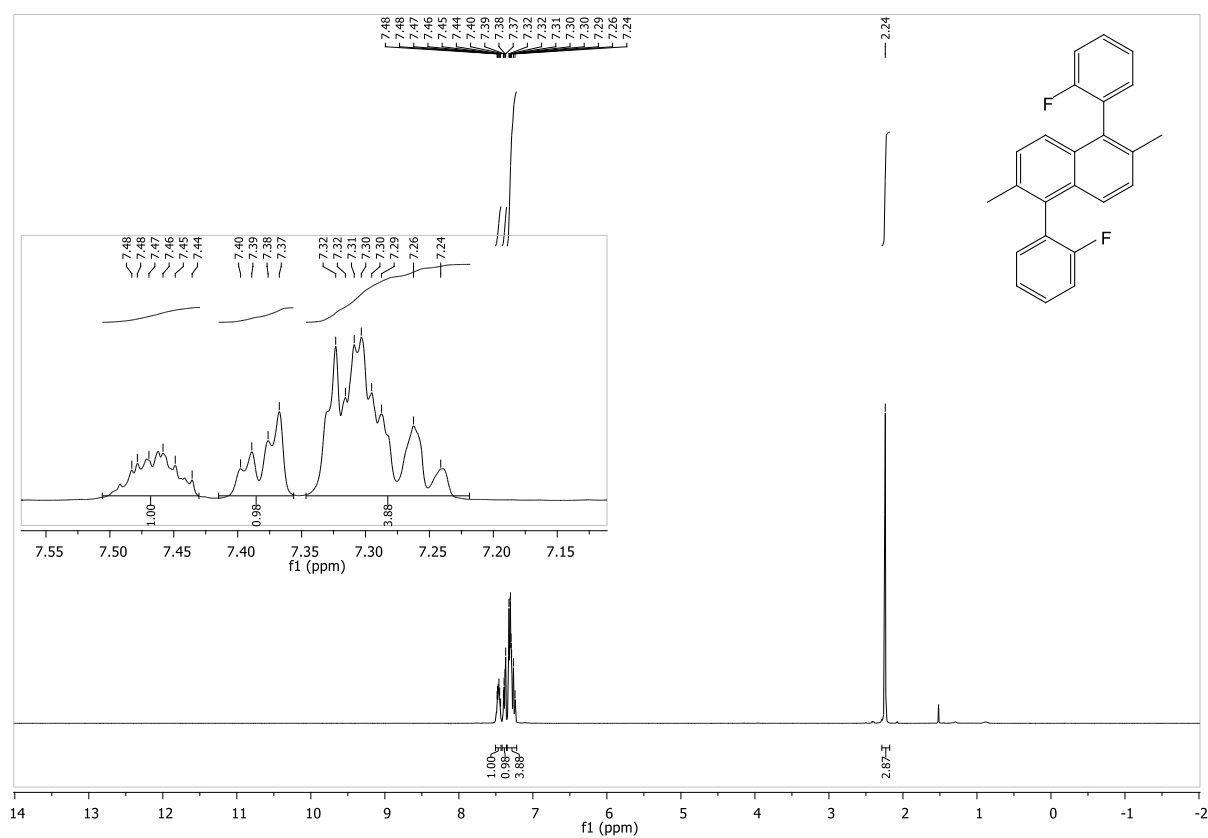


Figure 8.208: ^1H -NMR spectrum of 1,5-bis(2-fluorophenyl)-2,6-dimethylnaphthalene.

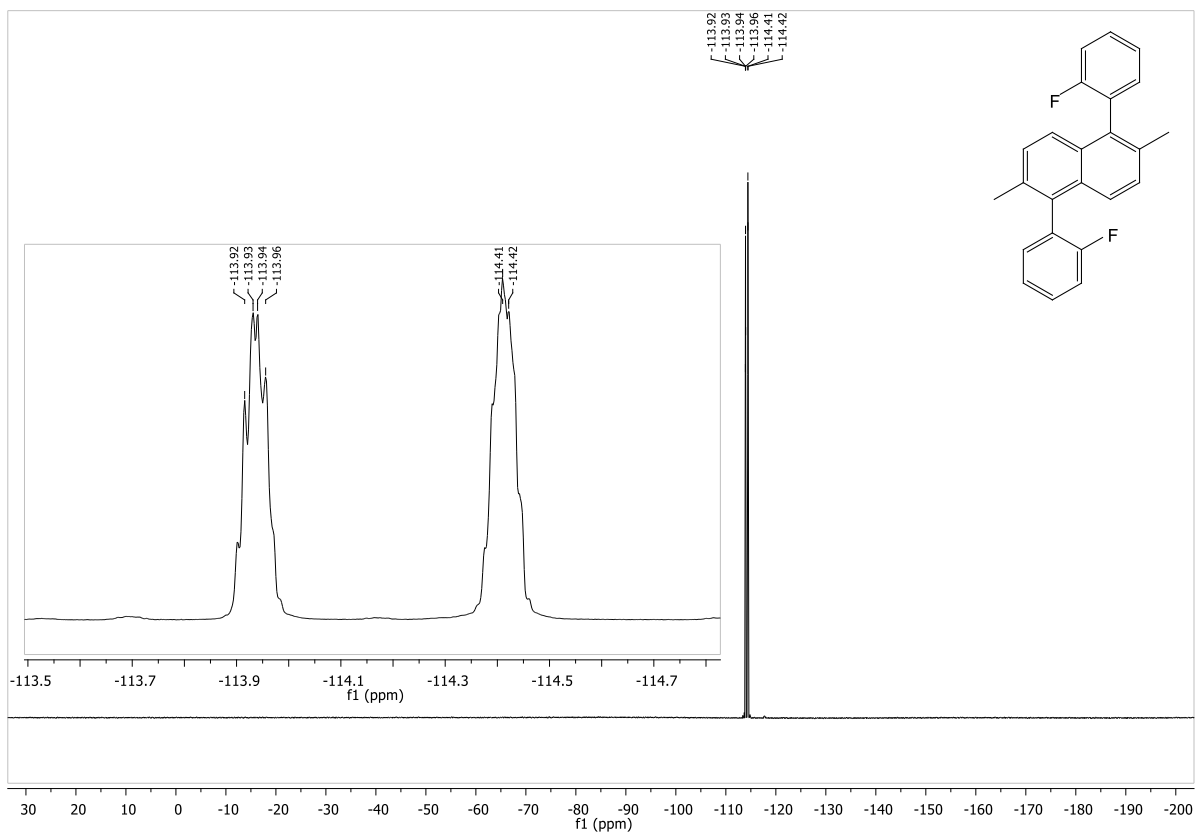


Figure 8.209: ^{19}F -NMR spectrum of 1,5-bis(2-fluorophenyl)-2,6-dimethylnaphthalene.

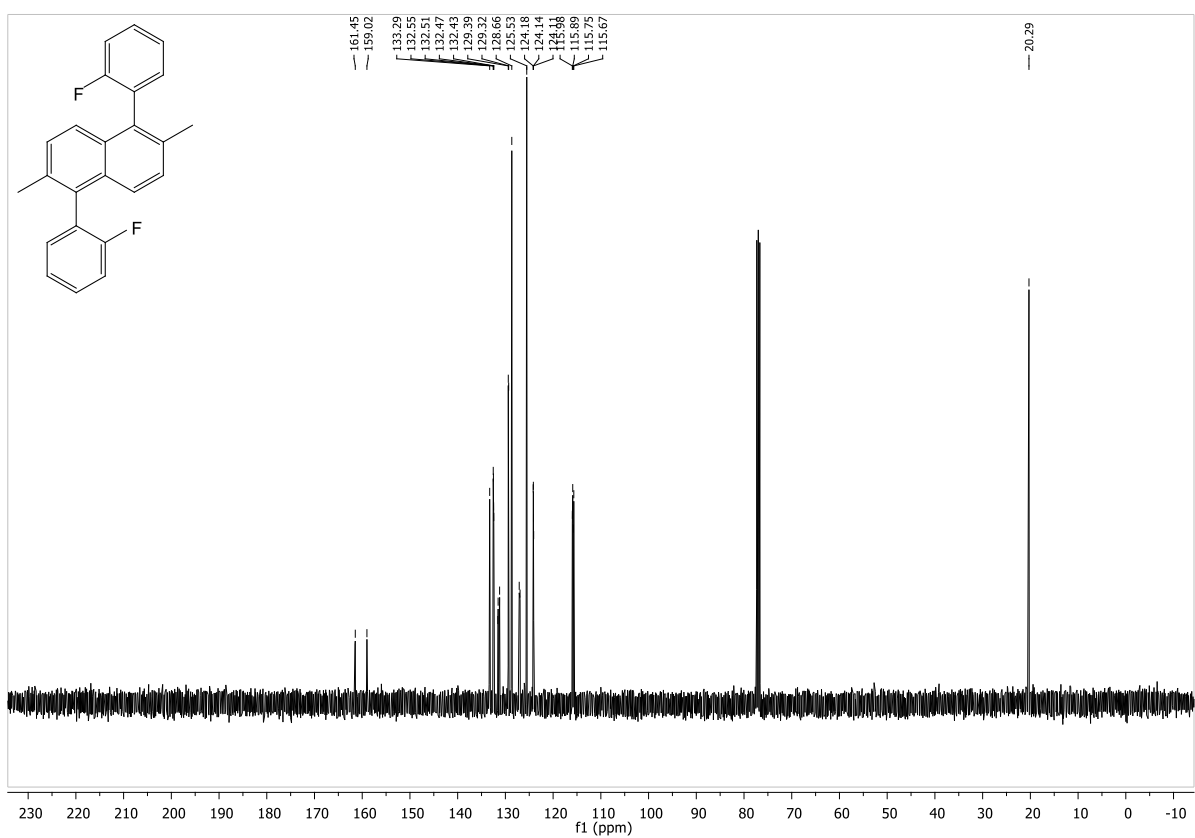


Figure 8.210: ^{13}C -NMR spectrum of 1,5-bis(2-fluorophenyl)-2,6-dimethylnaphthalene.

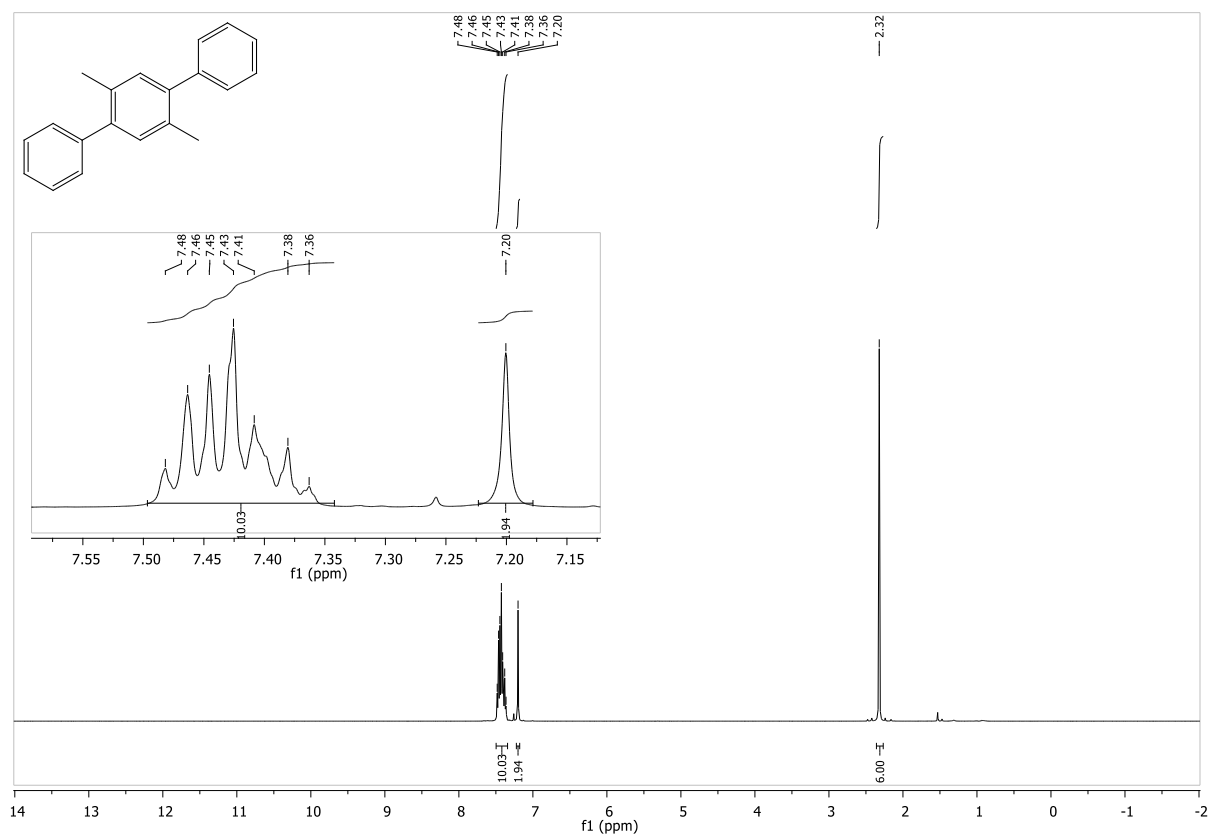


Figure 8.211: ¹H-NMR spectrum of 2',5'-dimethyl-1,1':4',1''-terphenyl.

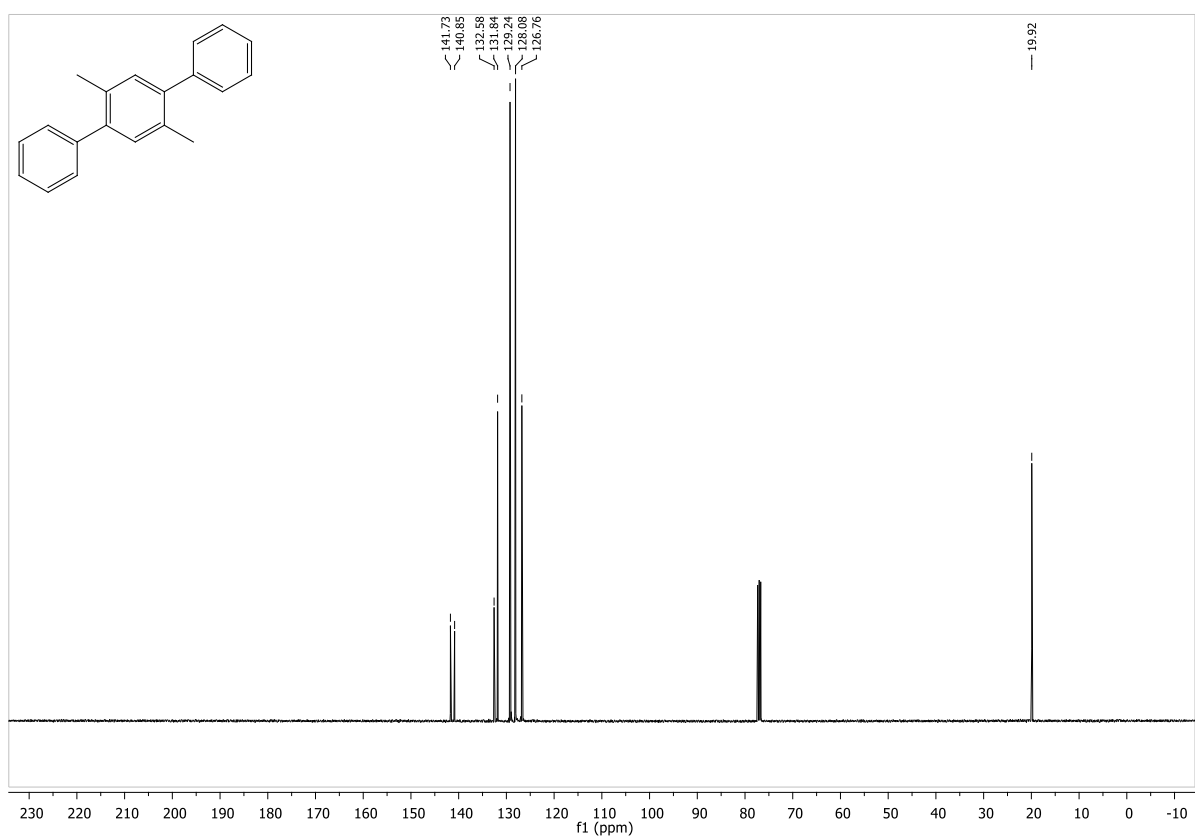


Figure 8.212: ¹³C-NMR spectrum of 2',5'-dimethyl-1,1':4',1''-terphenyl.

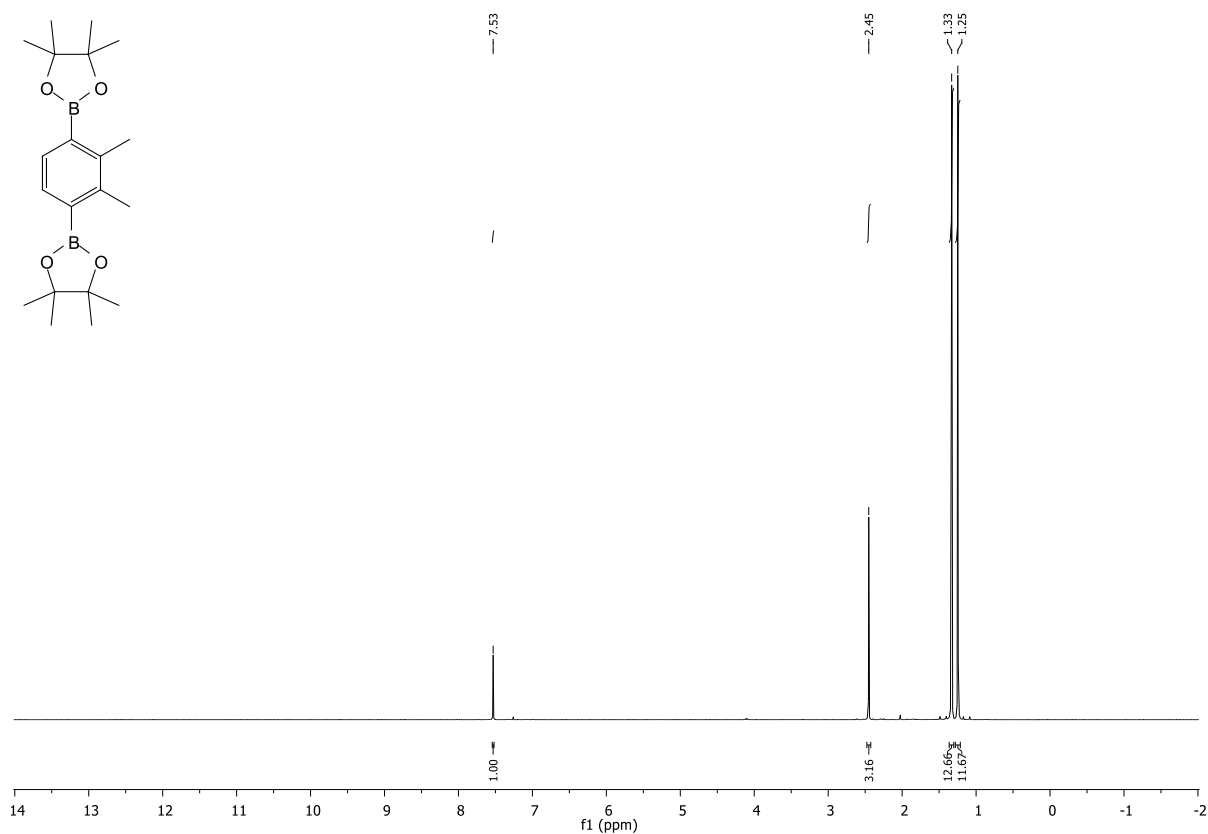


Figure 8.213: $^1\text{H-NMR}$ spectrum of 2,2'-(2,3-dimethyl-1,4-phenylene)bis(4,4,5,5-tetramethyl-1,3,2-dioxaborolane).

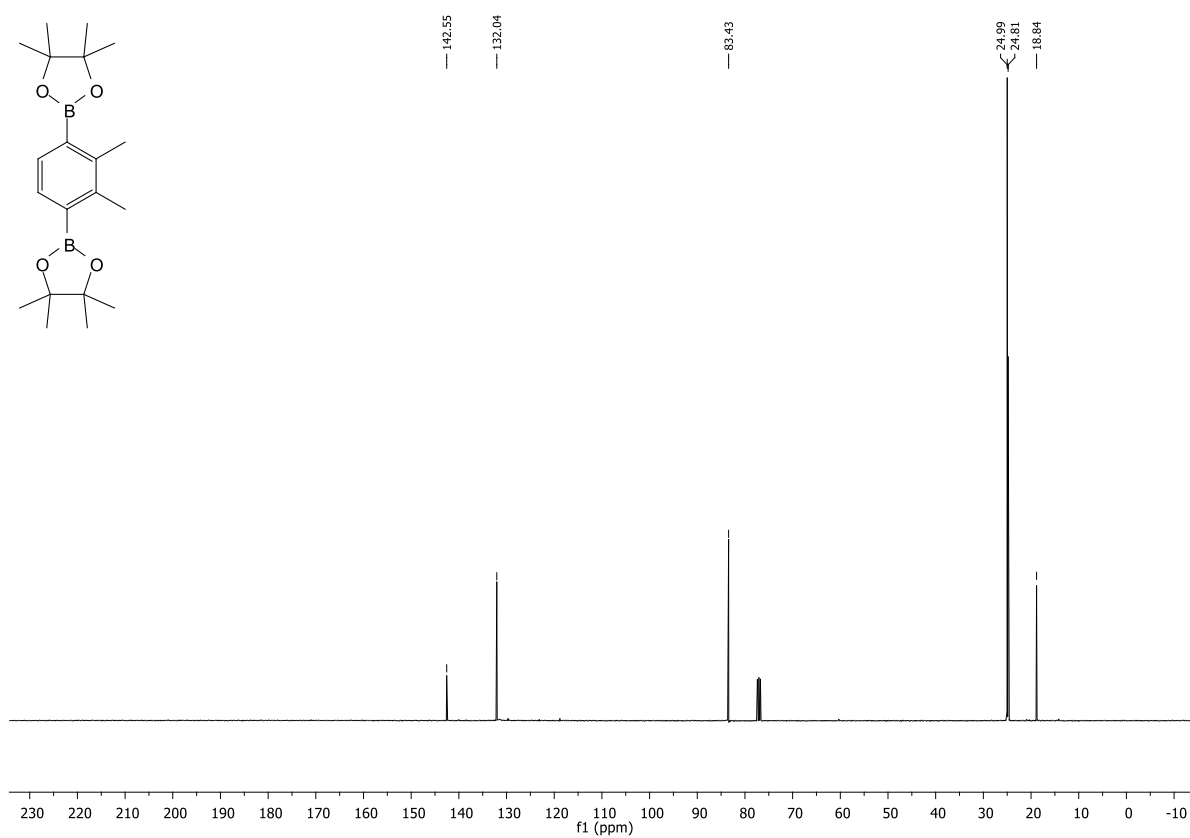


Figure 8.214: $^{13}\text{C-NMR}$ spectrum of 2,2'-(2,3-dimethyl-1,4-phenylene)bis(4,4,5,5-tetramethyl-1,3,2-dioxaborolane).

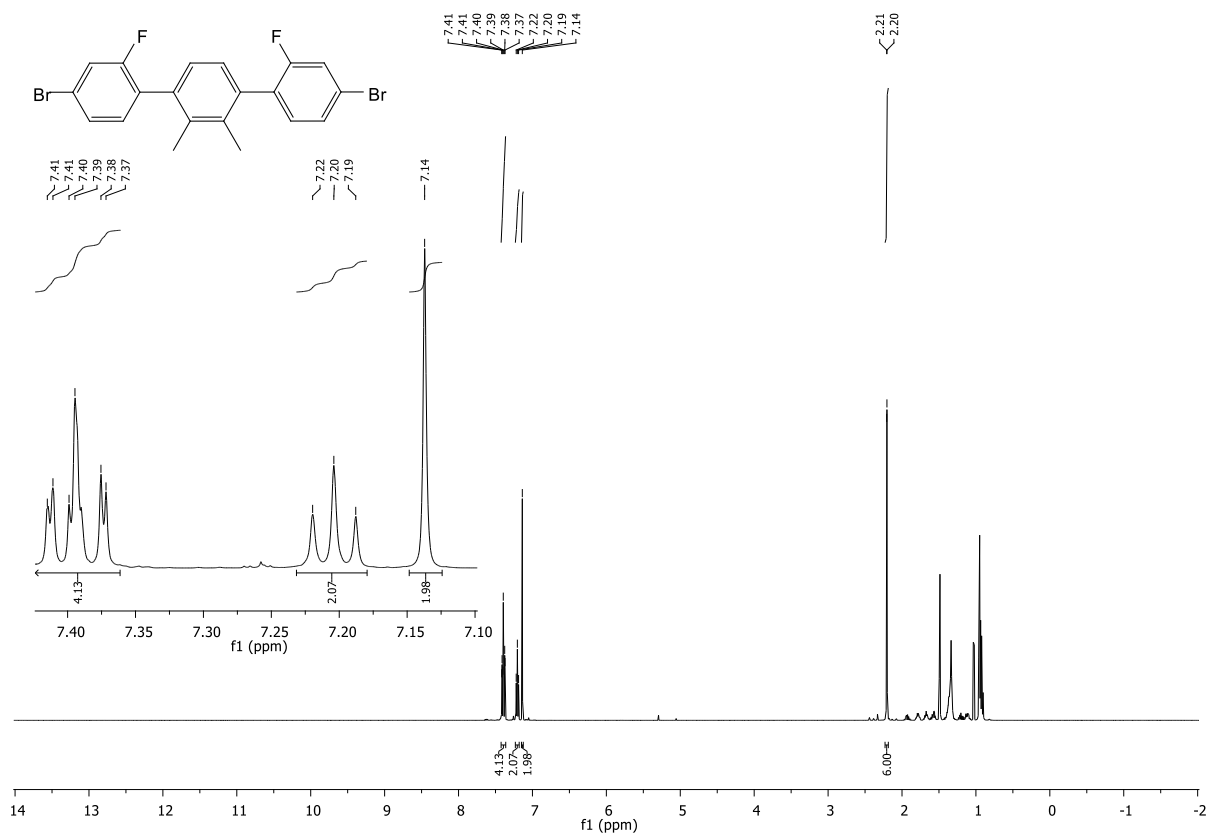


Figure 8.215: $^1\text{H-NMR}$ spectrum of 4,4'-dibromo-2,2''-difluoro-2',3'-dimethyl-1,1':4',1''-terphenyl.

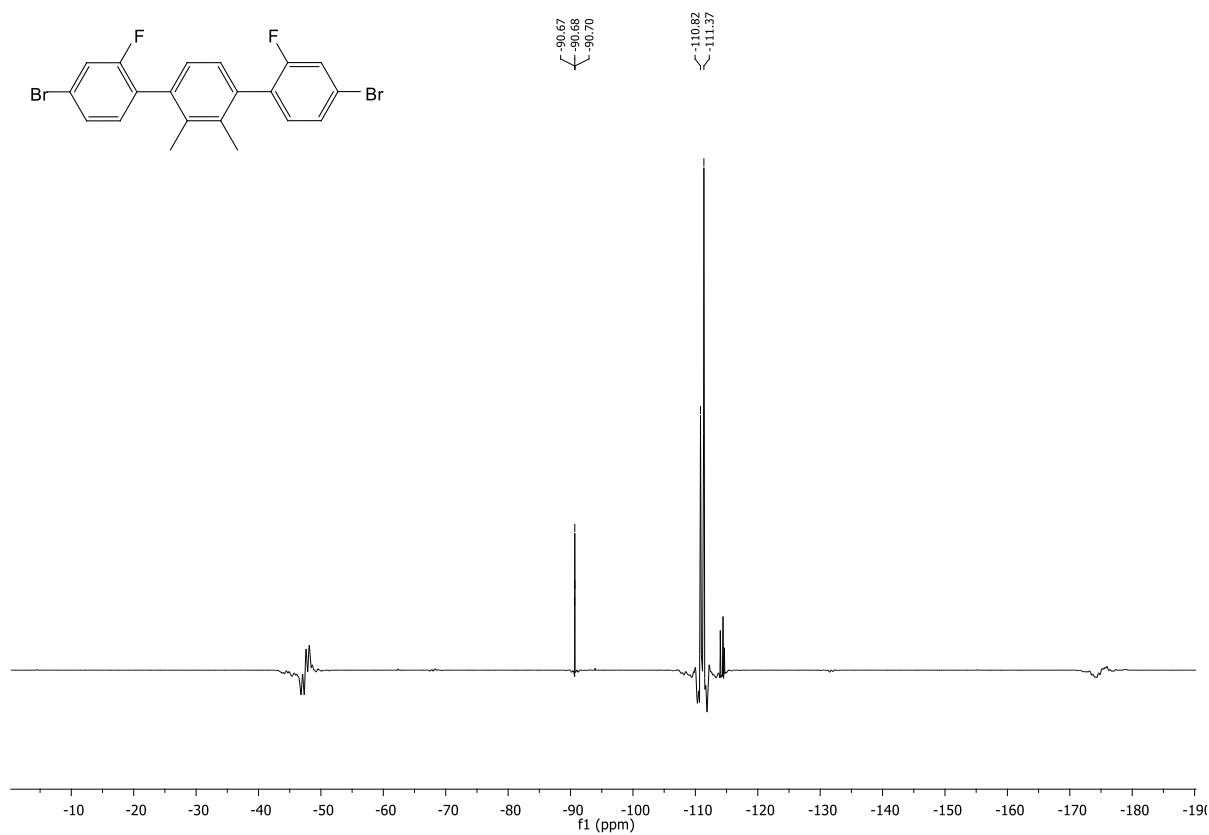


Figure 8.216: $^{19}\text{F-NMR}$ spectrum of 4,4'-dibromo-2,2''-difluoro-2',3'-dimethyl-1,1':4',1''-terphenyl.

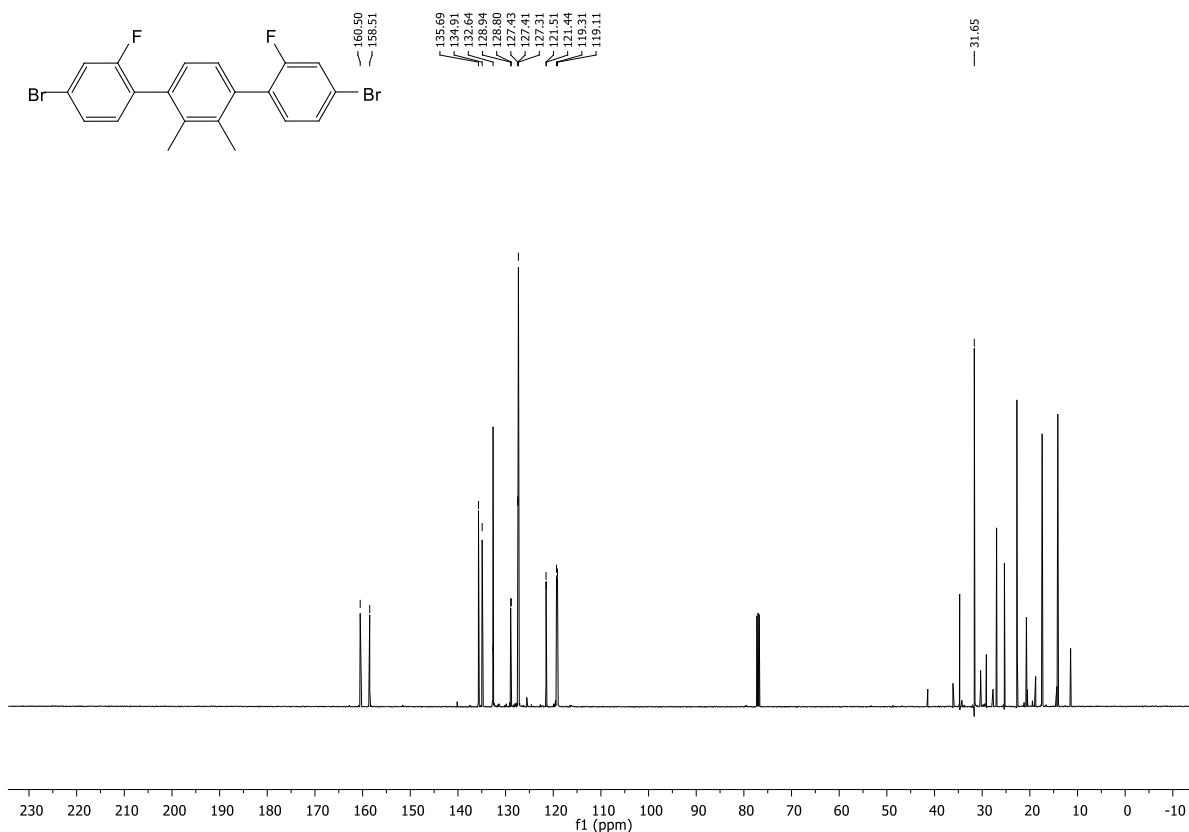


Figure 8.217: ^{13}C -NMR spectrum of 4,4''-dibromo-2,2''-difluoro-2',3'-dimethyl-1,1':4',1''-terphenyl.

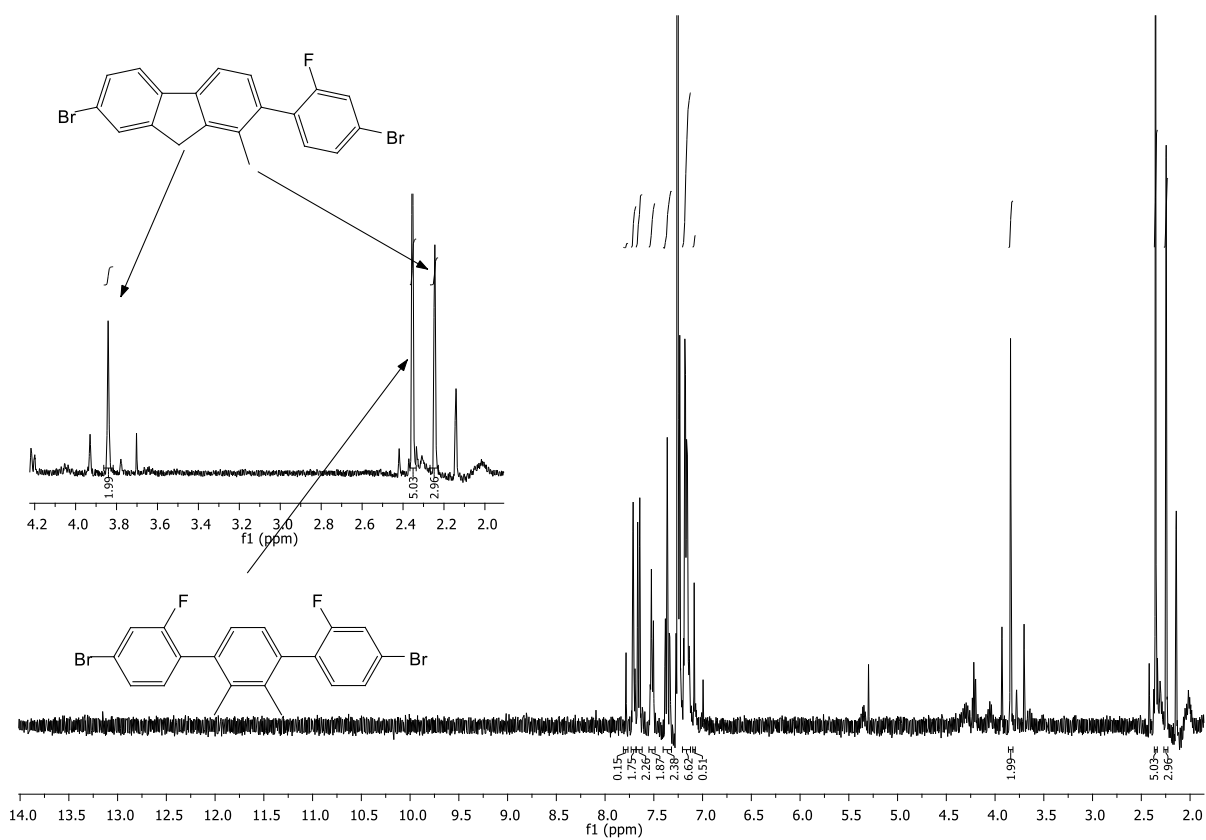


Figure 8.218: ^1H -NMR spectrum after reaction of 4,4''-dibromo-2,2''-difluoro-2',3'-dimethyl-1,1':4',1''-terphenyl.

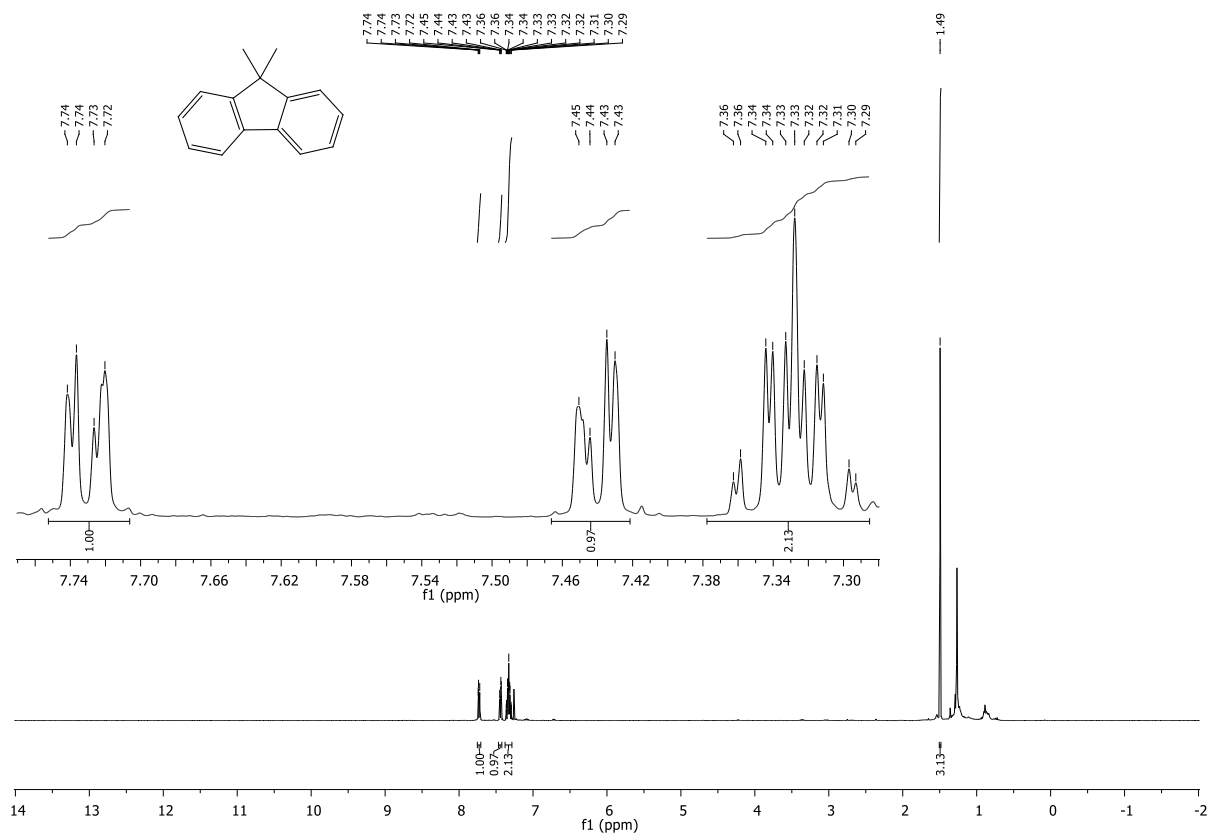


Figure 8.219: $^1\text{H-NMR}$ spectrum of 9,9-dimethyl-9H-fluorene.

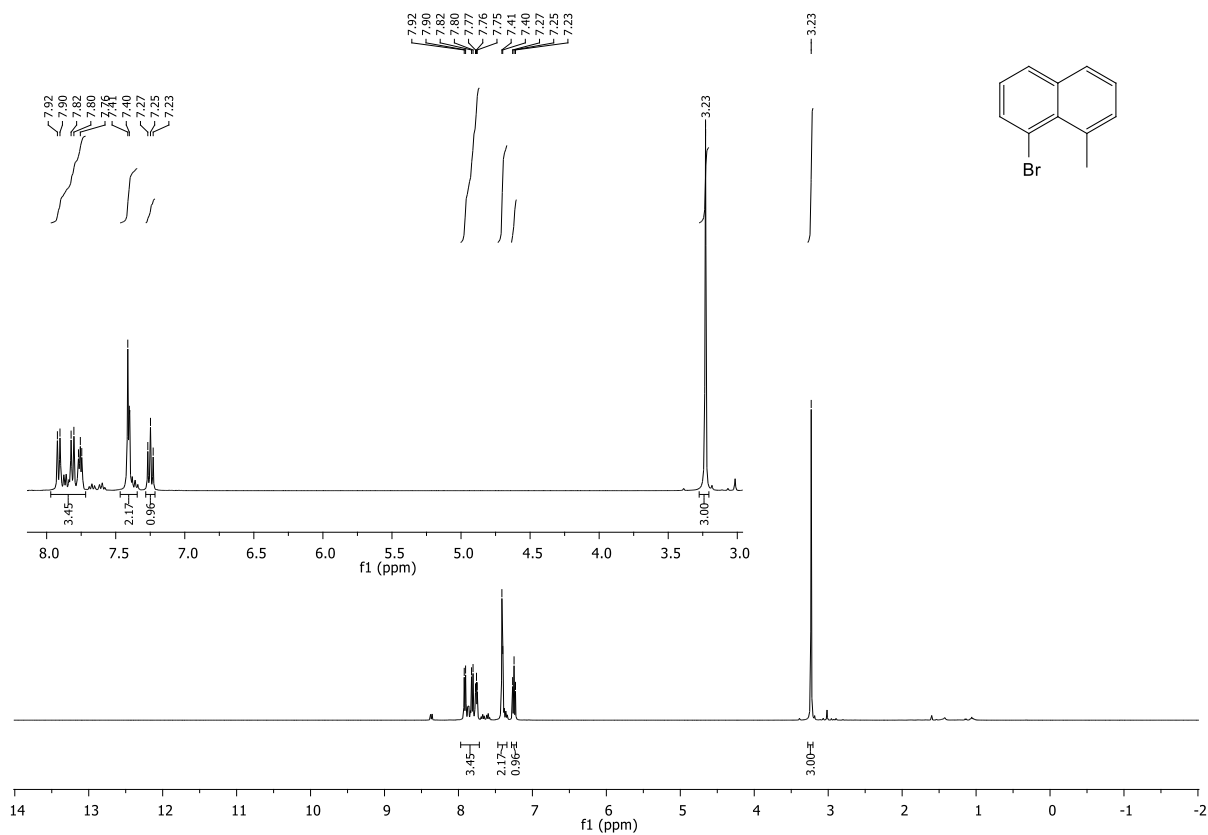


Figure 8.220: $^1\text{H-NMR}$ spectrum of 1-bromo-8-methylnaphthalene.

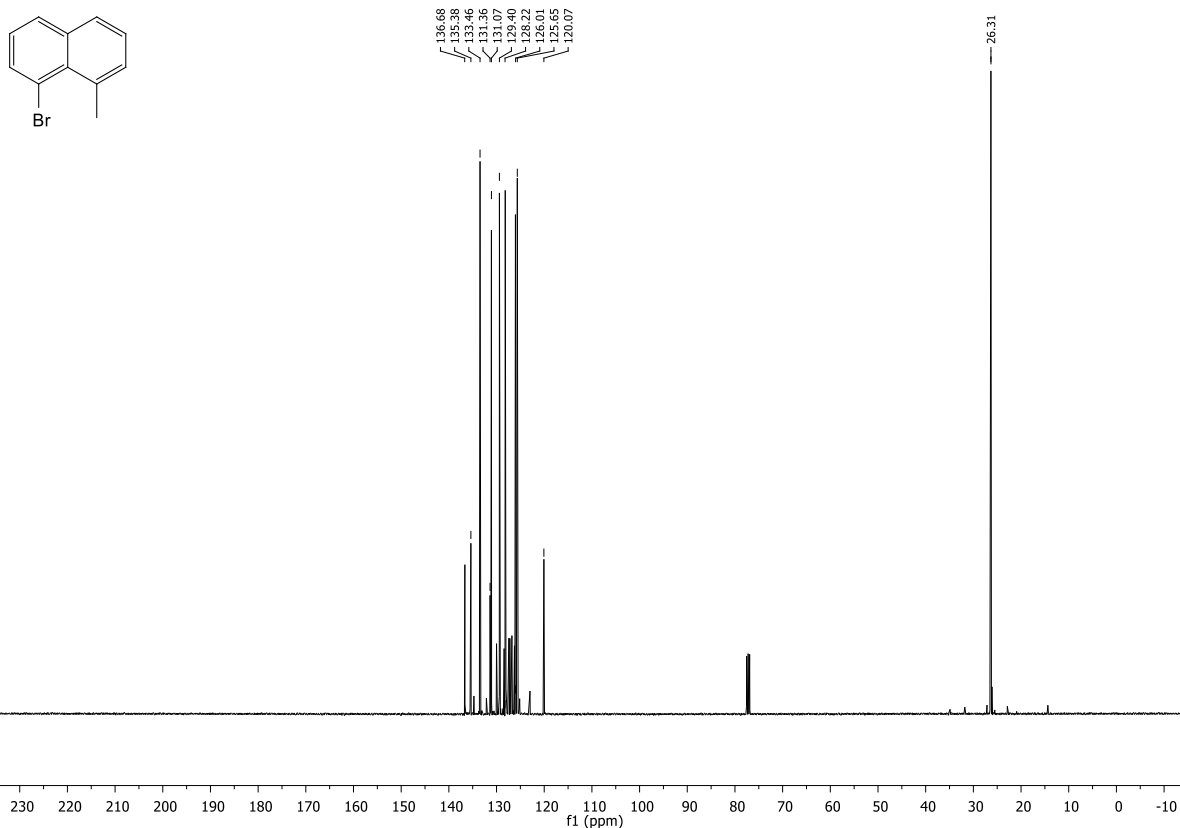


Figure 8.221: ^{13}C -NMR spectrum of 1-bromo-8-methylnaphthalene.

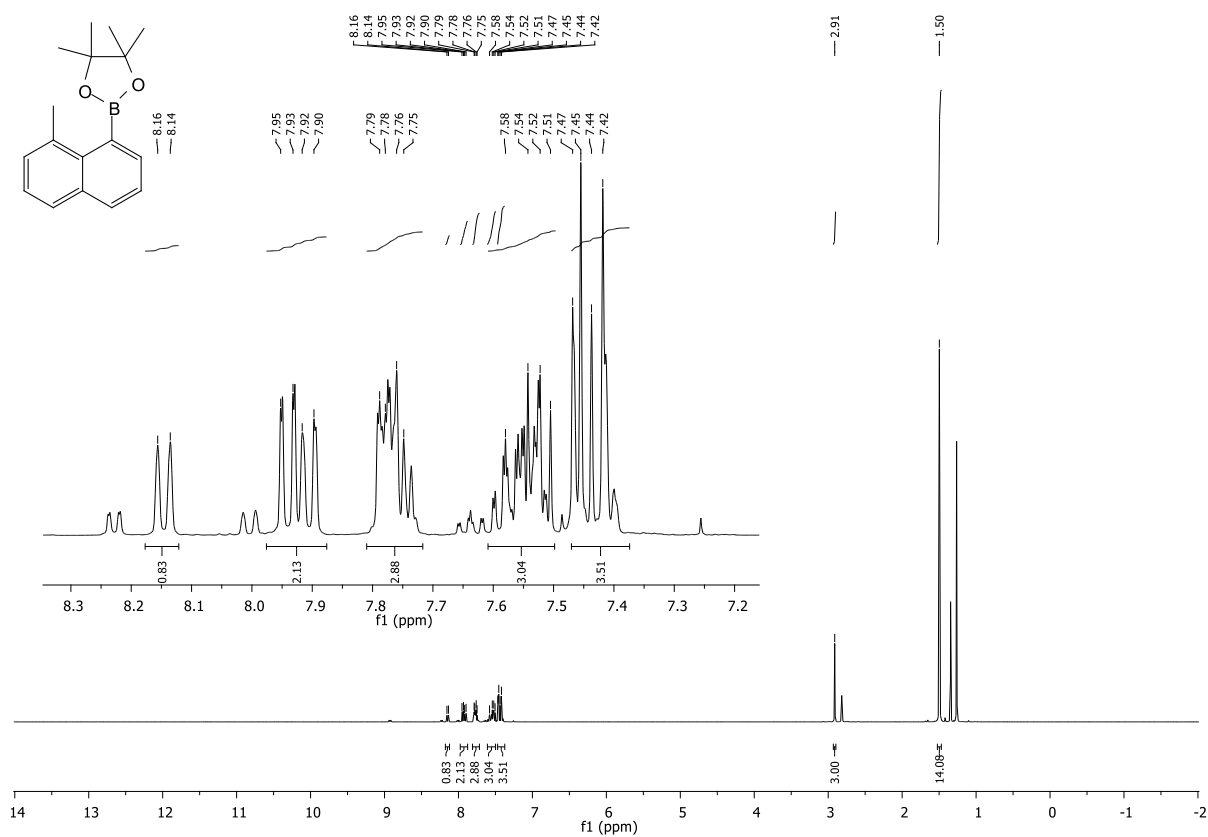


Figure 8.222: ^1H -NMR spectrum of 2-(8-bromonaphthalen-1-yl)-4,4,5,5-tetramethyl-1,3,2-dioxaborolane.

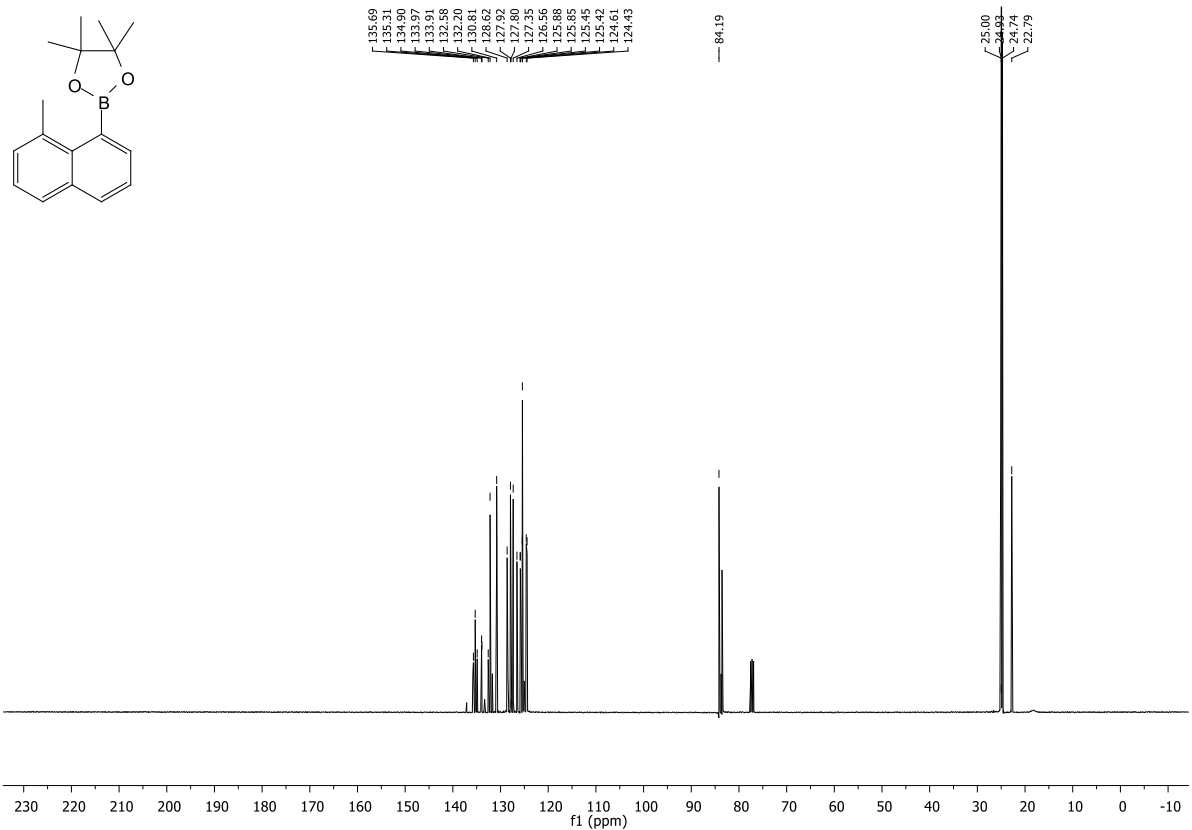


Figure 8.223: $^{13}\text{C-NMR}$ spectrum of 2-(8-bromonaphthalen-1-yl)-4,4,5,5-tetramethyl-1,3,2-dioxaborolane.

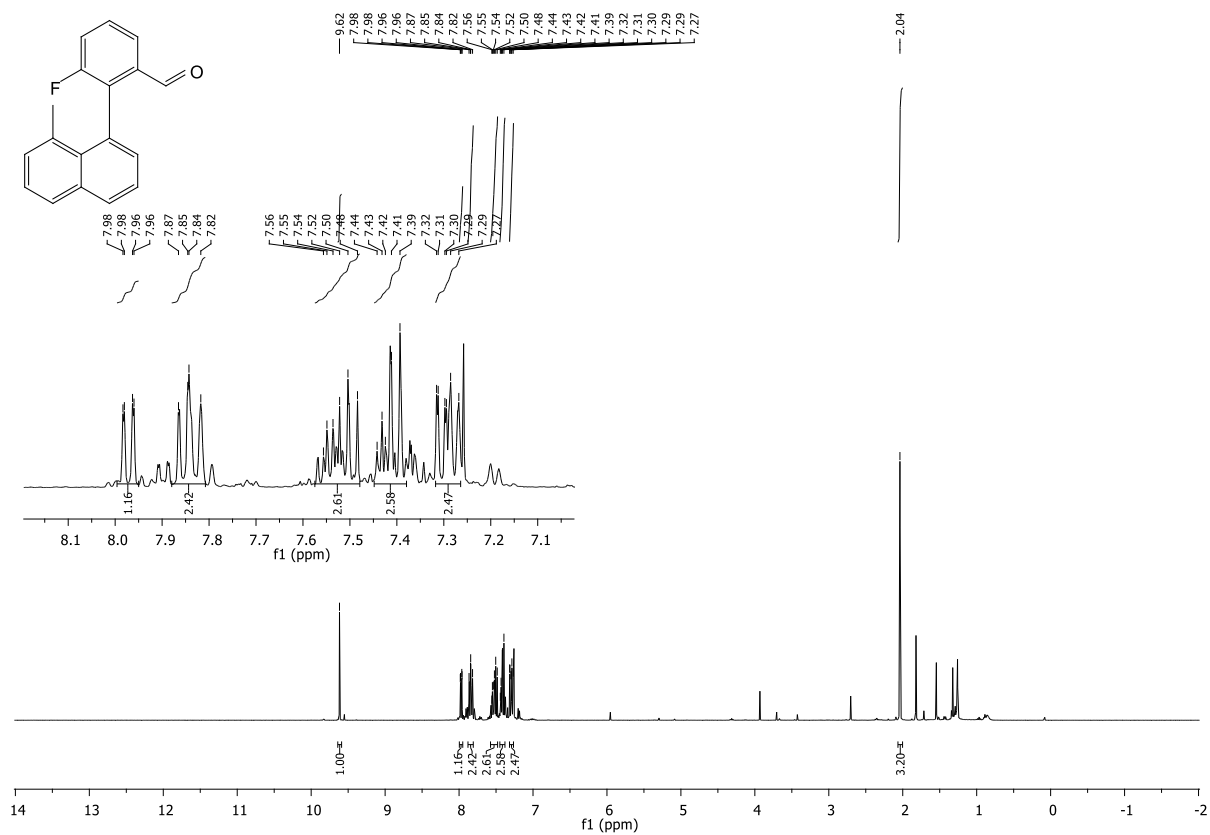


Figure 8.224: $^1\text{H-NMR}$ spectrum of 3-fluoro-2-(8-methylnaphthalen-1-yl)benzaldehyde.

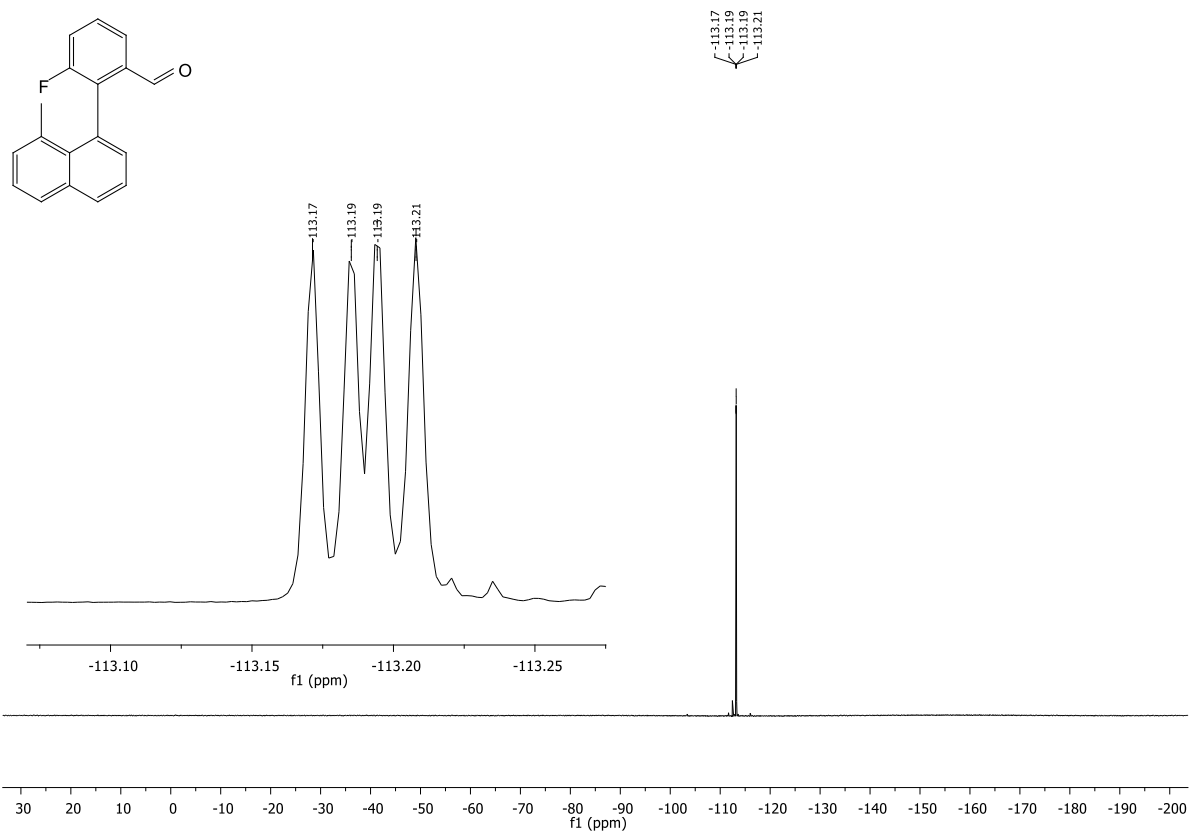


Figure 8.225: ¹⁹F-NMR spectrum of 3-fluoro-2-(8-methylnaphthalen-1-yl)benzaldehyde.

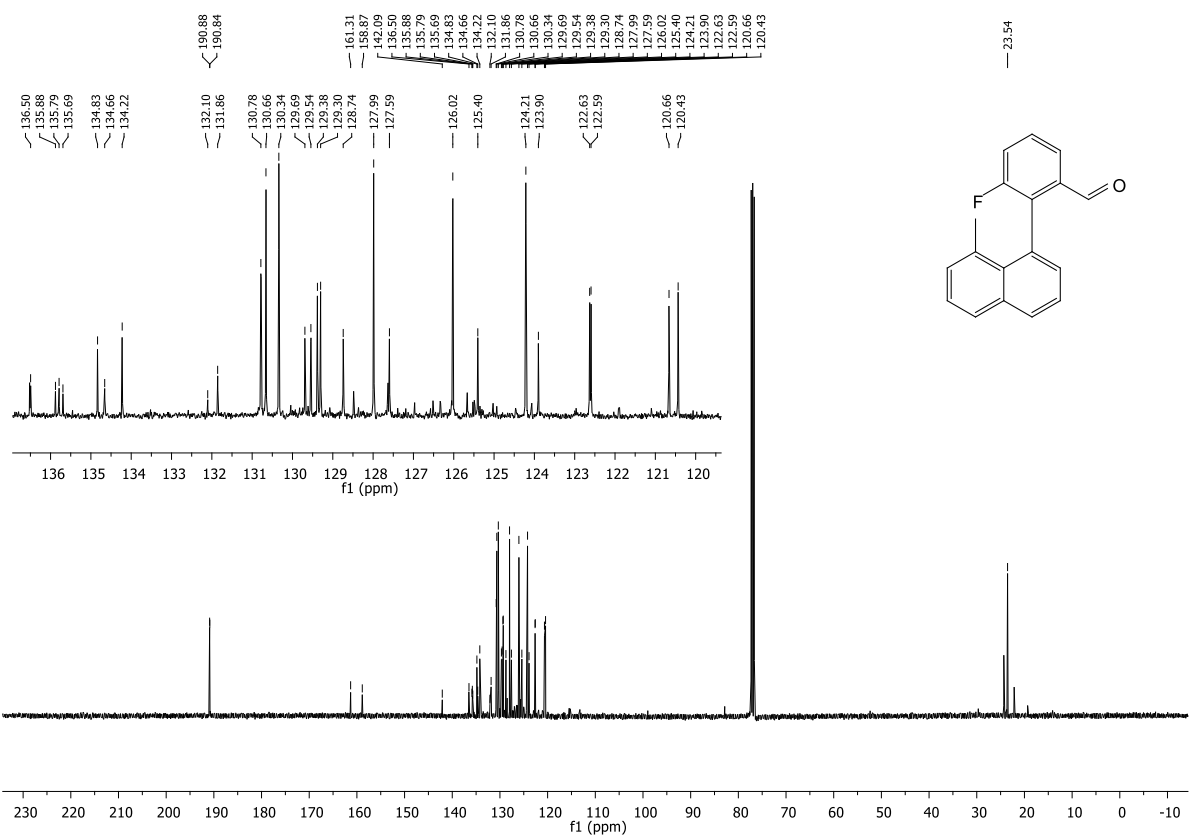


Figure 8.226: ¹³C-NMR spectrum of 3-fluoro-2-(8-methylnaphthalen-1-yl)benzaldehyde.

8.3.2. Synthesis of di-4-helicene derivates

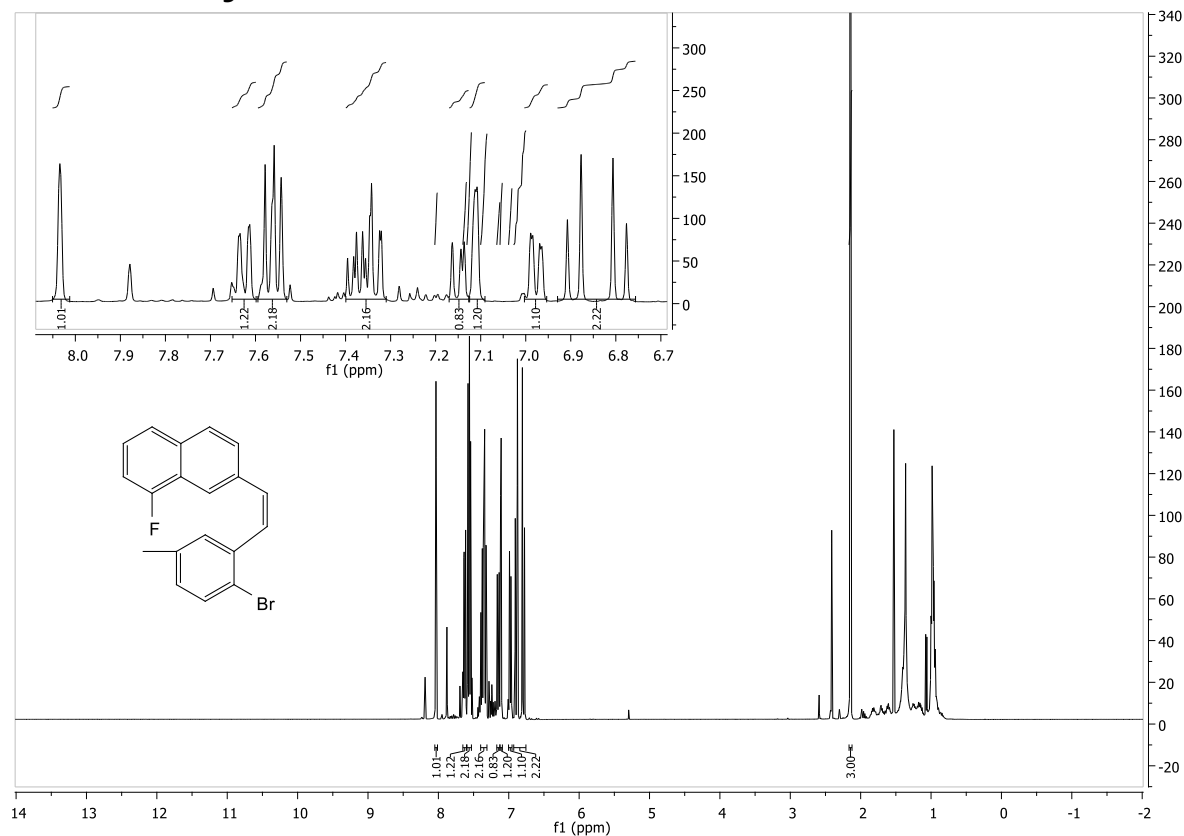


Figure 8.227: $^1\text{H-NMR}$ spectrum of (E) and (Z)-7-(2-bromo-5-methylstyryl)-1-fluoronaphthalene.

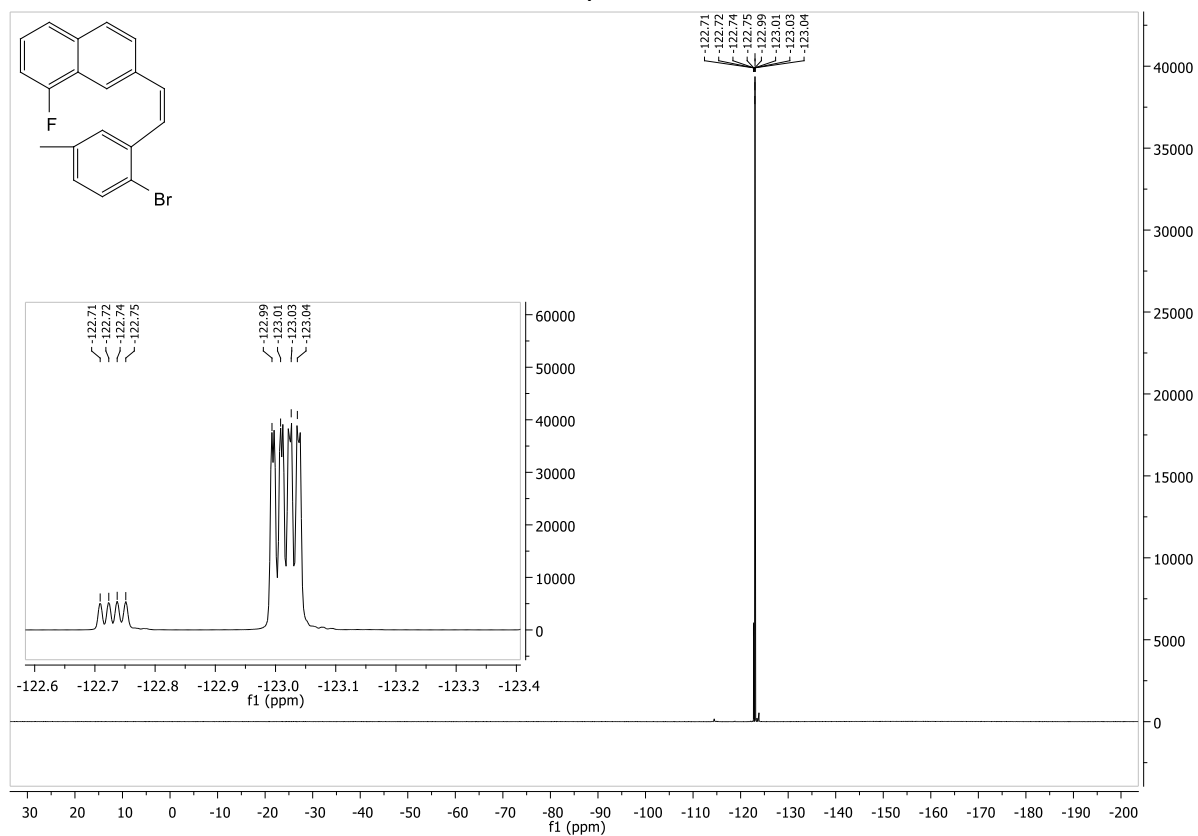


Figure 8.228: $^{19}\text{F-NMR}$ spectrum of (E) and (Z)-7-(2-bromo-5-methylstyryl)-1-

fluoronaphthalene.

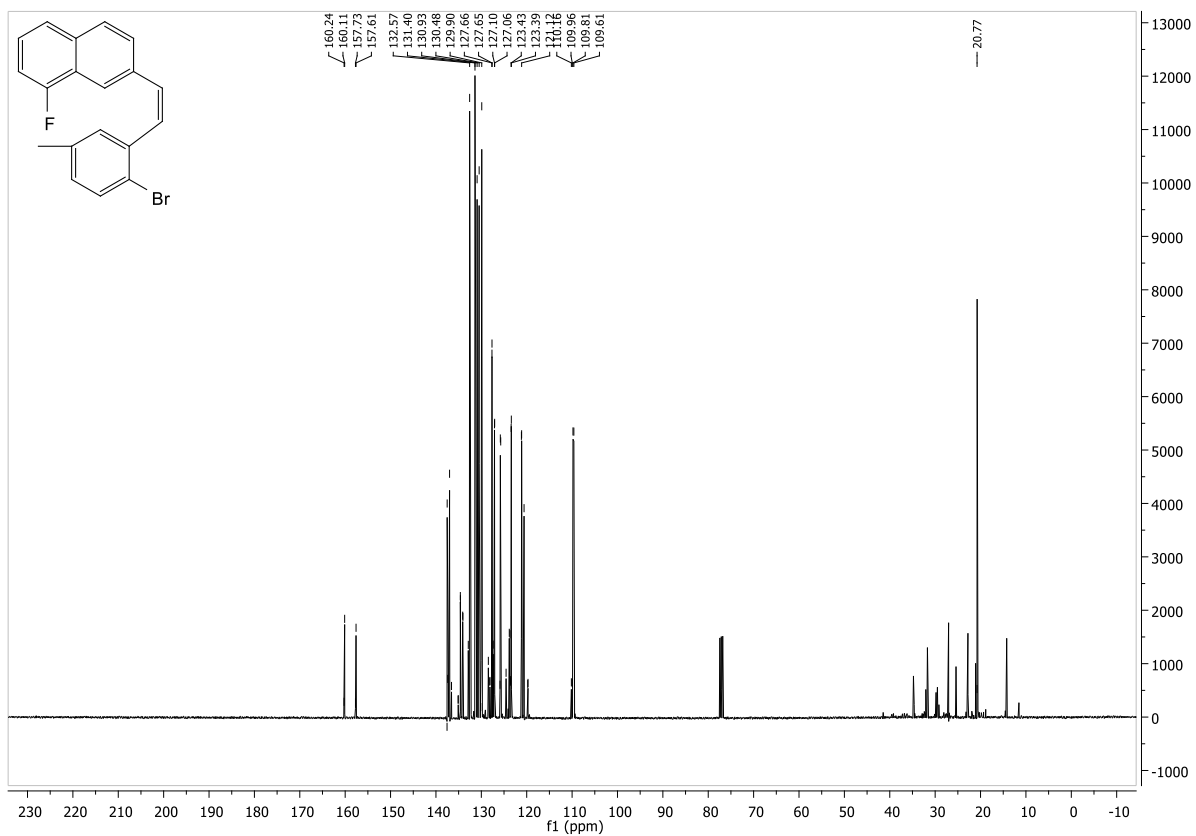


Figure 8.229: ^{13}C -NMR spectrum of (E) and (Z)-7-(2-bromo-5-methylstyryl)-1-fluoronaphthalene.

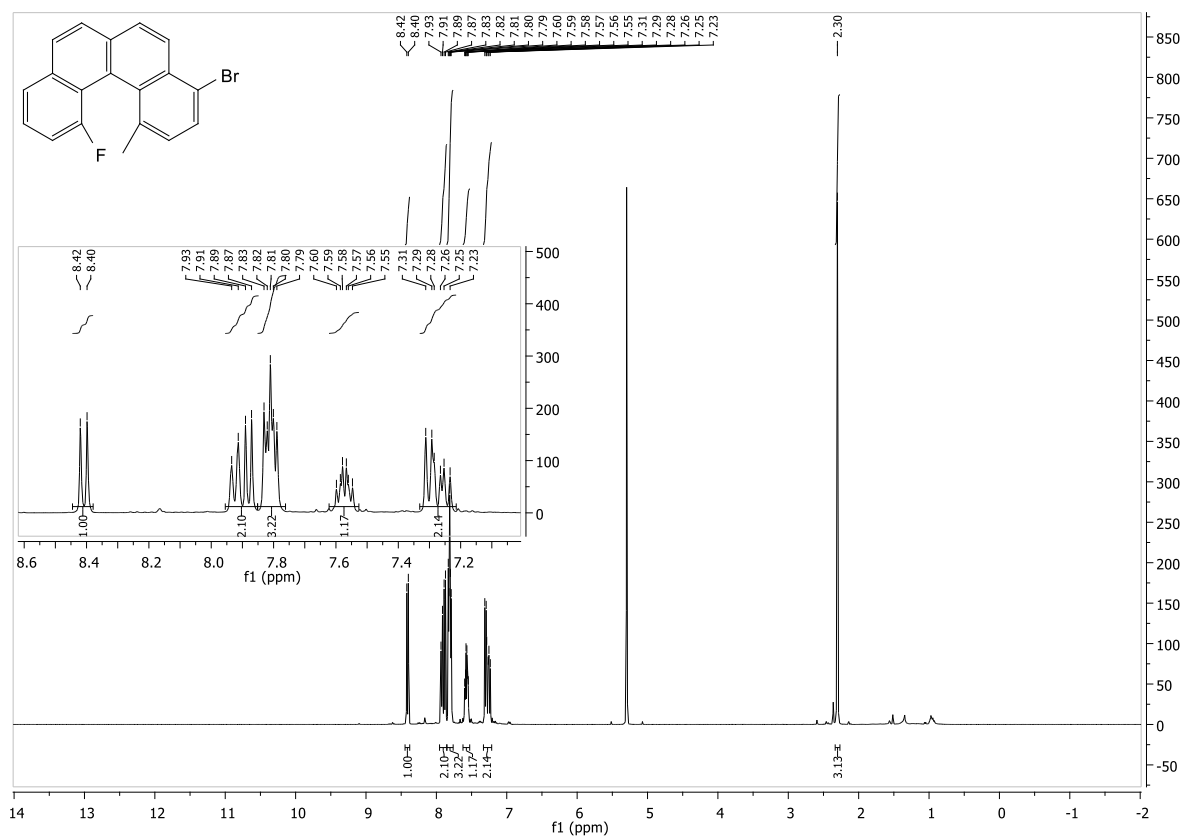


Figure 8.230: ¹H-NMR spectrum of 4-bromo-12-fluoro-1-methylbenzo[c]phenanthrene.

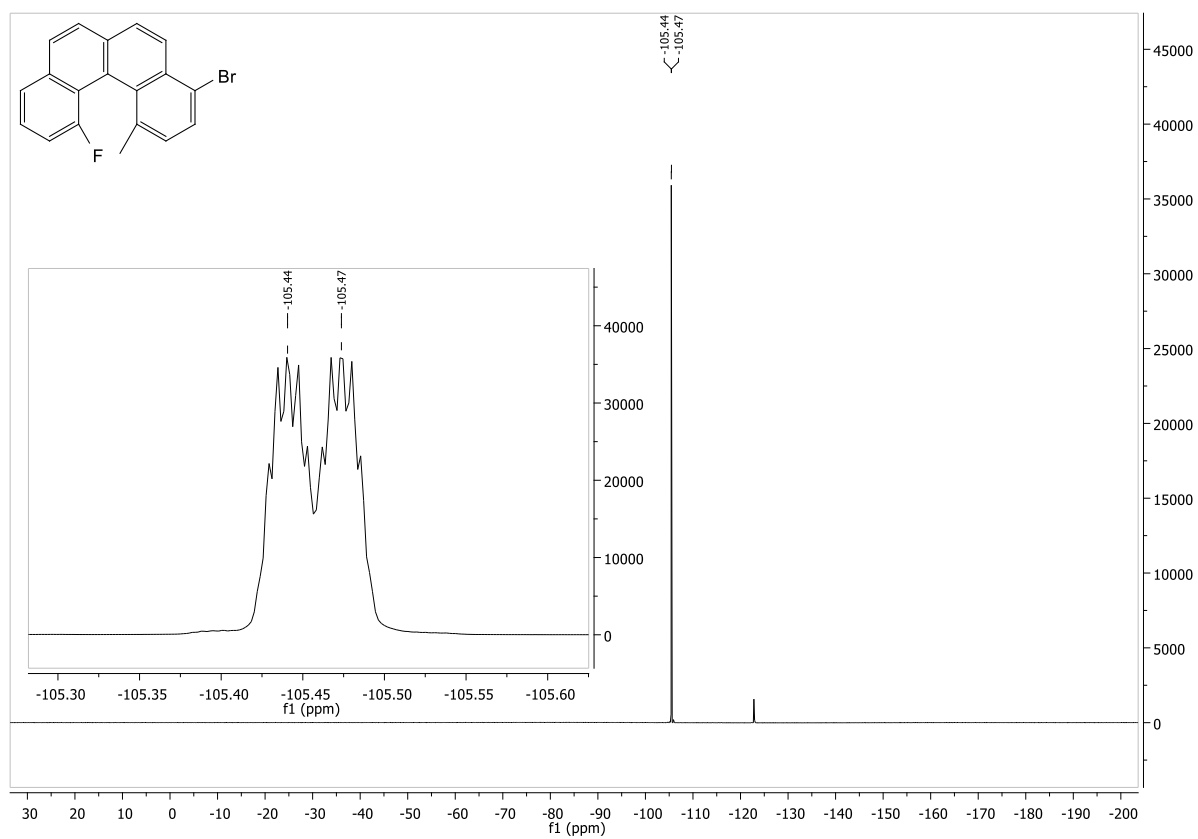


Figure 8.231: ¹⁹F-NMR spectrum of 4-bromo-12-fluoro-1-methylbenzo[c]phenanthrene.

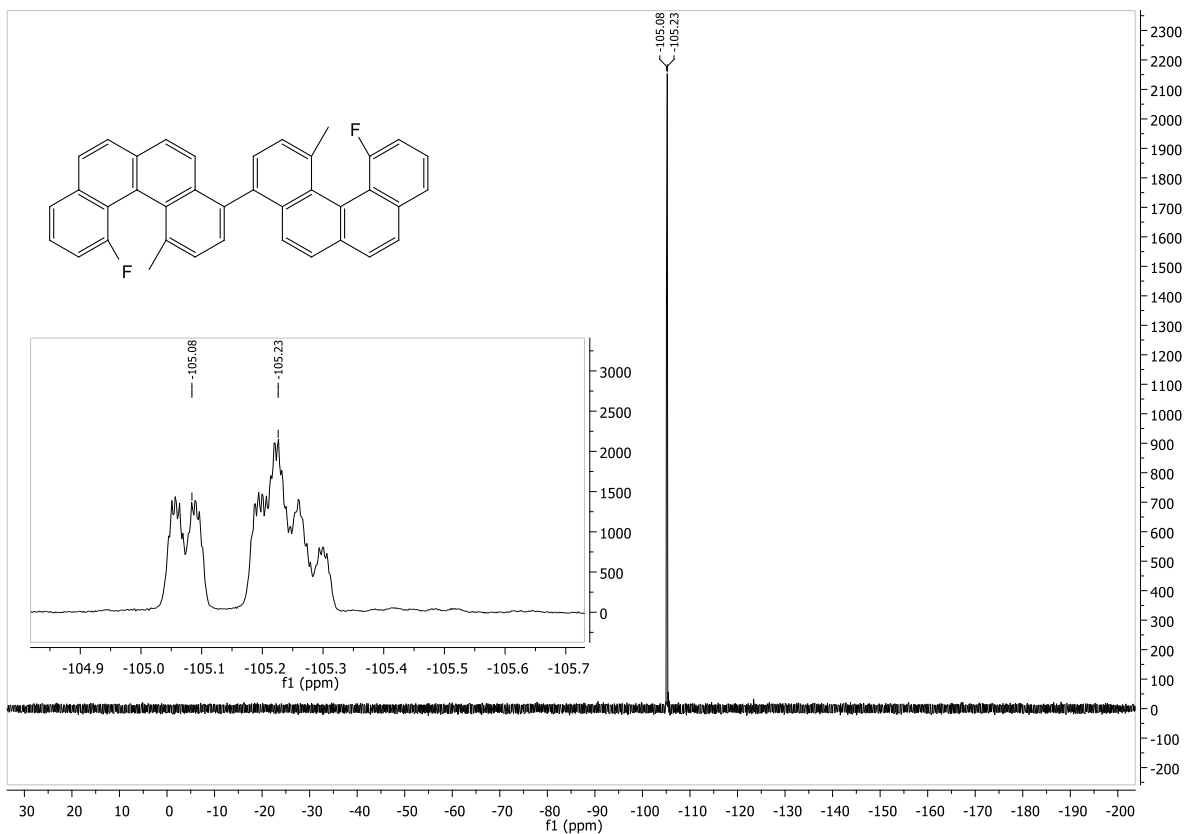


Figure 8.234: ^{19}F -NMR spectrum of 12,12'-difluoro-1,1'-dimethyl-4,4'-bibenzo[*c*]phenanthrene.

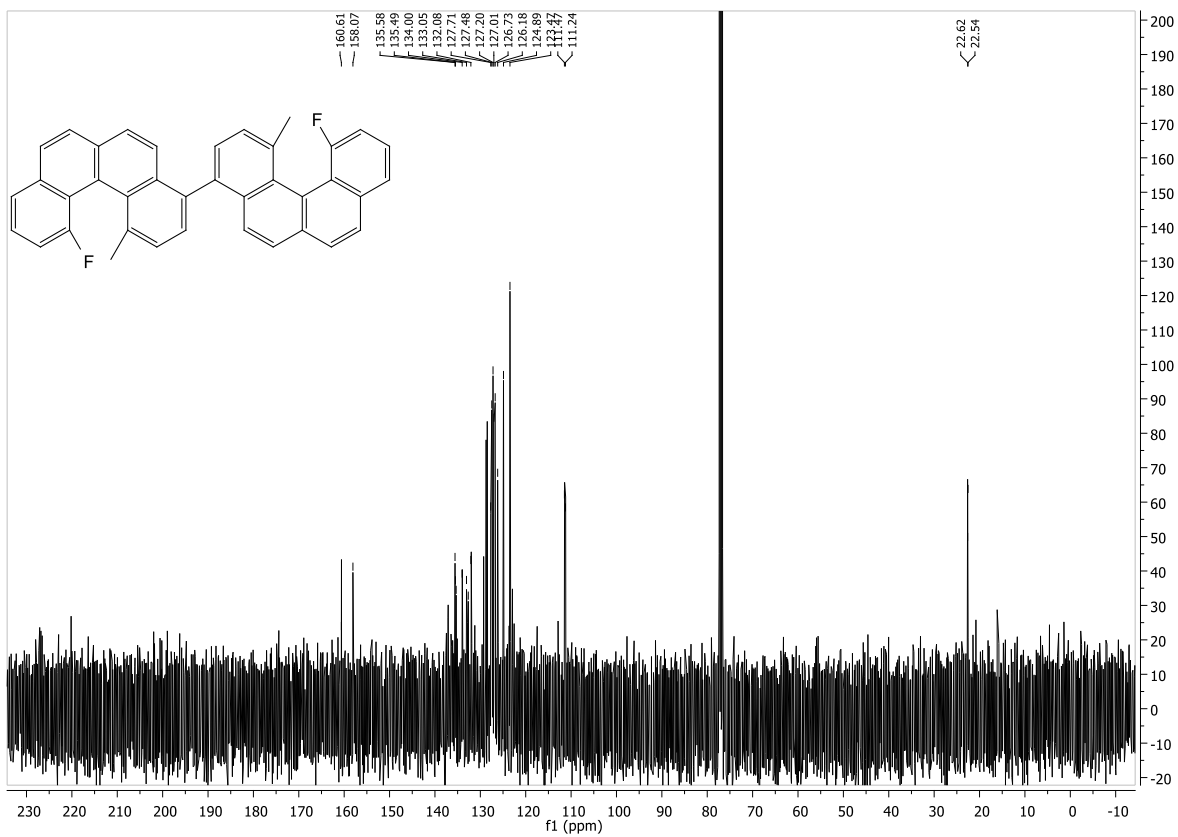


Figure 8.235: ^{13}C -NMR spectrum of 12,12'-difluoro-1,1'-dimethyl-4,4'-

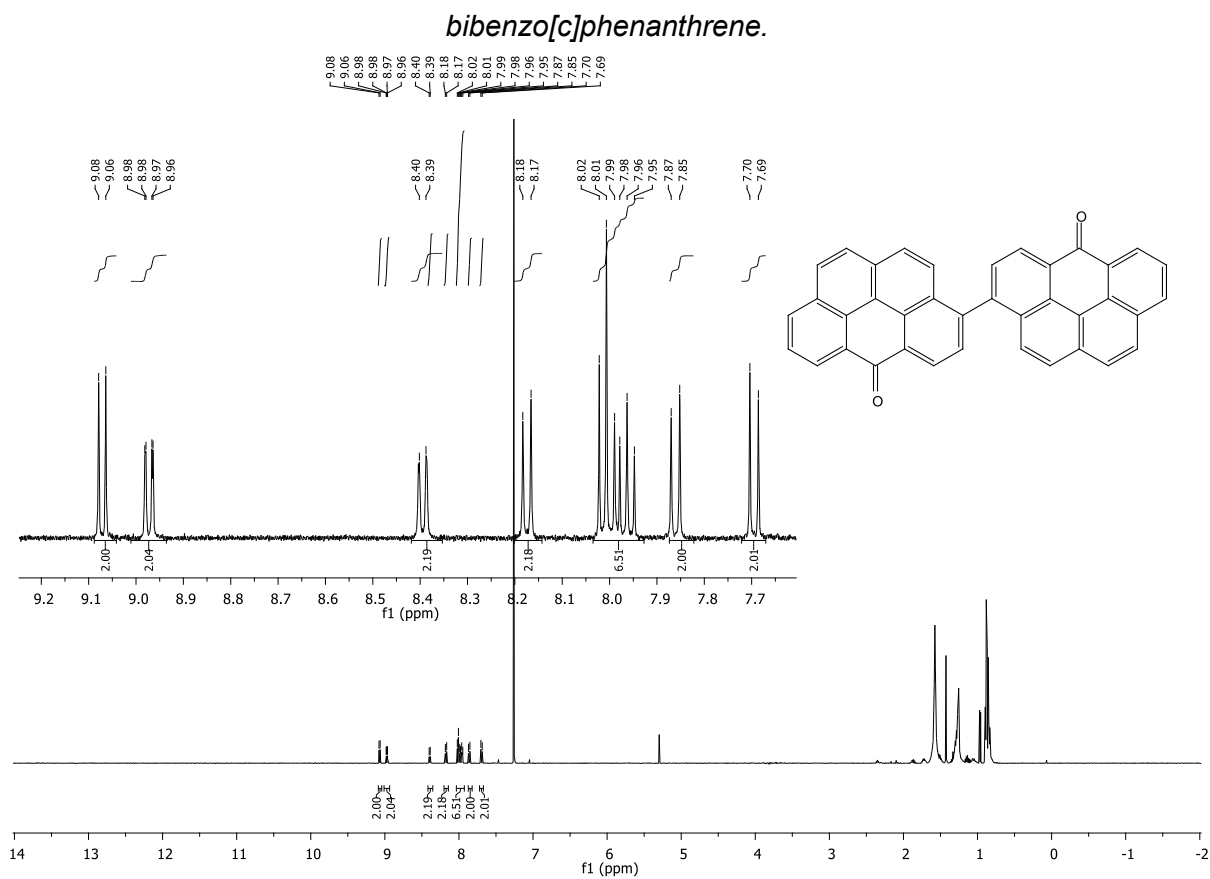


Figure 8.236: ¹H-NMR spectrum of 4,4'-bis(12-fluoro-1-methylbenzo[c]phenanthren-4-yl)-1,1'-biphenyl.

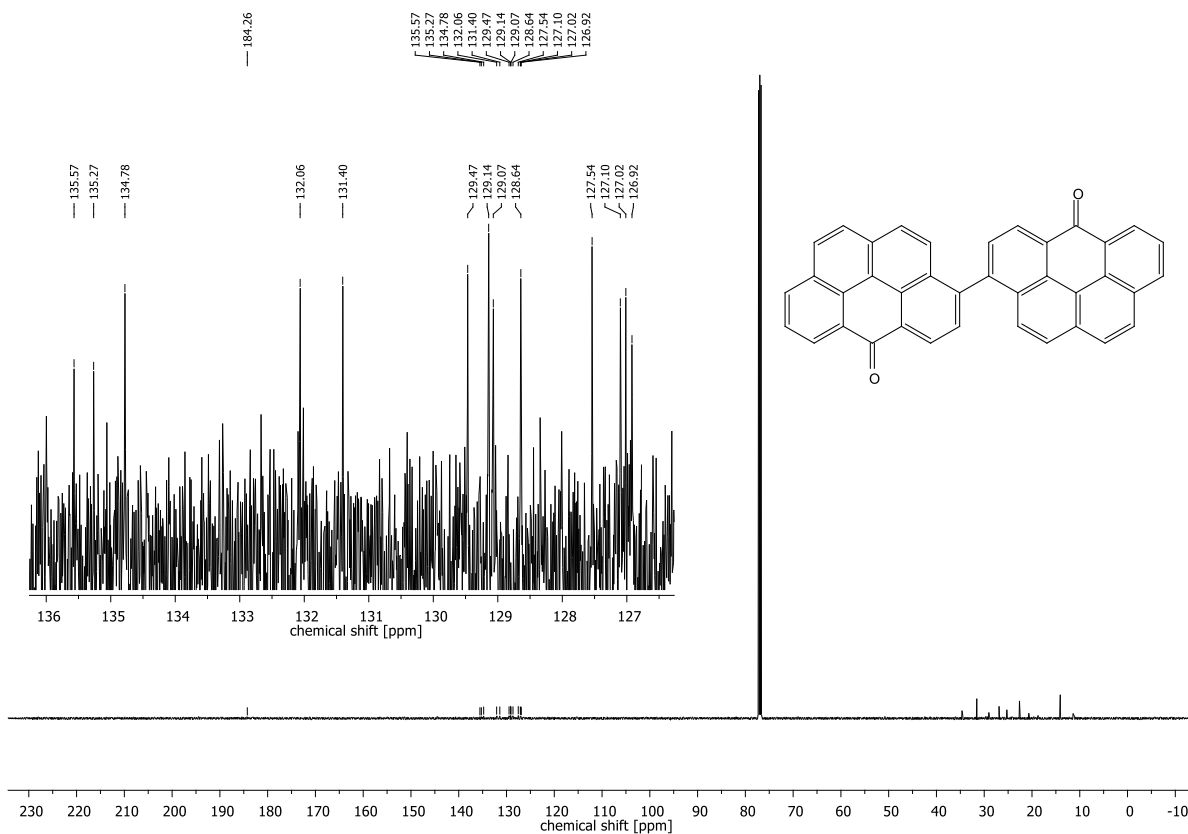


Figure 8.237: $^{13}\text{C-NMR}$ spectrum of 4,4'-bis(12-fluoro-1-methylbenzo[c]phenanthren-4-yl)-1,1'-biphenyl.

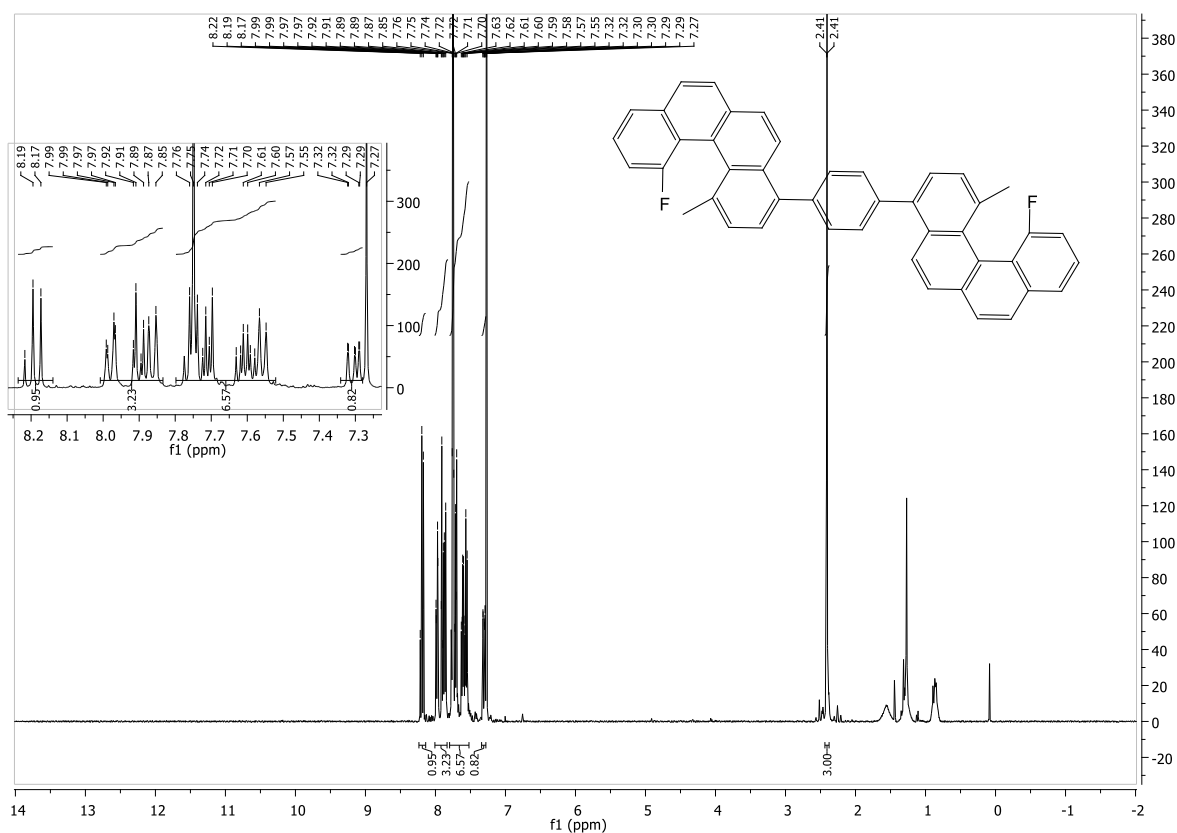


Figure 8.238: $^1\text{H-NMR}$ spectrum of 1,4-bis(12-fluoro-1-methylbenzo[c]phenanthren-4-yl)benzene.

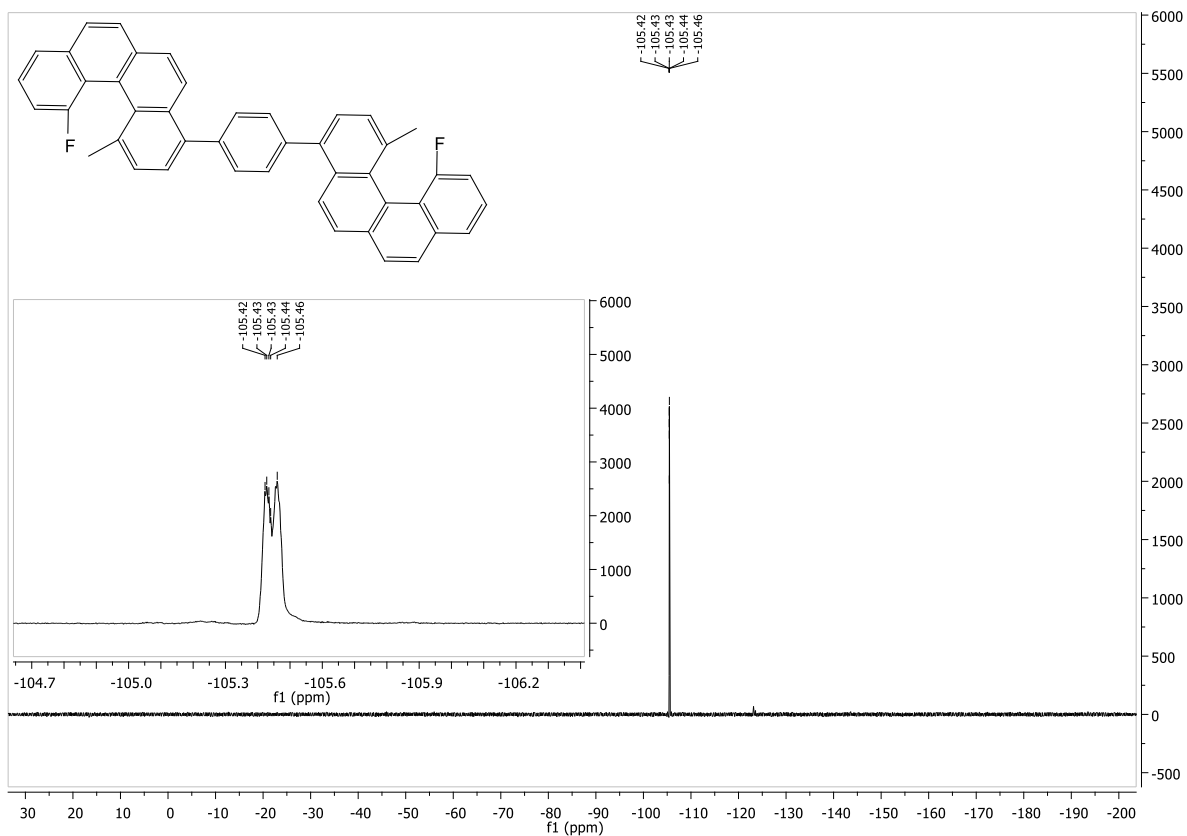


Figure 8.239: ^{19}F -NMR spectrum of 1,4-bis(12-fluoro-1-methylbenzo[c]phenanthren-4-yl)benzene.

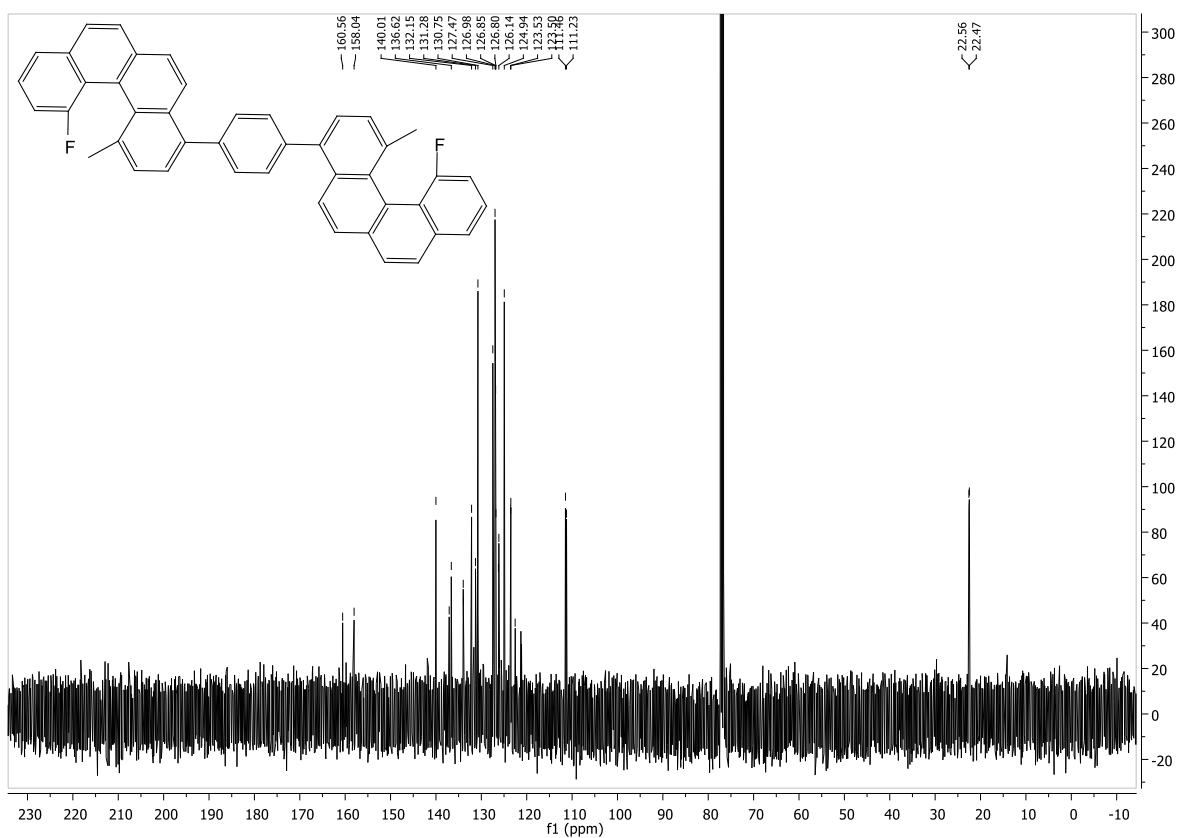


Figure 8.240: ^{13}C -NMR spectrum of 1,4-bis(12-fluoro-1-methylbenzo[c]phenanthren-4-yl)benzene.

yl)benzene.

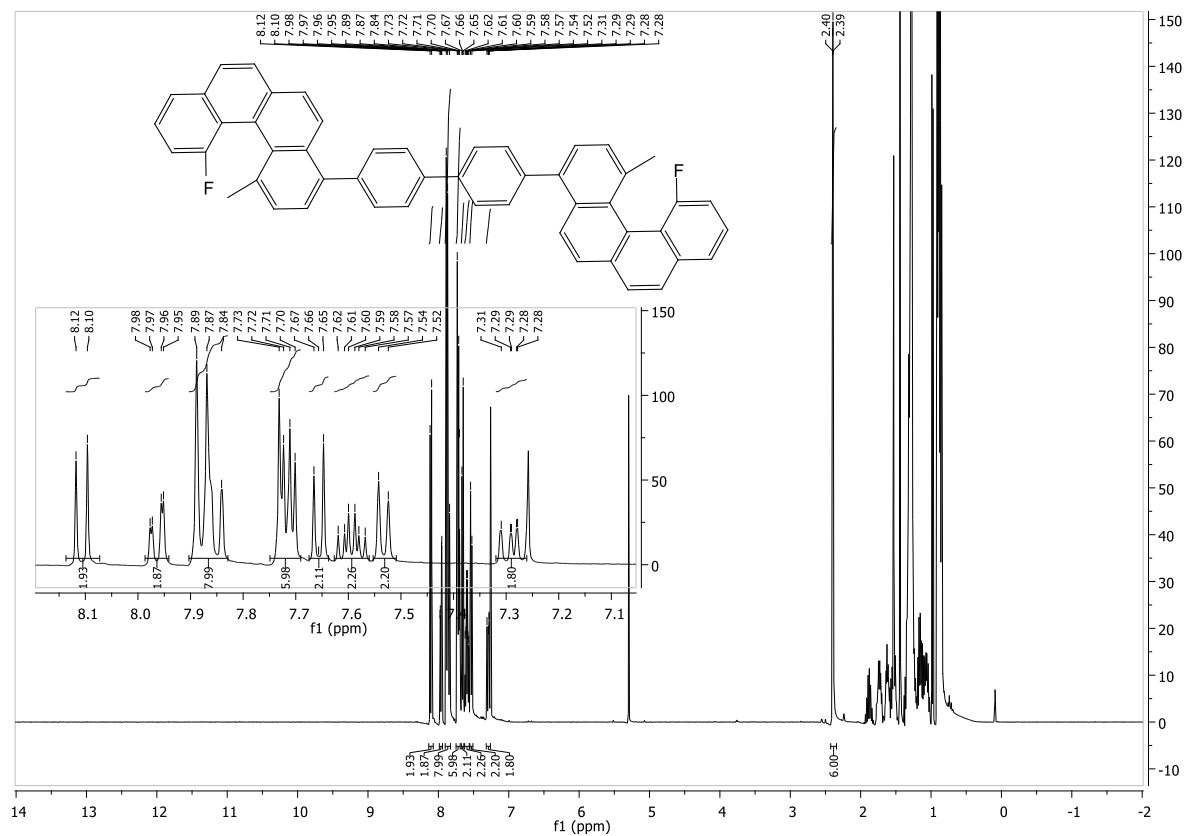


Figure 8.241: $^1\text{H-NMR}$ spectrum of 4,4'-bis(12-fluoro-1-methylbenzo[c]phenanthren-4-yl)-1,1'-biphenyl.

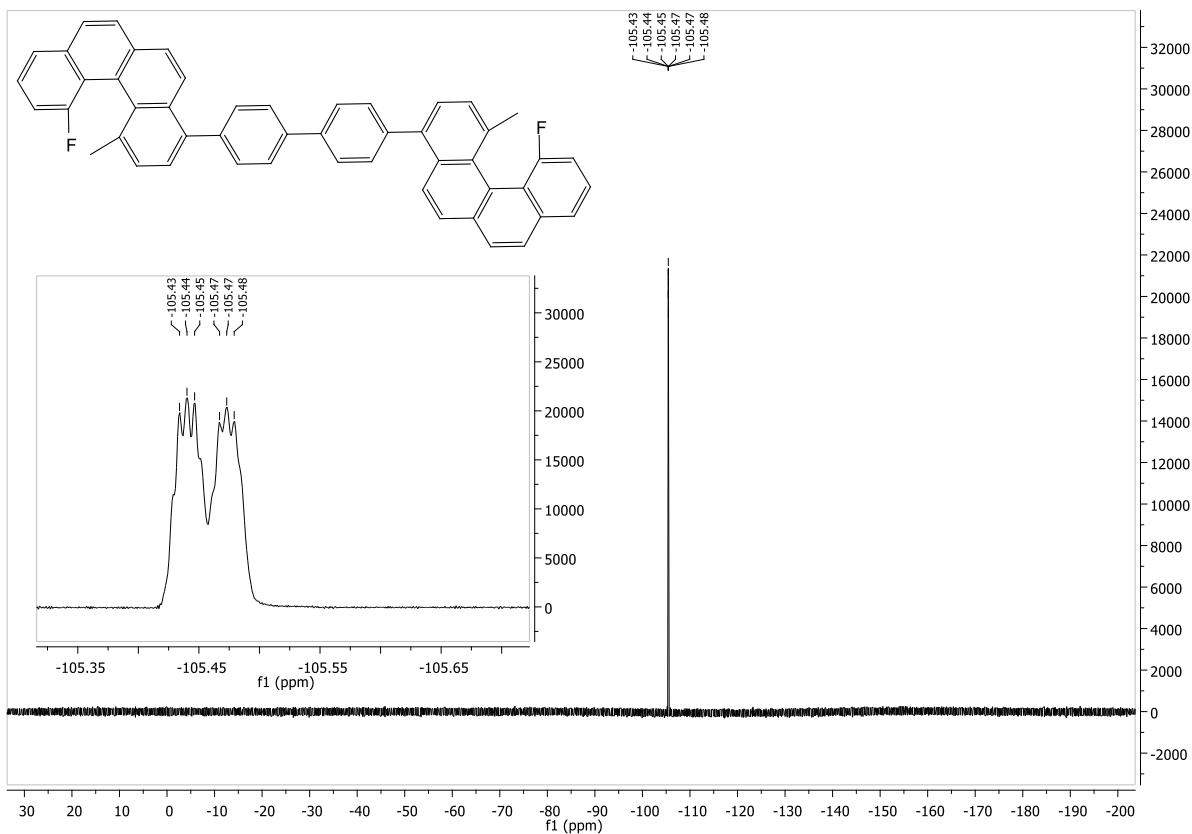


Figure 8.242: ^{19}F -NMR spectrum of 4,4'-bis(12-fluoro-1-methylbenzo[c]phenanthren-4-yl)-1,1'-biphenyl.

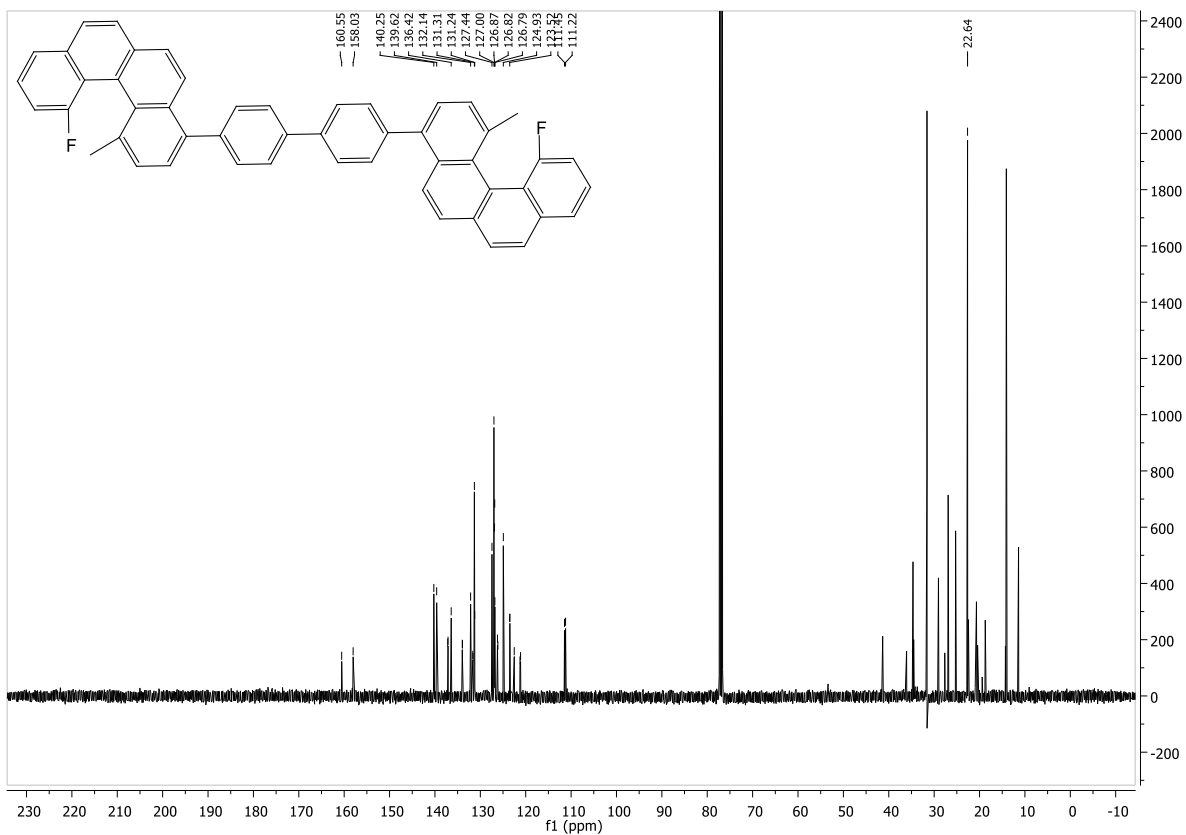


Figure 8.243: ^{13}C -NMR spectrum of 4,4'-bis(12-fluoro-1-methylbenzo[c]phenanthren-4-yl)-1,1'-biphenyl.

1,1'-biphenyl.

8.4. Screening the reactivity of different functional groups on Al₂O₃

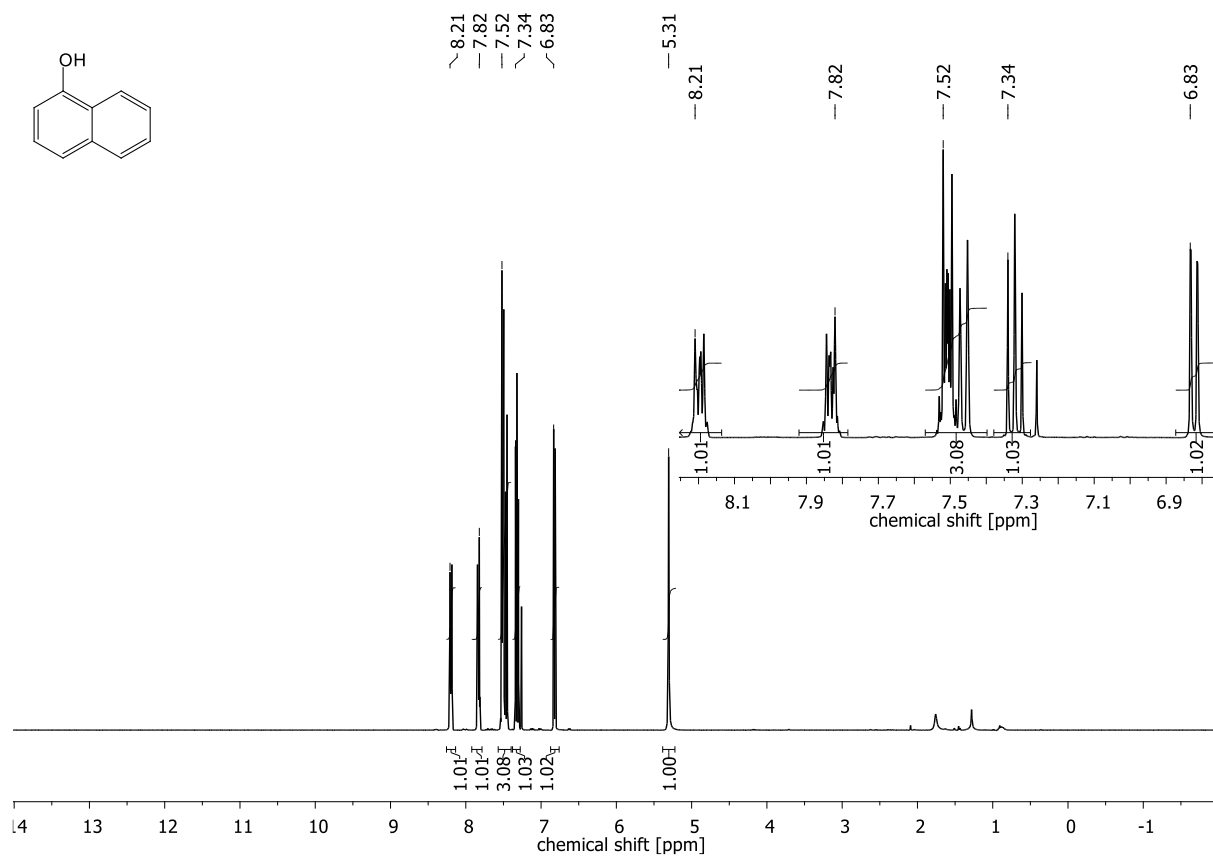


Figure 8.244: ¹H-NMR spectrum of naphthalen-1-ol

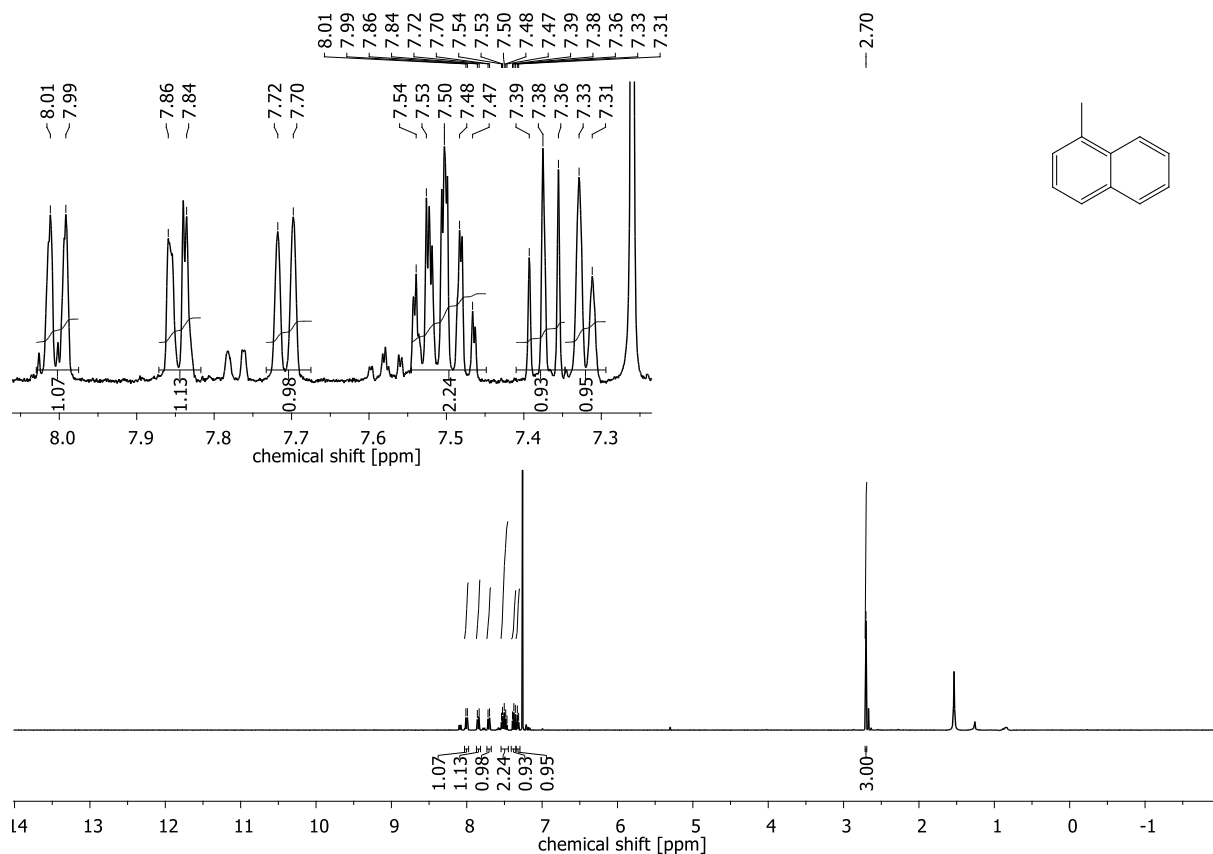


Figure 8.245: $^1\text{H-NMR}$ spectrum of 1-methylnaphthalene.

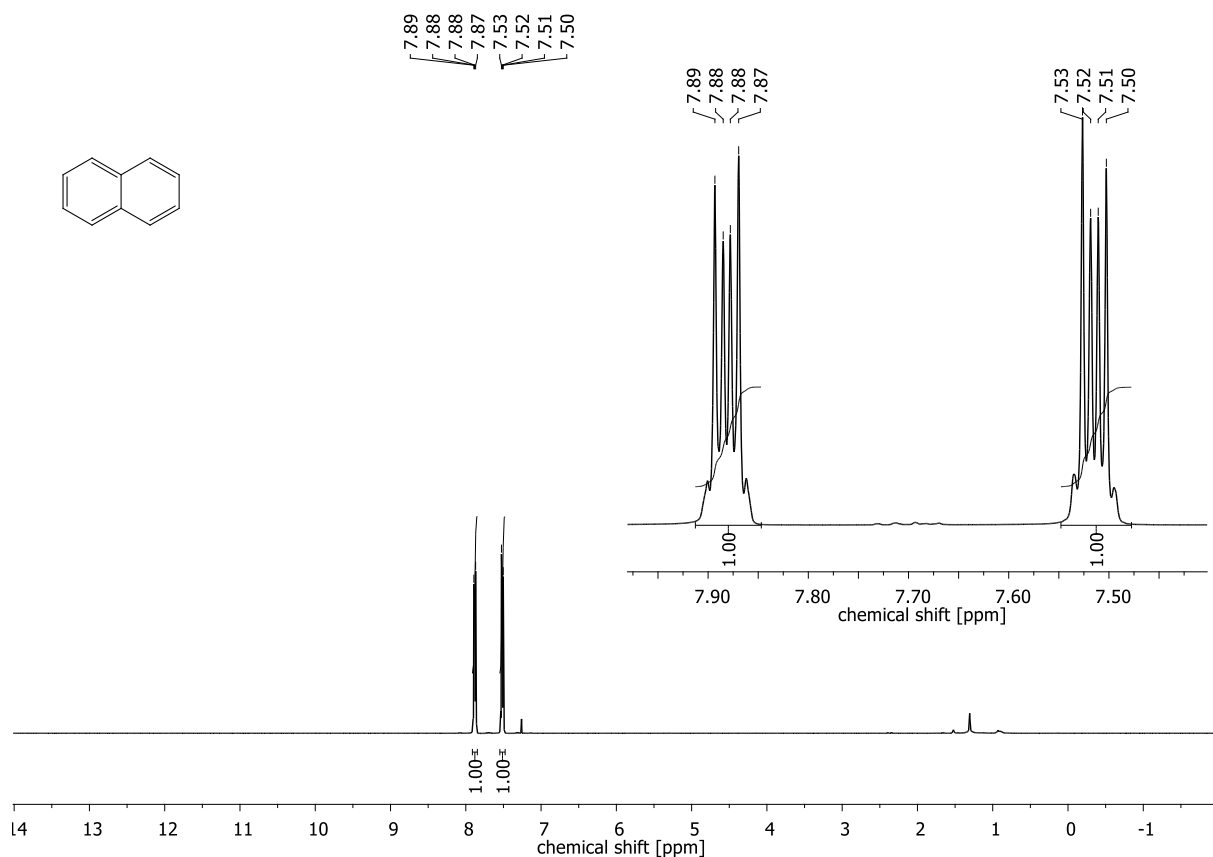


Figure 8.246: $^1\text{H-NMR}$ spectrum of naphthalene.

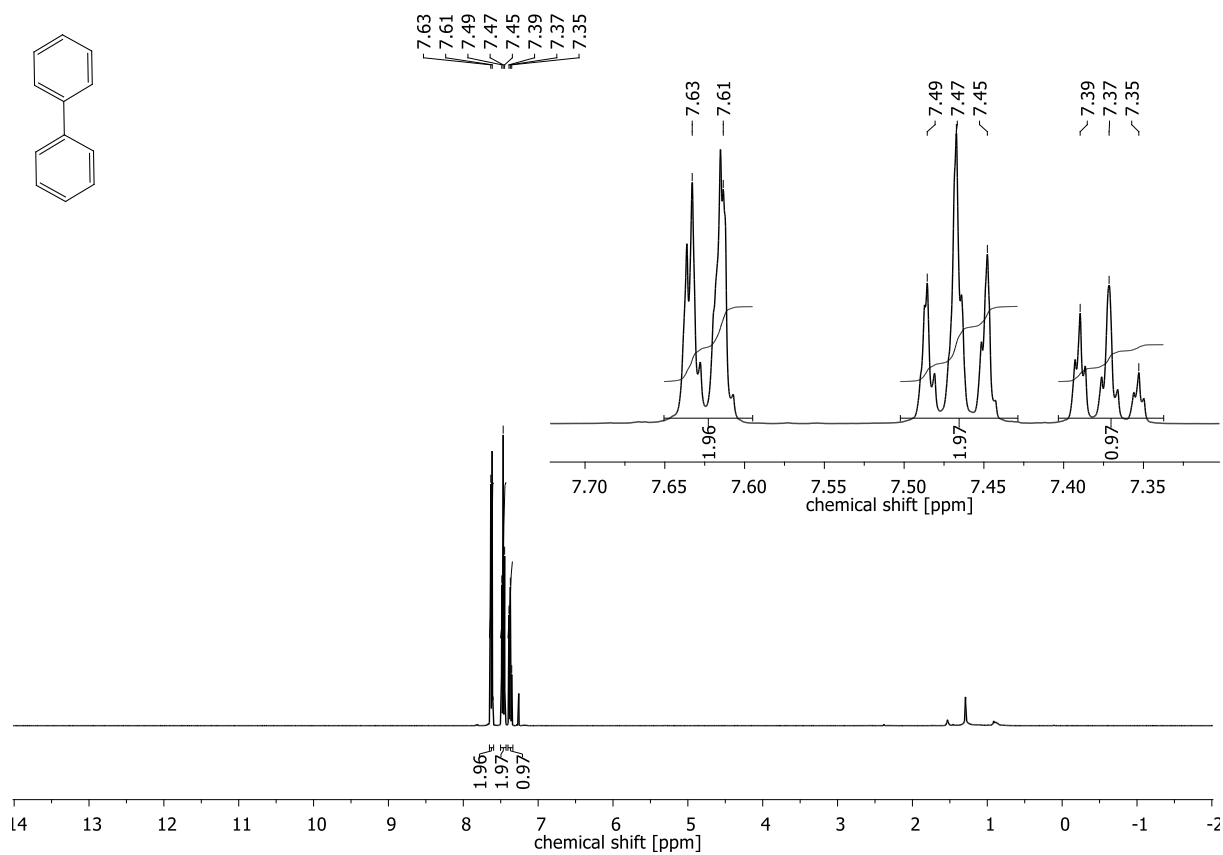


Figure 8.247: $^1\text{H-NMR}$ spectrum of 1,1'-biphenyl.

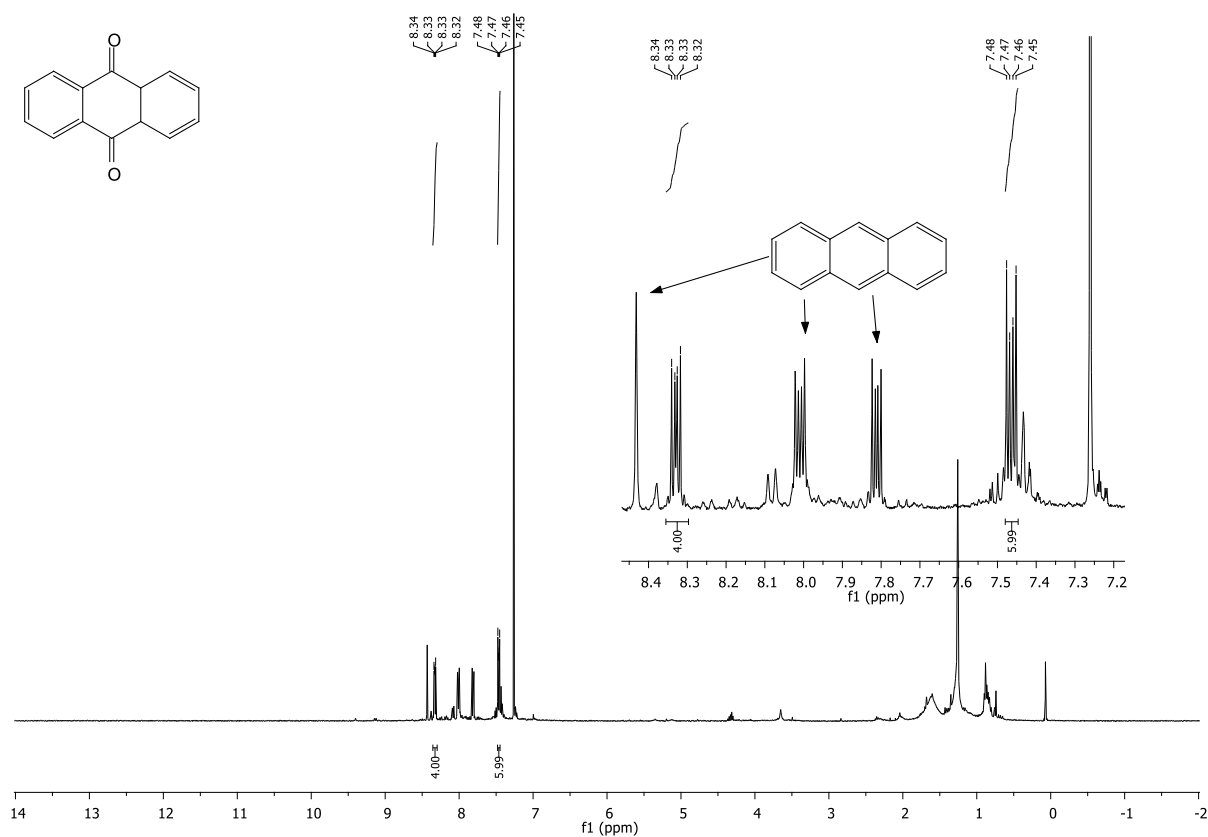


Figure 8.248: $^1\text{H-NMR}$ spectrum of 4a,9a-dihydroanthracene-9,10-dione and

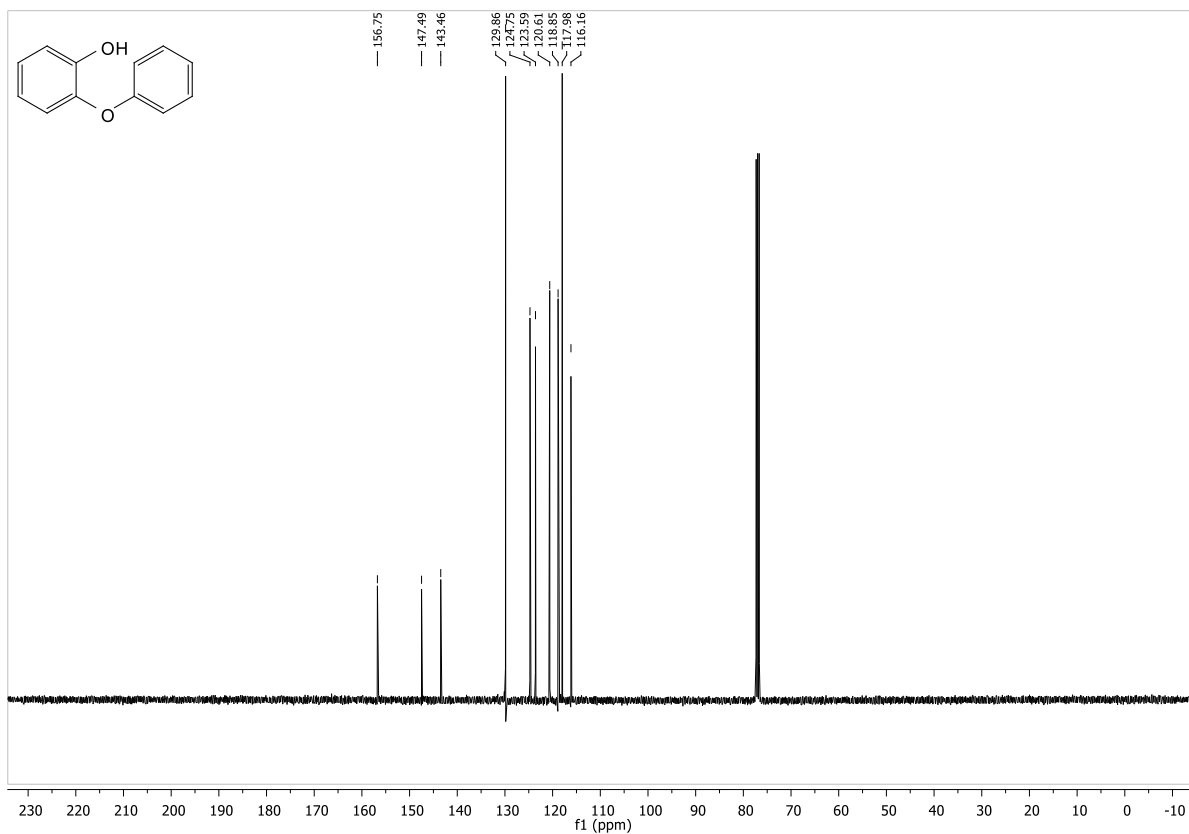


Figure 8.251: $^{13}\text{C-NMR}$ spectrum of 2-phenoxyphenol.

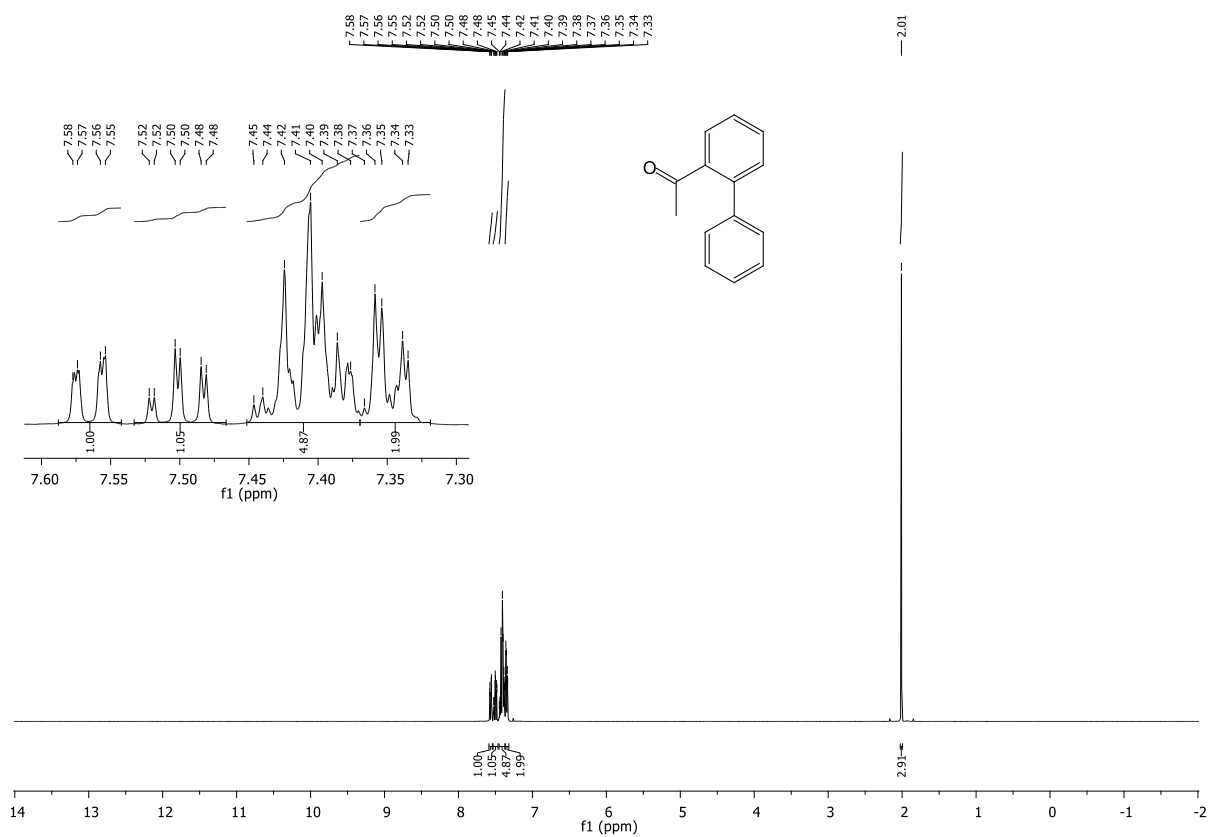


Figure 8.252: $^1\text{H-NMR}$ spectrum of 1-([1,1'-biphenyl]-2-yl)ethan-1-one.

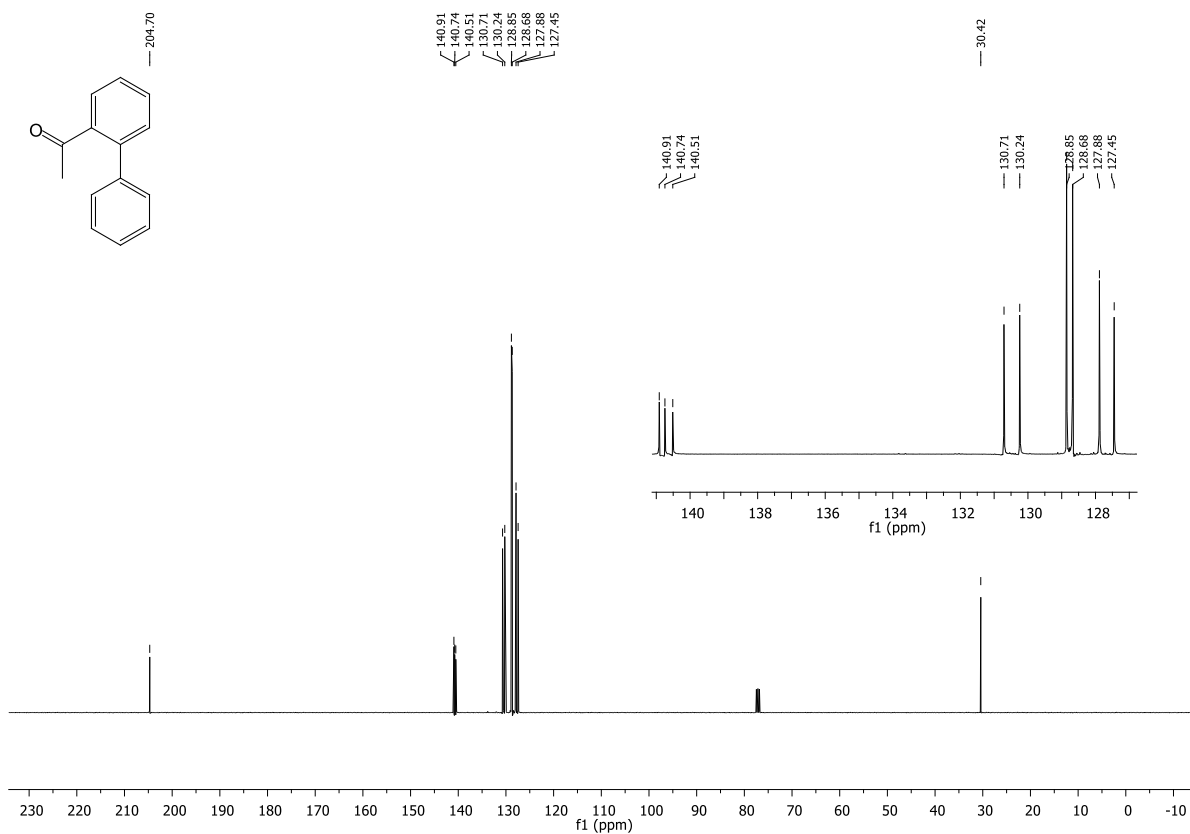


Figure 8.253: ^{13}C -NMR spectrum of 1-([1,1'-biphenyl]-2-yl)ethan-1-one.

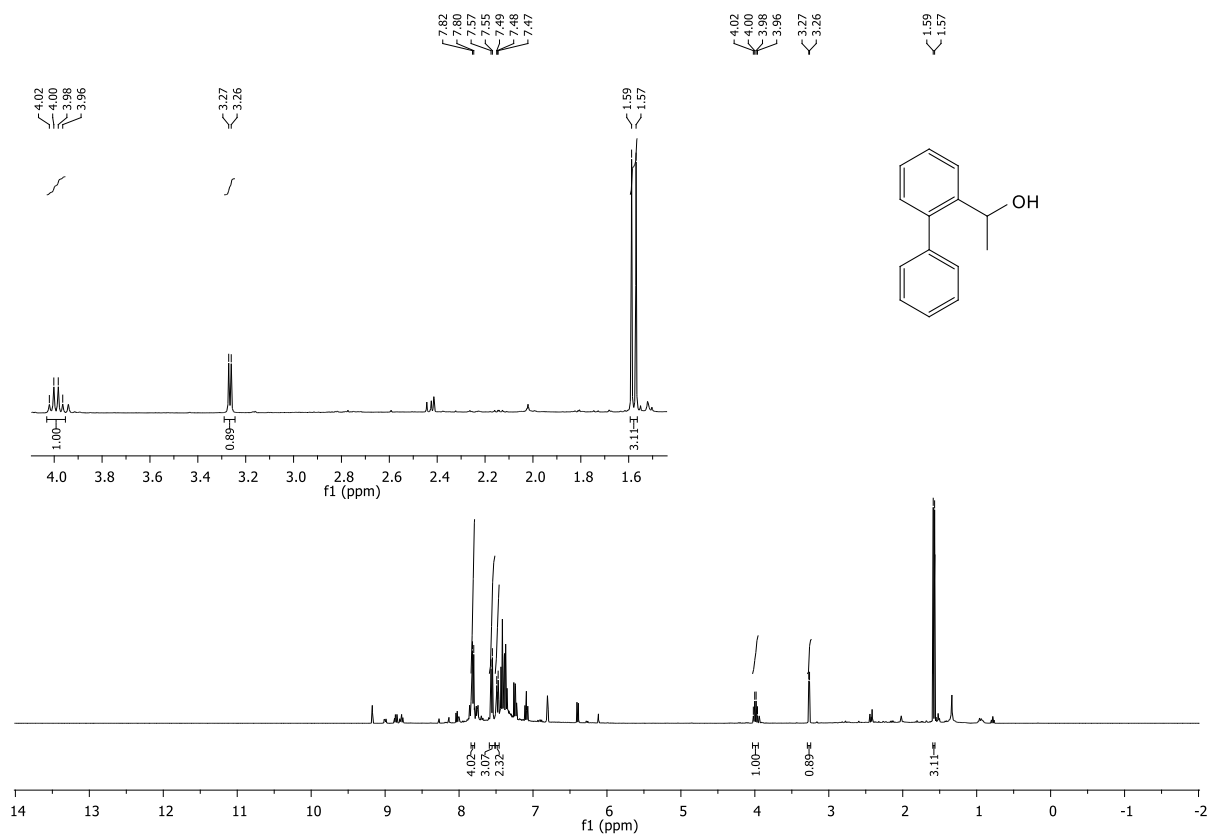


Figure 8.254: ^1H -NMR spectrum of 1-([1,1'-biphenyl]-2-yl)ethan-1-ol.

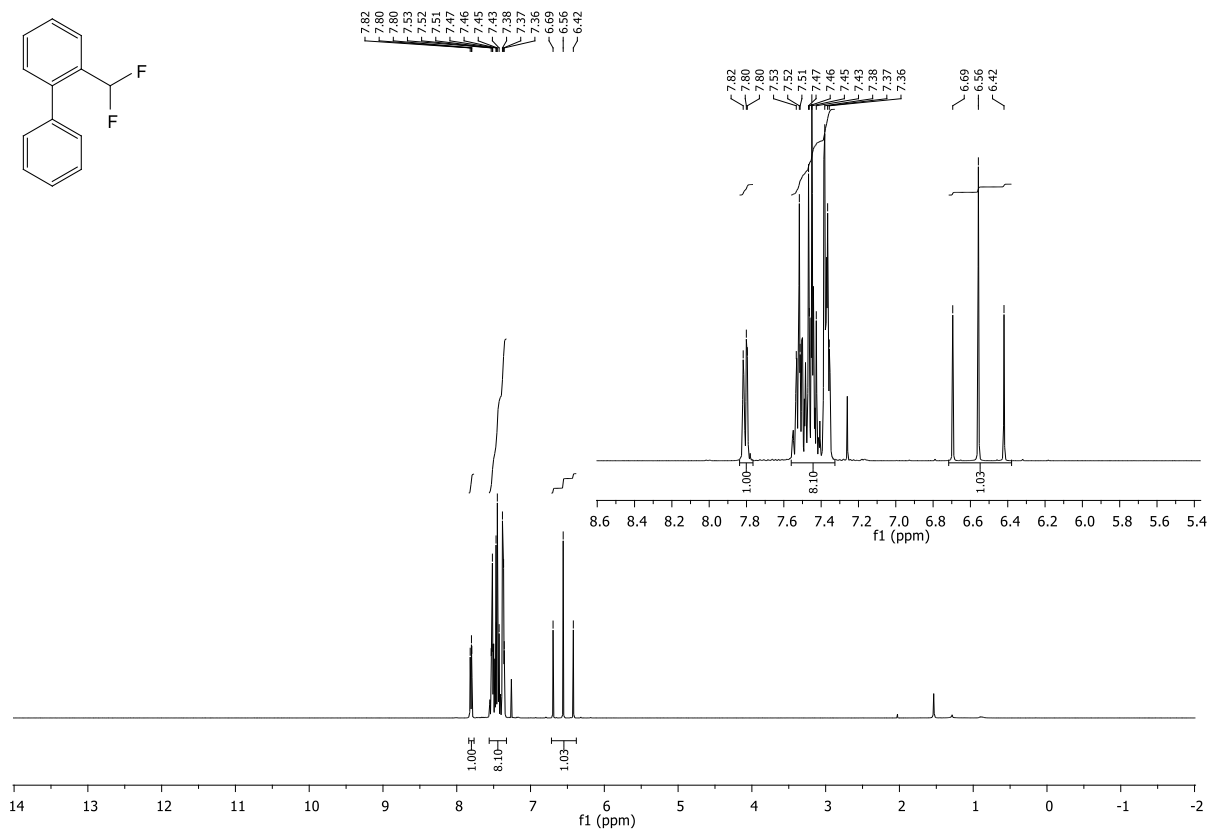


Figure 8.255: ¹H-NMR spectrum of 2-(difluoromethyl)-1,1'-biphenyl.

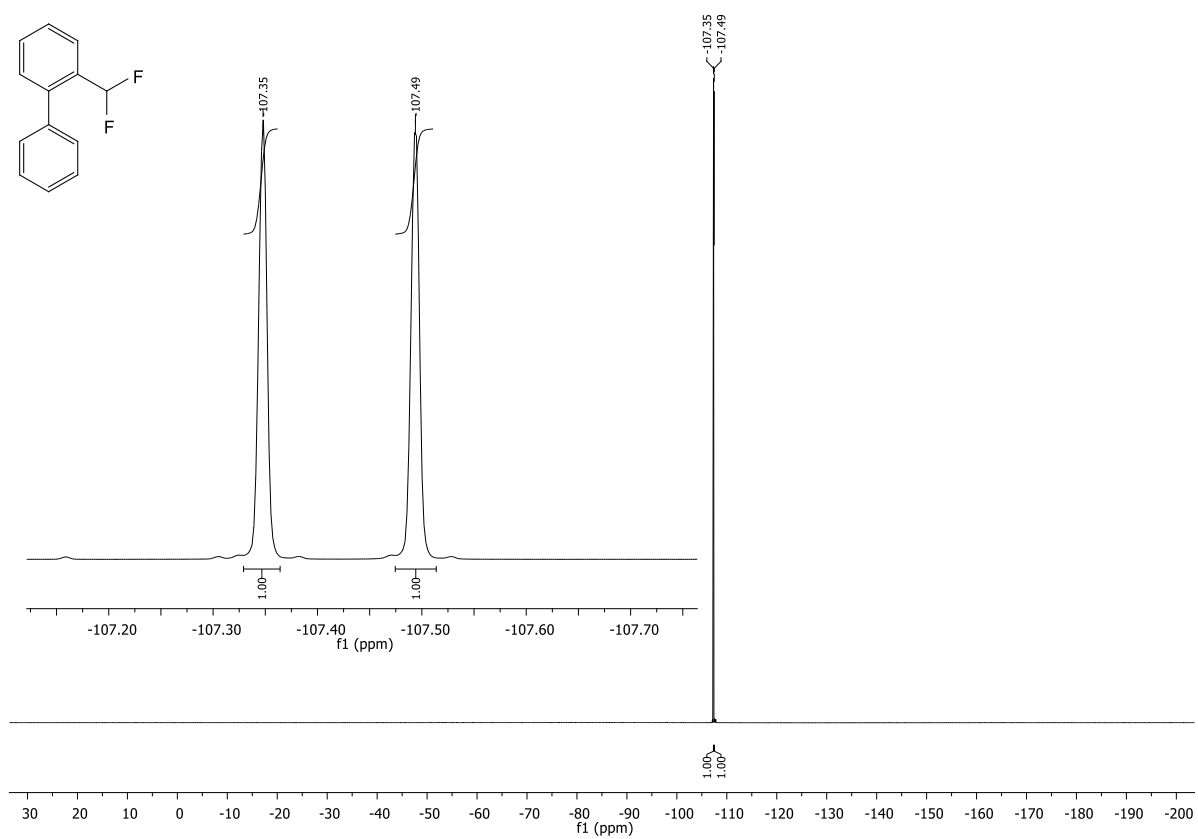


Figure 8.256: ¹⁹F-NMR spectrum of 2-(difluoromethyl)-1,1'-biphenyl.

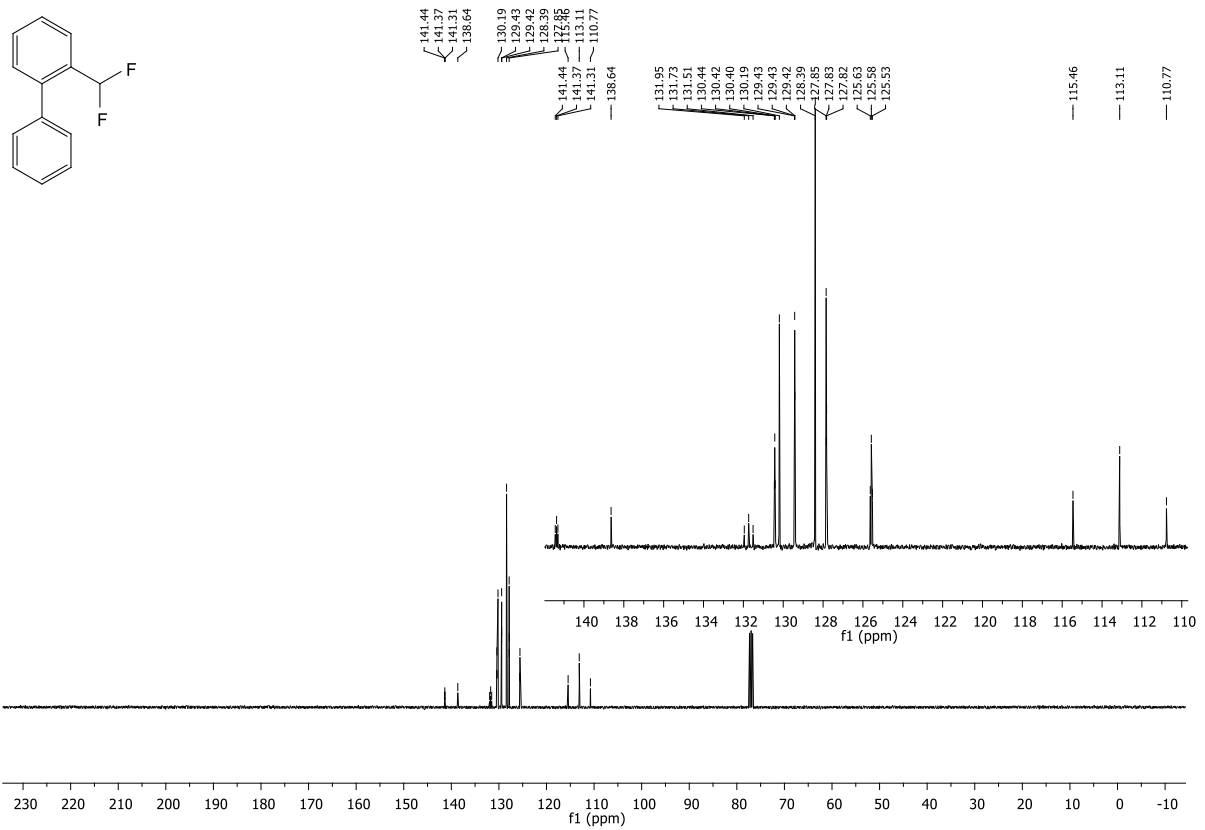


Figure 8.257: ^{13}C -NMR spectrum of 2-(difluoromethyl)-1,1'-biphenyl.

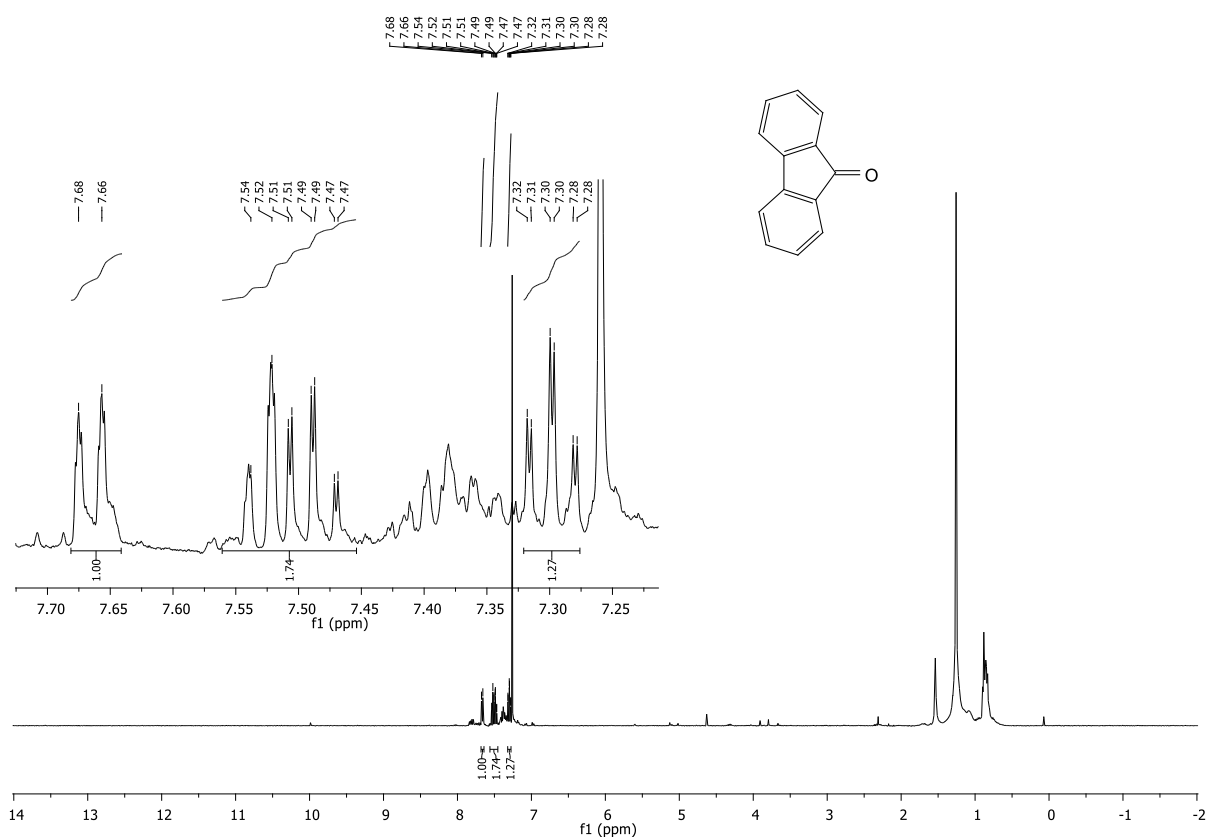


Figure 8.258: ^1H -NMR spectrum of 9H-fluoren-9-one.

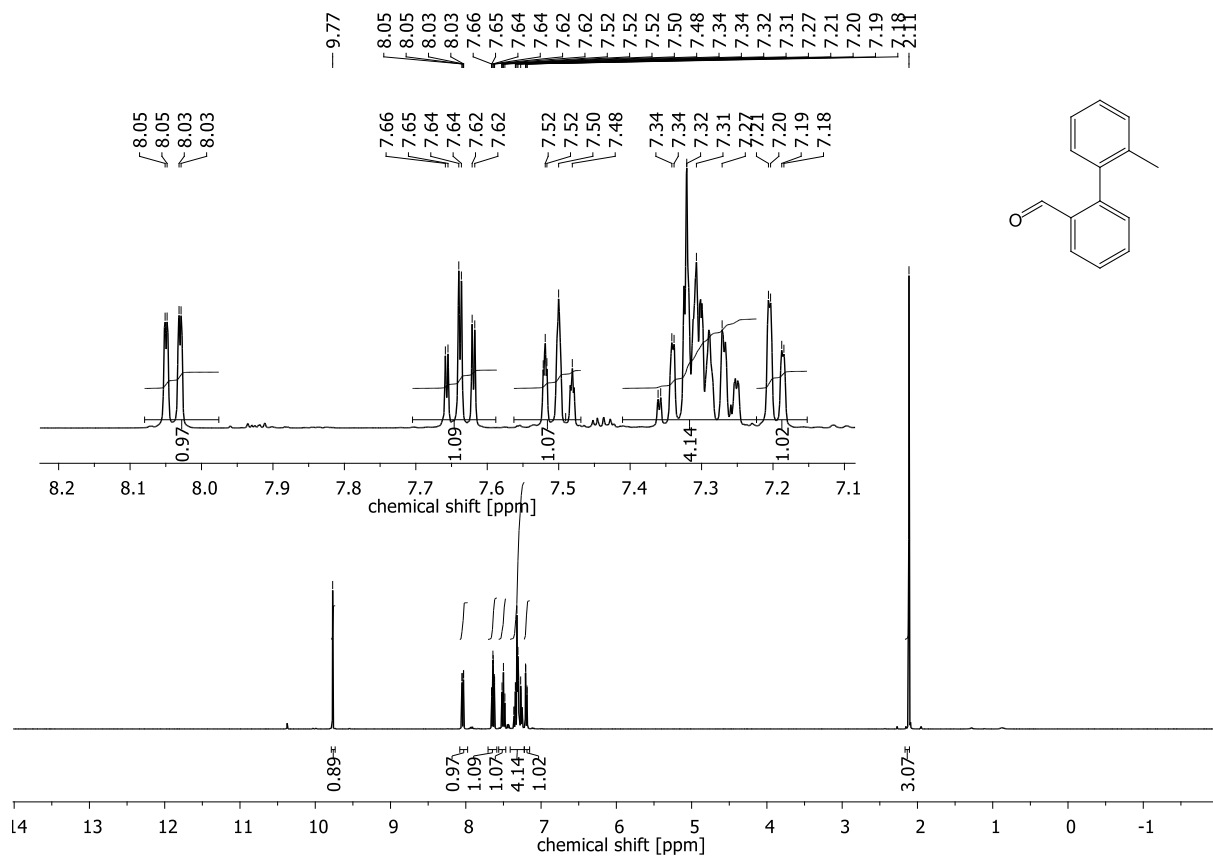


Figure 8.259: $^1\text{H-NMR}$ spectrum of 2'-methyl-[1,1'-biphenyl]-2-carbaldehyde.

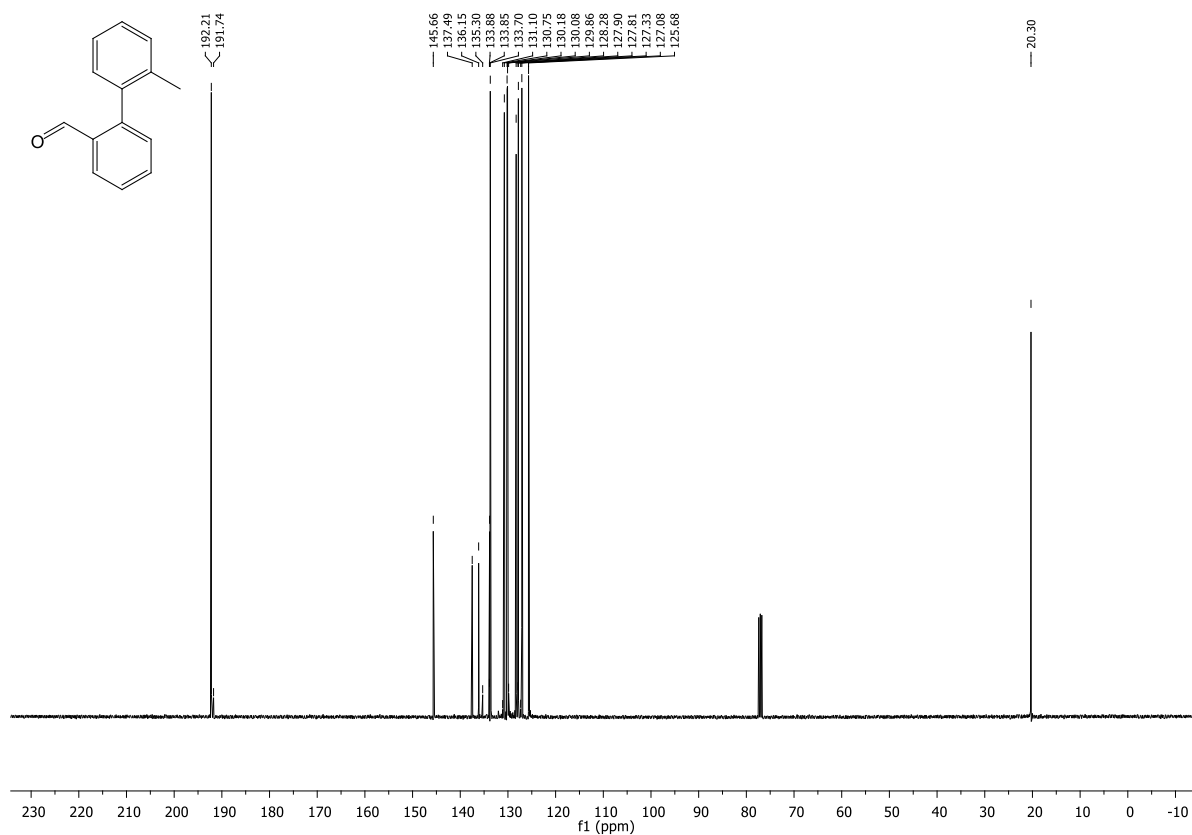


Figure 8.260: $^{13}\text{C-NMR}$ spectrum of 2'-methyl-[1,1'-biphenyl]-2-carbaldehyde.

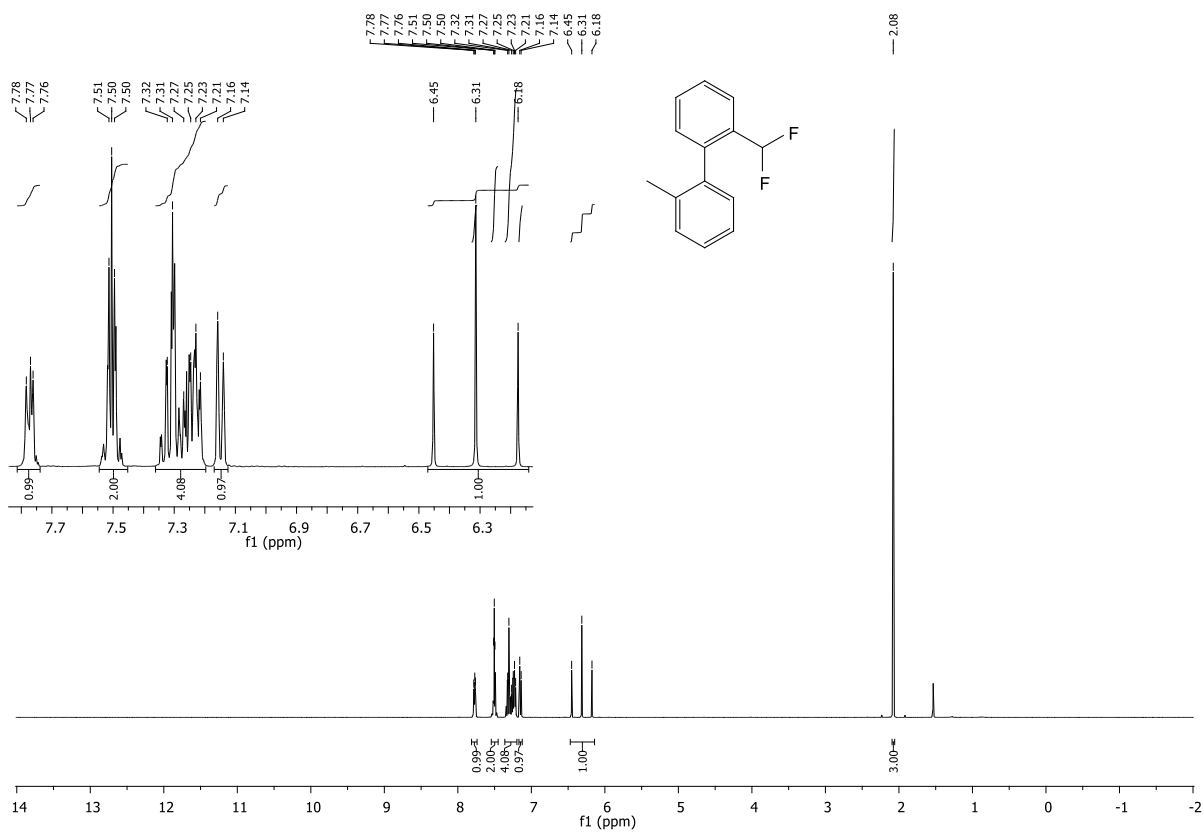


Figure 8.261: ¹H-NMR spectrum of 2-(difluoromethyl)-2'-methyl-1,1'-biphenyl.

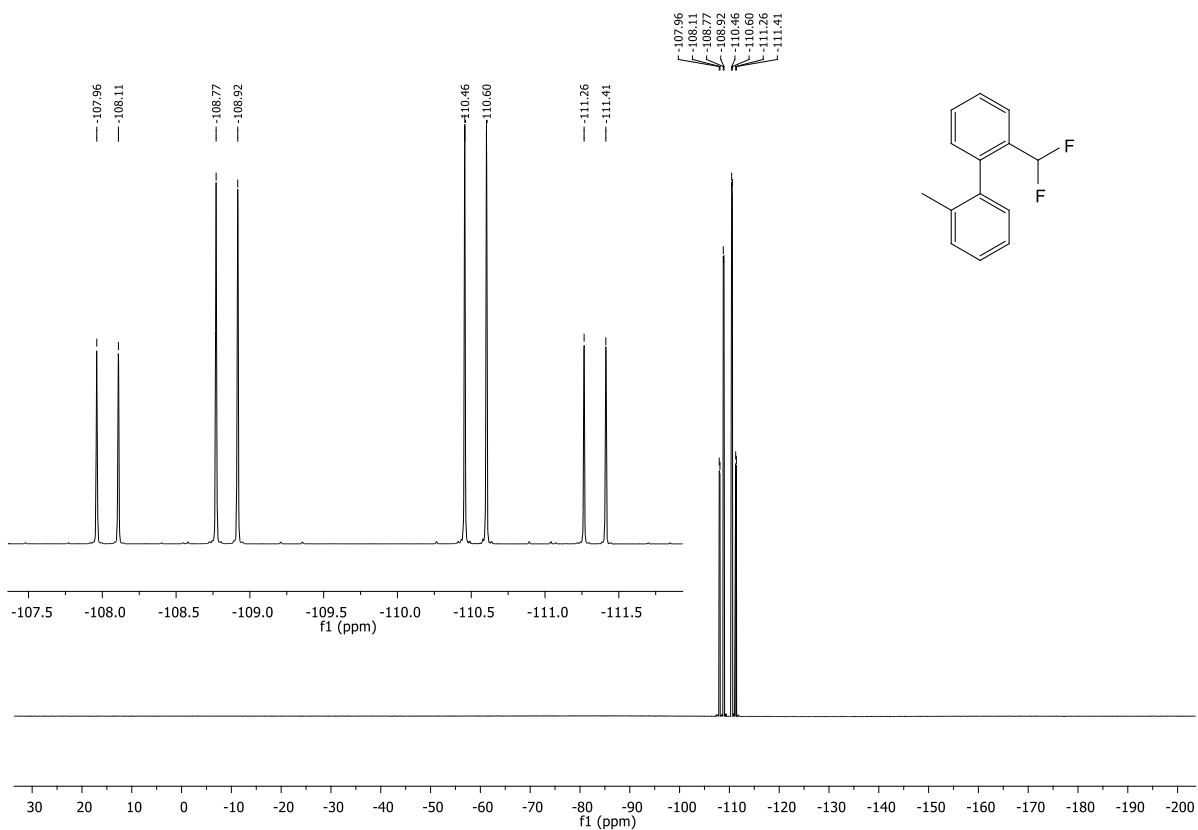


Figure 8.262: ¹⁹F-NMR spectrum of 2-(difluoromethyl)-2'-methyl-1,1'-biphenyl.

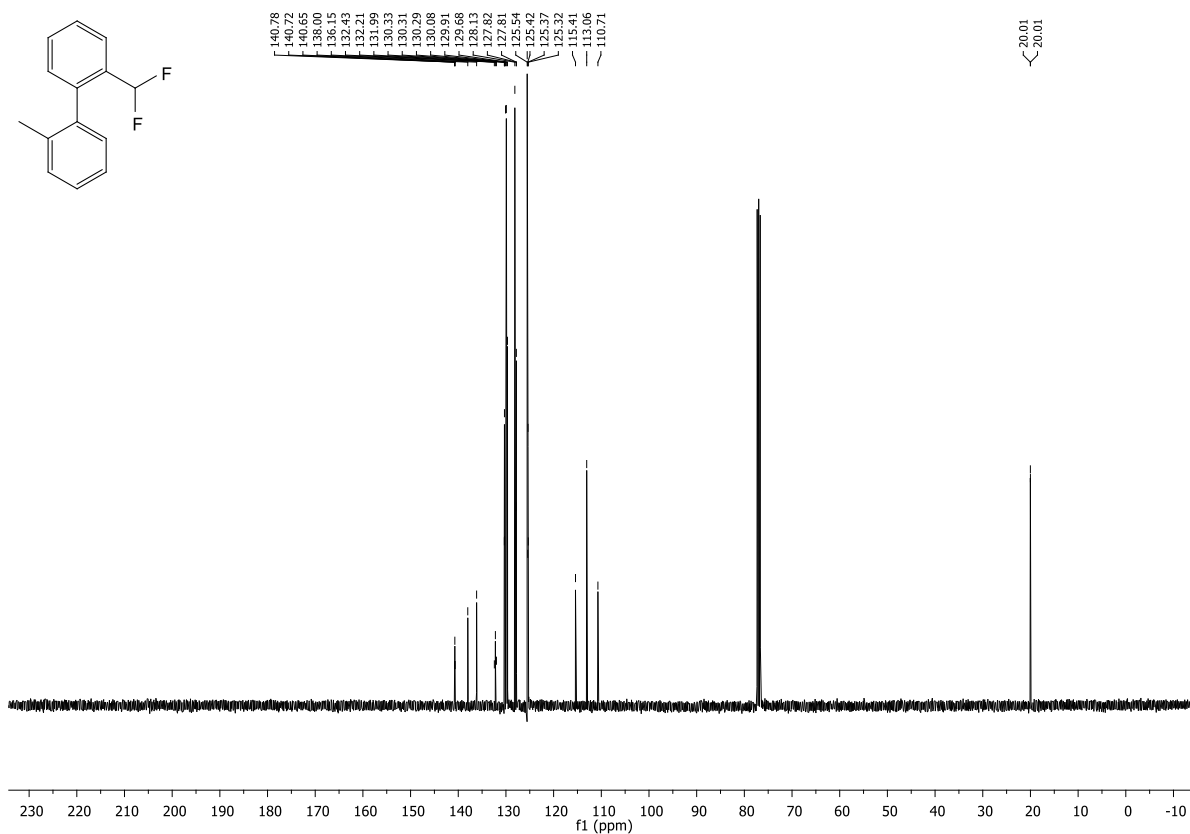


Figure 8.263: ^{13}C -NMR spectrum of 2-(difluoromethyl)-2'-methyl-1,1'-biphenyl.

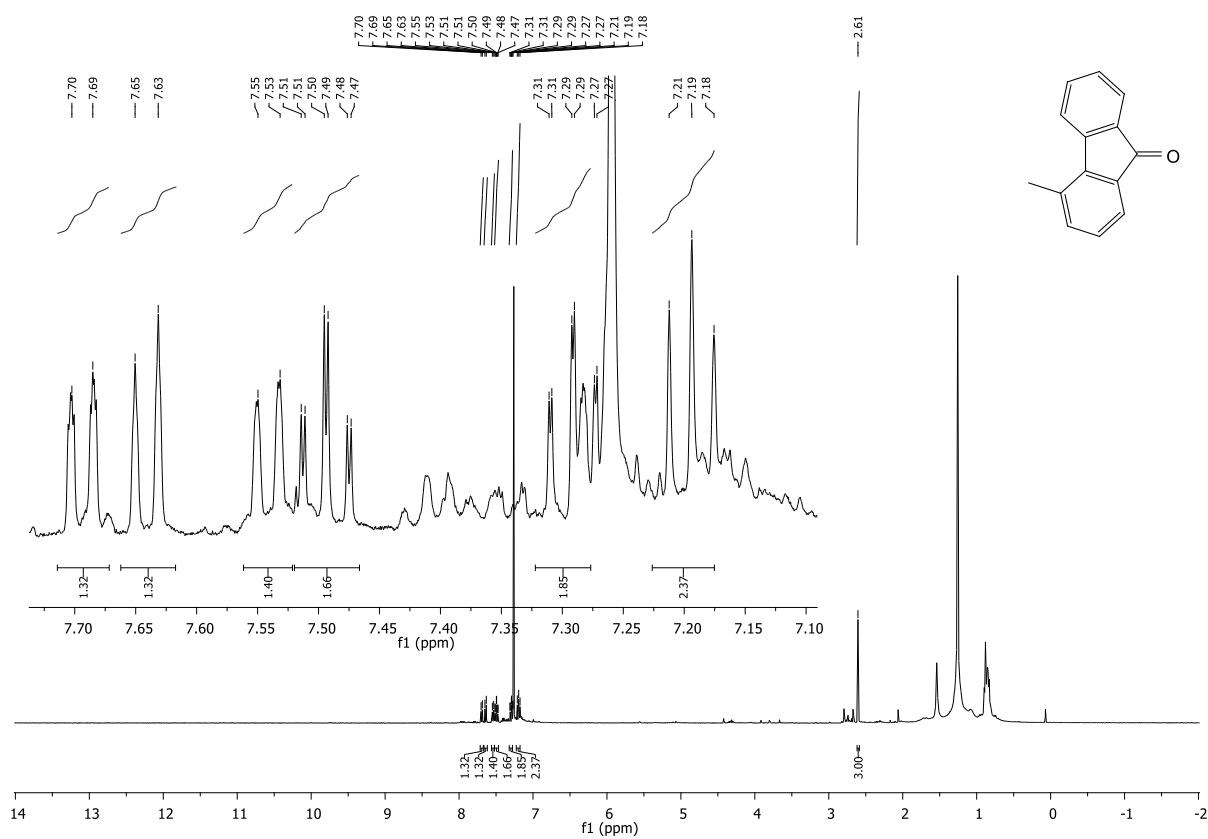


Figure 8.264: ^1H -NMR spectrum of 4-methyl-9H-fluoren-9-one.

8.5. Screening the reactivity of 2-ethynyl-1,1'-biphenyl on different metal oxides

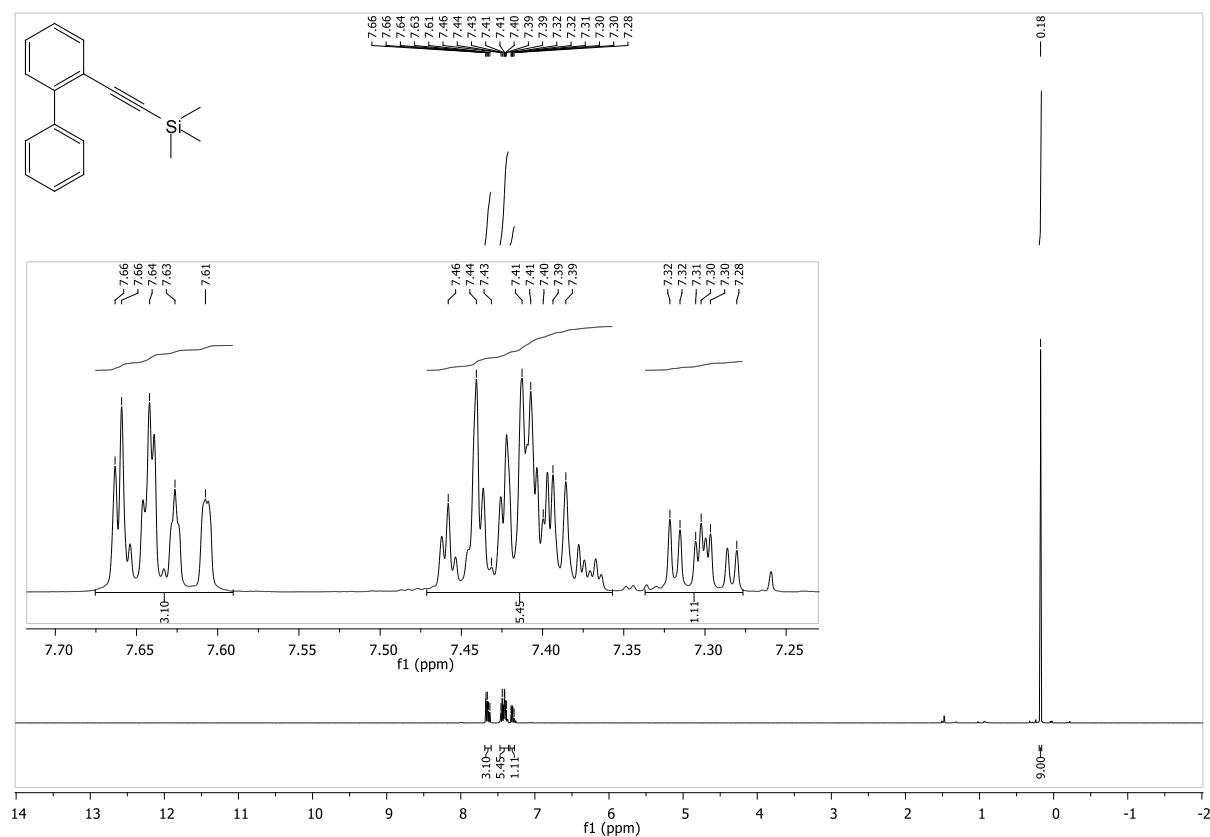


Figure 8.265: $^1\text{H-NMR}$ spectrum of ([1,1'-biphenyl]-2-ylethynyl)trimethylsilane.

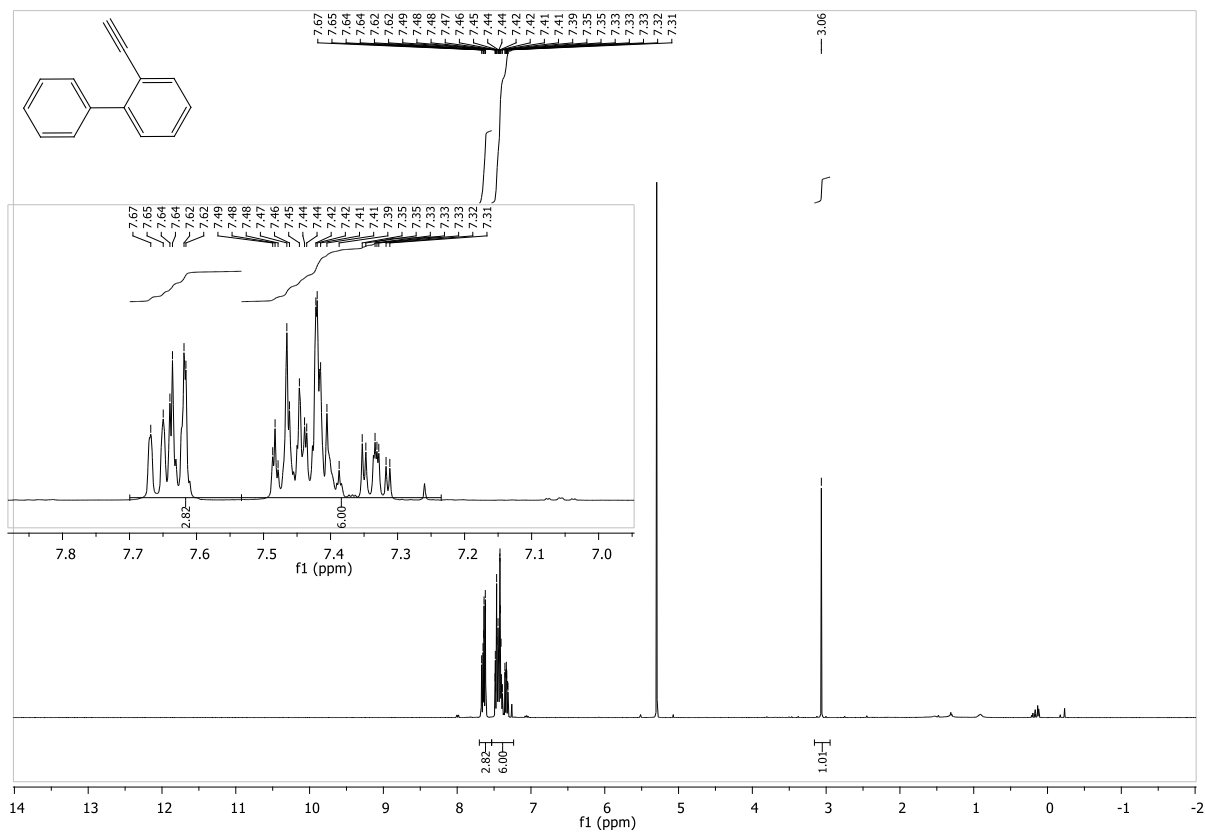


Figure 8.266: ¹H-NMR spectrum of 2-ethynyl-1,1'-biphenyl.

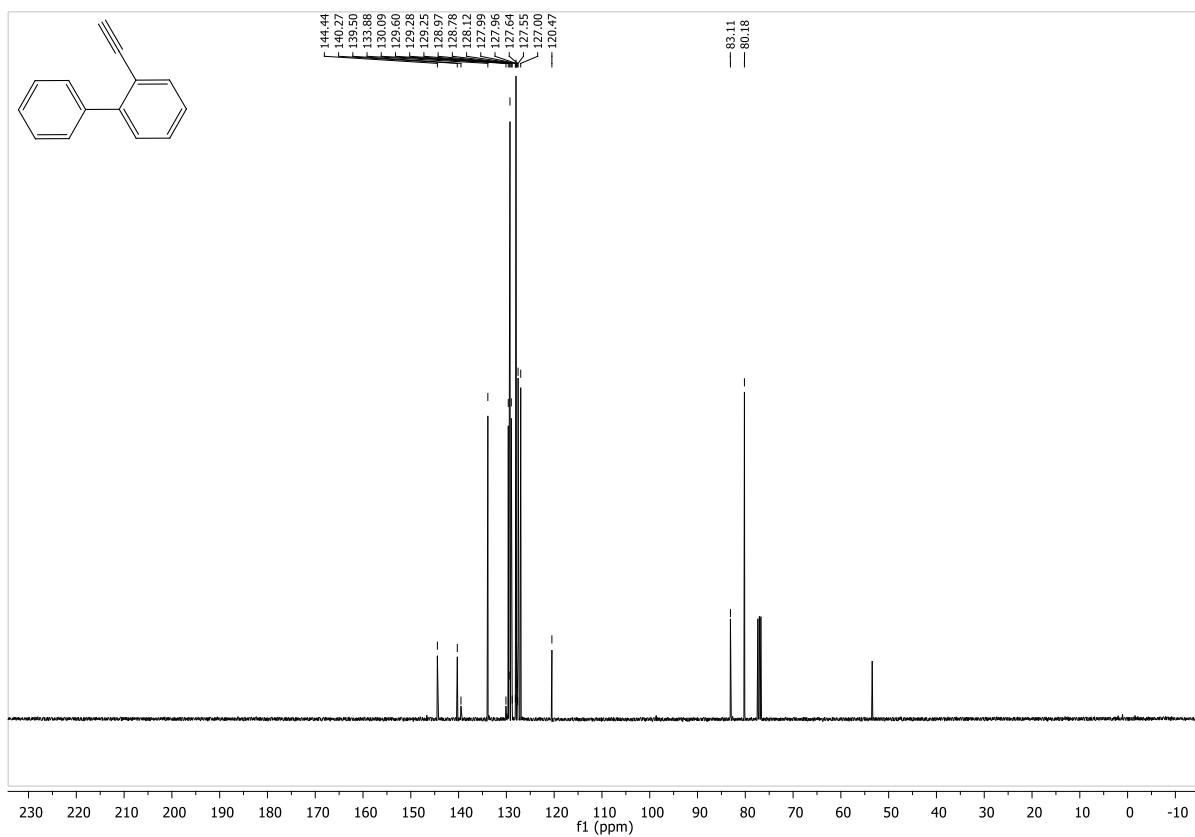


Figure 8.267: ¹³C-NMR spectrum of 2-ethynyl-1,1'-biphenyl.

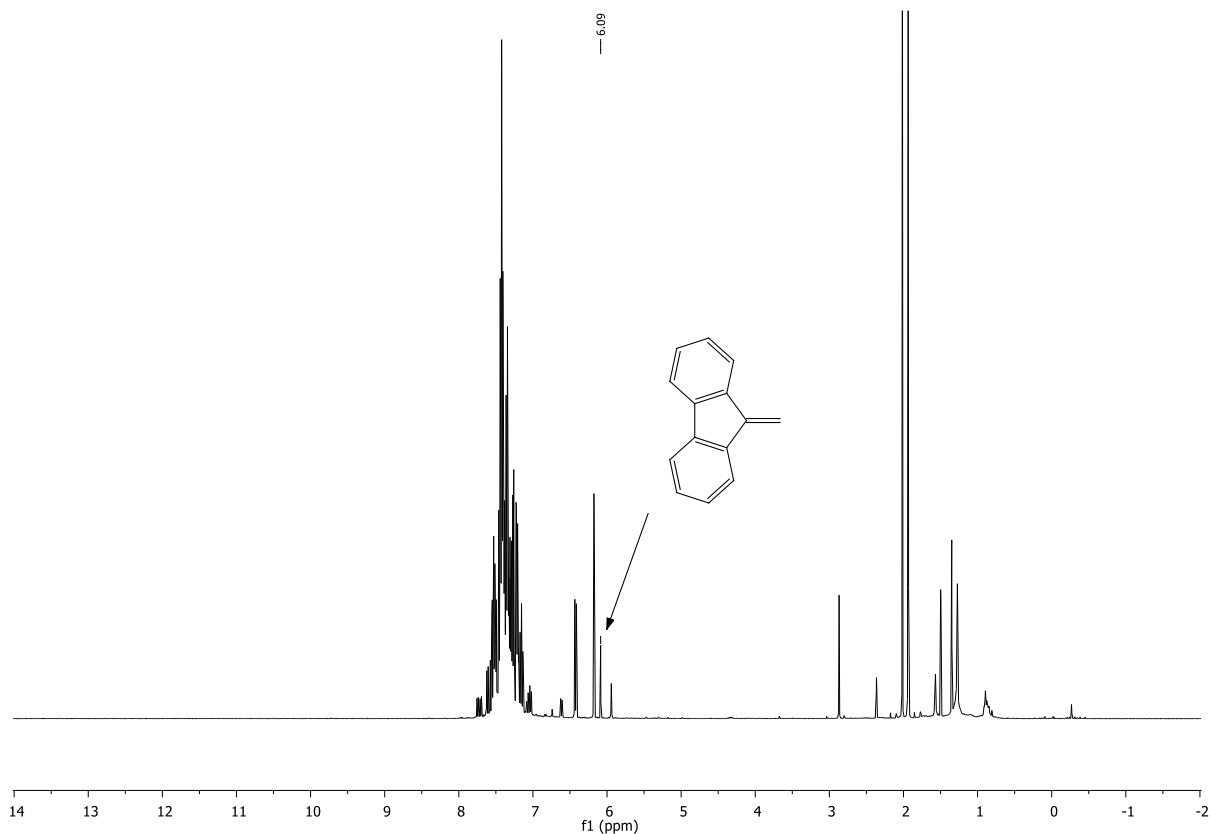


Figure 8.268: $^1\text{H-NMR}$ spectrum after reaction of biphenylacetylene on Nb_2O_3 at 90°C according to general procedure 1.

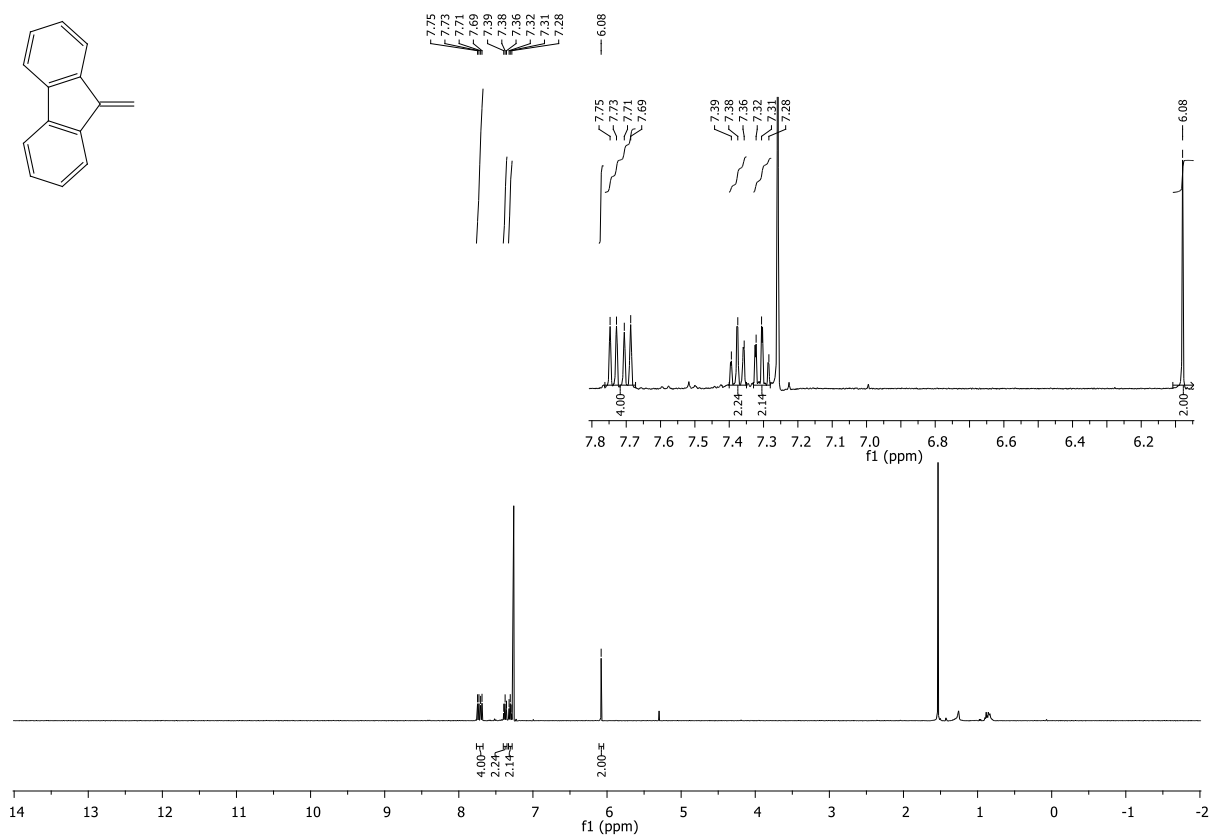


Figure 8.269: $^1\text{H-NMR}$ spectrum of 9-methylene-9H-fluorene.

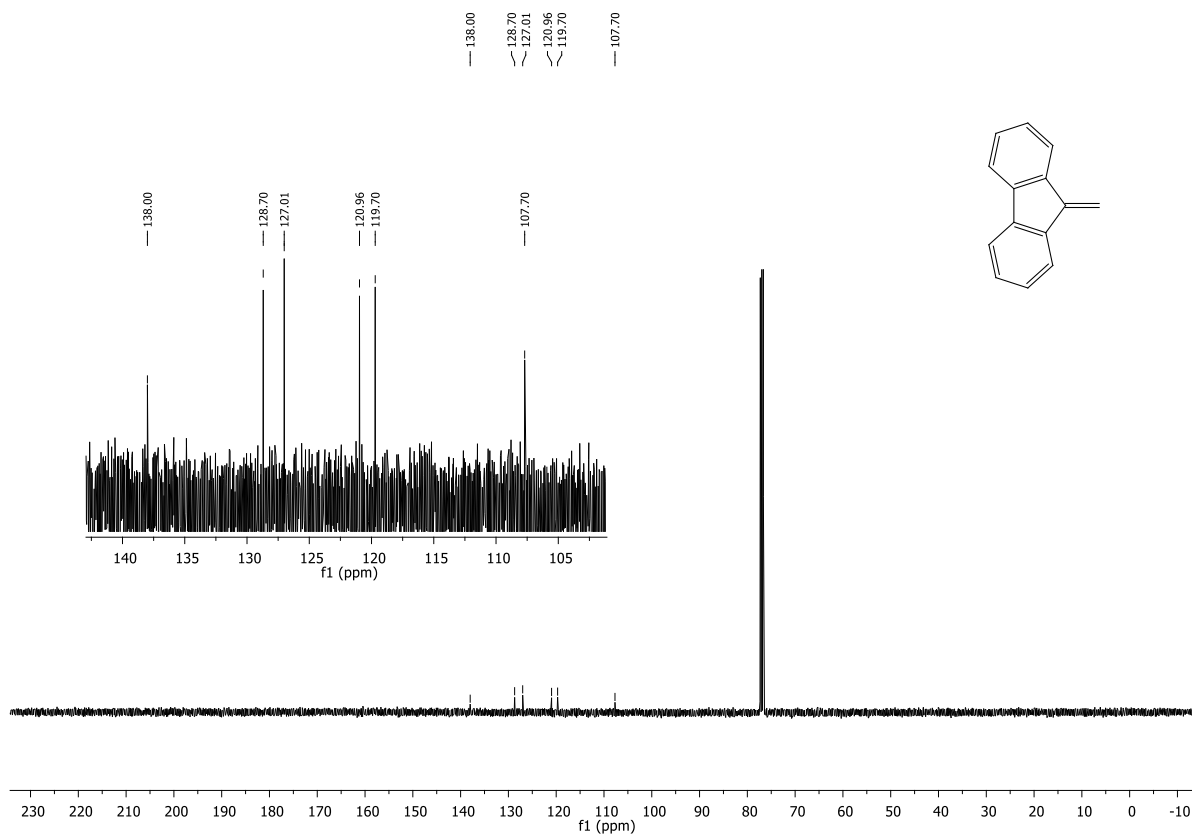


Figure 8.270: $^{13}\text{C-NMR}$ spectrum of 9-methylene-9H-fluorene.

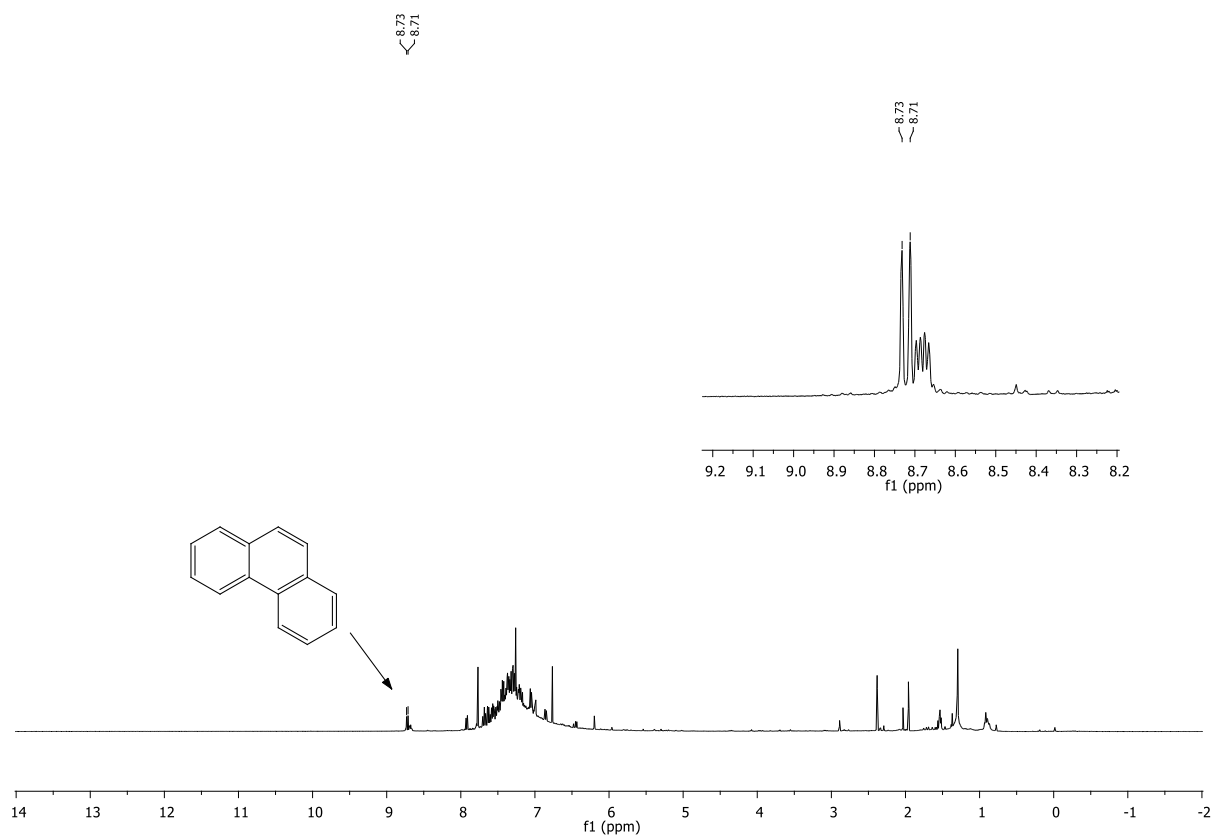


Figure 8.271: $^1\text{H-NMR}$ spectrum after reaction of biphenylacetylene on In_2O_3 at

200 °C according to general procedure 2.

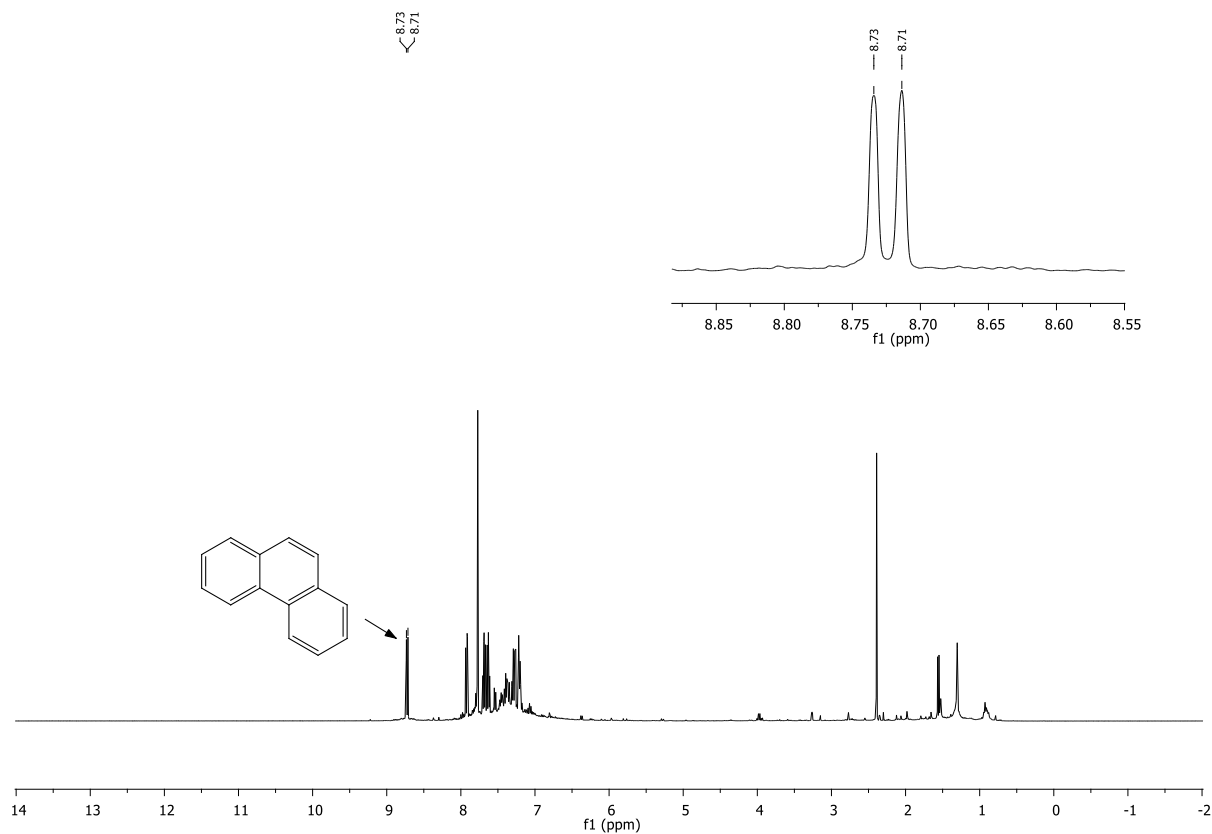


Figure 8.272: ¹H-NMR spectrum after reaction of biphenylacetylene on Ga₂O₃ at 200 °C according to general procedure 2.

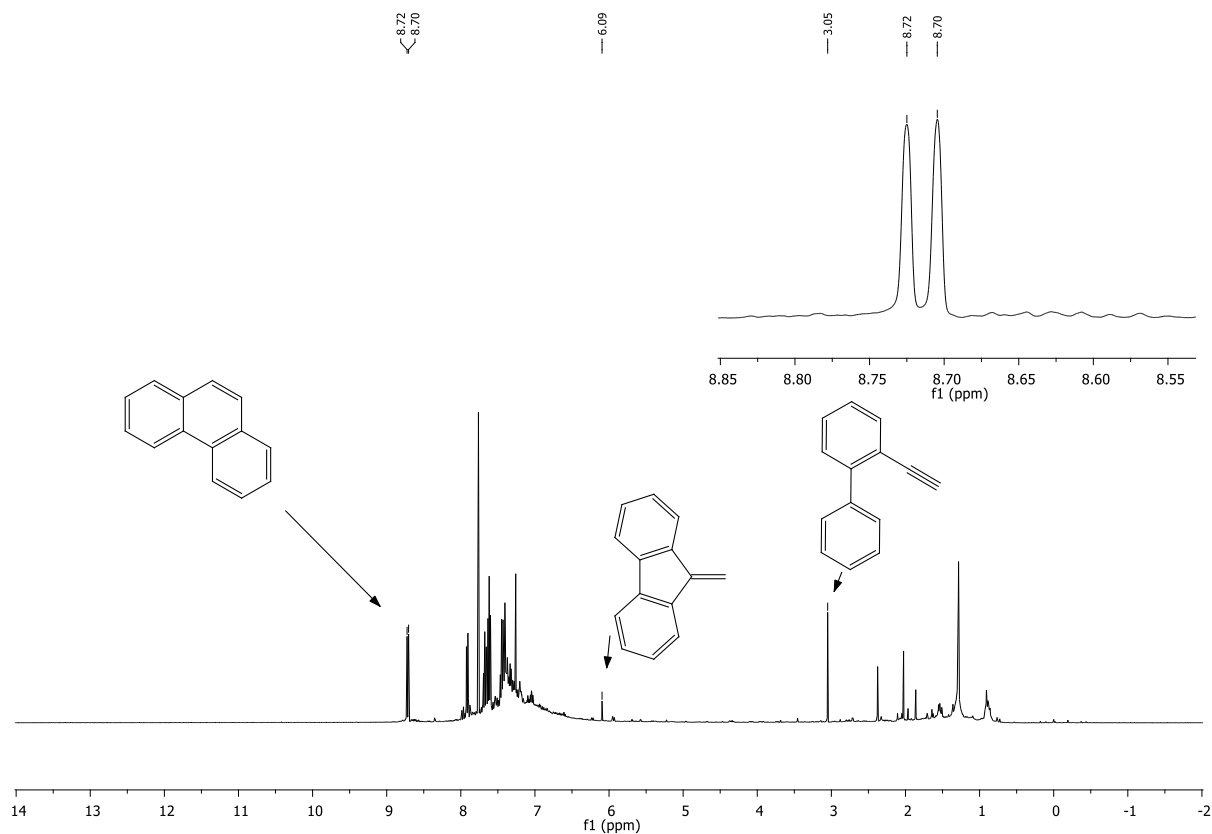


Figure 8.273: ¹H-NMR spectrum after reaction of biphenylacetylene on Ga₂O₃ at 100 °C

according to general procedure 2.

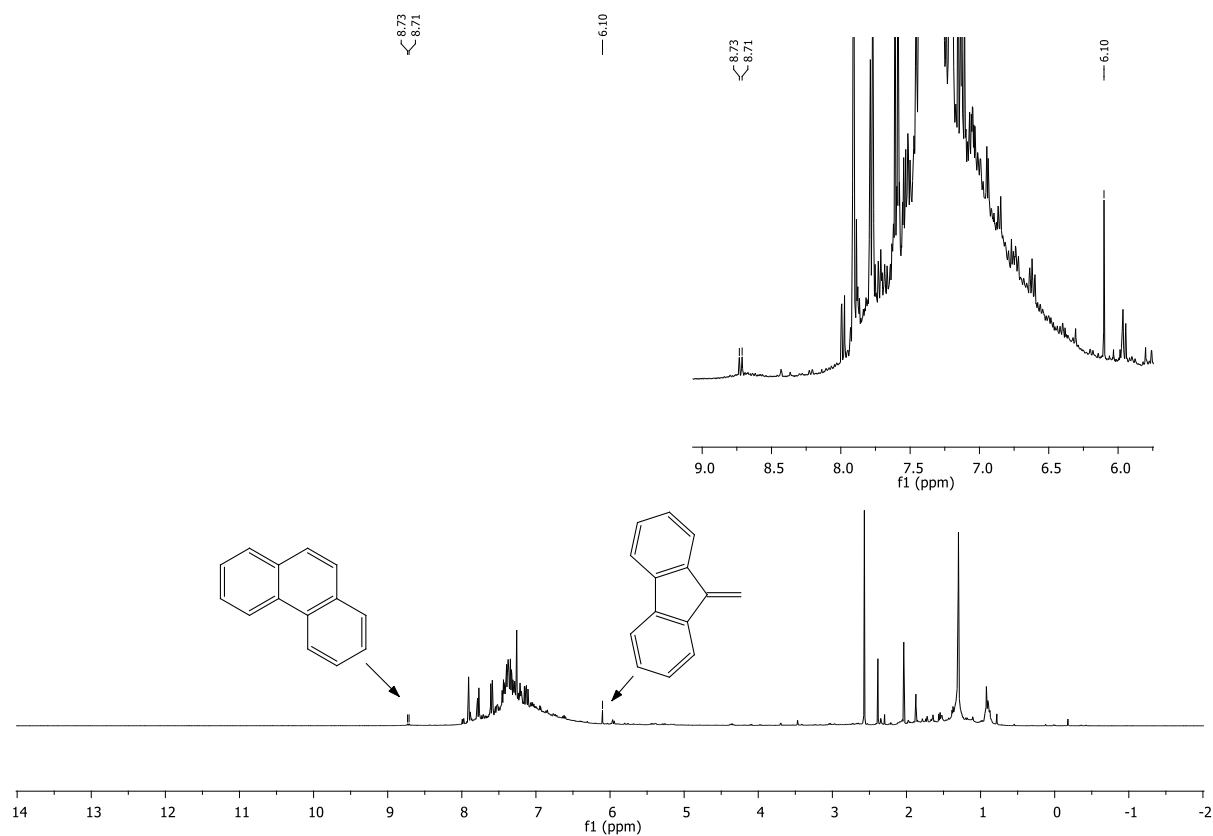


Figure 8.274: ¹H-NMR spectrum after reaction of biphenylacetylene on ZrO₂ at 100 °C according to general procedure 2.

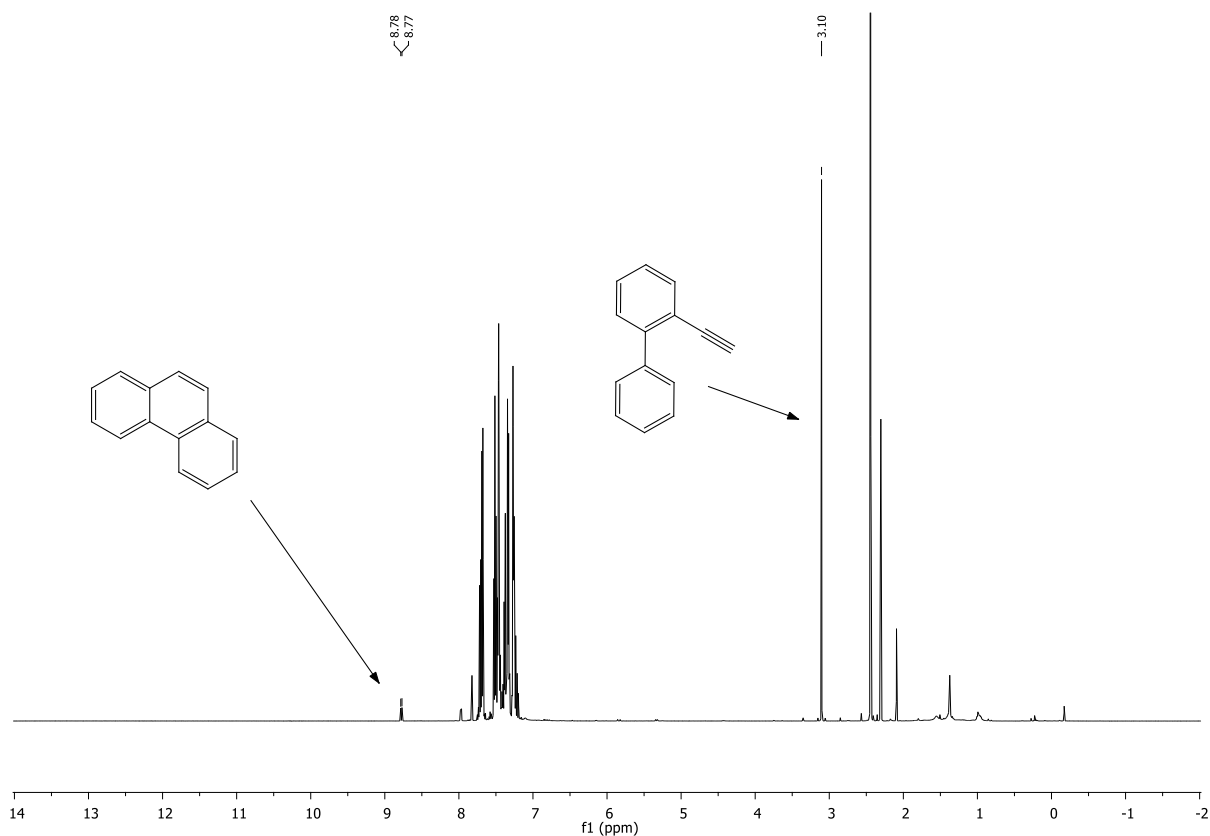


Figure 8.275: $^1\text{H-NMR}$ spectrum after reaction of biphenylacetylene on MoS_2 at $90\text{ }^\circ\text{C}$ according to general procedure 2.

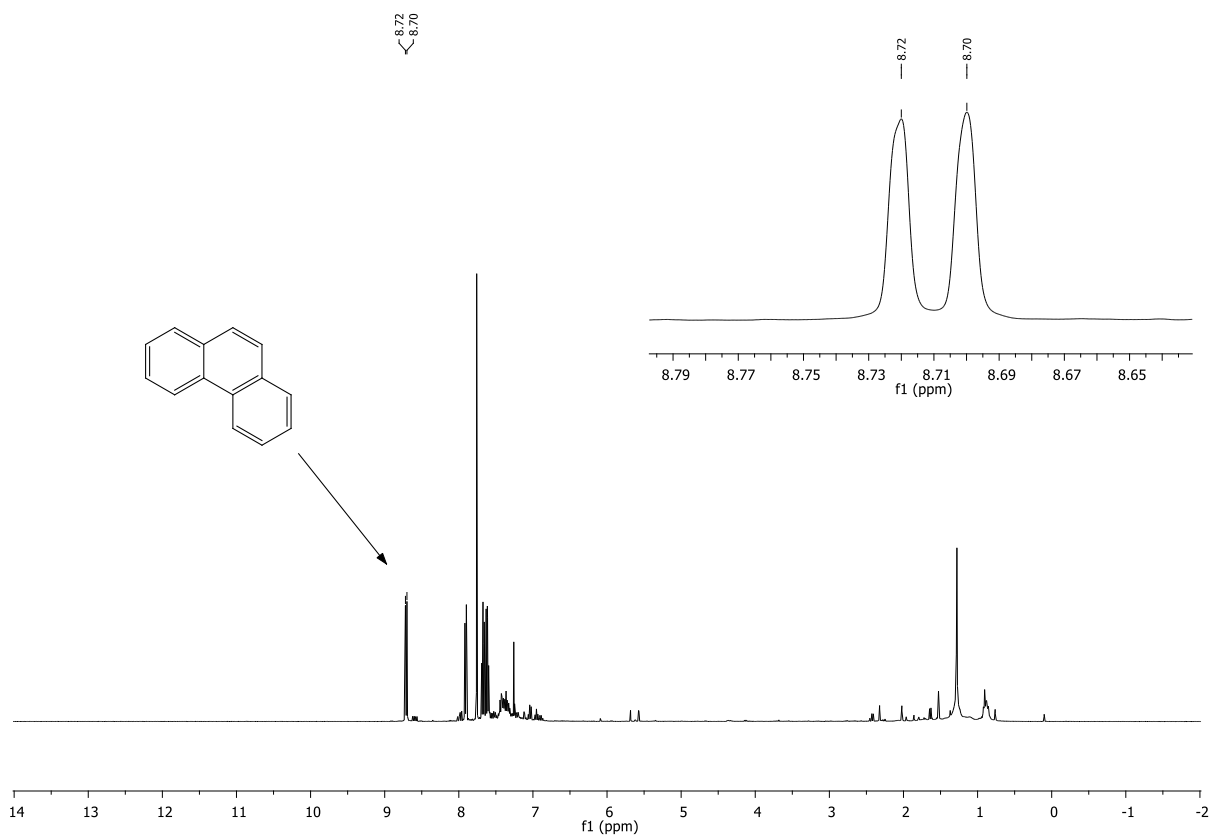


Figure 8.276: $^1\text{H-NMR}$ spectrum after reaction of biphenylacetylene on Zr_2O_3 at $400\text{ }^\circ\text{C}$

according to general procedure 2.

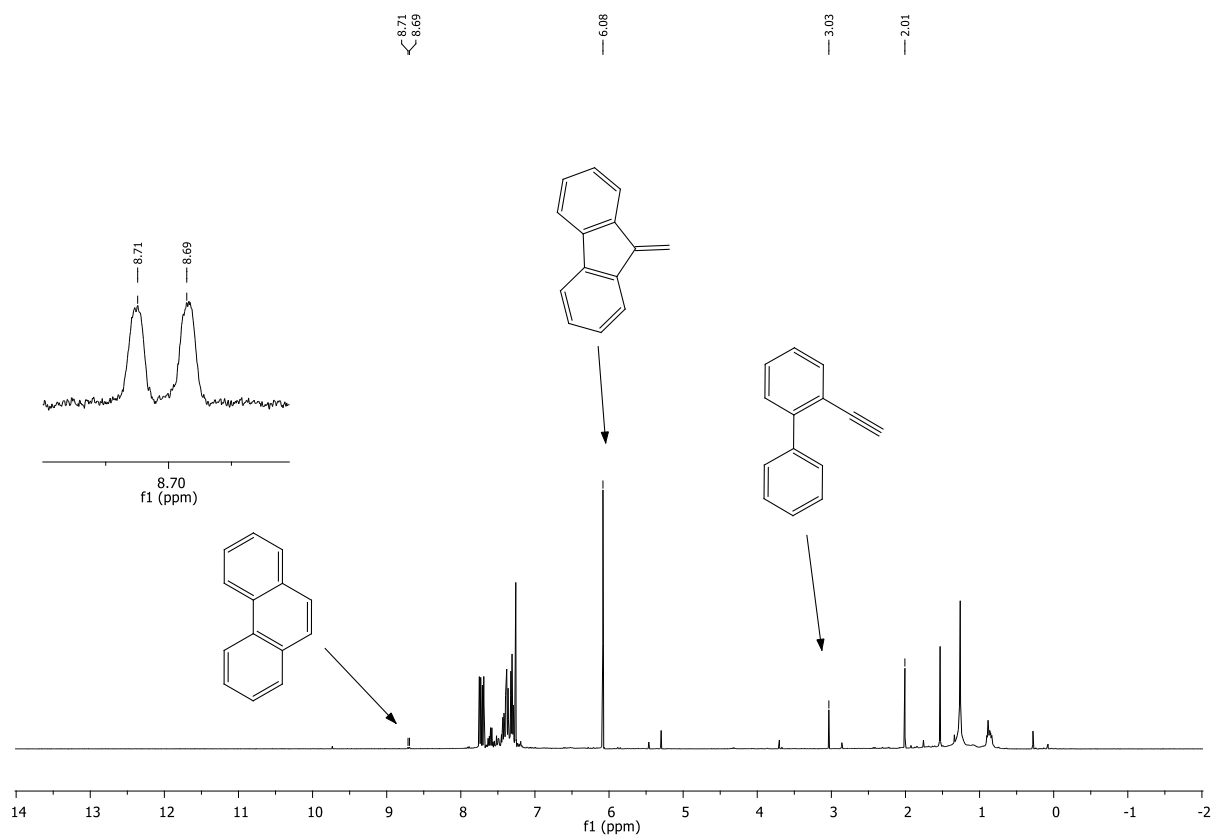


Figure 8.277: $^1\text{H-NMR}$ spectrum after reaction of biphenylacetylene on Zr₂₀ at 90 °C according to general procedure 1.

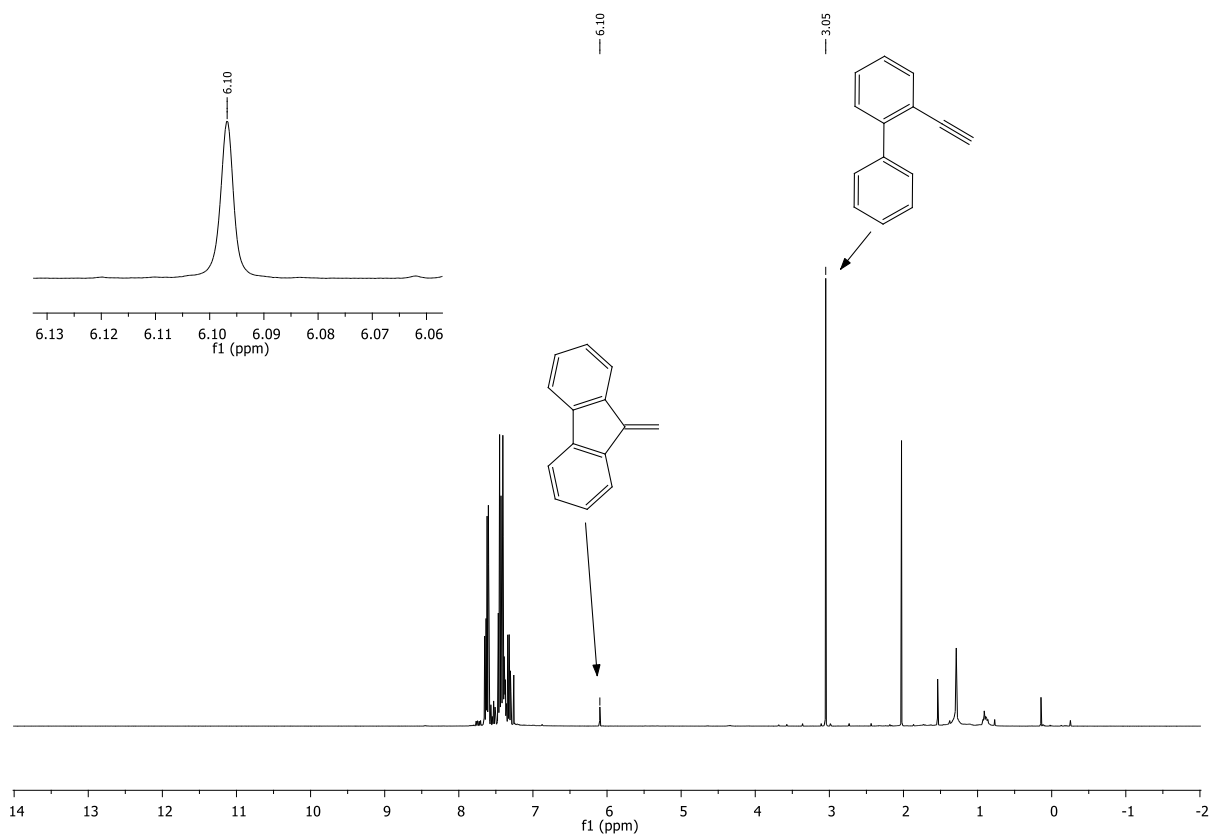


Figure 8.278: $^1\text{H-NMR}$ spectrum after reaction of biphenylacetylene on Si30 at 90 °C according to general procedure 1.

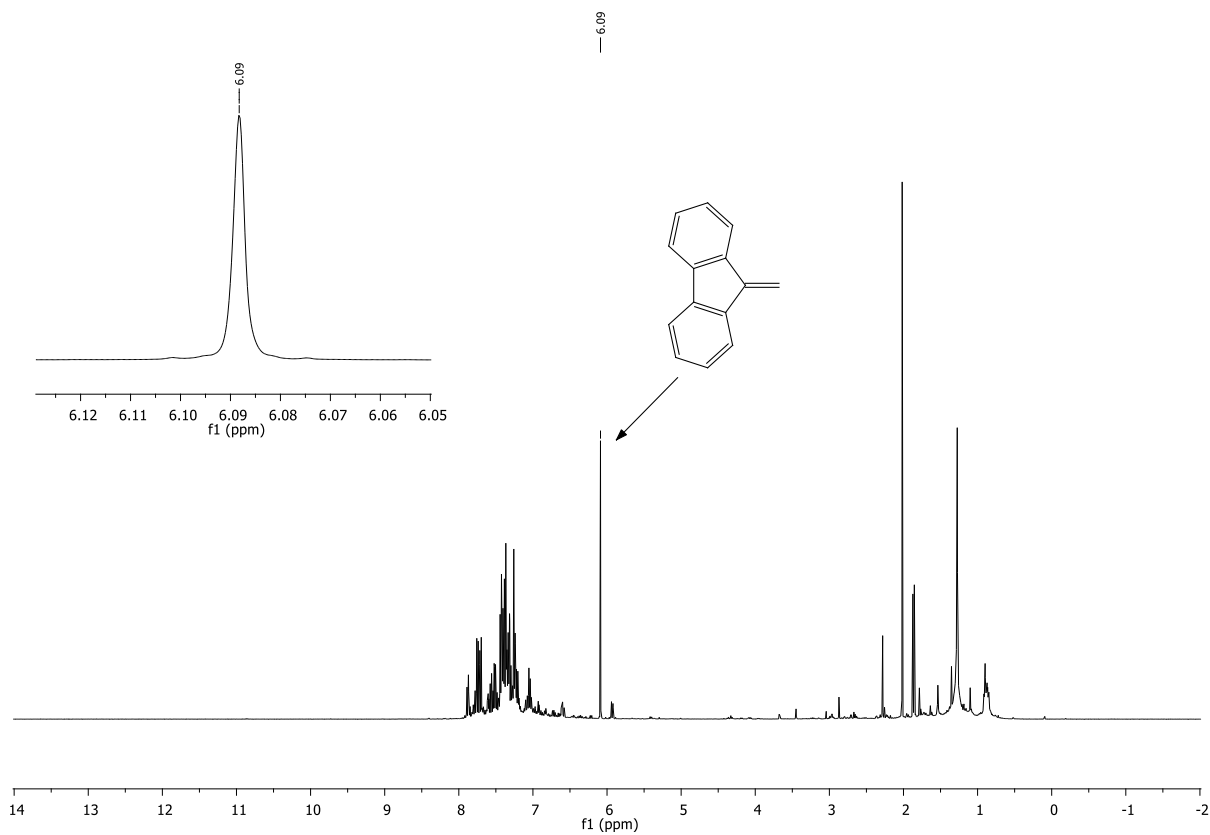


Figure 8.279: $^1\text{H-NMR}$ spectrum after reaction of biphenylacetylene on Si30 at 90 °C

according to general procedure 2.

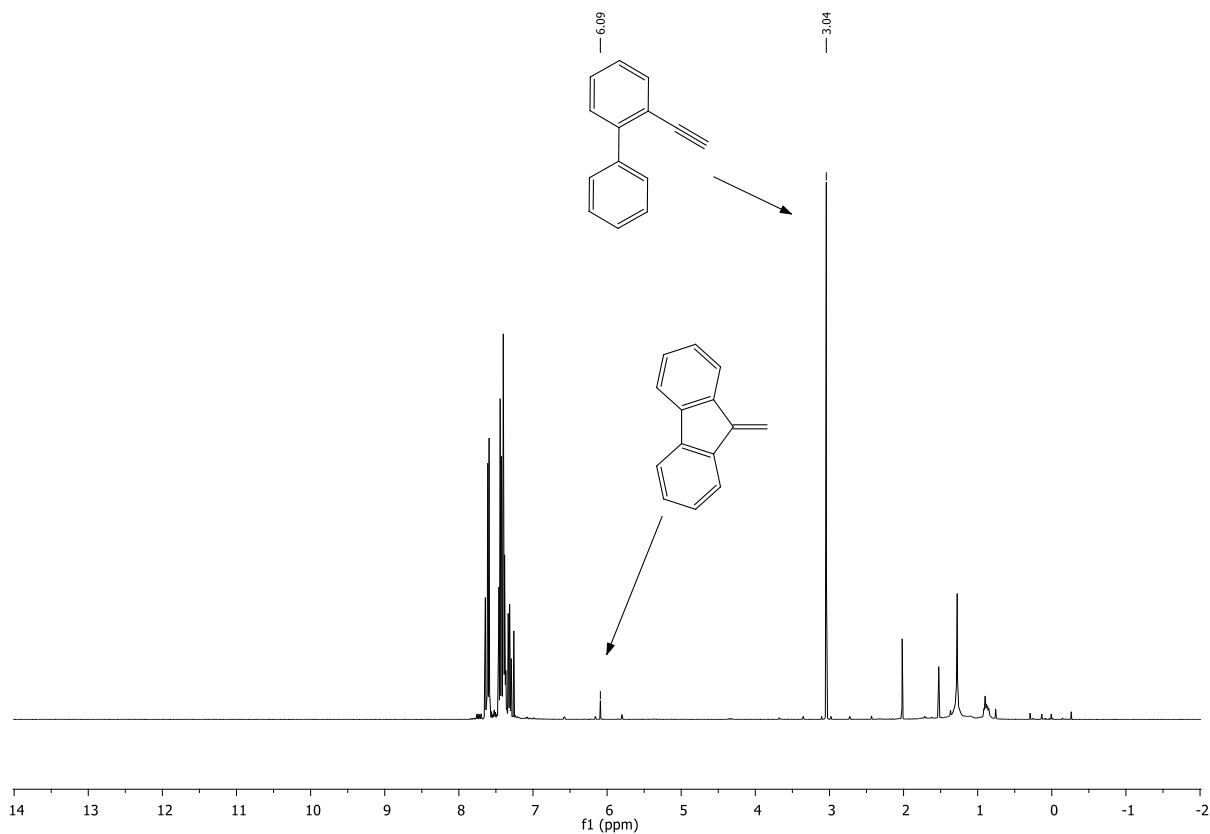


Figure 8.280: ¹H-NMR spectrum after reaction of biphenylacetylene on Si5 at 90 °C according to general procedure 1.

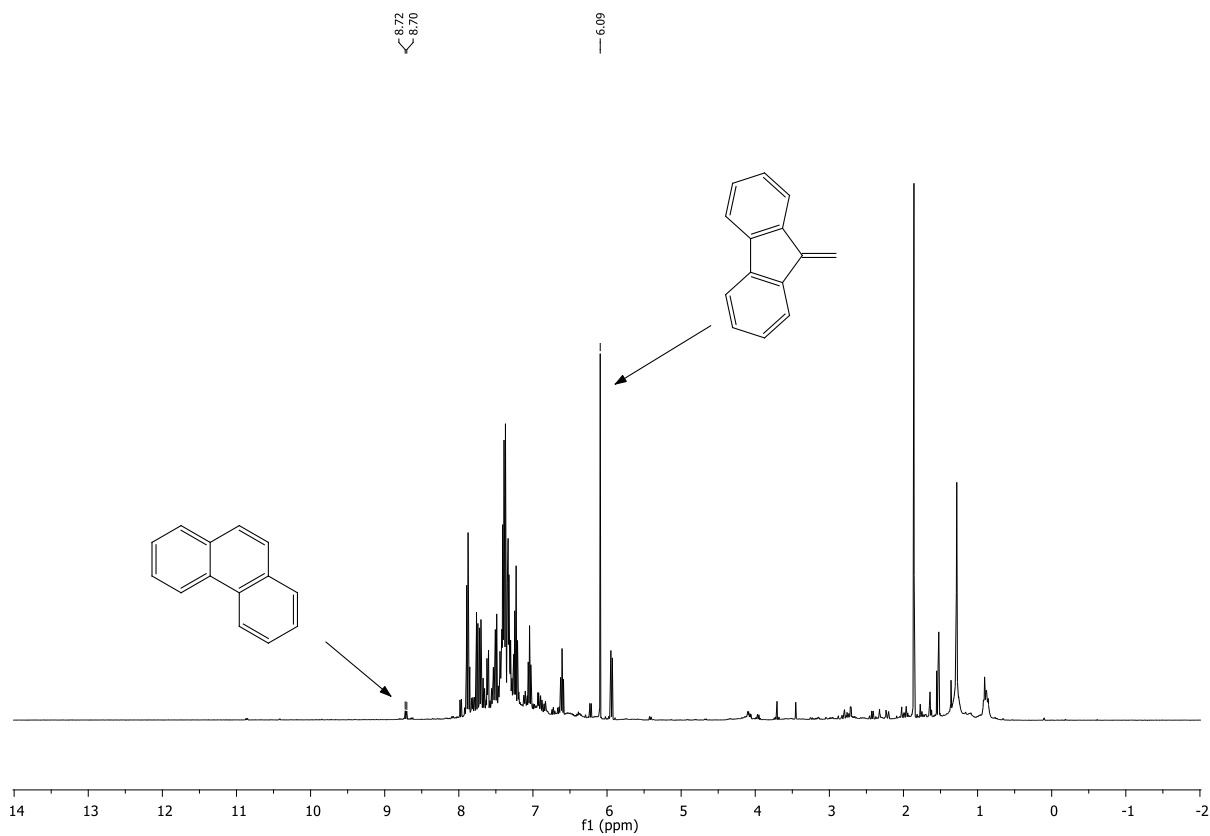


Figure 8.281: ¹H-NMR spectrum after reaction of biphenylacetylene on Si5 at 400 °C

according to general procedure 2.

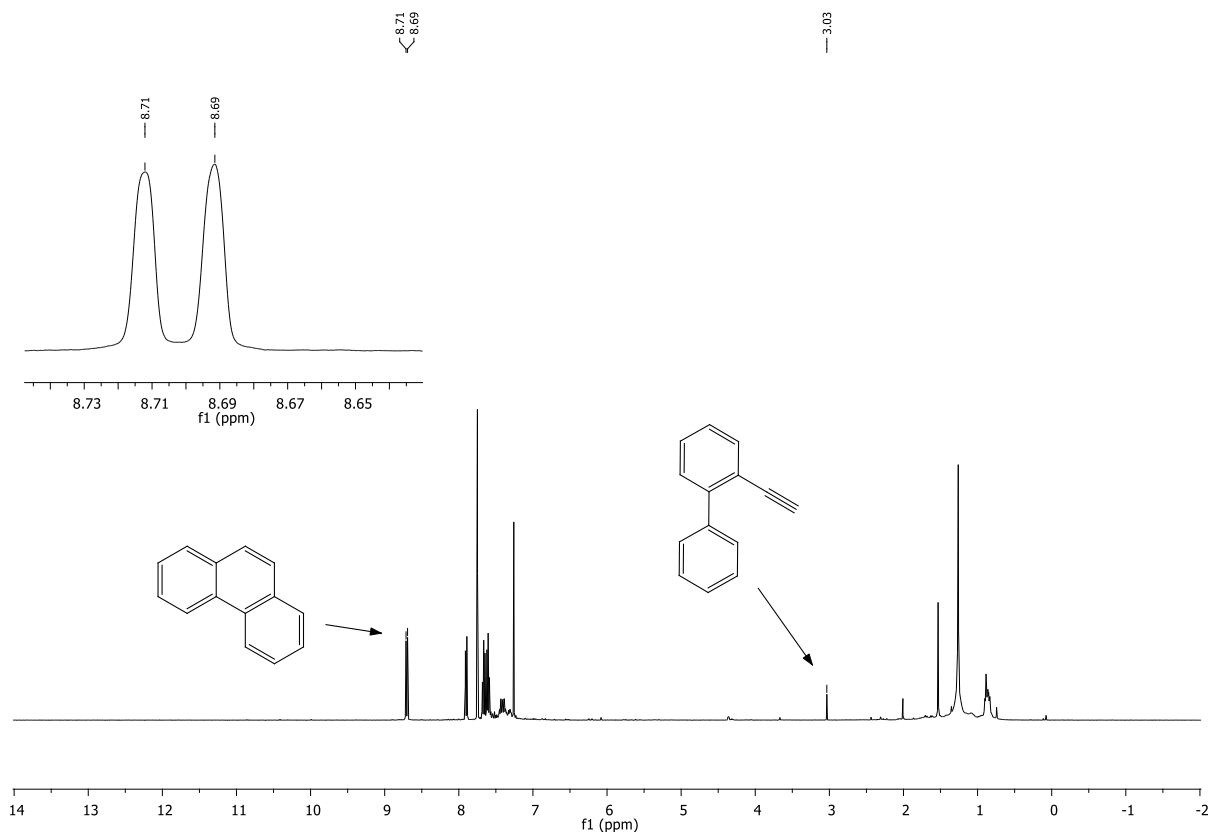


Figure 8.282: $^1\text{H-NMR}$ spectrum after reaction of biphenylacetylene on Ce20 at 400 °C according to general procedure 2.

8.6. Investigation for the soft pi-Lewis acidity of different alumina's terminations

Starting Material 7-(phenylethynyl)cyclohepta-1,3,5-triene

Datafile Name: AF619_001.lcd
Sample Name: AF619_
Sample ID: AF619_

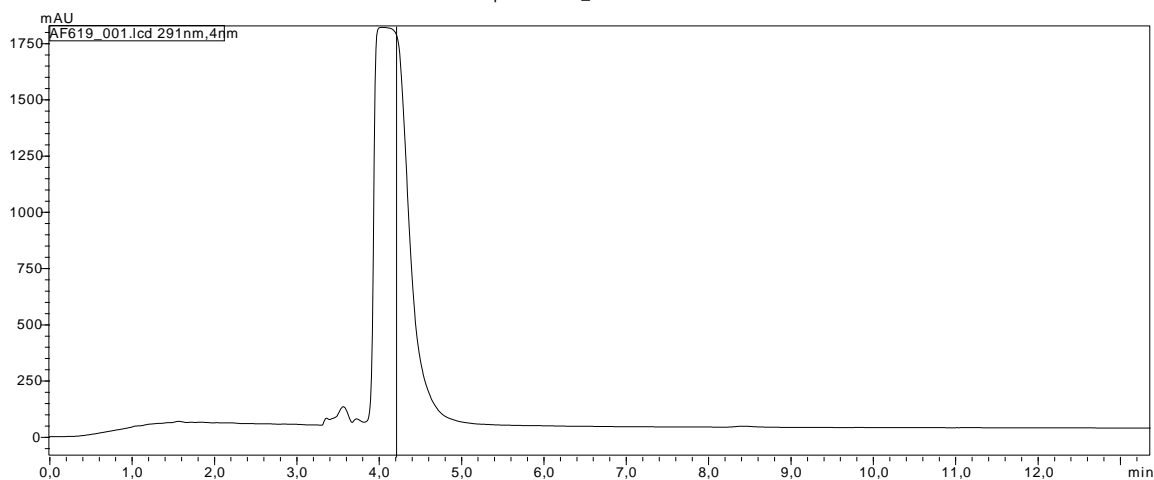


Figure 8.283: HPLC Chromatogram of 7-(phenylethynyl)cyclohepta-1,3,5-triene (SM) in toluol/methanol 1:9.

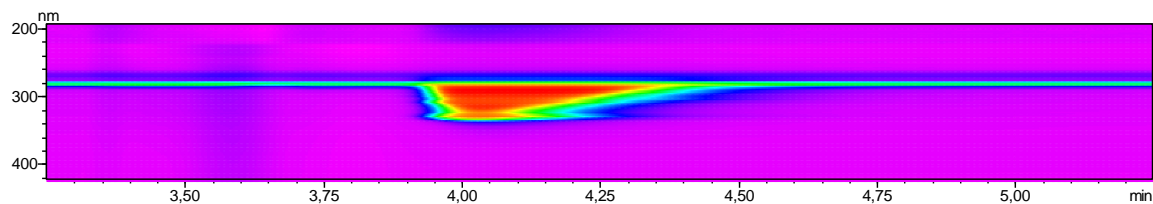


Figure 8.284: HPLC Contour view of 7-(phenylethynyl)cyclohepta-1,3,5-triene (SM).

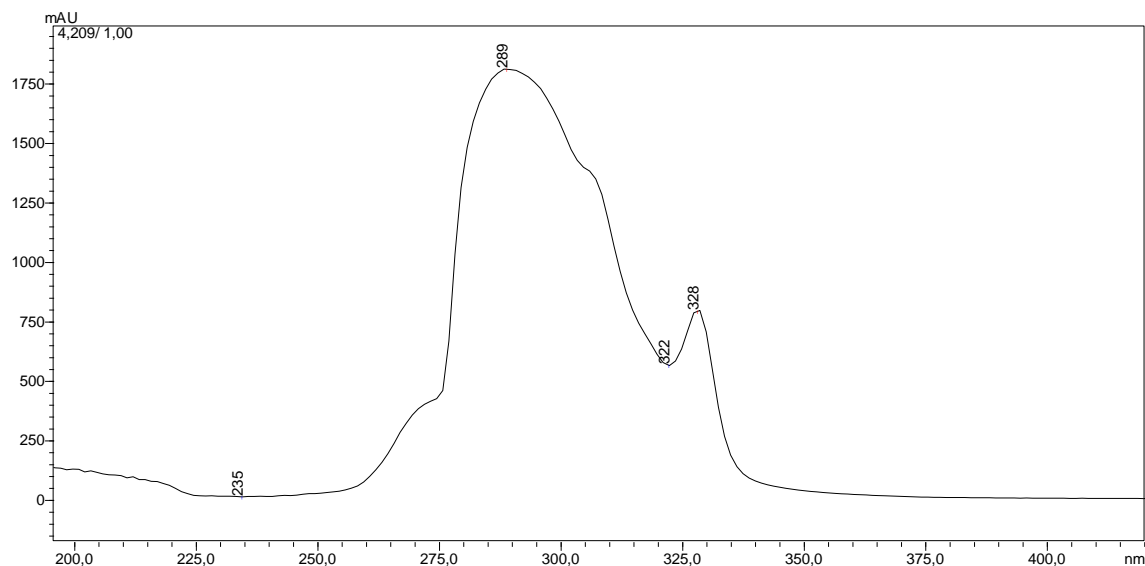


Figure 8.285: UV-vis-spectrum of 7-(phenylethynyl)cyclohepta-1,3,5-triene (SM).

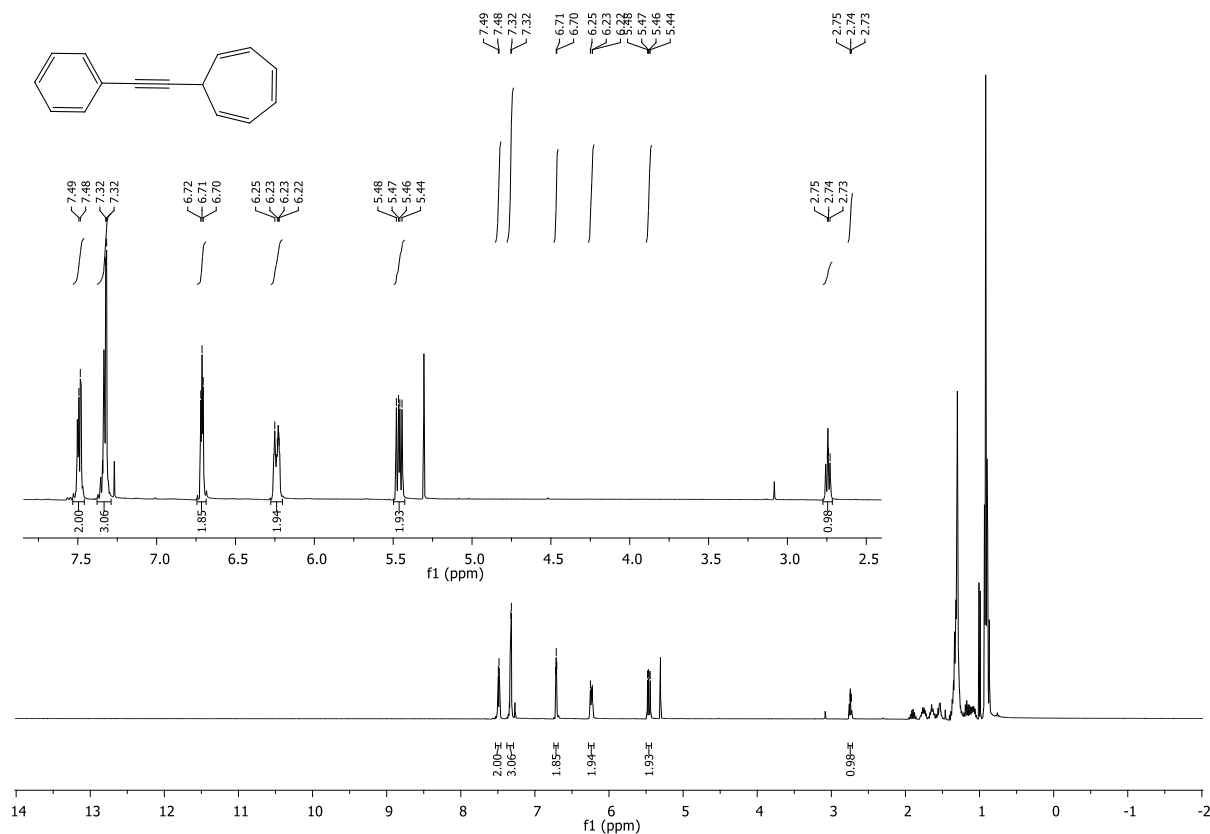


Figure 8.286: $^1\text{H-NMR}$ spectrum of 7-(phenylethynyl)cyclohepta-1,3,5-triene (SM).

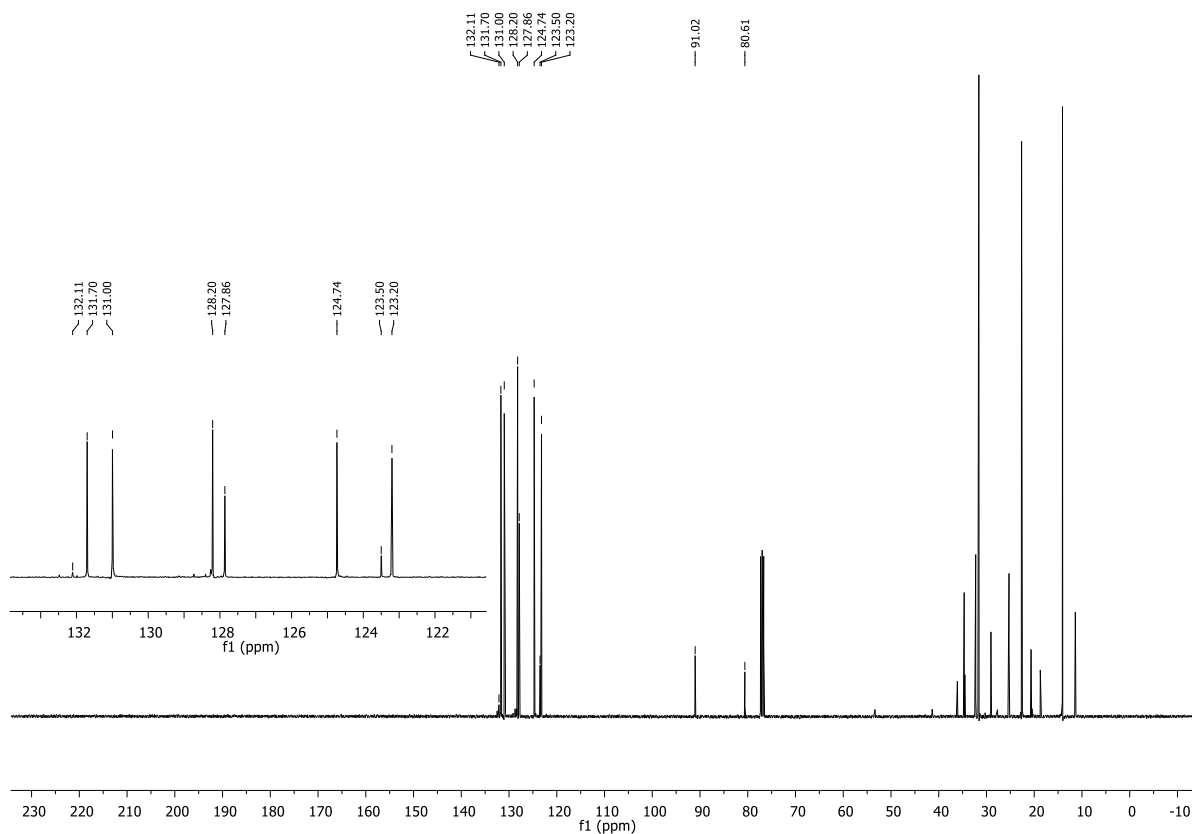


Figure 8.287: ^{13}C -NMR spectrum of 7-(phenylethynyl)cyclohepta-1,3,5-triene (**SM**).

Reaction on sampe 0 (our own alumina)

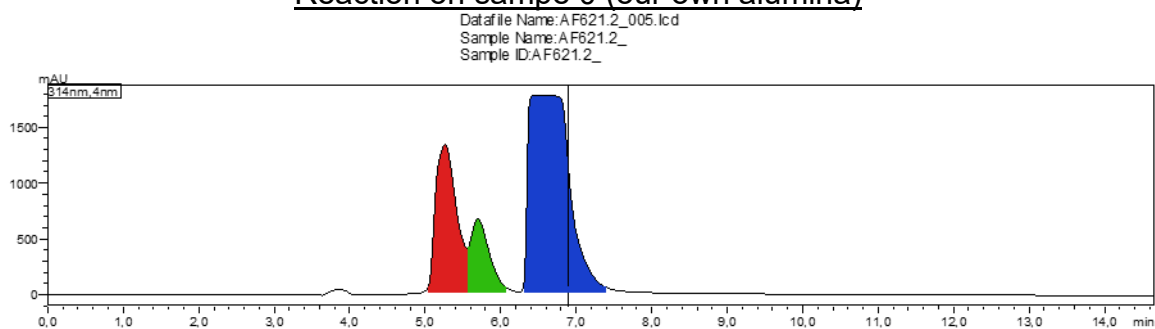


Figure 8.288: HPLC Chromatogram of reaction on sampe 0 in toluol/methanol 1:9.

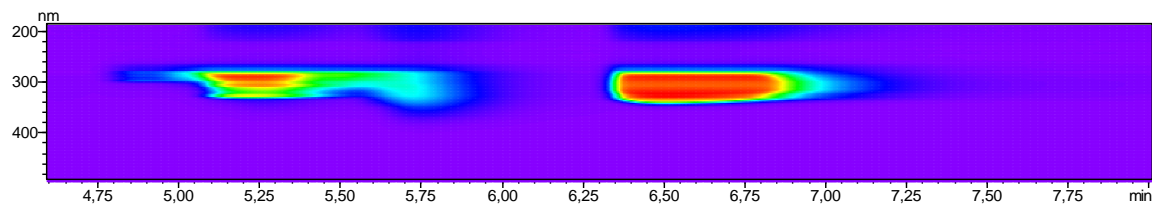


Figure 8.289: HPLC Contour view of reaction on sampe 0, **SM**(left signal), **Product 1** (middle signal) and **Product 2** (right signal).

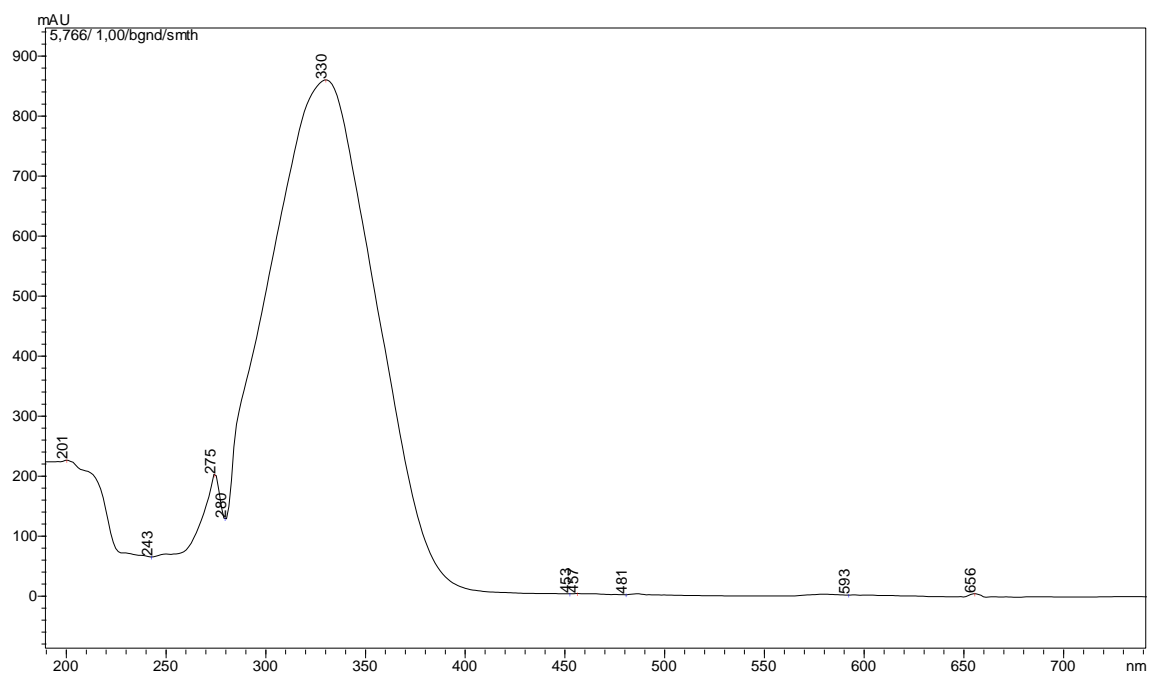


Figure 8.290: UV-vis-spectrum of Product 1.

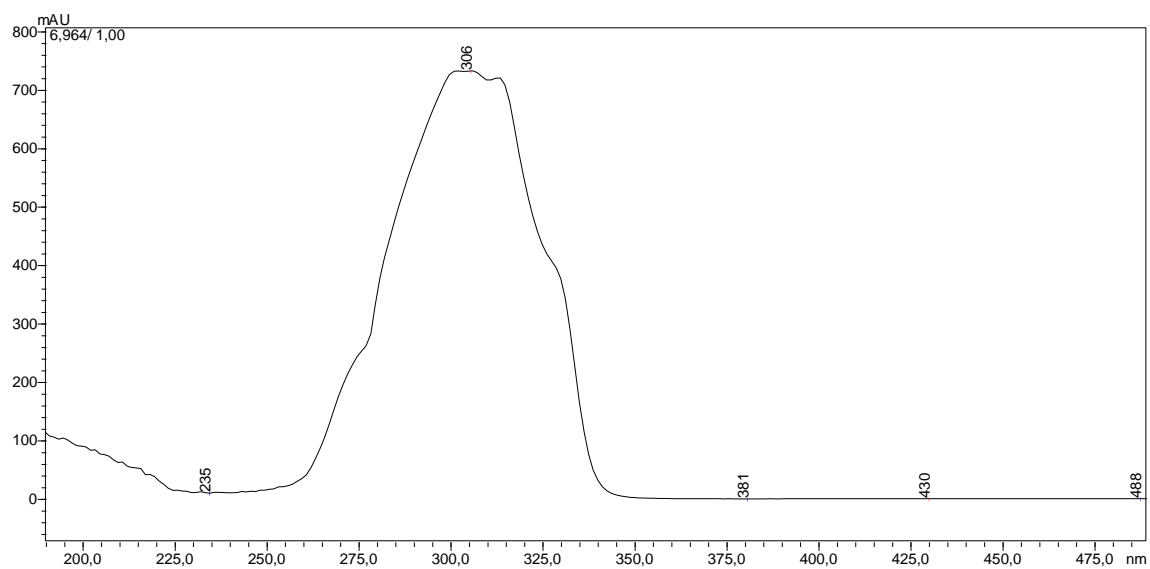


Figure 8.291: UV-vis-spectrum of Product 2 2-(cyclohepta-2,4,6-trien-1-yl)-1H-indene (right).

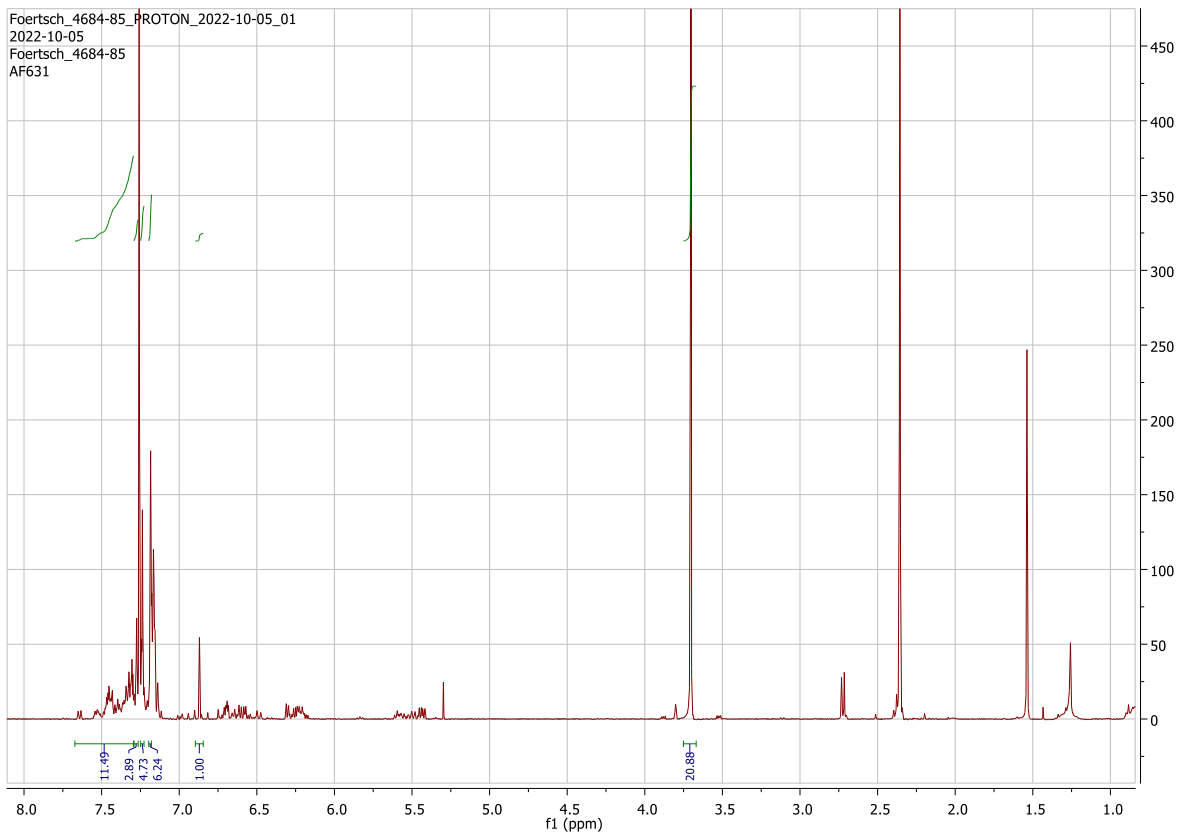


Figure 8.292: $^1\text{H-NMR}$ spectrum of AF631.

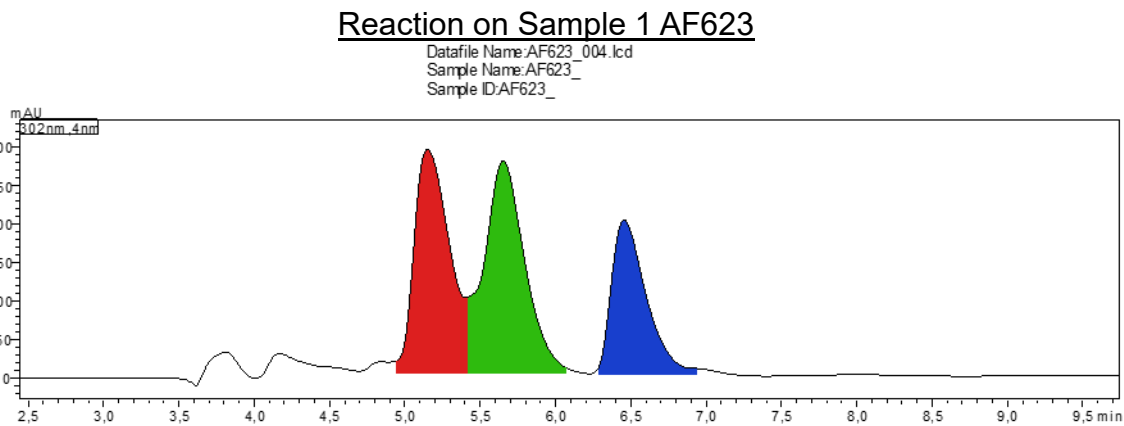


Figure 8.293: HPLC Chromatogram of reaction on Sample 1 623 in toluol/methanol 1:9.

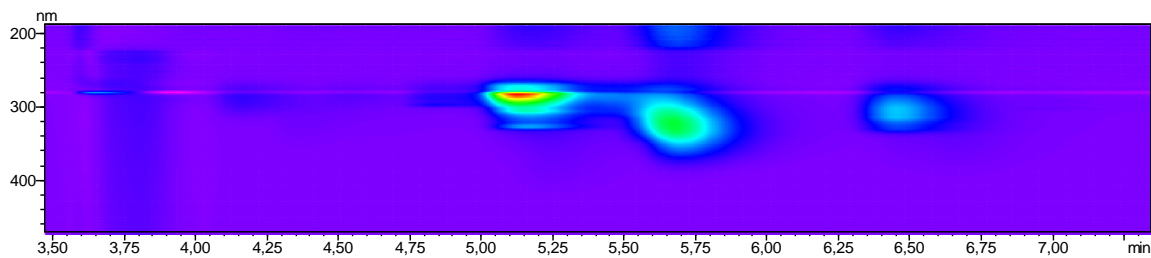


Figure 8.294: HPLC Contour view of reaction on Sample 1, **SM**(left signal), **Product 1** (middle signal) and **Product 2** (right signal).

Reaction on Sample 1 after purification AF623.2

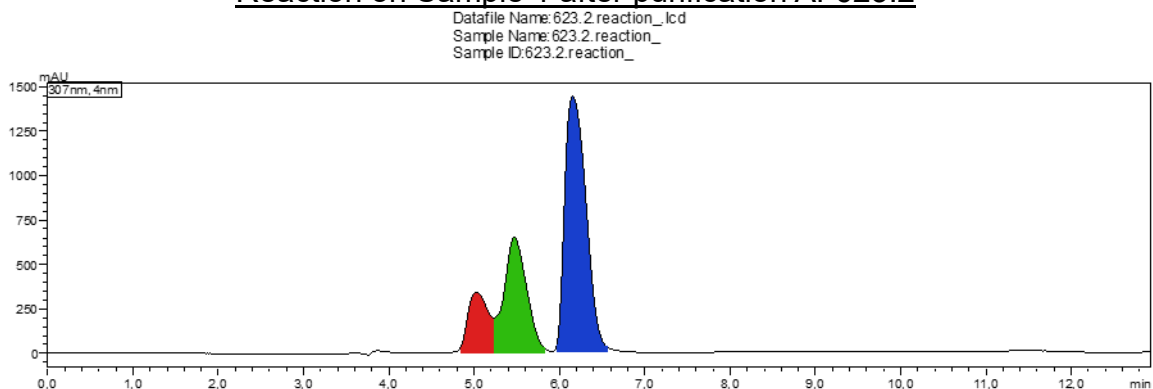


Figure 8.295: HPLC Chromatogram of reaction on Sample 1 after purification 623.2 in toluol/methanol 1:9.

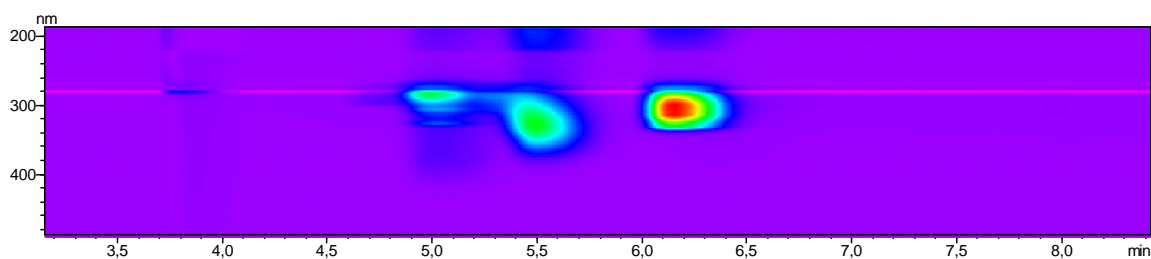


Figure 8.296: HPLC Contour view of reaction on Sample 1 after purification 623.2, **SM**(left signal), **Product 1** (middle signal) and **Product 2** (right signal).

Reaction on Sample 1 AF636

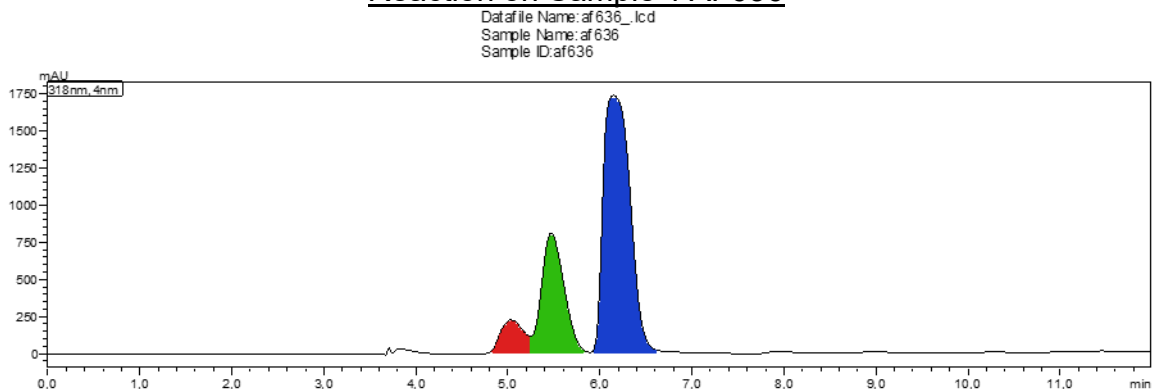


Figure 8.297: HPLC Chromatogram of reaction on Sample 1 636 in toluol/methanol 1:9.

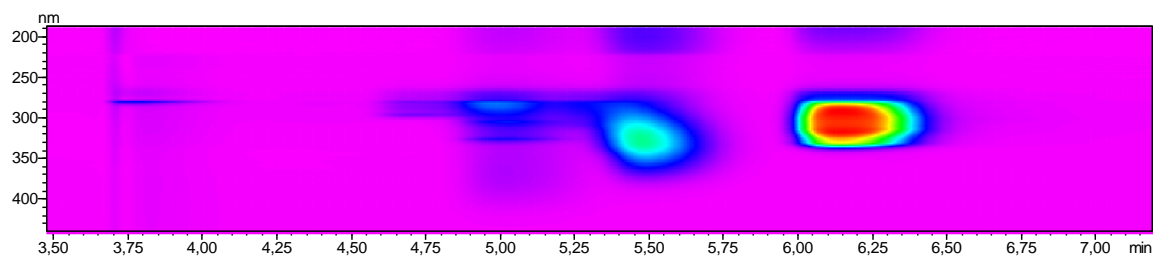


Figure 8.298: HPLC Contour view of reaction on Sample 1 636, SM(left signal), Product 1 (middle signal) and Product 2 (right signal).

Reaction on Sample 1 after purification AF636.2

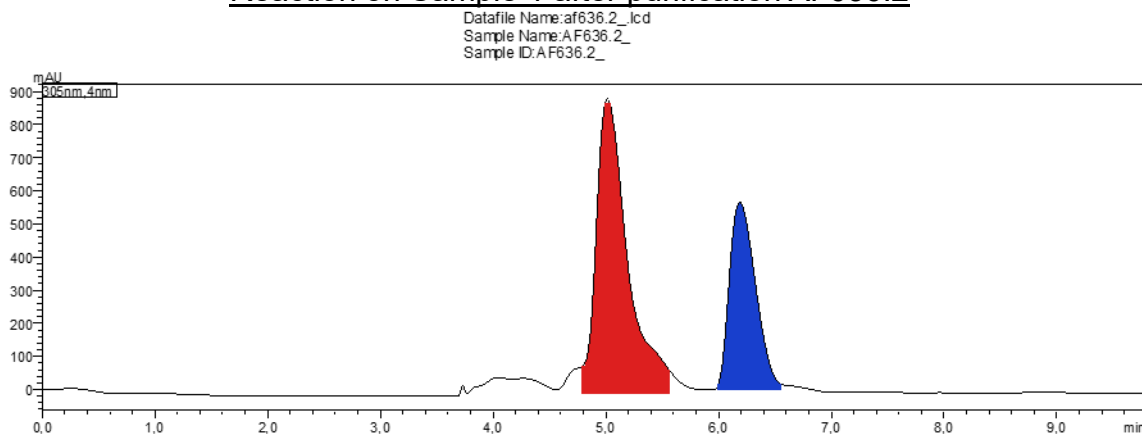


Figure 8.299: HPLC Chromatogram of reaction on Sample 1 after purification 636.2 in toluol/methanol 1:9

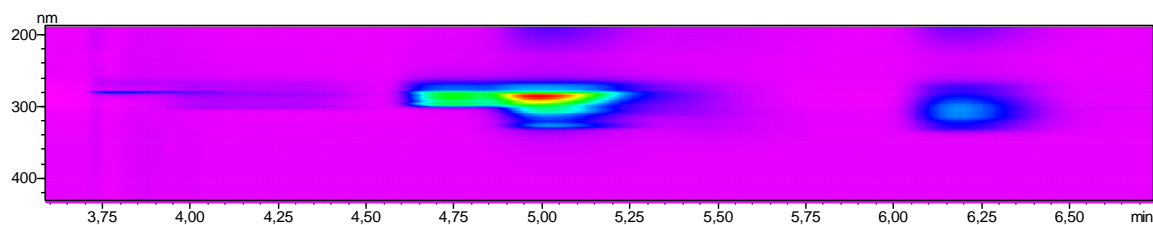


Figure 8.300: HPLC Contour view of reaction on Sample 1 after purification 636.2, SM(left signal), Product 1 (middle signal) and Product 2 (right signal).

Reaction on Sample 2 AF624

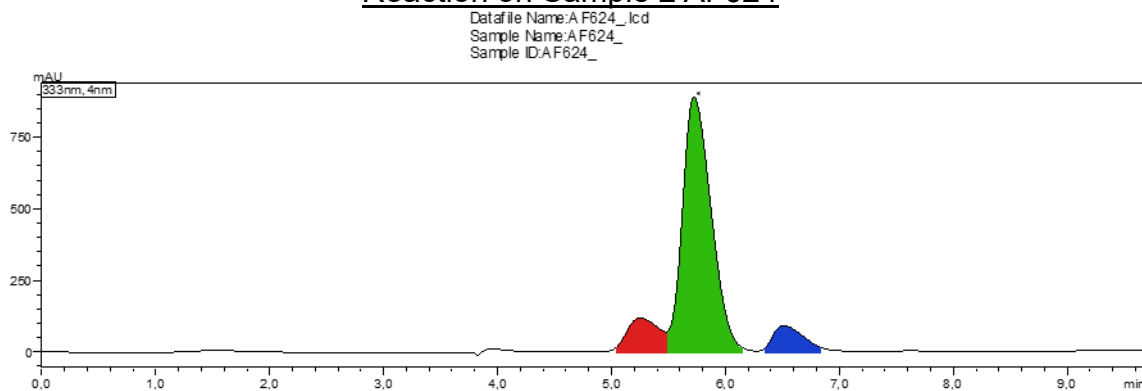


Figure 8.301: HPLC Chromatogram of reaction on Sample 2 624 in toluol/methanol 1:9.

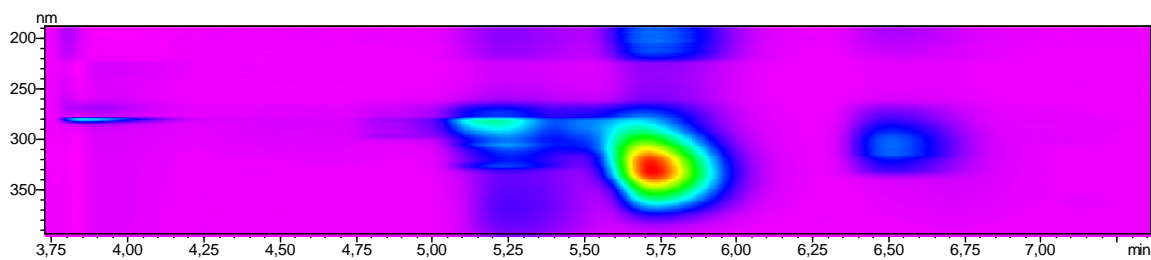


Figure 8.302: HPLC Contour view of reaction on Sample 2 624, **SM**(left signal), **Product 1** (middle signal) and **Product 2** (right signal).

Reaction on Sample 2 after purification AF624.2

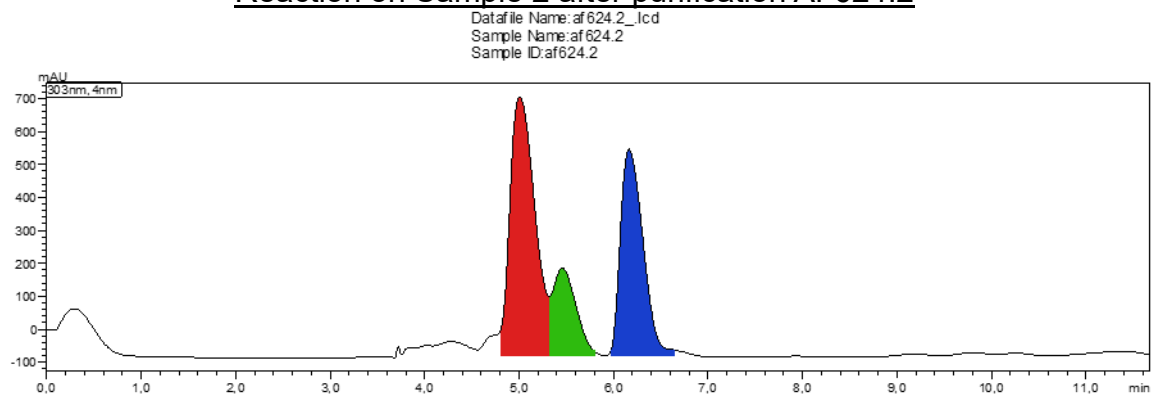


Figure 8.303: HPLC Chromatogram of reaction on Sample 2 after purification 624.2 in toluol/methanol 1:9.

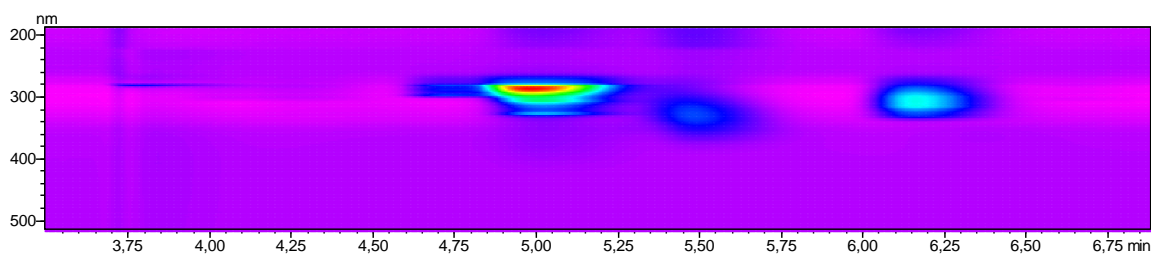


Figure 8.304: HPLC Contour view of reaction on Sample 2 after purification 624.2, **SM**(left signal), **Product 1** (middle signal) and **Product 2** (right signal).

Reaction on Sample 3 AF626

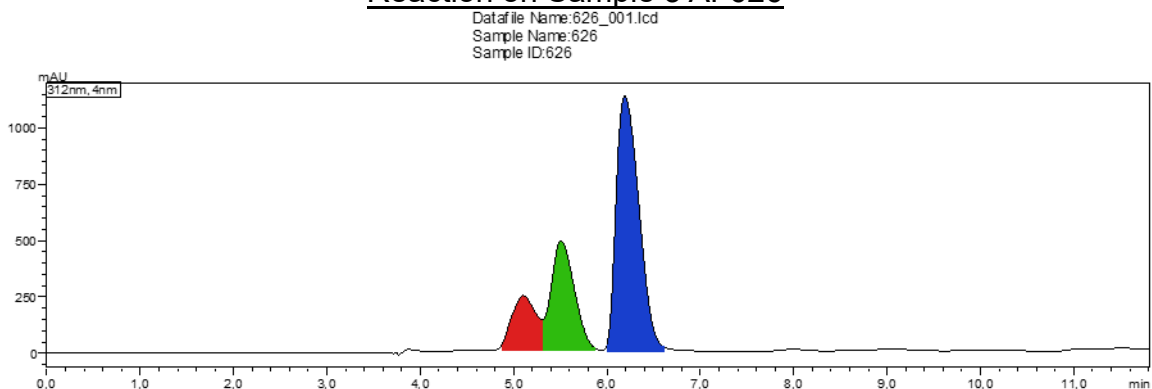


Figure 8.305: HPLC Chromatogram of reaction on Sample 3 626 in toluol/methanol 1:9.

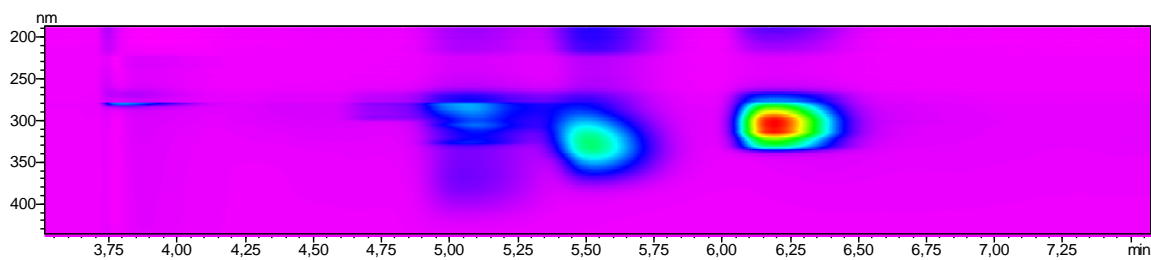


Figure 8.306: HPLC Contour view of reaction on Sample 3 626, SM(left signal), Product 1 (middle signal) and Product 2 (right signal).

Reaction on Sample 3 after purification AF626.2

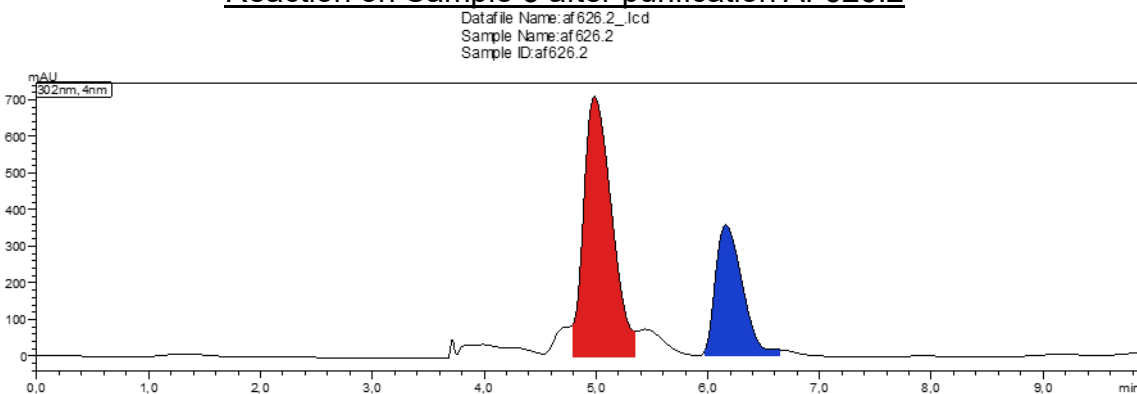


Figure 8.307: HPLC Chromatogram of reaction on Sample 3 after purification 626.2 in toluol/methanol 1:9.

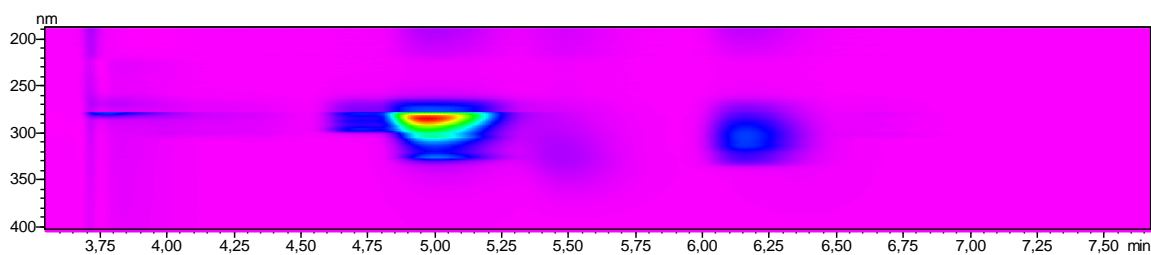


Figure 8.308: HPLC Contour view of reaction on Sample 3 after purification 626.2, SM(left signal) and Product 2 (right signal).

Reaction on Sample 4 AF627

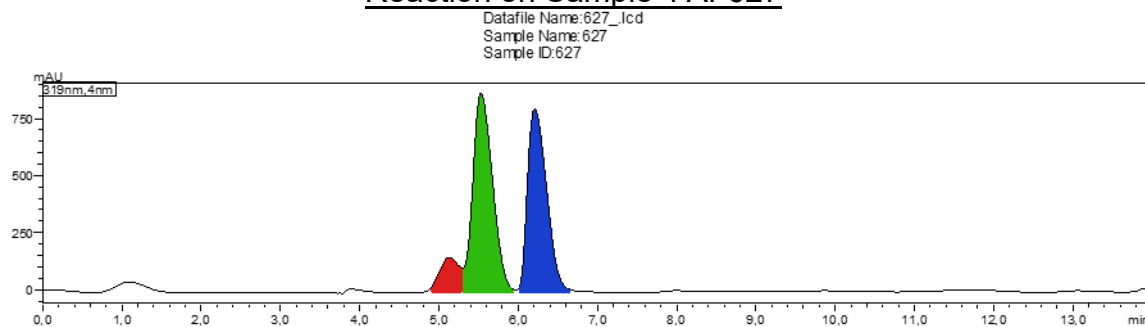


Figure 8.309: HPLC Chromatogram of reaction on Sample 4 627 in toluol/methanol 1:9.

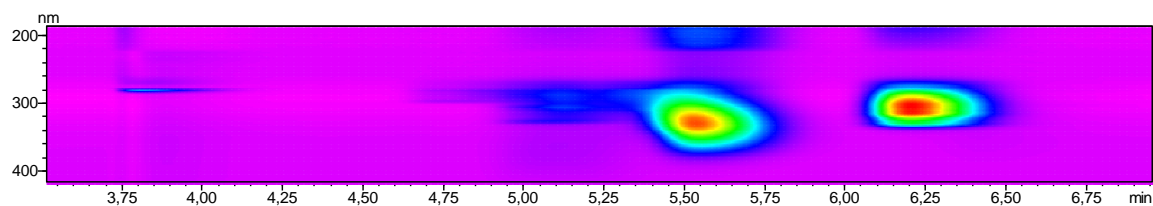


Figure 8.310: HPLC Contour view of reaction on Sample 4 627, **SM**(left signal), **Product 1** (middle signal) and **Product 2** (right signal).

Reaction on Sample 4 after purification AF627.2

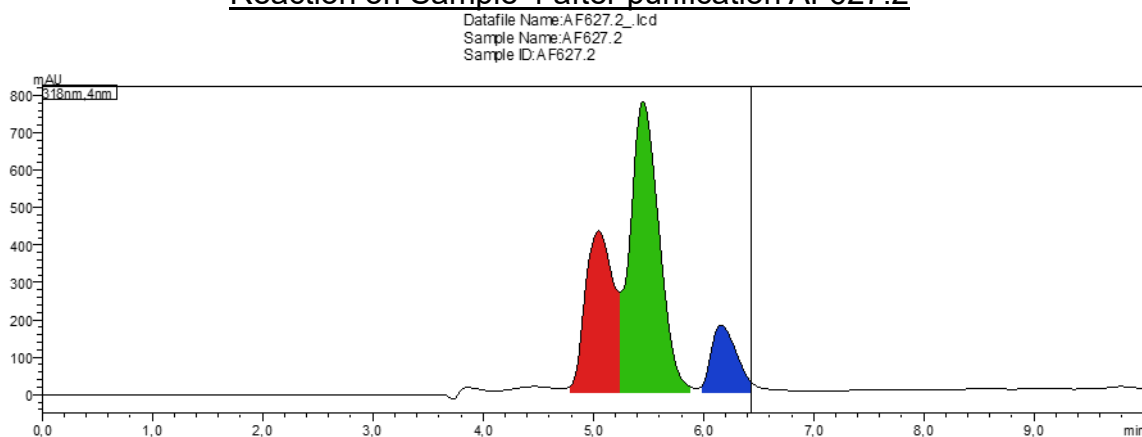


Figure 8.311: HPLC Chromatogram of reaction on Sample 4 after purification 627.2 in toluol/methanol 1:9.

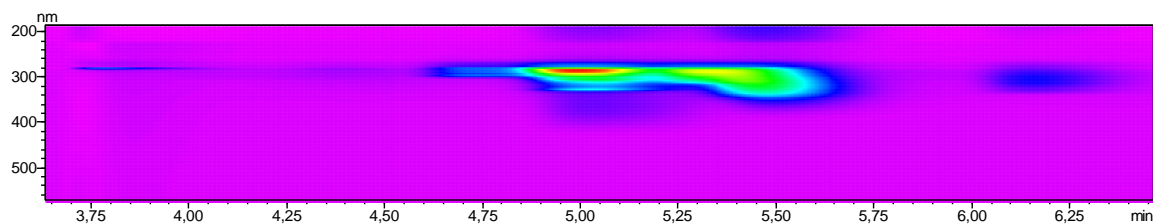


Figure 8.312: HPLC Contour view of reaction on Sample 4 after purification 627.2, **SM** (left signal), **Product 1** (middle signal) and **Product 2** (right signal).

Reaction on Sample 5 AF628

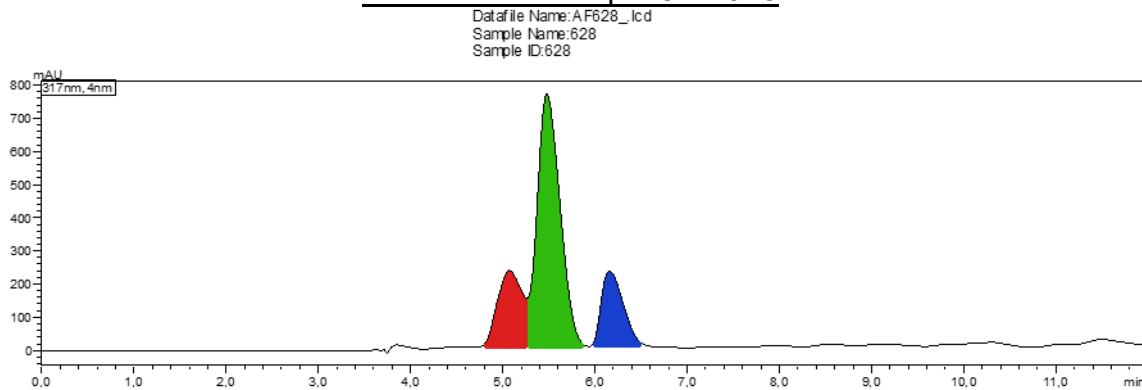


Figure 8.313: HPLC Chromatogram of reaction on Sample 5 628 in toluol/methanol 1:9.

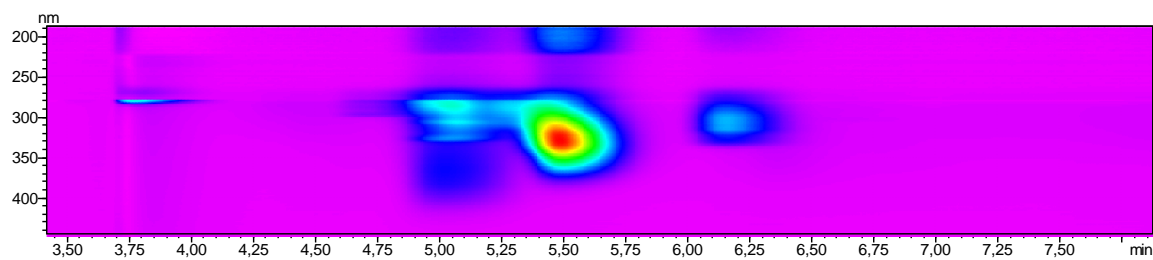


Figure 8.314: HPLC Contour view of reaction on Sample 5 628, SM(left signal), Product 1 (middle signal) and Product 2 (right signal).

Reaction on Sample 5 after purification AF628.2

Datafile Name: AF628.2_lcd
 Sample Name: AF628.2
 Sample ID: AF628.2

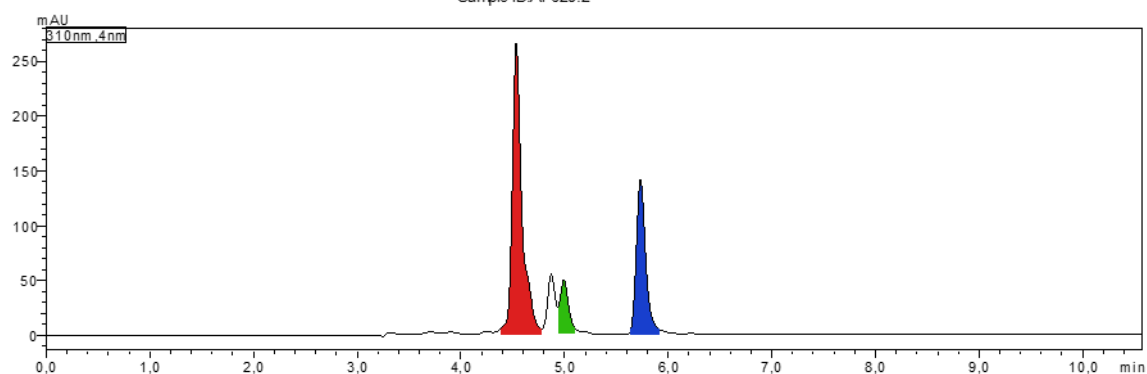


Figure 8.315: HPLC Chromatogram of reaction on Sample 5 after purification 628.2 in toluol/methanol 1:9.

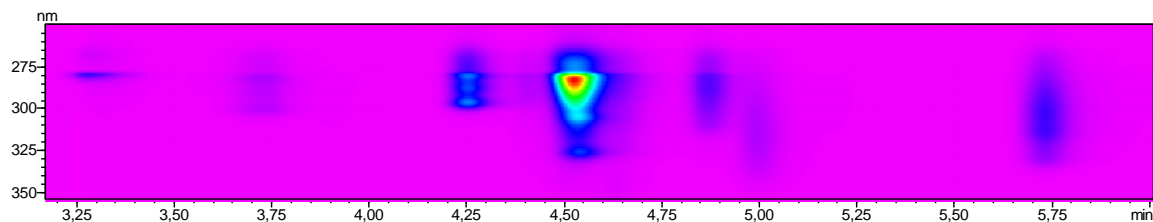


Figure 8.316: HPLC Contour view of reaction on Sample 4 after purification 628.2, SM(left signal), Product 1 (middle signal) and Product 2 (right signal).

Reaction on Sample 6 AF634

Datafile Name: af634_lcd
 Sample Name: af634
 Sample ID: af634

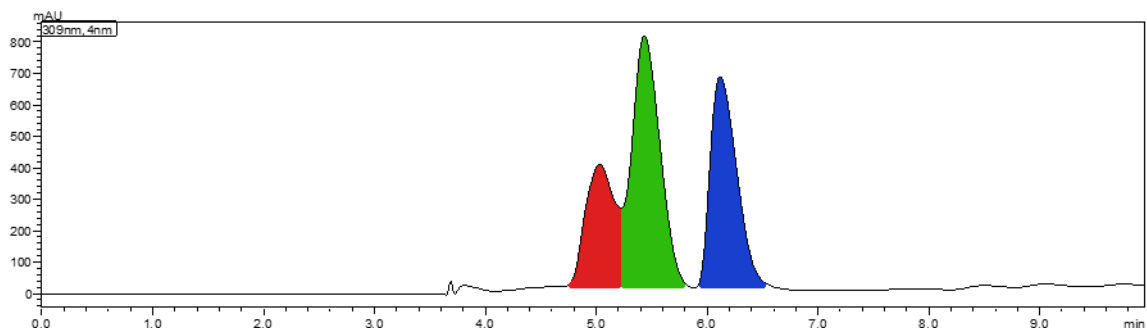


Figure 8.317: HPLC Chromatogram of reaction on Sample 6 634 in toluol/methanol 1:9.

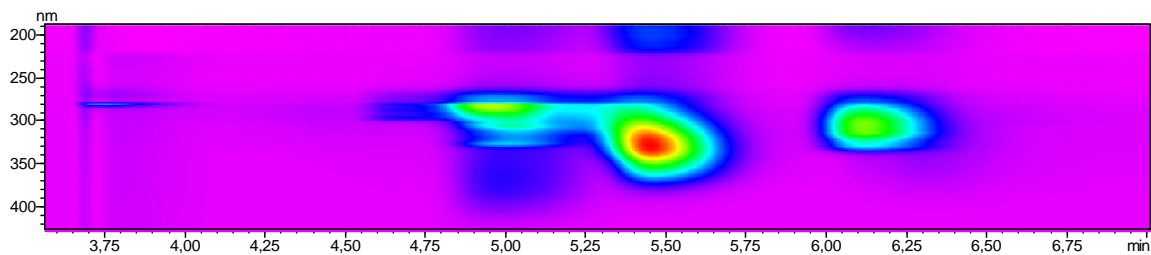


Figure 8.318: HPLC Contour view of reaction on Sample 6 634, SM(left signal), Product 1 (middle signal) and Product 2 (right signal).

Reaction on Sample 6 after purification AF634.2

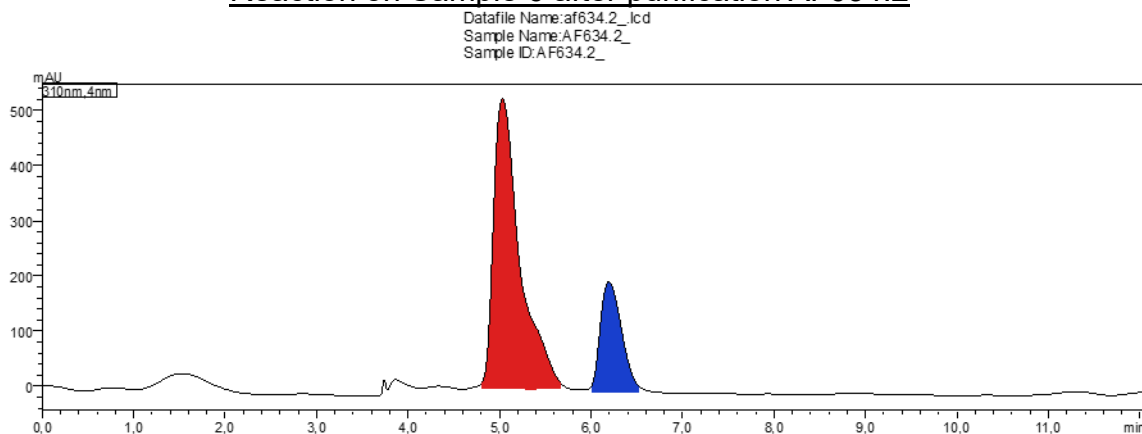


Figure 8.319: HPLC Chromatogram of reaction on Sample 6 after purification 634.2 in toluol/methanol 1:9.

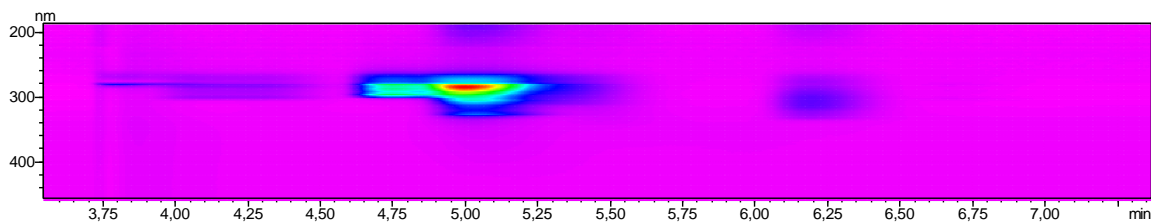


Figure 8.320: HPLC Contour view of reaction on Sample 6 after purification 634.2, SM(left signal) and Product 2 (right signal).

Reaction on Sample 7 AF635

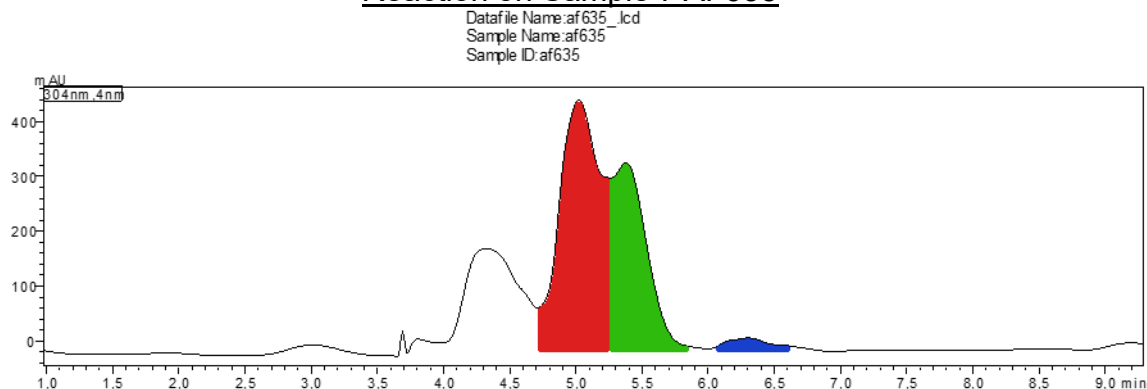


Figure 8.321: HPLC Chromatogram of reaction on Sample 7 635 in toluol/methanol 1:9.

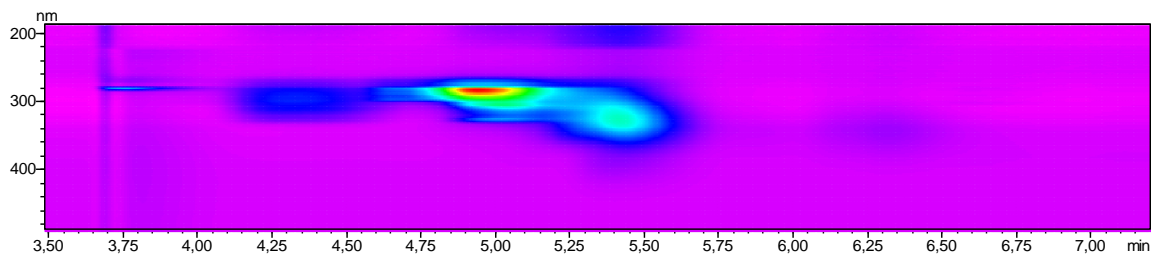


Figure 8.322: HPLC Contour view of reaction on Sample 7 635, SM(left signal), Product 1 (middle signal) and Product 2 (right signal).

Reaction on Sample 7 after purification AF635.2

Datafile Name: af635.2_.lcd
 Sample Name: AF635.2_
 Sample ID: AF635.2_

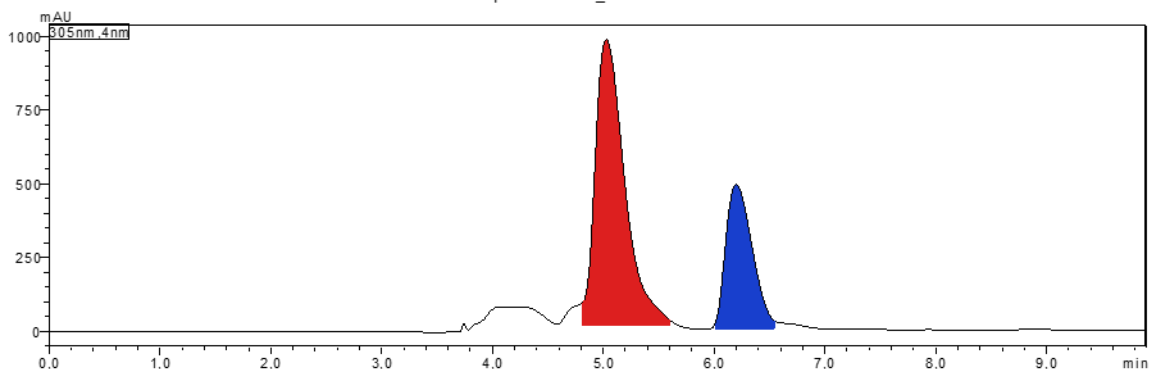


Figure 8.323: HPLC Chromatogram of reaction on Sample 7 after purification 635.2 in toluol/methanol 1:9.

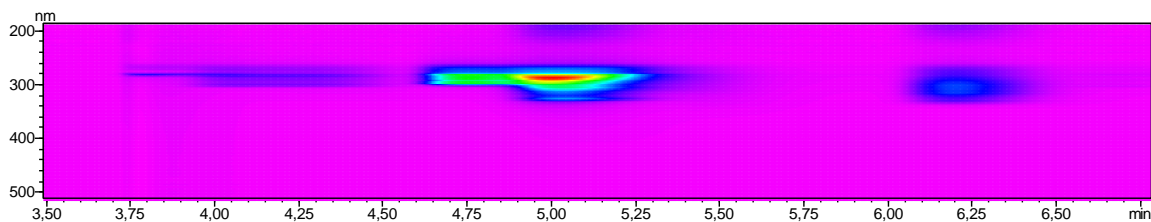


Figure 8.324: HPLC Contour view of reaction on Sample 7 after purification 635.2, SM(middle signal), Product 2 (right signal).

Reaction on Sample 8 AF632

Datafile Name: AF632.lcd
 Sample Name: AF632
 Sample ID: AF632

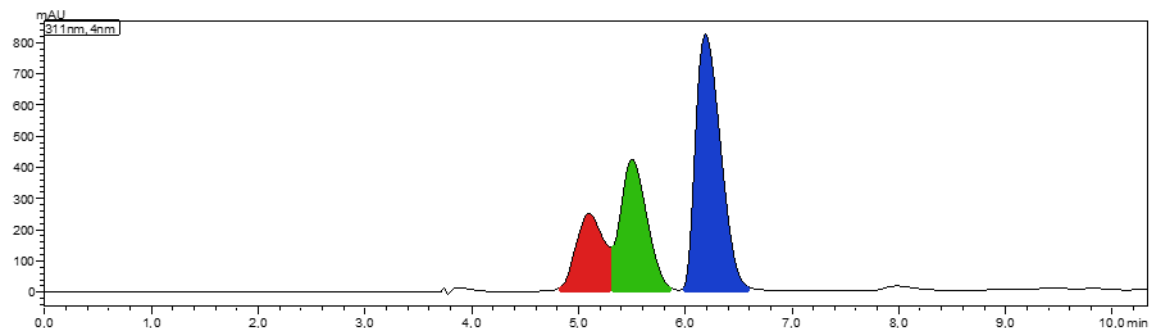


Figure 8.325: HPLC Chromatogram of reaction on Sample 8 632 in toluol/methanol 1:9.

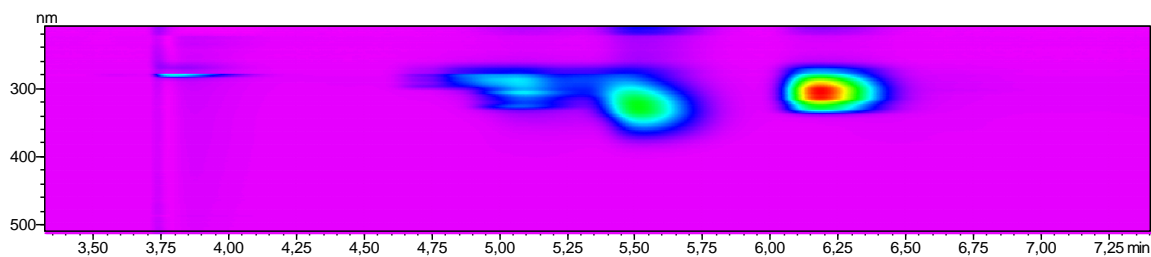


Figure 8.326: HPLC Contour view of reaction on Sample 8 632, **SM**(left signal), **Product 1** (middle signal) and **Product 2** (right signal).

Reaction on Sample 8 after purification AF632.2

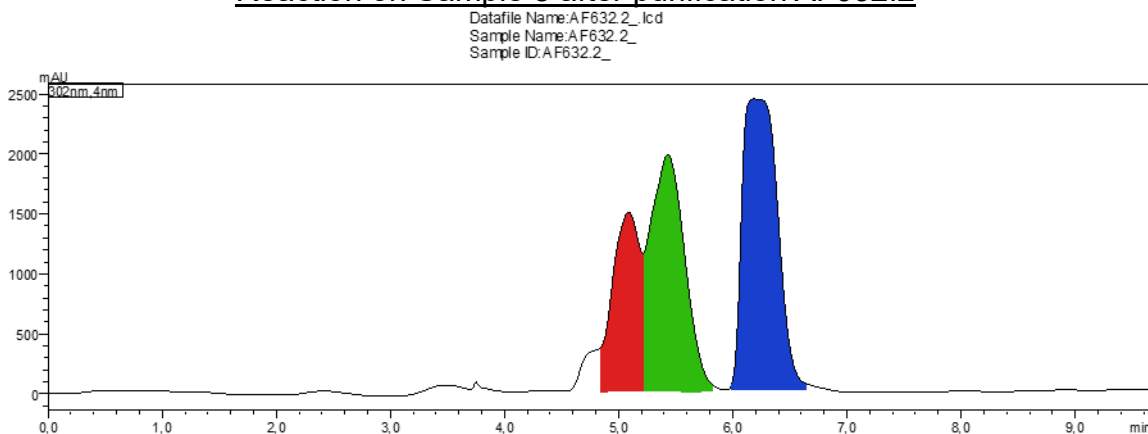


Figure 8.327: HPLC Chromatogram of reaction on Sample 8 after purification 632.2 in toluol/methanol 1:9.

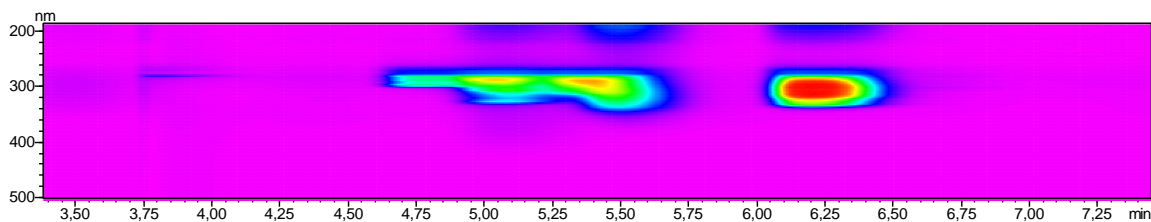


Figure 8.328: HPLC Contour view of reaction on Sample 8 after purification 632.2, **SM**(left signal), **Product 1** (middle signal) and **Product 2** (right signal).

Reaction on Sample 9 AF631

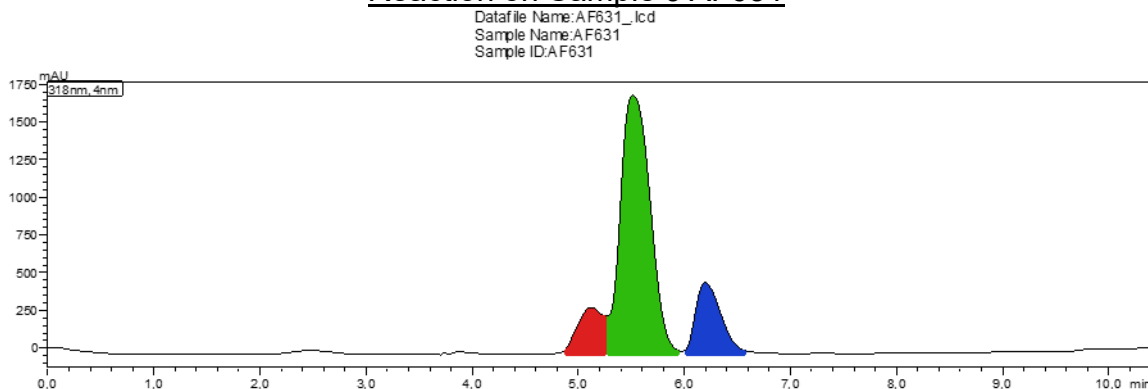


Figure 8.329: HPLC Chromatogram of reaction on Sample 9 631 in toluol/methanol 1:9.

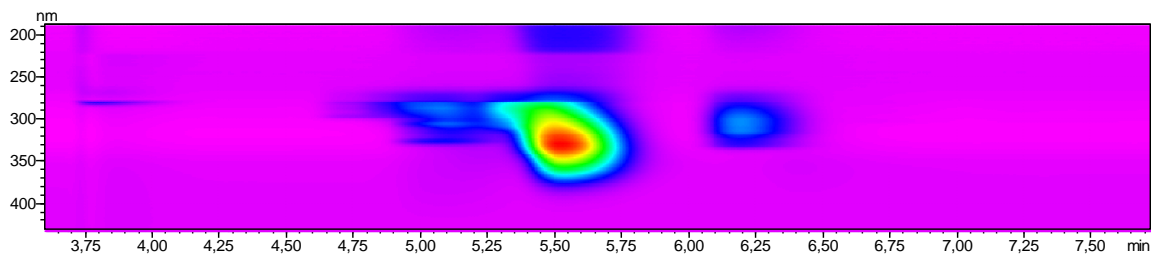


Figure 8.330: HPLC Contour view of reaction on Sample 9 631, **SM**(left signal), **Product 1** (middle signal) and **Product 2** (right signal).

Reaction on Sample 9 after purification AF631.2

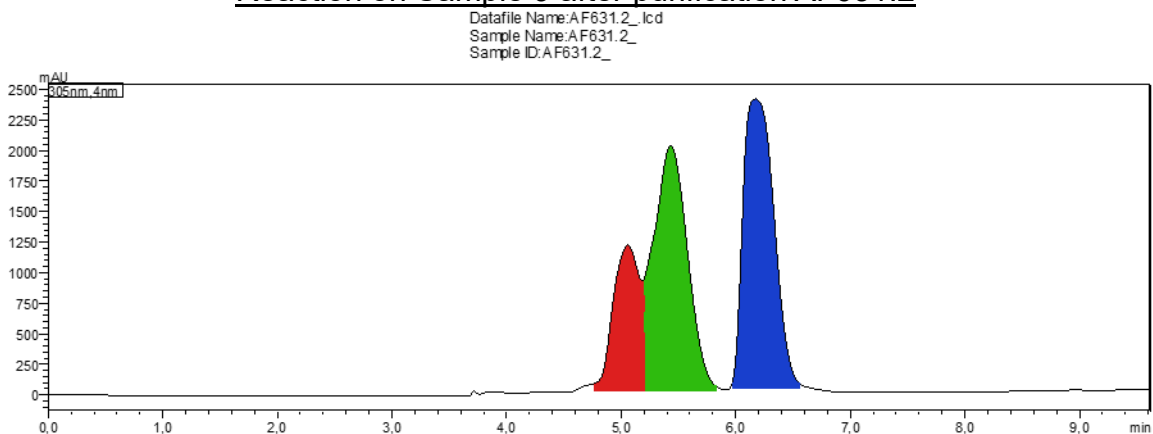


Figure 8.331: HPLC Chromatogram of reaction on Sample 9 after purification 631.2 in toluol/methanol 1:9.

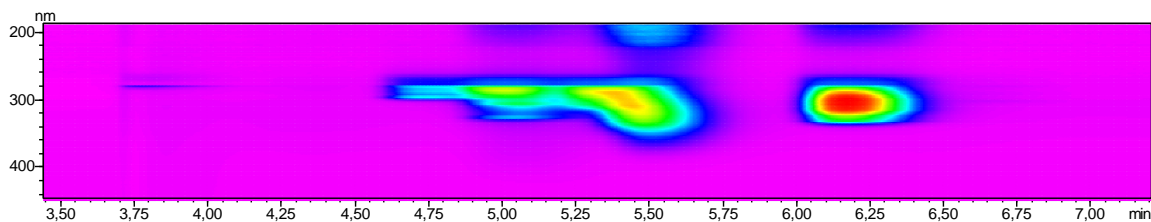


Figure 8.332: HPLC Contour view of reaction on Sample 9 after purification 631.2, **SM**(left signal), **Product 1** (middle signal) and **Product 2** (right signal).

Reaction on Sample 10 AF630

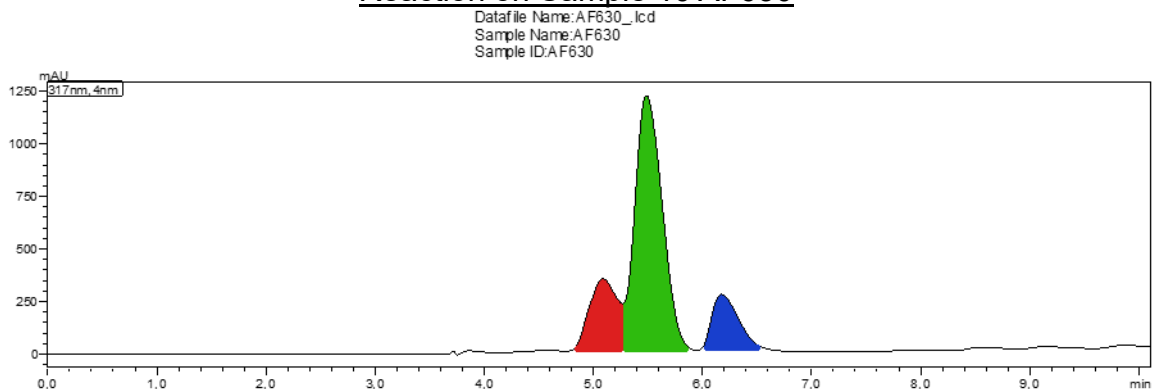


Figure 8.333: HPLC Chromatogram of reaction on Sample 10 630 in toluol/methanol 1:9.

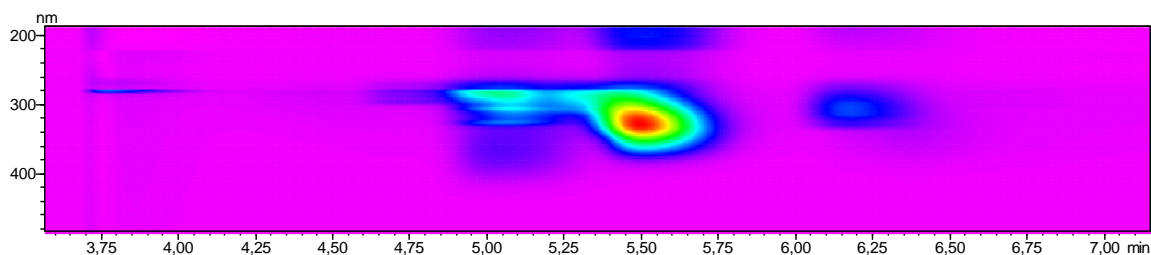


Figure 8.334: HPLC Contour view of reaction on Sample 10 630, **SM**(left signal), **Product 1** (middle signal) and **Product 2** (right signal).

Reaction on Sample 10 after purification AF630.2

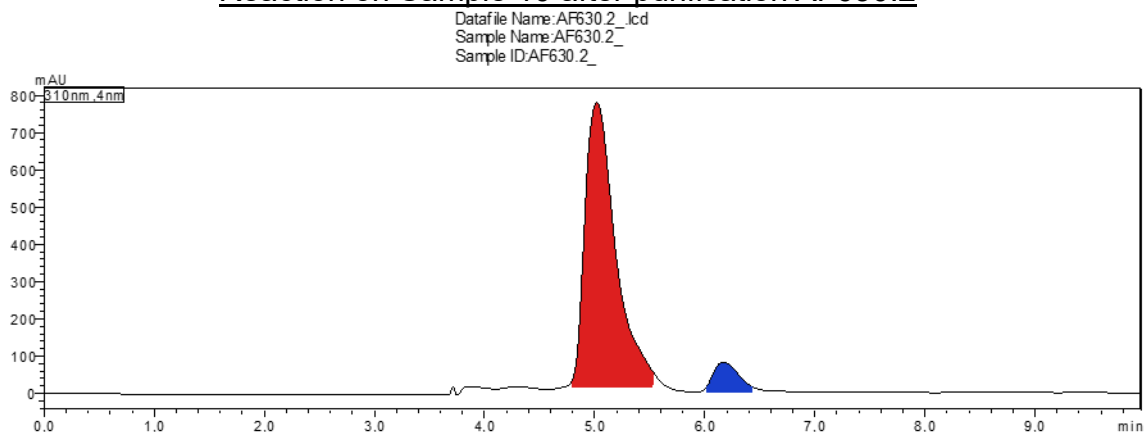


Figure 8.335: HPLC Chromatogram of reaction on Sample 10 after purification 630.2 in toluol/methanol 1:9.

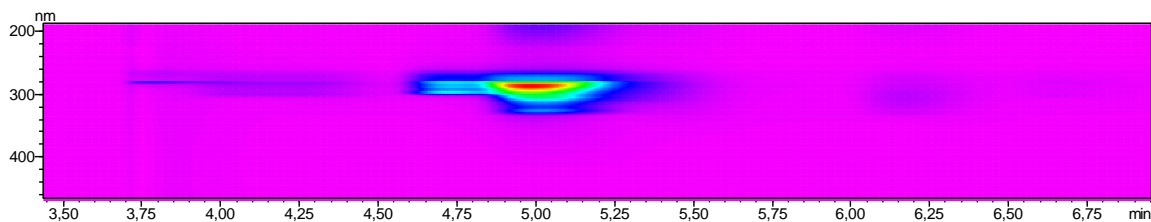


Figure 8.336: HPLC Contour view of reaction on Sample 10 after purification 630.2, **SM**(left signal), **Product 1** (middle signal) and **Product 2** (right signal).

Reaction on Sample 11 AF629

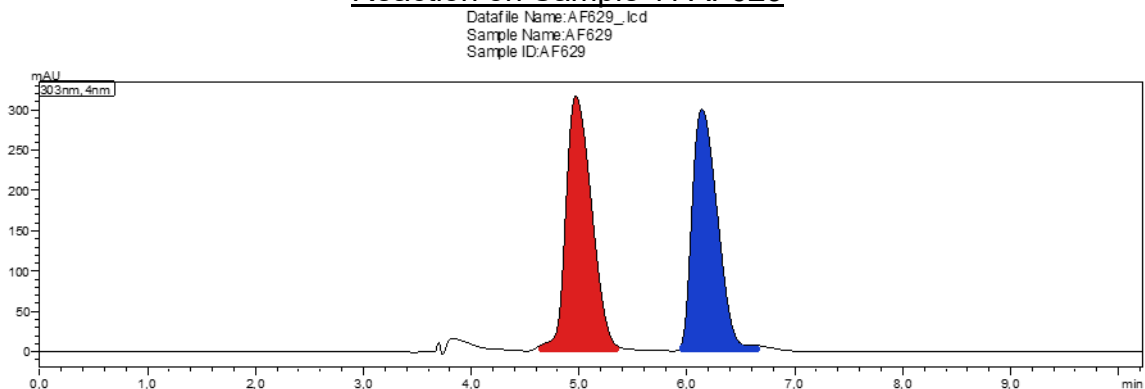


Figure 8.337: HPLC Chromatogram of reaction on Sample 11 629 in toluol/methanol 1:9.

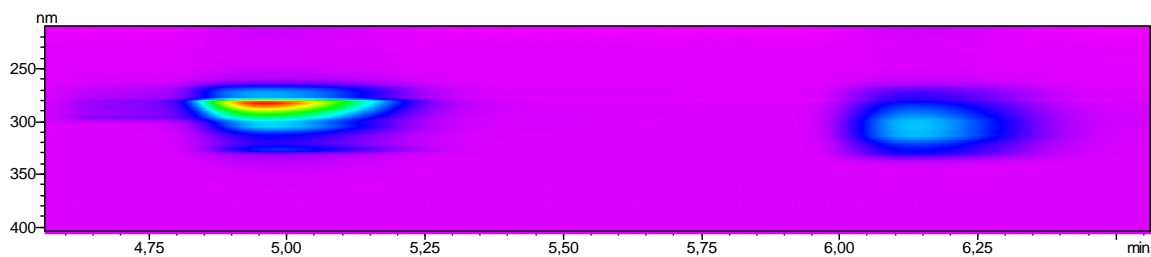


Figure 8.338: HPLC Contour view of reaction on Sample 11 629, **SM**(left signal) and **Product 2** (right signal).

Reaction on Sample 11 after purification AF629.2

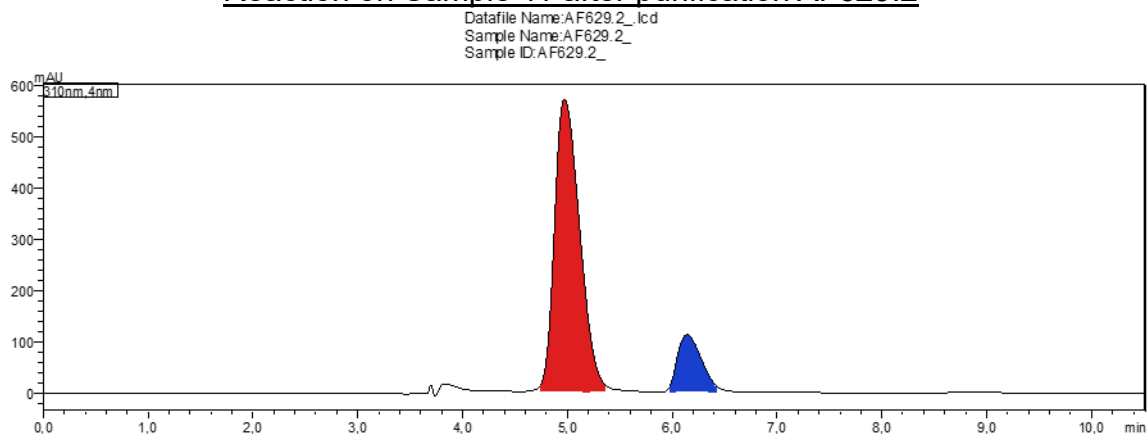


Figure 8.339: HPLC Chromatogram of reaction on Sample 11 after purification 629.2 in toluol/methanol 1:9.

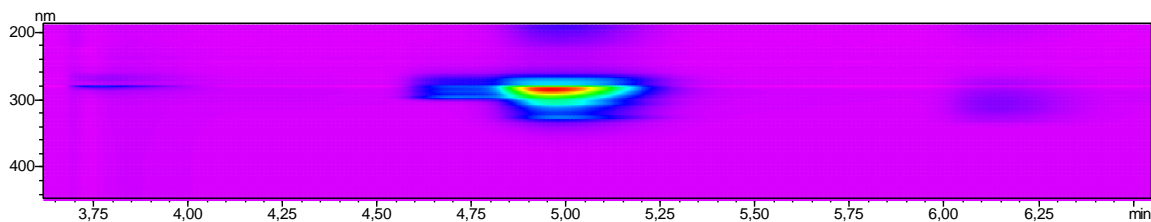


Figure 8.340: HPLC Contour view of reaction on Sample 11 after purification 629.2, **SM**(left signal) and **Product 2** (right signal).

8.7. Homodimerization of terminal Alkyne- Model molecule with different temperatures

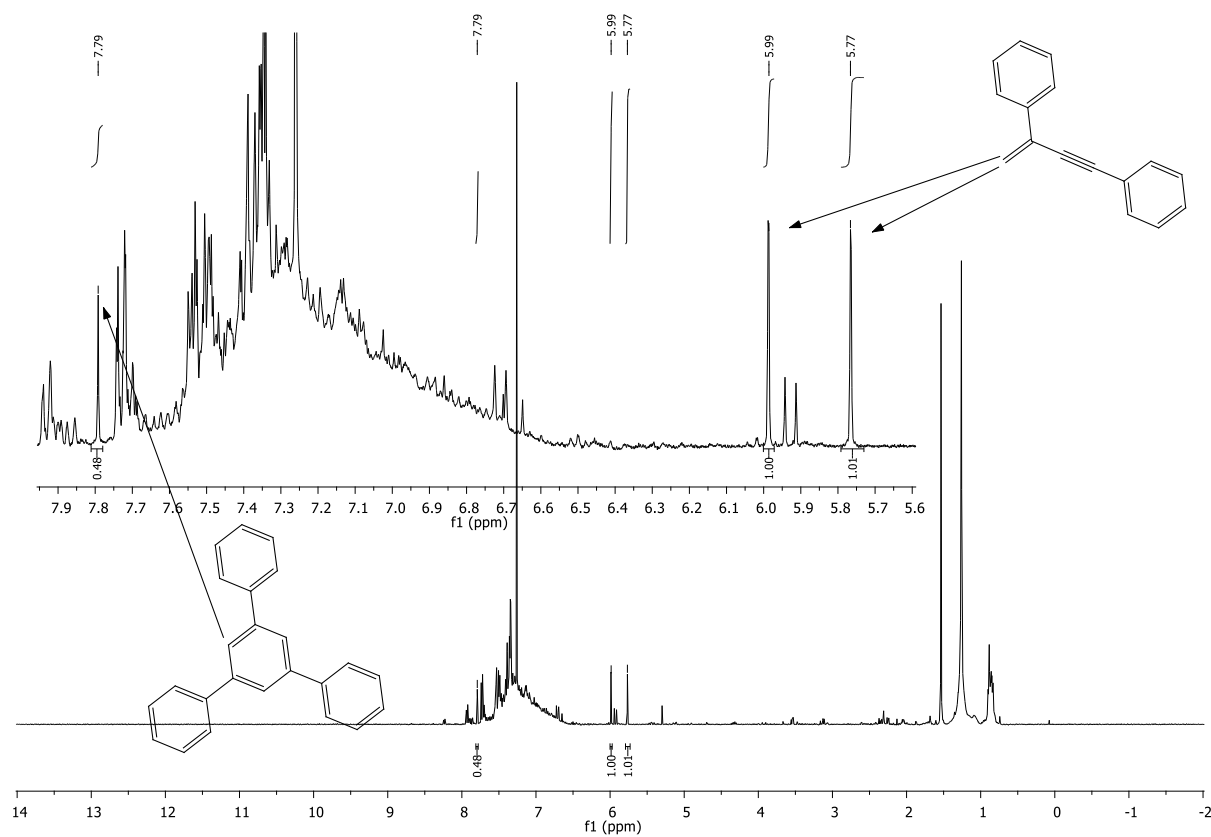


Figure 8.341: ¹H-NMR spectrum of dimerization and trimerization of phenylacetylene at 20 °C for 3 d.

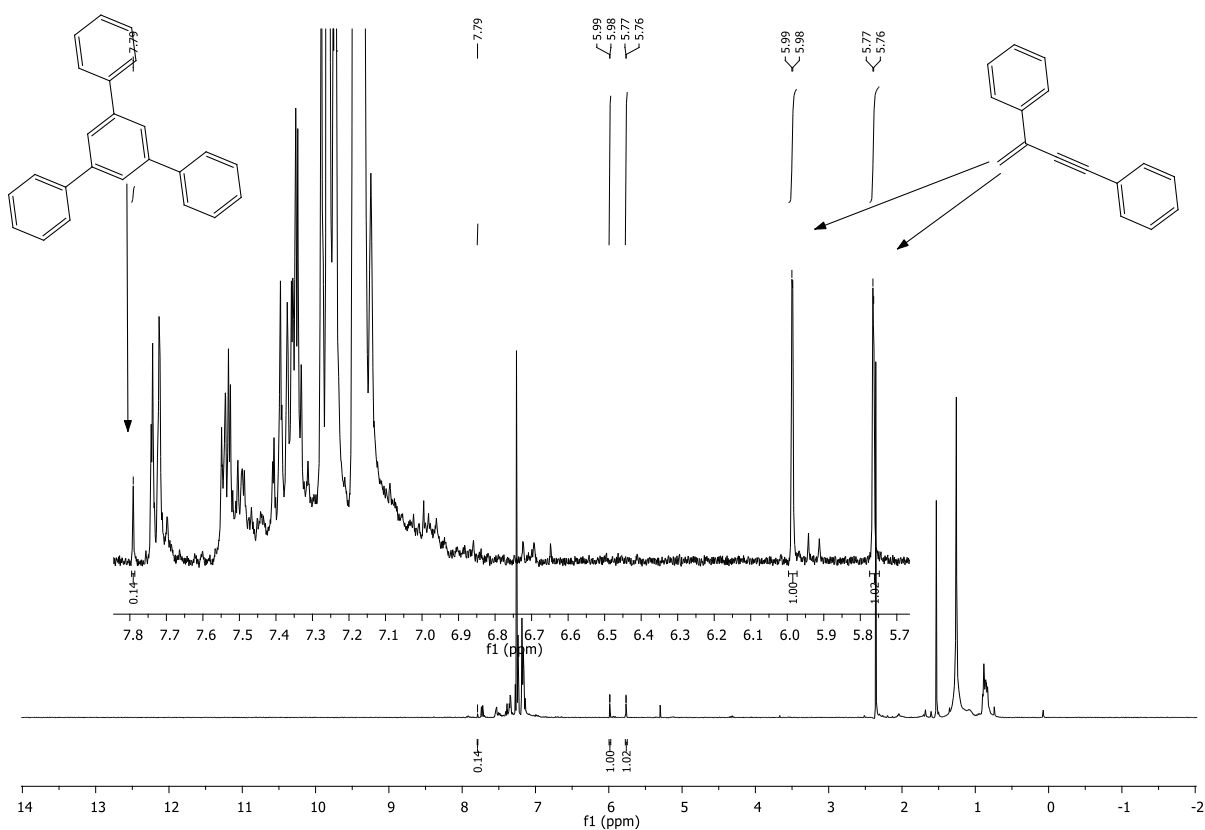


Figure 8.342: $^1\text{H-NMR}$ spectrum of dimerization and trimerization of phenylacetylene at $40\text{ }^\circ\text{C}$ for 2 h.

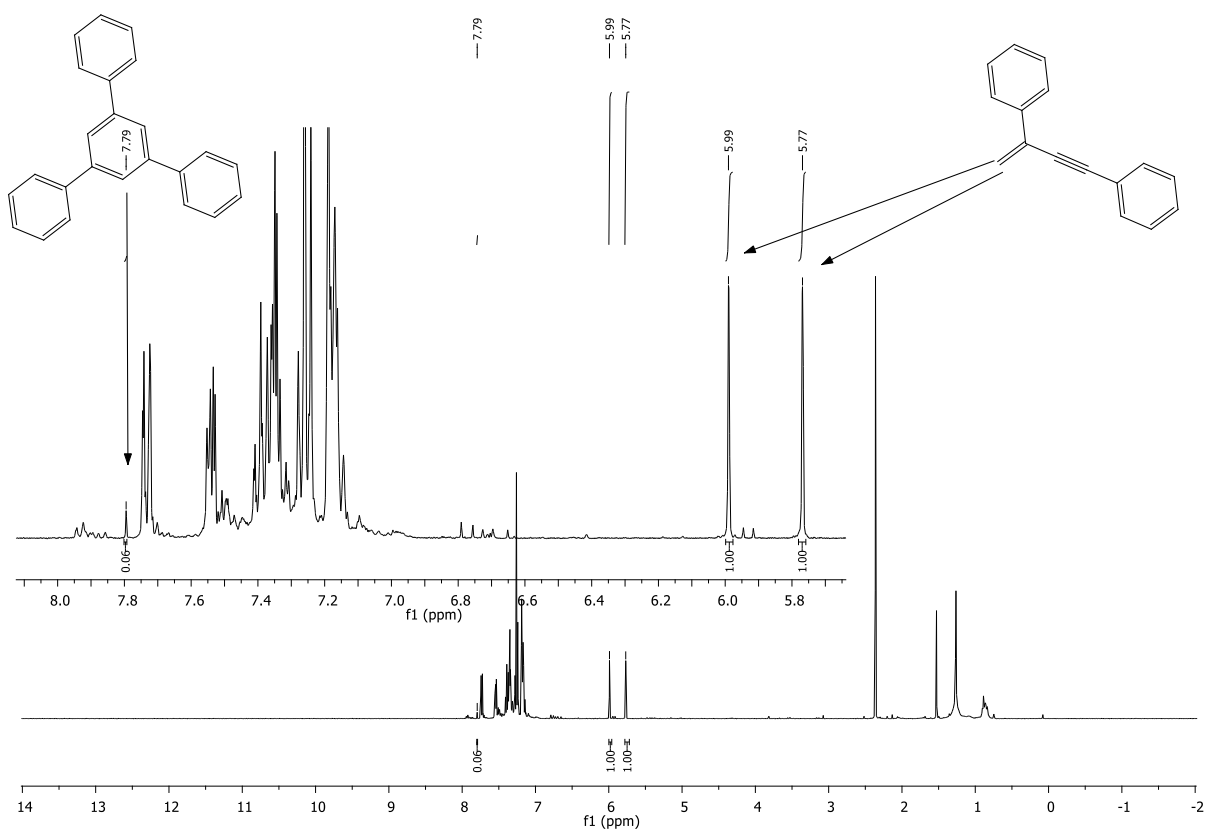


Figure 8.343: $^1\text{H-NMR}$ spectrum of dimerization and trimerization of phenylacetylene at $60\text{ }^\circ\text{C}$ for 2 h.

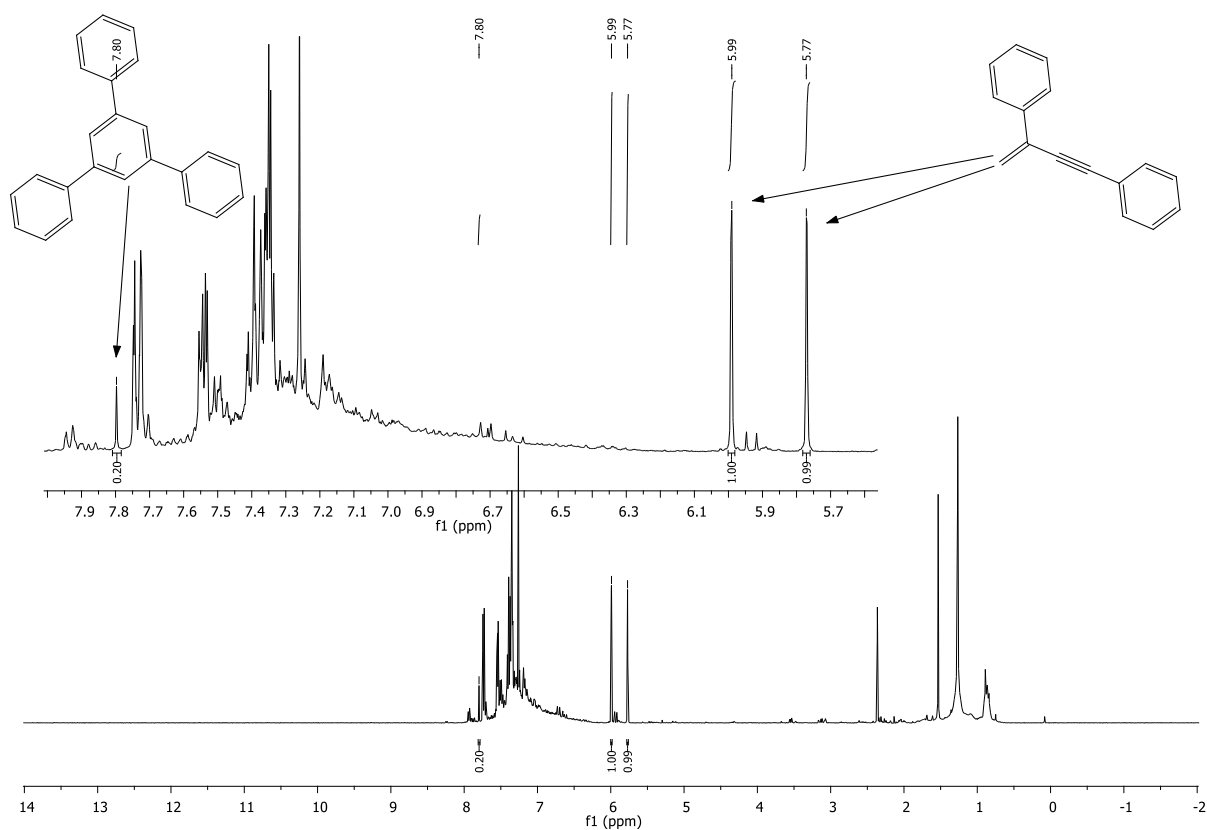


Figure 8.344: $^1\text{H-NMR}$ spectrum of dimerization and trimerization of phenylacetylene at $60\text{ }^\circ\text{C}$ for 6 h.

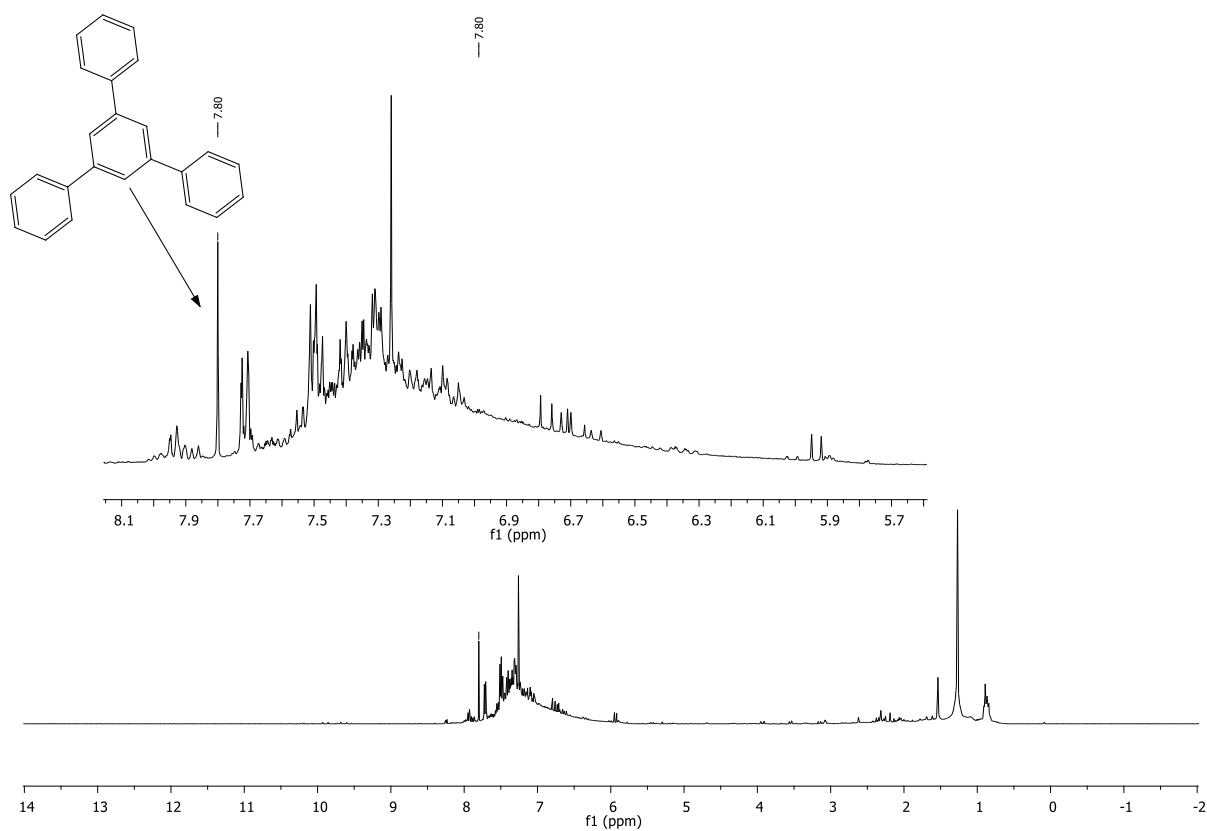


Figure 8.345: $^1\text{H-NMR}$ spectrum of trimerization of phenylacetylene at $90\text{ }^\circ\text{C}$ for 2 h.

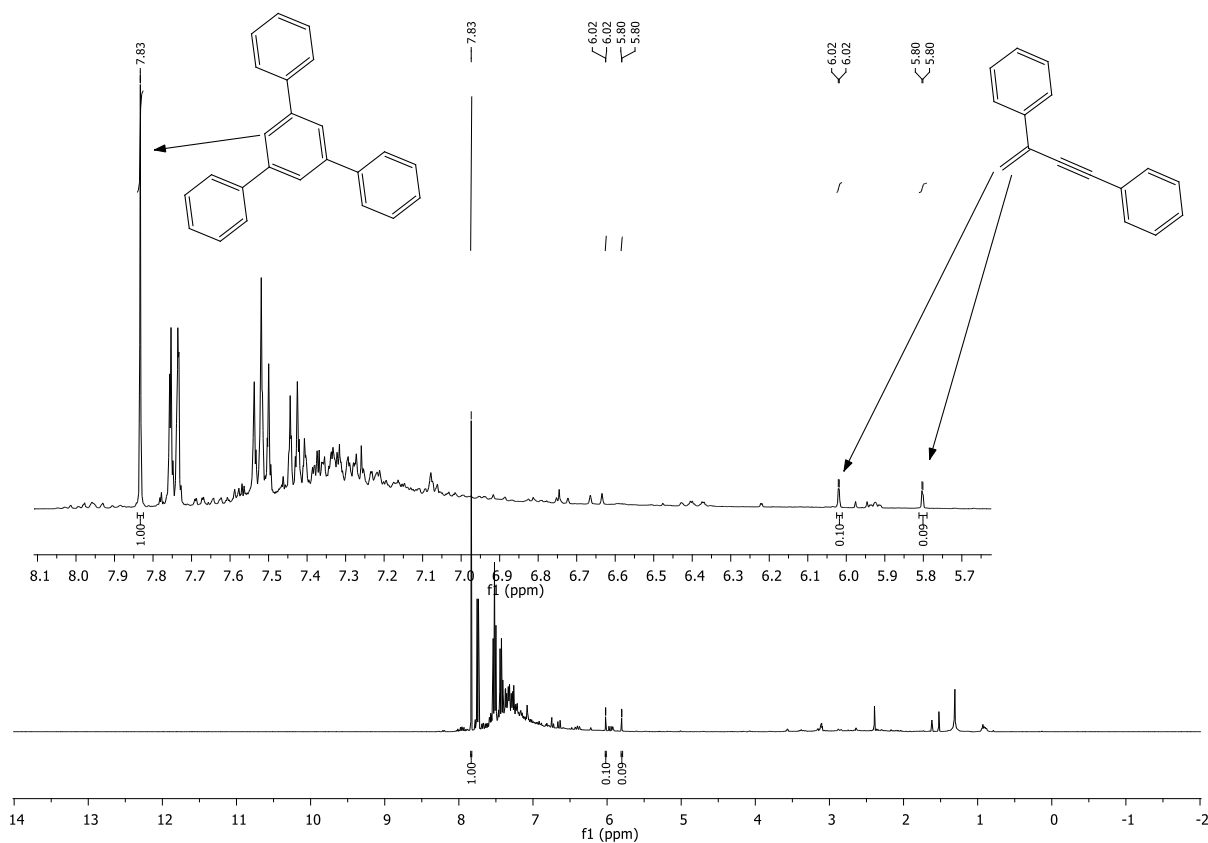


Figure 8.346: $^1\text{H-NMR}$ spectrum of dimerization and trimerization of phenylacetylene at $120\text{ }^\circ\text{C}$ for 2 h.

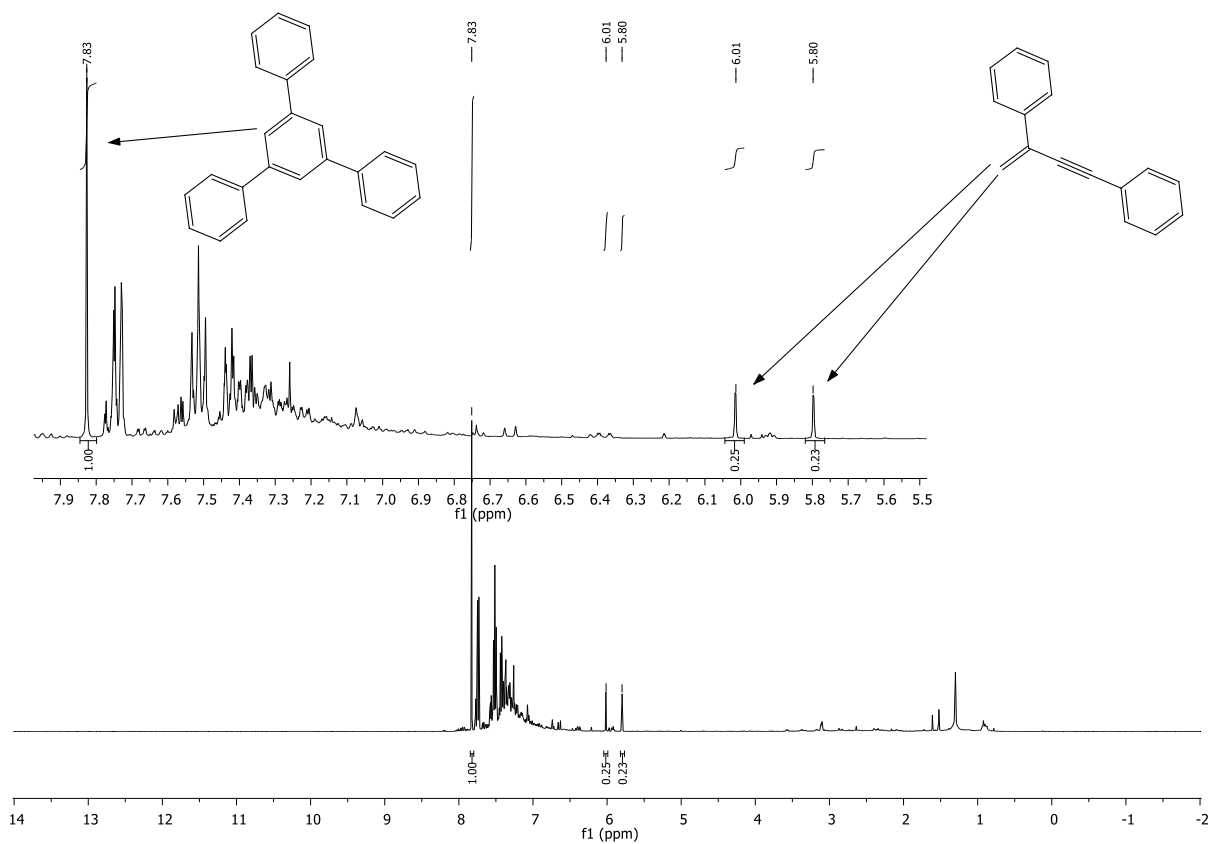


Figure 8.347: $^1\text{H-NMR}$ spectrum of dimerization and trimerization of phenylacetylene at $120\text{ }^\circ\text{C}$ for 2 h.

150 °C for 2 h.

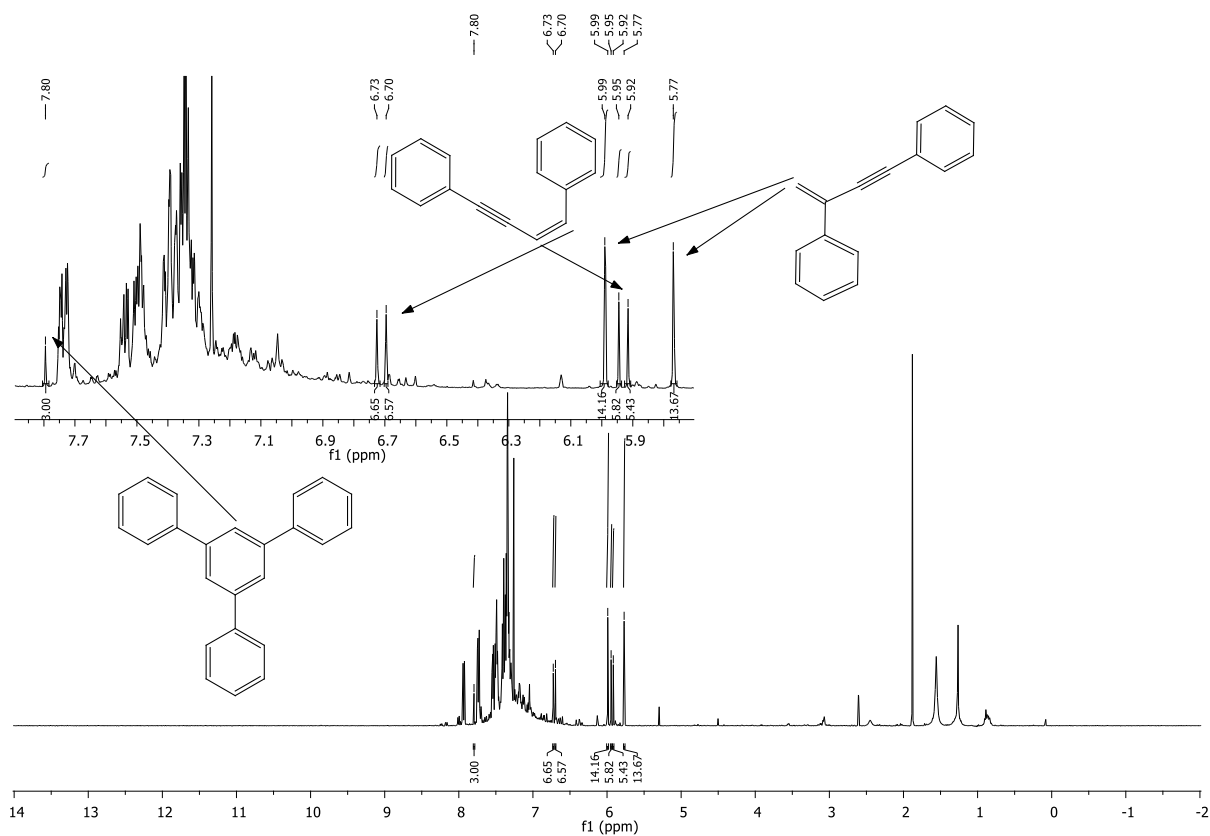


Figure 8.348: $^1\text{H-NMR}$ spectrum after reaction according to general procedure 9 on PURAL MG30 ($\text{Al}_2\text{O}_3 / \text{MgO} = 70 / 30$).

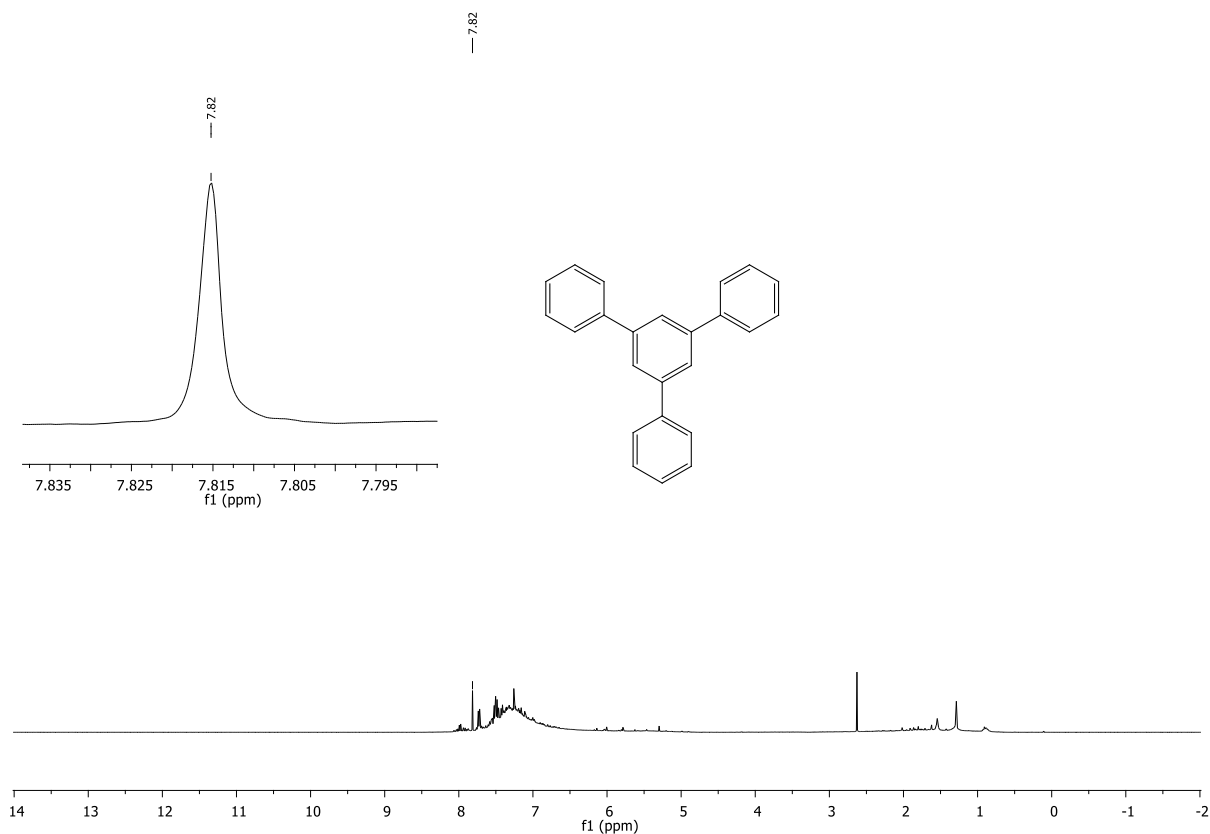


Figure 8.349: $^1\text{H-NMR}$ spectrum after reaction according to general procedure 9 on SIRAL 30 ($\text{Al}_2\text{O}_3 / \text{SiO}_2 = 70 / 30$)

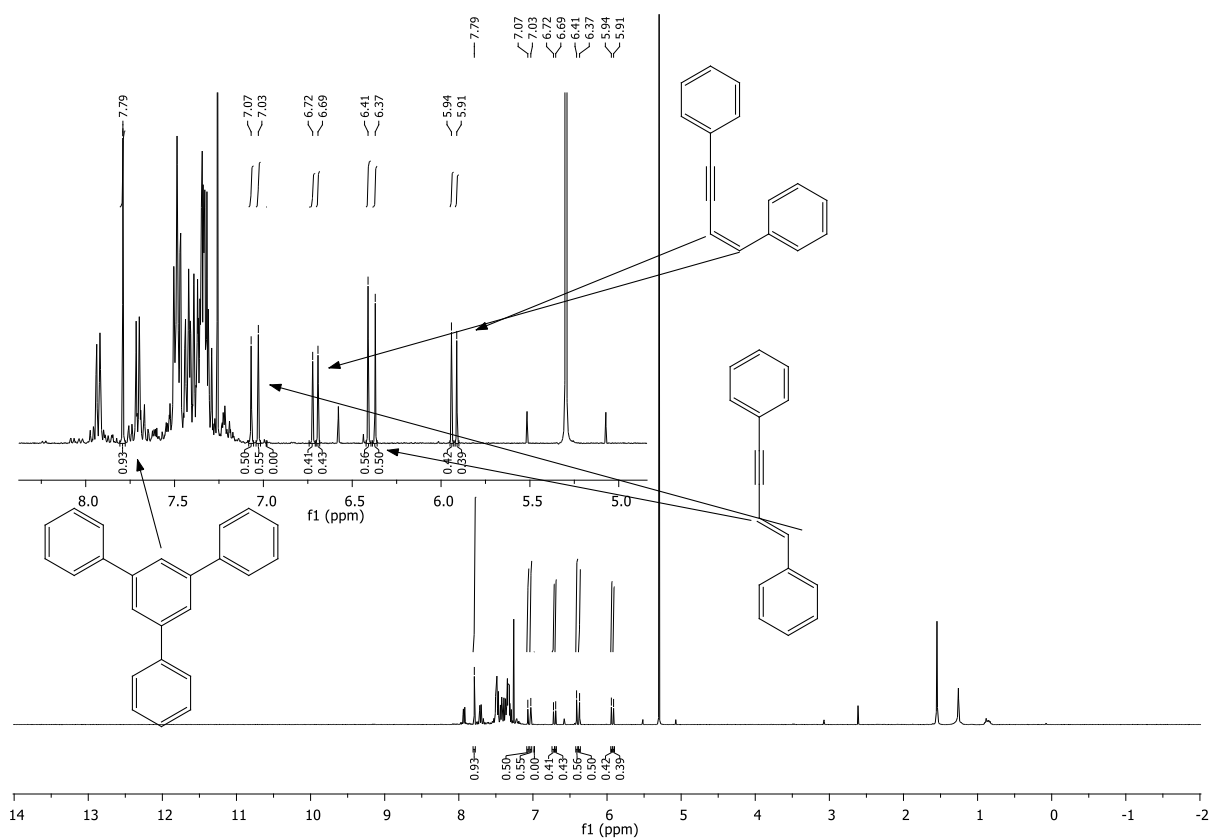


Figure 8.350: $^1\text{H-NMR}$ spectrum after reaction according to general procedure 9 on Puralox

SCFa-160/Ce20 ($\text{Al}_2\text{O}_3 / \text{CeO}_2 = 80 / 20$).

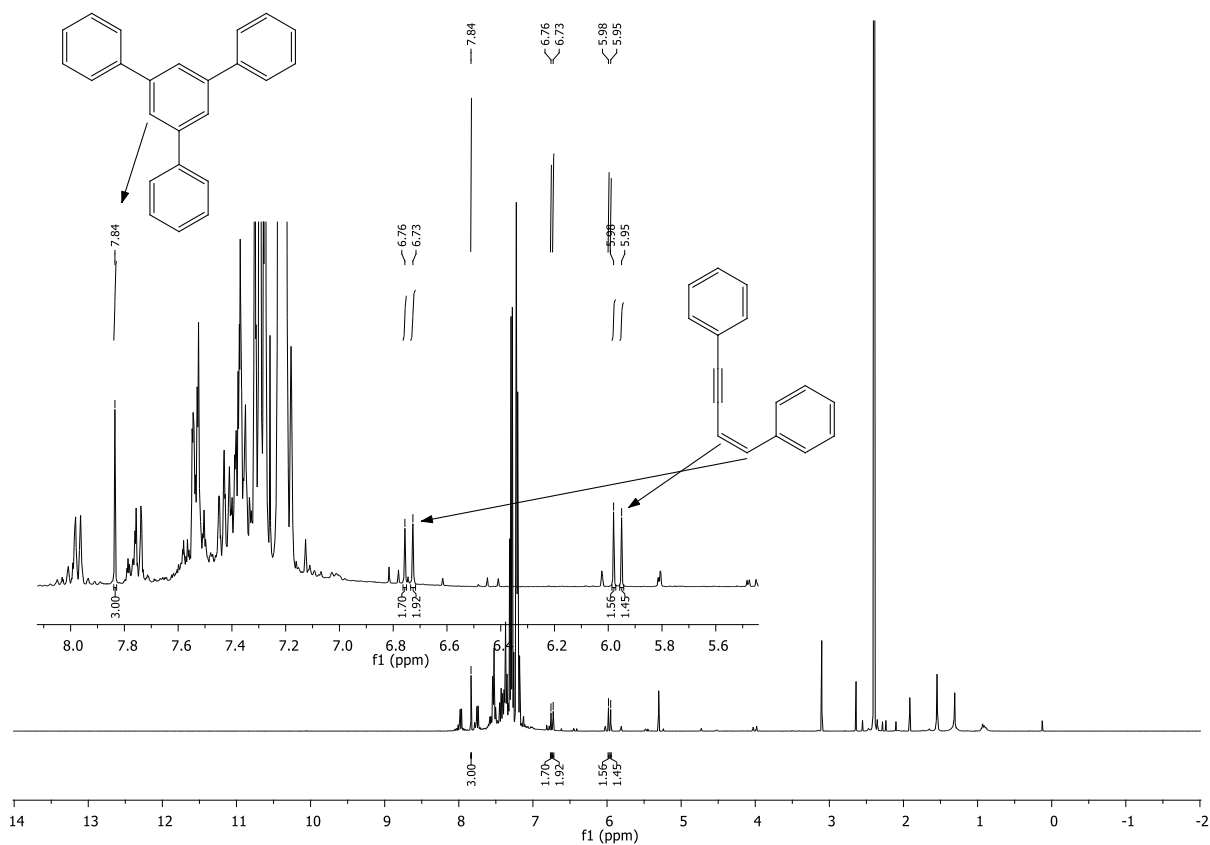


Figure 8.351: $^1\text{H-NMR}$ spectrum after reaction according to general procedure 8 on Puralox SCFa-160/Ce20 ($\text{Al}_2\text{O}_3 / \text{CeO}_2 = 80 / 20$).

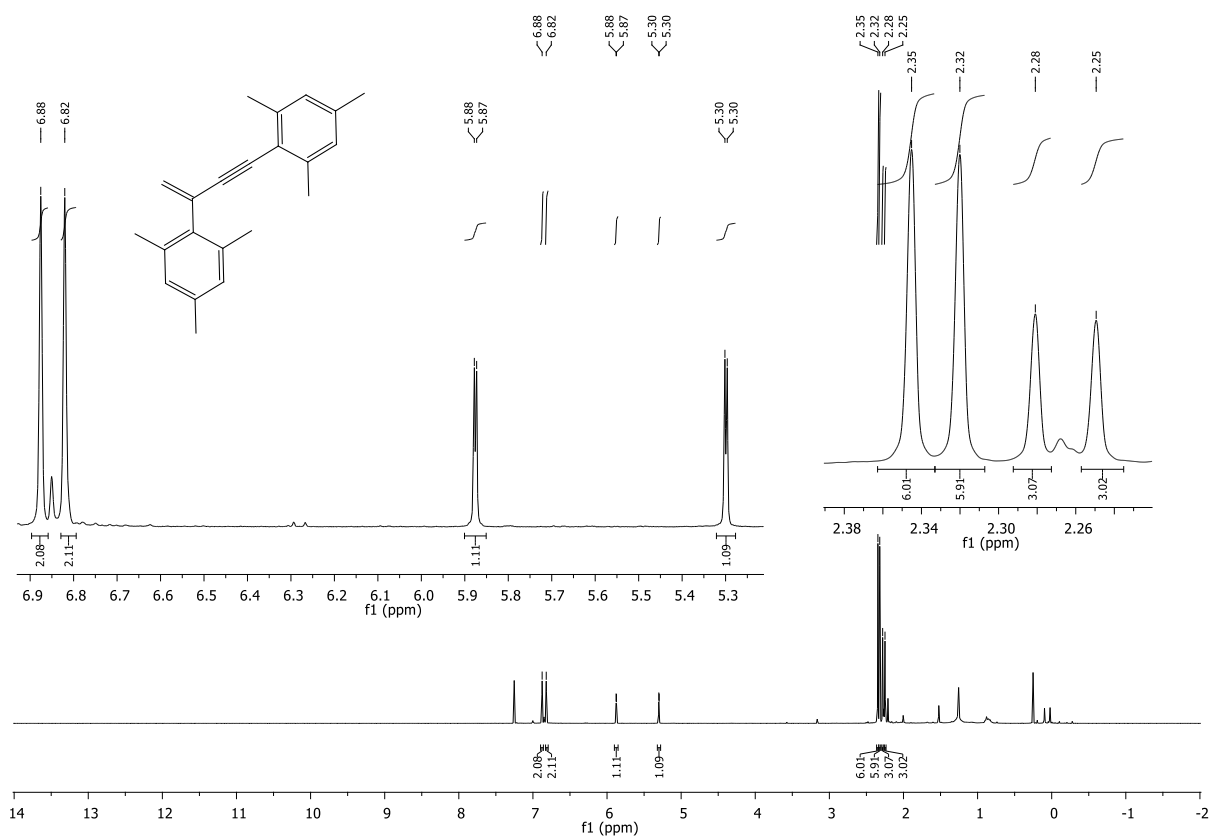


Figure 8.352: ¹H-NMR spectrum of 2,2'-(but-3-en-1-yne-1,3-diyl)bis(1,3,5-trimethylbenzene).

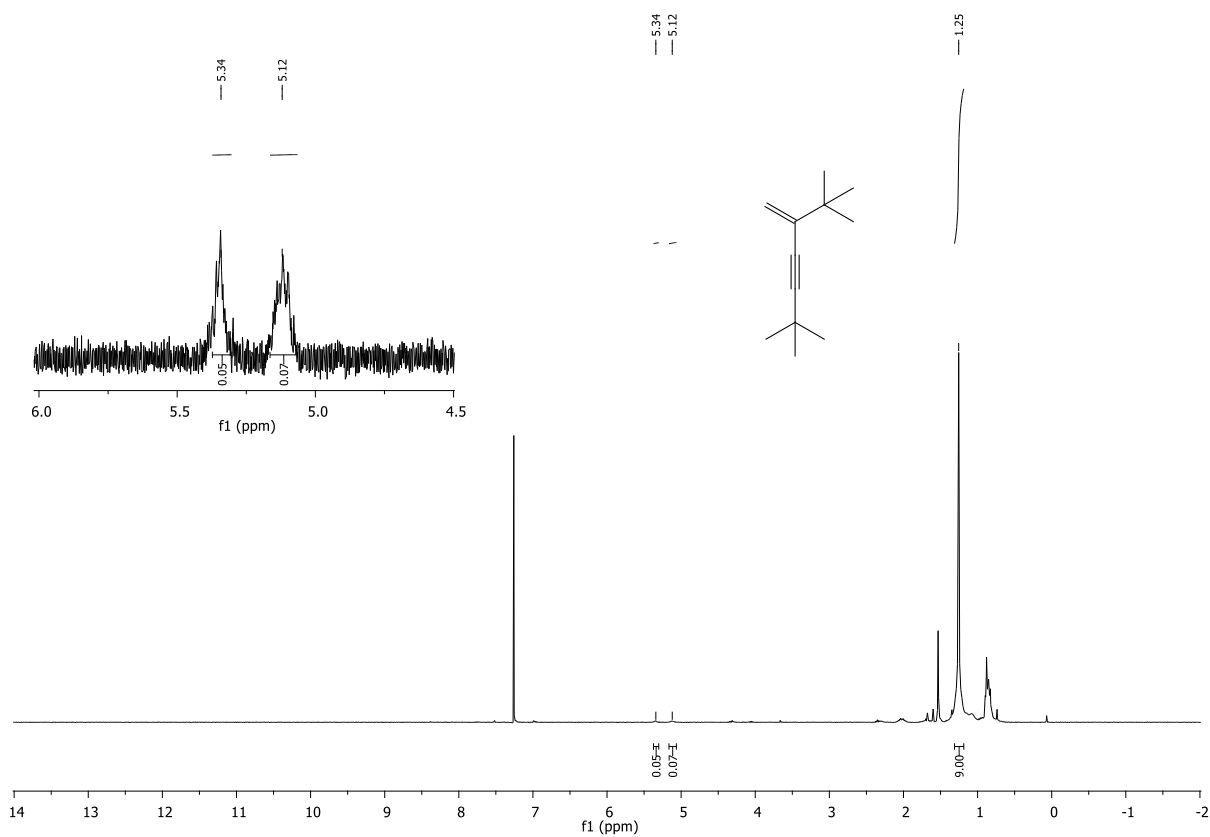


Figure 8.353: ¹H-NMR spectrum of 2,2,6,6-tetramethyl-5-methylenehept-3-yne.

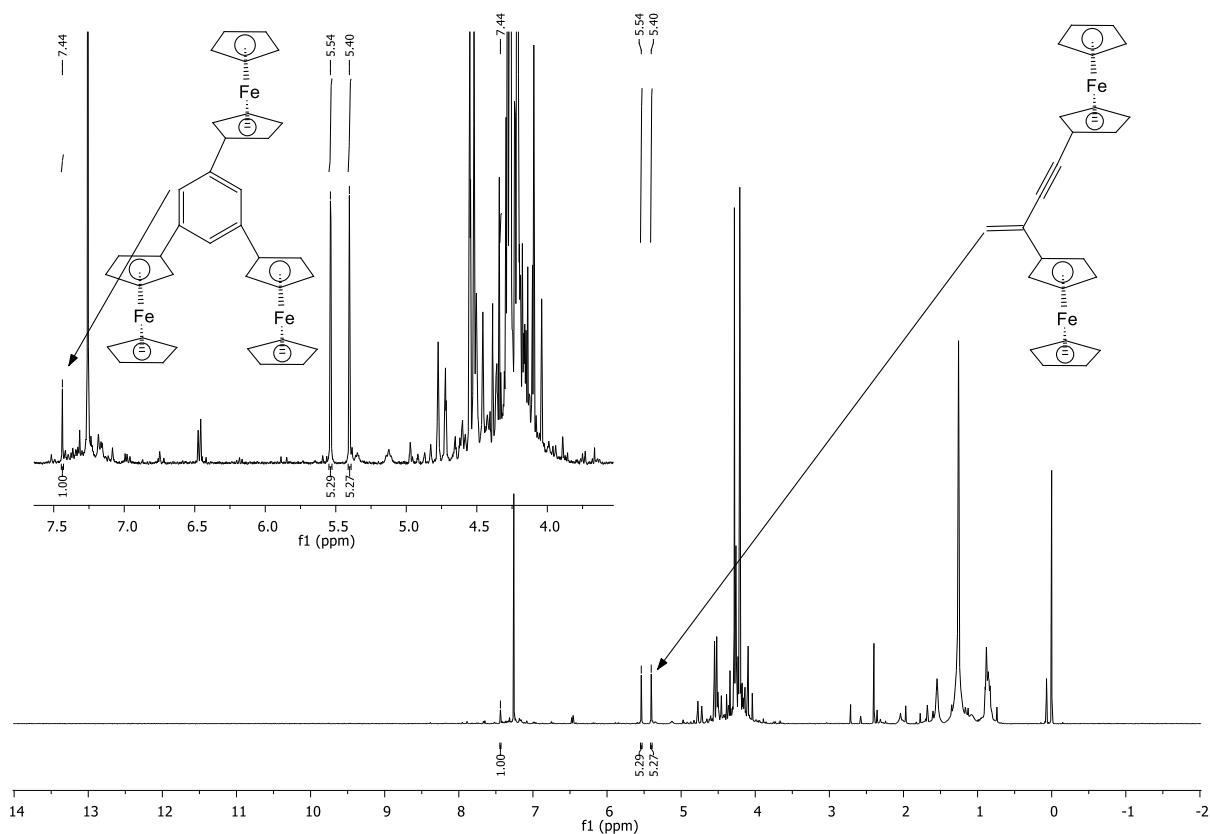


Figure 8.354: $^1\text{H-NMR}$ spectrum after reaction of ferrocene acetylene on Al_2O_3 at $60\text{ }^\circ\text{C}$ for 4 h.

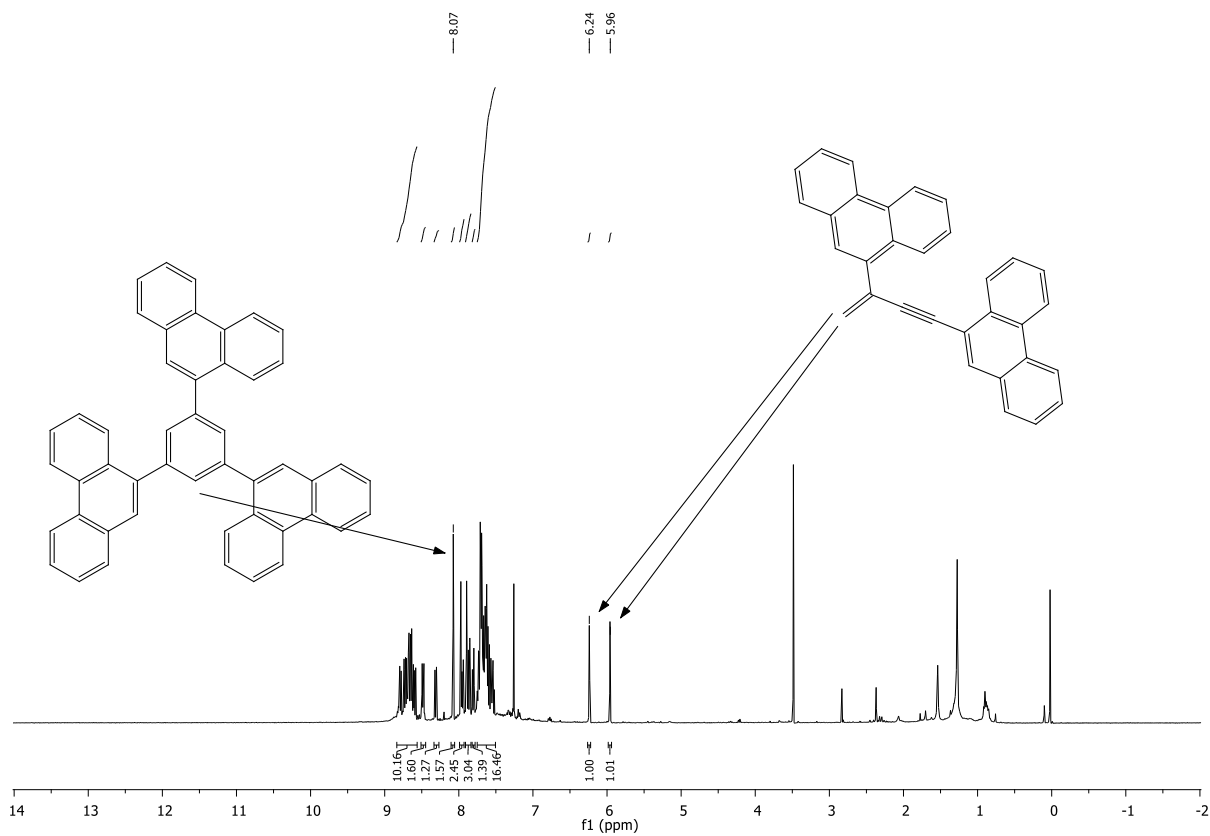


Figure 8.355: $^1\text{H-NMR}$ spectrum after reaction of 9-ethynylphenanthren on Al_2O_3 at $120\text{ }^\circ\text{C}$

for 4 h.

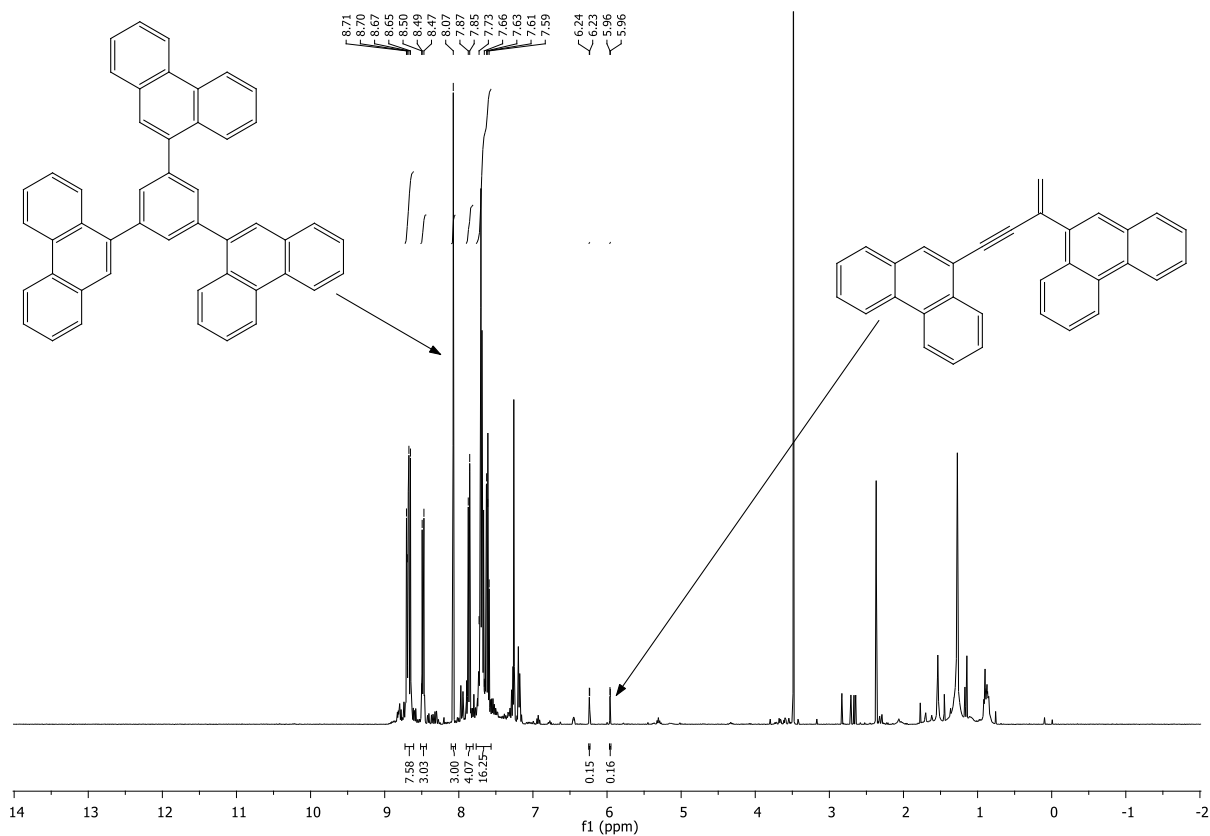


Figure 8.356: $^1\text{H-NMR}$ spectrum after reaction of 9-ethynylphenanthren on Al_2O_3 at 60°C for 4 h.

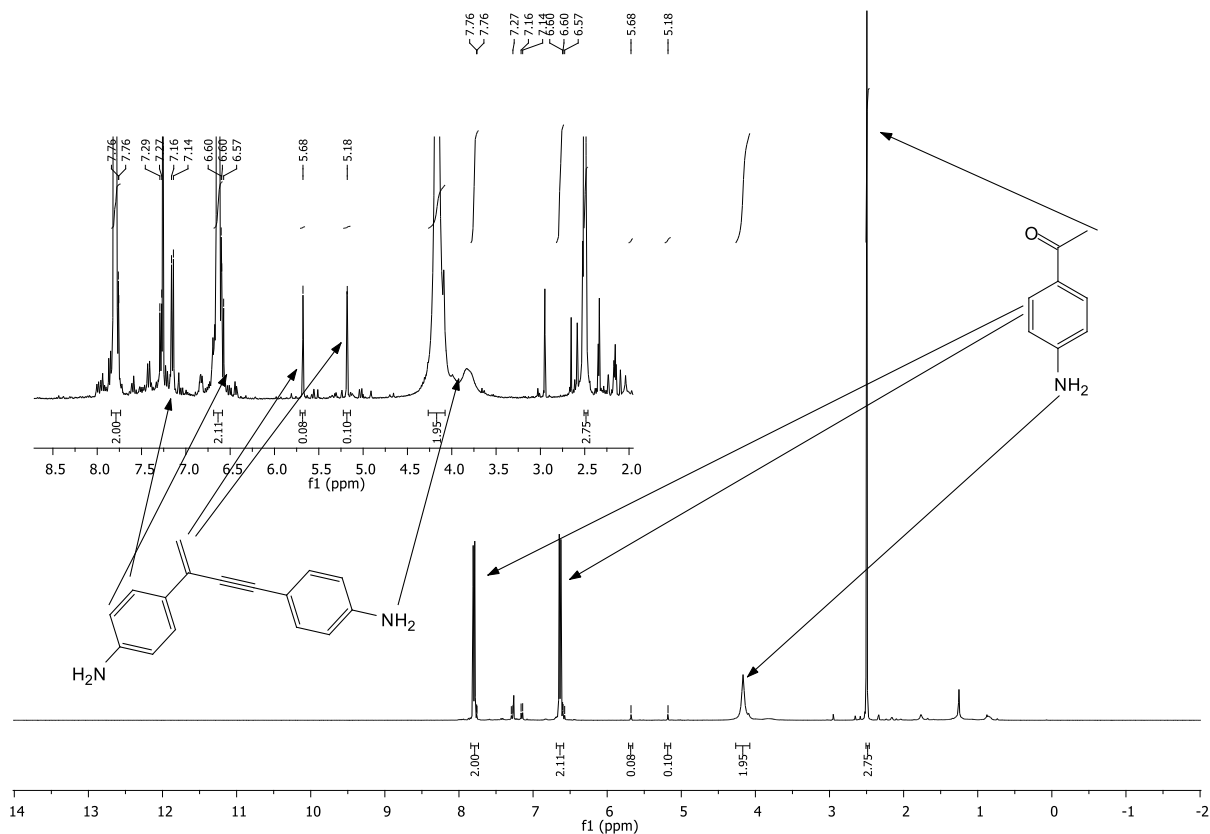


Figure 8.357: $^1\text{H-NMR}$ spectrum after reaction of 4-ethynylaniline on Al_2O_3 at $120\text{ }^\circ\text{C}$ for 4 h.

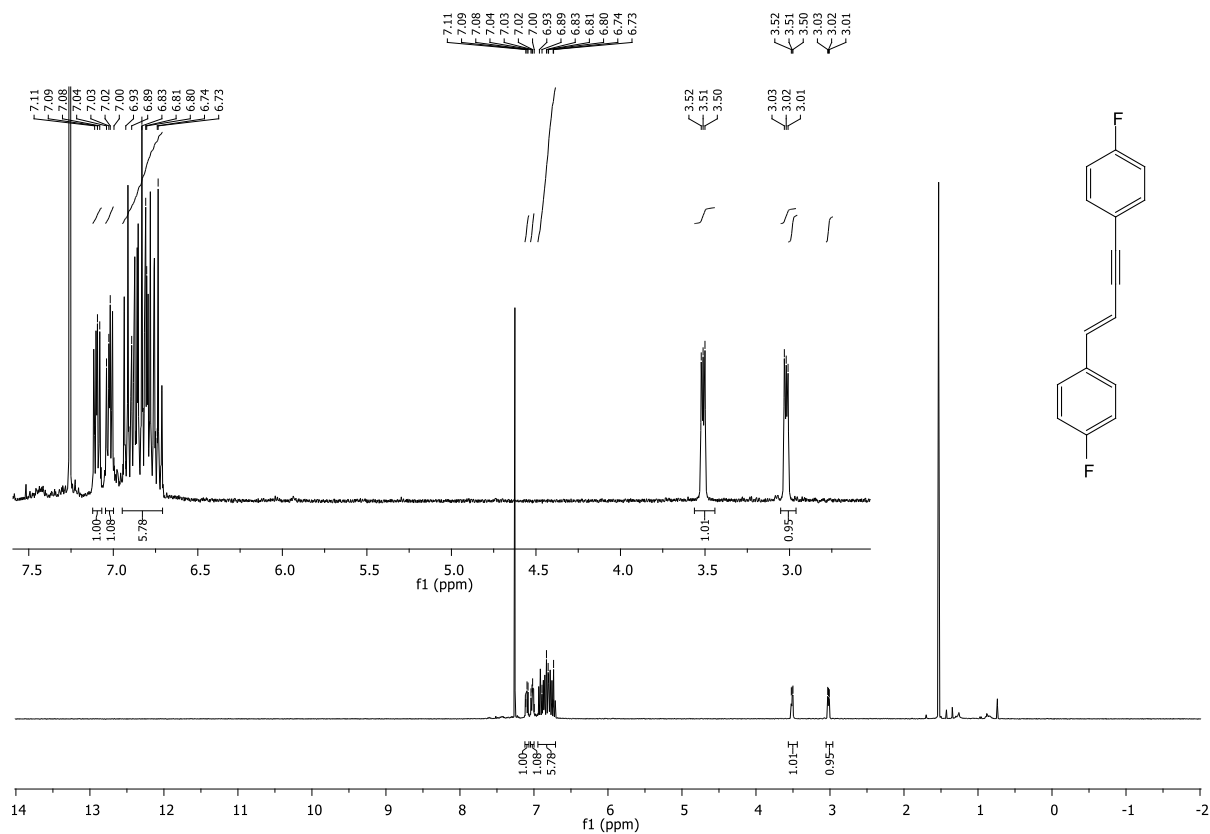


Figure 8.358: $^1\text{H-NMR}$ spectrum of head to head dimer of 1-ethynyl-4-fluorobenzene.

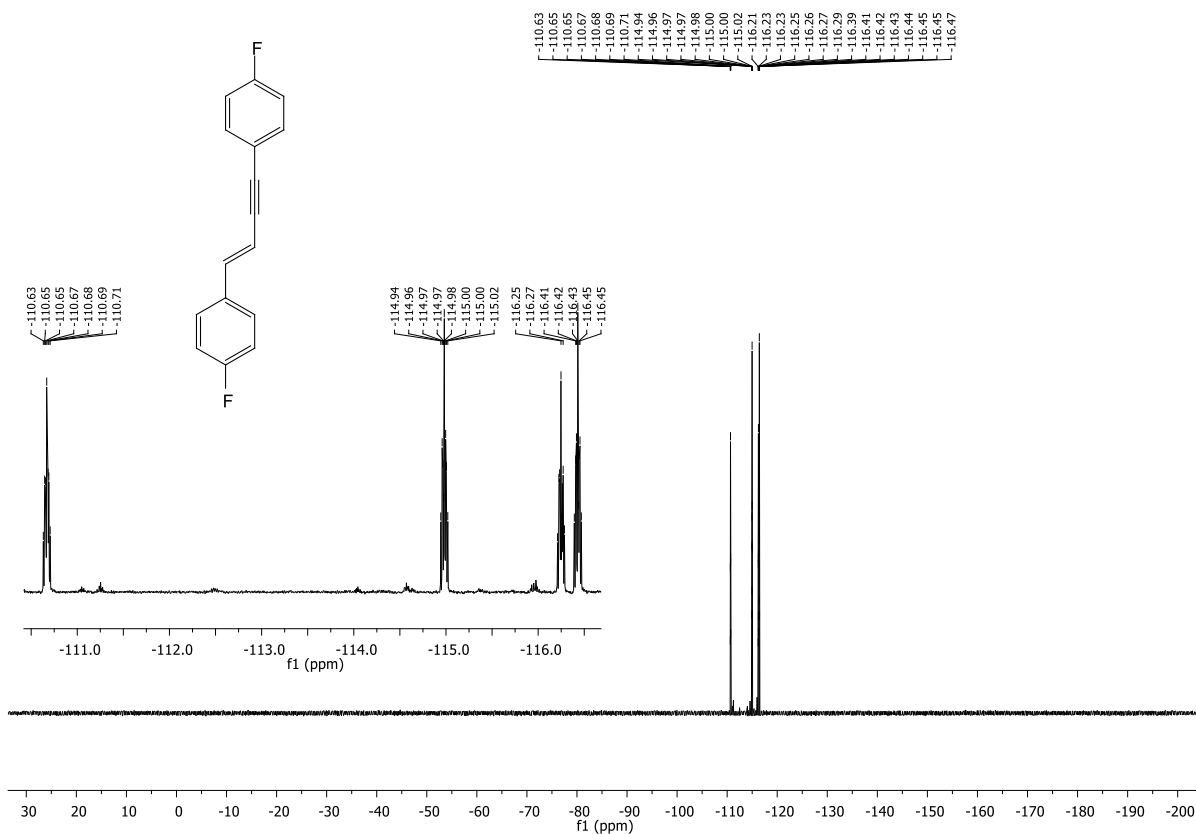


Figure 8.359: ^{19}F -NMR spectrum of head to head dimer of 1-ethynyl-4-fluorobenzene.

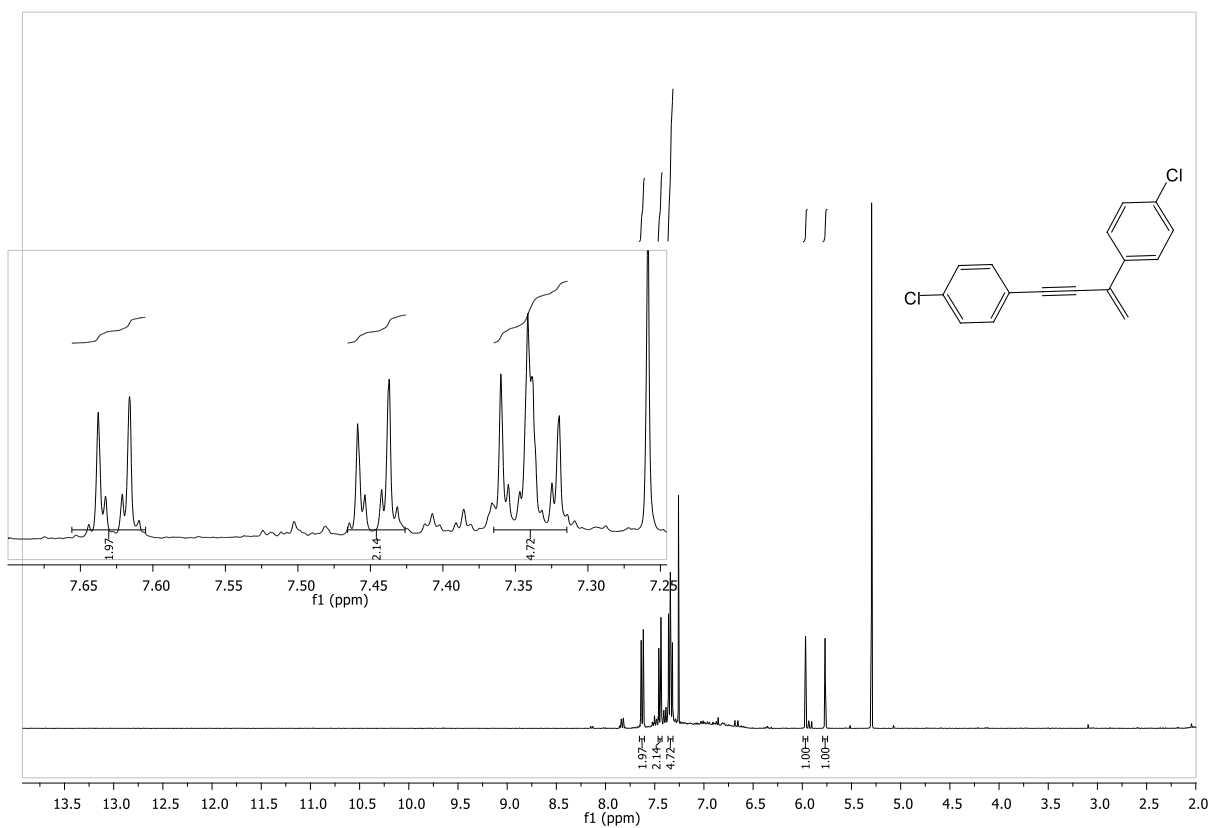


Figure 8.360: ^1H -NMR spectrum of 4,4'-(but-3-en-1-yne-1,3-diyl)bis(chlorobenzene).

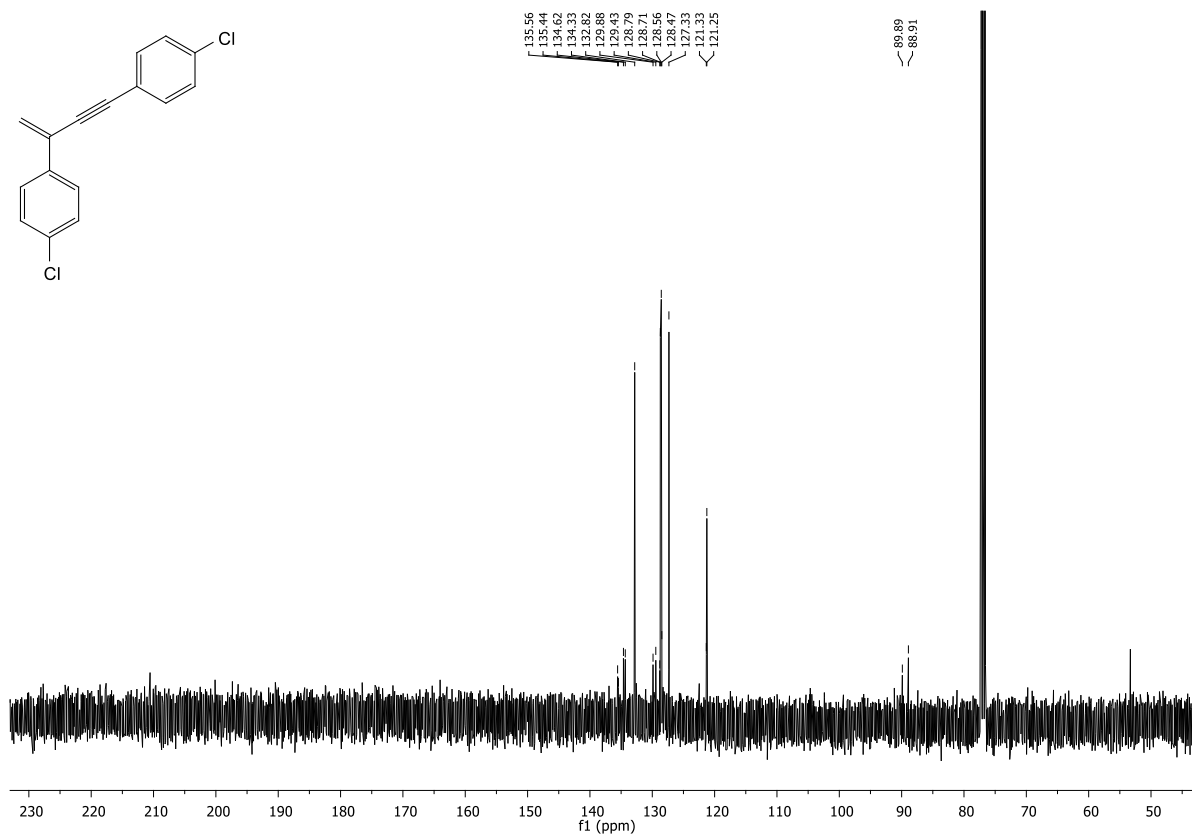


Figure 8.361: $^{13}\text{C-NMR}$ spectrum of 4,4'-(but-3-en-1-yne-1,3-diyl)bis(chlorobenzene).

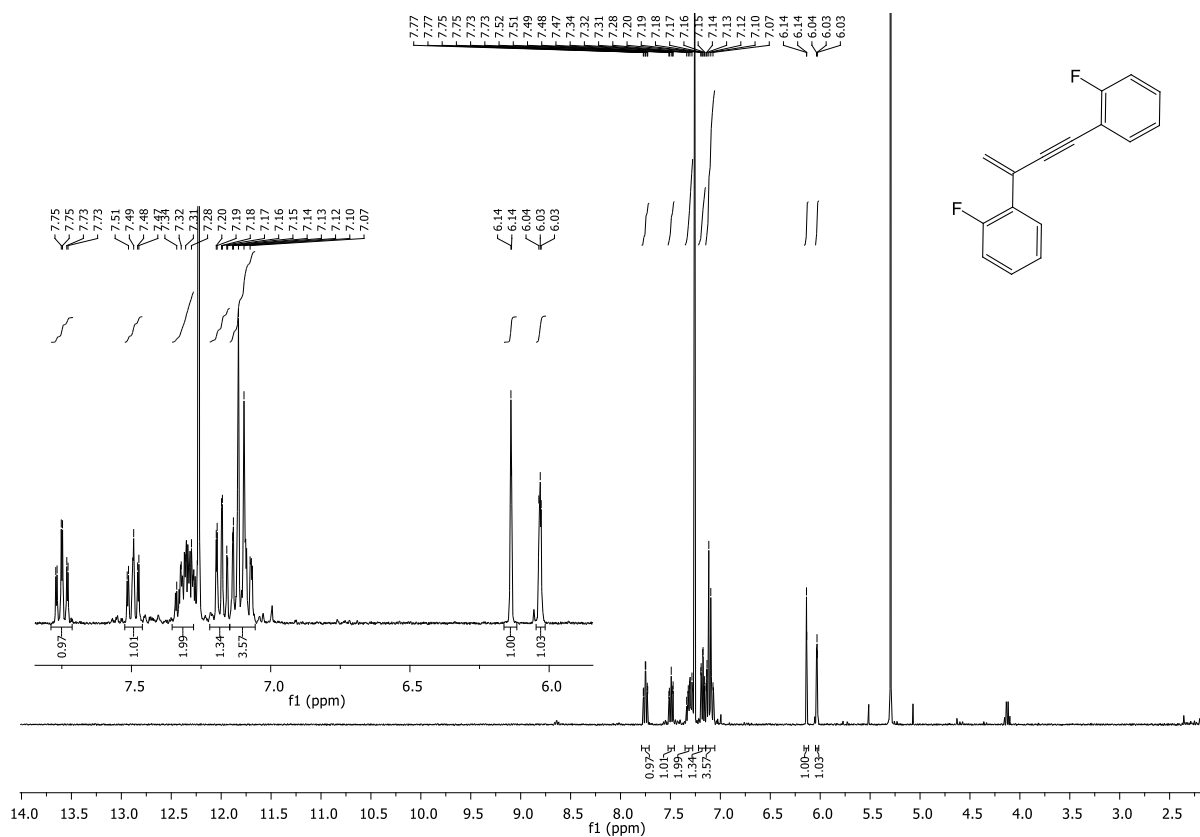


Figure 8.362: $^1\text{H-NMR}$ spectrum of 2,2'-(but-3-en-1-yne-1,3-diyl)bis(fluorobenzene).

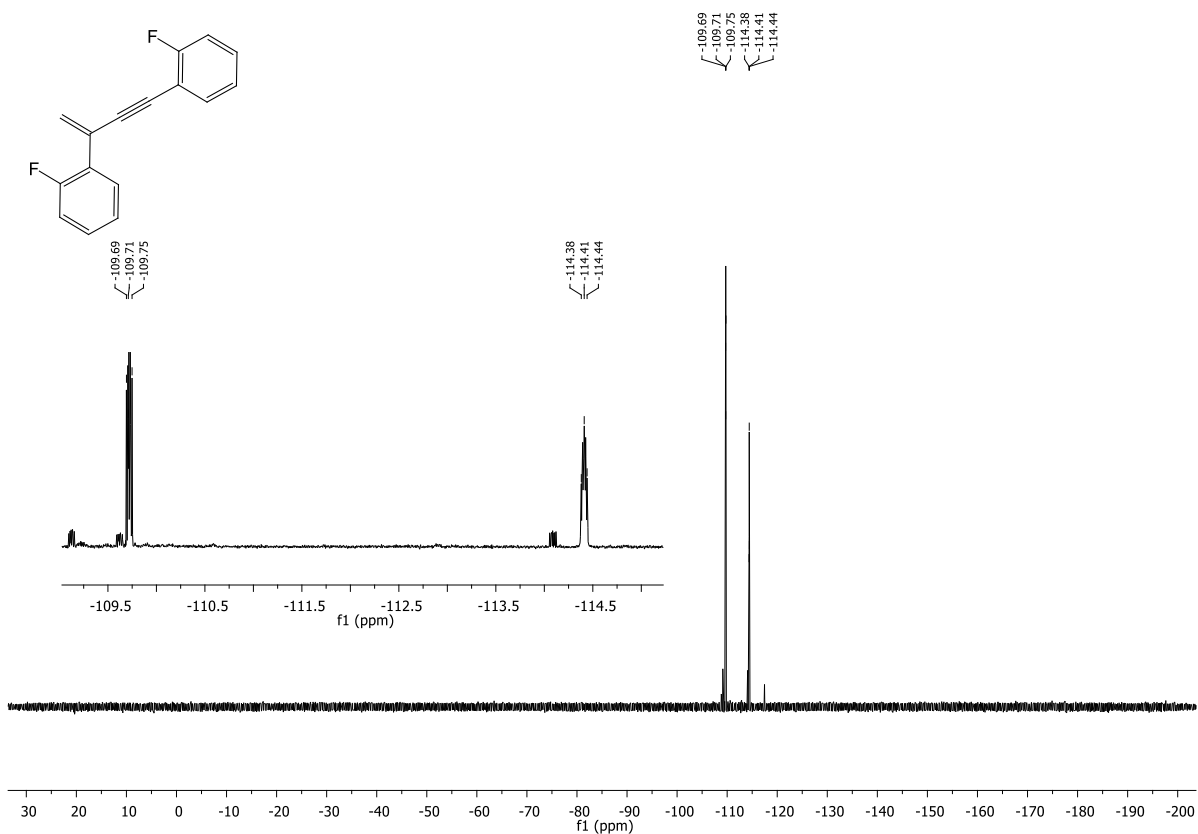


Figure 8.363: ^{19}F -NMR spectrum of 2,2'-(but-3-en-1-yne-1,3-diyl)bis(fluorobenzene).

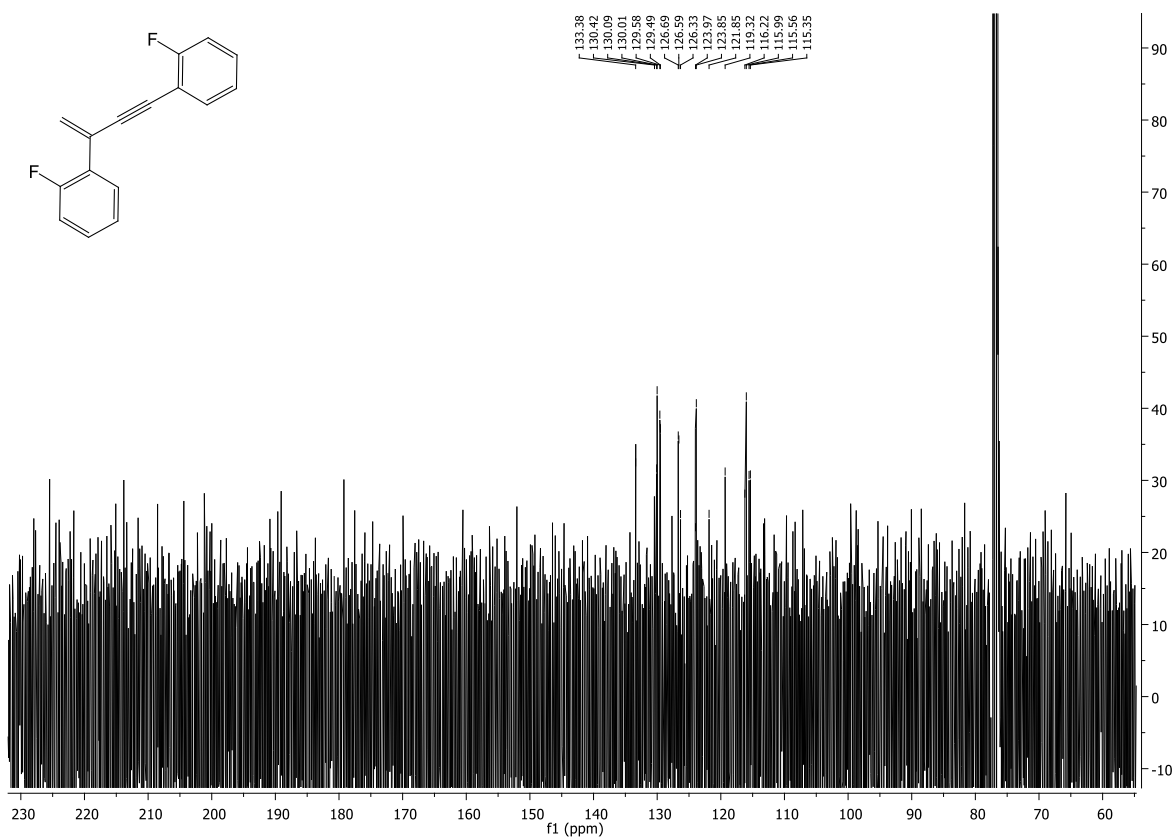


Figure 8.364: ^{13}C -NMR spectrum of 2,2'-(but-3-en-1-yne-1,3-diyl)bis(fluorobenzene).

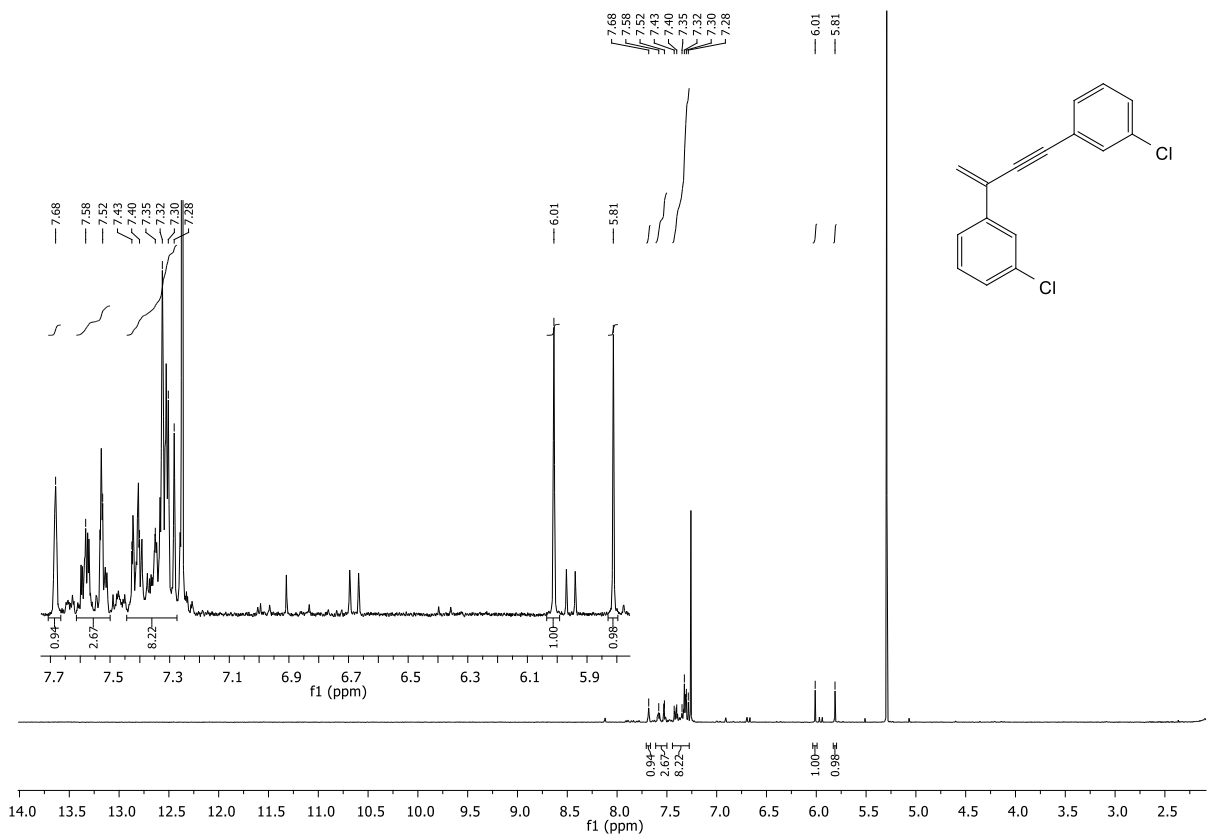


Figure 8.365: ¹H-NMR spectrum of 3,3'-(but-3-en-1-yne-1,3-diyl)bis(chlorobenzene).

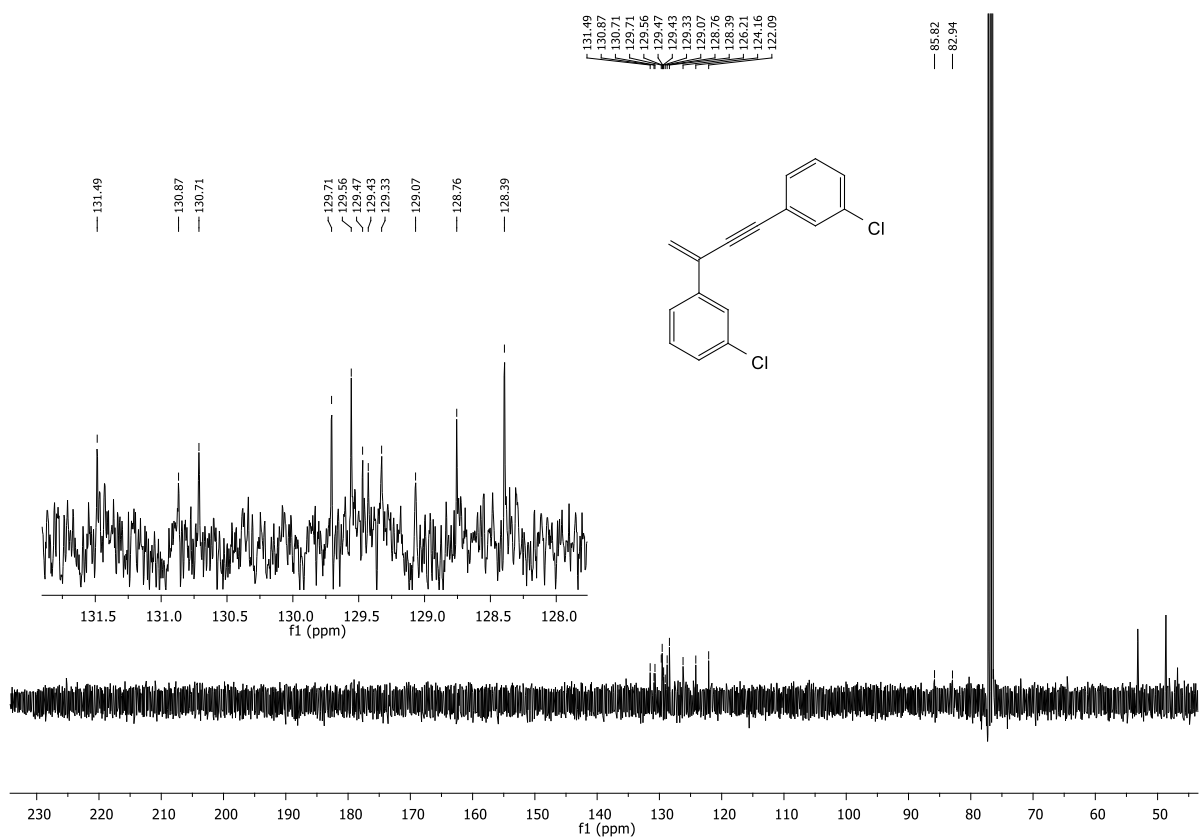


Figure 8.366: ¹³C-NMR spectrum of 3,3'-(but-3-en-1-yne-1,3-diyl)bis(chlorobenzene).

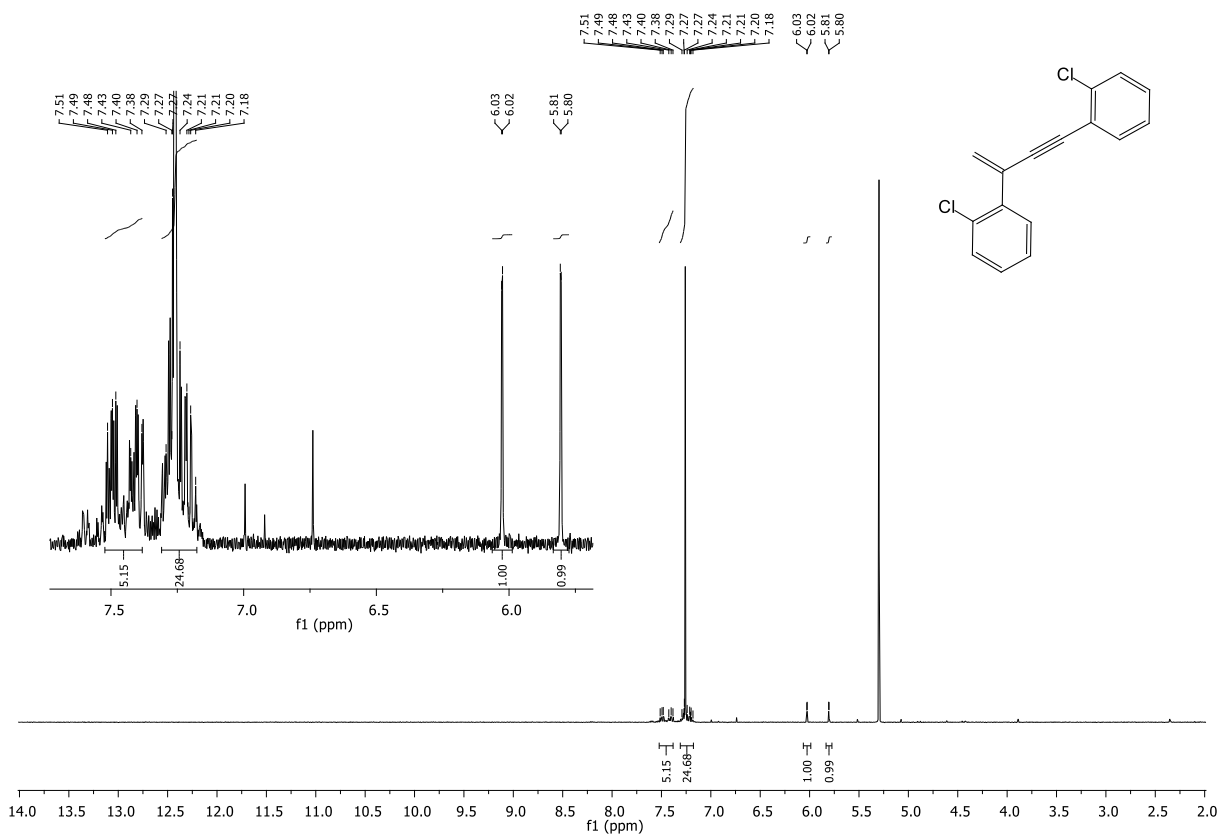


Figure 8.367: ¹H-NMR spectrum of 2,2'-(but-3-en-1-yne-1,3-diyl)bis(chlorobenzene).

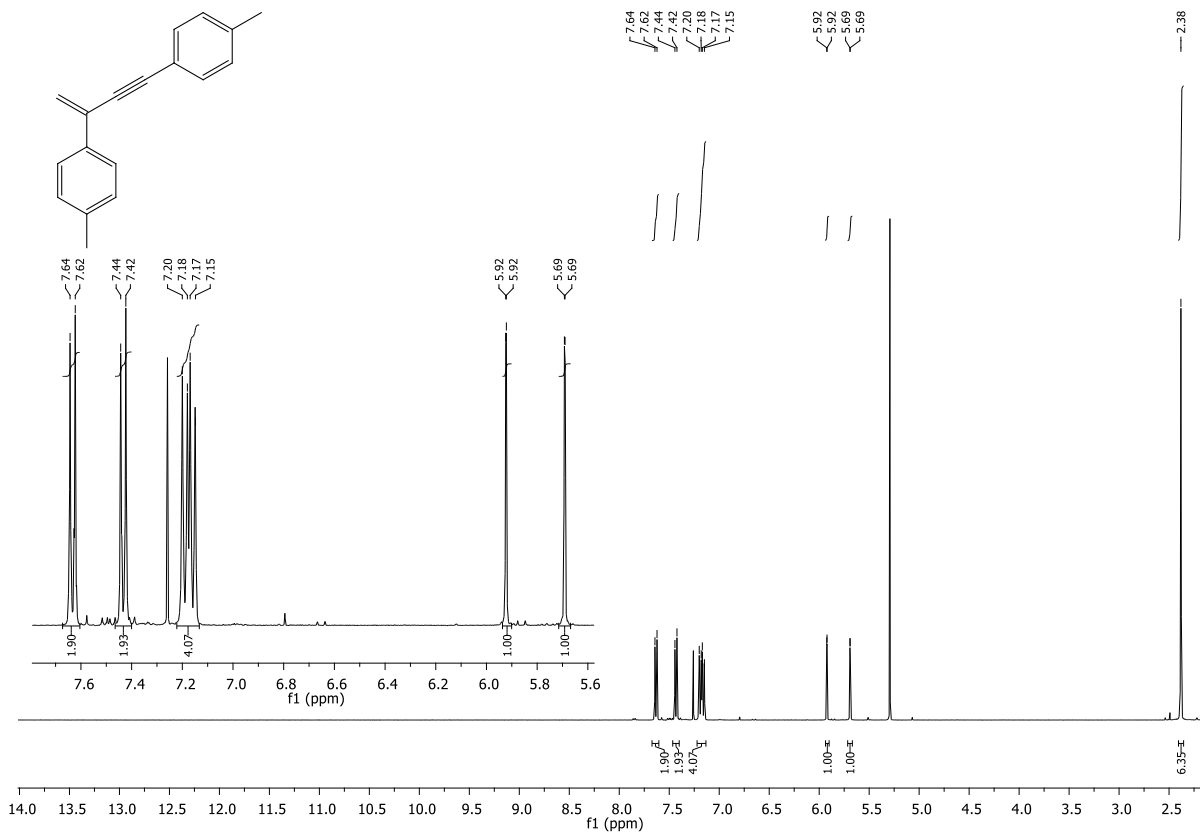


Figure 8.368: ¹H-NMR spectrum of 4,4'-(but-3-en-1-yne-1,3-diyl)bis(methylbenzene).

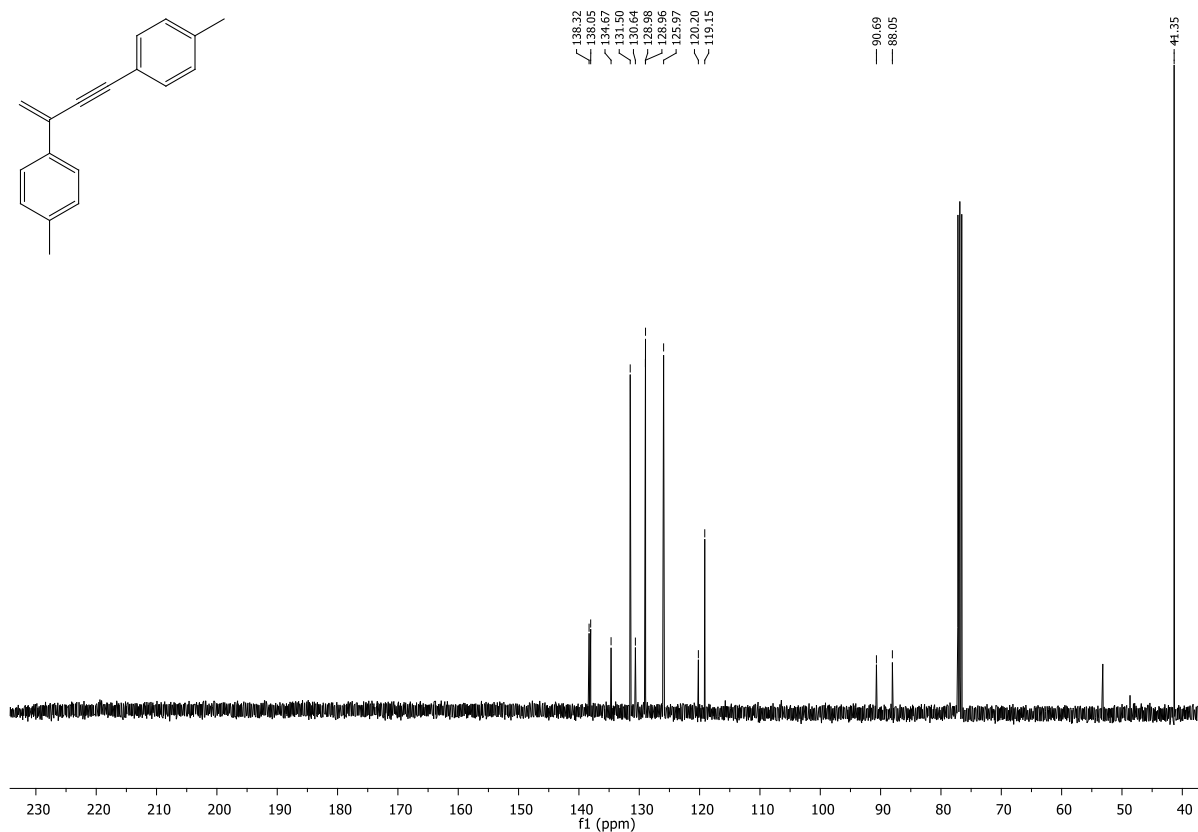


Figure 8.369: $^{13}\text{C-NMR}$ spectrum of 4,4'-(but-3-en-1-yne-1,3-diyl)bis(methylbenzene).

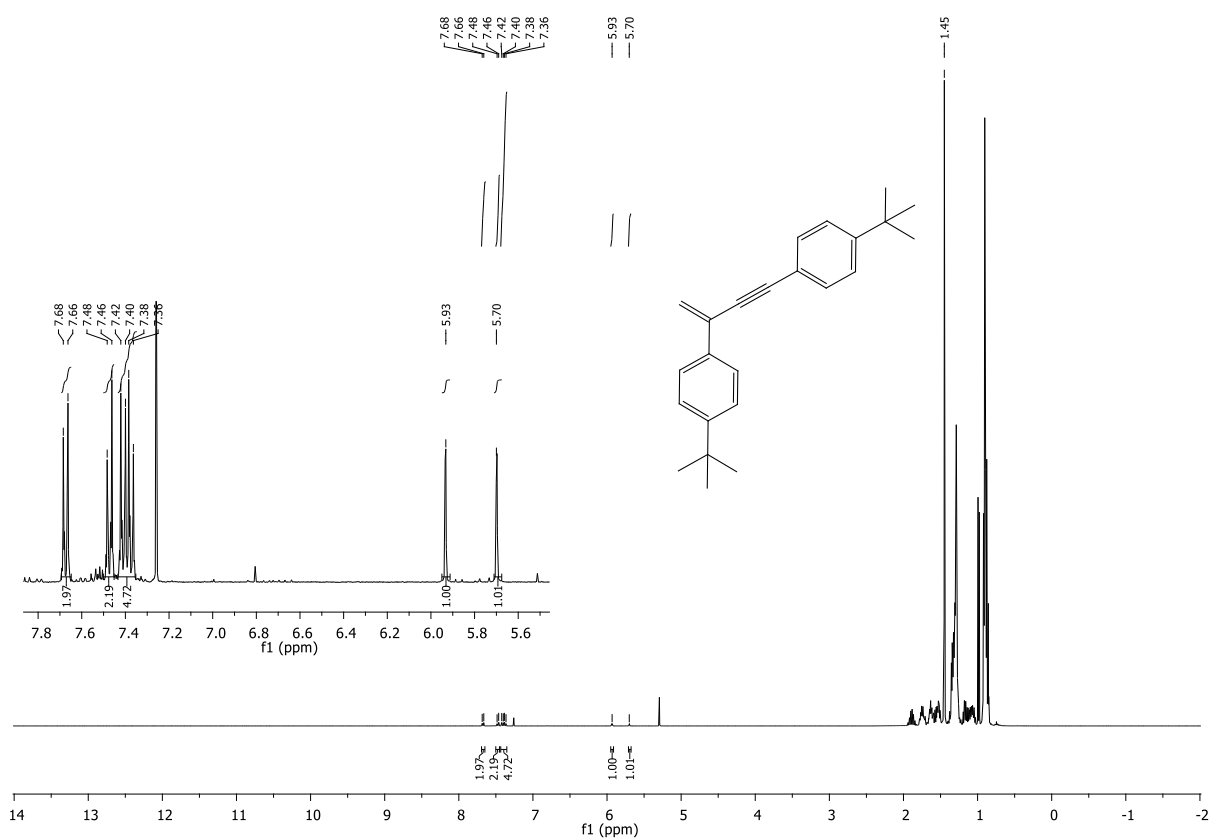


Figure 8.370: $^1\text{H-NMR}$ spectrum of 4,4'-(but-3-en-1-yne-1,3-diyl)bis(tert-butylbenzene).

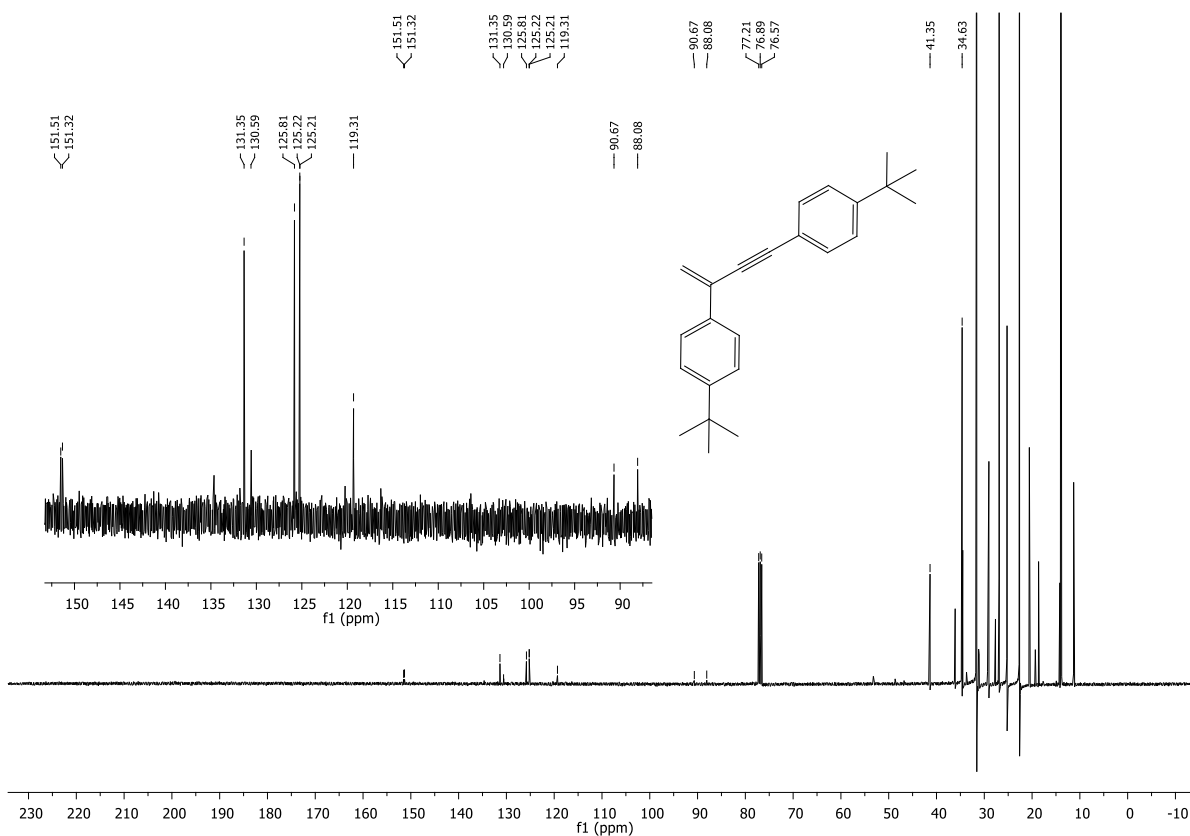


Figure 8.371: ^{13}C -NMR spectrum of 4,4'-(but-3-en-1-yne-1,3-diyl)bis(tert-butylbenzene).

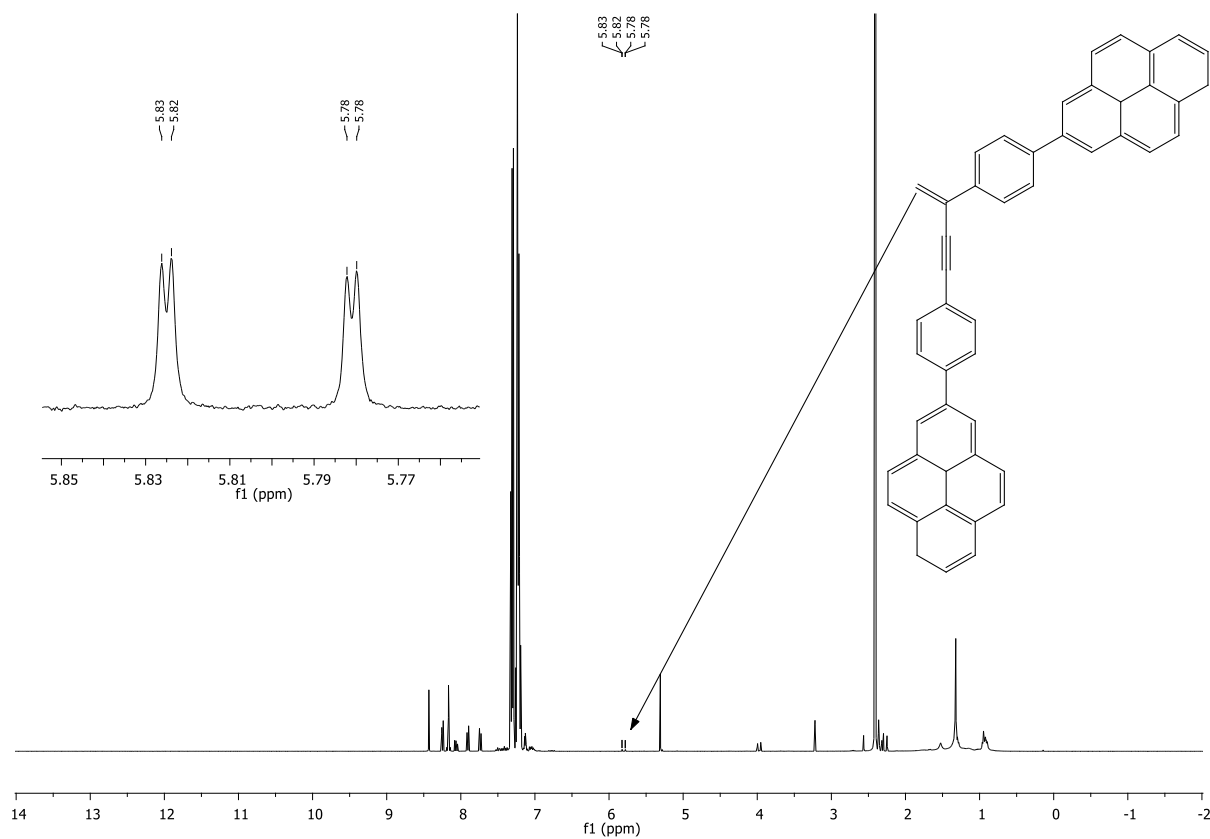


Figure 8.372: ^1H -NMR spectrum after reaction of 7-(4-ethynylphenyl)-1,5a1-dihdropyrene on Al_2O_3 .

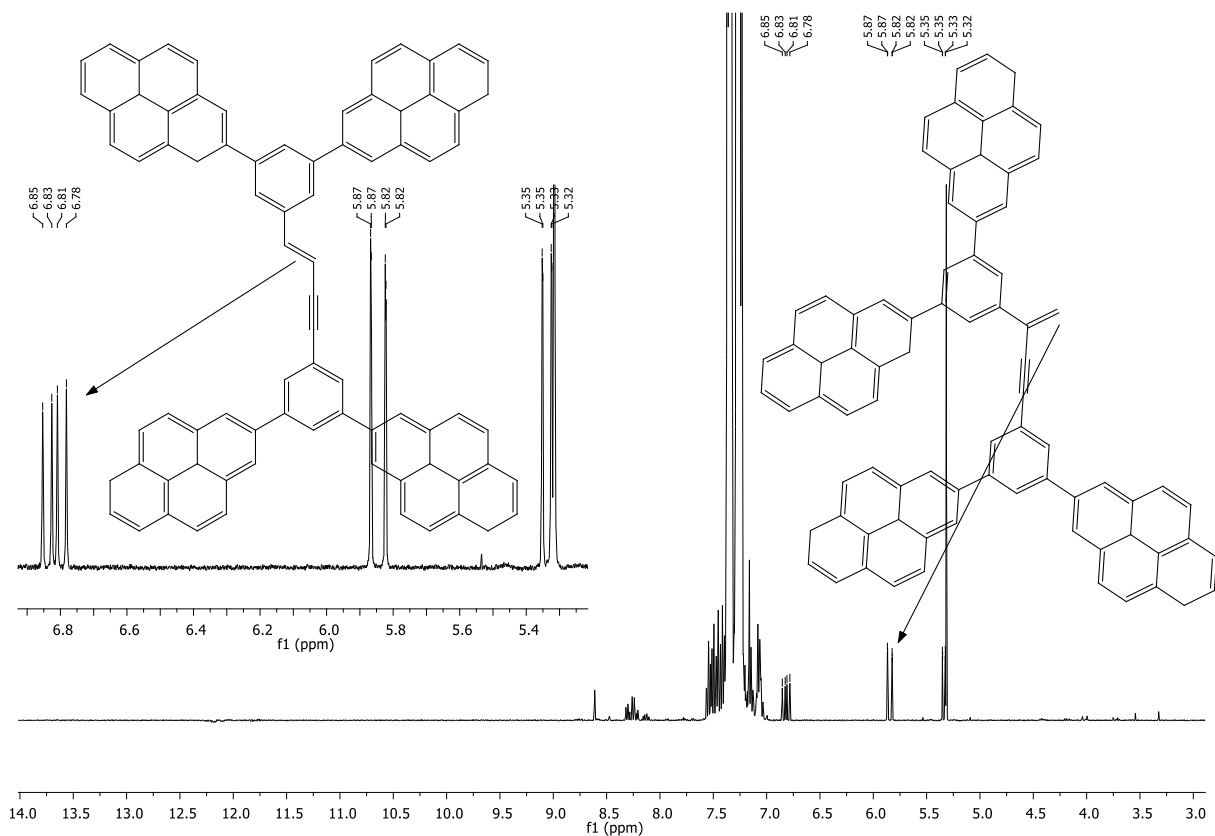


Figure 8.373: $^1\text{H-NMR}$ spectrum after reaction of 7,7'-(5-ethynyl-1,3-phenylene)bis(1,5a1-dihydropyrene) on Al_2O_3 .

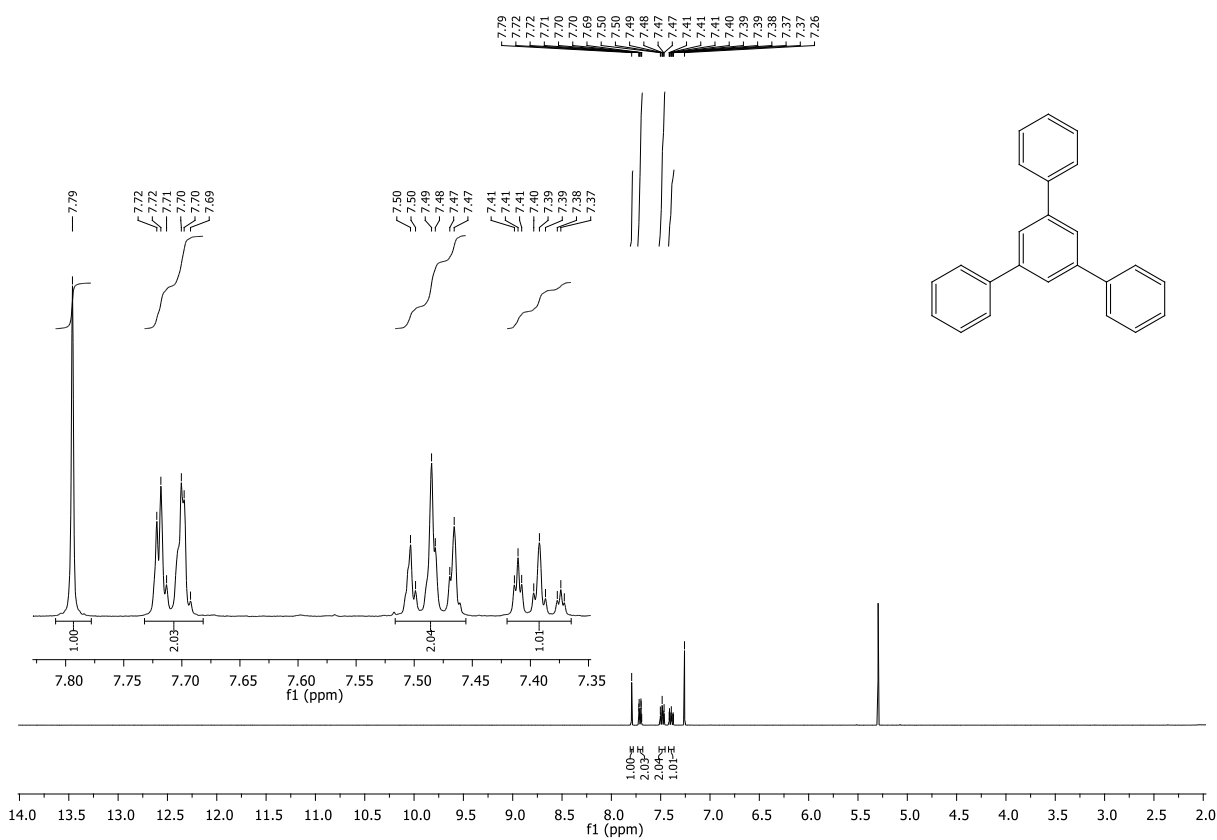


Figure 8.374: $^1\text{H-NMR}$ spectrum of 5'-phenyl-1,1':3,1''-terphenyl.

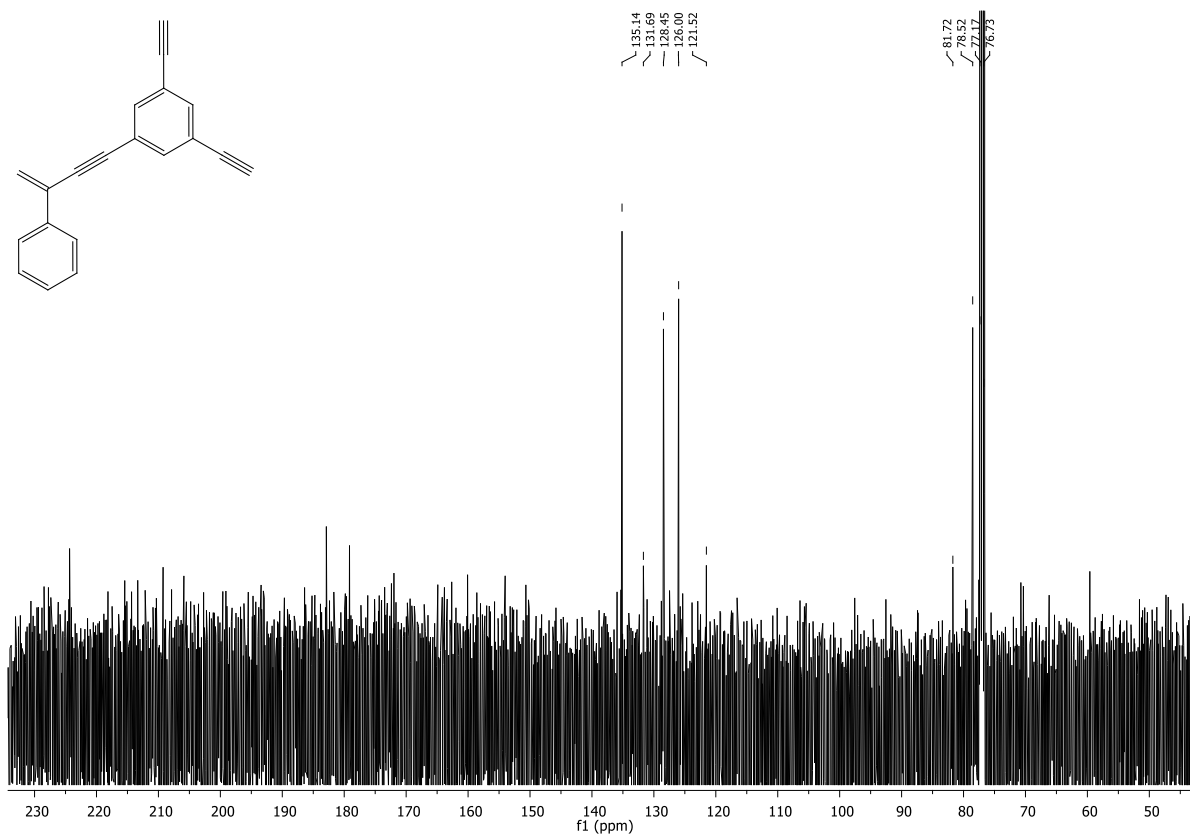


Figure 8.377: ^{13}C -NMR spectrum of 1,3-diethynyl-5-(3-phenylbut-3-en-1-yn-1-yl)benzene.

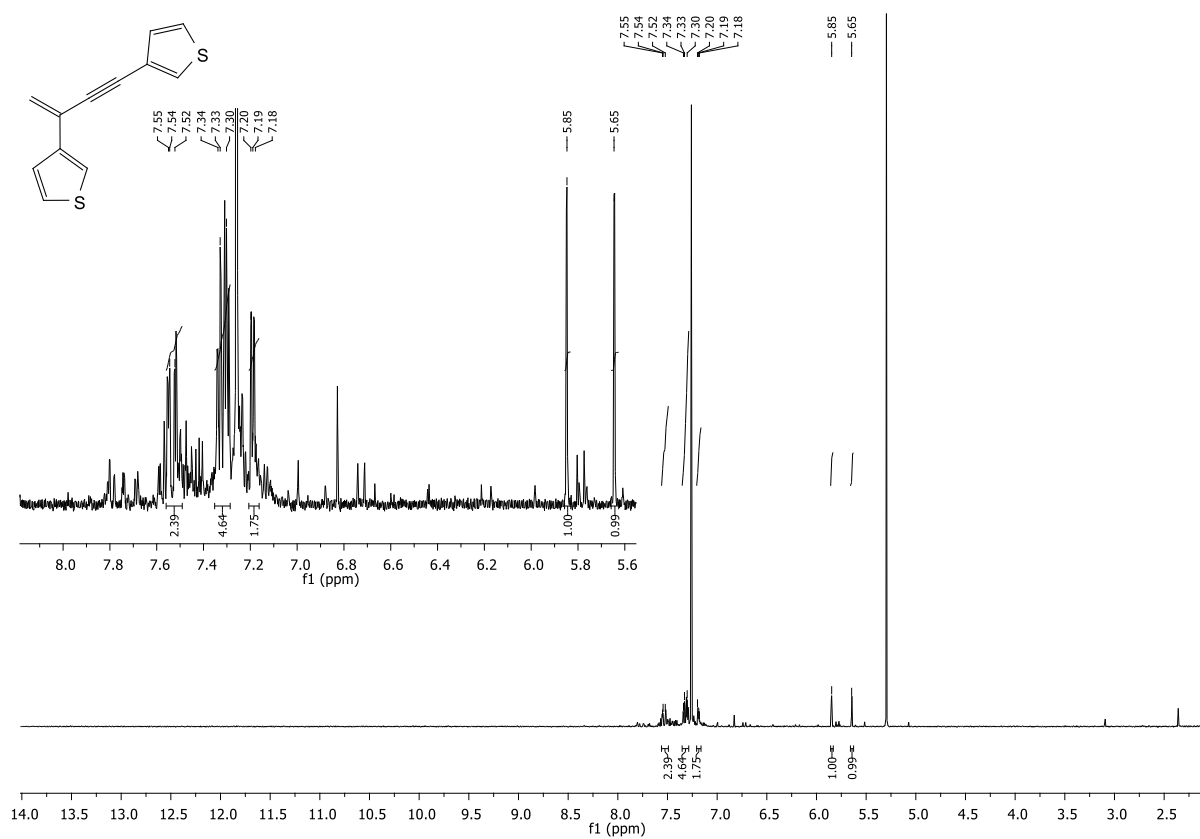


Figure 8.378: ^1H -NMR spectrum of 3,3'-(but-3-en-1-yne-1,3-diyl)dithiophene.

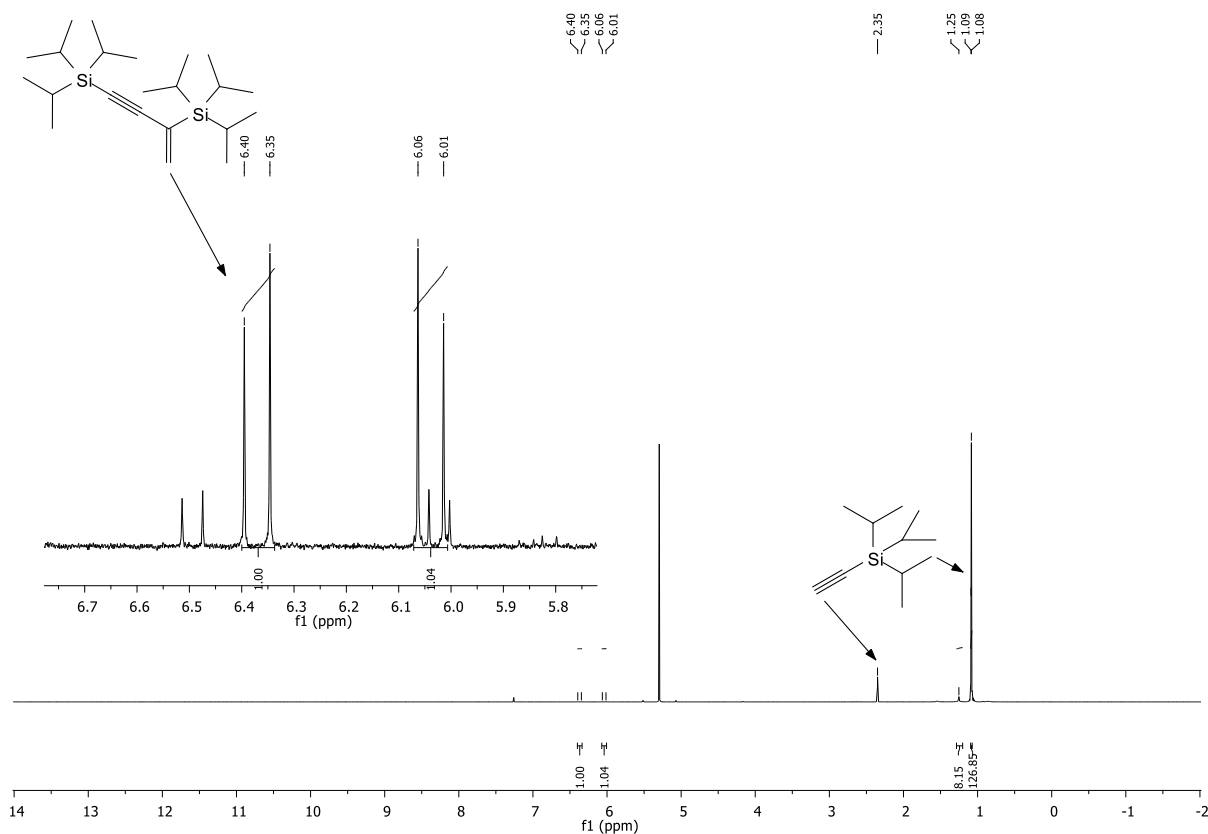


Figure 8.379: $^1\text{H-NMR}$ spectrum after reaction of ethynyltriisopropylsilane.

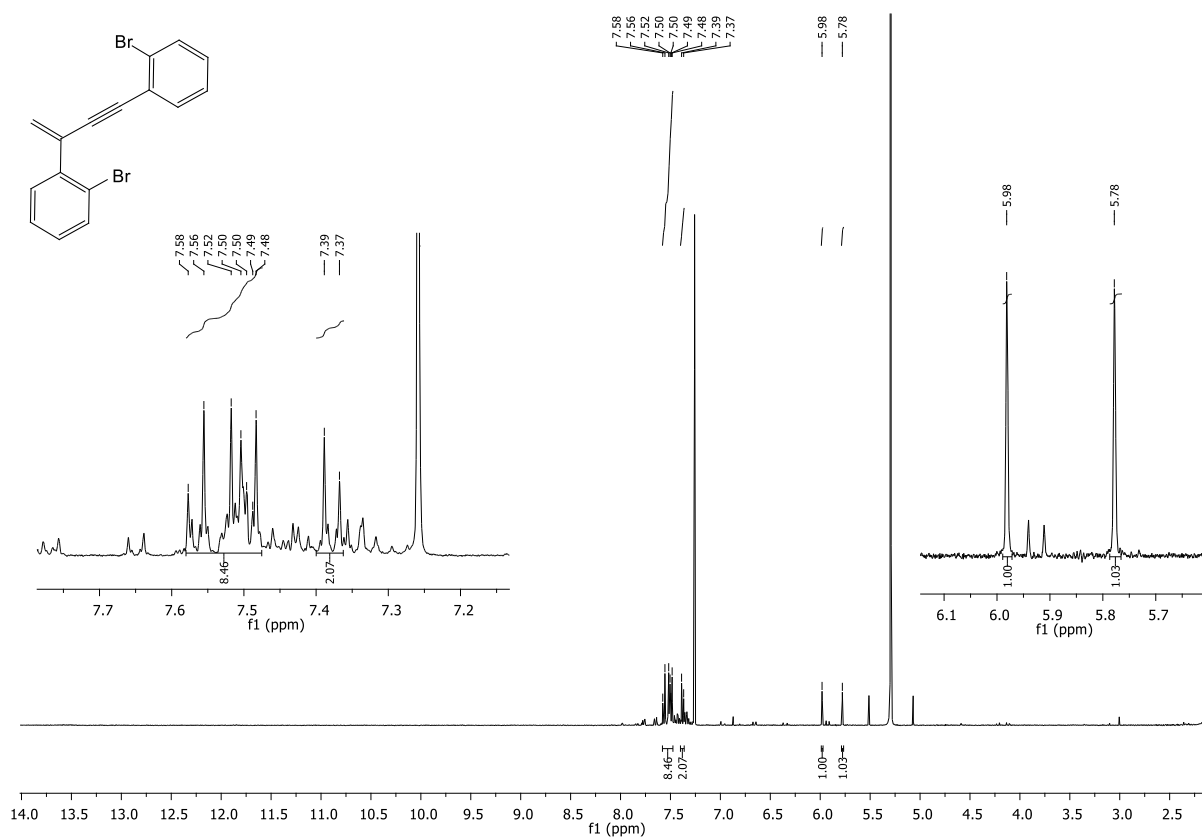


Figure 8.380: $^1\text{H-NMR}$ spectrum of 2,2'-(but-3-en-1-yne-1,3-diyl)bis(bromobenzene).

8.8. Hydrochlorination of terminal Alkynes on Al_2O_3

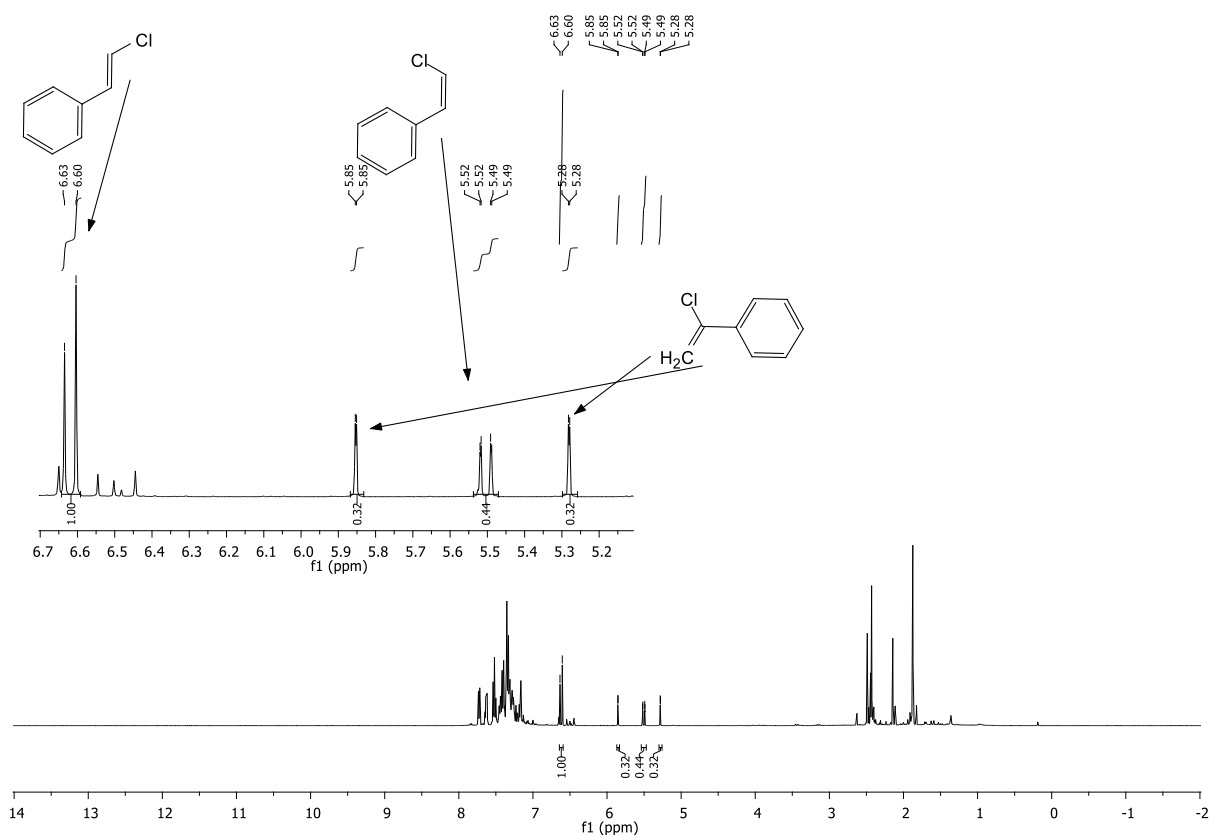


Figure 8.381: $^1\text{H-NMR}$ spectrum after chlorination of phenylacetylene.

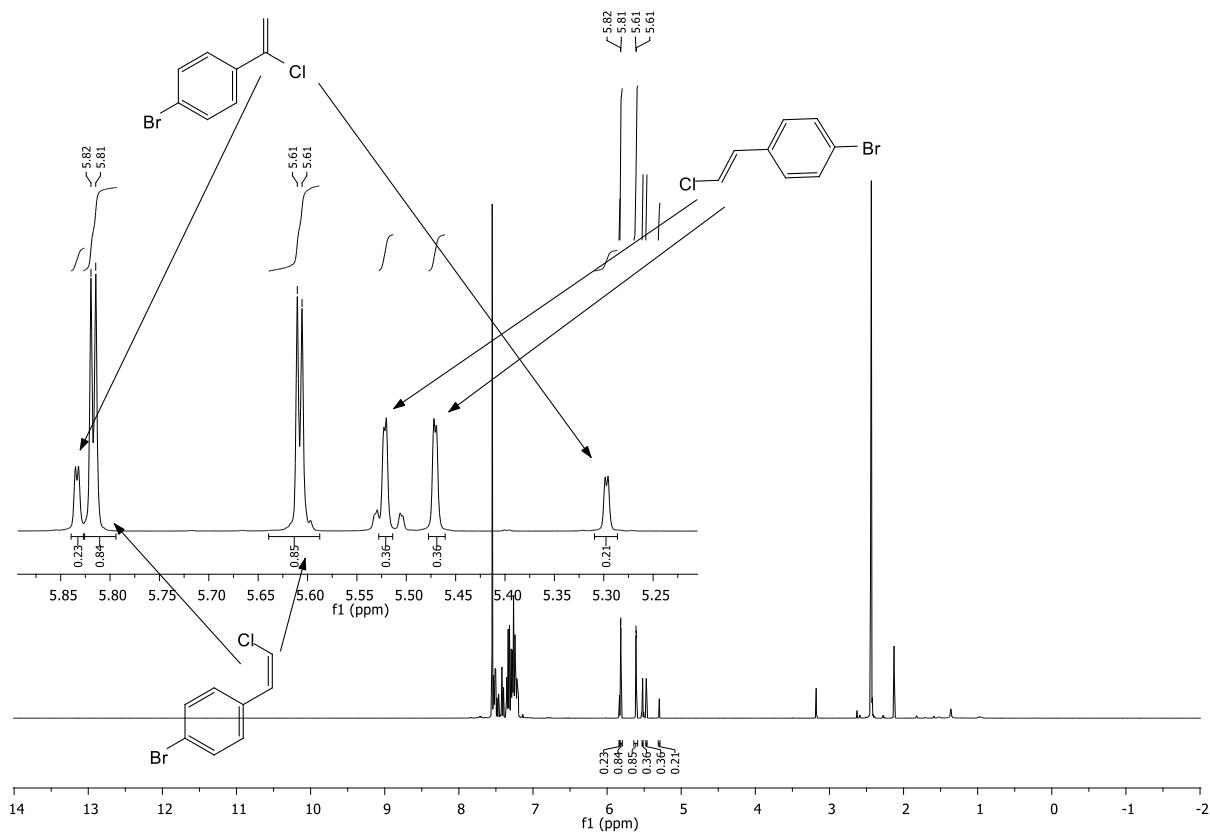


Figure 8.382: $^1\text{H-NMR}$ spectrum after chlorination of 1-bromo-4-ethynylbenzene

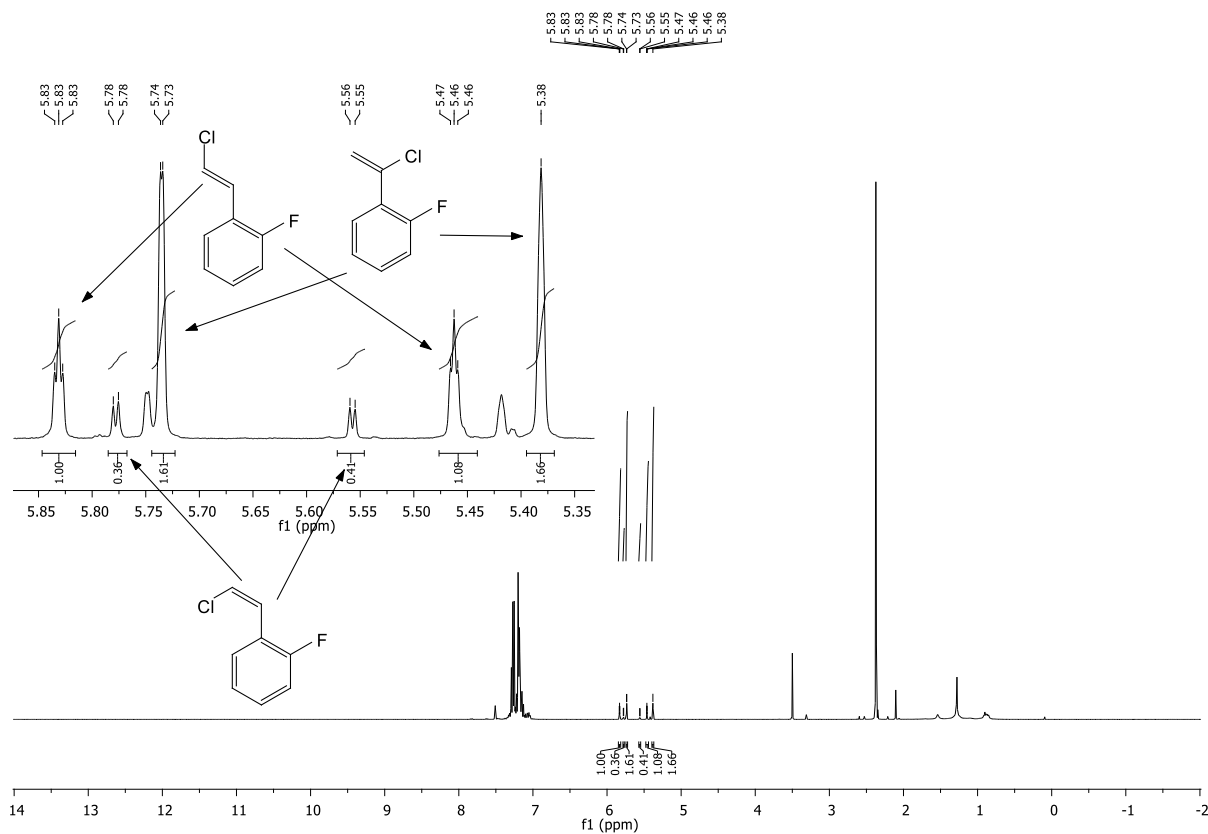


Figure 8.383: $^1\text{H-NMR}$ spectrum after chlorination of 1-ethynyl-2-fluorobenzene.

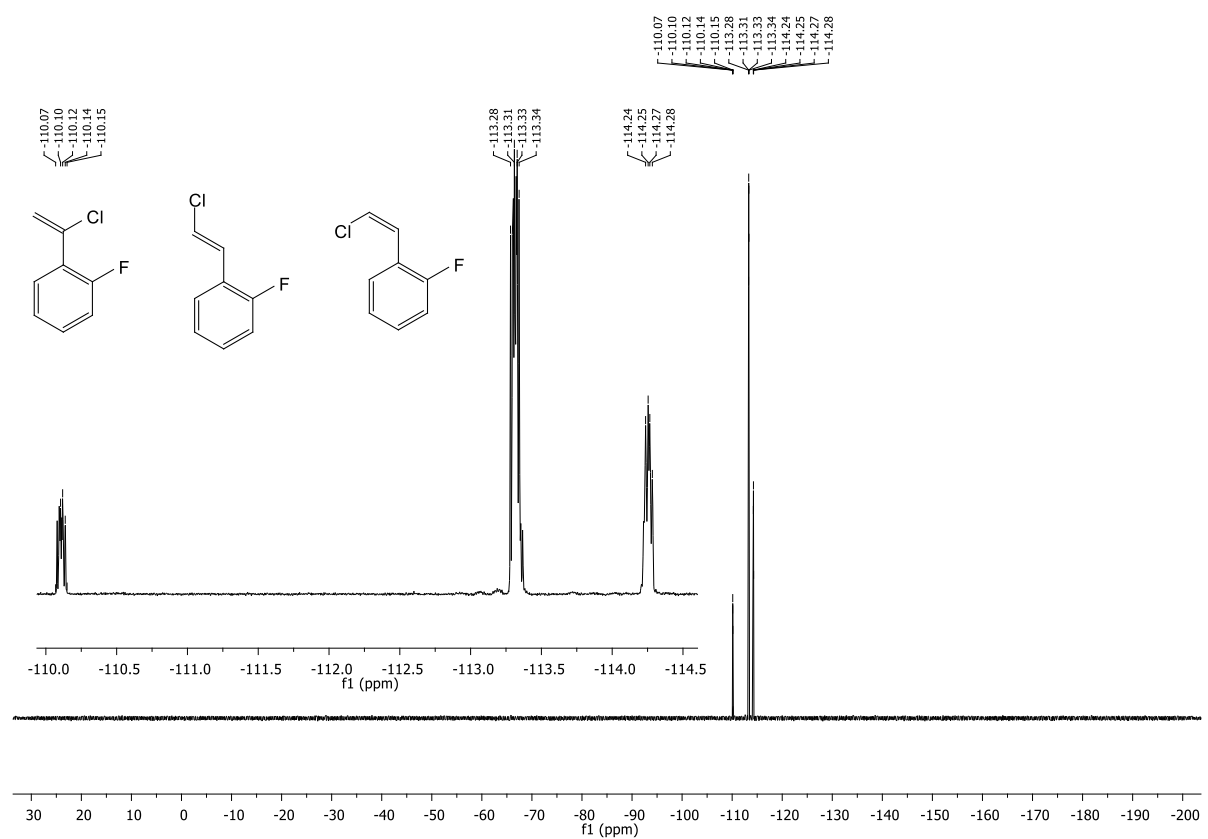


Figure 8.384: $^{19}\text{F-NMR}$ spectrum after chlorination of 1-ethynyl-2-fluorobenzene.

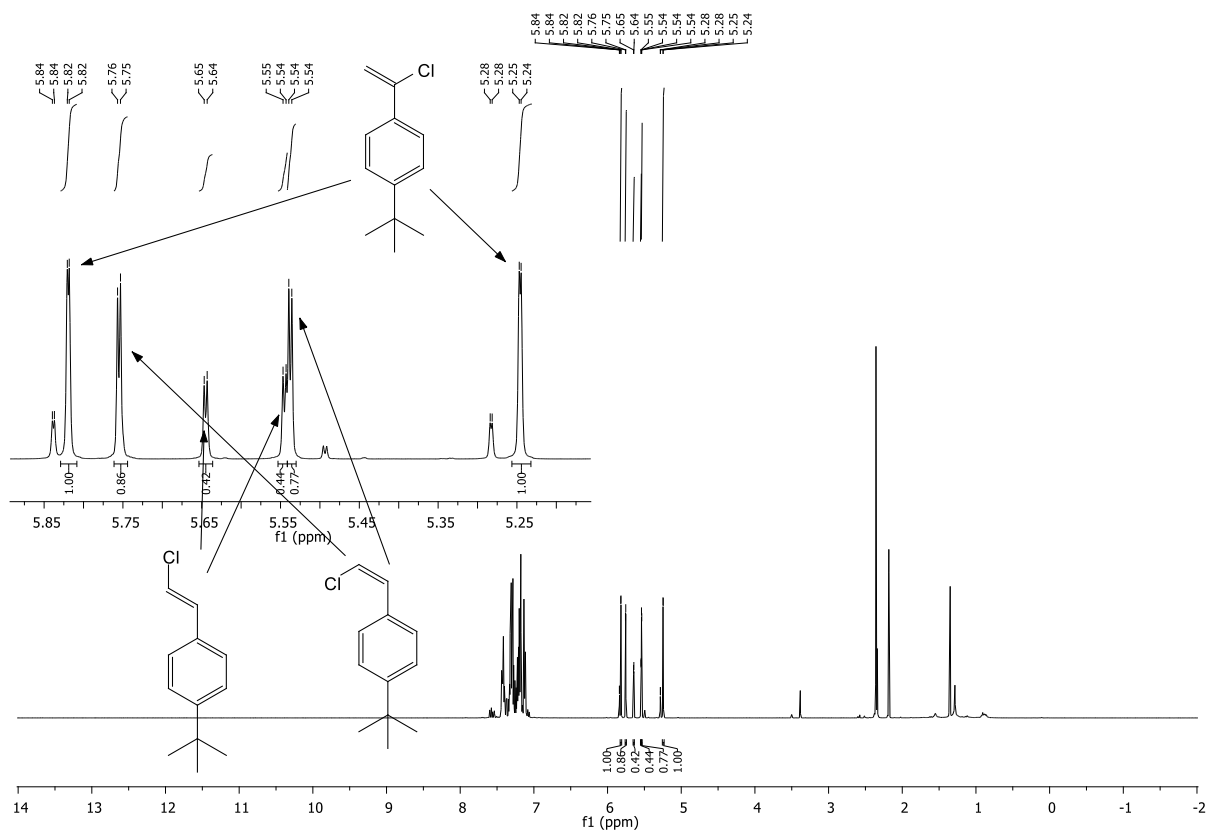


Figure 8.385: $^1\text{H-NMR}$ spectrum after chlorination of 1-(tert-butyl)-4-ethynylbenzene.

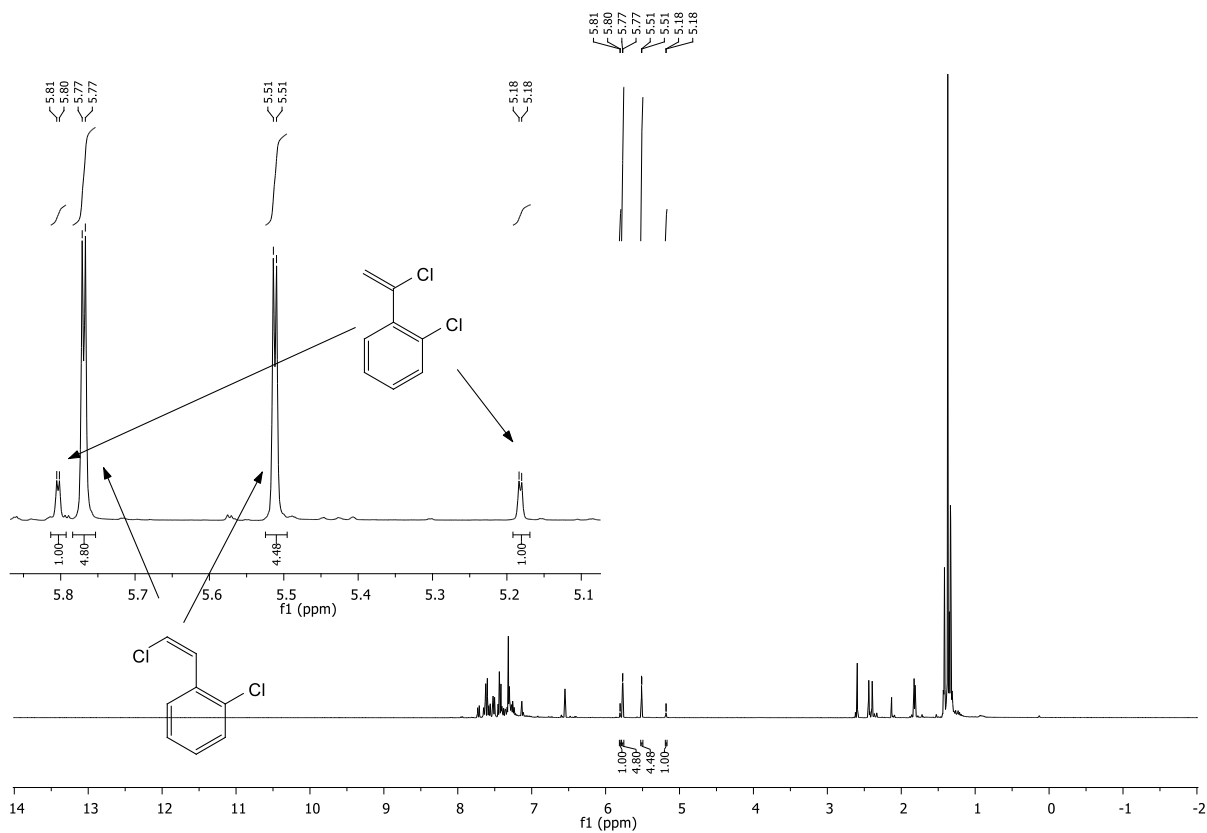


Figure 8.386: $^1\text{H-NMR}$ spectrum after chlorination of 1-chloro-2-ethynylbenzene.

Eidesstattliche Erklärung

Hiermit erkläre ich, Andreas Förtsch, die vorliegende Arbeit „Investigation of metal oxides mediated construction and reactivity of polycyclic aromatic hydrocarbons“ selbständig und ohne fremde Hilfe verfasst zu haben. Es wurden keine anderen als die von mir angegebenen Quellen und Hilfsmittel benutzt. Die den benutzten Werken wörtlich oder inhaltlich entnommenen Stellen sind als solche kenntlich gemacht worden. Ich erkläre, die Angaben wahrheitsgemäß gemacht, keine vergeblichen Promotionsversuche unternommen und keine Dissertation an einer anderen wissenschaftlichen Einrichtung zur Erlangung eines akademischen Grades eingereicht zu haben. Ich bin weder vorbestraft noch sind gegen mich Ermittlungsverfahren anhängig.

Publikationsliste

1. Akhmetov, V., Förtsch, A., Feofanov, M., Troyanov, S., & Amsharov, K. (2020). Folding of fluorinated oligoarylenes into non-alternant PAHs with various topological shapes. *Organic chemistry frontiers*, 7(10), 1271-1275.
2. Feofanov, M., Förtsch, A., Amsharov, K., & Akhmetov, V. (2021). Solid-state construction of zigzag periphery via intramolecular C–H insertion induced by alumina-mediated C–F activation. *Chemical Communications*, 57(92), 12325-12328.

ANDREAS FÖRTSCH

PROJEKTMANAGER F&E

Berufserfahrung

01/2023-05/2023



Projektmanager F&E bei Iolitec,

- Entwicklung neuer Ionischer Flüssigkeiten für Batterie-Elektrolyte und Metallabscheidung für Elektroden.
- Prozessoptimierung von Synthesen mit Blick auf Rentabilität, Sicherheit und Umweltschutz.
- Projektmanagement in Zusammenarbeit mit Universitäten, Forschungseinrichtungen und anderen Unternehmen (CaSino, HILUGEN).

11/2019-12/2022



Wissenschaftlicher Mitarbeiter der *Martin-Luther-Universität Halle-Wittenberg*,

- **Doktorarbeit** zum Thema „Investigation of metal oxides mediated construction and reactivity of polycyclic aromatic hydrocarbons“ bei Prof. Amsharov

04/2019-06/2019



Wissenschaftliche Hilfskraft im Arbeitskreis von Prof. Amsharov *Friedrich-Alexander-Universität Erlangen-Nürnberg*

- Übergang zur Doktorarbeit

04/2015 – 05/2015



Wissenschaftliche Hilfskraft

Friedrich-Alexander-Universität Erlangen-Nürnberg

Betreuung von Pharmazie Studenten des Praktikums Physikalischen Chemie I

09/2014 -01/2015



Wissenschaftliche Hilfskraft

Friedrich-Alexander-Universität Erlangen-Nürnberg

Betreuung von Pharmazie Studenten des Praktikums
Physikalischen Chemie II

Bildungsweg

10/2014 - 04/2019



Master of Science Chemie

Friedrich-Alexander-Universität Erlangen-Nürnberg

- Kernmodule: Anorganische Chemie, Organische Chemie, Physikalisch Chemie
- Wahlmodule: Molekulare Materialien, Katalyse
- Masterarbeit bei Prof. Amsharov über „Background Investigation Towards Elusive Heptagon Containing Polycyclic Aromatic Hydrocarbons by Cyclodehydrofluorination“
- Abschlussnote: 2,4

10/2015 – 02/2016



Auslandssemester

Imperial College London

Forschungsarbeit bei Prof. William

- „Synthesis and characterization of pentadentate yttrium phosphasalen and salen rac-lactide initiators and study of the structure-selectivity relationship“

10/2011 - 10/2014



Bachelor of Science Chemie

Friedrich-Alexander-Universität Erlangen-Nürnberg

- Bachelorarbeit bei Prof. Harder über „Chemistry of trispyrazolylborate aluminium complexes: terminal hydroxyde and oxyde species“
- Abschlussnote: 2,1

09/2003 - 06/2011



Abitur

Paul-Pfinzing-Gymnasium Hersbruck

- Facharbeitsthema „Epoxidharz-Klebstoffe“
- Abschlussnote: 2,2